UCRL-18043

cy. 2

INORGANIC MATERIALS RESEARCH DIVISION
Annual Report 1967

RECEIVED
LAWRENCE
RADIATION LABORATORY
JUL 2 1968
LIBRARY AND
DOCUMENTS SECTION

TWO-WEEK LOAN COPY

This is a Library Circulating Copy which may be borrowed for two weeks. For a personal retention copy, call Tech. Info. Division, Ext. 5545

UCRL-18043 cy. 2

Lawrence Radiation Laboratory
University of California Berkeley

Metallurgical Engineering

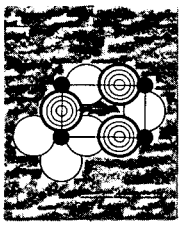

Chemistry

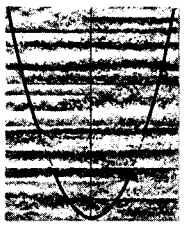

Solid-State Physics

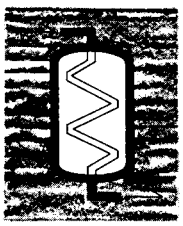

Chemical Engineering

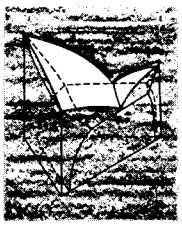

Ceramic Engineering

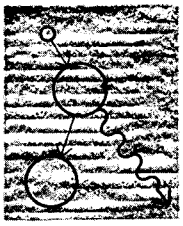

Nuclear Engineering

DISCLAIMER

This document was prepared as an account of work sponsored by the United States Government. While this document is believed to contain correct information, neither the United States Government nor any agency thereof, nor the Regents of the University of California, nor any of their employees, makes any warranty, express or implied, or assumes any legal responsibility for the accuracy, completeness, or usefulness of any information, apparatus, product, or process disclosed, or represents that its use would not infringe privately owned rights. Reference herein to any specific commercial product, process, or service by its trade name, trademark, manufacturer, or otherwise, does not necessarily constitute or imply its endorsement, recommendation, or favoring by the United States Government or any agency thereof, or the Regents of the University of California. The views and opinions of authors expressed herein do not necessarily state or reflect those of the United States Government or any agency thereof or the Regents of the University of California.

UCRL-18043
UC-2 General, Miscellaneous,
and Progress Reports
TID-4500 (51st Ed.)

INORGANIC MATERIALS RESEARCH DIVISION ANNUAL REPORT, 1967

March 1968

Lawrence Radiation Laboratory
University of California
Berkeley, California

Work done under
U.S. Atomic Energy Commission
Contract No. W-7405-eng-48

Printed in the United States of America
Available from
Clearinghouse for Federal Scientific and Technical Information
National Bureau of Standards, U.S. Department of Commerce
Springfield, Virginia 22151
Price: Printed Copy $3.00; Microfiche $0.65

INORGANIC MATERIALS RESEARCH DIVISION

ANNUAL REPORT, 1967

Contents

GENERAL INTRODUCTION 1

I. CHEMISTRY

A. Inorganic Chemistry 7

B. Chemical Thermodynamics 21

C. Solid-State Chemistry and Physics . . . 27

D. Electrochemistry 47

E. Physical Chemistry 73

F. Nuclear Science 99

II. METALLURGY

A. Crystal Imperfections 107

B. Kinetics of Dislocation Mechanisms . . 115

C. Relation of Structure to Properties in Crystal 119

D. High-Strength Materials 131

E. High-Field Superconductivity 141

F. Thermodynamics of Metal System 151

III. CERAMIC SCIENCE

A. High-Temperature Reactions 155

B. Microstructure and Behavior of Ceramic Materials; Glass-Metal Systems. . . . 161

C. Development and Behavior of Microstructures in Ceramic Systems . . 171

IV. SOLID-STATE PHYSICS

A. Theoretical Solid-State Physics . . . 183

B. Magnetic Properties of Solids 185

C. Far-Infrared Properties of Solids. . . 187

D. Superconductivity 193

E. Experimental Solid-State Physics and Quantum Electronics 195

F. Nuclear Spin Interactions 197

IMRD STAFF FOR 1967 199

DEGREES AWARDED 205

1967 RESEARCH SEMINARS. 207

KEY-WORD-PLUS-TITLE SUBJECT AND AUTHOR INDEX 209

INORGANIC MATERIALS RESEARCH DIVISION

ANNUAL REPORT, 1967

GENERAL INTRODUCTION

Leo Brewer, Division Head
Victor F. Zackay, Associate Head

The Division has continued to grow, and by the end of 1967 the number of graduate students had increased to 172 (see Fig. 1). A total of 48 advanced-degree theses were filed during the year (see Fig. 2).

The publications of the Division continued to increase, with 138 publications to technical journals or as chapters of books during 1967. Three new books were published by principal investigators of IMRD: Preparative Inorganic Reactions, by William Jolly (Interscience Publishers, 1967); An Atomistic Approach to the Nature and Properties of Materials, by Joseph A. Pask (John Wiley and Sons, 1967); Materials Data Book for Engineers and Scientists, by Earl R. Parker (McGraw-Hill Books Company, 1967).

The program of the IMRD is being materially increased by the new programs of Assistant Professors R. Herm, R. Shen, and G. Rochlin who have made excellent progress during 1967 in setting up their equipment. Dr. Charles Harris from MIT, who was appointed Assistant Professor in the Department of Chemistry, was added as a principal investigator. His investigations will be primarily concerned with the electron distribution in transition-metal complexes. Dr. Marshal Merriam was granted a year's leave to continue his research on superconductivity at the Indian Institute of Technology in Kanpur, India. His replacement for the duration of his leave is Dr. Robert Hammond who will be in charge of the research group until Merriam's return.

A number of IMRD principal investigators received professional honors and served in University administrative positions during the year. Professor Earl R. Parker was named to the presidency of the American Society for Metals, and Professor Leo Brewer was appointed as an associate director of the Lawrence Radiation Laboratory. Professor Harold S. Johnston is serving as Dean of the Department of Chemistry, while Professor Bruce Mahan was appointed vice-chairman of the Chemistry Department. Professor Charles W. Tobias continued as chairman of the Department of Chemical Engineering, as did Professor Jack Washburn as Chairman of the Department of Mineral Technology. Professor Alan W. Searcy and Professor Robert E. Connick ended their terms of office as Vice-Chancellors and returned to full-time teaching and research. Professor John Newman was awarded the Young Author's Award by the Electrochemical Society.

During the year Professor Richard Fulrath spent three months on sabbatical leave at Leeds University, England.

In the past year, Professor Gareth Thomas completed a six-month critical evaluation of ultrahigh-voltage electron microscopes. In this evaluation, Professor Thomas traveled

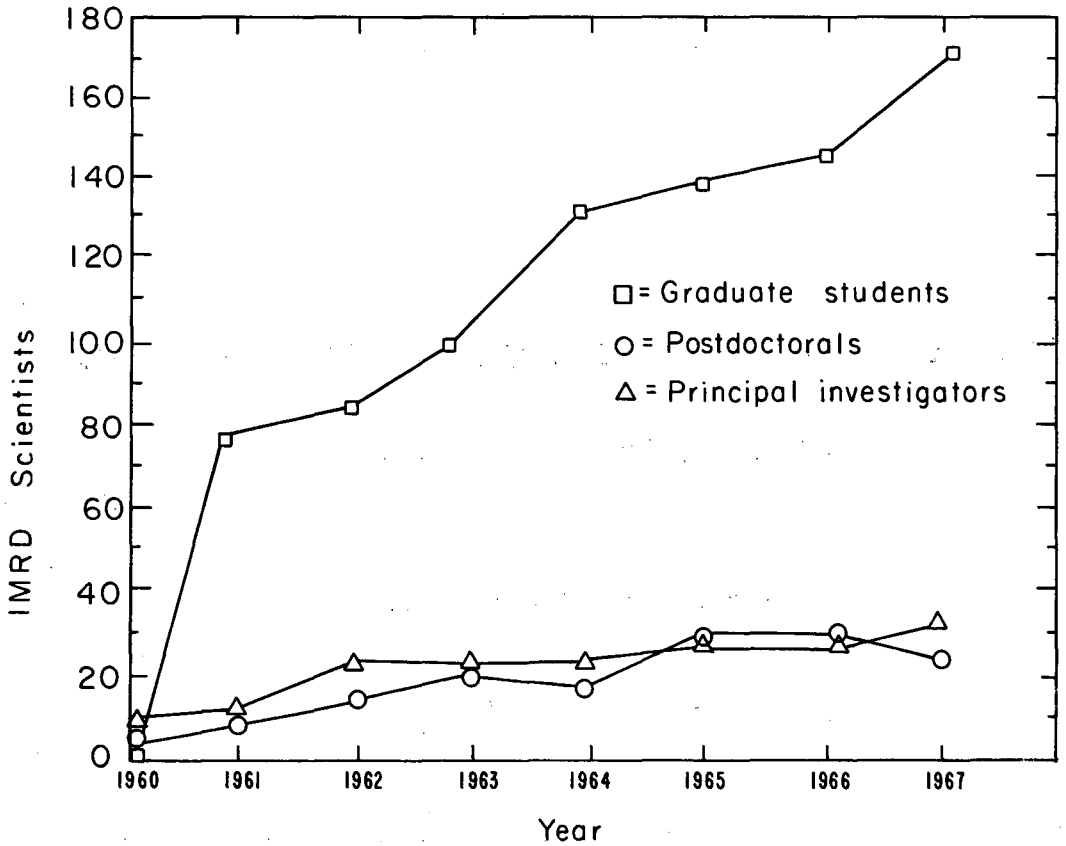

XBL683 – 2108

Figure 1

throughout the free world and was successful in obtaining working time on the largest instruments. By actually performing critical experiments on these microscopes, which varied in voltage from 200 to 1000 kV, Professor Thomas was able to evaluate the capabilities of the various designs, as well as to establish desirable future projects for our own machine which will be operating in the coming year. This critical evaluation of machines in use and in construction has been written as a report for the Atomic Energy Commission and should serve as a valuable guide for those contemplating buying and using these units.

As in the past years, IMRD continued to host a series of weekly seminars based on the current research interests of the Division and on the research of visiting speakers. Among the speakers were Dr. Y. L. Shen, Bell Telephone Laboratory, Murray Hill, New Jersey; Gideon Hirsch, Chemical Engineering Division, Argonne National Laboratory, Argonne, Illinois; Dr. E. G. Bauer, Crystal Physics Branch, U.S. Naval Ordnance Test Station, China Lake, California; Prof. H. R. Thirsk, Department of Physical Chemistry, University of Newcastle-upon-Tyne, England; Robert L. Park, Sandia Laboratory, Albuquerque, New Mexico; Dr. David Ragone, General Atomic, San Diego, California; Prof. Roger Parsons, Department of Physical Chemistry, University of Bristol, England; Dr. Igor Borisovich Borovskiy, Metallo-Physics Laboratory, A.A. Baykov Institute of Metallurgy, U.S.S.R. Academy of Sciences; Dr. Lloyd S. Williams, Chemical Research Laboratory, Commonwealth Scientific and Industrial Organization, Melbourne, Australia; Dr. Myron Strongin, Brookhaven National Laboratory, Upton, New York; Dr. Allen Metherell, Cavendish Laboratory, Cambridge, England; Dr. P. Schuepp, Department of Physics, University of Toronto, Canada; Dr. George Verhaegen, Universite Libre, Brussels, Belgium; Dr. Fred E. Stafford, Northwestern University, Evanston, Illinois; Prof. J. Kistemaker, F.O.M., Institute for Atomic and Molecular Physics, The Netherlands; Prof. J. C. Sohm, University of Grenoble, France; Dr. Steven M. Copley, Advanced Materials Research and Development Laboratory, Pratt and Whitney Division, United Aircraft Corporation, Middletown, Connecticut; and Prof. A. T. DiBenedetto, Washington University, Department of Chemical Engineering, St. Louis, Missouri.

Plans were finalized for the Fourth International Materials Symposium to be sponsored by IMRD which will be presented during June of 1968. The subject will be Structure and Chemistry of Solid Surfaces. Co-chairmen for this conference will be Professor Gabor Somorjai of IMRD and the University of California, Berkeley, Professor R. Gomer of the University of Chicago, and Professor R. Wallis, University of California at Irvine.

The policy adopted in 1965 of instituting salary reductions for graduate students who had not completed their degree work within five years was continued. During the first two years of operation of this policy, the notification of students after four years of study was sufficient to stimulate completion of their theses before the end of the fifth year. However, during the past year, it was necessary to apply the salary reduction in two instances.

The second annual review symposium of the Inorganic Materials Research Division was held as a continuation of the series launched last year. This symposium is aimed at facilitating interaction between IMRD and other laboratories in the materials-science field, and providing a regular review of the program by the AEC's Division of Research. Present for the two-day meeting were five representatives of the AEC, six invited reviewers, and about 50 guests representing several LRL divisions, UC departments, and other universities and laboratories. The sessions were open to faculty, students, and all other scientific associates of the UC campus. The program consisted of brief reviews of current research at IMRD. AEC representatives at the symposium were W. Sheely, L. Ianniello, R. Epple, R. Kandel, and J. Coleman. Invited reviewers were C. Barrett, P. Duwez, M. Simnad, J. Franklin, N. Nachtrieb, and D. Stevenson.

REPRESENTATIVE HIGHLIGHTS OF THE RESEARCH PROGRAM

Methods have been developed for fixing heat capacities and other properties of metals under high pressure. The determination of the annihilation spectrum of positrons has been shown to be applicable to the determination of

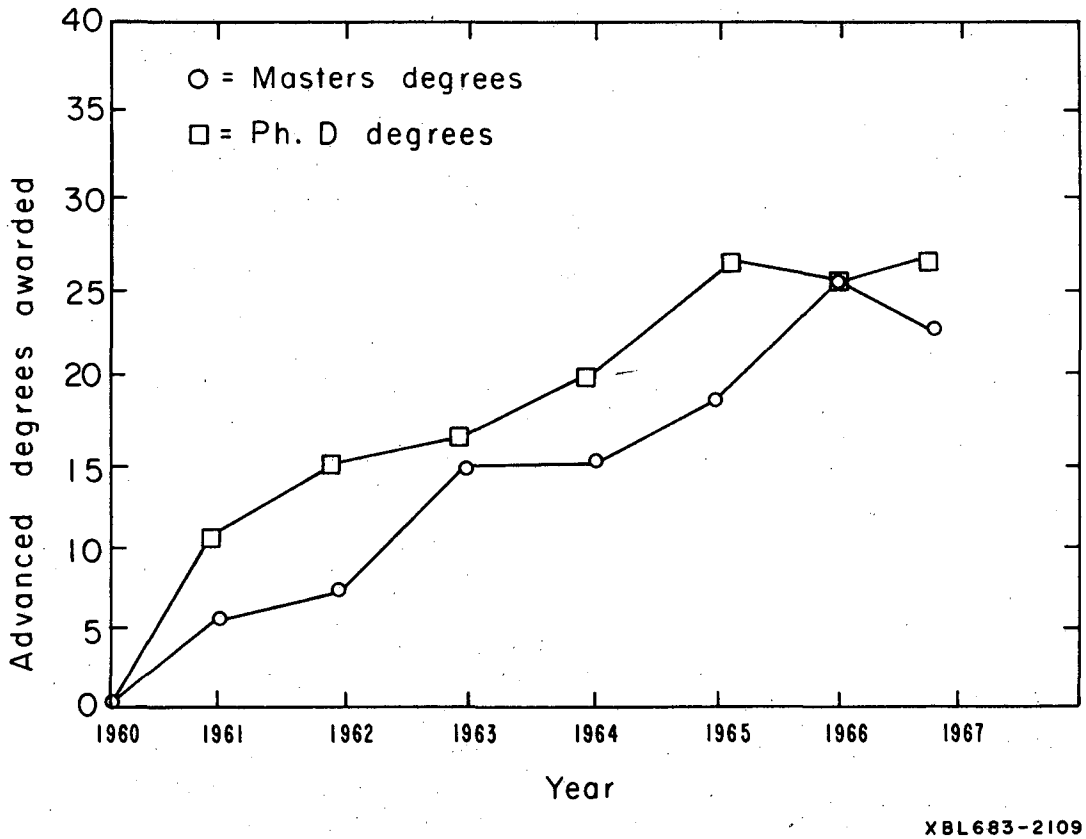

Figure 2

heat capacities of most metals under pressure. (See G. Jura, Sec. IC., p. 37.)

^{17}O NMR has been used to measure the very rapid rates of exchange of water molecules in the first coordination sphere of paramagnetic transition ions such as Ti(III), hydrolyzed polymers of Cr(III), VO^{++}, and Fe(III) and its hydrolyzed species, and to provide information on the structural arrangements of the water molecules. (See R. E. Connick, Sec. IA, p. 7.)

A phase-shift method has been used to detect intermediates in gas-phase reactions such as ClO and ClOO produced by the photolysis of Cl_2 in the presence of O_2 and HO_2 produced by the photolysis of O_3 in the presence of H_2O_2. (See H. S. Johnston, Sec. IE, p. 87.)

Measurements of transport properties of aqueous nitric acid and ammonium nitrate have been combined with literature data for other binary systems to develop a method of calculation of fundamental transport properties. (See J. Newman, Sec. ID., p. 61.)

NMR measurements for the ternary systems HNO_3-DNO_3-H_2O and $HClO_4$-$DClO_4$-H_2O have shown the presence of many species. These measurements have been combined with vapor-pressure data to evaluate dissociation constants for the equilibria among the various species. (See O. Redlich, Sec. IE., p. 94.)

Studies of ion-ion recombination have led to both an empirical and sound theoretical understanding of termolecular ion recombination which now provides predictions of the recombination rates in systems of almost arbitrary temperature and composition. For the first time, a complete energy and angular-distribution measurement for products and scattered reactants has been carried out for ion-molecule reactions. This information allows an unprecedented insight into the detailed dynamics of these reactions and provides a challenging test of the several theories of reaction rates. (See B. Mahan, Sec. IE., p. 73.)

A general mechanism has been worked out for the reaction between germane and a solution of amides in liquid ammonia to form potassium germyl, germanium imide, and hydrogen. Potassium germyl has been reacted with diborane to produce potassium germyltrihydroborate, KH_3GeBH_3. (See W. Jolly, IA., p. 10.)

Heat-capacity measurements on He^4 have been carried out between 0.3 and 2.5°K which allow evaluation of the equilibrium phase diagram and most of the thermodynamic properties of the hcp and bcc solids and liquid II. (See N. Phillips, Sec. IC., p. 28.)

The study of the mechanism of sublimation for sodium chloride single crystals has demonstrated the important effect of dislocations and divalent impurities upon the rate of sublimation. (See G. Somorjai, Sec. IC., p. 39.)

A fundamental understanding of the structural damage occurring during irradiation is difficult to achieve, since the defects introduced are of atomic dimensions. Further, the structural changes induced during irradiation cannot be observed, since at the usual experimental temperatures employed, the defects introduced quickly anneal out or otherwise change their configurations. Both these difficulties were overcome by placing a target specimen in a field-ion microscope that was mounted directly in the beam of an 88-inch cyclotron and bombarded at liquid-helium temperatures. The resulting damage and the recovery processes that occurred with increasing temperature could be observed on an atomistic scale. (See J. Washburn, Sec. IIA., p. 109.)

Fundamental studies on TRIP (Transformation-Induced Plasticity) Steels has continued and from these studies many interesting results of a scientific and engineering nature have emerged. It appears likely that the practical results of this research will be quickly taken up by industry. The practical directions of this development will undoubtedly be in the form of a whole new family of high-strength, high-ductility alloys with superior engineering properties. (See V. F. Zackay and E. R. Parker, Sec. IID., p. 131.)

In a study of the structural factors that influence the high-field characteristics of the high-T_c (20.4°K) compound $Nb_3(Al,Ge)$ discovered by Matthias et al., it was found that a "peak" in superconductivity existed at fields between about 140 and 200 kG at critical currents as high as 10^3 A/cm^2. The upper critical field of this compound is greater than 220 kG — at least as high as that of the better-known A15 compounds of Nb_3Sn and V_3Ga. (See L. Brewer, E. R. Parker, and V. F. Zackay, Sec. IIE., p. 144.)

Densification of MgO powders with admixtures of LiF under moderate pressures at temperatures of about 1000°C, with a subsequent heat treatment at about 1300°C, has resulted in transparent polycrystalline MgO. The formation of an LiF melt in which MgO is slightly soluble during hot pressing allows distribution of material by a liquid-phase sintering mechanism while the bulk of the liquid is being squeezed out. The kinetics are thus controlled by a viscous flow rather than a diffusion mechanism. The remainder of the LiF is removed by vaporization from the surface during the heat treatment. (See J. Pask, Sec. IIIB., p. 163)

A technique has been developed to measure quantitatively the wavelength of the periodic segregation in spinodally decomposed solutions. The technique was evolved by combining the information obtained from the electron-transmission patterns and the electron-diffraction patterns and with the aid of an analysis based on Lorentz deflections. (See G. Thomas, Sec. IIC., p. 119.)

The exchange of energy between a tungsten filament and room-temperature neon, nitrogen, argon, krypton, and mixtures of argon with oxygen were determined over a wide range of filament temperatures and gas pressures. For nonreactive gases the thermal accommodation coefficient was found to be independent of gas pressures between 10^{-7} and 5×10^{-5} atm. At high temperatures for the reactive gas, oxygen, the pressure dependence of the energy exchange was pronounced. (See A. Searcy, Sec. IIIA., p. 155.)

The diffusion kinetics in the Fe-MgO, NiO-MgO, and Fe_2O_3 systems were investigated with particular emphasis placed on the relationship between atomistic mechanisms and structural changes. The existence of Fe^{+3} ions and their location in the lattice in the Fe-MgO (vacuum) and Fe_2O_3-MgO (air) systems were determined by the use of electron paramagnetic resonance, optical spectroscopy, and Mossbauer analyses. (See J. A. Pask, Sec. IIIB., p. 161.)

The effect of orientation on the rate of strain hardening of ordered β-phase AgMg (CsCl structure) was investigated. The anisotropic strain-hardening behavior was interpreted in terms of dislocation interactions. (See J. Dorn, Sec. IIB., p. 115.)

The effect of pressure on high-temperature dissolution was studied in a system consisting of sodium disilicate glass and oxidized nickel microspheres. The relationship of the saturation concentration of nickel in the glass as a function of applied pressure was obtained and was found to be consistent with free-energy considerations. (See R. Fulrath, Sec. IIIC., p. 171.)

Chemistry

I. CHEMISTRY

A. INORGANIC CHEMISTRY

1. ^{17}O NMR STUDIES OF WATER EXCHANGE OF PARTIALLY COMPLEXED VANADYL ION

Kurt Wüthrich*

Vanadyl ion, VO^{2+}, in aqueous solution has one strongly bonded oxygen attached to the vanadium and an undetermined number of water molecules (waters) in contact with the metal ion. It is generally assumed that there are four equivalent waters in a square arrangement next to the vanadyl oxygen and one further water opposite the vanadyl oxygen, so that the species has tetragonal symmetry.

Our earlier NMR results indicated slow exchange of some waters in and out of the first coordination sphere. In order to clarify whether these waters were the four equivalent waters or the one axial water, experiments were performed with partially chelated vanadyl ions. The studies were carried out by measuring the broadening of the ^{17}O resonance of water by the various metal chelates. The EDTA complex gave almost no broadening, as would be expected when the metal ion is completely chelated. Two bidentate ligands, 5-sulfosalicylic acid and Tiron showed an enhancement of the broadening in the 1:1 complexes but very little broadening in the 1:2 complexes. The tridentate ligand iminodiacetic acid gave enhanced broadening. These results are consistent with the hypothesis that the exchange responsible for the broadening is attributable to the four equivalent waters — not the axial water. A similar conclusion has been reached by Reuben and Fiat[1] from a measurement of the number of slowly exchanging waters of the vanadyl ion, which they found to be four.

The enhancement of the broadening by these ligands was shown by a study of the temperature dependence of the broadening to arise from an increase in the rate of exchange of the waters relative to uncomplexed vanadyl ion. At 25°C the lifetime of the water molecules on the 1:1 Tiron complex is 10^3-fold shorter than on vanadyl ion.

Two quadridentate ligands, nitrilotriacetic acid and 2-picolyliminodiacetic acid, gave very little broadening. Models of these complexes show that the four equivalent water positions of vanadyl ion can be occupied only if the axial position is eliminated. In addition the 2-picolyliminodiacetate ion would have to have its four coordinating groups in a plane below the vanadium such that these four groups and the vanadyl oxygen would form a square pyramid with the vanadium inside and appreciably above the base of the pyramid. There is evidence from x-ray structural determinations that vanadyl ion does assume such a geometry in certain solids,[2] and it seems likely that the hydrated ion has such a geometry. The axial water would be held much less tightly than the four pyramidal waters, and the first-sphere coordination number of the vanadium is perhaps better thought of as five than six.

In the case of uncomplexed vanadyl ion there are small effects arising from the axial water and waters in the second coordination sphere that become apparent at low temperatures. These are being studied in order to get information on the second coordination sphere.

---

* Present address: Bell Telephone Laboratories, Murray Hill, New Jersey.

1. J. Reuben and D. Fiat, Inorg. Chem. 6, 579 (1967).
2. R. Dodge, D. H. Templeton, and A. Zalkin, J. Chem. Phys. 35, 55 (1961).

2. NUCLEAR MAGNETIC RESONANCE RELAXATION OF OXYGEN-17 BY FERRIC ION IN AQUEOUS SOLUTION*

Malcolm R. Judkins†

The ^{17}O NMR signal in aqueous perchloric acid solutions of ferric ion was studied as a function of temperature, frequency, and solution composition in order to separate the

various effects arising from ferric ion and its hydrolyzed species. The principle species affecting the ^{17}O NMR width by water exchange were found to be Fe^{3+}, $FeOH^{2+}$, and $Fe_3(OH)_4^{5+}$.

The ferric ion produces line broadening arising from exchange out of both a first and an outer coordination sphere. The first-coordination-sphere waters exchange slowly enough to be in the exchange-controlled region. The outer-coordination-sphere exchange, is rapid, and the ^{17}O nuclear spin is probably relaxed by a combination of scalar coupling and $\Delta\omega$ mechanisms. The first- and outer-coordination sphere effects cannot be separated unequivocally, and consequently the exchange lifetime can be given only approximately as $\sim 3\times10^{-3}$ sec at 25°C for a solution containing 0.375 M $Fe(ClO_4)_3$, 1.705 M $HClO_4$, and 0.730 M $NaClO_4$.

It appears that $FeOH^{2+}$ and $Fe_3(OH)_4^{5+}$ are in the relaxation-controlled region for the water exchange. Only an upper limit for the lifetime of waters in the first coordination sphere can be given: 2×10^{-6} and $6\times10^{-}$ sec for $FeOH^{2+}$ and $Fe_3(OH)_4^{5+}$, respectively. The relaxation seems to be a consequence of both scalar coupling and $\Delta\omega$ mechanisms. The species $Fe_2(OH)_2^{4+}$ does not appear to contribute importantly to the line broadening, possibly because of a low magnetic moment.

* Abstract from UCRL-17561, May 1967.
† Present address: Pigments Division, E. I. Dupont de Nemours, Wilmington, Del.

3. EFFECT OF COMPLEXING ON LIFETIMES OF WATER MOLECULES IN THE FIRST COORDINATION SPHERE OF NICKEL ION

Kenneth Kustin*

It is known that partial complexing of a metal ion can produce important changes in the rate at which water molecules remaining in the first-coordination-sphere exchange with the solvent water. These effects are not well understood. Experiments are underway to study a variety of complexes of nickel ion, using the broadening of the nuclear magnetic resonance of oxygen-17 as a measure of the water exchange rate.

* On sabbatical leave from Brandeis University, Waltham, Mass.

4. PROTON EXCHANGE FROM THE FIRST COORDINATION SPHERE OF HYDROLYTIC POLYMERS OF CHROMIUM(III)

Ronald Lee

The temperature dependence of the transverse nuclear relaxation time, T_2, for the protons of water molecules attached to chromic ion has been measured and discussed previously.[1-3] Such temperature studies can often lead to the actual rate of proton exchange from the first coordination sphere of the paramagnetic species to the bulk waters of the solution, or at worst, to a lower limit of such an exchange; in the case of chromic ion the actual rate was obtained. One difficulty in proton work of this type has been the uncertainty as to whether the line broadening is due to the exchange of the entire water molecule, the exchange of the protons off the water molecule, or a combination of both. In the case of chromic ion, the exchange of the entire water molecule is not in question, since Cr^{3+} with its d^3 system exchanges its waters very slowly.[4] It is expected that the hydrolyzed polymers of Cr^{3+}, namely the dimeric and trimeric species[5] would do the same. This has been verified for the dimer.[6]

The present study concerns the line-broadening of the proton resonance in perchlorate solutions of the dimer, $[Cr(H_2O)_4OH]_2^{4+}$, and the trimer, thought to be $[Cr_3(OH)_4(H_2O)_{10}]^{5+}$.

Dimer

In the region from 2 to 60°C, the linewidth increases with increasing temperature, indicating an exchange-controlled region. The data appear to indicate two different sites of proton exchange, although further studies must be performed before the conclusion can be accepted with certainty. A dependence of the linewidth on hydrogen-ion concentration must be considered. This leads to some difficulty, since the presence of high hydrogen-ion concentration can shift this species, a doubly bridged dimer, to a singly bridged dimer in the following reversible reaction:[5]

$$[(H_2O)_4Cr(OH)_2Cr(H_2O)_4]^{4+} + H_3^{+}O \rightleftharpoons [(H_2O)_5Cr-\overset{H}{O}-Cr(H_2O)_5]^{5+}.$$

It has been found that the singly bridged species gives a much greater linewidth at room temperature than the dimer. Thus even a small

amount of the singly bridged species can cause ambiguity in the data. The temperature region studied will be extended; lower temperatures can be reached by depressing the freezing point with $LiClO_4$. Since it is not known whether the bridging protons are exchanging, it is hoped that a doubly bridged dimeric species with other ligands containing no exchangable protons can be prepared and then studied to answer this question.

Trimer

A temperature study as a function of hydrogen-ion concentration has been performed. In the region from -4 to 64°C, the data indicate an exchange-controlled region, and can be analyzed to result from a hydrogen-ion-dependent step. Unfortunately, the trimer begins to decompose to the hexaquochromium(III) ion at ~75°C with the concentrations used, so it appears unlikely that data concerning the relaxation-controlled region can be obtained directly. The temperature will, however, be extended below 0°C, and further studies with respect to $[H^+]$ will be made.

1. R. Hausser and G. Laukien, Z. Physik 153, 394 (1967).
2. T. Swift and T. Stephenson, Inorg. Chem. 5, 1100 (1966).
3. N. Bloembergen and L. Morgan, J. Chem. Phys. 34, 842 (1961).
4. J. Hunt and H. Taube, J. Chem. Phys. 19, 602 (1951).
5. Sister Gertrude Thompson, C.S.J., Hydrolytic Polymerization in Cr(III) Solutions, (Ph.D. Thesis), UCRL-11410, June 1964.
6. R. Kolaczkowski and R. Plane, Inorg. Chem. 3, 322 (1964).

5. WATER EXCHANGE ON Ti(III)

Herbert Charles

The rate of H_2O^{17} exchange from the first coordination sphere of Ti(III) to the bulk solution is being investigated by NMR techniques. Since Ti(III) is susceptible to air oxidation and to hydrolysis, it is necessary to analyze for Ti(III) and H^+ as well as for paramagnetic impurities in the commercially available stock solution of $TiCl_3$. Spectrographic analysis was used to establish a lower limit for possible paramagnetic impurities. A separate more sensitive check for Mn(II) impurities was made using ESR by comparing the ESR signal from the commercial Ti(III) solution against a sample containing a known concentration of Mn(II).

A glass electrode was used to measure the hydrogen-ion concentration of the commercially available $TiCl_3$ solution. The glass electrode was calibrated against a solution containing a known amount of hydrogen ion approximately equal to that of the $TiCl_3$ solution. Sufficient $LaCl_3$ was added to the known HCl solution to simulate the ionic strength contributions due to Ti(III) and Ti(IV).

The temperature dependence of the linewidth was then extended to approximately 60°C. The data are consistent with a chemical-exchange-controlled region at low temperature and a relaxation-controlled region above ~20°C.

6. RESEARCH PLANS FOR CALENDAR YEAR 1968

Robert E. Connick

The proton-exchange studies of chromium (III) polymers will be extended to complete the known polymers. Polymeric complexed species will be prepared where some or all of the non-bridging oxygens are replaced by nitrogens, in order to determine the effect of such replacement on the proton exchange rate and in an attempt to distinguish between the different proton environments present in the uncomplexed polymers.

Some measurements will be made of proton NMR relaxation in waters in the first coordination sphere of vanadyl ion. Under favorable conditions such studies can be made to yield the longitudinal relaxation time for the electron spin resonance, a quantity which is not directly observable by other methods at high magnetic fields.

The interpretation of the oxygen-17 NMR relaxation brought about by cupric ion still has some uncertainties. Additional information on the system will be obtained by making a large variation in the field strength. In the case of gadolinium such measurements yielded T_1 of the electronic system and gave an unambiguous identification of this quantity relative to the rate of chemical exchange.

A variety of partially complexed nickel-ion species will be studied by ^{17}O NMR to determine the effect of complexing on the rate of water exchange.

Investigation of the water exchange rate for the first coordination sphere of Ti^{3+} will be completed.

7. 1967 PUBLICATIONS

Robert E. Connick and Associates

Technical Journals

1. D. Fiat and R. E. Connick, Magnetic Resonance Studies of Ion Solvation. The Coordination Number of Gallium (III) Ions in Aqueous Solutions, J. Am. Chem. Soc. 88, 4754 (1966).
2. K. Wuthrich and R. E. Connick, Nuclear Magnetic Resonance Relaxation of Oxygen-17 in Aqueous Solutions of Vanadyl Perchlorate and the Rate of Elimination of Water Molecules from the First Coordination Sphere, Inorg. Chem. 6, 583 (1967).

UCRL Reports

1. M. R. Judkins, Nuclear Magnetic Resonance Relaxation of Oxygen-17 in Aqueous Solutions of Ferric Ion (Ph.D. Thesis), UCRL-17561, May 1967.
2. K. Wuthrich and R. E. Connick, Nuclear Magnetic Resonance Studies of the Coordination of Vanadyl Complexes in Solution and the Rate of Elimination of Coordinated Water Molecules, UCRL-17526, May 1967.

8. STUDIES OF WEAK ACIDS

a. Intrinsic Basicity of the Hydroxide Ion*

William L. Jolly

Liquid ammonia is a much more basic solvent than water, and therefore one expects protonic acids to be more completely ionized (stronger) in ammonia than in water. However, the pK of water in liquid ammonia is 18, and the pK of water in water is 16.[1] Thus, in liquid ammonia, the ionization constant of water is 100 times smaller than it is in water. The explanation which has been offered for this behavior is that the hydroxide ion is abnormally strongly stabilized in water by hydrogen bonding and that consequently water in water is an abnormally strong acid.[1]

The intrinsic basicity of the hydroxide ion is much greater than that which can be achieved in a solvent such as water or alcohol. Unfortunately, hydroxides are not appreciably soluble in nonhydroxylic solvents. However, alkali metal hydroxides need not be dissolved to bring about the ionization of weak acids. Solid sodium hydroxide and potassium hydroxide are very effective in the preparation of salts. From readily available thermodynamic data we calculate the following equilibrium constants:

$$2KOH(s)+H^+(aq) = K^+(aq)+KOH\cdot H_2O(s) \qquad K = 10^{31}$$

$$2NaOH(s)+H^+(aq) = Na^+(aq)+NaOH\cdot H_2O(s) \qquad K = 10^{23}\ .$$

We see that any acid with an aqueous pK less than 31 should react with potassium hydroxide to form the potassium salt, and any acid with an aqueous pK less than 23 should react similarly with sodium hydroxide. Of course these reactions only have meaning for nonaqueous solvents, because it is not possible, for example, to have both KOH and $KOH\cdot H_2O$ in equilibrium with a solution that is aqueous in the usual sense. The free energy of transfer of a salt or a neutral species from water to another solvent is rather small, and so we can consider these reactions and their calculated equilibrium constants to be approximately valid for any solvent:

$$2KOH(s)+HA = K^++A^-+KOH\cdot H_2O \qquad K = 10^{31-pK_{HA}}$$

$$2NaOH(s)+HA = Na^++A^-+NaOH\cdot H_2O \qquad K = 10^{23-pK_{HA}}\ .$$

We have found several reactions of this type to be synthetically useful. By simply stirring powdered reagent grade KOH with solutions of the appropriate weak acids in 1,2-dimethoxyene, we have prepared, in quantitative yield, solutions of the potassium salts of germane, ethylgermane, cyclopentadiene, indene, and fluorene. The reactions are much easier and safer to carry out than the usual reactions of dispersed metal suspensions with weak acids. Using the solutions prepared from KOH as intermediates, we have made a variety of derivatives, such as CH_3GeH_3, $CH_3GeH_2C_2H_5$, ferrocene, nickelocene, and bis-indenyliron (II):

$$CH_3Cl + K^+ + GeH_3^- \rightarrow CH_3GeH_3 + KCl$$

$$CH_3Cl + K^+ + C_2H_5GeH_2^- \rightarrow CH_3GeH_2C_2H_5 + KCl$$

$$FeCl_2 + 2K^+ + 2C_5H_5^- \rightarrow Fe(C_5H_5)_2 + 2KCl$$

$$NiCl_2 + 2K^+ + 2C_5H_5^- \rightarrow Ni(C_5H_5)_2 + 2KCl$$

$$FeCl_2 + 2K^+ + 2C_9H_7^- \rightarrow Fe(C_9H_7)_2 + 2KCl\ .$$

* Abstracted from J. Chem. Educ. 44, 304 (1967).
1. W. L. Jolly, J. Phys. Chem. 58, 250 (1954).

b. Deprotonation of Weak Acids*

William L. Jolly

Alkali metal salts of very weak protonic acids commonly have been prepared by three methods that do not require a metal salt of the acid as a starting material: (1) reaction with strong bases, (2) direct reaction with alkali metals, and (3) cleavage of halo derivatives with alkali metals. It is the purpose of this communication to show that the thermodynamic limitations of each of these methods may be defined in terms of acid pK values.

Reaction with Strong Bases

In this method the weak acid is treated with an alkali metal salt of a still weaker protonic acid, sometimes using one of the protonic acids as a solvent. The pK of the acid whose salt is used as a reactant is an approximate upper limit to the pK values of the acids whose salts can be formed in this type reaction.

Reaction with Alkali Metals

In the second method the weak acid is treated with an alkali metal, usually suspended in a finely divided state in a polar solvent. For example, the sodium salt of indene may be prepared by the reaction of indene with a dispersion of sodium in tetrahydrofuran:

$$C_9H_8 + Na \rightarrow Na^+ + C_9H_7^- + 0.5H_2 \quad .$$

Reactions of this type may be broken into two parts:

$$HA = H^+ + A^-$$

$$M + H^+ = 0.5H_2 + M^+ \quad .$$

If we make the approximation that the free energy of formation of the dissolved salt is the same as that for the salt dissolved in water, then we may readily calculate the pK value of the weakest acids that can react in this way by using the free energy of formation of the appropriate alkali metal ion. Thus we calculate limiting pK values of 51, 46, and 49 for lithium, sodium, and potassium, respectively.

Cleavage by Alkali Metals

In the third method, the salt of a weak acid is formed by the reaction of an alkali metal with a halo derivative of the weak acid. For example, sodium phenyl is readily formed by the reaction of finely divided sodium with chlorobenzene:

$$2Na + C_6H_5Cl \longrightarrow Na^+C_6H_5^- + NaCl \quad .$$

Reactions of this general category (in which a metal M reacts with a halide AX) may be broken into three parts:

$$HA = H^+ + A^-$$

$$AX + H = HA + X$$

$$2M + X + H^+ = MX + M^+ + H \quad .$$

Obviously, for a given alkali metal and a given halogen, the overall driving force depends not only on the pK of the acid, but also on the difference in the dissociation energies of the H-A and X-A bonds. Now, almost all of the acids for which this third method is practical are hydrocarbons. Thus we are principally concerned with the differences in the dissociation energies of C-H bonds and the corresponding C-X bonds. To the precision with which we may assume that the latter differences are constant on going from one weak carbon acid to another, we may estimate the highest pK for which this type of reaction is thermodynamically possible. By considering the alkali metals lithium, sodium, and potassium, and the halogens chlorine, bromine, and iodine, we find that the theoretical limiting pK value varies from 119 (for the cleavage of a chloro compound by potassium) to 102 (for the cleavage of an iodo compound by sodium). Obviously, it is unlikely that any hydrocarbon will be found whose alkali metal salts cannot be made by this method because of thermodynamic limitations.

* Abstracted from Inorg. Chem. 6, 1435 (1967).

9. STUDIES OF THE HYDRIDES OF SILICON, GERMANIUM, TIN, AND PHOSPHORUS

a. Reactions of Silane, Germane, and Stannane with Metal- and Amide-Ammonia Solutions*

Douglas S. Rustad and William L. Jolly

Germane reacts with liquid ammonia solutions of potassium or potassium amide at -77° to form potassium germyl, germanium imide ($Ge(NH)_2 \cdot xNH_3$), and hydrogen gas. The fraction of the germane converted to germanium imide increases with increasing potassium concentration, but remains constant with increasing potassium amide concentration. Amide ion is an intermediate in the reaction of germane with metal-ammonia solutions. In the case of silane, the main reaction is ammonolysis, whereas in the case of stannane, no ammonolysis occurs. A general mechanism is proposed to explain the results.

* Abstracted from Inorg. Chem. 6, 1968 (1967).

b. Reaction of Potassium Germyl with Lewis Acids

Douglas S. Rustad,† Paul M. Kuznesof, and William L. Jolly

The principal reaction between diborane and potassium germyl, when the reagents are in the stoichiometric ratio or when potassium germyl is in slight excess, is

$$KGeH_3 + 1/2\ B_2H_6 \rightarrow KGeH_3BH_3\ .$$

The physical and chemical properties of the product are consistent with the formulation potassium germyltrihydroborate, the anion consisting of a hydroborate ion in which one of the hydrogen atoms has been replaced by a germyl group (or the equivalent: a germyl ion coordinated to a borane group). Hydrolysis of aqueous solutions proceeds slowly in the presence of base (either added or formed by the self-hydrolysis reaction) but proceeds rapidly upon the addition of acid.

$$H^+ + 3H_2O + GeH_3BH_3^- \rightarrow 3H_2 + GeH_4 + B(OH)_3\ .$$

The salt melts at 98 to 99° with little apparent decomposition. The decomposition of the salt which occurs at 200°C corresponds to a hydride shift from germanium to boron, with subsequent decomposition of the GeH_2 moiety:

$$KGeH_3BH_3 \xrightarrow{\Delta} [GeH_2] + KBH_4$$

$$\Delta \downarrow$$

$$H_2 + GeH_2 + GeH_4 + Ge_2H_6 + Ge_3H_8 + Ge\ .$$

The infrared and NMR spectra of $KGeH_3BH_3$ are consistent with the $GeH_3BH_3^-$ structure.

Potassium germyl reacts with CO_2 in 1,2-dimethoxyethane to give a salt, $KGeH_3CO_2$. Infrared and ultraviolet spectra suggest a structure for the anion analogous to that of the acetate ion. A bathochromic shift in the ultraviolet spectrum relative to acetate is consistent with the relative band positions of organosubstituted analogs. The NMR spectrum of the salt in D_2O shows a single resonance at -4.30 ppm (TMS ext. std.). Titrations of aqueous solutions yield, for 2-germaacetic acid, pK = 3.5, a value which may be compared with pK = 4.75 for acetic acid. The potassium salt hydrolyzes slowly in moist air. Aqueous solutions are about 2% hydrolyzed in 20 hours at 25°; hydrolysis is complete in 15 hours at 80°. The hydrolysis yields one mole of GeH_4; subsequent acidification of the solution gives another mole of CO_2:

$$GeH_3CO_2^- + H_2O \rightarrow GeH_4 + HCO_3^-$$

$$HCO_3^- + H^+ \rightarrow H_2O + CO_2\ .$$

In acid solution, hydrolysis gives one mole of carbon monoxide and nonreproducible amounts of GeH_4 ($GeH_4/CO \approx 0.5$). A solution at pH 2 is about 50% hydrolyzed in 30 min at 30°; hydrolysis in 1 M H^+ is complete in 15 hours at 25°. The two hydrolysis routes are analogous to the decarboxylations of organic carboxylates and the decarbonylations of organic carboxylic acids.

† Present address: University of the West Indies, Kingston, Jamaica.

c. Investigation of the Disproportionation of Digermane

Robert Dreyfuss and William L. Jolly

Digermane (Ge_2H_6) decomposes in liquid ammonia solution to give germane (GeH_4) and a solid hydride of nonstoichiometric composition. The net reaction may be written as

$$(4-x)\ Ge_2H_6 \rightarrow (6-2x)\ GeH_4 + 2GeH_x.\quad 0 < x < 4$$

The value of x decreases with increasing reaction temperature and with increasing reaction time. Crude experiments indicate a similar digermane decomposition in aqueous sodium hydroxide, but the aqueous reaction goes to a measurable extent only if solid hydroxide is present.

The nature of the solid from the disproportionations is now our principal interest. When in contact with liquid ammonia, this solid is colorless and soluble at -63°, yellow at warmer temperatures, and blood red at room temperature. On removal of the ammonia, the solid becomes yellow.

It is planned to see if our solid GeH_x is similar in nature to that which Glarum and Kraus[1] prepared by the reaction of bromobenzene with sodium germyl. The reaction with sodium in ammonia will be studied.

A preliminary proton magnetic-resonance study of the liquid-ammonia disproportionation at low temperatures shows peaks corresponding to germane and digermane, as well as several peaks at higher fields. These change in number and intensity as the reaction proceeds. It is hoped that better spectra will be obtained to permit identification of the soluble

germanium-hydrogen species.

1. S. N. Glarum and C. A. Kraus, J. Am. Chem. Soc. 72, 5398 (1950).

d. The Chemistry of Stannane

John R. Webster and William L. Jolly

It was reported last year that SnH_3Cl (unlike SnH_3Br and SnH_3I, which decompose at room temperature to SnH_4, H_2, and stannous halide in a 1:1:1 mole ratio), decomposes to Sn, H_2, SnH_4, $SnCl_2$, and HCl. Further investigation has indicated that the Sn in the decomposition products of SnH_3Cl is probably a secondary product from the decomposition of SnH_4, which is formed in the initial reaction. Thus the only products after 1 hour from SnH_3Cl are SnH_4, H_2, $SnCl_2$, and HCl. The stoichiometric data indicate that the following two reactions take place:

$$2SnH_3Cl \rightarrow SnH_4 + SnCl_2 + H_2$$

$$3SnH_3Cl \rightarrow 2SnH_4 + SnCl_2 + HCl \ .$$

Stannane is partially hydrolyzed by cold aqueous hydrochloric acid, and a metastable intermediate product is formed. After unreacted SnH_4 is removed at low temperature, further hydrolysis occurs on warming the solution to room temperature. The reaction may be represented as follows:

$$SnH_4 \xrightarrow[-78^\circ C]{8\underline{M}\ HCl} X + H_2$$

$$X \xrightarrow[25^\circ C]{8\underline{M}\ HCl} Sn^{2+} + 2\ H_2$$

The ratio of H_2 evolved at 25° to that at -78 is 2:1. Preliminary experiments on SnH_4 hydrolysis in aqueous 40% $HClO_4$ at low temperatures have given similar results. Although the results in 40% $HClO_4$ were not as well defined as those in 8M HCl, it is felt that the species X may be SnH_3^+ (with anion Cl^- or ClO_4^-), which on warming is hydrolyzed to stannous ion and two moles of hydrogen. Attempts to isolate SnH_3^+ by formation of a salt with BF_4^- have failed. Similarly, addition of BCl_3 to the reaction of SnH_4 in liquid HCl in hopes of isolating $SnH_3^+BCl_4^-$ were unsuccessful.

e. Phosphine*

Sudarshan D. Gokhale† and William L. Jolly

In this synthesis, experimental details are given for the laboratory preparation of phosphine by the pyrolysis of phosphorous acid:

$$4H_3PO_3 \rightarrow 3H_3PO_4 + PH_3 \ .$$

This is the most convenient method known and the yields approach 100%.

* Abstracted from Inorg. Syn. 9, 56 (1967).
† Present address: Wyandotte Chemical Corp., Wyandotte, Mich.

10. BORON HYDRIDE CHEMISTRY

William L. Jolly, Theresa Schmitt, and Francis Wang

Potassium hydroborate reacts with 8M HCl at -70° to form 2 moles of hydrogen per mole of hydroborate and a solution which yields another 2 moles of hydrogen when warmed above -20°. Diborane reacts slowly with 8M HCl at -75° to form 2 moles of hydrogen per mole of diborane; 4 more moles of hydrogen is evolved upon warming the solution above -20°. These and other data suggest that, in both reactions, the aquated BH_2^+ ion is formed at the low temperature.*

Attempts to precipitate salts of the $(H_2O)_2BH_2^+$ cation from cold 8M HCl solutions using the anions BF_4^- and $B_{12}H_{12}^{2-}$ have been unsuccessful.

The hydrolysis of $(CH_3)_4NB_3H_8$ in alcohol-water-HCl solutions proceeds stepwise, as evidenced by differing hydrogen evolution when carried out at -65 and 0°, and by the formation of a soluble species with strong reducing power. Probably the species $(H_2O)_2BH_2^+$, is involved.

* Abstracted from Inorg. Chem. 6, 344 (1967).

11. SULFUR-NITROGEN CHEMISTRY

A. Adducts of Sulfur Nitride with Boron Trihalides

Kenneth J. Wynne† and William L. Jolly

Sulfur nitride in methylene chloride reacts with BF_3 to form burgundy-colored crystals of $S_4N_4 \cdot BF_3$ and with BCl_3 to form red-orange needles of $S_4N_4 \cdot BCl_3$. The BF_3 adduct decomposes reversibly to S_4N_4 and BF_3 when heated, whereas the BCl_3 adduct sublimes with slight decomposition. The properties of the adducts are consistent with structures in which the Lewis acid is coordinated to a nitrogen atom of an S_4N_4 ring, as in $S_4N_4 \cdot SbCl_5$. The boron trifluoride in $S_4N_4 \cdot BF_3$ may be displaced by BCl_3 or $SbCl_5$. In an attempt to displace BCl_3 from $S_4N_4 \cdot BCl_3$ with $SbCl_5$, the adduct $S_4N_4 \cdot BCl_3 \cdot SbCl_5$ formed. This reaction was unexpected because no diadducts were found in the reaction of S_4N_4 with either excess BCl_3 or $SbCl_5$. The conversion of $S_4N_4 \cdot BCl_3$ to $S_4N_4 \cdot SbCl_5$ may be effected by treating $S_4N_4 \cdot BCl_3$ with $SbCl_5$ to give $S_4N_4 \cdot BCl_3 \cdot SbCl_5$, followed by heating this substance in vacuo at 90° to form $S_4N_4 \cdot SbCl_5$ and BCl_3.

* Abstracted from Inorg. Chem. 6, 107 (1967).
† Present address: University of Georgia, Athens, Ga.

b. Studies of the Thermal Splitting of S_4N_4

R. Lyle Patton and William L. Jolly

Sublimation of S_4N_4 in vacuo through a hot zone containing Ag wool at 300° results in initial evolution of N_2 and conversion of the Ag to Ag_2S. This Ag_2S catalytically converts further S_4N_4 to S_2N_2 and small amounts (2 to 10%) of $(SN)_x$. Attempts using more readily available catalysts (e.g., glass wool and Cu turnings) in the hot zone have not been as successful as the above method.

A dark red-orange material is trapped on a -196° cold finger placed immediately above a 300° zone of glass wool through which S_4N_4 is sublimed. When this material is slowly warmed in vacuo to room temperature, a rapid decomposition to S_4N_4 and $(SN)_x$ occurs, and a minute amount of the red-orange material (which also converts to S_4N_4 and $(SN)_x$ when warmed) sublimes to a closely-placed -196° cold spot. These results indicate the presence of unstable volatile species such as SN radicals or short $(SN)_x$ chains.

c. Reactions of Disulfur Dinitride with Antimony Pentachloride and Boron Trihalides

R. Lyle Patton and William L. Jolly

Various adducts can be formed by the reaction, in dicholoromethane, of disulfur dinitride with antimony pentachloride, boron trichloride, and boron trifluoride. Addition of solutions of the Lewis acids to solutions of S_2N_2 at 20° yields the corresponding 1:1 Lewis acid-S_4N_4 adducts. In the cases of $SbCl_5$ and BCl_3, adducts of S_2N_2 can be prepared by changing the order of mixing and/or lowering the temperature. Thus addition of S_2N_2 to an equimolar amount of $SbCl_5$ at 20° produces crystalline $S_2N_2 \cdot SbCl_5$; addition to an excess of $SbCl_5$ produces crystalline $S_2N_2 \cdot (SbCl_5)_2$. The $S_2N_2 \cdot SbCl_5$ may be formed from $S_2N_2 \cdot (SbCl_5)_2$ either by driving off one mole of $SbCl_5$ in vacuo at 90° or by reaction with one mole of S_2N_2 in dichloromethane. Further addition of S_2N_2 to $S_2N_2 \cdot SbCl_5$ produces $S_4N_4 \cdot SbCl_5$. $S_2N_2 \cdot SbCl_5$ sublimes in vacuo at 60° with only slight decomposition. Reaction of S_2N_2 with excess BCl_3 at -78° yields a product of composition, $S_2N_2 \cdot (BCl_3)_2$, which loses one mole of BCl_3 upon warming to 0° to form $S_2N_2 \cdot BCl_3$. The latter reaction may be reversed by treatment with BCl_3 at -78°. $SbCl_5$ displaces BCl_3 from $S_2N_2 \cdot BCl_3$ to form $S_2N_2 \cdot SbCl_5$ and $S_2N_2 \cdot (SbCl_5)_2$. A second (perhaps polymeric) modification of $S_2N_2 \cdot BCl_3$ forms when a mixture of S_2N_2 and BCl_3 in dichloromethane is warmed to 0°. This second form is unreactive toward BCl_3 and $SbCl_5$. Most of the above adducts have been characterized by their infrared spectra.

d. S_4N_4-H_2SO_4 Solutions

Steven Lipp and William L. Jolly

When S_4N_4 is treated with 100% H_2SO_4 at room temperature an orange solution is formed. ESR analysis of this solution has shown it to contain a paramagnetic species.[1] The spectrum consists of a quintet of relative intensities 1:2:3:2:1, with g value of 2.011 and splitting constant A = 3.2 gauss. The spectrum is consistent with a paramagnetic species containing two equivalent nitrogen atoms. On the low-field and high-field sides of the spectrum some small peaks of approximately 0.1 to 0.5% of the main peak intensity can be seen. These additional low intensity peaks have the same splitting as the major quintet, and, like the quintet, are sharper on the low-field side.

We believe that these smaller peaks are due to the splitting by natural-abundance (~0.7%) of ^{33}S. From the relative intensities

of the peaks we calculate that there is one sulfur atom for each two nitrogens. It was previously reported[1] that the paramagnetic species was positively charged. Thus, its formula would be SN_2^+, with the possible addition of an undeterminable number of oxygen and (or) hydrogen atoms to give the general formula $SN_2O_xH_y^+$.

The initial ultraviolet-visible spectrum of this solution shows four absorbances. The absorbances at 4560 and 3510Å decrease at different rates, while a quintet of peaks around 4000Å and a very intense peak at 2160Å increase. After complete reaction, the ratio of the peak intensities of the quintet is 1.0:1.5:1.3:0.8:0.4, with roughly equal splitting of approximately 90Å.

Conductivity and cryoscopy have been used to examine this solution. We find that both of these techniques give results which are concentration-dependent. Further study of the system of S_4N_4 in H_2SO_4 will be required to determine the identity of the species in solution and their concentrations.

1. D. Chapman and A. G. Massey, Trans. Faraday Soc. 58, 1291 (1962).

e. S_4N_4-Ammonia Solutions

Kenneth J. Wynne and William L. Jolly

Concentrated solutions of S_4N_4 in liquid ammonia show two peaks in the ^{14}NMR spectrum—one due to a nitrogen compound derived from the S_4N_4 and one due to the solvent NH_3. Quantitative studies of the peak areas show that the ratio of nitrogen atoms in the nitrogen compound to the total number of sulfur atoms in solution is 1:1. It seems unlikely that this result can be explained in terms of simple dissolution of $S_4N_4 \cdot NH_3$ molecules, inasmuch as spectral[1] and chemical[2] evidence indicate that a deep-seated reaction takes place, possibly with formation of S_2N_2. Molecular-weight studies of the dissolved species would be helpful in determining the nature of the species.

1. M. Goehring, Quart. Rev. 10, 437 (1956).
2. J. T. Nelson and J. J. Lagowski, Inorg. Chem. 6, 1292 (1967).

f. Tetrasulfur Tetranitride*

Millena Villena-Blanco and William L. Jolly

Tetrasulfur tetranitride can be prepared in good yield by passing ammonia into a solution of S_2Cl_2 in carbon tetrachloride.

$$6S_2Cl_2 + 16NH_3 \rightarrow S_4N_4 + 8S + 12NH_4Cl$$

In this detailed synthesis, those experimental features are emphasized which, if neglected, can cause difficulty.

* Abstracted from Inorg. Synthesis 9, 98 (1967).

g. Sulfur Nitrogen Chlorides*

William L. Jolly and Keith D. Maguire†

The usual directions for preparing sulfur nitrogen chlorides call for the starting material S_4N_4, a compound that is neither readily available commercially nor easily prepared. It has been shown that $S_3N_2Cl_2$ may be conveniently prepared from the readily available materials ammonium chloride and disulfur dichloride and that $S_3N_2Cl_2$ may be easily converted to S_4N_3Cl, S_3N_2Cl, or $S_3N_3Cl_3$. The present syntheses are based on the reactions:

$$4S_2Cl_2 + 2NH_4Cl \rightarrow S_3N_2Cl_2 + 8HCl + 5S$$

$$3S_3N_2Cl_2 + S_2Cl_2 \rightarrow 2S_4N_3Cl + 3SCl_2$$

$$3S_3N_2Cl_2 + 3Cl_2 \rightarrow 2S_3N_3Cl_3 + 3SCl_2$$

$$3S_3N_2Cl_2 \rightarrow 2S_3N_3Cl + 2NSCl + SCl_2.$$

* Abstracted from Inorg. Synthesis 9, 102 (1967).
† Present address: Pennsalt Chem. Company, King of Prussia, Pa.

12. STUDIES OF PENTAAMMINE COMPLEXES OF COBALT, RHODIUM, AND IRIDIUM

a. The Aquation of the Nitropentaamminecobalt(III) Ion in Sulfuric Acid Solutions*

Arlo D. Harris,† Robert Stewart, David Hendrickson, and William L. Jolly

We have previously observed that, in concentrated sulfuric acid, the nitropentaamminecobalt(III) ion is converted to the bisulfatopentaamminecobalt(III) ion via the aquopentaamminecobalt(III) ion.[1] This result was rather surprising in view of the low activity of water in concentrated sulfuric acid and in view of the fact that the original nitro complex possesses no cobalt-oxygen bond. Therefore, in order to obtain information about the mechanism of the reaction, we have studied the kinetics of the reaction as a function of the sulfuric acid concentration and have used oxygen-18 as a tracer to determine the source of the oxygen atom in the aquopentaamminecobalt(III) ion.

The pseudo-first-order rate constants ($k = -d \ln [Co(NH_3)_5NO_2^{2+}]/dT$) were obtained from linear plots of the logarithm of the $Co(NH_3)_5NO_2^{2+}$ concentration vs time. At sulfuric acid concentrations from 0.94 to 55.74%, k is constant. For sulfuric acid concentrations above 57%, k may be calculated from the relation $k = (4\pm2)\times10^{-11}\ h_o\ sec^{-1}$, where h_o is the antilog of $-H_o$, the Hammet acidity function. We conclude that in the concentrated acid solutions a reaction path which is first-order in hydrogen ion activity predominates.

Isotopic analysis of three different samples of $[Co(NH_3)_5H_2O]Br_3$, isolated from the reaction of $[Co(NH_3)_5NO_2]SO_4$ with ~90% sulfuric acid containing about 4% oxygen-18 showed that the coordinated water contained about 0.2% ^{18}O, essentially the fraction present in normal oxygen samples. We therefore conclude that the oxygen of the coordinated water molecule came principally from the coordinated NO_2^- ion.

The mechanism for the conversion of the nitro complex to the aquo complex in concentrated sulfuric acid solutions must account for the first-order dependence on hydrogen ion activity and the fact that one of the NO_2^- oxygen atoms ends up in the coordinated water molecule. We suggest the rate-determining step

$$(NH_3)_5CoNO_2^{2+} + H^+ \xrightarrow{k_1}$$

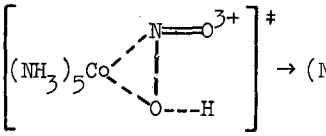

The proton may be considered as assisting the displacement of the nitrosyl ion. This step would be followed by a rapid protonation of the hydroxy intermediate

$$Co(NH_3)_5OH^{2+} + H^+ \rightarrow Co(NH_3)_5H_2O^{3+} \quad .$$

In dilute sulfuric acid solutions, the aquo complex is the final product. In concentrated sulfuric acid solutions, the aquo complex is converted at a finite rate to the bisulfato complex.[1]

---

* Abstracted from Inorg. Chem. 6, 1052(1967).
† Present address: Department of Chemistry, California State College, Fullerton, Calif.

1. W. L. Jolly, A. D. Harris, and T. S. Briggs, Inorg. Chem. 4, 1064 (1965).

b. Proton Magnetic Resonance Spectra of Rhodium and Iridium Complexes in Sulfuric Acid

David N. Hendrickson and William L. Jolly

Proton magnetic resonance spectra of rhodium(III) and iridium(III) complexes in sulfuric acid have been observed. Results, including some for analogous cobalt(III) complexes, are summarized in Table I.12.B-I. It was found that rhodium and iridium pentaammine complexes have only one proton resonance, whereas cobalt pentaammine complexes typically show two peaks in the ratio of four to one, assignable to the cis and trans ammine protons, respectively.

Exchange with the solvent was ruled out as an explanation for the loss of the second peak in the rhodium and iridium pentaammines. This was accomplished by quantitative NMR techniques, integrating the spectrum of a sulfuric acid solution of $(Rh(NH_3)_5Br)Br_2$ and NH_4Br. With the assumption that there is no intramolecular ammonia exchange, it seems that the cis and trans proton resonances are degenerate within our resolution.

Table I.12 B-I. Proton chemical shifts of ammine complexes

Complex	Chemical shift, ppm vs TMS Co(III)[a]	Rh(III)	Ir(III)
$(M(NH_3)_6)^{3+}$	-3.59	-3.82	
$(M(NH_3)_5Cl)^{2+}$	-3.76 cis -3.09 trans	-3.78	-4.55
$(M(NH_3)_5H_2O)^{3+}$	-4.16 cis -2.91 trans		-4.68
$(M(NH_3)_5NCS)^{2+}$	-3.99 cis -3.53 trans		-4.58
$(M(NH_3)_5Br)^{2+}$	-3.87 cis -3.16 trans	-3.80	
$(M(NH_3)_5HSO_4)^{2+}$	-3.84 cis -2.92 trans	-4.13	
trans$(M(NH_3)_4Cl_2)^+$	-3.93	-3.85	
trans$(M\ en_2Cl_2)^+$	-5.22 NH_2 -3.65 CH_2	-4.60 NH_2 -3.18 CH_2	

a. W. L. Jolly, A. D. Harris, and T. S. Briggs, Inor. Chem. 4, 1064 (1965).

13. STUDIES IN LIQUID AMMONIA

a. Kinetics of Metal-Acid Reactions in Liquid Ammonia

Leonardo Prizant and William L. Jolly

A special conductivity cell, with a low-temperature thermostated bath, has been built for studying the rate of reaction of alkali metals with very weak protonic acids in liquid ammonia. Preliminary work has indicated that satisfactory data should be obtainable for protonic acids such as anilines, urea, and other amino compounds.

b. A Glass pH Electrode in Liquid Ammonia

Robert Shiurba and William L. Jolly

By replacing the internal solution of a Beckman cation-sensitive glass electrode with AgCl-saturated 8M HCl, we have obtained a glass electrode which can be used to measure ammonium ions (solvated protons) in liquid ammonia at its boiling point (-33°).

Using a Cu, $Cu(NH_3)_2^+$ reference electrode without liquid junction, we have shown that the Nernst Law is obeyed over an ammonium chloride concentration range 0.005 to 0.5M.

A satisfactory reference electrode with liquid junction has been made using the asbestos capillary junction of a commercial calomel electrode. The reference electrode was a copper wire inserted into a solution of CuCl and $NaNO_3$ in a mixture of isopropylamine and dimethyl sulfoxide.

c. Reversibility of the Reaction of Alkali Metals with Liquid Ammonia*

Ernest J. Kirschke† and William L. Jolly

Ammoniated electrons exist in solutions of the alkali metal amides in liquid ammonia which have reached thermodynamic equilibrium with hydrogen gas. By using both electron spin resonance and optical spectroscopy to measure the electron concentration, an equilibrium constant of 5×10^4 was measured for the reaction

$$e_{am}^- + NH_3 = NH_2^- + 1/2H_2,$$

and 3×10^9 for the reaction

$$Na^+ + e_{am}^- + NH_3 = NaNH_2(s) + 1/2H_2$$

at 25°. From the temperature coefficients of these reactions, the approximate $\Delta H°$ values of -16 and -12 kcal/mole, respectively, were obtained.

* Abstracted from Inorg. Chem. 6, 855 (1967).
† Present address: U.S. Naval Weapons Laboratory, Dahlgren, Va.

14. STUDIES OF MISCELLANEOUS NITROGEN COMPOUNDS

a. Molecular Structure of Sodium α-Oxyhyponitrite

David N. Hendrickson

The molecular structure of sodium α-oxyhyponitrite, $Na_2N_2O_3$, is being investigated by mass spectrometric studies of the products of decomposition of the N^{15}-labelled salt. The compound was prepared from unlabelled NH_2OH and labelled $EtONO_2$. Preliminary results of the reaction of the labelled $Na_2N_2O_3$ with Ag^+,

$$N_2O_3^{2-} + Ag^+ \rightarrow Ag + NO + NO_2^- ,$$

indicate that most of the ^{15}N ends up in the NO_2^-. Thus it appears that there are two kinds of N atoms in $N_2O_3^{2-}$.

b. Nitrogen NMR Chemical Shifts

David N. Hendrickson and Paul M. Kuznesof

Wave functions derived from a self-consistent molecular orbital theory with complete neglect of differential overlap[1] are being used to calculate the NMR shielding constants for the nitrogen nuclei in NO_3^-, NO_2^-, NO_2^-, and NH_4^+. Only the local contributions to the shielding of the nitrogen nucleus are considered in each case. A complete valence atomic orbital basis set is used for the molecular orbitals.

Thus far, eigenfunctions and eigenvalues have been obtained for the electronic states of NO_3^- and NO_2^- through limited configuration interaction. For nitrite we obtained for the three lowest allowed electronic states the eigenvalues 2.16 ($^1B_1$), 4.91 ($^1B_2$), and 6.03 ($^1A_1$) ev. The observed transition energies are 3.50, 4.20, and 5.95 ev. The 3.50 ev state has been shown to have B_1 symmetry. Previous calculations with only the pi system self-consistent gave two allowed bands at 2.93 ($^1B_1$) and 5.75 ev ($^1B_2$), and a forbidden $^1A_2$ band at 4.40 ev.[2] In the case of the nitrate ion the two lowest allowed bands were calculated as 5.15 and 8.15 ev, both of $^1E'$ symmetry. The spectrum of NO_3^- shows bands at 4.10 and 6.26 ev. With only the pi system self-consistent, only one allowed transition of E' type is predicted at 6.22 ev.[2]

1. J. A. Pople, D. P. Santry, and G. A. Segal, J. Chem. Phys. 43, S130, S136 (1965).
2. K. McEwen, J. Chem. Phys. 34, 547 (1961).

15. RESEARCH PLANS FOR CALENDAR YEAR 1968

William L. Jolly

Studies of the Hydrides of Germanium and Tin

A Kolbe electrolytic oxidation of the $GeH_3CO_2^-$ ion will be attempted, with the aim of preparing Ge_2H_6 analogously to the synthesis of C_2H_6 from $CH_3CO_2^-$. Other planned work includes a kinetic study of the hydrolyses of $GeH_3CO_2^-$, the preparation of silicon and tin analogs of $GeH_3CO_2^-$, and studies of the reaction of $KGeH_3$ with other Lewis acids. Further studies of the hydrolysis of SnH_4 in cold 40% $HClO_4$ will be carried out to see how well the results agree with those in cold 8M HCl. The physical and chemical properties of the product of the low-temperature reaction of SnH_4 and NH_3 will be investigated.

Boron Hydride Chemistry

We plan to attempt identification of the intermediates in the aqueous acid hydrolysis of the $B_3H_8^-$ ion and of other boron hydride species such as tetraborane and the methyl-substituted diboranes. The reaction of diborane with water at low temperatures yields various metastable products; their nature will be investigated by both stoichiometric and by infrared studies.

Sulfur-Nitrogen Chemistry

A gas-flow saturation method will be used to determine the vapor pressure of $S_3N_3Cl_3(g)$ over $S_3N_3Cl_3(s)$. Inasmuch as we already have information about the vapor pressure of NSCl(g) over $S_3N_3Cl_3(s)$, these data will permit calculation of thermodynamic functions for the gaseous trimerization reaction. We will attempt to grow crystals of $S_2N_2 \cdot SbCl_5$ and $S_2N_2(SbCl_5)_2$ satisfactory for X-ray structural studies. Cryoscopy, ESR, ultraviolet- and visible-spectroscopy, and conductivity studies of the S_4N_4-H_2SO_4 system will continue in our effort to determine the species present in solution.

Studies of Pentaammine Complexes of Cobalt, Rhodium, and Iridium

Future plans include NMR double irradiation of the nitrogen to remove broadness in the proton spectra. Proton NMR studies of dimeric cobalt ammines and pentaammineruthenium(II) complexes will be carried out.

Studies of Liquid Ammonia and Miscellaneous Nitrogen Compounds

The exploratory studies outlined in Sections 13 and 14 will be followed up with full-scale investigations. We hope to be able to compare the kinetic reactivities of various acids toward the ammoniacal electron with the acidities of the same acids. We also hope that the glass pH electrode in liquid ammonia can be developed into a practical device for following titrations of acids and bases in liquid-ammonia systems.

16. 1967 PUBLICATIONS

William L. Jolly and Associates

Technical Journals

1. H. Bloom and W. L. Jolly, Silicon Production Process, U.S. Patent 3,322,503, May 30, 1967.
2. S. Gokhale and W. L. Jolly, Phosphine, Inorg. Syntheses 9, 56 (1967).
3. A. D. Harris, R. Stewart, D. Hendrickson, and W. L. Jolly, The Aquation of the Nitropentaamminecobalt(III) Ion in Sulfuric Acid Solutions, Inorg. Chem. 6, 1052 (1967).
4. W. L. Jolly, The Deprotonation of Weak Acids, Inorg. Chem. 6, 1435 (1965).
5. W. L. Jolly, editor, Preparative Inorganic Reactions, Vol. 3 (Interscience Publ., New York, 1967).
6. W. L. Jolly, The Intrinsic Basicity of the Hydroxide Ion, J. Chem. Ed. 44, 304 (1967).
7. W. L. Jolly and T. Schmitt, Evidence for BH_2^+ in Cold Acidic Solutions, Inorg. Chem. 6, 344 (1967).
8. W. L. Jolly and K. Maguire, Sulfur Nitrogen Chlorides, Inorg. Syntheses 9, 102 (1967).
9. E. Kirschke and W. L. Jolly, The Reversibility of the Reaction of Alkali Metals with Liquid Ammonia, Inorg. Chem. 6, 855 (1967).
10. D. Rustad and W. L. Jolly, Reactions of Silane, Germane, and Stannane with Metal- and Amide-Ammonia Solutions, Inorg. Chem. 6, 1986 (1967).
11. M. Villena-Blanco and W. L. Jolly, Tetrasulfur Tetranitride, Inorg. Syntheses 9, 98 (1967).
12. K. Wynne and W. L. Jolly, Adducts of Sulfur Nitride with Boron Trihalides and Antimony Pentachloride, Inorg. Chem. 6, 107 (1967).

UCRL Reports

1. W. L. Jolly, Inorganic Synthesis with Electric Discharges, UCRL-17519, April 1967.
2. W. Jolly, D. Rustad, T. Birchall, and D. Chazan, The Deprotonation of Weak Acids with Potassium Hydroxide, UCRL-17487, March 1967.
3. W. L. Jolly and A. D. Norman, Hydrides of Groups IV and V, UCRL-17760, Aug. 1967.
4. A. D. Norman, J. R. Webster, and W. L. Jolly, Silane, Stannane, Silane-d_4, Germane-d_4, and Stannane-d_4, UCRL-17486, April 1967.
5. D. Rustad, I. Reactions of Silane, Germane, and Stannane with Metal- and Amide-Ammonia Solutions, II. Preparation and Reactions of Potassium Germyltrihydroborate, $KGeH_3BH_3$ (Ph.D. Thesis), UCRL-17602, June, 1967.
6. D. Rustad and W. L. Jolly, Reactions of Silane, Germane, and Stannane with Metal- and Amide-Ammonia Solutions, UCRL-17534, April 1967.

B. CHEMICAL THERMODYNAMICS

1. RADIATIVE LIFETIMES OF EXCITED ELECTRONIC STATES OF ATOMS AND MOLECULES

Paul T. Cunningham

The phase-shift apparatus[1] has been used to measure the radiative lifetimes of excited states in a number of atoms[2] in high-temperature atomic beams. The results are outlined in Table IB.1-I.

Table IB.1-I. Lifetimes of some atomic states.

Element	State	Lifetime (nsec)
Na	$3p^2P^0$	16.2±0.3
Cu	$4p^2P^0$	7.2±0.3
Ag	$5p^2P^0_{3/2}$	6.7±0.4
Ag	$5p^2P^0_{1/2}$	7.5±0.4
Al	$4s^2S_{1/2}$	7.05±0.3
Al	$3d^2D$	13.7±0.4
Ga	$5s^2S_{1/2}$	7.6±0.4
Ga	$4d^2D$	7.7±0.3
In	$6s^2S_{1/2}$	7.5±0.3
In	$5d^2D_{3/2}$	7.9±0.5
In	$5d^2D_{5/2}$	7.9±0.5
Tl	$7s^2S_{1/2}$	7.65±0.2
Tl	$6d^2D_{3/2}$	6.9±0.4
Pb	$7s^3P^0_1$	6.05±0.3
Bi	$7s^4P_{1/2}$	5.9±0.2

The apparatus has been modified to permit measurement of states with longer lifetimes. Speed-of-light calibration measurements over a path length of 100 ft have been completed.

1. L. Brewer, C. G. James, R. G. Brewer, F. E. Stafford, R. A. Berg, and G. M. Rosenblatt, Rev. Sci. Instr. 33, 1450 (1962).
2. P. T. Cunningham and J. K. Link, J. Opt. Soc. Am. 57, 1000 (1967).

2. SPECTROSCOPIC INVESTIGATIONS OF HIGH-TEMPERATURE SPECIES TRAPPED AT LOW TEMPERATURES IN INERT MATRICES

J. Ling-Fai Wang, Baldwin A. King, and C. Beat Meyer*

Absorption studies have been made of Mg and Ca atoms in rare gas matrices, and absorption and fluorescence studies have been carried out on Cu, Ag, and Au trapped either alone or together in matrices of Ar, Kr, Xe, and SF_6. Additional experiments are in progress. It is hoped that such studies will shed light on the origin of the fine structure of these spectra and clarify the role of long-range solute-solute interactions.

* With Department of Chemistry, University of Washington, Seattle, Wash.

3. INORGANIC SYNTHESES IN LOW-TEMPERATURE MATRICES, NONAQUEOUS SOLVENTS, AND COCONDENSATION SYSTEMS

David Solan, J. Ling-Fai Wang, and Baldwin A. King

The radicals are produced by high temperatures, and quickly passed by a line-of-sight path to a 77°K surface, where they are cocondensed with a normal volatile compound, the other reactant. The reaction proceeds at the surface, and the large amounts of energy produced are quickly conducted away to the liquid nitrogen coolant, thus preventing the products from decomposing. The products, sometimes very unique, are then characterized and their properties determined. Cocondensation reactions with GeH_2 and GeF_2 have failed to produce new products. SiF_2 plus GeH_4 gave an homologous series of compounds, $GeH_3Si_nF_{2n}H$(n=1 to 3) plus the compound, GeH_3SiF_3. The PF_2

radical has been shown to form from the cracking of P_2F_4. Electron-spin-resonance studies at 77°K showed only an intense broad line. Matrix infrared and mass spectrometric investigations of this radical are contemplated. When P_2F_4 is passed through a 750° furnace at 5 mm pressure, a radical other than PF_2 forms which undergoes cocondensation reactions. The products of these reactions are unstable, and only one new compound has been found in high enough yields to be analyzed. The characterization of this compound is still continuing, but it appears to be P_4F_6.

Experiments on the reaction between SF_6 and alkali atoms in liquid ammonia are continuing, but the product is not clearly characterized yet.

Magnesium atoms and oxygen atoms have been simultaneously trapped in rare gas matrices. When the matrix was warmed to the temperature at which oxygen atoms could diffuse, the magnesium atom spectrum vanished and a banded molecular spectrum appeared. If further experiments demonstrate that diatomic MgO has been synthesized in the matrix, this technique will be extended to other high temperature molecules to characterize their spectra under low-temperature conditions.

4. IODINE PREDISSOCIATION AND RECOMBINATION STUDIES

Joel Tellinghuisen

To investigate the possibility of a spontaneous predissociation of the B state of I_2, we devised a special radiation cell with an iodine discharge lamp affixed to one end and fitted with two Suprasil quartz windows for photomultiplier observation of absorption and fluorescence of the iodine atomic radiation produced by the discharge lamp. Gaseous I_2 in the cell, on irradiation with light in the banded region of the B state (5000Å to 6300Å) will produce iodine atoms, which will absorb and re-emit the atomic radiation from the lamp. The amount of fluorescence or absorption observed with a "solar-blind" photomultiplier can be related to the concentration of iodine atoms in the cell. By varying the temperature of a cold finger, the I_2 pressure in the cell may be controlled, and an [I] vs [I_2] relationship can be drawn. A proper steady-state treatment of the molecular processes occurring in the cell predicts a functional relationship from which a value for the rate constant for spontaneous predissociation k_p may be determined. Ultimately it may be possible to determine k_p as a function of the region of excitation in the B state and thereby fix the spontaneous predissociative contribution to the measured lifetimes for I_2.[1]

To propose a sensible reaction mechanism for the steady-state treatment, we must know more about the recombination of iodine atoms under the conditions of the experiment described above. A flash photolysis experiment was designed to study recombination from the standpoint of the disappearance of the iodine atoms. Present sketchy results indicate the disappearance is first order with respect to [I] and inversely dependent on [I_2] in the pressure range 5 to 200 microns, pointing to wall recombination as the dominant recombination process in this pressure region with a cell diameter of 3 cm.

The recombination investigation will be expanded to include higher [I_2] regions and renewal of some of the classic I_2-inert gas studies.[2,3] The results should be helpful in better understanding the predissociation situation.

1. A. Chutjian, J. Link, and L. Brewer, J. Chem. Phys. 46, 2666 (1967).
2. M. I. Christie, R. G. W. Norrish, F. R. S., and G. Porter, Proc. Roy. Soc. (London) A216, 152 (1952).
3. D. L. Bunker and N. Davidson, J. Am. Chem. Soc. 80, 5085 (1958).

5. PSEUDOPOTENTIAL CALCULATIONS ON ATOMS AND DIATOMIC MOLECULES

Joel Tellinghuisen

A pseudopotential approach to the problem of calculating electronic energies of atoms and molecules is being used to investigate the anomalous bonding behavior of the alkali diatomic molecules and molecular ions, M_2 and M_2^+. From experimental results the dissociation energies of the ions are known to be approximately 50% greater than those of the corresponding neutral molecules, although the force constants are smaller and the mean internuclear distances larger for the ions as expected.[1] A straightforward application of molecular orbital theory fails to predict the correct relative bond energies, probably because correlation effects of the valence electrons on the highly polarizable cores has not been properly accounted for. It was hoped that a pseudopotential treatment might lend itself nicely to the incorporation of such effects in a manner that would maintain a simple, lucid connection between physical intuition and the resulting numbers.

The suggestion of Cohen and Heine for use of a perturbation treatment with a model

Hamiltonian has been taken as the starting point in the calculations.[2] Neglecting the last term, their Eq. (28) reads

$$(H + V_R)\phi = H_M\phi + [(V-V_M)\phi - \Sigma_t \phi_t \langle\phi_t|(V-V_M)|\phi\rangle] = E\phi$$
$$= H_M\phi + V_p\phi,$$

where the Σ_t indicates the summation over all core states. Expansion of ϕ over a suitable basis set and use of the variational principle can yield a "best" ϕ for the chosen H_M, and the perturbation V_p is calculated and added later. For V_M a cutoff Coulomb potential ($V_M = -1/r$ for $r \geq r_0$ or $V_M = 0$ for $r < r_0$) has been used. For the "true potential" V we have considered simply the nucleus and the average undistorted electronic distribution in the Na^+ ion as determined from the wave functions of Sachs.[3] His functions were also taken as the correct core functions ϕ_t.

Results have been encouraging. Expanding in a basis of Slater-type orbitals (STO's) and taking r_0 to be a reasonable 2.4 to 2.8 atomic units (a.u.) the calculations yield the ground-state atomic Na dissociation energy within about 5%, and give better values for several excited S states. Results are even better for the P and D states. Including an additional perturbation term of the form $-\alpha/r^4$ ($r > r_{core}$), where α is a calculated polarizability[4] for Na^+ can give values that are exactly equal to experiment for a favorably chosen r_{core} lying in the range 2.4 to 2.8 a.u. (in this case about 2.6). For the Na_2^+ ion the basis functions used were a set of two-center "dog-bone" orbitals of the form $X = Re^n\exp(-\eta\ Ro)$ where $Re = (r_a^2 + r_b^2)^{1/2}$ and $Ro = r_a + r_b$. Expanding over only five such functions and obtaining the necessary matrix elements by a crude numerical integration procedure led to values of the dissociation energy within 50% of experiment; inclusion of the $-\alpha/r^4$ term with the same parameters used in the atomic calculation yielded a dissociation energy within several percent of the best experimental value.

Present efforts are directed at setting up procedures to do the molecular computations over an STO basis set. Much more accurate numerical integration procedures have been devised to calculate the integrals that cannot be solved with ease in closed form. When these new computation routines are completed and tested, they will be used to recalculate Na_2^+ and later Na_2. It should then be a simple matter to apply this pseudopotential approach to the calculation of energies for other alkali diatomics, and with appropriate extensions, for many-electron-bonded molecules.

1. Yuan-tseh Lee and B. H. Mahan, J. Chem. Phys. 42, 2893 (1965).
2. M. H. Cohen and V. Heine, Phys. Rev. 122, 1821 (1961).
3. L. M. Sachs, Phys. Rev. 124, 1283 (1961).
4. M. Born and M. Göppert-Mayer, Handbuch der Physik 24r2 (Julius Springer, Berlin, 1933) p. 738.

6. DETERMINATION OF THE ELECTRONIC PARTITION FUNCTION OF SCANDIUM MONOFLUORIDE BY MOLECULAR-BEAM FLUORESCENCE

David Green

The molecular-beam method used previously to fix the ground-state of LaO[1] has been extended to ScF. King furnace equilibrium studies of the intensities of the green $^1\Pi$-$^1\Sigma^+$ and red $^3\phi$-$^3\Delta$ transitions have given the relative transition probabilities. From these data the expected relative intensity of the transitions in the molecular beam may be calculated assuming no radiative intersystem decay. The relative fluorescent intensity at various beam path lengths indicates that both the $^1\Sigma^+$ and $^3\Delta$ states of ScF persist at least as long as 10^{-4} sec, which is the transit time in the beam. A maximum energy separation has been estimated[2] to be 2000 cm^{-1}.

The thermodynamic free-energy function is dependent upon the degeneracies and energies of low-lying states. This work indicates the partition function should include electronic contributions from both the $^1\Sigma^+$ and $^3\Delta$ states. In addition a $^1\Delta$ which has not been observed should be thermodynamically important.

1. L. Brewer and R. Walsh, J. Chem. Phys. 42, 4055 (1965).
2. D. W. Green, Molecular-Beam Studies of Scandium Monofluoride, Part I, UCRL-17961, January 1968.

7. MAGNESIUM OXIDE SPECTRUM AND CALCULATIONS

David Green

The spectral region from 3600 to 4000Å is complicated by extensive overlap of MgO, MgOH, and perhaps other emitters. Computer calculations have been made[1] from known spectroscopic constants to determine the band heads of MgO in this region. Higher terms in the rotational energy cannot be neglected in these calculations. Observed[2,3] but previously unassigned features show excellent agreement with

calculated heads.

Experimental observations of MgO spectra in a flow arc are nearly complete. Several features predicted by calculation but not previously reported have now been observed. Other spectra features in this region have the appearance of MgO band heads not belonging to known electronic transitions and will be investigated further. The spectral region to the violet of these transitions will be searched for other MgO transitions.

It is hoped that a complete search of the near ultraviolet, visible, and near infrared spectral regions will give some indications as to the energies of the triplet states of MgO which have been predicted.[4]

1. D. W. Green, Calculated Violet Band Heads of Magnesium Oxide, UCRL-17878, Oct. 1967.
2. D. S. Pesic, Proc. Phys. Soc. (London), A76, 844 (1960).
3. D. S. Pesic and A. G. Gaydon, Proc. Phys. Soc. (London) A73, 244 (1959).
4. L. Brewer, Principles of High Temperature Chemistry, in Proceedings of the R. A. Welch Foundation Conferences on Chemical Research, VI. Topics in Modern Inorganic Chemistry (R. A. Welch Foundation, Houston, Texas,1962), Chap. 3, pp. 47-92.

8. ANALYSIS OF ROTATIONAL PERTURBATIONS USING ISOTOPIC SHIFTS

David Green and Helen Johansen

A method has been formulated for the analysis of rotational perturbations using observed spectral shifts of rotational lines. The data are fit to an analytical function of $J(J+1)$ by using a computer program. From the parameters of the least-squares fit, the spectroscopic constants of the perturbing state may be inferred. Isotopic molecules allow the determination of T_e, B_e, α_e, D_e, ω_e and $\omega_e x_e$ for the perturbing state. Low-lying electronic states whose spectra have not yet been analyzed may be accurately characterized by their effect on observed states.

This method is presently being tested by computer for the limitations caused by inaccurate experimental data. Experimental tests of the method may be done using the CN molecule where the perturbations have been analyzed.[1] If these tests are successful, we will analyze such molecules as CaO, where several lowlying states have been observed only through perturbations.[2]

1. N. H. Keiss and H. P. Broida, J. Mol. Spectry. 7, 194 (1961).
2. M. Hultin and A. Lagerqvist, Arkiv for Fysik 2, 471 (1951).

9. TRANSITION-METAL ALLOY SYSTEMS

Paul Wengert

The Zr compounds of Ru, Os, Rh, Ir, Pd, Pt, Ag, and Au have been studied. Limits on the Gibbs free energy of formation of these compounds were determined by observing high-temperature reactions of ZrC with the above elements. ZrC was found to be in equilibrium with Ru, Os, $ZrRh_3$, $ZrIr_3$, $ZrPd_3$, $ZrPt_3$, Ag, and Au. Such an equilibrium between the ZrT_3 type compounds indicates that $\Delta F_f(ZrT_3)$ is less than -11.5 kcal/g-atom at 298°K for these alloys. Since ZrC exists in equilibrium with Ru, Os, Ag, and Au, no Zr compounds of these elements are more stable than ZrC; therefore, they have a ΔF_f greater than -46.2 kcal/mole of Zr at 298°K. No ternary compounds were found. The high stability of the compounds of Zr with Rh, Ir, Pd, and Pt with a decrease to both the left and right in the periodic table confirms the predictions of the Engel theory of metals.

10. COMPILATIONS

Norman Lofgren

The compilations of thermodynamic properties of the gaseous diatomic oxides and of the compounds of molybdenum are continuing slowly.

11. RESEARCH PLANS FOR CALENDAR YEAR 1968

Leo Brewer

Radiative Lifetimes of Excited Electronic States of Atoms and Molecules

The new frequency range which was installed in the lifetime apparatus last year will be calibrated further against known lifetimes. For example, measurements of the lifetime of the $^3P_1$ state of mercury are in progress. The lifetime of the B state of I_2 will be compared further with results from other lifetime apparatus. Future work will concentrate on measurements of the second excited states in the principal series of the alkali metals and on diatomic molecules (particularly the $B^2\Sigma$ state of CN).

Spectroscopic Studies of High-Temperature Species in Low-Temperature Matrices

Studies of interactions between Cu, Ag, and Au atoms in low-temperature matrices will be continued. The effect of dimerization upon the spectra will be studied, as well as the effect of asymmetry of environment introduced by use of a mixture of matrix atoms or molecules. It is hoped to be able to use a variety of fluorinated hydrocarbons of increasing polarity to determine the effect of electric field upon the spectra of atoms and diatomic molecules, with ultimate extension to trapping in alkali and silver halide matrices. The effect of temperature variation upon the spectra will be studied from 4°K up to the upper temperature limit in each matrix where diffusion becomes rapid.

Inorganic Syntheses in Low-Temperature Matrices and Nonaqueous Solvents

The synthesis of high-temperature species such as MgO and CaO by matrix trapping of the atoms and reaction upon warming to diffusion temperatures will be carried out in an effort to establish the ground electronic states and to find intercombination spectra.

Electron-transfer reactions between metallic atoms and SF_6 to form SF_6^- will be studied in matrices and in liquid ammonia. Cocondensation experiments at 20 and 77°K are planned for the radicals formed by decomposition of P_2F_4 in a search for new types of inorganic compounds.

Iodine Predissociation and Recombination Studies

Studies of photodissociation of iodine will be continued to determine the rate constant for spontaneous predissociation.

Pseudopotential Calculations for Atomic and Diatomic Molecules

The previous calculations for sodium will be extended and more accurate numerical procedures devised to allow more reliable recalculation for Na_2^+ and Na_2.

Magnesium Oxide Spectra

An attempt will be made to analyze features between 3600 and 4000Å which do not correspond to the calculated band heads expected for the two known transitions of this region. A more complete search from the ir to the uv will be made for bands that might be analyzable.

Analysis of Rotational Perturbations Using Isotopic Shifts

The proposed new method will be tested with various trial molecules and then applied to CaO^{16} and CaO^{18} in an effort to fix the ground electronic state and the low-lying electronic states of the CaO molecule.

Transition-Metal Alloy Systems

The study of extraordinarily stable transition-metal compounds will be extended to a check of the prediction of the Engel theory that there should be a maximum of stability as a platinum group metal is combined with metals of the left-hand side of the periodic table varying from the second to sixth group. The stability of a given compound will be checked by equilibrating with carbides or nitrides or by vapor-pressure measurements.

Compilations

It is hoped that sufficient time can be found during the next year to complete the compilations of thermodynamics properties of gaseous diatomic oxides and of the compounds of molybdenum.

12. 1967 PUBLICATIONS

Leo Brewer and Associates

Technical Journals

1. L. Brewer, Bibliography of the High Temperature Chemistry and Physics of Gases and Gas-Condensed Phase Reactions (International Union of Pure and Applied Chemistry, Commission of High Temperature and Refractories) Nos. 22-25 (1967).
2. L. Brewer, Future Developments in the Spectroscopy of High-Temperature Molecules, in High-Temperature Chemistry, J. L. Margrave ed. (National Academy of Science-National Research Council, Washington, D.C., 1967), Publ. 1470, pp. 3-18.
3. L. Brewer, Viewpoints of Stability of Metallic Structures, in Battelle-Geneva Colloquium on Phase Stability in Metals and Alloys, P. Rudman, J. Stringer, and R. L. Jaffe, eds. (McGraw-Hill Book Co., New York, 1967), pp. 39-61, 241-9, 344-6, and 560-8.
4. L. Brewer, A Most Striking Confirmation of

the Engel Metallic Correlation, Acta. Met. 15, 553 (1967).
5. A. Chutjian, J. Link, and L. Brewer, Measurement of Lifetimes and Quenching Cross Sections of the B State of I_2, J. Chem. Phys. 46, 7,2666 (1967).
6. P. T. Cunningham and J. K. Link, Measurement of Lifetimes of Excited States of Na, Tl, In, Ga, Cu, Ag, Pb, and Bi by the Phase Shift Method, J. Opt. Soc. Am. 57, 1000-7 (1967).

UCRL Reports

1. L. Brewer and R. Hauge, Near Infrared Bands of Diatomic CaO and SrO, UCRL-17670, July 1967.
2. D. Green, Calculated Violet Band Heads of MgO, UCRL-17878, October 1967.

C. SOLID-STATE CHEMISTRY AND PHYSICS

1. HEAT CAPACITY OF DILUTE Fe IN Cu ALLOYS

John C. F. Brock* and Norman E. Phillips

We have measured the heat capacity of several dilute alloys of Fe in Cu between approximately 0.1 and 1°K. The results for 0.1 and 0.05% alloys are shown in Fig. IC.1-1, where they are compared with earlier measurements at the higher temperatures.[1] The prediction of a concentration-independent linear term[2,3] in the heat capacity is only approximately verified. Actually, there is a weak concentration dependence of the linear term in the concentration range 0.1 to 0.3% Some preliminary results for more dilute alloys suggest that the linear term becomes more nearly proportional to concentration in agreement with Nagaoka's calculations[4] for the interaction suggested by Kondo to explain the electrical resistivity of alloys of this type.[5]

* Present address: University of Witwatersrand, Johannesburg, South Africa.

1. J. P. Franck, F. D. Manchester, and D. L. Martin, Proc. Roy. Soc. (London) A263, 494 (1961).
2. A. W. Overhauser, J. Phys. Chem. Solids 13, 52 (1960).
3. W. Marshall, Phys. Rev. 118, 1519 (1960).
4. Y. Nagaoka, Phys. Rev. 138, A1112 (1965).
5. J. Kondo, Progr. Theoret. Phys. (Kyoto) 32, 37 (1964).

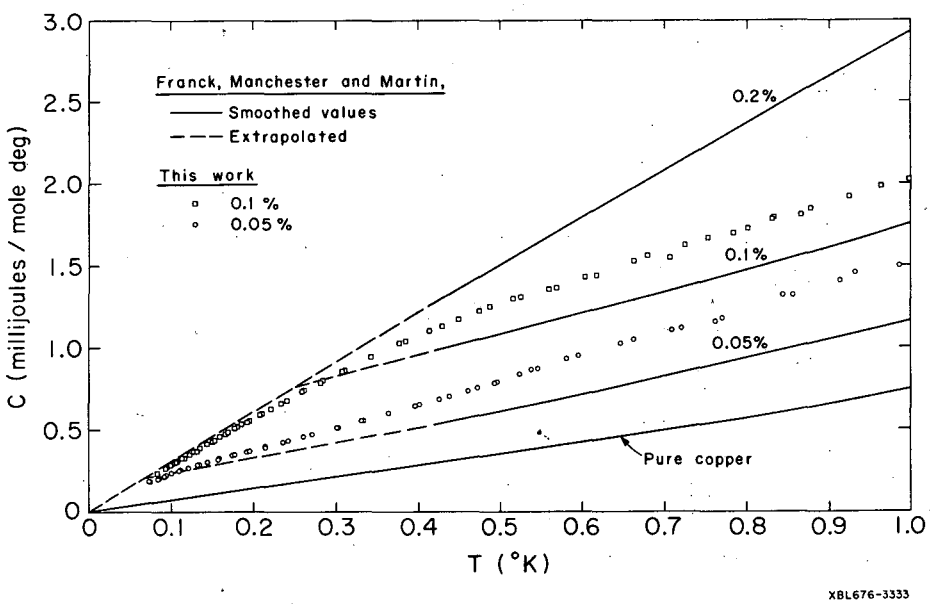

Fig. IC.1-1. Heat capacity of some dilute Fe-in-Cu alloys.

2. HEAT CAPACITY OF A Ni-Rh ALLOY*

Norman E. Phillips, Baylor B. Triplett, and David W. Woody

A number of recent theoretical papers[1-3] have predicted that interactions of conduction electrons with low-energy spin density fluctuations will lead to an enhancement of the effective mass at low temperatures and an associated logarithmic term in the electronic heat capacity. Nickel-rhodium has been identified as a system in which this effect occurs[4] and we have made heat-capacity measurements between 0.05 and 5°K to verify the predicted temperature dependence. Preliminary results indicate approximate agreement with theory above 0.1°K, but possible discrepancies at lower temperatures.

* We are indebted to E. Bucher for supplying the $Ni_{0.62}Rh_{0.38}$ sample and for communication of experimental results in advance of publication.

1. S. Doniach and S. Engelsberg, Phys. Rev. Letters 17, 750 (1966).
2. N. F. Berk and J. R. Schrieffer, Phys. Rev. Letters 17, 433 (1966).
3. D. J. Amit, J. S. Kane, and H. Wagner, Phys. Rev. Letters 19, 425 (1967).
4. E. Bucher, W. F. Brinkman, J. P. Maita, and H. J. Williams, Phys. Rev. Letters 19, 1125 (1967).

3. HEAT CAPACITY OF SOLID bcc AND hcp He^4

James K. Hoffer and Norman E. Phillips

Before the discovery of the bcc phase of solid He^4 would have anomalous thermal properties near the melting curve.[1] Although early measurements on bcc He^4 indicated the predicted anomalous dependence of C_V on volume,[2] later measurements cast doubt on this result, but were of insufficient precision to settle the question.[3]

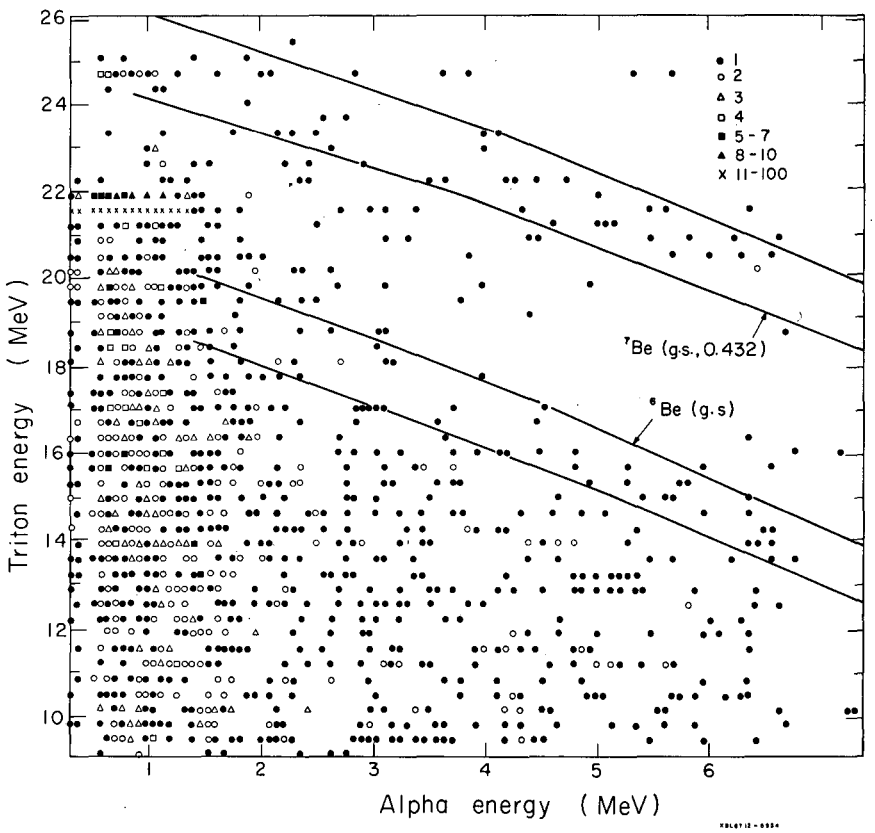

Fig. IC.3-1. Heat capacity of bcc He^4.

We have made C_V measurements on He^4 covering the entire bcc phase and the low-density portion of the hcp phase, down to sufficiently low temperatures to permit an evaluation of the entropy as a function of V and T. The hcp phase is found to have no anomalous properties, and no linear term in the heat capacity. As a consequence of improved precision and the success of our attempt to measure C_V of the supercooled bcc phase, we are able to determine the thermodynamic properties of this phase unambiguously. The results, shown in Fig. IC. 3-1, show that the heat capacity has a normal volume dependence. The Gruneisen parameters are found to be similar to other monatomic solids at equivalent densities. The data however do clearly show a smooth rapid rise in C_V shortly before the onset of melting. This is the only indication of any anomalous properties in the bcc phase, and corresponds to a rapid increase in $(\partial\alpha K^{-1}/\partial T)_r$ as the phase boundary is approached. Having also made precision volume measurements we are able to redefine the V-T phase diagram, which is then seen to have a more reasonable shape than those reported from earlier work.

1. L. Goldstein, Phys. Rev. 122, 726 (1961).
2. G. Ahlers, Phys. Rev. 135, A10 (1964).
3. D. O. Edwards and R. C. Pandorf, Phys. Rev. 144, 143 (1966).

4. THE CONSTANT-VOLUME HEAT CAPACITY OF COMPRESSED HELIUM II

Charles G. Waterfield, James K. Hoffer, and Norman E. Phillips

At present there are no reported values for the constant-volume heat capacity of He^4 below 1.2°K at molar volumes other than at vapor pressure.[1] The manner in which the thermal excitations vary with pressure and temperature is not only of theoretical interest but also is reflected in the melting curve, as described later. Theoretically,[2,3] at the lowest temperatures the only occupied energy states correspond to longitudinal phonons with energy, ϵ, related to momentum, P, by $\epsilon=\mu_I P$ (μ_I being the velocity of first sound). With increasing temperature higher energy states, termed rotons, are occupied, with energy now given by

$$\epsilon = \Delta + (P^2 - P_0^2)/2\mu,$$

where Δ is the energy gap from the ground state, and μ is an effective mass. This form of dispersion curve has been confirmed by inelastic neutron scattering.[4] The heat capacity can be considered as the sum of contributions from both phonons and rotons

$$C_v = C_{ph} + C_r,$$

or more fully

$$C_v = \frac{16}{15}\Pi^5 \frac{k^4 \bar{V} T^3}{h^3 \mu_I^3} + \left[\frac{2k^{3/2}\bar{V}}{(2\Pi)^{3/2}\hbar^3} \left(\mu^{1/2} P_0^2\right) \left(\Delta/k\right)^2 \times \left\{ T^{-3/2} + \frac{kT^{-1/2}}{\Delta} + \frac{3}{4}\left(\frac{k}{\Delta}\right)^2 T^{1/2} \right\} \cdot e^{-\Delta/kT} \right].$$

Analysis of C_v enables one to study the density variation of the energy gap (Δ/k) and the composite parameter ($\mu^{1/2}$ P_0^2).

We have made accurate C_v measurements from ~0.3°K upwards on liquid ^4He at saturated vapor pressure and at five molar volumes between that and the freezing line. Our values for C_{ph} are in good agreement with sound-velocity measurements at low temperatures.[5] The values obtained for the roton parameters are shown in Figs. IC.4-1 and 4-2 and are compared with those obtained by others using different methods. There is seen to be a general agreement about Δ/k but not about $\mu^{1/2}$ P_0^2, and on the whole the parameters derived from fountain pressures[6] seem in best agreement. As expected we find that the limit of the pure phonon region decreases rapidly in temperature as the molar volume decreases. The roton parameters become increasingly temperature-dependent at lower volumes, leading to deviations from the elementary theory above a certain temperature, which in the case of the lowest volumes studied is as low as ~0.9°K.

1. J. Wiebes, C. G. Niels-Hakkerburg, and H. C. Kramers, Physica 23, 625 (1957).
2. L. Landau, J. Phys. USSR 5, 71 (1941); 11, 91 (1947).
3. L. Goldstein, Phys. Rev. 89, 597 (1953).
4. D. G. Henshaw and A. D. B. Woods, Phys. Rev. 121, 1266 (1961).
5. K. R. Atkins and R. A. Stasior, Can. J. Phys. 31, 1156 (1953).
6. C. J. N. van den Meijderburg et al., Physica 27, 197 (1961).
7. C. Baghosian and H. Meyer, Phys. Rev. 152, 200 (1966).
8. R. L. Mills, Ann. Phys. 35, 410 (1965).

5. MELTING CURVE OF He^4

Norman E. Phillips, James K. Hoffer, and Charles G. Waterfield

At temperatures below that at which roton excitation becomes important, the heat capacity of liquid He^4 is less than that of the solid

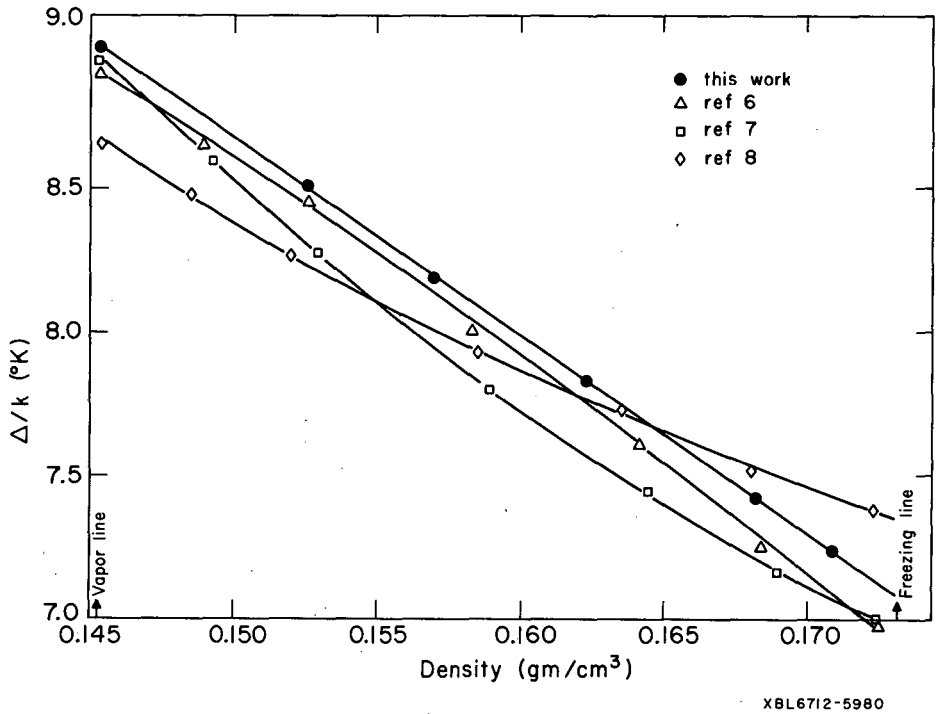

Fig. IC.4-1. Roton energy gap for liquid HeII as a function of density.

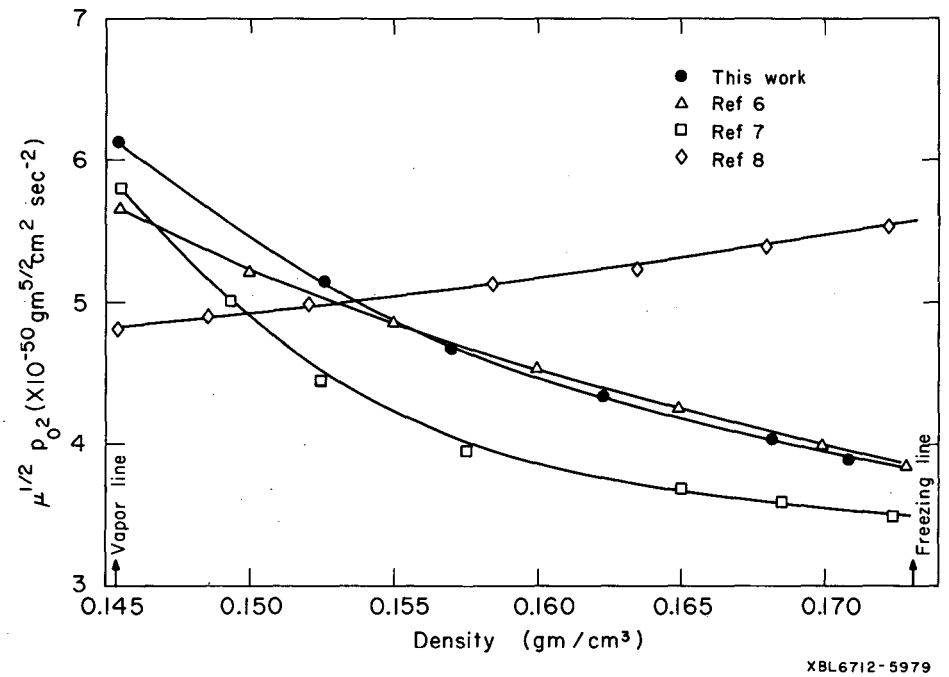

Fig. IC.4-2. $\mu^{1/2}\ P_0^2$ as a function of density.

because of the absence of transverse phonons in the liquid. This leads to a region in which it is in equilibrium, and consequently a minimum in the melting pressure and maxima in the volume-temperature equilibrium curves. The derivatives of these curves are related to the entropies of the solid, liquid, and mixed phases by

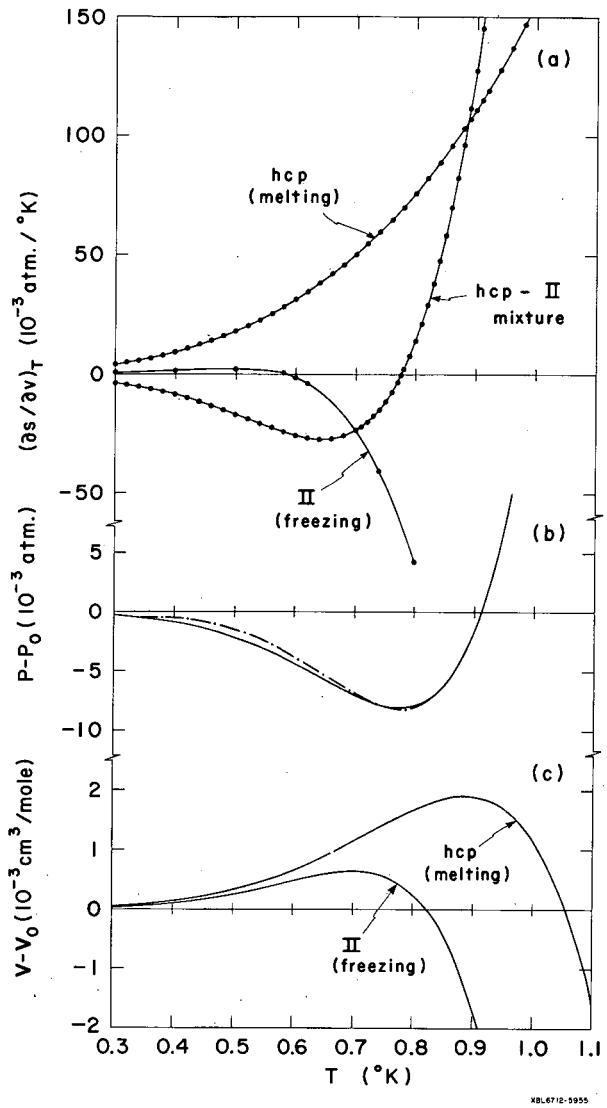

Fig. IC.5-1. (a) $(\partial S/\partial V)_T$ for hcp (solid) He^4, II (liquid), and hcp-II mixtures. (b) Melting pressure of He^4. The dashed line represents smoothed values measured by Straty and Adams.[1] (c) Freezing and melting volumes of liquid He^4 II and solid hcp He^4.

$$\frac{dP}{dT} = \left(\frac{\partial S_m}{\partial V_m}\right)_T = \frac{\Delta S}{\Delta V} ,$$

$$\frac{dV_\ell}{dT} = V_\ell K_\ell \left\{\left(\frac{\partial S_\ell}{\partial V_\ell}\right)_T - \left(\frac{S_m}{V_m}\right)_T\right\} ,$$

and

$$\frac{dV_s}{dT} = V_s K_s \left\{\left(\frac{\partial S_s}{\partial V_s}\right)_T - \left(\frac{\partial S_m}{\partial V_m}\right)_T\right\} ,$$

where the subscripts m, ℓ, and s refer to mixture, liquid, and solid respectively, and K is the compressibility. Figure IC.5-1 shows values of $(\partial S/\partial V)_T$ obtained from our heat-capacity data and the resulting values of the melting pressure and melting and freezing volumes, all relative to their values at 0°K. Our values of $P-P_0$ are in reasonable agreement with recent direct measurements[1] and in quantitative agreement (when we use our own values of the various parameters) with a theoretical analysis.[2]

1. G. C. Straty and E. D. Adams, Phys. Rev. Letters 17, 290 (1966).
2. L. Goldstein and R. L. Mills, Phys. Rev. 159, 136 (1967).

6. HEAT CAPACITY OF SOME SILVER CLATHRATE SALTS*

Mary M. Conway and Norman E. Phillips

Superconductivity has recently been reported in some silver clathrate salts of formula $(Ag_7O_8)^+ X^-$, in which $X^- = NO_3^-$, F^-, and BF_4^- at transition temperatures of 1.04, 0.3, and 0.15°K respectively.[1] Because of the unusual structure of these superconductors, we undertook heat-capacity measurements to verify the existence of bulk superconductivity and to determine the electronic density of states and Debye temperatures θ_0. The results for the NO_3^- clathrate, shown in Fig. IC.6-1, verify the presence of a bulk superconductivity transition. From the transition temperatures in various fields, H_{c2} can be measured and used to deduce a value of 2 for the Landau-Ginzburg parameter, in marked disagreement with the value reported earlier.[1]

We have also measured the heat capacity of the HF_2^- salt. As shown in Fig. IC.6-2 it has a relatively broad, perhaps incomplete transition. The measurements in a magnetic field support the suggestion that its superconducting transition may be influenced by the presence of paramagnetic ions.[2] The

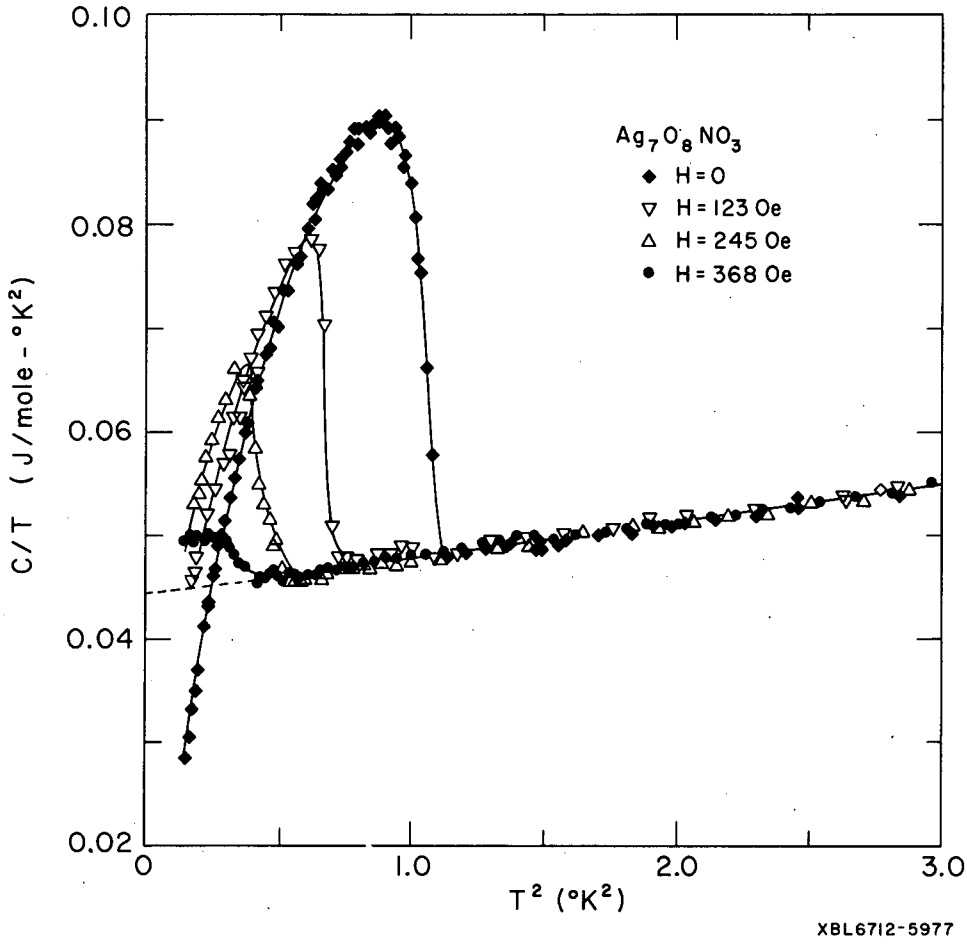

Fig. IC.6-1. Heat capacity of $Ag_7O_8NO_3$.

striking feature of these results however is the large change in θ_0 and density of states (measured by the coefficient of the electronic heat capacity γ) brought about by substitution of the HF_2^- ion for the NO_3^- ion, as shown in Fig. IC.6-2. The results for the two salts are summarized in Table IC.6-I.

Table IC.6-I. Parameters related to superconducting properties of $Ag_7O_8NO_3$ and $Ag_7O_8HF_2$.

	T_c (°K)	θ_0 (°K)	γ mJ/mole-°K^2
NO_3^-	1.03	85.3	0.446
HF_2^-	0.7-1.4	129	0.725

* We are indebted to Dr. T. H. Geballe for supplying the samples and for communication of experimental results in advance of publication.

1. M. B. Robin, K. Andres, T. H. Geballe, N. A. Keuhler, and D. B. McWhan, Phys. Rev. Letters 17, 917 (1966).
2. T. H. Geballe, private communication.

7. HEAT CAPACITY OF MOLYBDENUM

John C. F. Brock* and Norman E. Phillips

To search for further evidence for a second energy gap in transition-metal superconductors, we have measured the heat capacity of a high-purity molybdenum sample. The normal

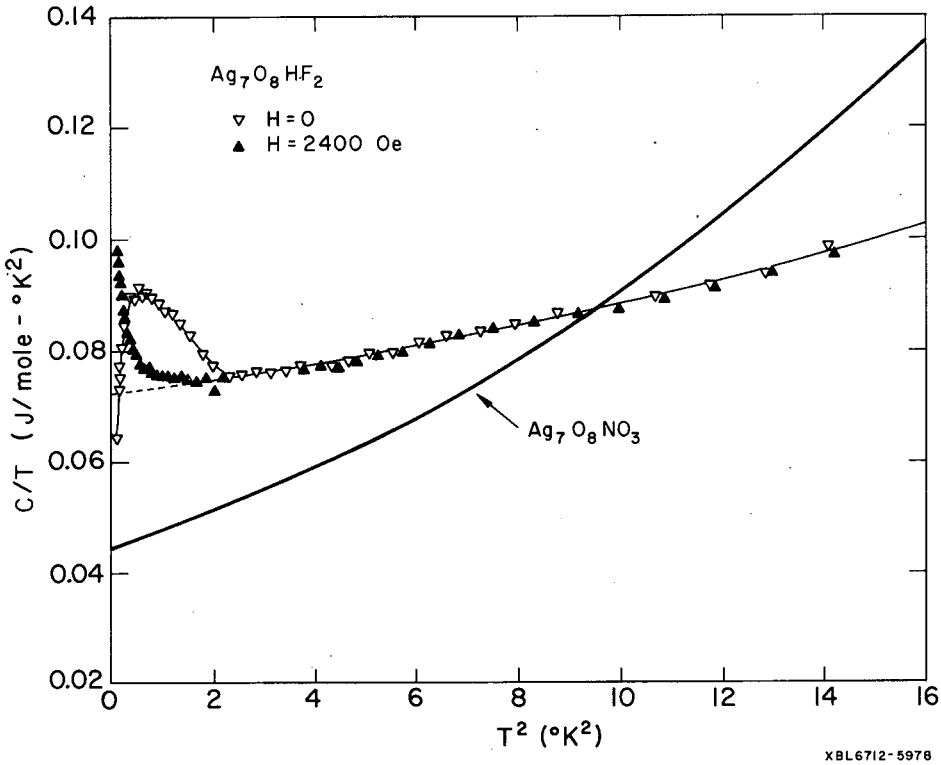

Fig. IC.6-2. Heat capacity of $Ag_7O_8HF_2$. The normal-state heat capacity of $Ag_7O_8NO_3$ is shown for comparison.

state heat capacity was measured between 0.1 and 6°K, and the superconducting-state heat capacity from 0.08 to T_c. Deviations from a simple BCS type of temperature dependence, somewhat similar to those found[1] in V, Nb, and Ta, were observed in the superconducting state.

* Present address: University of Witwatersrand, Johannesburg, S. Africa.

1. L. Y. L. Shen, N. M. Senozan, and N. E. Phillips, Phys. Rev. Letters 14, 1025 (1965).

8. HEAT CAPACITY OF METALS UNDER PRESSURE

Schubert S. B. Wang, Mary M. Conway, and Norman E. Phillips

We have constructed an improved high-pressure cell for low-temperature calorimetry of metals. The material used has a substantially smaller heat capacity in the region below 1°K than the earlier cell and will thus permit more accurate measurements. Its heat capacity has been measured between 0.3 and 20°K in 0-, 1000-, and 5000-Oe magnetic fields.

9. He^3-He^4 DILUTION REFRIGERATOR

Baylor B. Triplett and Norman E. Phillips

A He^3-He^4 dilution refrigerator has been constructed for use in a metal, vibration-isolated dewar. Apart from electrical wiring, the refrigerator is ready for testing.

10. RESEARCH PLANS FOR CALENDAR YEAR 1968

Norman E. Phillips

Heat Capacity of Metals Under Pressure

The improved high-pressure cell will be used to extend the measurements on α-U and α-Ce to a range of pressures. It should be possible to decide whether the low-temperature anomaly in the heat capacity of α-U really disappears at 10 kbar and whether the density of states in α-Ce is strongly pressure-dependent, as would be expected if there is an appreciable 4f contribution to the electron wave functions. We are considering building another cell that would hold pressures of 20 kbar.

High-Magnetic-Field, Low-Temperature Calorimetry

The He^3-He^4 dilution refrigerator and a He^3 evaporation refrigerator will both be used in conjunction with the 60-kG magnet for the measurement of heat capacities in magnetic fields. Measurements will be made on some rare earth metals to attempt a separation of the electronic and magnetic contributions to the heat capacity, and on superconductors containing magnetic impurities.

Heat Capacity of Dilute Alloys

The measurements on dilute Fe-in-Cu alloys will be extended to lower concentrations and to higher temperatures.

Heat Capacity of Helium

We are considering several new applications of the apparatus in which the heat-capacity measurements on solid and liquid He^4 have been made. The possibilities include high precision C_V measurements at the λ line and measurements on He^3 and He^3-He^4 solutions.

11. 1967 PUBLICATIONS

Norman E. Phillips and Associates

Technical Journals

1. J. C. Ho and N. E. Phillips, Upper Limit for the Magnetic Hyperfine Field in Antiferromagnetic Chromium, J. Appl. Phys. 38, 1153 (1967).

12. THE FERMI MOMENTUM OF ALUMINUM FROM 0 TO 100 KBARS*

James J. Burton† and George Jura

The zero-pressure annihilation spectrum of the positron source was obtained initially. It was assumed that pressure changes in the annihilation spectrum of the source were small in comparison to the total pressure change in the spectrum, and possible changes in the source spectrum were neglected in analyzing the data. The source contributed roughly one-third of the total annihilation spectrum.

Annihilation spectra were taken at 0, 27, 54, 81, and 108 kbars. The pressure calibration was based on the phase transitions of bismuth in the same geometry using silver chloride as the pressure transmitter. In going from 0 to 100 kbars, the γ emission rate of the source was found to decrease by 20%; this was not surprising, as in Mossbauer studies to 100 kbars the intensities of the Fe^{57} lines have been found to decrease as much as 80% because of deformation of the anvils. The raw data at each pressure were corrected for the pressure and time decrease in count rate. The aluminum spectrum at each pressure was obtained by subtracting the source spectrum from the corrected data assuming that the ratio of total source to total aluminum counts was constant over the pressure range of interest and that the shape of the source spectrum did not vary with pressure. The results for the Fermi momentum at each pressure did not depend greatly on these two assumptions.

At each pressure studied, the central portion of the observed annihilation spectrum of the aluminum was fit with a parabola. In fitting the data with a parabola we neglect the effects due to the finite resolution of the experimental apparatus and the finite width of the source; errors introduced by this assumption are small compared to the statistical uncertainty in the results.

The Fermi momenta at the five pressures examined are plotted in Fig. IC.12-1 as a function of pressure. The line in this figure is the Fermi momentum curve predicted by the free-electron model assuming three free electrons per atom and using the volume data for aluminum of Bridgman[1] and Jamieson.[2] Figure IC.12-1 shows that the Fermi momentum of aluminum is very accurately described by the free-electron model within the errors of this experiment.

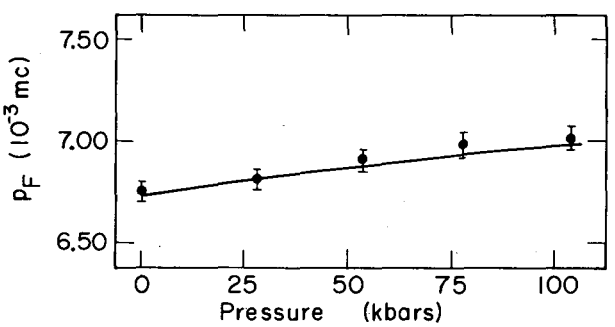

XBL673-2390

Fig. IC.12-1. The Fermi momentum of aluminum as a function of pressure. The line is that predicted by the free-electron model.

We have found that the Fermi momentum of aluminum to 100 kbars is very accurately described by the free-electron model. This is intuitively reasonable as the Fermi surface of aluminum at zero pressure is fairly close to that predicted by the free-electron model assuming three electrons per atom. We would not expect the number of free electrons to increase with pressure, as this would involve stripping core electrons off the aluminum ions, which is energetically unfavorable.

Melz[3] has found in experiments to 7 kbars that the Fermi surface of aluminum does not grow as predicted by the free-electron model. Ashcroft[4] showed in an OPW calculation that the zero-pressure Fermi surface of aluminum can be fitted with two Fourier coefficients of a weak pseudopotential:

$$V_{111} = 0.0179 \text{ Ry}$$

$$V_{200} = 0.0562 \text{ Ry}.$$

Melz obtained the pressure derivatives of the pseudopotential coefficients based on form factors proposed by Harrison.[5]

$$\frac{dV_{111}}{dP} = 1.6\times10^{-4} \text{ Ry/kbar}$$

$$\frac{dV_{200}}{dP} = 2.1\times10^{-4} \text{ Ry/kbar}.$$

He found that these pressure derivatives adequately explained his data.

Using Melz's[3] values of the derivatives of the pseudopotential coefficients we have calculated the average value of the momentum at the Fermi surface for a number of pressures between 0 and 100 kbars, assuming that the coefficients are linear in pressure. The calculated average momenta at the Fermi surface agreed with the values obtained from the free-electron model to within 0.1% over the entire range. Though the band gaps of aluminum are pressure-dependent, very little of the Fermi surface lies close to the zone boundaries. Thus the average momentum at the Fermi surface does not depend strongly on the band gaps so long as the gaps are small.

This work suggests that positron annihilation studies of Fermi momenta may be an excellent tool for investigating either the pressure dependence of the volume of free-electron metals or the high-pressure electronic properties of metals for which the pressure dependence of the volume is well established. Positron annihilation would be most useful for studying metals with a large compressibility because of the difficulties involved in getting sufficient accuracy in the data and the difficulties involved in getting sufficient accuracy in the data and the weak expected volume dependence of the results.

---

* Abstracted from UCRL-17464, March 1967.

† Present address: Department of Chemistry, University of Illinois, Urbana, Illinois.

1. P. W. Bridgman, Proc. Am. Acad. Arts Sci. 76, 55 (1948).
2. J. C. Jamieson, High Pressure Measurement (Butterworths, Washington, D.C., 1963), p. 389.
3. P. J. Melz, Phys. Rev. 152, 540 (1966).
4. N. W. Ashcroft, Phil. Mag. 8, 2055 (1963).
5. W. A. Harrison, Phys. Rev. 131, 2433 (1963).

13. SURFACE-PHASE TRANSFORMATIONS ON A MOLECULAR SURFACE

James J. Burton† and George Jura

Low-energy electron-diffraction work on the surfaces of metals shows changes on some metals which have been interpreted as phase changes on the surface. Calculations have been made for the 100 face of solid argon to see whether such a transition can be accounted for on the basis of known energy functions of the crystal. Such transformations are shown to be thermodynamically possible. Indeed, the results obtained in this investigation are such that an upper temperature limit is determined for such a transition.

The energy of the various surfaces were determined using a Lennard-Jones 6-12 potential. The vibrations of the atoms were approximated by the Einstein model. The Einstein approximation for the vibrational modes is poor, but the differences that are necessary for this calculation were essentially the same when the Nernst-Lindemann approximation was used. Since the Nernst-Lindemann modification is closer to the true vibrational frequency distribution, more credence can be placed in the results than one would anticipate from the use of the Einstein model alone.

The process considered is transformation of a single layer of the 100 face of argon from its normal configuration to the so-called 2×1 configuration, alternate rows of the normal lattice are shifted one half of the length of the crystallographic unit cell. If F_o is the free energy of the normal surface and F that of the transformed surface, then a transition will occur whenever

$$\Delta F = F - F_o \leq 0.$$

Since

$$F = E - TS,$$

where E is determined from the potential energy and S from the Einstein treatment of the vibrations of the atoms, and the thermodynamic quantities refer to unit area, the problem lies in the calculation of E and S for both configurations.

Only the top layer of the crystal was permitted to relax. If further layers were treated more generally, the computed temperature for the transition would be reduced.

In the entropy calculation, the contribution of the top two layers must be considered, since the expansion of the first layer tends to reduce the force constant of the atoms in the second layer of atoms. The entropy change of the atoms in the second layer is almost 10% of those in the top layer.

Normally, the zero-point energy is neglected in calculations of this kind. However, the change in zero-point energy is appreciable, and it must be considered.

The effect of the hardness of the potential was also investigated. This was done by varying the power of the repulsive term in the potential. It was found that the steeper the repulsive potential, the higher the temperature at which the transition would occur. Thus, this result would indicate that such a transition on the surface could be found only for the more compressible metals; a prediction in accord with experiment.

The experimental work indicates that the transformed surface exists in domains, estimated to contain between 20 and 40 atoms per domain. The domains would introduce a configuration entropy in the calculation. For the 100 surface of argon the results are summarized in the equation,

$$F = 4.83 - (0.0592+0.1335/N)T,$$

where N is the number of atoms in the domain. For N = 0 the transition temperature is 81.5 °K, while for a domain size of 40 atoms, the calculated value of the transition temperature is reduced to 77.5°K. Both of these values are below the normal melting point of argon, 83.9°K.

One other interesting computation was performed, the effect of the creation of a vacancy on the surface. In the transformed surface, there are two kinds of sites, co responding to those atoms in a normal lattice position, and the shifted atoms. Energetically, it was much more difficult to form a vacancy in the normal position of the transformed lattice than in the normal surface. In the up position, it is easier, energetically to create a vacancy. When the calculations were made to find the relaxations about a vacancy in the up position, it was found that the surrounding atoms moved to the normal lattice site. In effect, a change was started which transformed all of the atoms in a shifted line to the normal lattice positions. Thus, this calculation predicts that as the temperature is increased and the number of vacancies must increase, that the transformed surface will transform back to the normal lattice. This prediction is in accord with experiment and is a likely explanation of the observed behavior.

A few calculations of the effect of impurities have also been made, but these showed no features that call for comment at present.

The techniques developed here also permit a more general theoretical treatment of the problem of adsorption.

---

† Present address: Department of Chemistry, University of Illinois, Urbana, Illinois.

14. RESISTIVITY OF PHOSPHOROUS

John Pryzbylinski and George Jura

The original work on the resistivity of phosphorous was done on a 3/16-in. diam disk. This work showed that phosphorous became metallic at pressures above 125 kbars. The existence of a pressure gradient in the sample was of no consequence to prove the metallic nature at a pressure of 140 kbars. Later Jamieson reported transitions in phosphorous at around 100 kbars. An attempt was made to determine the resistivity of phosphorous when not under a gradient. Obviously, it was expected that the resistance would exhibit a discontinuity when the phase change occurred.

A hoop of phosphorous was made in a geometry that would decrease the gradient to less than 0.5%. A great difficulty was observed when the resistivity measurements were started. After a pressure increment, hours would pass without the resistance becoming constant with time. It was not unusual for 12 hours to pass before the resistance became constant to within 0.1%, less than the accuracy within which the measurements were being made. Thus, several months were required for an isothermal determination of the resistance as a function of the pressure.

No discontinuity was observed at the pressures at which the transition was reported.

The lack of a discontinuity does not indicate the lack of a transition. Such a behavior had been observed earlier with lanthanum. If lanthanum is taken as a model, the determination at a higher temperature would show the discontinuity. However, it is not believed that the time required for such an investigation is worthwhile.

15. HEAT CAPACITIES OF METALS UNDER PRESSURE

Walter Stark† and George Jura

The methodology of determining heat capacities by an electric pulse has been completed. The determination of the heat capacity of iron has been completed to a pressure of 100 kbars, and from 150°K to room temperature. At some of the pressures, the data extend to 77°K.

At present available instrumentation restricts the use of the method to those metals whose specific resistance is 5μΩ-cm or greater at room temperature. This restriction, which precludes only about four metals from the developed technique, could be removed if a preamplifier such as the Tektronix 1A7 were developed having a voltage compensator that extends to higher voltages. For the magnitude of the currents that are required, the voltage compensator is inadequate. The restriction given is based on the use of a preamplifier such as the Tektronix Type W.

If a constant current of magnitude I is pulsed through a wire of resistance R, and its temperature derivative of resistance is R', and dE/dt is the rate of change of the voltage across the wire with time, it is easy to show that, in the limit of t = 0

$$C_p = I^3 RR'/dE/dt.$$

In an actual experiment, dE/dt is measured as a function of I, and the heat capacity determined from the slope of the line in a plot of dE/dt vs I^3. A typical example is shown in Fig. IC.15-1.

The major experimental difficulty lies in the determination of 0 time. There is a rise time of the current in the sample. This period is about 10 to 15 μsec. The question of whether or not this is sufficiently close to zero was tested experimentally. The original trace of voltage versus time is linear provided a sufficiently fast sweep rate is employed. The initial slope was found to be independent of the slope from the fastest to the slowest of all possible rates. Further consideration of the problem of the heat loss, using as a model the infinitely long wire as treated by Jaeger, indicates that no error is made even with this uncertainty in zero time. The heat loss initially is so low that it may be neglected. This is no longer true at 100 μsec. The theoretical consideration supports the experimental result. The estimated error in the specific heats using the above formula is about 5%.

In principle, the heat capacity can also be determined if it is assumed that a steady state can be reached in the system by the use of a pulse of long duration. This has been done in several instances. The precision of the method is considerably lower than the former. It is not capable of better than 30%. When both methods have been used, the results have been in agreement within the monstrous error of the steady-state method.

Since iron is quite incompressible, little variation in the heat capacity as a function of pressure can be expected. In the isothermal compression to 100 kbars, the heat capacity is essentially constant. If all of the determinations that have been made are averaged, there is about a 1% decrease in the heat capacity in going from 25 to 100 kbars. Since this number is considerably smaller than the inherent error, it is probably safest to conclude that the heat capacity is essentially unchanged. It is also evident that the temperature data cannot be used to safely determine the variation of the Debye temperature with pressure.

A feature of particular interest that was observed in this investigation was the temperature dependence of the resistance of iron. At pressures of 20 kbars and higher, the resistance of iron could be expressed as

$$R = R_o T^{3/2}.$$

The 3/2-power dependence on temperature certainly is not one that would be expected from generally known theories. The temperature dependence has been observed for iron at one atmosphere from about 4 to 20°K. Two explanations have been advanced: (1) a magnon interaction, and (2) a band shift. The present work yields no answer. However, an answer could be obtained from similar determination on the transition metals, those that have a magnetic moment and those that do not. If the 3/2-power dependence were noted for all ferromagnets, but not for the other transition metals, the magnon interaction would be indicated. If this effect were observed to be random, then it would be safe to conclude that it was a band effect. A single experiment on nickel showed the 3/2-power dependence. These studies have not advanced beyond this stage.

The present results agree with all of the information that is available on the equation of state of iron.

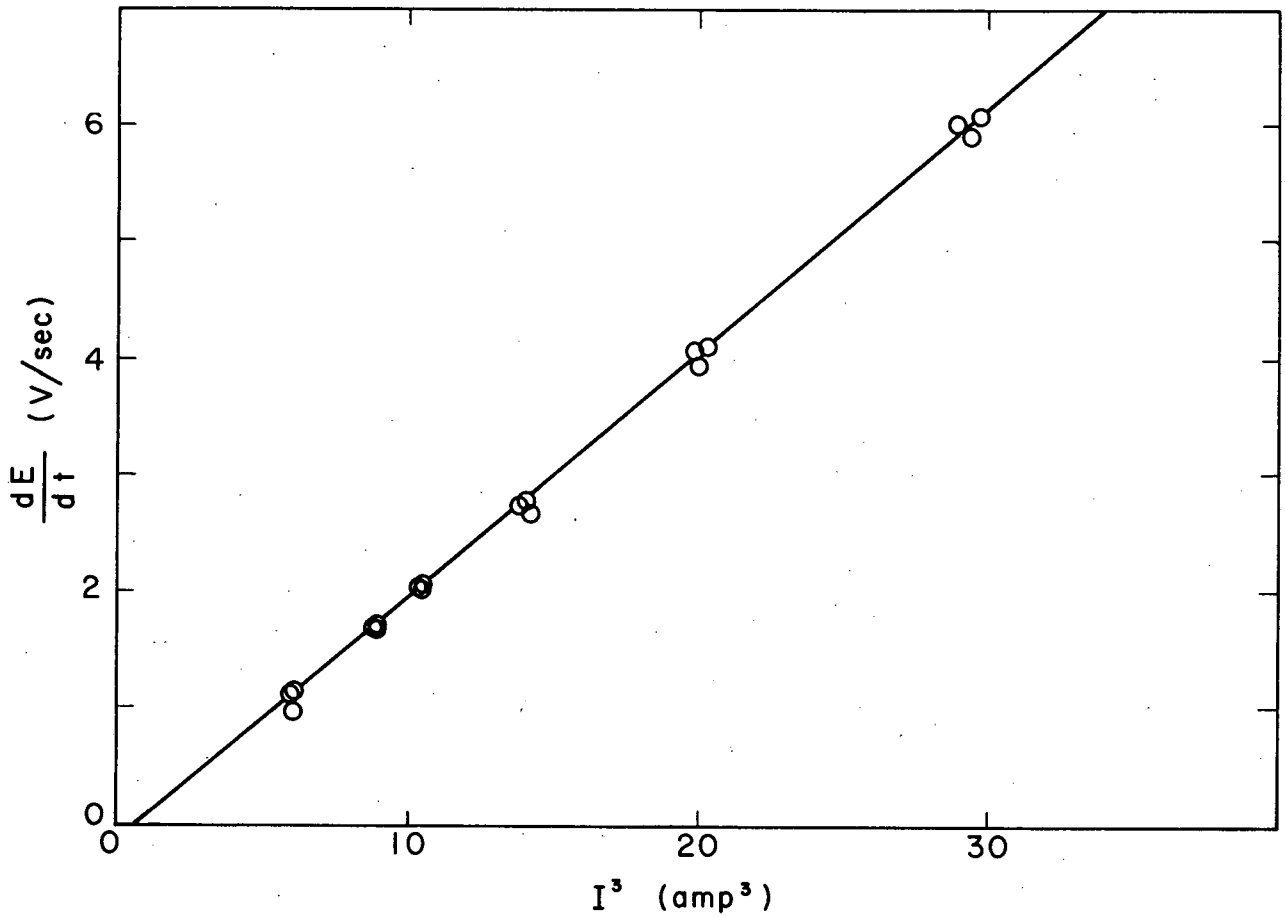

XBL672-948

Fig. IC.15-1. Typical plot of dE/dt versus I^3 for iron.

Since the technique has been developed, it is evident that these investigations can be carried forward for all except a few metals.

† Present address: Sandia Corporation, Las Vegas, New Mexico

16. RESEARCH PLANS FOR CALENDAR YEAR 1968

George Jura

A more general and hopefully better than ever treatment of some problems in physical adsorption will be undertaken.

The development of more precise techniques for the determination of Mössbauer spectra under pressure will be studied. A cam drive has been constructed, tested, and is now being rebuilt. It is hoped that during the year the hyperfine structure of Dy^{161} can be resolved, determined, and analyzed. The spectrum of tin is also scheduled.

Positron annihilation is also to be continued. The modifications introduced this year in an attempt to obtain better results failed because of the placement of the source by Health Chemistry. There is to be a return to the original procedure. Potassium and bismuth are to be investigated in that order. Hopefully the entire year will not be occupied by studies of these two metals.

Work will be continued on specific-heat determinations.

17. 1967 PUBLICATIONS

George Jura and Associates

Technical Journals

1. J. J. Burton and G. Jura, Self-Diffusion in Solid Argon: The Activation Energy, J. Phys. Chem. Solids 28, 705 (1967).
2. J. J. Burton and G. Jura, Surface Distortion in FCC Solids, J. Phys. Chem. 71, 1937 (1967).
3. J. J. Burton and G. Jura, The Configuration and Energy of Defects on the (100) Surface of a Molecular Crystal, Proceedings of the Symposium on Fundamentals of Gas-Surface Interactions, Salzburg and Smith, eds. (Academic Press, New York, 1967).
4. D. Phillips and G. Jura, The Electrical Resistance of Bismuth from 25 to 90 Kilobars, Trans. AIME 239, 1 (1967).
5. D. Raimondi and G. Jura, The Effect of Pressure on the Mössbauer Effect of Fe^{57} in Nickel Metal, J. Appl. Phys. 38, 5 (1967).
6. D. Raimondi and G. Jura, An Experimental Equation of State for Al to the Debye Approximation, J. Phys. Chem. Solids 28, 1419 (1967).

UCRL Reports

1. J. J. Burton, I. Relaxations in a Molecular Crystal. II. The Fermi Momentum of Aluminum from 0 to 100 Kilobars (Ph. D. Thesis), UCRL-17479, May 1967.
2. J. J. Burton and G. Jura, Phase Transformations on Solid Surfaces, UCRL-17343 Rev., April 1967.
3. J. J. Burton and G. Jura, The Fermi Momentum of Aluminum from 0 to 100 Kbars, UCRL-17464, March 1967.
4. W. Stark, Jr., Thermal Pulsing of Metals Under High Pressure (Ph.D. Thesis), UCRL-17454, April 1967.

18. VAPORIZATION KINETICS OF SOLIDS

a. Evaporation Mechanism of Sodium Chloride

Joseph E. Lester† and Gabor A. Somorjai

The studies to uncover the evaporation mechanism of NaCl single crystals have been completed. The vacuum evaporation rates have been investigated using a microbalance in the temperature range 450 to 650°C. The total evaporation rate from the (100) face of the high purity crystals was found to depend on the dislocation density. Samples with low dislocation density (etch-pit count ~ $1\times10^6/cm^2$) vaporize at a rate lower by a factor of two than the maximum rate calculated from the equilibrium pressure (Fig. IC.18-1a.). The evaporation rate of crystals having high dislocation densities ($\sim10^7/cm^2$) was equal to the maximum equilibrium rate (Fig. IC.18-1b). Mass spectrometric investigations revealed that the vapor consists of monomer and dimer molecules, the dimer concentration being roughly 5 to 30 mole % of the vapor [NaCl (solid) $\rightarrow$ (1-X)NaCl (vapor) + X/2 Na_2Cl_2(vapor)] in the temperature range of interest (Fig. IC.18-2). The activation energies of vaporization are 52.6±1 and 62.1±1 kcal/mole of vapor for the monomer and the dimer molecules, respectively. The monomer-to-dimer ratio remains unchanged for the vaporizing crystals of different dislocation densities. Although the activation energies of vaporization may change somewhat (2 to 4 kcal) the difference [ΔH^*(dimer) - ΔH^*(monomer)] remains constant within the accuracy of the measurements (5%).

Monovalent ion impurities (OH^-, Br^-, O_2^-) had no effect on the vaporization characteristics. Divalent ion impurity (Ca^{2+}) in concentrations as small as 10^2 ppm has increased the activation energies of vaporization.

These experimental results can be explained if we assume that the molecules (both NaCl and Na_2Cl_2) are formed at sites (kinks) in the ledges on the surface. Most of these ledges of approximately monatomic height are formed where dislocations intersect the surface. Increase in the dislocation density will increase the number of ledge nucleation sites and thus increase the density of kinks on the surface. Therefore the total evaporation rate increases.

Their mean free paths away from the ledge for both monomer and dimer molecules are very small (a few lattice spacings). There is no equilibrium between the monomers and the dimers on the surface, as indicated also by the constant value of the monomer-to-dimer ratio. This vaporization model is further supported by the fact that divalent impurity (Ca^{2+}) increased the activation energy of vaporization It is apparent that the binding energy of a sodium chloride molecule is larger in the neighborhood of a divalent ion.

† Present address: Department of Chemistry, Northwestern University, Evanston, Illinois.

b. Evaporation Mechanism of Gallium Arsenide Single Crystals

Catherine Lou and Gabor A. Somorjai

The evaporation rates of the (111) and ($\bar{1}\bar{1}\bar{1}$) crystal faces of GaAs have been measured in the temperature range 700 to 900°C using a microbalance. The solid dissociates upon

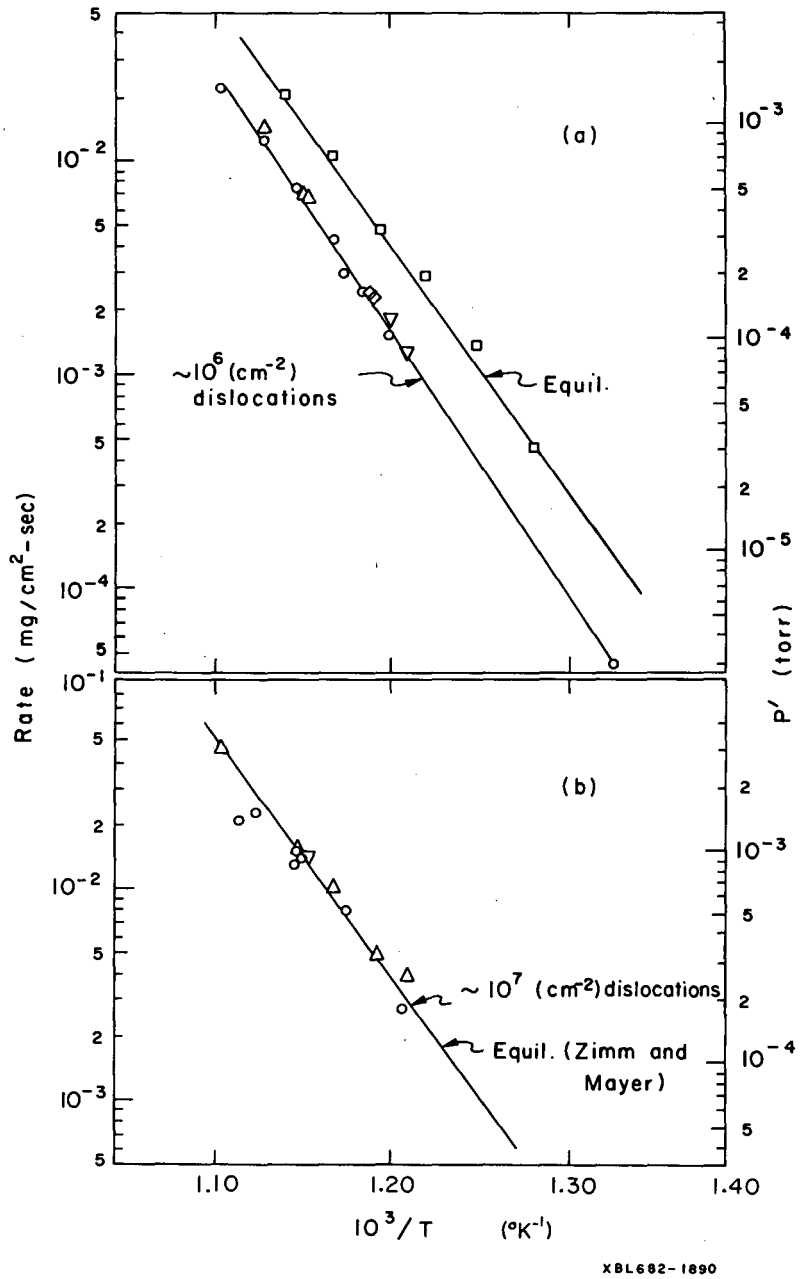

Fig. IC.18-1 (a) Evaporation rates of low-dislocation density single crystals as a function of temperature; (b) evaporation rates of high-dislocation density NaCl crystals as a function of temperature.

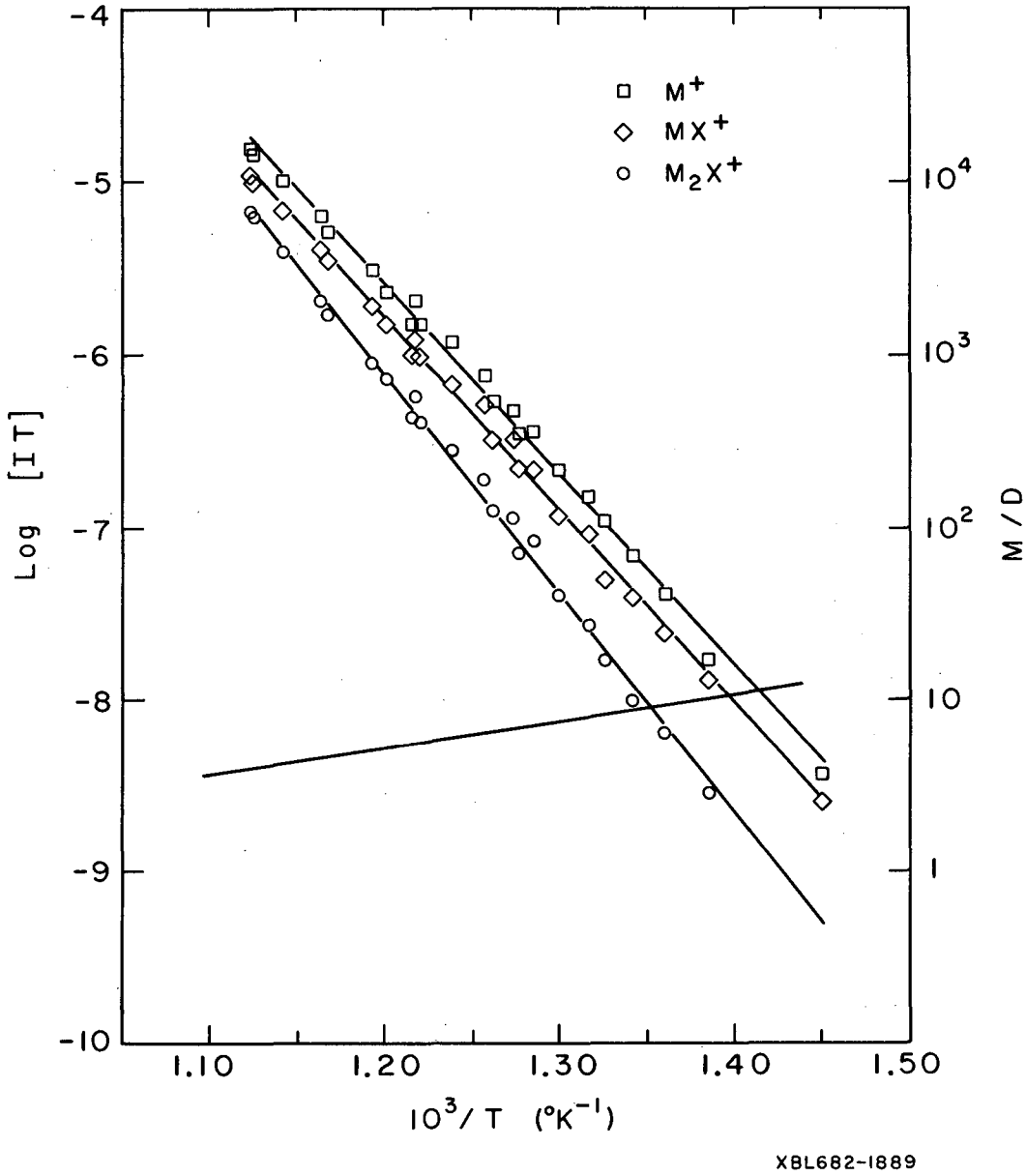

Fig. IC.18-2 The intensities of the 23, 58, and 81 mass peaks as a function of temperature.

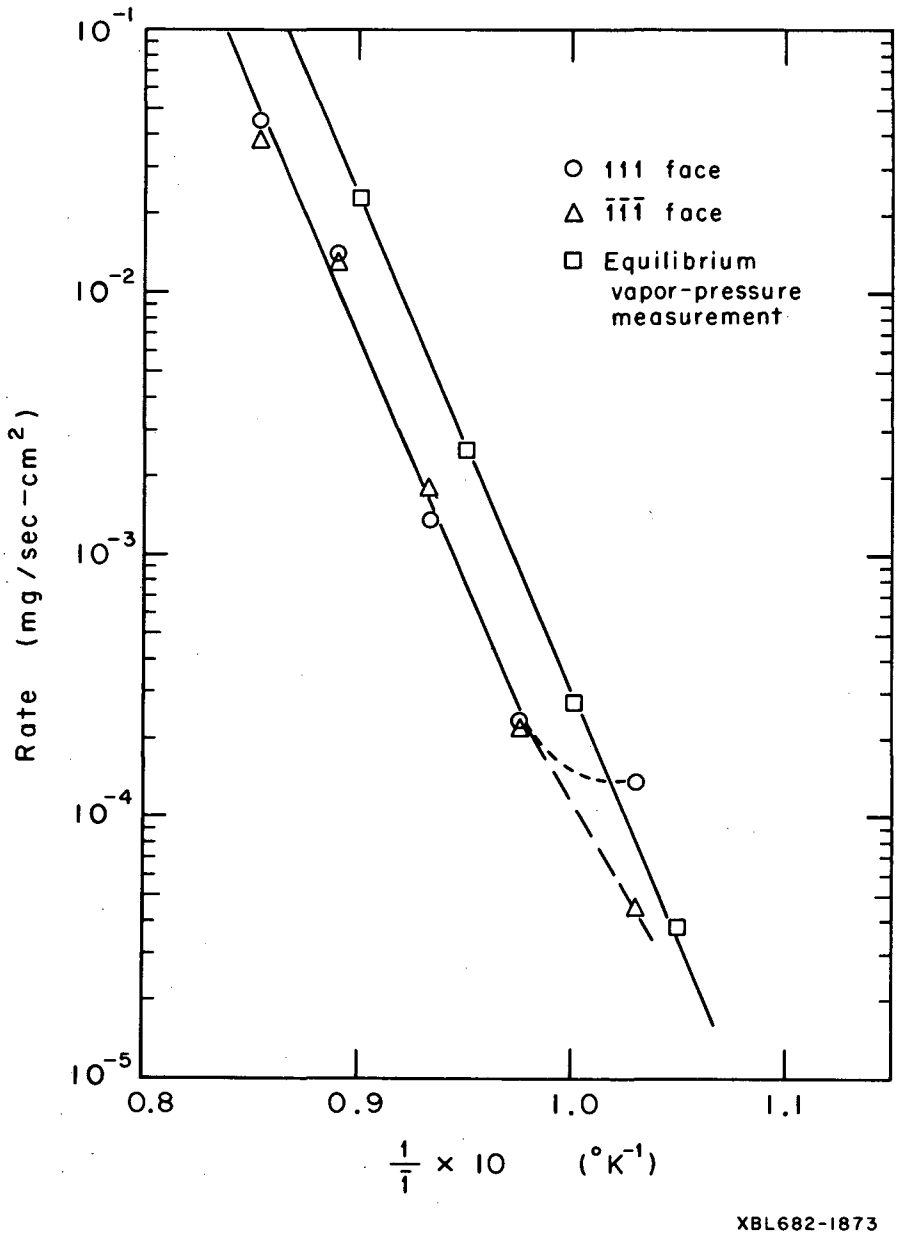

Fig. IC.18-3. Evaporation rate of GaAs single crystals as a function of temperature.

evaporation; arsenic molecules vaporize, while at elevated temperatures (>750°C) gallium (liquid) remains on the vaporizing surface. The evaporation rate was found to be lower by a factor of three than the maximum rate calculated from equilibrium vapor-pressure measurements (Fig. IC.18-3). At low temperatures (<750°C) the vacuum evaporation rates of the gallium (111) and arsenic ($\bar{1}\bar{1}\bar{1}$) crystal faces seem to be different (Fig. IC. 18-3). We have found that excess gallium increased the evaporation rate of the (111) face to the maximum equilibrium value at 800°C. It is apparent that gallium liquid catalyzes the vaporization reaction.

c. Evaporation Rate of Ice Single Crystals

J. Gordon Davy and Gabor A. Somorjai

The evaporation rates of the c face of hexagonal single crystals of ice have been measured in the temperature range -100 to -40°C using a microbalance. At low temperatures (< -60°C) the evaporation rate is near the maximum rate as predicted from equilibrium vapor-pressure studies. Above -60°C, the evaporation rates seem to decrease with respect to the maximum rates. This phenomena is being investigated.

d. High-Temperature Vaporization Mechanisms[1]

Gabor A. Somorjai

Experimental information about the vaporization mechanism of solids has been obtained from evaporation-rate measurements which are carried out far from equilibrium. In such studies one stable face of a single crystal should be used. Vacuum evaporation rates of solids that undergo structural rearrangement, dissociation, or association upon vaporization are, in general, markedly lower ($\alpha \ll 1$) than the maximum evaporation rate ($\alpha = 1$) predicted by the Hertz-Knudsen-Langmuir equation. The rate-controlling step in the vaporization process, in most cases, is a surface reaction followed by the rapid desorption of the vaporizing species. It is expected that most refractory compounds (carbides, oxides, borides, and nitrides) can have vacuum evaporation rates which are several orders of magnitude lower than the maximum rate derived from equilibrium studies. Several mechanisms leading to congruent and noncongruent vaporization are discussed. The vaporization characteristics of the different groups of refractory solids are summarized. Experiments are suggested to elucidate the mechanism of vaporization of refractory materials.

1. G. A. Somorjai, High-Temperature Vaporization Mechanisms, UCRL-17628, June 1967.

19. SURFACE STUDIES BY LOW-ENERGY ELECTRON DIFFRACTION

a. Studies of the Clean (100), (111), and (110) Crystal Faces of Platinum

Hylan B. Lyon[+] and Gabor A. Somorjai

These studies have been completed. Several surface structures have been discovered, both ordered and disordered, which have well-defined temperature ranges of stability. The properties of these surface structures have been investigated in detail. The Debye temperatures which characterize the mean displacement of the surface atoms perpendicular to the surface planes were measured for all three faces. The average value of the surface Debye temperature is 110°K and shows little variation from face to face. The Debye temperature of bulk platinum is 234°K.

The intensity of the specularly reflected electron beam (00 reflection) has been analyzed as a function of electron energy. A model has been developed which accounts for many of its properties. The adsorption of oxygen on the (100) face of platinum has also been investigated.

+ Lt.-Comdr. Lyon has returned to active duty with the U. S. Navy.

b. The Mean Displacement of Surface Atoms in Palladium and Lead Single Crystals

Richard M. Goodman, Helen H. Farrell, and Gabor A. Somorjai

The intensity of specularly reflected (00 reflection) low-energy (5- to 500-eV) electrons has been measured as a function of temperature for the (100) and (111) faces of palladium and for the (111) face of lead in the temperature ranges 25 to 600°C and 25 to 225°C, respectively. From the data the root-mean-square displacements $\langle \mu_\perp \rangle$ of surface atoms perpendicular to the surface planes and the surface Debye temperatures have been calculated. The mean vibrational amplitudes of surface atoms are 40 to 100% larger than for bulk atoms. There is little difference between the surface mean displacements of different crystal orientations; $\langle \mu_\perp \rangle$ appears to be relatively insensitive to changes of surface structure or surface density. The experimental results correlate well with those obtained for platinum and silver single-crystal surfaces. It is believed that all monatomic fcc crystal surfaces should have mean displacements markedly larger than that in the bulk.

c. Low-Energy Electron-Diffraction Study of Solid and Liquid Lead

Richard M. Goodman and Gabor A. Somorjai

The melting of the (111) crystal face of lead has been investigated. The diffraction chamber was modified so that one can continuously monitor the diffraction pattern as the crystal is melted, and above and below the melting point. The temperature of the crystal

surface can also be controlled accurately. It was found that the surface of the lead crystal melts at the melting point in the bulk (327°C). The crystal can be easily regrown maintaining the (111) orientation upon slowly cooling the melt below the freezing point. Rapid quenching favors the formation of crystallites with (100) crystal faces.

The intensity of the diffracted beam decreases rapidly at higher beam voltages (> 150 eV) due to the large Debye-Waller factor and absorption effects. Low-energy electron-diffraction studies of other liquid metals (Sn, etc.) are in progress.

d. Low-Energy Electron-Diffraction Study of α-Alumina (Al_2O_3) and Quartz (SiO_2) Surfaces

Theodore M. French, Joseph Morabito, and Gabor A. Somorjai

Diffraction patterns have been obtained from both the (0001) faces of the hexagonal α-alumina and quartz single crystals. The surface preparation (polishing, etching) plays an important role in obtaining the ordered surface which gives reproducible diffraction features. At high temperatures (>800°C) ion bombardment destroys the ordered surface of SiO_2, while it has no apparent effect at 25°C because of the surface space charge which repels the noble gas ions. The surface charge on these high-resistivity crystals can be reduced by applying a beam voltage pulsing technique.

Quartz undergoes several phase transformations between 25 and 1200°C ($\alpha \rightarrow \beta$, cristobalite → tridymite). These are under investigation at present, along with several other properties of SiO_2 and Al_2O_3 surfaces.

e. Low-Energy Electron-Diffraction Study of Aluminum

Helen H. Farrell and Gabor A. Somorjai

In order to determine the unique position of surface atoms (structure analysis), the relative intensities of the diffracted beams should be analyzed in terms of a diffraction theory. The aims of these investigations are two-fold: (1) to carry out accurate intensity measurements using the different crystal faces of aluminum single crystals, and (2) to develop and apply a theory of electron scattering to low-energy electron diffraction.

So far we have studied the (100) face of aluminum. After suitable surface preparation diffraction patterns have been obtained. The ordered surface does not seem to oxidize or become contaminated rapidly. It can be maintained in ultrahigh vacuum for extended periods of time. Unlike platinum, gold, and palladium surfaces, the Al (100) face does not form different surface structures as a function of temperature. The surface retains the same periodicity which is characteristic of the bulk unit cell.

f. Low-Energy Electron-Diffraction Studies at Low Temperatures

Joseph Morabito and Gabor A. Somorjai

A crystal holder has been developed which allows the study of crystal surfaces in the range from -195 to 500°C. The first low-temperature investigations will be carried out using silver single crystals. The physical adsorption of different gases on silver surfaces will be studied.

g. Low-Energy Electron-Diffraction Study of Surface Reactions on (100) Platinum

Alan E. Morgan and Gabor A. Somorjai

Platinum is used as a catalyst in many gas-phase reactions, (oxidation of ammonia, hydrogenation of hydrocarbons, etc.). The mechanisms and kinetics of reactions on the (100) surface of platinum are being investigated using LEED. The reactants and products are detected with a quadrupole mass spectrometer. The effects of temperature, gas pressure, and in particular, the presence of ordered surface structures on the reactions are being studied. These structures might be due to rearrangements of the platinum surface atoms with temperature or to gases adsorbed on the surface in ordered arrays.

The Pt(100) - (5x1) surface structure is formed by heating the crystal above 200°C in ultrahigh vacuum. The properties of this structure, both in vacuo and in the presence of various gases (O_2, H_2, N_2, CO, CO_2, CH_4, C_2H_4, and Xe), are being examined. In addition, adsorption of these gases on the (100) face of platinum is being investigated, with particular reference to the discovery of further surface structures.

20. SOLID-STATE REACTIONS

a. Sodium in Silicon Single Crystals

Whalun Szeto and Gabor A. Somorjai

The diffusion rate and solubility of sodium in silicon single crystals have been studied in the temperature range 500 to 900°C. Sodium was introduced by immersing the silicon samples into molten sodium at the desired temperature. It was found that sodium rapidly diffuses into silicon, and the diffusion rates are comparable to that of lithium. Sodium is a donor in silicon, and the free-electron concentration in the intrinsic crystal can be increased by more than three orders of magnitude by in-diffusion of sodium ($> 10^{16}$ cm^{-3}). At elevated temperatures (> 700°C) molten sodium dissolves silicon, and the dissolution rate increases more rapidly with increasing temperature than the diffusion rate.

Sodium ions can also be drifted in p-type silicon by applying an electric field (500 eV) at a low temperature of 90°C. It is likely that sodium-drifted silicon or germanium crystal can be used as nuclear detectors. They may have better temperature stability, or they may be less sensitive to the presence of impurities than lithium-drifted nuclear detectors.

21. RESEARCH PLANS FOR CALENDAR YEAR 1968

Gabor A. Somorjai

Studies of the interaction of velocity-selected molecular beams of gases (O_2, CO, CH_3, etc.) with metal single-crystal surfaces will be initiated. These investigations will be a part of our continuing research effort to explore the elementary steps of chemical surface reactions. The energy distribution of inelastically scattered electrons will be studied to verify the nature of the electron-surface atom interactions.

Vaporization-kinetics studies will be made of noncongruently vaporizing solids.

Investigations of the mechanism of photodecomposition of different solids will be initiated.

22. 1967 PUBLICATIONS

Gabor A. Somorjai and Associates

Technical Journals

1. H. B. Lyon and G. A. Somorjai, Low-Energy Electron-Diffraction Study of the Clean (100), (111), and (110) Faces of Platinum, J. Chem. Phys. 46, 2539 (1967).
2. H. B. Lyon, A. M. Mattera, and G. A. Somorjai, Low-Energy Electron-Diffraction Study of Face-Centered-Cubic Metals, in Proc. International Conference on Fundamentals of Gas-Surface Interaction, 1967 (Academic Press, New York, 1967).
3. A. M. Mattera, R. M. Goodman, and G. A. Somorjai, Low-Energy Electron-Diffraction Study of the (100) Face of Silver, Gold, and Palladium, Surface Sci. 7, 26 (1967).
4. G. A. Somorjai, Note on the Anomalous Surface Structures of Gold, Surface Sci. 8, 98 (1967).
5. G. A. Somorjai and J. E. Lester, Evaporation Mechanism of Solids, in Progress in Solid State Chemistry, Vol. 4 (Pergamon Press, New York, 1967), Chapter 2.
6. G. A. Somorjai, Small Angle X-Ray Scattering and Low Energy Electron Diffraction Studies of Catalyst Surfaces in X-Ray and Electron Methods of Analysis, (Plenum Press, 1968), p. 101.

UCRL Reports

1. A. Chutjian and G. A. Somorjai, Structure Analysis of Low-Energy Electron-Diffraction Patterns Using an Optical Analog, UCRL-17126, January 1967.
2. R. M. Goodman, H. H. Farrell, and G. A. Somorjai, The Mean Displacement of Surface Atoms in Palladium and Lead Single Crystals, UCRL-17837, September 1967.
3. R. M. Goodman, H. H. Farrell, and G. A. Somorjai, The Properties of the Specular Low-Energy Electron Beam Scattered by Face-Centered-Cubic Metal Single-Crystal Surfaces, UCRL-17983, December 1967.
4. D. A. Jenkins, A Technique for Drifting Lithium into Germanium, UCRL-17317, Jan. 1967.
5. J. E. Lester, Kinetics of Vaporization of Sodium Chloride (Ph.D. Thesis), UCRL-17794, November 1967.
6. J. E. Lester and G. A. Somorjai, The Effect of Dislocations on the Vaporization Rate of NaCl Single Crystals, UCRL-18014, December 1967.
7. H. B. Lyon, Jr., Low-Energy Electron-Diffraction Study of Low-Index Platinum Single Crystal Surfaces (Ph.D. Thesis), UCRL-17549, June 1967.
8. J. M. Morabito and G. A. Somorjai, Low-Energy Electron-Diffraction, The Technique and its Application to Metallurgical Science, UCRL-17942, November 1967.
9. G. A. Somorjai, Surface Chemistry, UCRL-18018, December 1967.
10. G. A. Somorjai, High-Temperature Vaporization Mechanisms, UCRL-17628, June 1967.

D. ELECTROCHEMISTRY

1. OPTICAL STUDIES OF INTERFACIAL PHENOMENA

Rolf H. Muller and Rolf F. Steiger

Ellipsometry of metal-gas interfaces has been conducted as a first step toward interpretation of the more complex optical behavior of metal-electrolyte interfaces. Adsorption experiments on optically polished 316 stainless steel surfaces, carried out with many nitrogen-diluted vapors at atmospheric pressure, confirmed the sensitivity of the technique to partial monolayer coverages. An example of such measurements is given in Fig. ID.1-1. The ellipsometer measurements also showed variations between film-free metal surfaces after seemingly identical treatments. Ultrahigh vacuum techniques are expected to remove this uncertainty.

Extensive modification of a commercial ellipsometer has been completed. The resulting instrument, shown in Fig. ID.1-2, provides more space for the specimen under study and allows its vertical displacement by a motor-driven spindle. The new base plate makes it possible to combine several different light sources with both ends of the ellipsometer and, thus, to convert easily from linear to elliptic polarization incident on the specimen. The use of a synchronous light chopper in conjunction with a phase-sensitive detector has greatly alleviated the previously experienced noise problems with the extremely low photomultiplier signals, which must be measured near optical extinction.

Theoretical studies on the technique of ellipsometry have shown the necessity to differentiate sixteen, rather than the previously employed four, "zones" for the unambiguous derivation of relative phase Δ and amplitude $\tan\psi$ from ellipsometer readings. A previously unexplained disagreement in phase between measurements and computations has been traced to arbitrary choices in coordinate systems. A graphical prediction of relative phase and

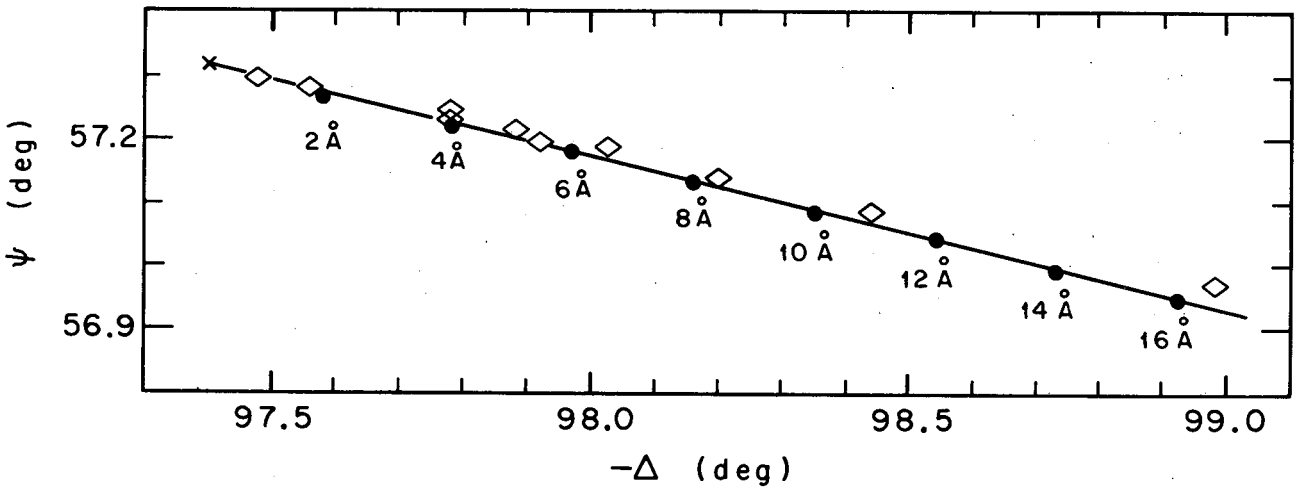

XBL682-1874

Fig. ID.1-1. Adsorption of n-propanol on 316 stainless steel. Ellipsometer measurement of relative amplitude attentuation $\tan\psi$ and phase difference Δ between components polarized parallel and normal to the plane of incidence. × measured bare surface; ◇ measured film-covered surface with 10% increments in vapor partial pressure; ● computed ψ and Δ values for 2-Å increments in film thickness, using measured bare-surface data and film refractive index 1.385.

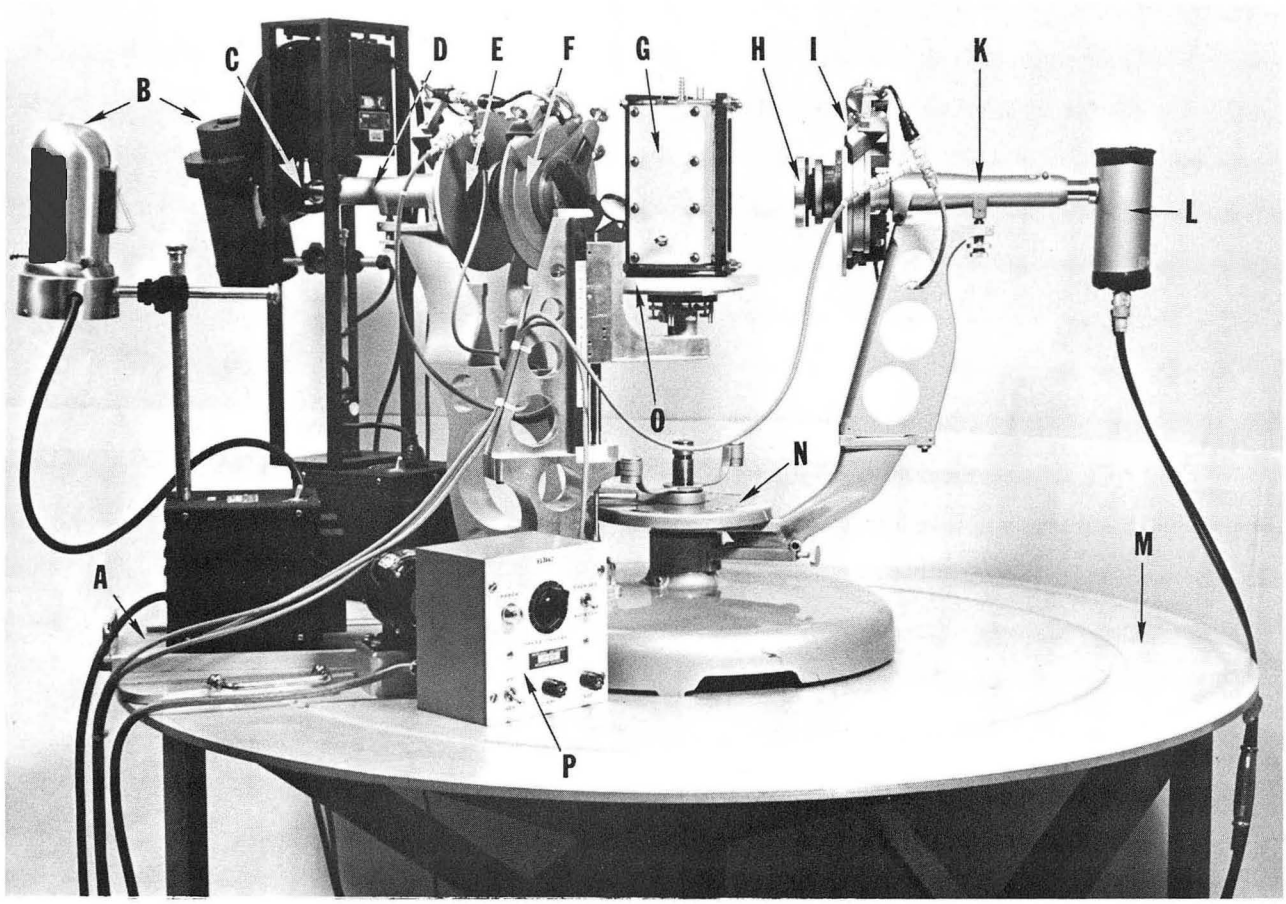

XBB 682-860

Fig. ID.1-2. Modified ellipsometer, elliptic polarization incident. (A) movable carriage for light sources, (B) exchangeable monochromatic light sources, (C) light chopper and generator of reference signal for phase-sensitive detector, (D) collimator tube with pinhole entrance, (E) polarizer circle with illuminated scale, (G) cell with specimen surface, (H) iris diaphragm for control of observed specimen area, (I) polarizer circle with illuminated scale, (K) telescope tube with pinhole exit, (L) photomultiplier, (M) base plate for exchange of light sources and conversion to linear polarization incident, (N) angle of incidence circle, (O) specimen table with vertical movement, and (P) motor drive control unit for specimen table.

amplitude for reflection from a thin transparent film on a metal substrate has been found to closely approximate exact computer-generated solutions. The model used provides also a good physical insight into the fundamental factors of ellipsometry.

Measurements on the effect of cell windows on ellipsometer results have shown that a cell containing the surface under study must be constructed such that its windows are penetrated by the light beam at right angles. Alignment errors of ±1° then affect ψ and Δ by less than 0.01°. Computational correction for the effect of the windows otherwise requires a much more precise knowledge of the angle of incidence, typically to ±0.03°.

The combination of ellipsometry and low-energy electron diffraction has been initialed for the study of gas adsorption and surface-reaction phenomena.* The two techniques complement each other, since one is sensitive to surface coverage, the other to surface structure.

The ultrahigh vacuum attainable in the equipment also allows the determination of optical constants of atomically clean single-crystal metal surfaces at different temperatures. Strain-free, plano-parallel windows have been mounted on an existing low-energy electron-diffraction apparatus, and a new base plate for the ellipsometer optical components has been built which allows their rapid and reproducible connection and disconnection with the diffraction system required for bakeout of the latter. First observations have demonstrated the feasibility of the measurements and pointed out the necessity to develop treatments of the single-crystal surfaces which maintain optical flatness while exposing the undisturbed lattice structure.

* In cooperation with Professor G. Somorjai.

2. SURFACE CALORIMETRY

Rolf H. Muller and Ramesh C. Gupta

Techniques have been developed for the measurement of thermal effects associated with adsorption and electrochemical reactions at plane interfaces.

Several thermopiles with up to 27 junctions located immediately below a metal-covered 3-cm^2 surface of a cube of epoxy resin were constructed (see Fig. ID.2-1). Performance tests for different time functions of energy release were conducted by resistive heating of the metal surface. The signals obtained agreed to within 20% with expected results derived from a new theoretical treatment of time-dependent heat release, for which a computer program has been written. The use of measured, rather than literature, values for the thermal properties of the materials employed is expected to yield still better agreement. The detection limit for short-term heat releases of 26 ergs/cm^2 (8×10^{-7} cal/cm^2) achieved to date is due to noise, which is still several times higher than that expected from the characteristics of the circuit components.

Performance tests with pyroelectric temperatures probes of barium titanate ceramic are in progress. Noise and insulation losses in the electrostatic voltage measurement have been greatly reduced, but comparison with the theory derived earlier on the response of pyroelectric detectors in nonuniform-temperature fields is not yet possible.

A thermostat has been built to contain the surface-calorimetry experiments and provide a constant reference temperature for the heat sink. The thermostat consists of four concentric copper cans separated by foamed styrene insulators. The temperature of the outer can is controlled by circulating water. This thermostat provides uniform temperatures with variations of less than 10^{-9}°C/min.

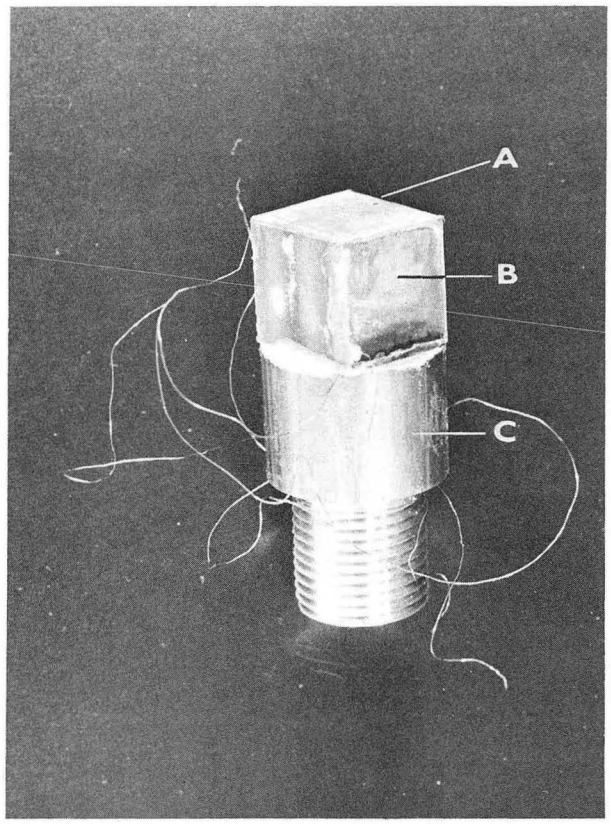

XBB 682-859

Fig. ID.2-1. Thermopile for measurement of heat effects at planar interfaces. (A) a 1.7- by 1.7-cm planar interface with 27 thermocouple junctions located 125μ below the surface and 200-Å-thick nichrome coating on top for resistive-heating tests, (B) thermopile body with 77μ-diam (chromel-constantan) thermocouple wires embedded in epoxy resin, (C) copper heat sink in thermal contact with reference junctions on bottom face of thermocouple body.

3. RESEARCH PLANS FOR CALENDAR YEAR 1968

Rolf H. Muller

Metal single-crystal surfaces shown by low-energy electron diffraction to be atomically clean will be characterized by reflection of

polarized light for determination of their complex refractive index at different temperatures. Gas adsorption on such surfaces will be studied by ellipsometry in conjunction with mass spectrometry.

The optical effect of birefringent films on the reflection of polarized light, to be expected from adsorbed oriented molecules, will be treated theoretically and results compared with suitable measurements.

The sensitivity of multiple-thermocouple temperature probes for surface calorimetry is hoped to be further improved by use of substrates with lower thermal conductivity and couples of higher thermoelectric constants. Techniques for the vapor deposition of such materials which have shown promise will be perfected. The response of pyroelectric crystals to time-dependent heat release on one of their surfaces will be compared to the theoretical model for their behavior. Measurement of heats of immersion at controlled potential will be initiated.

The surface of metals after anodic dissolution at high rate will be examined by optical and electron microscopy to define the structural factors important for the dissolution process.

The traveling-laser interferometer will be used for the microscopic description of local heterogeneous mass-transfer conditions.

4. 1967 PUBLICATIONS

Rolf H. Muller and Associates

Journal Articles

1. R. H. Muller, Optical Studies of Electrolyte Films on Gas Electrodes, J. Electrochem. Soc. 114, 651 (1967).
2. M. M. Sharma and R. K. Gupta, Mass Transfer Characteristics of Plate Columns Without Downcomer, Trans. Inst. Chem. Engrs. 45, T169-T 175 (1967).

UCRL Reports

1. R. H. Muller, Choice of Coordinate System in Ellipsometry, UCRL-17841, Sept. 1967.
2. R. H. Muller and J. R. Mowat, Reflection of Polarized Light from Film Covered Surfaces, UCRL-17128, Feb. 1967.

5. FUNDAMENTAL STUDIES OF IONIC MASS TRANSFER

a. Travelling-Laser Interferometer for Mass-Transfer Studies

Kirk W. Beach, Rolf H. Muller, and Charles W. Tobias

A modified Mach-Zehnder laser interferometer with an electrochemical flow cell for the study of mass-transfer boundary layers under forced and free convection has been constructed. Alignment of the optical elements has confirmed the expected advantages of the present design. Observation of the concentration profiles in mass transfer boundary layers during copper deposition from copper sulfate solutions has been initiated.

Spurious diffraction patterns, a common problem with laser illumination, due to scattering from optical imperfections such as dust particles, have been greatly reduced by careful cleaning of all optical components and introduction of a spatial filter immediately preceding the film plane.

The effect of light deflection, due to refractive-index gradients, on the resulting fringes is being evaluated theoretically. This will allow correction of errors in the apparent boundary-layer thickness.

A holographic technique is being studied for possible observation of three-dimensional, natural convection cells[1] which appear above a horizontal cathode.

1. R. G. Hickman and C. W. Tobias, Ionic Mass Transport by Combined Free and Forced Convection, Z. Phys. Chem. (Leipzig) 229, 145-166 (1965).

b. Current and Potential Distribution in Convective Mass Transfer at Plane-Plate Electrodes

J. Robert Selman and Charles W. Tobias

Preparations were made for a systematic exploration of unsteady-state effects and deposit-roughness effects on the shape of limiting current curves. In part the study will use rotating disks of Cu in $CuSO_4$-H_2SO_4-H_2O solution and of Ni in $K_3Fe(CN)_6$-$K_4Fe(CN)_6$-KOH-H_2O solution; potential-current-time curves

are now being recorded for various rates of galvanostatic current increase. In a second stage, mass-transfer between parallel plates will be used, and sectional currents will be measured.

To improve the flow and current capacity of the parallel-plate channel circuit used so far a design study was made. A particular aim was to include the practically important region of highly turbulent mass-transfer in the exploration of limiting current curves, as well as a design suitable for study of very high current densities. The new design aims at realizing Reynolds numbers of 125,000. The present circuit is now being adapted for gravity-flow, as a transition before the new design is carried out.

To improve the ease with which sectional currents and potentials, as well as time-logged data, can be treated, a magnetic-tape recording system has been added to the digital data-logging equipment. A general-purpose program for tabulating, plotting, and cross-plotting sectional data is now available. The determination of physical properties of the $CuSO_4$-H_2SO_4-H_2O system was continued, with special emphasis on accurate determination of solution composition. Density, viscosity, and refractive index were measured for 0.05M and 0.1M $CuSO_4$ solutions over a wide range of sulfuric acid concentration.

c. Supersaturation During Electrolytic Gas Evolution

Charles Bon and Charles W. Tobias

Prior theoretical studies of electrolytic bubble growth had indicated that the rate of bubble growth is controlled by mass transfer of dissolved gas to the growing bubble.[1] The solution near a gas-evolving electrode may therefore be expected to be highly supersaturated with gas. An experimental study was performed aimed at measuring the concentration of dissolved hydrogen near the electrode surface during electrolytic hydrogen evolution. A cell was built which contained measuring electrodes reversible to hydrogen at accurately known distances from the platinum cathode. This was accomplished by embedding platinum foils into the cell walls in such a way that their edge was exposed to the electrolyte. The measuring electrode closest to the working electrode was a distance of 0.001 in. During an experiment, potentials of the measuring electrodes with respect to the cathode were measured simultaneously by using a high-impedance multichannel digital voltmeter.

Typical concentration profiles which illustrate the high degree of supersaturation found especially at high current densities are shown in Fig. ID.5-1. From measured concentration profiles the hydrogen flux at the electrode was determined and compared to the flux calculated from Faraday's law. Good agreement between the results was obtained, as illustrated in Table ID.5-I.

Table ID.5-I. Comparison between measured and calculated hydrogen flux at electrode.

Current Density	Hydrogen flux calculated from Faraday's law	Hydrogen flux determined from measured concentration gradient (Fig. ID.5-1)
(mA/cm^2)	($moles/cm^2$-sec)	($moles/cm^2$-sec)
39.5	2.04×10^{-7}	2.56×10^{-7}
3.95	2.04×10^{-8}	2.26×10^{-8}
0.395	2.04×10^{-9}	2.42×10^{-9}

Surface-renewal theory was used to predict the hydrogen concentration at the cathode surface. The theory correctly predicts the observed square-root dependence of the surface concentration on the current density. The calculated absolute values lie somewhat below the measured values, the discrepancy probably being due to impeded bubble nucleation. Even without specifically taking into account nucleation of bubbles, surface-renewal theory gives an adequate description of expected mass transfer rates during electrolytic gas evolution.

1. H. Cheh and C. W. Tobias, On the Dynamics of Hemispherical Phase Growth in Nonuniform Temperature Fields, UCRL-17415, March 1967; Mass Transfer to Spherical Drops or Bubbles at High Re, UCRL-17424, March 1967; On the Dynamics of Hemispherical Phase Growth in Nonuniform Concentration Fields, UCRL-17439, March 1967.

6. DYNAMICS OF POROUS ELECTRODES

a. Reaction Distribution in Flooded Porous Electrodes

Richard Alkire, Edward A. Grens II, and Charles W. Tobias

Experimental determination of reaction distributions in flooded porous electrodes is necessary to test the validity of the proposed mathematical models for such electrodes and as a method of evaluation of electrode kinetic parameters at the internal surface of porous matrices. No such measurements are available

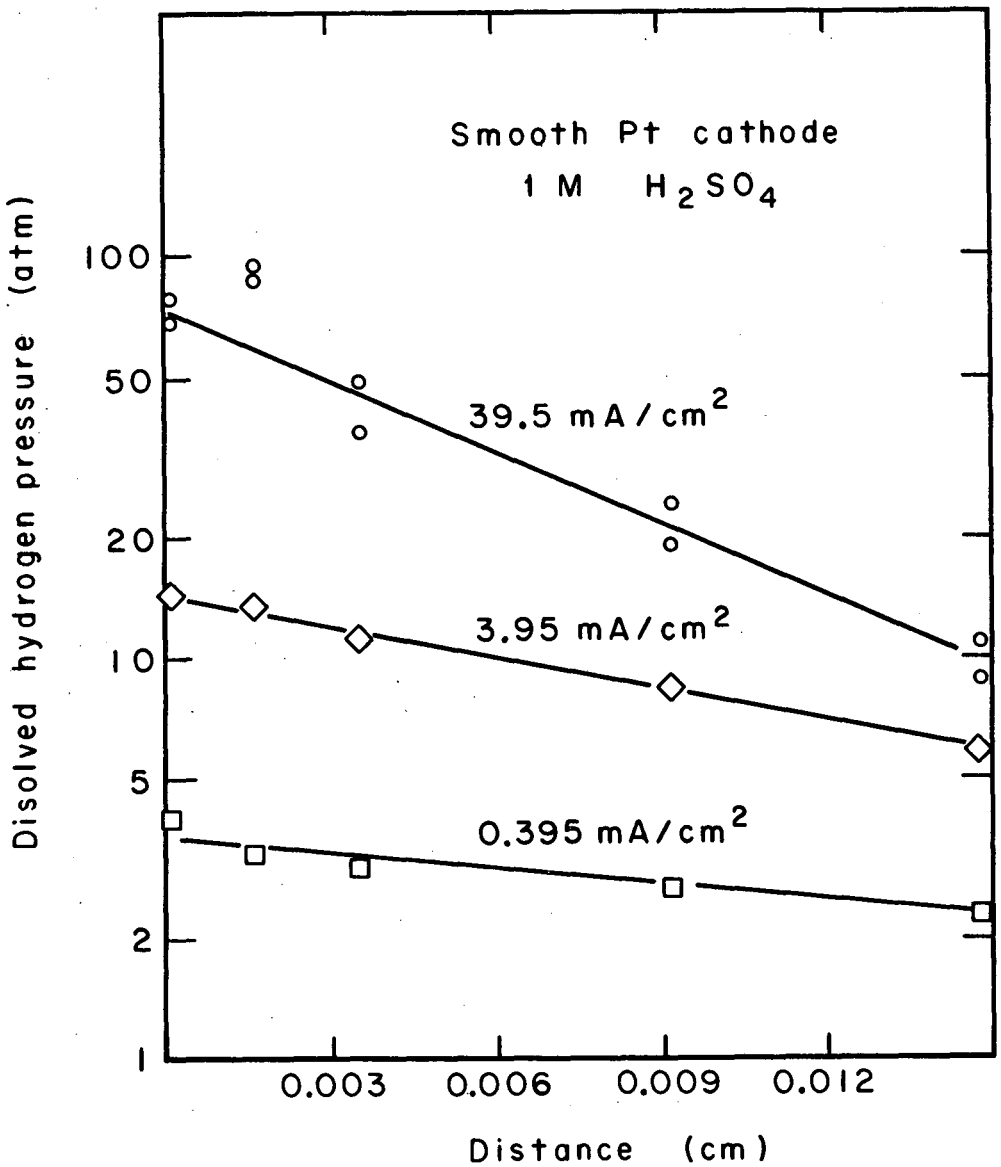

XBL682-1875

Fig. ID.5-1. Measured concentration profiles of dissolved hydrogen versus distance from electrode.

because of difficulties involved in simulating porous electrode behavior.

A new technique is being developed for measuring the reaction distribution within flooded porous electrodes without sectioning or otherwise altering the electrodes before and during operation. This method consists of dissolving a porous metal anode to such an extent that the porosity of the matrix changes from its original value. The resulting change in porosity distribution is equivalent to the time-average current distribution during dissolution. A post-electrolysis examination is then conducted by impregnating the reacted electrode with epoxy resin, sectioning, taking photomicrographs, and measuring porosity as a function of distance from the external surface.[1]

Porous electrodes of extremely uniform porosity and well-known geometry have been

fabricated by winding a coil of small-diameter wire in hexagonal array, sintering, and cutting electrodes from the fused mass. The void spaces between the wires constitute the pores. Suitable sintering conditions were determined from the results of thirteen preliminary tests. The coil was wound by a specially designed semi-automatic device used in conjunction with a variable-speed lathe. The porosity of the electrodes is 5.32±0.27% (see Fig. ID.6-1).

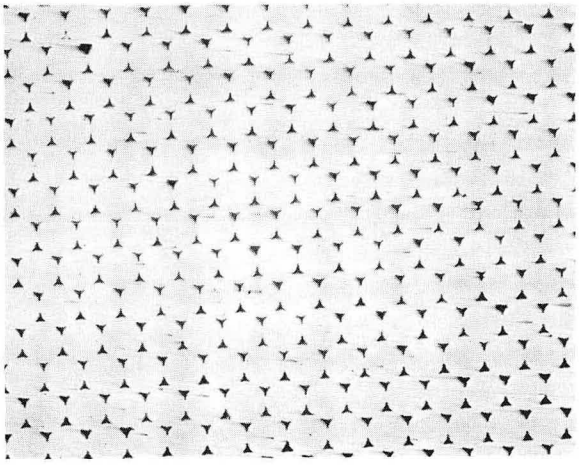

XBB 682-858

Fig. ID.6-1. Copper electrode of defined porosity.

Present theories describe only events within the pore and do not consider behavior of the external (visible) surface of the electrode. Therefore we have masked the external surface from electrochemical reaction by vapor-depositing a platinum layer 800Å thick. The deposition was carried out at a low angle, so that Pt did not enter the pores and mask the internal surface.

The existing theoretical framework established by earlier work in our group[2] is being extended. The reaction distribution within porous electrodes is calculated as a function of time in the pseudo-steady state, with allowance for the changing porosity of the matrix and for the convective flow due to volumetric expansion during dissolution.

1. R. Alkire, Reaction Distribution in a Porous Anode (M.S. Thesis), UCRL-16114, June 1965.
2. J. S. Newman and C. W. Tobias, J. Electrochem. Soc. 109, 1183 (1962); E. A. Grens II and C. W. Tobias, Ber. Bunsenges. Phys. Chem. 68, 236 (1964).

b. The Effect of Periodic Meniscus Displacements on the Performance of Porous Gas Electrodes*

Jean-Pierre Roussillon and Edward A. Grens II

The influence of periodic movement of the gas-electrolyte interface in a film-type porous gas electrode was studied experimentally for the oxygen cathode in 2N potassium hydroxide electrolyte. A single silver capillary tube of 150μ i.d. was used as a cathode. The interface motion was obtained by displacement of the electrolyte in a closed compartment by a small piston driven mechanically at a controlled frequency and amplitude. Response of the cathode potential relative to the mercury-mercuric oxide reference electrode was measured under galvanostatic conditions. The results obtained could not be quantitatively interpreted because of the deviation of conditions in the capillary electrode from design conditions. These included the resistance of extraneous ionic current paths and local variations in electrode kinetic behavior along the pore wall. Nevertheless, qualitative effects of the meniscus movement were observed; they were characterized by a periodic response of the cathode potential of a few millivolts amplitude. These effects indicate a decrease in overpotential during the advance of the meniscus toward the gas-filled portion of the capillary, and an increase during motion in the opposite direction, as might be expected on the basis of film-electrode models.

* Abstract of UCRL-17594, August 1967.

7. ELECTROCHEMISTRY IN NONAQUEOUS SOLVENTS

a. Viscosity of Concentrated Solutions of Calcium in Liquid Ammonia in the Temperature Interval -40 to -70°C

Jonathan P. Earhart and Charles W. Tobias

The viscosity of concentrated solutions of calcium in liquid ammonia was determined in the concentration interval from 3.4 to 8.9 mole-% calcium at temperatures from -40 to -70°C. The modified cross-arm viscometer used for the measurements was calibrated at each of the temperatures at which measurements were made. A minor surface-tension correction was made using the surface tension of sodium-ammonia solutions in the absence of such data for calcium-ammonia solutions. An analysis of possible errors indicates that the results are accurate to ±5%.

The viscosity of concentrated solutions at concentrations near the two-phase region (about 40% of saturation) is nearly equal to the viscosity of pure liquid ammonia at the same temperature. At -40°C a solution with a concentration of 8.9 mole-% calcium (83% of saturation) has a viscosity more than twice that of the pure solvent. Similar increases in viscosity with increasing concentration were found at all temperatures between -40 and -70°C (Fig. ID.7-1). This is the opposite of the effect in sodium- and potassium-ammonia solutions where the viscosity decreases with increasing concentration. A possible explanation for these results may lie in the increased degree of order in calcium-ammonia solutions.

b. Thallium-Thallous Halide Reference Electrodes in Propylene Carbonate

Friedrich G. K. Baucke and Charles W. Tobias

A search has been continued[1] for a reference electrode of the second kind in propylene carbonate (PC) solutions. The electrodes

Tl(Hg)/TlCl(sat'd), LiCl(10^{-3}M),

Tl(Hg)/TlBr(sat'd), LiBr(0.1M),

and

Tl(Hg)/TlI(sat'd), KI(0.1M),

with thallium concentrations of the amalgam

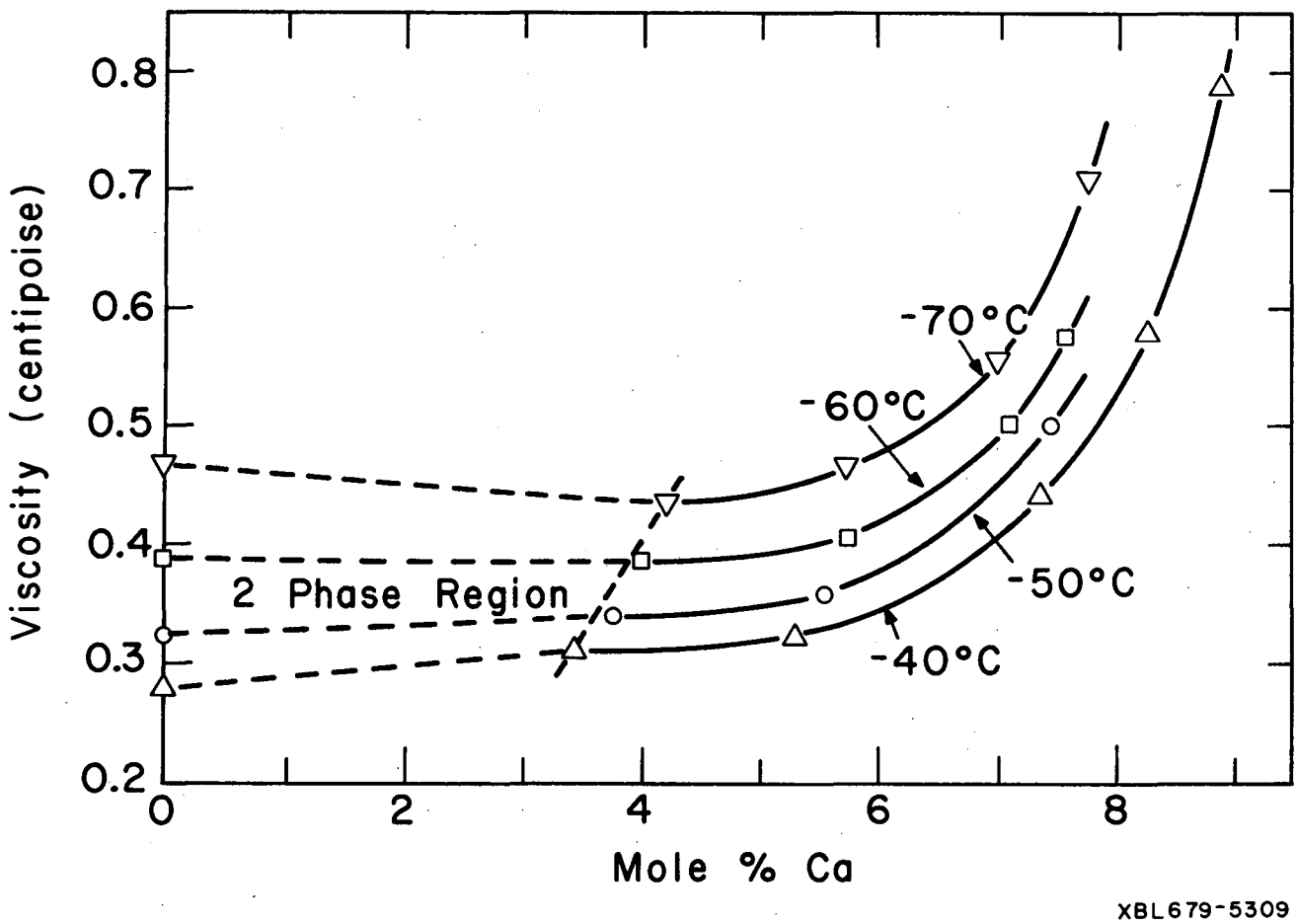

Fig. ID.7-1. Viscosity of calcium-ammonia solutions.

ranging from 1 to 20 at.-%, and the electrode

$$Tl/TlCl(sat'd),\ LiCl(10^{-3}M),$$

with electrolytically formed thallous chloride have been studied at 30°C and were found to be well suited:

1. Bias potentials of amalgam electrodes were below 0.5 mV; those of thallium electrodes were below 0.1 mV over the test period of six months.
2. Polarization measurements up to current densities of 10^{-6} A/cm^2 showed linear dependence of the overpotentials on currents without hysteresis. The approximate effective exchange current density of the amalgam electrode with 9 at.-% thallium and thallour chloride as sparingly soluble electrolyte was found to be on the order of 2 to 5×10^{-5} A/cm^2.
3. Electromotive forces of amalgam concentration cells including solid thallium electrodes agreed within 0.1 mV with values of such electrodes in aqueous thallous sulfate given by Richards and Daniels.[2]

The solubilities of thallous chloride, bromide, and iodide were found to be of the order of 1 to 5×10^{-6} moles/l.

1. F. G. K. Baucke and C. W. Tobias, IMRD Annual Report 1966, UCRL-17330, March 1967, pp. 42-43.
2. T. W. Richards and F. Daniels, J. Am. Chem. Soc. 41, 1732 (1919).

c. Rotating-Disk System for Metal Deposition from Nonaqueous Solvents

Friedrich G. K. Baucke, Dieter Landolt, and Charles W. Tobias

Meaningful study of the deposition of active metals from nonaqueous solvents requires the use of highly purified solvents and careful exclusion of oxygen and water. A knowledge of prevailing mass-transfer conditions during the deposition process is desirable, because of the usually low solubility of the dissolved salts and because of the strong influence of mass transfer on the structure of the obtained deposits. Hydrodynamics and mass-transfer characteristics of the rotating-disk electrode system are well understood theoretically. An experimental setup was designed to be used in metal deposition studies under inert-atmosphere conditions (Fig. ID.7-2). The setup consisted mainly of two parts -- a rigidly mounted drive and a detachable cell unit. The drive unit contained a feedback-regulated dc motor and a mercury contact unit providing electrical contact to the rotating axle. The electrochemical cell was constructed in a way that during experiments the electrolyte was separated from the atmosphere by an antichamber through which argon flowed continuously. Filling of the cell with solvent and all handling of chemicals was done in a dry box. During transport of the cell between dry box and drive unit, it was sealed hermetically by means of a specially designed seal involving a slight raising or lowering of the rotation axle. Stainless steel electrodes embedded in teflon and screwed onto the axle were used as working electrodes. Electrode potentials were measured against a reference electrode of the second kind. Preliminary experiments directed towards the deposition of potassium and calcium from propylene carbonate were carried out in the system.

8. ELECTROLYSIS AT EXTREMELY HIGH CURRENT DENSITIES

a. Stoichiometry of Copper Dissolution at High Current Densities

Kimio Kinoshita, Dieter Landolt, Rolf H. Muller, and Charles W. Tobias

The stoichiometry of electrochemical copper dissolution in various electrolytes was investigated both in a flow-channel apparatus under forced convention conditions and in a H cell under natural convection.

The results of anodic weight-loss determinations in the forced convection system showed a marked influence of flow rate, current density, and electrolyte compositions on the apparent valence of the dissolved product. It was shown that the change in the apparent valence coincided with a stepwise increase in cell voltage when plotted as a function of current density. The behavior is illustrated for the Cu/KNO_3 system in Fig. ID.8-1. In view of results obtained independently from potential measurements and from optical observations it must be concluded that the observed change in apparent valence is related to the formation of an anodic layer. In order to substantiate results obtained by weight loss determinations, dissolution experiments were carried out in a stagnant solution of 3N KCl in an H-cell. After passage of a given amount of charge under constant current conditions the electrolyte solution was analyzed chemically for Cu^+ and Cu^{++}.

Cu^+ was determined by adding Fe^{3+} to an aliquot and then titrating the Fe^{2+} obtained

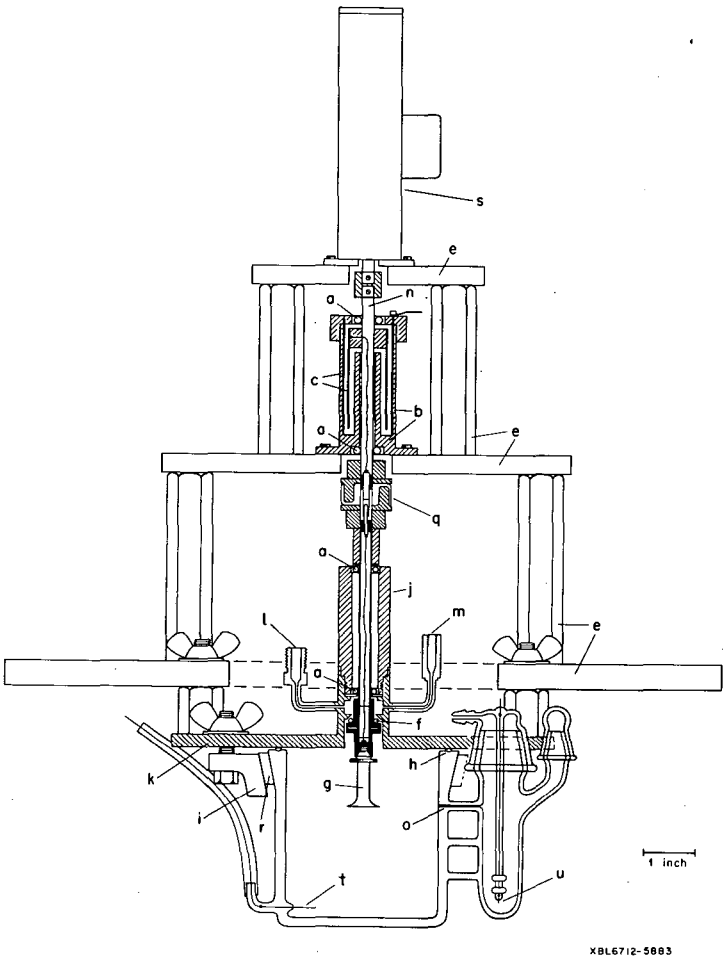

Fig. ID.7-2. Rotating-disk electrode for metal deposition from nonaqueous solvents.

by Cu^{+} oxidation with Ce^{4+}. The total amount of copper in the solution was determined in another aliquot by first oxidizing all Cu^{+} to Cu^{2+} with Na_2O_2 and then titrating the Cu^{2+} using the conventional iodine-thiosulfate method. In addition to analyzing the solution, the weight loss of the anode was determined in each experiment. The results obtained by the two independent methods for determining the valence of the dissolution products showed excellent agreement. This would indicate that in the experiments performed under natural convection conditions in the Cu/KCl system, no oxygen was liberated at the anode, i.e., the only anodic reaction was the dissolution of copper to Cu^{+} and Cu^{2+}.

b. Electrode Potentials and Surface Characteristics in High-Current-Density Copper Dissolution

Dieter Landolt, Kimio Kinoshita, Rolf Muller, and Charles W. Tobias

An analysis of published literature data on electrochemical machining (ECM) had indicated that under most conditions employed technically ohmic losses in the electrolyte account for most of the observed overall cell voltage. Electrode potentials seemed to be of the same order of magnitude as those observed in low-current electrolysis. The exact measurements of electrode potentials is difficult,

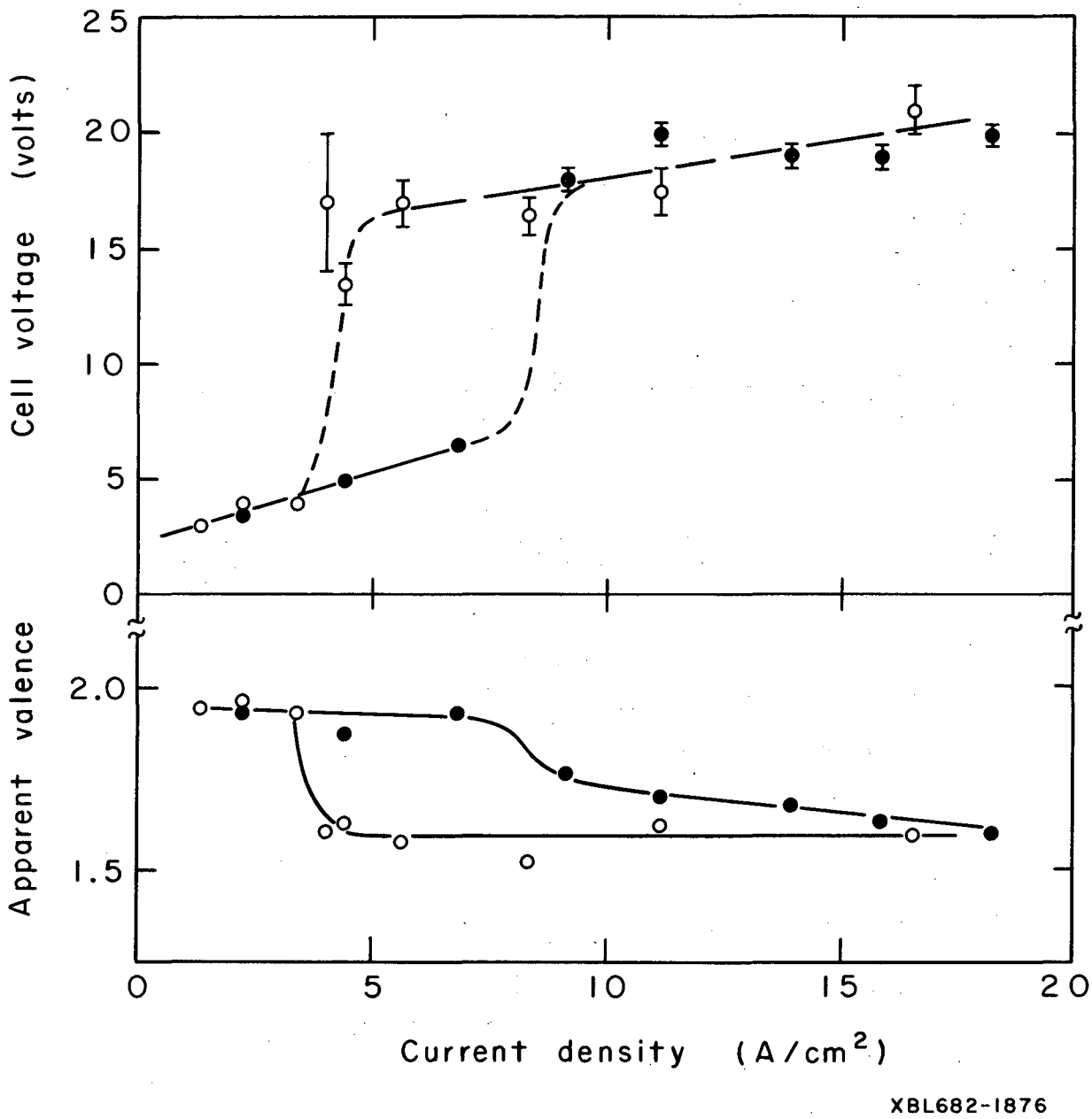

Fig. ID.8-1. Variation of apparent valence and of cell voltage with current density during anodic copper dissolution in 2N KNO_3. ● Flowrate 200 cm/sec, 0 Flowrate 30 cm/sec.

however, because of the large IR drops involved and because of the rapidly dissolving anode.

An experimental investigation of the potential current behavior of copper dissolution in potassium nitrate solution at extremely high current density was initiated. A flow channel cell of 0.5-mm gap width contained mechanically polished copper electrodes (99.999% purity) of 0.0167-cm^2 surface area embedded in epoxy. Constant current steps of definite length corresponding to the dissolution of approximately 10 μ were applied, using a mercury-relay switching circuit. The time behavior of cell voltage and electrode potentials was followed by means of an oscillograph having a time resolution of approximately 1 msec (Fig. ID.8-2). Current densities applied ranged up to 150 A/cm^2 at linear flow rates of up to 2500 cm/sec. After each run the electrode surfaces were studied under a microscope.

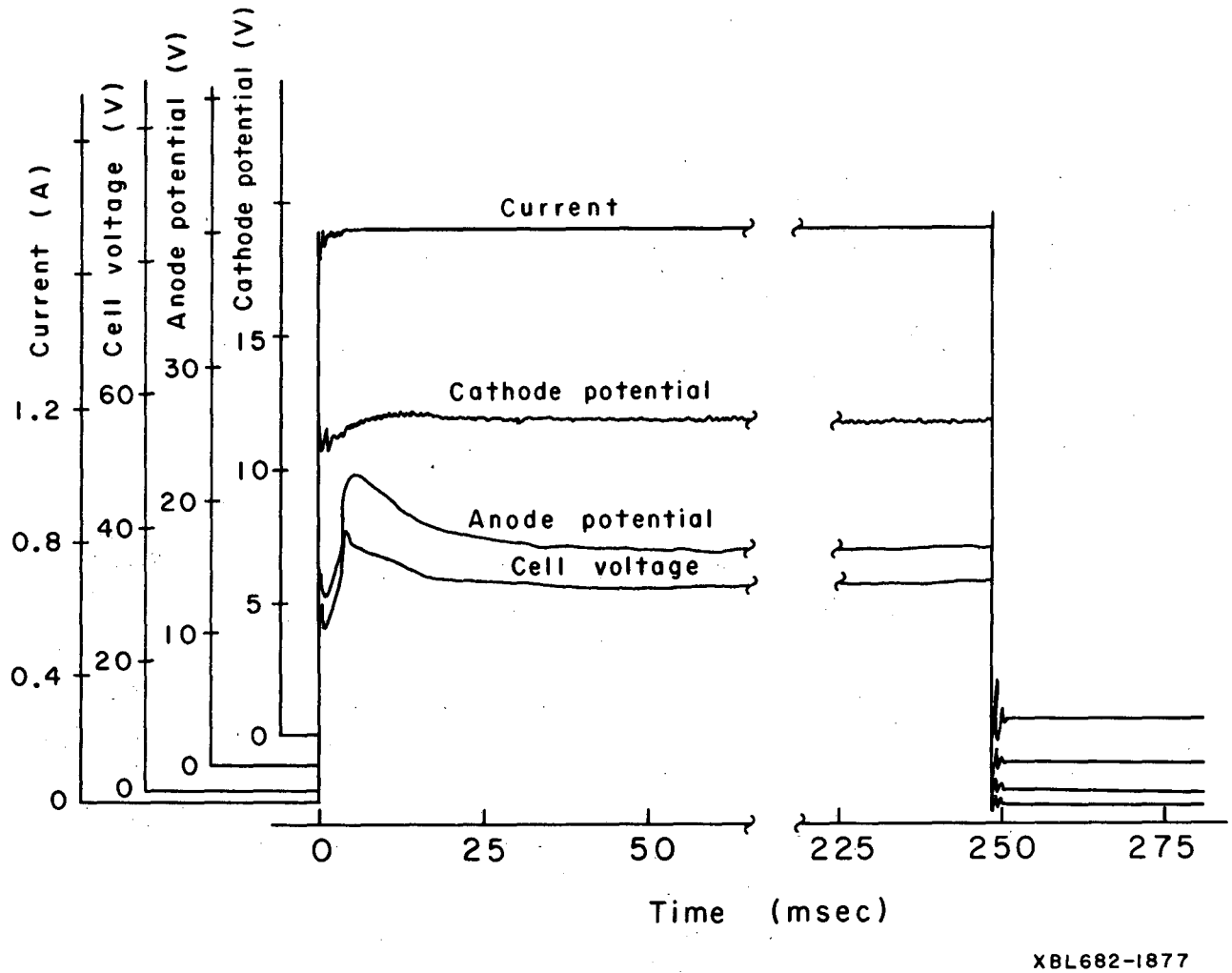

Fig. ID.8-2. Potential vs time behavior during copper dissolution in 2N KNO_3 at constant current. Current density: 100 A/cm^2; flow rate: 1000 cm/sec.

The results obtained show that under certain conditions a steep rise of the anode potential in the order of 10 V occurs, which has to be attributed to the formation of an anodic layer. The onset of this passivation effect is strongly dependent on flow rate and current density, thus indicating an influence of prevailing mass-transfer conditions.

Figure ID.8.2 illustrates a further characteristic of the potential time behavior observed in the "passive" region, especially at high current densities. After an initial rise the anode potential, and hence the cell voltage, drops again, reaching a value somewhere between the original step value and the peak value. This overshooting effect indicates a change of the initial structure of the anode layer, which might possibly be due to thermal effects. The decay of the anode potential after the current was switched off was too rapid to allow subtraction of ohmic contributions from the overall anode potential decay curve. Further studies of decay curves using oscilloscopic

techniques are planned.

The appearance of the anode surfaces after dissolution was different for the two potential regions discussed. Etching was observed in the absence of the passivation effect, while pitting, preferentially along grain boundaries, occurred in the "passive" region at high anode potential (Fig. ID.8-3). Studies have been initiated for studying the mechanism of pit formation by means of electron-microscope replica techniques.

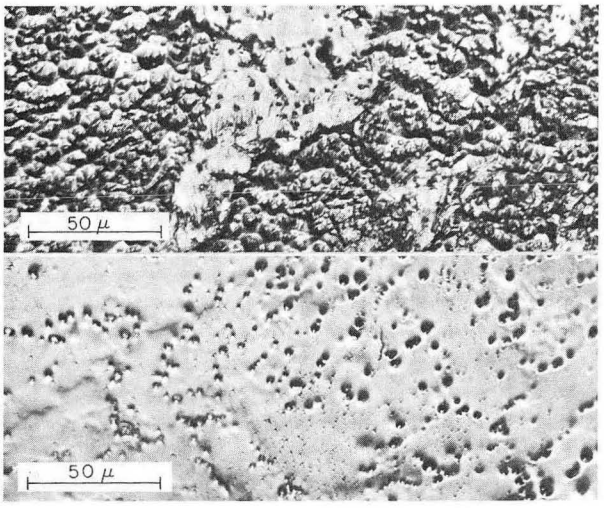

XBB 682-857

Fig. ID.8-3. Surface of copper anodes after passage of 23 coulomb/cm^2 at constant current density of 54 A/cm^2. Electrolyte flow rates were 400 cm/sec (pitted surface) and 1000 cm/sec (etched surface).

c. Optical Study of Cathodic Gas Evolution During High-Current-Density Electrolysis

Dieter Landolt, Kimio Kinoshita, Rolf H. Muller, and Charles W. Tobias

During electrochemical machining (ECM) large amounts of hydrogen are liberated at the cathode. Gas present between the electrodes may affect the electrolysis conditions in several ways: 1) increased ohmic resistance of the electrolyte and possible change in current distribution on the electrodes, 2) changed hydrodynamic conditions due to two-phase flow, 3) possible initiation of gaseous discharge (sparking), e.g., associated with a contiguous gas blanket at the cathode.

An experimental study using high-speed stop-motion photography was initiated aimed at the determination of the size and distribution of hydrogen bubbles generated during high-current-density electrolysis. The study should also provide for the observation of possible solid dissolution products generated at the anode.

The experimental setup used was the same as described in Sec. b. A camera attached to a microscope objective was placed on one side of the electrolytic cell, a high-intensity microflash unit on the other. The flash unit allowed exposure times as short as 0.5 μsec, necessary to stop the motion of bubbles moving at speeds of several hundred cm/sec. The triggering of the flash unit was synchronized with the cell current switching circuit. This allowed pictures to be taken after passage of equal amounts of charge under all conditions. A telecentric aperture, optimized for maximum lens resolution and depth of field, was placed in the focal plane of the microscope objective. Exposure tests using various extremely sensitive films were performed. Preliminary photographs (Fig. ID.8-4) demonstrate the strong influence of flow rate and current density on size and distribution of the bubbles.

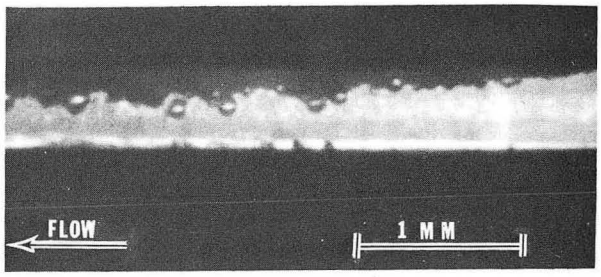

XBB 682-856

Fig. ID.8-4. Cathodically generated hydrogen bubbles. Current density: 50 A/cm^2; electrolyte flow rate: 200 cm/sec.

9. MECHANISM OF ELECTROPOLISHING

Kaoru Kojima and Charles W. Tobias

In the electropolishing of metals such as copper, steel, and nickel, phosphoric acid has been used extensively as a solvent. Experimental evidence has been presented in the literature that mass transfer plays an important role in establishing electropolishing conditions. An understanding of the role of mass transfer during anodic copper dissolution in phosphoric acid solutions requires not only the consideration of mass transfer of phosphoric acid but also that of copper phosphate (copper dissolution product) and water.

The limiting current for the dissolution process was calculated by using an "effective" binary diffusion equation[1]

$$N_i = -c\mathscr{D}_{im} \nabla X_i + X_i \sum_j N_j \qquad (1)$$

and

$$\sum_i J_i^* = 0, \qquad (2)$$

where i stands for phosphoric acid, copper phosphate, or water. The boundary conditions are: 1) at the anode surface the concentration of phosphoric acid is zero, and 2) the flux of copper phosphate is related to the flux of phosphoric acid by a defined stoichiometric relation. It was found that in concentrated acid solution, most of the concentration change occurs in a thinner layer adjacent to the anode than one would expect by calculating a corresponding diffusion-layer thickness for dilute solutions. This effect is due to an increase of viscosity of the solution in that layer which we call here the viscous-diffusion layer. The calculated limiting current for a rotating-disk electrode is shown by a solid curve in Fig. ID.9-1 and fits observed values[1] of limiting current within about 10% error (Fig. ID.9-1).

In dilute phosphoric acid solution, the effect of the viscous layer diminishes and the limiting current may be calculated by conventional methods.

For convenient estimation of the limiting current in concentrated phosphoric acid solutions, the following correlations were found to fit published literature data:

$$i = K(1.553)(2F)\mathscr{D}_{cum}^{2/3}\, \nu^{-1/6} n^{1/2} C_t$$ (for rotat-disk anode[1])

$$i = K(0.896)(2F)\mathscr{D}_{cum}^{2/3}\, \nu^{-1/6} V_\infty^{1/2} C_t$$ (for laminar flow between two parallel-plate electrodes[2])

$$i = K(2F) \cdot \frac{\mathscr{D}_{cum} C_t}{\delta_D}$$ (for capillary diffusion[3])

In the above expressions $\mathscr{D}_{cum}$ is the diffusion coefficient of copper phosphate in phosphoric acid-water solution, and C_t is the total concentration of phosphoric acid plus water. The value of K is 0.0318 for rotating disk, 0.0175 for laminar flow between two parallel-plate electrodes, and 0.0548 for anodic dissolution through a capillary tube.

1. Z. Zembura, Bull. Acad. Polonaise Sci. XI, 271 (1963).
2. T. P. Hoar and G. P. Rothwell, Electrochim. Acta 9, 135 (1964).
3. S. I. Krichma and K. F. Afendik, Dokl. Akad. Nauk. SSSR 159, 405 (1964).

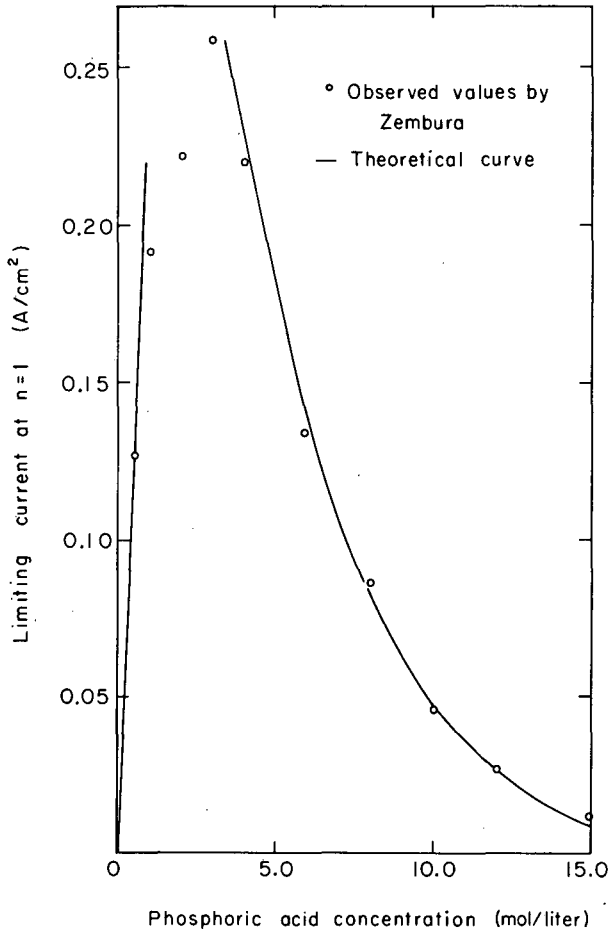

Fig. ID.9-1. Relation between limiting current at n = 1 RPS and the concentration of phosphoric acid at 25° C (rotating-disk anode).

10. RESEARCH PLANS FOR CALENDAR YEAR 1968

Charles W. Tobias

The double-beam laser interferometer using a laser as a light source will be used for the study of concentration gradients at electrode surfaces under forced-convection conditions.

The transient response of copper dissolution and deposition systems to potentiostatic and galvanostatic ramp functions will be investigated using a rotating-disk electrode. Studies will continue on the longitudinal distribution of current and potential on cathodes in a channel-type cell in laminar and turbulent flow.

Studies of the reaction distribution and overpotential behavior within pores by anodic dissolution of copper electrodes of uniform, well-defined porosity will be completed.

Exploration of the possibilities for the electroreduction of reactive metals in propylene carbonate and related solvents will be continued. Emphasis will be placed on the groups IVb, Vb, and VIb metals.

The investigation of the stoichiometry of copper dissolution at extremely high current density will be extended to include chemical analysis of gaseous and solid reaction products. Surface characteristics of dissolved electrodes and potential behavior will be investigated in various electrolytes. A method allowing potential transient measurements in the microsecond range will be developed. High-speed stop-motion photography will be applied to the study of the influence of cathodically generated hydrogen gas on the overall cell behavior during high-current density metal dissolution.

Paralleling our theoretical work on the mechanism of "smoothing" and electropolishing, experimental work will be initiated on copper anodes in phosphoric acid and in other electrolytes.

11. 1967 PUBLICATIONS

Charles W. Tobias and Associates

Technical Journals

1. H.Y. Cheh and C.W. Tobias, Dynamics of Hemispherical Phase Growth in Nonuniform Temperature Fields, Phys. Fluids 10, 2087 (1967).
2. R.E. Davis, G.L. Horvath, and C.W. Tobias, The Solubility and Diffusion Coefficient of Oxygen in Potassium Hydroxide Solutions, Electrochim. Acta 12, 287-297 (1967).
3. N. Ibl and D. Landolt, Zur Kinetik der Chlorat-Bildung bei der NaCl Elektrolyse, Chem. Ing. Technik 39, 706-712 (1967).
4. C.W. Tobias, Editor, Advances in Electrochemistry and Electrochemical Engineering, Vol. 5 (John Wiley and Sons, New York, 1967).

UCRL Reports

1. F.G.K. Baucke and C.W. Tobias, Thallium Amalgam-Thallous Halide Reference Electrodes in Propylene Carbonate, UCRL-17892, November 1967.
2. H. Y. Cheh, On the Mechanisms of Electrolytic Gas Evolution (Ph.D. Thesis), UCRL-17324, February 1967.
3. H. Cheh and C. W. Tobias, On the Dynamics of Hemispherical Phase Growth in Nonuniform Concentration Fields, UCRL-17439, March 1967.
4. H. Cheh and C. W. Tobias, Mass Transfer to Spherical Drops or Bubbles at High Re, UCRL-17424, March 1967.
5. H. Cheh and C. Tobias, On the Dynamics of Hemispherical Phase Growth in Nonuniform Temperature Fields, UCRL-17415, March 1967.
6. J. P. Earhart, The Viscosity of Concentrated Solutions of Calcium in Liquid Ammonia in the Temperature Interval of -40 to -70°C (M.S. Thesis), UCRL-17858, Oct. 1967.
7. N. Ibl and D. Landolt, On the Mechanism of Anodic Chlorate Formation in Dilute NaCl Solutions, UCRL-17461, November 1967.
8. R. N. O'Brien, The Rotating-Disc Electrode, Hydrodynamic Boundary and Diffusion Layers by Laser Interferometry, UCRL-17348-Rev., January 1967.
9. W. Smyrl and C. W. Tobias, The Effect of Diffusion of a Sparingly Soluble Salt on the EMF of a Cell without Transference, UCRL-17685, July 1967.
10. W. Smyrl and C. W. Tobias, Thermodynamic Properties of LiCl in Dimethyl Sulfoxide, UCRL-17686, July 1967.

12. TRANSPORT PROPERTIES OF CONCENTRATED ELECTROLYTIC SOLUTIONS

Thomas W. Chapman† and John Newman

The development of the optical-diffusion technique described in previous reports[1,2] has been completed, and the method has yielded diffusion coefficients for aqueous potassium chloride solutions within a few tenths of a percent of the well-established standard values. Subsequent measurements have provided the diffusivity of nitric acid in water at 25°C and concentrations up to 3M. No previous diffusion data for this system were available.

The literature for physical and transport property data of binary aqueous electrolytic solutions has been surveyed thoroughly. It was found that there are 32 cases for which complete transport property data are available for a system at a particular temperature and over a concentration range. In order to seek general correlations, we calculated from these experimental data more fundamental transport properties, which were referred to previously.[1] The behavior of the calculated properties is much more systematic than that of the measured quantities.

We interpret the behavior of the "ionic diffusion coefficients" defined by the general flux relations in terms of the effects of various ions on the structure of water. The value of this coefficient at high dilution is proportional to the limiting ionic equivalent conductance, and its variation at higher concentrations depends on the nature of both the particular ion and its counter ion. In general, ions which tend to disrupt the structure of water may be associated with maxima in ionic diffusion coefficients. With structure-making ions such maxima are usually not observed unless the counter ion is strongly structure breaking. The decrease of ionic diffusion coefficients at high concentrations does not correlate quantitatively with solution viscosity.

A complete description of the experimental method as well as the interpretation of the transport properties is given in a recent report.[3]

† Present address: Dept. of Chemical Engineering, University of Wisconsin, Madison, Wisc.

1. T. W. Chapman and J. Newman, Transport Properties of Concentrated Electrolytic Solutions, in Inorganic Materials Research Division Annual Report, 1965, UCRL-16658, February 1966, pp. 68-69.
2. T. W. Chapman and J. Newman, Transport Properties of Concentrated Electrolytic Solutions, in Inorganic Materials Research Division Annual Report, 1966, UCRL-17330, March 1967, p. 48.
3. T. W. Chapman, The Transport Properties of Concentrated Electrolytic Solutions, (Ph.D. Thesis), UCRL-17768, November 1967.

13. MOVING-BOUNDARY TRANSFERENCE NUMBERS

Paul Milios and John Newman

A rigorous expression relating the transference number to moving-boundary measurement data has been derived. The transference number of 0.213 M NH_4NO_3 was measured at 25°C.

The moving-boundary system is described by the following equations:
A material balance,

$$\frac{\partial c_i}{\partial t} = -\frac{\partial N_i}{\partial x} = -\frac{\partial c_i v_i}{\partial x}, \qquad (1)$$

a current equation,

$$i = F \Sigma z_i N_i , \qquad (2)$$

a statement of electroneutrality,

$$\Sigma z_i c_i = 0 , \qquad (3)$$

a transport equation by

$$c_i \frac{\partial \mu_i}{\partial x} = RT \sum_j \frac{c_i c_j}{c_T \mathcal{D}_{ij}} (v_j - v_i) , \qquad (4)$$

and a definition of the transference number for a single salt solution,

$$t_+ = \frac{z_+ c_+ (v_+ - v_0)}{z_+ c_+ (v_+ - v_0) + z_- c_- (v_- - v_0)} . \qquad (5)$$

(See Newman[1] for a discussion of these equations.) Equation (5) defines a transference number with respect to the solvent. This is the transference number that is usually reported in the literature.

Equations (1-5) can be manipulated to yield the expression for the transference number,[2]

$$t_1 = -a_B z_3 \left[\frac{c_3}{c_0}\right]_A \left[\frac{FV}{It} + \frac{M_e}{z_2 \rho_e} + \frac{b_B}{z_2 \nu_2 a_B}\right] . \qquad (6)$$

Equation (6) is applicable when the boundary is rising and the anode is a dissolving metal. Analogous expressions apply to other experimental arrangements. The quantities a_B and b_B are defined by the equation

$$c_{0B} = a_B + b_B c_B . \qquad (7)$$

The subscripts in Eqs. (6) and (7) have the following significance: 1 refers to the leading ion, 2 to the following ion, 3 to the common ion, 0 to the solvent, A to the leading solution far removed from the boundary, B to the following solution far removed from the boundary, and e refers to the dissolving electrode.

The quantity V is the volume through which the boundary moves when current I is passed for time t. These are the variables that are measured in an experimental determination of a transference number.

Equation (7) is equivalent to a linear density-concentration curve and is used only over the range of concentration present in solution B. As this range can be made small,[2] the linear representation is adequate.

The transference number of 0.213 M NH_4NO_3 at 25°C was measured. The boundary was formed and contained in a Tiselius cell, and its displacement was measured using Schlieren optics. Silver nitrate was used as the following solution. Conditions were such that Eq. (6) was applicable. The result is $t_+ = 0.5140 \pm 0.0024$.

1. J. Newman, Transport Processes in Electrolytic Solutions, Adv. Electrochem Electrochem. Engr. 5, 87-135 (1967).
2. P. Milios, A Theoretical Analysis of the Moving Boundary Measurement of Transference Numbers (M.S. Thesis), UCRL-17807, September 1967.

14. CURRENT DISTRIBUTION ON A ROTATING-DISK ELECTRODE

Vinay Marathe and John Newman

The current distribution for the deposition of copper on a rotating disk is being studied experimentally for comparison with the theoretical predictions reported earlier.[1]

The thickness of the deposit will be proportional to the current density at the point. Thus measurement of the deposit thickness at various points would yield the current distribution. The hydrodynamics and the assumption of a counter electrode at infinity impose a limit on the disk size. Also the deposit should be thinner than the diffusion boundary layer ($\approx 4\times10^{-3}$ cm). This necessitates measurement of variations in very small thicknesses over a small distance.

The possibilities of employing some of the conventional methods for thin film thickness measurements were investigated. Interference microscopy gives results to the accuracy of $\lambda/2$ (λ = wavelength of the source) but cannot be used since the deposit is not smooth enough to give an interference pattern. Radiographic methods give the amount of deposit (g/cm^2) directly, thus eliminating the need for any assumption about the density of the deposit. Among the several disadvantages of the method is the requirement of a high initial source activity to reduce the statistical errors inherent in radiation intensity measurements.[2]

The variation in thickness is measured by optical observation of the deposited layer. The electrolyte is copper sulfate with sulfuric acid as supporting electrolyte. Deposition is done at 25±0.1°C in a 14-cm-diam by 10-cm-high cell until the maximum thickness of the deposit does not exceed the diffusion boundary-layer thickness. The disk is embedded in epoxy resin before cutting it, so that the deposit surface is not burred during cutting. It is then polished down to a diameter and etched with a solution of 50 cc ammonium hydroxide and 20 cc 30% hydrogen peroxide in 50 cc water, so that the deposited layer can be distinguished from the disk due to differences in grain structure. The deposit distribution is then obtained from microphotographs, as shown in Fig. ID.14-1.

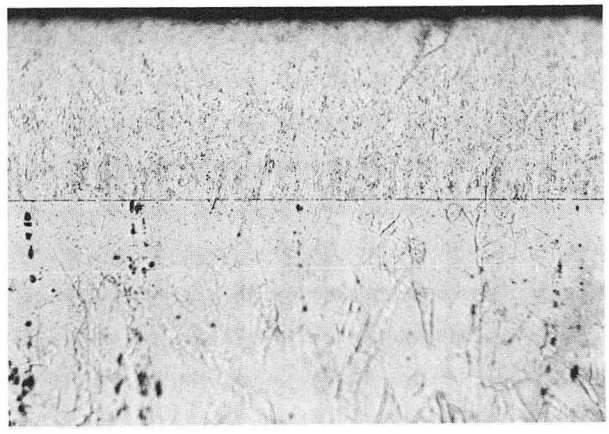

XBB 682-855

Fig. ID.14-1. Microphotograph of copper deposit on part of a copper disk (magnification about 200×).

The theoretical current distribution is obtained by a computer program and depends on parameters involving the transport properties and concentration of the electrolyte and the disk size.

1. J. Newman, Current Distribution on a Rotating Disk below the Limiting Current, J. Electrochem. Soc. 113, 1235-1241 (1966).
2. J. F. Cameron, The Uses of Radioactive Isotopes in Nondestructive Testing, Prog. Nondestructive Testing 2, 91-164 (1960).

15. CONCENTRATION PROFILE AND DIFFUSION COEFFICIENT IN A STAGNANT DIFFUSION CELL*

Limin Hsueh and John Newman

In a previous paper,[1] the effect of variations of physical properties has been taken into consideration in solving the equations of fluid motion and convective diffusion for a rotating disk electrode. There was no way to measure the concentration profile near the electrodes or to invert the measured diffusion coefficient into the differential diffusion

coefficient. Consequently, a simpler geometry and hydrogynamic system--a stagnant diffusion cell-- is chosen for study, thus keeping the assumptions in solving the convective-diffusion equation as few as possible, in order to improve our understanding of the basic laws of mass transfer in electrolytic solutions.

The theoretical analysis is similar to the previous one,[1] i.e., numerical solution of the coupled equations of continuity and of convective diffusion simultaneously for a one-dimensional unsteady-state diffusion with account for the variation of physical properties and nonzero interfacial velocity at electrodes. The concentration profile of a $CuSO_4$ system at 0.4M has been plotted in terms of the concentration ratio c/c_∞ vs the dimensionless distance ξ in Fig. ID.15-1. Here ξ is defined as $y/(4D_\infty t)^{1/2}$, where y is the normal distance from the electrode, D_∞ is the diffusivity at the bulk concentration, and t is the time of diffusion. This is compared with the case of constant physical properties. The results will be verified experimentally by optical observations.

The flux at the electrode in terms of $(1/c_\infty)(dc/d\xi)$ at $\xi = 0$ is plotted as a function of concentration in Fig. ID.15-2. The sharp variation at the dilute end may be attributed to the strong diffusivity change in dilute solutions. For the case of constant physical properties, $(1/c_\infty)(dc/d\xi)$ at $\xi = 0$ is a constant. This is in contrast to the case of the rotating disk electrode, where it is a function of the Schmidt number.

It is desirable to obtain the differential diffusion coefficient from the integral diffusion coefficient which is measured by a stagnant diffusion cell or a rotating disk electrode. This is because of the relatively simple experimental setup and the easily measurable quantities, time t and current density i, in addition to the less time required for a single measurement in comparison with other optical measurements.[2]

A computer program was worked out and tested successfully for the system of copper sulfate. With the measured value of $i\sqrt{t}$ at various concentrations, the differential

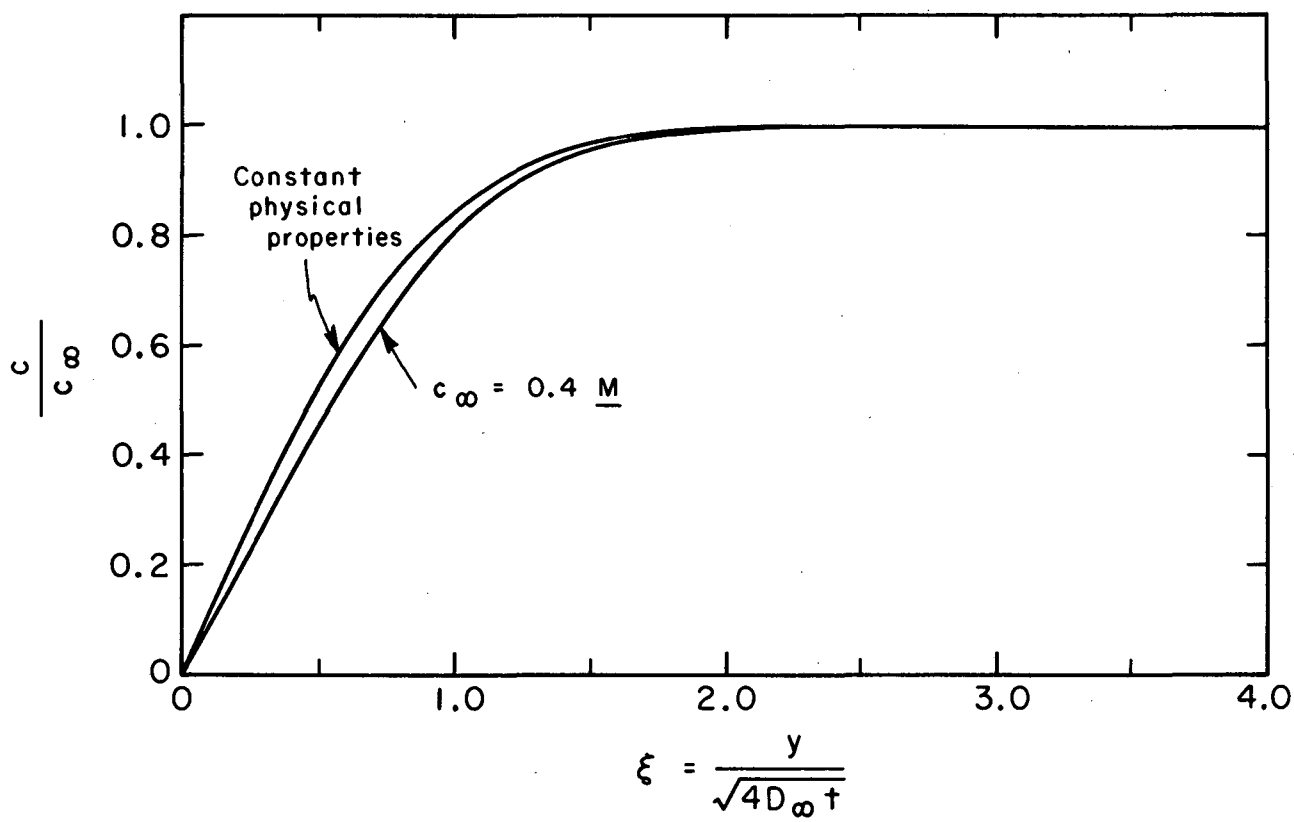

Fig. ID.15-1. Concentration profile in a stagnant diffusion cell for copper sulfate solutions at 25°C.

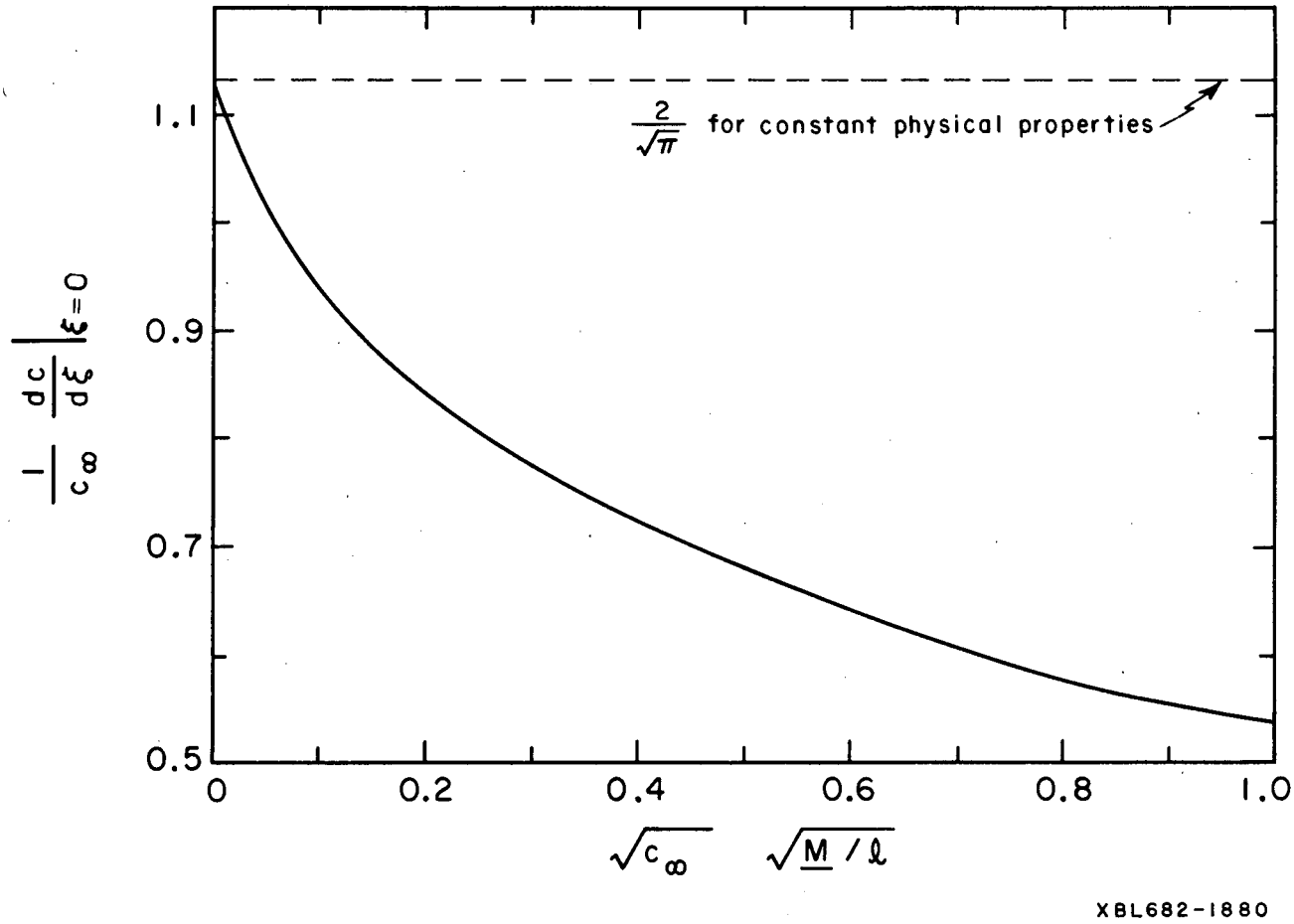

Fig. ID.15-2. Concentration dependence of the flux in a stagnant diffusion cell for copper sulfate solutions at 25°C.

diffusion coefficient can be calculated by an iterative method. However, a probable disadvantage that may limit the applicability of this method is the high ohmic potential drop associated with a solution of a single electrolyte.

The analysis described above is also applicable to the dropping-mercury electrode or any other electrolytic mass transfer system where the penetration model of diffusion can be applied.

* This work is supported by the Petroleum Research Fund, administered by the American Chemical Society.

1. J. Newman and L. Hsueh, The Effect of Variable Transport Properties on Mass Transfer to a Rotating Disk, Electrochim. Acta 12, 417-427 (1967).
2. T. W. Chapman, The Transport Properties of Concentrated Electrolytic Solutions (Ph.D. Thesis), UCRL-17768, Nov. 1967.

16. FLOW TUNNEL WITH MOVING WALLS

Ping Huei Sih and John Newman

The moving-wall water tunnel designed by Thomas Atkins[1] has been tested and modified. The major problems in the original design were the driving mechanism and the centering of the moving belts. Changes were made so that some of the difficulties were reduced or eliminated.

In the original design there was too much friction between the moving belts and the supporting plates, and the gears were small and fragile, so that it was difficult to keep the belts moving without stripping the gears. This has been corrected by introducing stronger and bigger gears with a different linkage to give more positive driving power. In addition, ducts were made on the plates to increase the thickness of the liquid layer between the belts and the plates. Since in this case the frictional force is inversely proportional to the

thickness, friction is reduced. Also, this arrangement eliminated slipping between the driving rollers and the belts.

In order to avoid the migration of belts to one side or the other of the rollers, all the rollers were tapered from the center. Also, the end rollers were made adjustable to give more flexibility in controlling the tension of the belts. Originally, each belt was made by joining a piece of mylar film along a 45-deg. cut. This was not desirable, because it was not symmetrical. After a series of tests, a vee-shaped splice was selected.

The construction of the whole system has been completed. Since we shall study a mass-transfer problem in the tunnel, the velocity profile will be measured by a hot-wire anemometer. The method does not introduce foreign material into the system; therefore, there will not be any interference with mass-transfer processes.

1. T. Atkins, in Inorganic Materials Research Division Annual Report, 1964, UCRL-11889, February 1965, Fig. ID.24-1.

17. LAMINAR FREE CONVECTION AT A VERTICAL ELECTRODE IN THE PRESENCE OF SUPPORTING ELECTROLYTE

J. Robert Selman and John Newman

Free convection at a vertical plate is described by an equation of motion for the vertical velocity, coupled to the equation of convective diffusion by means of the buoyancy term. In the case of an electrolytic solution subject to electrolysis, the equations of convective diffusion for the several species all contain additional terms due to migration in the electric field; the equations themselves are coupled by means of the electroneutrality condition. For such solutions, characterized by a high Schmidt number, it is also possible to circumvent the nonlinearity of the equation of motion by assuming asymptotic behavior ($Sc \to \infty$), i.e., an infinitely thin diffusion layer within the region of nonzero velocity, and neglecting inertial effects in the equation of motion but not in the equation of convective diffusion. The equations can be further simplified by a similarity transformation and by stretching the coordinates with respect to the quantity $Sc^{1/4}$.[1] Upon linearization, the equations in difference form constitute a coupled tridiagonal matrix and can be solved by a procedure outlined elsewhere.[2]

The average current density $\bar{i}$ can be expressed as a Nusselt number:

$$\overline{Nu} = \frac{\bar{i}\, S_R\, L}{nF\, \mathcal{D}_R \Delta c_R},$$

which employs the diffusivity $\mathcal{D}_R$ of the reacting ion R, a characteristic length L, and reaction stoichiometry parameters of the reacting ion, according to:

$$\sum_i S_i M_i^{z_i} \rightarrow ne^- .$$

For a multicomponent system this number can now be related to the Grashof number characteristic for free convection and employing properties of species R

$$Gr_R = \frac{g\alpha_R \Delta c_R L^3}{\nu^2},$$

and to the Schmidt number Sc_R, by

$$\overline{Nu} = \gamma_R(0)\ (Gr_R\ Sc_R)^{1/4} .$$

The average shear stress at the electrode is expressed likewise:

$$\frac{\bar{\tau}_o}{L\rho g \alpha_R \Delta c_R} = -\ \phi_R(0)\ (Gr_R\ Sc_R)^{-1/4} .$$

When the amount of supporting electrolyte is increased but the reacting ion concentration kept constant, the coefficients $\gamma_R(0)$ and $\phi_R(0)$ are influenced directly by migration and indirectly by the densification of the solution at the electrode, which is not accounted for by the number Gr_R. To separate the effects a Grashof number based on total density difference is used:

$$Gr = \frac{g\Delta\rho L^3}{\nu^2 \rho_\infty}$$

$$\overline{Nu} = \gamma(0)\ (Gr\ Sc_R)^{1/4}$$

$$\bar{\tau}_o / Lg\Delta\rho = -\ \phi(0)\ (Gr\ Sc_R)^{-1/4} ,$$

where

$$\gamma(0) = \gamma_R(0)\left(\frac{\sum_i \alpha_i \Delta c_i}{\alpha_R\ c_R}\right)^{-1/4}$$

$$\phi(0) = \phi_R(0)\left(\frac{\sum_i \alpha_i \Delta c_i}{\alpha_R \Delta c_R}\right)^{-3/4} .$$

As a preliminary check, the equations were solved for a binary solution (e.g., $CuSO_4$-H_2O)

and the results compared with information available for free-convection heat transfer at high Prandtl numbers. To this end the current density and shear stress at the wall were related to Grashof and Schmidt numbers based on physical properties of the binary salt:

$$\overline{Nu}_S = \frac{\overline{iS}_R L(1-t_R)}{nF\mathcal{D}_S \Delta C_s} = \frac{z_i \nu_R (1-t_R)\mathcal{D}_R}{\mathcal{D}_S}\,\overline{Nu}$$

$$= \gamma_S(0)(Gr_S Sc_S)^{1/4}$$

$$\frac{\bar{\tau}_o}{Lg\Delta\rho_S} = -\,\phi_S(0)(Gr_S\, Sc_S)^{-1/4}\,,$$

where

$$\gamma_S(0) = \gamma_R(0)(1-t_R)\left(\frac{\mathcal{D}_R}{\mathcal{D}_S}\right)^{3/4}\left(\frac{\alpha_R}{\alpha_S}\right)^{1/4}$$

$$\phi_S(0) = \phi_R(0)\left(\frac{\mathcal{D}_R}{\mathcal{D}_S}\right)^{1/4}\left(\frac{\alpha_R}{\alpha_S}\right)^{3/4}.$$

The values obtained were $\gamma_S(0) = 0.67001$ and $\phi_S(0) = 0.93308$. These can be compared with values from the literature, given in Table ID.17-I. Also included are values for $\gamma_S(0)$ computed in a separate numerical solution excluding migration but including the inertial terms in the equation of motion.

Table ID.17-I. $\gamma_S(0)$ and $\phi_S(0)$ as a function of Sc number.

	Sc→	10	100	1000	∞*
$\gamma_S(0)$	This work	0.6200	0.6533	0.6653	0.6703
	Ostrach[3]	0.6200	0.6532	0.6649	
	Schuh[4]	0.649	0.692	0.692	
$\phi_S(0)$	This work				0.9328
	Ostrach[3]	0.8434	0.9005	0.9225	

* In the asymptotic limit of large Schmidt number, the inertial terms are dropped from the equation of motion.

Solutions were next obtained for the system $CuSO_4$-H_2SO_4-H_2O, both on the assumption of incomplete dissociation to HSO_4^- and of complete dissociation to $SO_4^=$. The results are expressed in Fig. ID.17-1 as $\gamma(0)/\gamma_S(0)$ and $\phi(0)/\phi_S(0)$, while the solid lines indicate values of the analogous $\gamma(0)/\gamma_S(0)$ obtained for a rotating disk and a growing mercury drop (in part published earlier[5]). Figure ID.17-2 gives the concentration increase of the H^+ ion at the electrode, again compared to values for the rotating disk and growing drop.

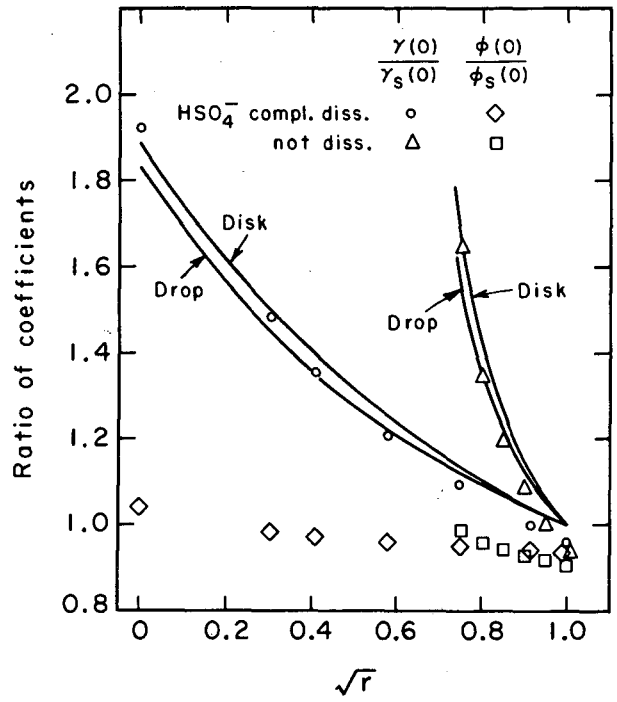

Fig. ID.17-1. Influence of migration on current and shear stress at the electrode. Solid curves represent earlier calculations on rotating-disk and dropping-mercury electrodes.

$$\left(r = \frac{C_{H_2SO_4}}{C_{H_2SO_4} + C_{CuSO_4}}\right)$$

To assess the practical importance of the dissociation of HSO_4^-, computations were made for the case of a rotating disk, while accounting for a variable degree of dissociation by means of a dissociation constant K = 0.01. The results, in all cases, are very close to the limit of incomplete dissociation, i.e., a solution containing H^+, HSO_4^-, and Cu^{++} only (Table ID.17-II).

From Fig. ID.17-1 it is apparent that, in the limit of pure diffusion, the current in the case of natural convection does not tend to the value valid for a binary solution (or for heat transfer as $Pr \to \infty$). In this respect behavior is different from that of the rotating-disk or growing-drop electrode, where forced convection takes place. The coupling of velocity profile with concentration profile, in combination with disparity of the diffusion coefficients of the ionic species, causes an additional depression of the current in the limit of pure diffusion.

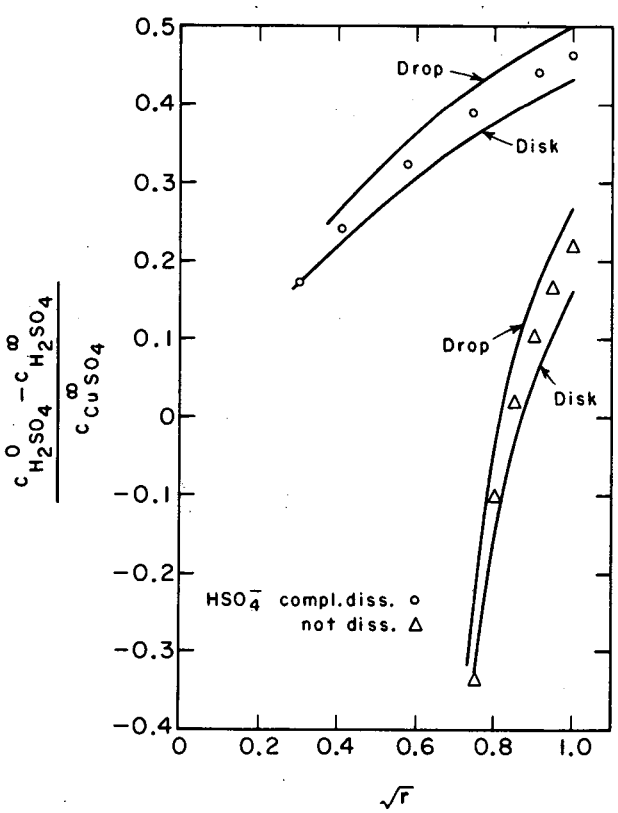

Fig. ID.17-2 Influence of migration on composition of solution at the electrode. Solid curves represent earlier calculations on rotating-disk and dropping-mercury electrodes.

$$\left(r = \frac{c_{H_2SO_4}}{c_{H_2SO_4} + c_{CuSO_4}} \right)$$

Table ID.17-II. Ratio $\gamma(0)/\gamma_s(0)$ for solutions of variable dissociation, expressed as percentage of the same ratio for the case of no dissociation of HSO_4^-.

$\sqrt{r}$	$c_{H_2SO_4}$		
	1.5M	1.0M	0.5M
0.95	99.94	99.91	99.82
0.90	99.87	99.80	99.60
0.85	99.76	99.64	99.27
0.80	99.54	99.29	98.52
0.75	98.18	97.29	95.05

$$\left(r = \frac{c_{H_2SO_4}}{c_{H_2SO_4} + c_{CuSO_4}} \right)$$

Work is being continued on the system $K_3Fe(CN)_6$-$K_4Fe(CN)_6$-KOH-H_2O.

1. G. W. Morgan and W. H. Warner, J. Aero. Sci. 23, 937-948 (1956).
2. J. Newman, Numerical Solutions of Coupled, Ordinary Differential Equations, UCRL-17739, August 1967.
3. S. Ostrach, An Analysis of Laminar-Free Convection Flow and Heat Transfer About a Flat Plate Parallel to the Direction of the Generating Body Force, NACA Rep. 1111, 1953.
4. Morgan and Warner, ref. 1, p. 942.
5. J. Newman, Effect of Ionic Migration on Limiting Currents, Ind. Eng. Chem. Fundamentals 5, 525 (1966).

18. POTENTIALS OF CELLS WITH LIQUID JUNCTIONS

William H. Smyrl and John Newman

All cells used to obtain standard cell potentials contain liquid junctions. In order to extract thermodynamic information, it is necessary to account for the effect of the diffusion phenomena on the cell potential. It may be possible to ignore the effect under certain conditions, and it is desirable to know what these conditions are. The procedure is to determine the concentration profiles, or to calculate them from the laws of diffusion, and along with the transport and thermodynamic properties of the junction region, to calculate the "liquid-junction potential."

The potentials of cells with liquid junctions are well known for a few systems. In particular, for activity coefficients of unity, a concentration profile for restricted diffusion yields the Planck equation, a concentration profile for a continuous-mixture junction yields the Henderson equation, and Guggenheim has derived the result for free diffusion from an initially sharp boundary (with equal ionic diffusion coefficients). The present work[1] extends the treatment of these junctions to include the activity coefficient correction. The system of diffusion of a sparingly soluble salt away from the solid is treated also and is of significance for cells which employ an electrode of the second kind. The calculations have been made using Guggenheim's extension of the Debye-Hückel equation for the activity coefficients of solutions of several electrolytes. For the HCl-KCl junction, the results agree satisfactorily with experimental data. The junctions NaCl-$HClO_4$ and HCl-KNO_3, chosen because all the Guggenheim β coefficients are known, were also treated, but there are no experimental results with which to compare the calculated results. Diffusion of AgCl away from solid AgCl into a solution of HCl has a negligible effect on the cell potential, except in very dilute solutions of HCl ($\sim 10^{-5}$ molal), according to our calculations. A proposal has been made for tabulating the results of cells with liquid junctions.

1. W. H. Smyrl and J. Newman, Potentials of Cells with Liquid Junctions, UCRL-17986, May 1968.

19. MASS TRANSFER AND ELECTROCHEMICAL SYSTEMS

John Newman

Current distribution and mass transfer in electrochemical systems have been reviewed[1] in a sequel of the fundamentals of transport processes in electrolytic solutions,[2] thus providing a basis for the development of design procedures for electrochemical systems.

Three minor contributions are related to several mass-transfer problems. The use of an integral equation[3] for the diffusion layer on a rotating disk electrode promises to eliminate a computational problem encountered earlier.[4] The basic equation of polarographic limiting currents can be written

$$I_{avg} = 3.5723\ nF\ c_\infty\ D_1^{1/2}\ Q^{2/3}\ T^{1/6} \times [1 + K(D_1^3\ T/Q^2)^{1/6}]\ ,$$

which coincides with Ilkovič's equation when $K = 0$. In the present work[5] it is shown that the coefficient K of the correction term has the value

$$K = \frac{14\Gamma(15/14)}{11\Gamma(11/7)} \left(\frac{3}{7}\right)^{1/2} \left(\frac{4\pi}{3}\right)^{1/3} = 1.4530.$$

The Lévêque equation applies to mass (or heat) transfer to the wall of a tube with fully developed laminar flow and a constant wall concentration. This has been extended[6] to greater distances from the beginning of the mass-transfer section:

$$\frac{J}{\pi R^2 (c_b - c_0)\langle v_z\rangle} = (48)^{1/3} Z^{2/3} \Theta_0'(0) + 4Z\Theta_1'(0) + 3\left(\frac{9}{2}\right)^{1/3} Z^{4/3} \Theta_2'(0) + O(Z^{5/3})$$

$$= 4.069792\ Z^{2/3} - 2.4Z - 0.4453787 Z^{4/3} + O(Z^{5/3}),$$

where

$$\Theta_0'(0) = 1/\Gamma(4/3) = 1.11984652, \quad \Theta_1'(0) = -0.6,$$

$$\Theta_2'(0) = -\frac{11/140}{\Gamma(4/3)} \left[\frac{\Gamma(5/3)}{\Gamma(4/3)}\right]^2 = -0.0899230.$$

Here J is the rate of mass transfer to the wall in a length z, $\langle v_z\rangle$ is the average velocity in the tube, and $Z \equiv zD/2\langle v_z\rangle R^2$.

1. J. Newman, Current Distribution and Mass Transfer in Electrochemical Systems, UCRL-17294, January 1967.
2. J. Newman, Transport Processes in Electrolytic Solutions, Adv. Electrochem. Electrochem. Engr. 5, 87-135 (1967).

3. J. Newman, The Diffusion Layer on a Rotating Disk Electrode, J. Electrochem. Soc. 114, 239 (1967).
4. J. Newman, Current Distribution on a Rotating Disk below the Limiting Current, J. Electrochem. Soc. 113, 1235-1241 (1966).
5. J. Newman, The Koutecký Correction to the Ilkovič Equation, J. Electroanal. Chem. 15, 309-312 (1967).
6. J. Newman, Extension of the Lévêque Solution, UCRL-17600, June 1967.

20. MASS TRANSFER TO THE REAR OF A CYLINDER AT HIGH SCHMIDT NUMBERS

John Newman

Recently it has been shown[1] how to calculate the rate of mass transfer to the rear of a sphere in Stokes flow at high Péclet numbers, where the usual diffusion-layer treatment breaks down. In the present work[2] this concept has been extended to arbitrary two-dimensional and axisymmetric bodies with rounded rear sides, at Reynolds numbers higher than those of "creeping flow" but still below those at which eddies are formed at the rear. This relieves an important constraint on the experimental verification because free convection should give less interference at these higher flow rates.

For the two-dimensional cylindrical bodies, the local Nusselt number in the rear region is found to be proportional to the Schmidt number to the one-sixth power, in contrast to the axisymmetric bodies where the local Nusselt number is of order unity. Figure ID.20-1 gives an idea of the mass-transfer rate near the rear and shows how it blends into the diffusion-layer solution at large distances from the rear. Here $\partial\bar{\Theta}/\partial Y$ at $Y = 0$ is proportional to the rate of mass transfer, and X is proportional to the distance from the rear.

1. P. H. Sih and J. Newman, Mass Transfer to the Rear of a Sphere in Stokes Flow, Intern. J. Heat Mass Transfer 10, 1749-1756 (1967).
2. J. Newman, Mass Transfer to the Rear of a Cylinder at High Schmidt Numbers, UCRL-17599, June 1967.

21. NUMERICAL SOLUTION OF COUPLED, ORDINARY DIFFERENTIAL EQUATIONS

John Newman

A wide variety of problems arising, for example, in fluid flow and electrochemical mass transfer can be reduced to coupled, ordinary, frequently nonlinear, differential

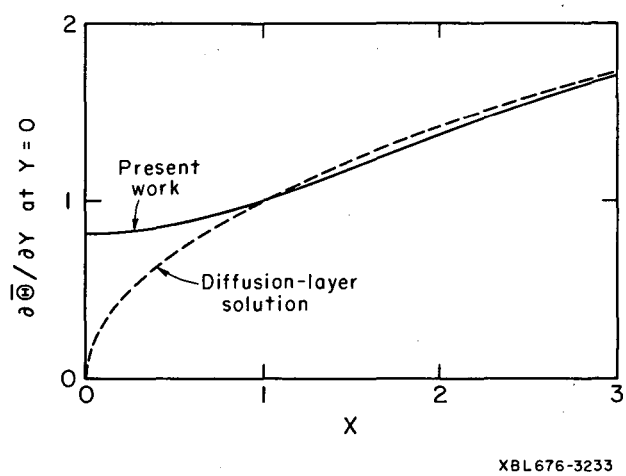

Fig. ID.20-1. Rate of mass transfer near the rear of a bluff two-dimensional body at large Schmidt numbers.

equations. The numerical solution of these problems becomes routine by the method developed here.[1] The equations are linearized about a trial solution and then put into finite-difference form. The resulting coupled tri-diagonal matrices can be solved readily on a high-speed digital computer, and the nonlinear problem can then be solved by iteration. The method is also applicable to stage-wise distillation problems, where the equations are already similar to the finite-difference approximation to differential equations.

1. J. Newman, Numerical Solution of Coupled, Ordinary Differential Equations, UCRL-17739, August 1967.

22. RESEARCH PLANS FOR CALENDAR YEAR 1968

John Newman

The current distribution for deposition of copper on a rotating disk will be measured and compared with theoretical predictions reported earlier. The current distribution for plane electrodes in the walls of a flow channel in laminar flow will be calculated taking into account ohmic potential drop, concentration variations near the electrodes, and electrode kinetics. Mass-transfer rates in the region near the rear of a cylinder or a sphere in laminar flow will be studied experimentally with an electrochemical system for verification of the theoretical calculations already reported. This will involve further development of the flow channel with moving walls.

Concentration profiles will be observed optically for migration in a cell with a stagnant electrolytic solution at the limiting current. Comparison with theoretical calculations should reveal whether it is necessary to consider hydrolysis and pH changes or low anode-current efficiencies in addition to the concentration dependence of transport properties in order to account for observed deviations from the predictions of dilute-solution theory.

The diffusion coefficients of aqueous solutions of potassium hydroxide will be measured by optical observation of restricted diffusion. Tables of existing measurements of the transport properties of binary electrolytic solutions will be completed. Additional measurements of transference numbers by the moving-boundary method and of conductivities will be made.

Currents limited by gas solubility and the effect of incomplete dissociation of bisulfate ions on limiting currents will be studied in a stagnant diffusion cell. The theoretical study of limiting currents for natural convection at vertical electrodes in the presence of supporting electrolyte will be completed.

23. 1967 PUBLICATIONS

John Newman and Associates

Technical Journals

1. Thomas W. Chapman and John Newman, Polarography in a Binary Salt Solution, J. Phys. Chem. 71, 241-245 (1967).
2. Limin Hsueh and John Newman, Mass Transfer and Polarization at a Rotating Disk Electrode, Electrochim. Acta 12, 429-438 (1967).
3. John Newman, Retardation of falling drops, Chem. Eng. Sci. 22, 83-85 (1967).
4. John Newman, Transport Processes in Electrolytic Solutions, Adv. Electrochem. Electrochem. Engr. 5, 87-135 (1967).
5. John Newman, The Diffusion Layer on a Rotating Disk Electrode, J. Electrochem. Soc. 114, 239 (1967).
6. John Newman and Limin Hsueh, The Effect of Variable Transport Properties on Mass Transfer to a Rotating Disk, Electrochim. Acta 12, 417-427 (1967).
7. John Newman, The Effect of Migration in Laminar Diffusion Layers, Intern. J. Heat Mass Transfer 10, 983-997 (1967).
8. John Newman, Internal Contamination of Buildings by Fallout, Health Physics 13, 991-999 (1967).
9. John Newman, The Koutecký Correction to the Ilkovič Equation, J. Electroanal. Chem. 15, 309-312 (1967).
10. C. D. Scott and John S. Newman, Heat Storage in Tunnel Walls, Ind. Eng. Chem. Fundamentals 6, 473-474 (1967).
11. Ping Huei Sih and John Newman, Mass Transfer to the Rear of a Sphere in Stokes Flow, Intern. J. Heat Mass Transfer 10, 1749-1756 (1967).
12. William H. Smyrl and John Newman, Double Layer Structure at the Limiting Current, Trans. Faraday Soc. 63, 207-216 (1967).

UCRL Reports

1. Thomas W. Chapman, The Transport Properties of Concentrated Electrolytic Solutions (Ph.D. Thesis), UCRL-17768, November 1967.
2. Marvin E. McDonald and John Newman, The Steady Laminar Flow Past a Circular Cylinder, UCRL-17374, February 1967.
3. Paul Milios, A Theoretical Analysis of the Moving Boundary Measurement of Transference Numbers (M.S. Thesis), UCRL-17807, September 1967.
4. John Newman, Current Distribution and Mass Transfer in Electrochemical Systems, UCRL-17294, January 1967.
5. John Newman, Mass Transfer to the Rear of a Cylinder at High Schmidt Numbers, UCRL-17599, June 1967.
6. John Newman, Extension of the Lévêque Solution, UCRL-17600, June 1967.
7. John Newman, Numerical Solution of Coupled, Ordinary Differential Equations, UCRL-17739, August 1967.

E. PHYSICAL CHEMISTRY

1. CAPTURE RADIUS FOR ION RECOMBINATION*

Eric K. Parks†

The concept of a critical capture radius[1] has been used for 40 years in the theory of three-body ion recombination. In this paper we rigorously derive expressions for the dependence of the value of the capture radius on the masses of the combining ions, and calculate the corresponding rate constants. The calculated rate constants are compared with some recently available experimental data,[2,3] and it is found that the use of the rigorously calculated capture radius leads to serious underestimates of the recombination rate constant.

* Abstracted from UCRL-17754 and a paper accepted for publication in the Journal of Chemical Physics.

† Present address: Department of Chemistry, Massachusetts Institute of Technology, Cambridge, Mass.

1. J. J. Thomson, Phil Mag. 47, 337 (1924).
2. G. A. Fisk, B. H. Mahan, and E. K. Parks, J. Chem. Phys. 47, 2649 (1967).
3. B. H. Mahan and J. C. Person, J. Chem. Phys. 40, 392 (1964).

2. GASEOUS-ION RECOMBINATION. V*

Bruce H. Mahan

Pitaevski's[1] formulation of the three-body ion-electron recombination rate constant based on the Fokker-Planck equation has been modified and extended so as to apply to the termolecular recombination of gaseous ions. The result is the following expression for the termolecular recombination rate constant:

$$k' = (8\pi^2/9)(\alpha e^2/\mu_{23})^{1/2}(e^2/kT)^3(m_3/M_{23})\ R,$$

where

$$R = \left\{4\left(\frac{m_2}{M_{23}}\right)^2 + 15\left(\frac{m_3}{M_{23}}\right)^2\left(\frac{\mu_{12}}{\mu_{13}}\right)^2 + \left(\frac{\mu_{12}}{\mu_{13}}\right)\left[5\left(\frac{m_2-m_3}{M_{23}}\right)^2 - 2\right]\right\}.$$

Here m_1, m_2, and m_3 are the masses of the spectator ion, the ion undergoing collision, and the neutral molecule, respectively, and μ_{ij} and M_{ij} stand for the reduced mass and sum of the masses of the particles i and j. The quantities α and e are the polarizability of the neutral and fundamental charge, and the other symbols have their usual meaning. A comparison between the calculated and experimental rate constants given in Table IE.2-I shows quite satisfactory numerical agreement.

Table IE.2-I. Calculated and experimental[2,3] rate constants.

System	Temp. (°K)		$k_{exp}\times10^{26}$ (cm^6/sec)	$k_{calc}\times10^{26}$ (cm^6/sec)
Tl_2I^+, TlI_2^-	Xe	530	3.0	0.86
	Ar	530	1.3	0.39
Tl_2Br^+, $TlBr_2^-$	Xe	590	2.0	0.70
	Ar	590	1.1	0.40
Tl_2Cl^+, $TlCl_2^-$	Xe	610	1.8	0.87
	Ar	610	1.2	0.37
NO^+, NO_2^-	He	300	4.1	3.6
	Ne	300	10.4	8.3
	H_2	300	5.8	5.6
	D_2	300	6.1	7.2

* Abstracted from UCRL-17821 and a paper accepted for publication in the Journal of Chemical Physics.

1. L. P. Pitaevski, Zh. Eksperim. i Teor. Fiz. 42, 1326 (1962). [English transl.: Soviet Phys.-JETP 15, 919 (1962)].
2. B. H. Mahan and J. C. Person, J. Chem. Phys. 40, 392 (1964).
3. G. A. Fisk, B. H. Mahan, and E. K. Parks, J. Chem. Phys. 47, 2649 (1967).

3. RATE OF ATTACHMENT OF GASEOUS ELECTRONS TO NITROGEN DIOXIDE*

Bruce H. Mahan and Isobel C. Walker†

Gaseous thermal electrons have been produced by the flash photoionization of nitric oxide and their concentration measured as a function of time by using a microwave-cavity resonance technique. The rates at which these gaseous electrons attach to NO_2 in the presence of several inert gases have been measured. The rate of attachment was found to be independent of the pressure of the inert gas in the range from 3 to 70 Torr. However, as Table IE.3-I shows, the apparent second-order rate constant does depend on the nature of the inert gas. The mechanism that accounts for these observations is

$$NO_2 + e \rightarrow (NO_2^-)^* \quad (1)$$

$$(NO_2^-)^* \rightarrow NO_2 + e \quad (2)$$

$$(NO_2^-)^* + M \rightarrow NO_2^- + M \quad (3)$$

$$(NO_2^-)^* + M \rightarrow NO_2 + M + e. \quad (4)$$

Table IE.3-I. Rate constants for electron attachment to NO_2.

Added Gas M	k(cc/molecule-sec)
He	2.0×10^{-11}
Ne	3.1×10^{-11}
Ar	4.5×10^{-11}
Kr	3.0×10^{-11}
Xe	2.5×10^{-11}
N_2	4.0×10^{-11}

Making the steady-state assumption for $(NO_2^-)^*$ and assuming $k_2<(k_3+k_4)M$, we get

$$\text{rate} = [k_1k_3/(k_3+k_4)]\,(NO_2)(e),$$

which is consistent with the experimental data.

* Abstracted from UCRL-17737 and J. Chem. Phys. 47, 3780 (1967).

† Present address: University of Stirling, Stirling, Scotland.

4. THE COLLISIONAL-RADIATIVE REACTION OF $O_2(^1\Delta_g)$*

Arnold M. Falick† and Bruce H. Mahan

The reaction

$$2\ O_2(^1\Delta_g) \rightarrow 2\ O_2(^3\Sigma_g^-) + h\nu\ (6340\text{Å})$$

has been studied using the four-line EPR spectrum of the J=2 level of $O_2(^1\Delta_g)$ to measure the reactant concentration. It was found that the rate of light emission depends on the square of the concentration of $O_2(^1\Delta_g)$, but not on the nature or concentration of inert gas in the range from 0.3 to 0.8 Torr. The mechanism proposed is

$$2\ O_2(^1\Delta_g) \rightleftharpoons O_4^{**} \overset{M}{\rightleftharpoons} O_4^*$$

$$O_4^{**} \rightarrow 2\ O_2 + h\nu$$

$$O_2^* \rightarrow 2\ O_2 + h\nu,$$

where O_4^{**} and O_4^* are two $O_2(^1\Delta_g)$ molecules unbound and bound respectively by the van der Waals potential. The overall rate constant was found to be $5\pm1\times10^{-23}$ cc/molecule-sec, which corresponds to a radiative lifetime of 3 sec for the complex O_4^*. This latter value is consistent with the radiative lifetime of 2 sec calculated from the integrated absorption coefficient.[1]

* Abstracted from UCRL-17744 and J. Chem. Phys. 47, 4778 (1967).

† Present address: Department of Chemistry, University of California, Santa Barbara, Calif.

1. H. Salow and W. Steiner, Z. Physik 99, 127 (1936).

5. INELASTIC SCATTERING OF N_2^+ BY HELIUM*

William R. Gentry,† Eric A. Gislason, Bruce H. Mahan, and Chi-wing Tsao

We have investigated the angular and energy distribution of N_2^+ scattered by helium at relative energies of 7.5 and 11.3 eV. Experiments were performed by allowing a well-collimated, momentum-analyzed beam of N_2^+ to impinge on He gas at 4×10^{-4} Torr in a scattering cell. Ions leaving the scattering cell entered a 90-deg spherical electrostatic energy analyzer and a quadrupole mass filter and were detected by an ion counter. The complete

detection system was mounted on a rotatable lid, so that the angular distribution of scattered ions could be determined.

For both relative energies the anticipated elastic scattering was found at small ($\chi < 50$-deg) center-of-mass angles. As the scattering angle increased, inelastic energy loss was detected, which increased to 2.0 and 3.5 eV at $\chi = 180$-deg for the 7.5 and 11.3 eV relative energy experiments, respectively. Such large fractional energy losses which correspond to rotational, vibrational, and perhaps electronic excitation of N_2^+ are quite unexpected. We expect future experiments with a variety of collision partners will clarify our understanding of the excitation process.

* Abstracted from UCRL-17647 and J. Chem. Phys. 47, 1856 (1967).
† Present address: Department of Chemistry, Massachusetts Institute of Technology, Cambridge, Massachusetts.

6. PRODUCT ENERGY AND ANGULAR DISTRIBUTIONS FROM THE REACTION OF N_2^+ WITH ISOTOPIC HYDROGEN MOLECULES*

William R. Gentry,† Eric A. Gislason, Yuan-tseh Lee,‡ Bruce H. Mahan, and Chi-wing Tsao

The purpose of this work was to investigate the dynamics of the reaction of N_2^+ with

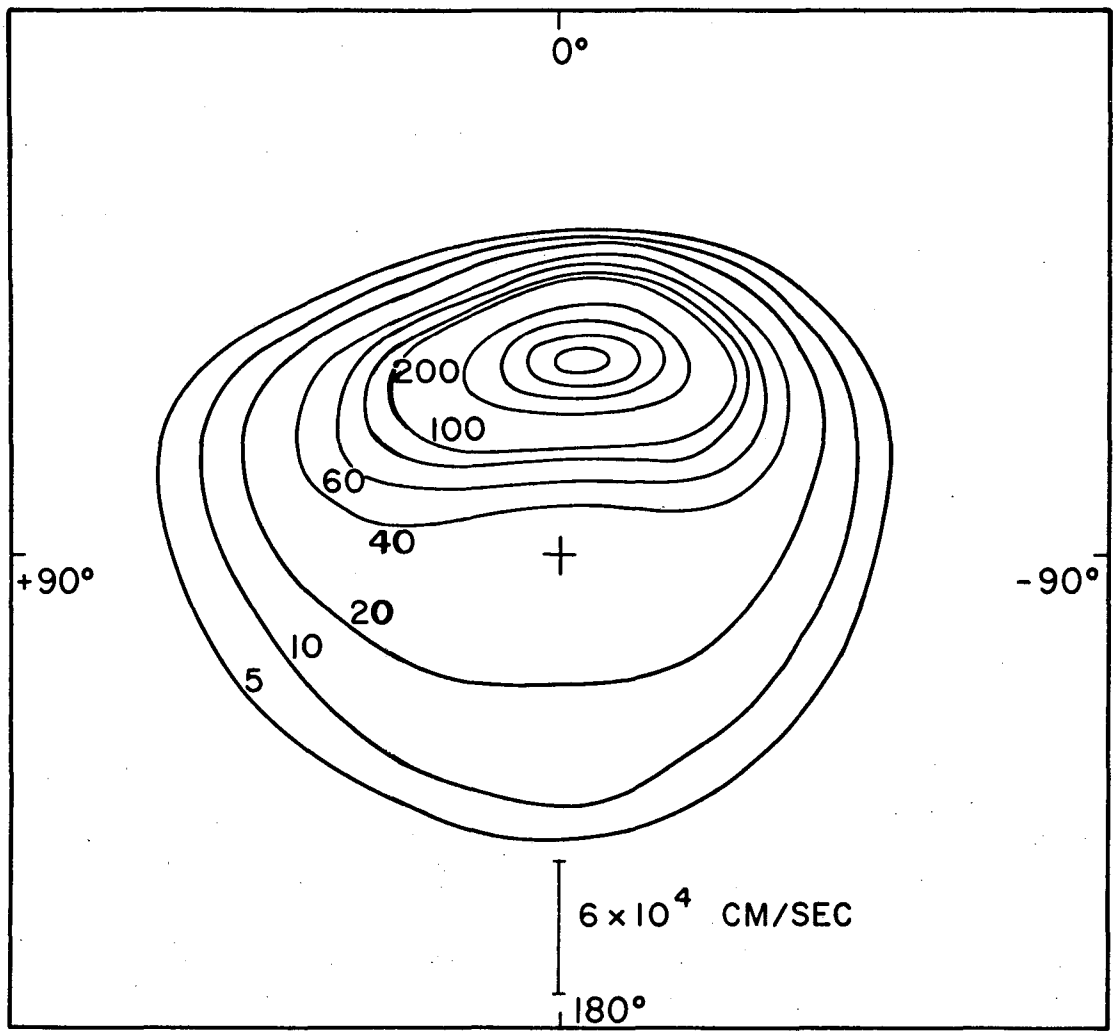

XBL 678-4780

Fig. IE.6-1. Contour map of N_2D^+ distribution in the center-of-mass coordination system. Reaction: $N_2^+ + D_2 \rightarrow N_2D^+ + D$ at 3.1-eV relative energy.

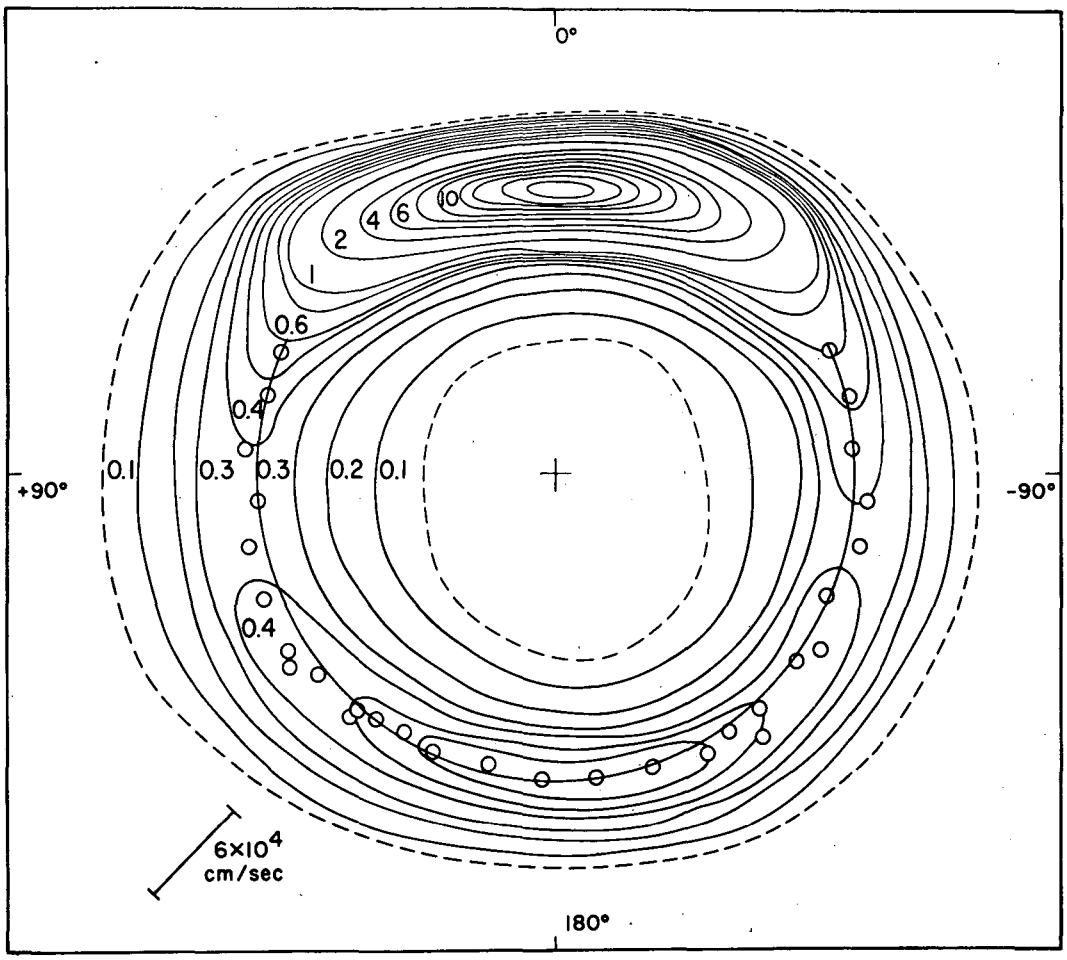

XBL 678-4799

Fig. IE.6-2. Contour map of N_2D^+ intensity produced from the reaction: $N_2^+ + D_2 \rightarrow N_2D^+ + D$ at 8.1-eV relative energy.

H_2, D_2, and HD. To do this, we directed a momentum-analyzed beam of N_2^+ through an isotropic scattering gas, and the energy and angular distribution of products and inelastically scattered reactant molecules were determined. By determining the angular distribution of products at several energies, and the energy distribution at various angles, enough data have been taken to permit the construction of contour maps of scattered-product intensity. Examples of these maps are given in Figs. IE.6-1 and IE.6-2. These are the first complete reaction-product intensity distributions that have been obtained by molecular beam techniques.

The general features of the reaction dynamics can be discerned from the intensity-contour maps. The scattering is symmetric about the initial relative-velocity vector (the 0 to 180-deg line in Figs. IE.6-1 and IE.6-2), except for small deviations attributable to instrumental effects. The asymmetry about X=90-deg indicates that the reactions proceed by a direct interaction mechanism rather than by a long-lived complex. The product intensity is particularly great at small angles and speeds close to the projectile speed. Such intense forward scattering is consistent with a predominant stripping process,[1] but the presence of large-angle scattering shows that rebound-reactive collisions occur and are important at all energies. The crater-like shape of the distributions observed for high projectile energies is a consequence of the instability of reaction products with zero relative translational energy and concomitant high internal energy. Analysis of these distributions shows that products scattered through small center-of-mass angles with respect to the direction of the N_2^+ projectile are more excited internally than those that have been formed by a recoil

type of collision.

Studies of the intensity of products formed in reactions with H_2, D_2 and HD indicate that for small-angle scattering, there is a large (factor of 10) isotope effect that favors hydrogen over deuterium in the products. A much smaller isotope effect favors deuterium over hydrogen in products formed by the recoil process.

* Abstracted from UCRL-17674 and Discussions of the Faraday Soc. 44, 137 (1967).

† Present address: Department of Chemistry, Massachusetts Institute of Technology, Cambridge, Massachusetts.
‡ Present address: Department of Chemistry, Harvard University, Cambridge, Massachusetts.

1. K. Lacmann and A. Henglein, Ber. Bunsenges. Physik. Chem. 69, 292 (1965).

7. DYNAMICS OF THE N_2^+-CH_4 REACTION

Eric A. Gislason, Chi-wing Tsao, Bruce H. Mahan, and Arthur Werner

Using our ion-molecule molecular-beam apparatus, we have investigated the reactive and nonreactive collisions of N_2^+ with CH_4. Some of the results for the reactive scattering are shown in Fig. IE.7-1, a contour map of the intensity of N_2H^+ formed by collision of 75-eV N_2^+ on methane. The detected product tends to be concentrated at angles close to the original direction of the N_2^+ projectile. The quantity Q is the difference between the exothermicity of the reaction and the internal excitation energy of the products. Virtually all products lie in the regions of negative Q, which indicates a high degree of excitation of both N_2H^+ and CH_3. This internal excitation tends to increase as the scattering angle increases.

The nonreactive scattering is shown in Fig. IE.7-2 for 75-eV N_2^+ on CH_4. Again as the scattering angle increases, the internal excitation of the product increases. For an angle as large as 45-deg, the most probable internal excitation is between 4.4 and 8.2 eV. It is not clear how this energy is disposed in the products. Possibilities include dissociation of the CH_4 to CH_3 and H or CH_2 and 2H, or excitation of the N_2^+ to the $A^2\Pi$ state (1.12 eV), the $B^2\Sigma$ state (3.2 eV), or the $C^2\Sigma$ state. Further studies with CD_4 targets may clarify this point.

8. ION-CYCLOTRON RESONANCE MASS SPECTROMETRY

Robert Horton, Richard M. Lambert, and Bruce H. Mahan

Ion cyclotron resonance is a relatively new form of mass spectrometry which offers certain features useful for the study of ion-molecule reactions. One of these is the possibility of using the double resonance technique for the establishment of reaction mechanisms. In one of our experiments, the ion detector was set to detect a modulated negative ion signal at mass 30. Then N_2O was introduced, and a modulated "heating" field at the cyclotron resonance frequency of mass 16 was turned on. A signal at mass 30 was detected, which indicated that the reaction

$$O^- + N_2O \rightarrow NO^- + NO$$

was occurring. Such a specific demonstration that a given daughter ion is due to the reaction of a particular parent ion makes it possible to deduce the elementary reactions, we have modified our instrument so as to be able to produce ions by modulated photoionization. Measurement of the phase of the modulated signal of daughter ions relative to the parent should permit the calculation of reaction rate constants. First attempts to do these experiments have been promising, but have not yet produced definite results.

9. MOLECULAR FRAGMENTATION BY ELECTRON IMPACT

Mien-Hsuing Cheng and Bruce H. Mahan

We have continued the development of an apparatus to measure the angular and energy distribution of ions produced by electron impact. When a molecular beam of N_2 is bombarded with 50-volt electrons, the N_2^+ ions have an angular distribution closely approximating the neutral molecular beam distribution, as expected. The N^+ ions, however, show an apparently isotropic angular distribution and kinetic energies of approximately 3 eV. These observations are consistent with recent experiments of Kieffer and Van Brunt.[1] We have also measured the angular distribution of N^+, O^+, NO^+, and N_2^+ from ionization of N_2O. At present, attempts are being made to remove extraneous factors which may be distorting these distributions.

1. L. J. Kieffer and R. J. Van Brunt, J. Chem. Phys. 46, 2728 (1967).

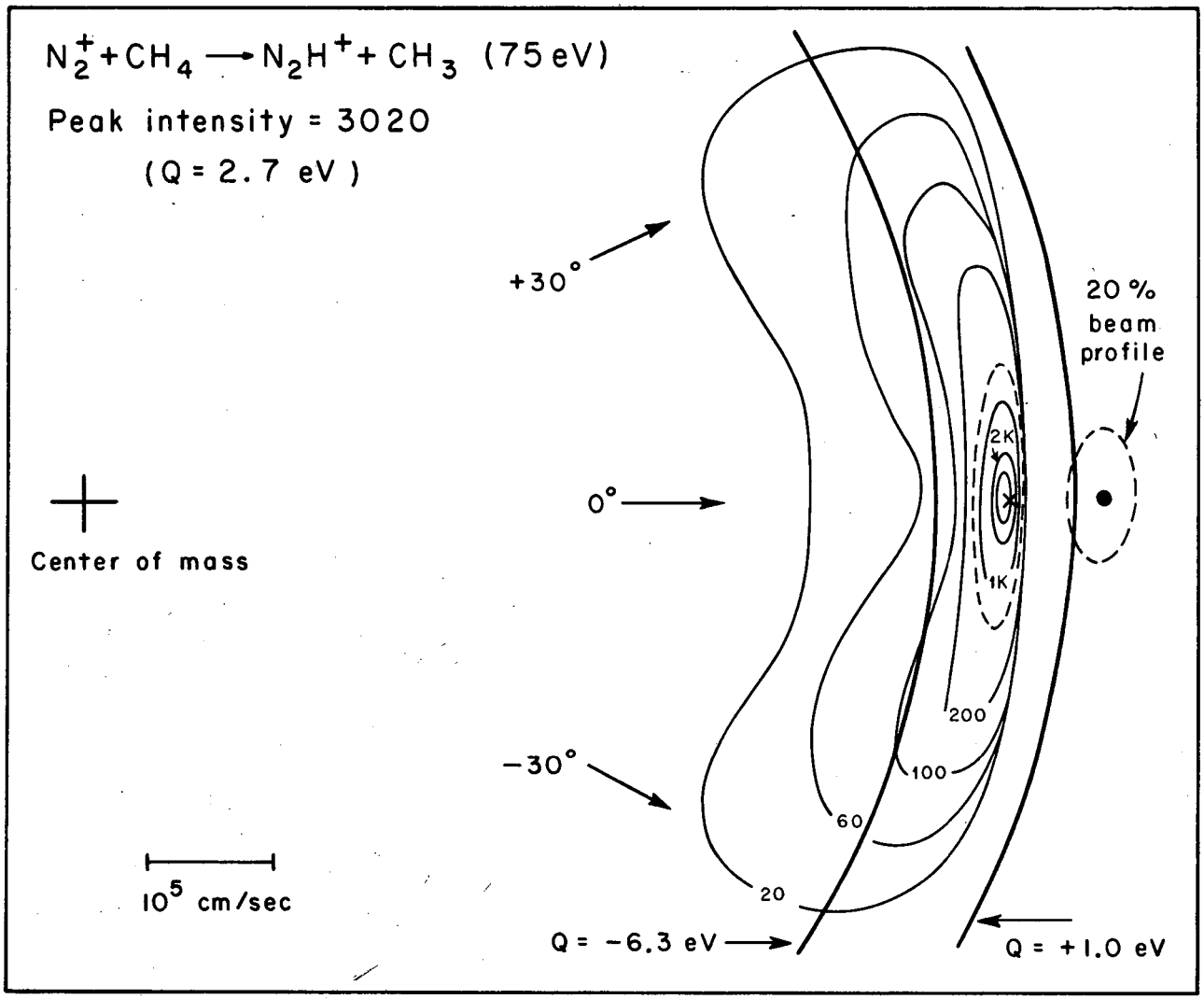

XBL682-1952

Fig. IE.7-1. Contour map of N_2H^+ intensity produced from the reaction $N_2^+ + CH_4 \rightarrow N_2H^+ + CH_3$ at 27.2 eV relative energy.

10. MASS SPECTROMETRY OF HIGH-PRESSURE IONIZED GASES

Michael Mosesman and Bruce H. Mahan

We are continuing studies of the concentrations of ions in photoionized nitric oxide at pressures up to 10 torr. Apparent equilibrium constants for the reactions

$$NO^+ + NO = N_2O_2^+$$

and

$$N_2O_2^+ + NO = N_3O_3^+$$

have been studied as a function of sampling pinhole size, pressure, temperature, and accelerating voltages in the sampling system. Some of our earlier data were found to be affected by gas cooling effects associated with expansion of the gas upon passing through the sampling pinhole. Use of smaller, laser-drilled pinholes has made this effect less serious. It is not yet clear that all extraneous factors that can distort the ion concentration ratios have been eliminated completely, and work is continuing to accomplish this. Our qualitative observations do show, however,

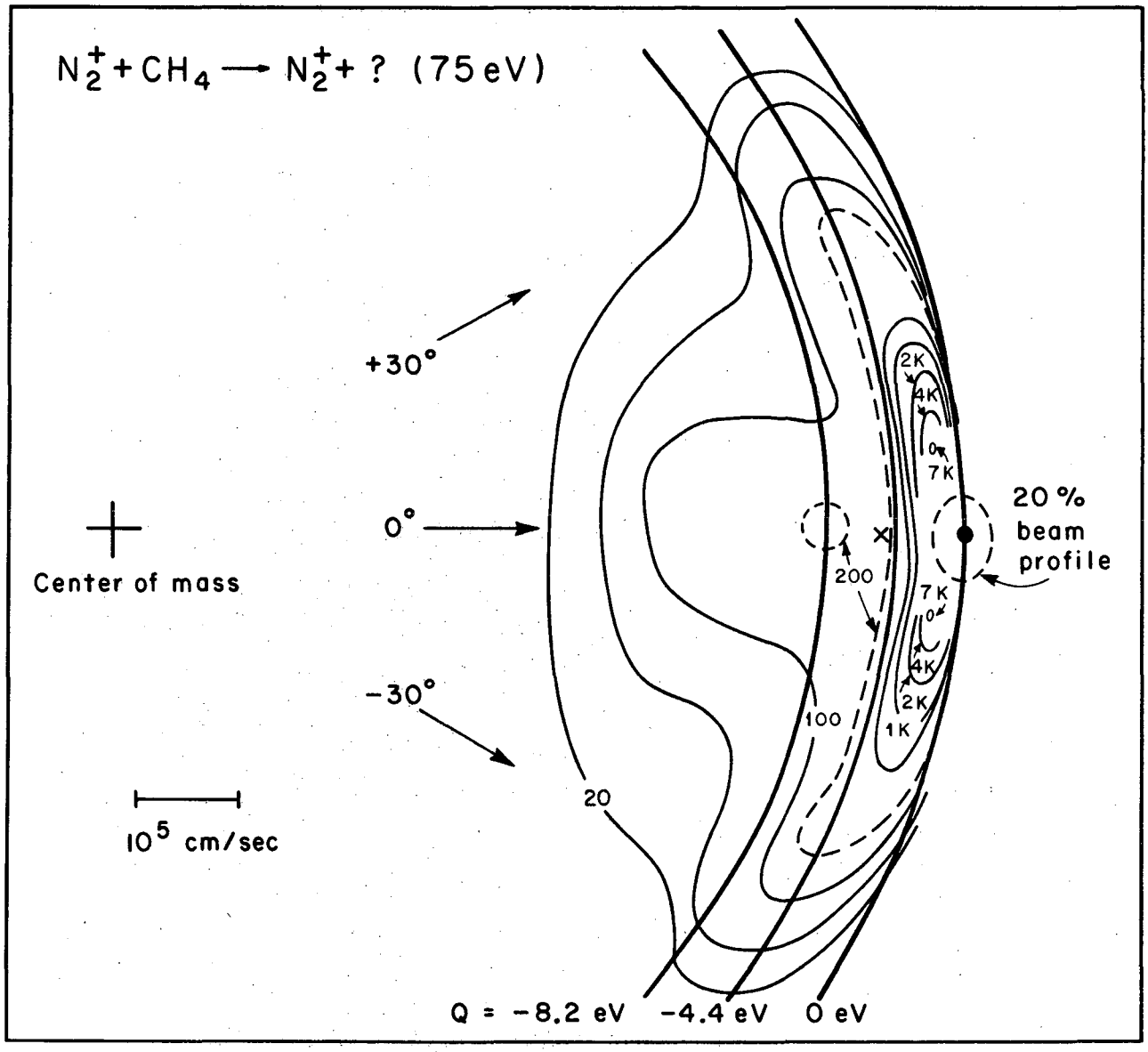

XBL682-1951

Fig. IE.7-2. Contour map of N_2^+ scattered by CH_4 at 27.2 eV relative energy.

that the association energy of the above reactions is of the order of 0.5 eV, and that while $N_2O_2^+$ is observed readily, $(NO^+)N_2$ is not observed under the same conditions of temperature and partial pressure. Thus, the ion-neutral bonding in $N_2O_2^+$ must involve more than the simple ion-induced dipole potential.

11. RESEARCH PLANS FOR CALENDAR YEAR 1968

Bruce H. Mahan

Work in 1968 will be mainly concerned with ion-molecule reactions, molecular ionization, and ion-neutral association. Molecular-beam studies of the reactions of simple ions like N^+, O^+, and C^+ with simple targets like H_2, D_2, and hydrocarbons will be carried out. The inelastic nonreactive scattering in such systems will also be studied.

Investigations of the dynamics of the fragmentation of molecular ions will continue, and ion-cyclotron resonance mass spectrometry will be used to study the reactions of negative ions and of positive ions produced by photoionization.

12. 1967 PUBLICATIONS

Bruce H. Mahan and Associates

Technical Journals

1. A. Falick and B. Mahan, The Collisional-Radiative Reaction of $O_2(^1\Delta_g)$, J. Chem. Phys. 47, 4778 (1967).
2. G. A. Fisk, B. Mahan, and E. K. Parks, Gaseous Ion Recombination Rates. IV., J. Chem. Phys. 47, 2649 (1967).
3. W. Gentry, E. Gislason, Y. Lee, B. Mahan, and C. Tsao, Product Energy and Angular Distributions from the Reaction of N_2^+ with Isotopic Hydrogen Molecules, Dis. Faraday Soc. 44, 137 (1967).
4. W. R. Gentry, E. A. Gislason, B. H. Mahan, and C. Tsao, Inelastic Scattering of N_2^+ by Helium, J. Chem. Phys. 47, 5 (1967).
5. B. Mahan, Resonant Transfer of Vibrational Energy in Molecular Collisions, J. Chem. Phys. 46, 1 (1967).
6. B. Mahan and I. C. Walker, Rate of Attachment of Gaseous Electrons to Nitrogen Dioxide, J. Chem. Phys. 47, 3780 (1967).

UCRL Reports

1. A.M. Falick, An EPR Study of the $O_2(^1\Delta_g)$ Molecule (Ph.D. Thesis), UCRL-17453, June 1967.
2. W. R. Gentry, A Beam Study of $N_2^+ + H_2$, HD, D_2 Reaction Dynamics (Ph.D. Thesis), UCRL-17813, September 1967.
3. W. R. Gentry, A Versatile Apparatus for Measuring Total and Differential Cross Sections for Ion Neutral Interactions, UCRL-17691, July 1967.
4. B. Mahan, Gaseous Ion Recombination Rates. V., UCRL-17827, September 1967.
5. E. Parks, The Capture Radius for Ion Recombination, UCRL-17754, August 1967.

13. LEAST-SQUARES-ADJUSTED ASSIGNMENTS FOR THE ESR SPECTRA OF FREE RADICALS IN SOLUTION

Alfred Bauder, Raymond Pao, and Rollie J. Myers

In most forms of spectroscopy even skilled spectroscopists still only utilize a fraction of the available data. While signals may be recorded for an entire spectrum only that part of the spectrum in the vicinity of certain maxima or minima are most commonly used in the final act of data reduction. The reasons for this are two-fold. First, one often has only a theoretical prediction of a spectrum in a limited region, and data reduction is done only for that region. Second, one often does not have the necessary method for including all the data for analysis, since a complete spectrum can contain a considerable amount of information. High-speed digital computational techniques have essentially solved this second problem, if the spectroscopic data are taken in a form that can be easily "read" by a computer. Since almost any kind of a spectroscopic instrument can now yield data which by off-line or on-line techniques are computer compatible, the major limitation now depends upon the first problem.

The electron-spin-resonance spectra of free radicals in solution can be readily predicted by a simple Hamiltonian. In addition, the theoretical line-shape function is Lorentzian and little or no deviation from this line-shape function is expected. Under these circumstances the entire ESR spectrum of a free radical in solution depends upon only a few parameters. There is one coupling constant for each proton, nitrogen, etc. in the radical. There is a g value for the center of the spectrum, and there is often only a single line-width parameter. Limitations in instrumentation demand three additional parameters - one for total intensity, and two for base-line offset and drift. The major problem in instrumentation is to provide an accurate indication of magnetic field. This was done by constructing a field-locked NMR probe so that magnetic field changes as small as 10^{-3} gauss are automatically measured by a frequency counter.

With our Honeywell-EI Automatic Data Logging System Model S6114, seven decimal figures of magnetic field and five decimal figures of ESR signal are recorded in 0.1 sec on magnetic tape in NRZ1 computer code. A series of computer programs[1] have been prepared to smooth these data and to fit them by least squares to a theoretical spectrum. The computer program continues to make a least-squares adjustment of the parameters until convergence is obtained.

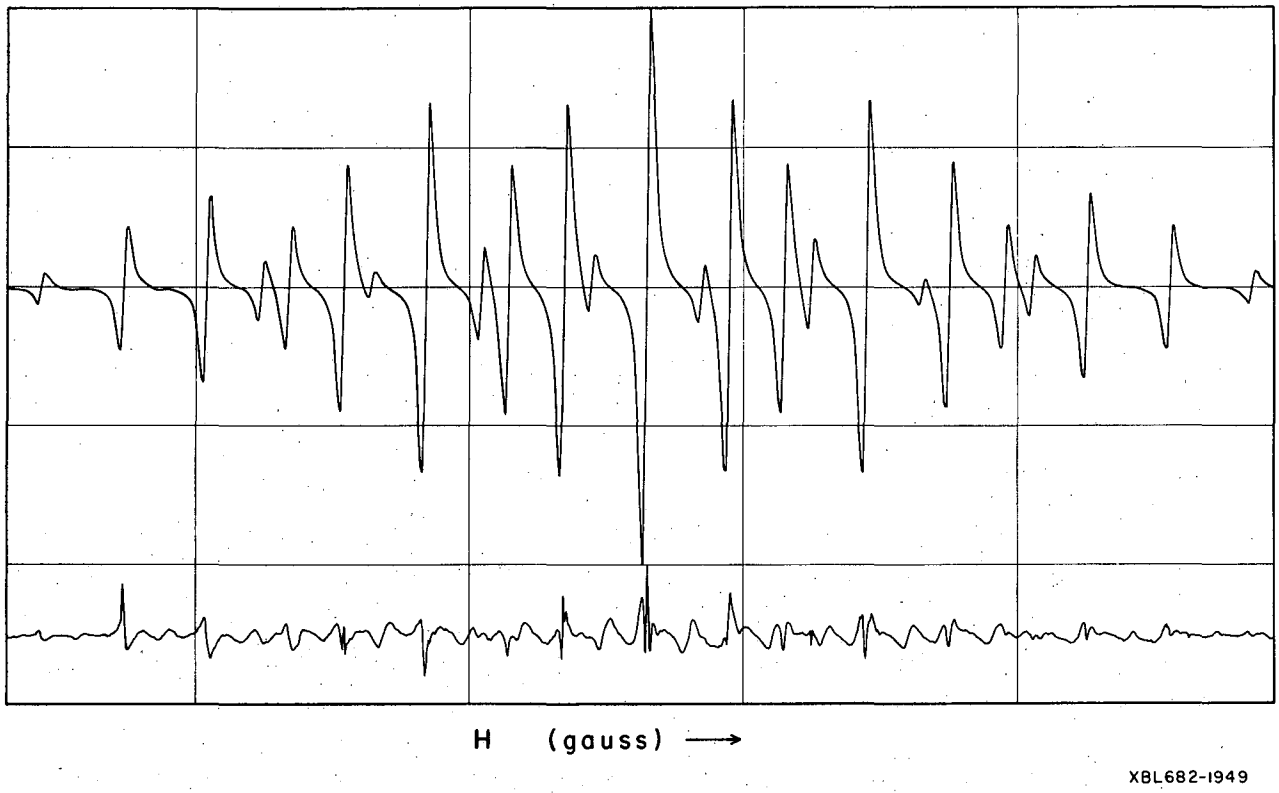

Fig. IE.13-1. Least-squares fit to ESR spectrum of pyrazine-radical anion. About one-half of the 2000 smoothed data points are shown. The lower error curve has a scale magnification of 2.762.

Figure IE.13-1 illustrates this method for the radical anion of pyrazine in liquid ammonia. This spectrum had been assigned previously and we obtained coupling constants for the two equivalent nitrogens and the four equivalent hydrogens. The least-squares-adjusted fit with the experimental spectrum is shown in this figure. Approximately 15,000 data points were smoothed to 2,000 points and the least-squares adjustment was made to these 2,000 points. The resultant coupling constants are ten times as accurate as were previously obtained.[2]

An interesting feature of the complete fit to the spectrum is shown in the error curve. On the side of each line in the main spectrum are weak (4%) C-13 satellite signals. Previous workers[3] had assigned this C-13 spectrum, but from our work their assignment appears to be in error, since they assigned two satellite lines on each side, while Fig. IE.13-1 shows only one.

1. A. Bauder and R. J. Myers, Least-Squares Curve Fitting of ESR Spectra, UCRL-17829, September 1967.
2. C. L. Talcott and R. J. Myers, Mol. Phys. 12, 549 (1967).
3. E. W. Stone and A. H. Maki, J. Chem. Phys. 39, 1635 (1963).

14. TEMPERATURE DEPENDENCE OF THE EPR SPECTRUM OF $Cu(H_2O)_6^{++}$ IN WATER

James J. Chang and Rollie J. Myers

The EPR spectrum of the hexaquocopper(II) ion in solution has been measured as a function of temperature at 9000 MHz. It has been known for some time that near 0°C the linewidth tends to decrease as temperature is increased, but that above 0° the linewidth increases as temperature is increased.[1] Several mechanisms have been proposed which adequately explain the low-temperature behavior of the spectrum.[2] However, there is as yet no good explanation which also explains the high-temperature behavior.

At room temperature the hexaquocopper(II) ion exhibits a single broad line in the EPR spectrum with a linewidth of about 150 gauss. However, since the common copper nuclei have a spin with I = 3/2, the spectrum is expected to be composed of four lines corresponding to transitions between the four hyperfine components. The single line is found to be a superposition of these four lines, and the hyperfine structure may be seen in the spectrum at 0°.[3] But, for a linewidth study, the linewidth of interest is that due to a single hyperfine component. However, the spectrum is only partially resolved, and moreover, the linewidths exhibit an m_I dependence so that an accurate determination of the linewidths for each of the hyperfine components is difficult. Also, an accurate determination of the constants of the spin Hamiltonian, which is necessary for an adequate understanding of the linewidths, is difficult to make for an unresolved spectrum.

To determine the spin-Hamiltonian parameters g and A and the linewidths, a least-squares fitting program has been used in connection with our data-acquisition equipment. The spectrum is digitally recorded on magnetic tape with a Honeywell-EI Automatic Data Logging System Model S6114. The magnetic tape is first processed by a program that smooths the spectrum and reduces the number of data points. The least-squares program fits a sum of Lorentzian lines to the experimental data points, using a second-order spin Hamiltonian.[4] The parameters that are fitted are g, A, and the linewidths. There are also parameters for base-line shift and base-line drift in the experimental spectrum. Good values for the parameters have been obtained in this manner.

Figure IE.14-1 is a graphical presentation of the results of the fit to the spectrum obtained at 0°C. The experimental points are represented by the crosses. The smooth curve is the theoretical spectrum fit to the points. The results of the fit to the spectrum at 40°C are presented in Fig. IE.14-2 to show the goodness of the fit for an unresolved spectrum. Spectra have been fitted over a temperature range from 0 to 50°C.

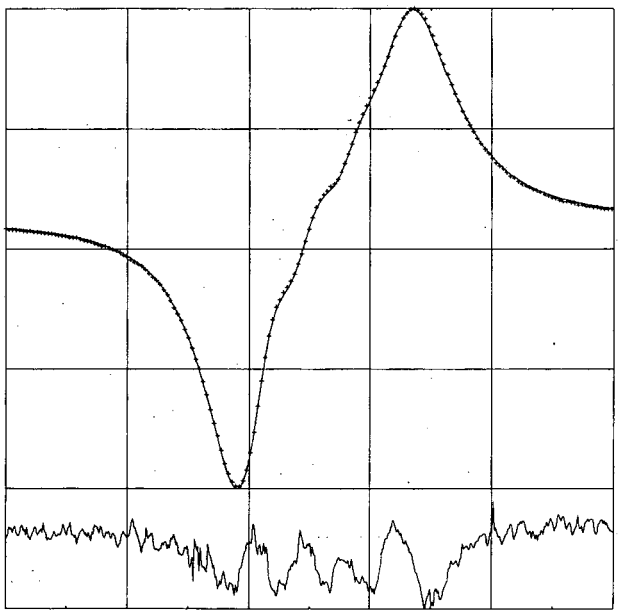

Fig. IE.14-1. Least-squares fit to $Cu(H_2O)_6^{+2}$ at 0°C. Note slight quartet structure in this spectrum. The lower error curve has a scale magnification of 15.11.

One possible mechanism for the high-temperature behavior is the rotational-spin-orbit mechanism due to Kivelson.[5] According to Atkins and Kivelson, the contribution to the linewidth due to this mechanism is given by

$$T_2^{-1} = (12\pi r^3)^{-1}(\Delta g_{\parallel}^2 + 2\Delta g_{\perp}^2)\, kT/\eta \ .$$

The linewidths may then be plotted as a function of T/η. The linewidths for $Cu(NH_3)_6^{++}$ in liquid ammonia determined by Spencer[1] may also be plotted. We may then compare the slopes of the lines. Since the hydrodynamic radii, r, of both species are about the same, the ratio of the slopes would be expected to be close to

$$\frac{(\Delta g_{\parallel}^2 + 2\Delta g_{\perp}^2)_{H_2O}}{(\Delta g_{\parallel}^2 + 2\Delta g_{\perp}^2)_{NH_3}}$$

if the rotational-spin orbit mechanism were the dominant mechanism. However, our experimental ratio and the theoretical ratio do not agree

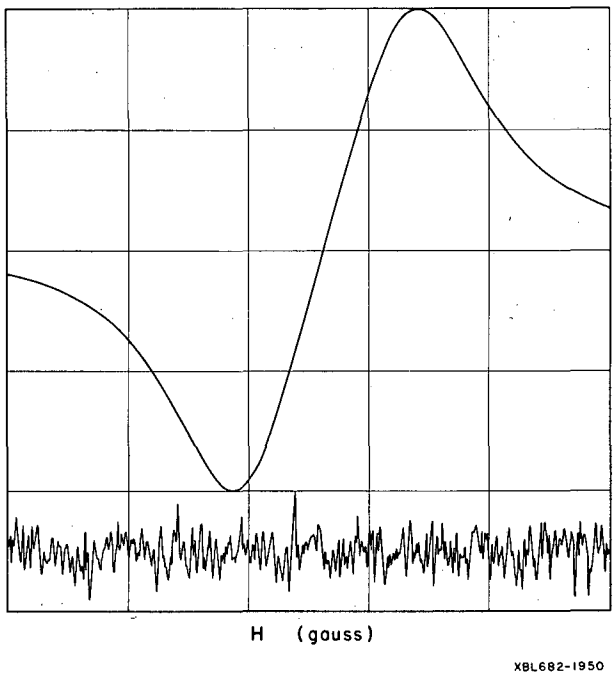

Fig. IE.14-2. Least-squares fit to $Cu(H_2O)_6^{+2}$ at 40°C. The lower error curve has a scale magnification of 11.519. Note complete absence of any obvious structure, but error curve shows essentially perfect fit by four hyperfine lines.

with each other by about a factor of two. One can conclude that either the hydrodynamic radii are not the same or we do not know the Δg values. Recently[6] it has been argued that the Δg values may be much smaller in solution for $Cu(H_2O)_6^{+2}$, but it may be very difficult to determine the correct Δg values for these solutions.

1. J. B. Spencer, Electron Spin Resonance Studies of Transition Metal Ion Complexes (Ph.D. Thesis), UCRL-16175, August 1965.
2. H. M. McConnell, J. Chem. Phys. 25, 709 (1956); see also V. I. Avvakumov, Sov. Phys. JETP 37, 1017 (1959); Eng. Trans. 10, 723 (1960).
3. R. G. Hayes, Electron Spin Resonance Linewidths (Ph.D. Thesis), UCRL-9873, September 1961.
4. A. Bauder and R. J. Myers, Least-Squares Curve Fitting of EPR spectra, UCRL-17829, September 1967.
5. P. W. Atkins and D. Kivelson, J. Chem. Phys. 44, 169 (1966).
6. W. B. Lewis, M. Alei, Jr., and L. O. Morgan, J. Chem. Phys. 45, 4003 (1966).

15. ELECTRON-SPIN-RESONANCE SPECTRA NEAR 1°K

David W. Pratt,† Akira Jindo,
W. Thomas Batchelder, and Rollie J. Myers

The pumping speed of our liquid helium dewar system has been improved so that spectra can now be taken down to 1.2°K. Our previous work on VCl_4 in $TiCl_4$ has been continued, and the source of our complex spectra has been determined.

In our previous work dilute samples of VCl_4 in $TiCl_4$ were quick-frozen in liquid nitrogen and then rather slowly cooled to liquid helium temperature. It was found that complex spectra were obtained, and exactly the same spectrum was never obtained after recooling the sample. Other workers[1] have made similar observations, and upon their suggestion we have checked the anisotropy of our samples.

To do this we have used a cylindrical cavity and a rotating magnet. When this was done we observed that our spectra were anisotropic. If the samples were slowly cooled by radiation in the dewar instead of being plunged into liquid nitrogen, about the same amount of anisotropy was observed. It seems quite clear now that, instead of polycrystalline glass, we are obtaining fairly large crystallites, so that over a volume of about 1cc all random orientations are not obtained. We have found however, that both CCl_4 and mineral oil have formed a good glass in our apparatus.

Since in our attempts at an assignment for VCl_4 in $TiCl_4$ we assume all random orientations, it is now clear why we could not assign these spectra. We shall have to obtain either a single crystal of $TiCl_4$ or find a better technique for forming glasses.

Work has also been done on single crystal of α-$NiCO_4 \cdot 6H_2O$. This is reported to be paramagnetic down to 1°K and its magnetic parameters have been well established.[2] At 9,000 MHz we observed some transition which can be ascribed to multiple quantum transitions for the Ni^{2+} ions. However, additional signals are observed which must be due to Co^{2+} impurity ions. It should be possible to use the Co^{2+} spectrum as a probe to study the behavior of the Ni^{2+} in this concentrated paramagnetic. The low temperatures are necessary for the Co^{2+} spectrum to be broadened above 1.5°K. This must be due to relaxation by the Ni^{2+} ions for most Co^{2+} spectra are quite sharp at 4.2°K. Many new effects are quite possible in concentrated paramagnetics and a study of such systems should prove to be particularly interesting.

† Present address: Department of Physics, University of California at Santa Barbara.

1. Dr. Rolf B. Johannsen, National Bureau of Standards, private communication.
2. R. A. Fischer, E. W. Hornung, G. E. Brodale, and W. F. Giauque, J. Chem. Phys. 46, 4945 (1967).

16. THE ESR SPECTRA OF THE RADICAL ANIONS OF METHYL-SUBSTITUTED NITROSOBENZENES

Carolyn L. Talcott and Rollie J. Myers

Several years ago we assigned the ESR spectrum of nitrosobenzene radical anion in liquid ammonia.[1] The analysis of the spectrum was quite simple, but the assignment of the coupling constants to specific hydrogens was difficult. Since the C-N-O bond is not linear, five separate proton coupling constants are obtained. The simplest choice of proton coupling constant is to expect that both ortho and both meta coupling constants would be close in value and that the para coupling constants would be essentially the unique one. Our final assignment was based upon these assumptions.

Other work[2] has indicated that these assumptions were wrong, and that one ortho was close to the para and that the other ortho formed the unique coupling constant. In order to have such a set of coupling constants one would seem to have a large asymmetry in the pi system of the molecule, and on theoretical grounds this appeared to be unlikely.

In order to test our assignment for nitrosobenzene, it is necessary to make substitutions for the protons. Deuterium substitution is chemically difficult, so we used methyl substitutions. It is well known that, except for certain degenerate systems, methyl substitutions have little effect on pi systems. The results for some methyl-substituted nitrosobenzenes are given in Table IE.16-I.

These data show clearly that one ortho coupling constant is close to the para, and that the other ortho forms the unique one. We have revised our assignment for nitrosobenzene accordingly, as shown in the table.

The remaining problem is the theoretical one of explaining why the ortho coupling constants differ by one gauss. The previously proposed α and β effects produce an asymmetry in the pi system but it is difficult to justify the large Hückel constants that must be used. An alternate mechanism is to assume a spin polarization mechanism utilizing the oxygen of the NO group with the adjacent CH bond. This can be called the Q effect. Calculations indicate that this is a reasonable model and it agrees with the data for o-nitrosotoluene, where one expects the larger ortho coupling to belong to the cis hydrogen.

Table IE.16-I. Coupling constants for methyl substituted radical anions of nitrosobenzene in liquid ammonia.[a]

Substitution	A (N)	A (ortho)	A (meta)	A (para)
para	8.21	3.94 3.04	1.12 1.12	4.28[b]
ortho	7.66	4.05 2.20[b]	1.20 0.99	4.05
----	7.97	3.99±.15 2.97	0.96 1.14	3.99±.15

a. values in gauss.
b. coupling constant for methyl protons.

1. D. H. Levy and R. J. Myers, J. Chem. Phys. 42, 3731 (1965).
2. E. J. Geels, R. Konaka, and G. A. Russell, Chem. Commun. 2, 13 (1965). P. B. Ayscough, F. P. Sargent, and R. Wilson, J. Chem. Soc. (B) 1966, 903.

17. NMR SPECTRUM OF CHLORINE-35 IN LIQUID VCl_4 AND $TiCl_4$

David W. Pratt* and Rollie J. Myers

The ^{35}Cl NMR spectrum of pure VCl_4 at room temperature consists of a broad line whose peak-to-peak width in a derivative presentation is approximately 2.25 KHz or 5.40 gauss. This is the kind of broad signal characteristic of ^{35}Cl signals in similar compounds like $TiCl_4$. However, the position of the VCl_4 resonance is temperature-dependent due to the Fermi-contact interaction with the odd electron in VCl_4.

Utilizing Cl^- in H_2O as reference, we have measured the position of the ^{35}Cl resonance in VCl_4 as a function of temperature. A plot of our results is shown in Fig. IE.17-1. It is well known that in a paramagnetic molecule at high temperatures the electron-nuclear coupling is reduced to zero for systems with a short spin-lattice relaxation time for the electron. From the slope of the line in Fig. IE.17-1, it can be determined that in VCl_4 that $A(^{35}Cl)/g\beta = +0.527 \pm 0.050$ gauss. This is of considerable value in our ESR work on VCl_4 of liquid helium temperatures. The positive sign for this A value is consistent with only π bonding between the vanadium and the chlorine for the

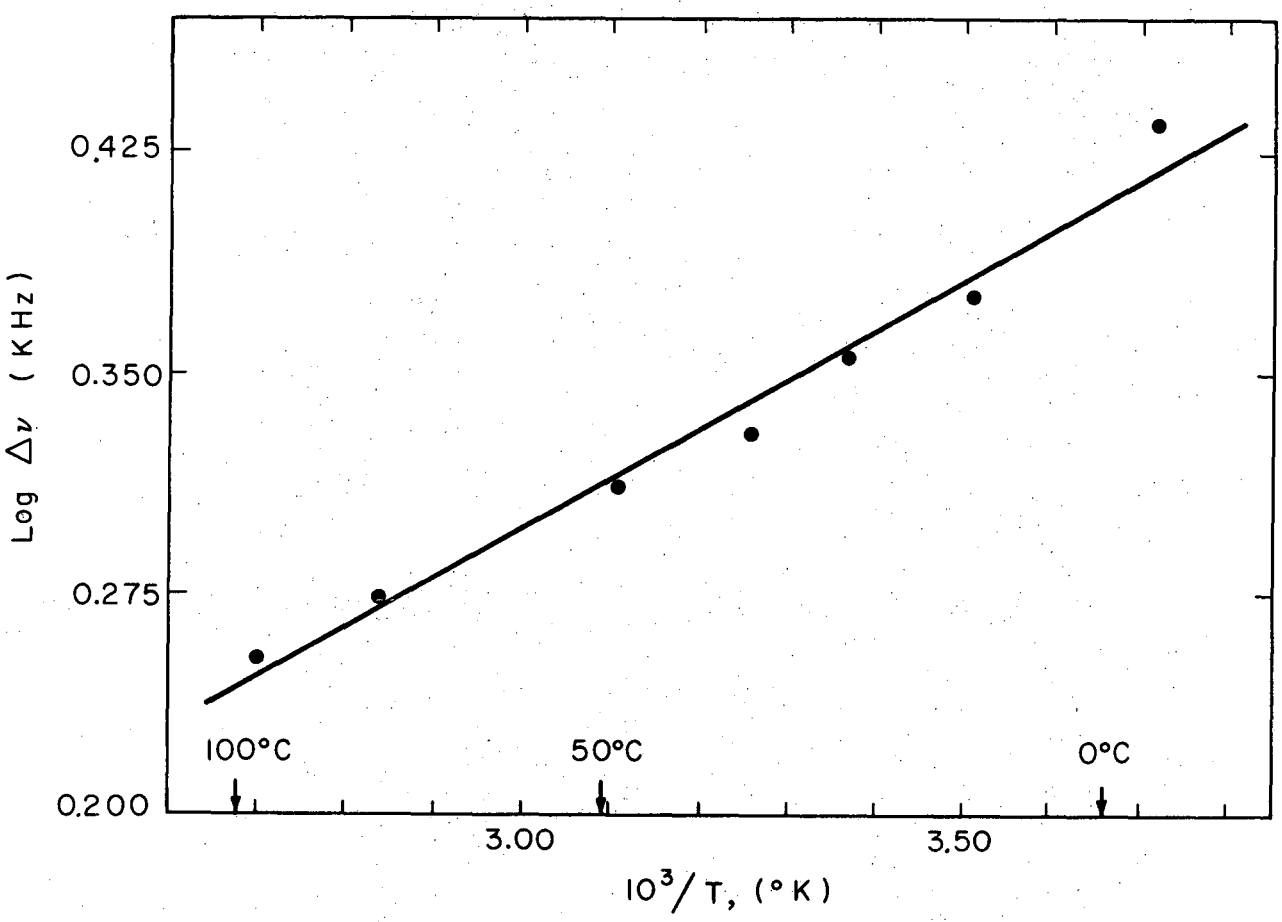

XBL673-2352

Fig. IE.17-1. NMR shift of ^{35}Cl in VCl_4 vs Cl^- from 0 to 100°C.

unpaired 3d electron.

The NMR linewidths for the VCl_4 and $TiCl_4$ have proven to be particularly interesting. The VCl_4 linewidth decreases nicely as the temperature is raised. This decrease is consistent with a possible combination of electron-spin relaxation and nuclear-quadrupole relaxation. However, the $TiCl_4$ linewidth decreases only slowly as the temperature is raised. This is in contradiction to the theory[1] of linewidth in liquids due to nuclear-quadrupole relaxation. It seems clear that the linewidth in $TiCl_4$ is more complicated than has been previously assumed, and similar systems should be investigated further.

---

* Present address: Department of Physics, University of California, Santa Barbara.

1. A. Abragam, The Principles of Nuclear Magnetism (Oxford Press, London, 1961), p. 346.

18. RESEARCH PLANS FOR CALENDAR YEAR 1968

Rollie J. Myers

The digital system will be extended so that one spectrometer will be all digital, including a digital sweep. Our present programs will be extended to include more possible variations in linewidth and line shape. The full potential of off-line operation will be explored.

The work near 1°K will be continued on single-crystal and glass systems. VCl_4 will be substituted in a single-crystal system, and its spin Hamiltonian and relaxation parameters will be finally established. Work will continue on $NiSO_4 \cdot 6H_2O$, $V(CO)_6$, and other systems being presently investigated.

In our gaseous radical work particular attention will be given to time-averaging techniques for short-lived species. The potential of vacuum-ultraviolet irradiation will also be explored. Techniques will also be developed for extending magnetic-resonance techniques to polyatomic radicals.

Work on transition-metal complexes in solution will be continued. Both normal ESR spectra and dynamic nuclear polarization will be utilized. Both NMR and ESR methods will be investigated for the problems of spin relaxation in solution.

19. 1967 PUBLICATIONS

Rollie J. Myers and Associates

Technical Journals

1. D. C. McCain and R. J. Myers, Spin-Lattice and Spin-Spin Relaxation Times for VO^{2+} in Aqueous Solution, J. Phys. Chem. 71, 192 (1967).
2. D. W. Pratt and R. J. Myers, The Electron Spin Resonance Spectrum of Vanadium Hexacarbonyl at Liquid Helium Temperatures, J. Am. Chem. Soc. 89, 6470 (1967).
3. C. L. Talcott and R. J. Myers, Electron Spin Resonance Spectra of the Radical Anions of Pyridine and Related Nitrogen Heterocyclics, Mol. Phys. 12, 549 (1967).

UCRL Reports

1. A. Bauder and R. J. Myers, Least-Squares Curve Fitting of EPR Spectra, UCRL-17829, September 1967.
2. D. W. Pratt, Magnetic Resonance Spectra of VCl_4 and Other Paramagnetic Species (Ph.D. Thesis), UCRL-17406, May 1967.
3. C. L. Talcott, Electron Spin Resonance Studies of Radicals Produced by Electrolysis (Ph.D. Thesis), UCRL-17743, September 1967.

20. SPECTRA AND LIFETIMES OF GAS-PHASE FREE RADICALS AT VERY LOW CONCENTRATIONS

Harold S. Johnston, E. D. Morris Jr., Thomas T. Paukert, and Jack van den Bogaerde

Photochemical reactions may occur with quite different mechanisms at high and at low light intensities.[1] Under conditions of high light intensities in flash photolysis, radicals are typically produced at a pressure of about 1 torr and with a half-life of about 10^{-5} seconds. With a moderately intense steady light source, the same reaction would give radical pressure of about 10^{-5} torr and half-life of about 1 sec.[1] We have in operation a general method of observing the infrared[2] or ultraviolet[3] spectra of radicals in low-intensity photolyses. This method, which gives both spectral and kinetic data at low light intensities, may be regarded as supplementary to high-intensity kinetic spectroscopy.

Upon photolysis of Cl_2 in the presence of O_2, the familiar ClO radical has been observed both by ultraviolet and infrared absorption. The postulated[4] but previously unseen peroxy radical ClOO has also been observed in both ultraviolet and infrared regions. In the ultraviolet region ClO has bands between 2700 and 2900Å and a continuum with a maximum at 2650Å; ClOO shows continuous absorption between 2200 and 2700Å with a maximum at about 2450Å. In the infrared region ClO absorbs around 940 cm^{-1} and ClOO shows a doublet at 1437 and 1450 cm^{-1}. So far, these spectra are of low resolution. Reaction rates as deduced from observed phase shifts are in fairly good agreement with results of flash photolysis, but some differences require further detailed study.

The photolysis of ozone in the presence of hydrogen peroxide gives evidence of gas-phase infrared absorptions by the elusive HO_2 radical. Although there is evidence of absorption at all three fundamental frequencies reported from matrix-isolation studies,[5] two of these regions show strong interference by H_2O and H_2O_2. The third frequency at 1125 cm^{-1} is sufficiently clear of interference to be used to get kinetic data on the HO_2 radical.

1. H. S. Johnston and F. Cramarossa, Advan. Photochem. 4, 1 (1965).
2. H. S. Johnston, G. E. McGraw, T. T. Paukert, L. W. Richards, and J. van den Bogaerde, Proc. Nat. Acad. Sci. 57, 1146 (1967).
3. E. D. Morris, Jr., current Ph.D. research.
4. G. Porter and F. J. Wright, Disc. Faraday Soc. 14, 23 (1953).
5. D. E. Milligan and M. E. Jacox, J. Chem. Phys. 38, 2627 (1963).

21. KINETICS OF NO_2 ELECTRONIC FLUORESCENCE

Stephen E. Schwartz and Harold S. Johnston

The molecule NO_2 absorbs radiation strongly from 3000 to 6000Å. Below 4000Å the molecule is dissociated to NO and O, and above 4000Å it fluoresces.[1-3] The fluorescence lifetime is a matter of great interest in molecular dynamics, since the observed radiative lifetime is greater by two orders of magnitude than that predicted from the absorption coefficient.[3,4]

By means of a phase-shift technique, we are measuring the lifetime as a function of the exciting wavelength, using a narrow (±12Å) spectral source tunable through the region 4000 to 6000Å. In some experiments the lifetime was measured over a wide range of wavelengths by a photomultiplier sensitive to 8000Å, and in other experiments filters provided a narrow (±50Å) range of observed fluorescence. This technique is designed to make efficient use of the available excitation light. Experimental conditions are typically 1μ pressure of NO_2 and a signal intensity of about 100 counts per second. Observed lifetimes are between 10 and 100 μsec.

We found that the size of the fluorescence cell has an effect on the measured lifetime. In its lifetime the thermal NO_2 molecule travels on the average 2 or 3 cm, a distance comparable to the dimensions of usual fluorescence cells. Experiments are now conducted in a 33-cm-diam, 22-liter bulb, and no effect of wall quenching is detectable in this case.

A series of experiments was made at 1.3μ, with an excitation half-width of 23Å and with broad-band detection. The lifetime as a function of excitation wavelength is given by Fig. IE.21-1. There is a general increase in lifetime as a function of excitation wavelength, as expected, but there are some fluctuations in this dependence. The inset shows the region around 5175Å as excited with a 12Å half-width.

Other experiments were made with variation of NO_2 pressure, with variation of exciting wavelength (4300 to 4800Å), and with variation of wavelength of observation (5020, 5590, and 7500Å). For excitation at 4800Å, the results are plotted according to the Stern-Volmer function in Fig. IE.21-2. The relation of slope to Stern-Volmer quenching rate constant is given by the fan inserted in the figure. The rate constant for hard-spheres collisions is 30×10^{-11} cc/particle-sec for NO_2. The quenching-rate constants are large, approaching the gas-kinetic value. However, the curved lines of Fig. IE.21-2 show

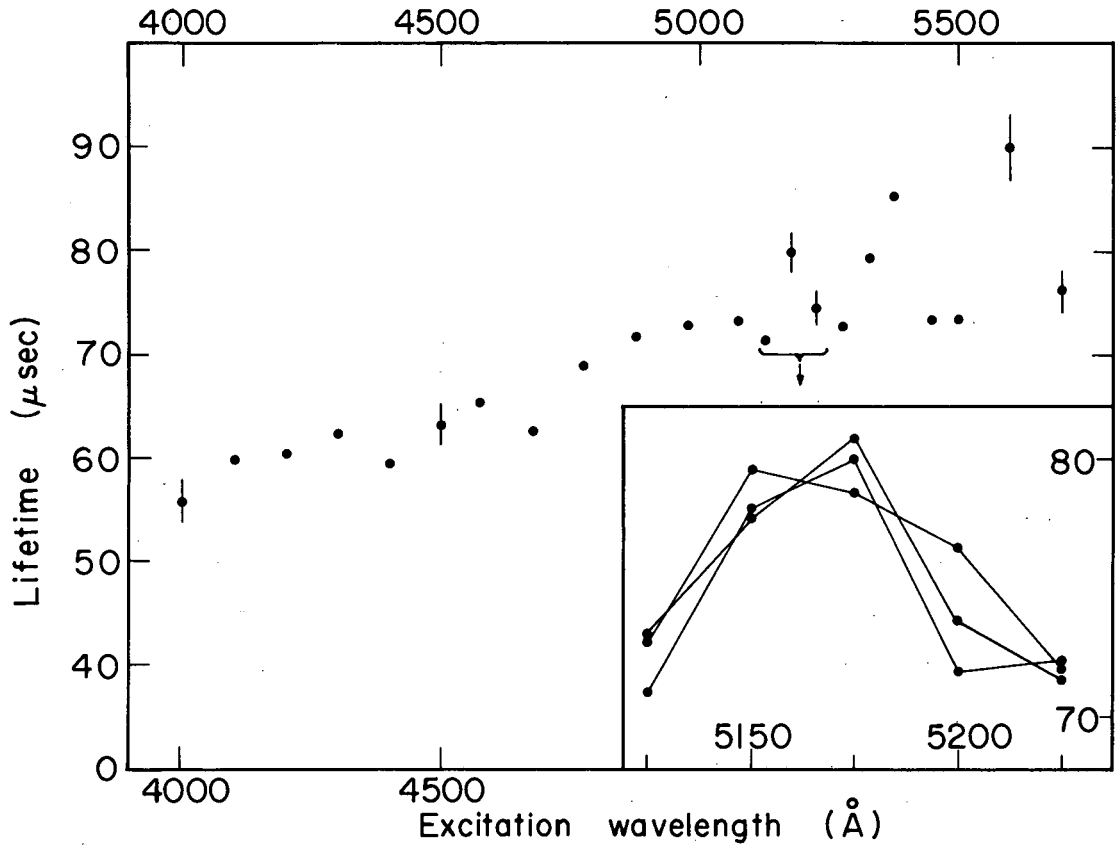

Fig. IE.21-1. Fluorescence lifetime of NO_2 gas at 1.3×10^{-3} torr pressure as a function of excitation wavelength. Half width of excitation light was 23Å. Error bars are typical and were determined from the scatter of several experiments. Inset shows individual data points for the region around 5175Å, excited with 12Å half width. Data points for the same run are connected; points within a run were taken in random order.

that there is a failure of the simple Stern-Volmer mechanism.

Figure IE.21-3 is a similar plot obtained with excitation at 4300Å, and there are striking differences between excitation at 4300 and 4800Å.

These experiments provide a broad range of independent variables, pressure of NO_2, excitation wavelength, and observation wavelength. The observables are lifetime and relative intensity of the fluorescence. These varied data are being interpreted in terms of the molecular dynamics of the excited electronic state; both experimental and theoretical studies are still in progress.

1. W. P. Baxter, J. Am. Chem. Soc. 52, 3920 (1930).
2. O. Heil, Z. Physik 77, 563 (1932).
3. D. Neuberger and A.B.F. Duncan, J. Chem. Phys. 22, 1693 (1954).
4. A. E. Douglas, J. Chem. Phys. 45, 1007 (1966).

22. CHEMILUMINESCENCE FROM IF

Stephen D. Gabelnick and Harold S. Johnston

The gas-phase reaction of fluorine and iodine is accompanied by chemiluminescence in the 4000 to 8000-Å wavelength region. The

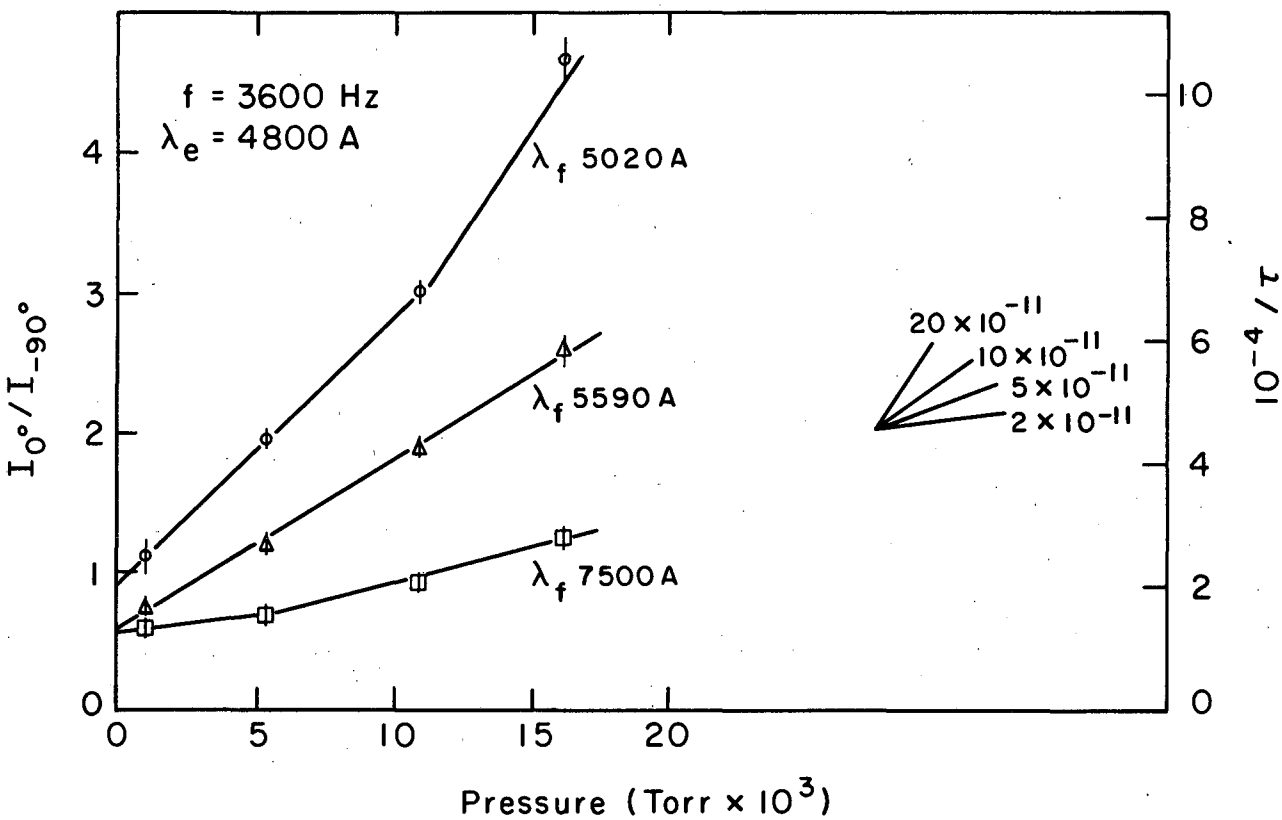

XBL682-1955

Fig. IE.21-2. Inverse lifetime plot of NO_2 fluorescence, excited at 4800Å and observed with interference filters at 5020 and 5590Å. Observation at 7500Å was accomplished with a Corning 7-69 filter. The left-hand coordinate axis is the ratio of in-phase to out-of-phase intensity. The right-hand axis gives the inverse of lifetime calculated under the assumption of Stern-Volmer kinetics. Error bars are determined from the scatter of the data. Equivalence of slope to the quenching-rate constant K_q in units of cc/molecule-sec is given by the fan.

emission has been attributed to the $^3\Pi_{0+} \rightarrow {}^1\Sigma_{0+}$ transition of the chemically unstable diatomic species iodine monofluoride, which had previously been observed in an iodine-fluorine flame by Durie.[1,2] We have found the relative intensities of the vibration-rotation bands of the spectrum to be dependent on the pressure inside the flow reactor, thus indicating that the vibrational deactivation process is competitive in rate with that of spontaneous emission. Making a reasonable estimate for the rate constant of vibrational-translational energy transfer for the reaction

$$IF\ (^3\Pi_{0+},\ v=1) + M \rightarrow IF\ (^3\Pi_{0+},\ v=0) + M,$$

one is able to calculate a radiative lifetime of 10^{-3}-10^{-4} sec for the excited electronic state of iodine monofluoride from the variation of intensity with pressure.

In order to obtain relative populations of the vibrational quantum levels of the excited state of IF, one must determine the Franck-Condon overlap factors. These have been calculated using Rydberg-Klein-Rees potentials[3-5] for both the upper and lower

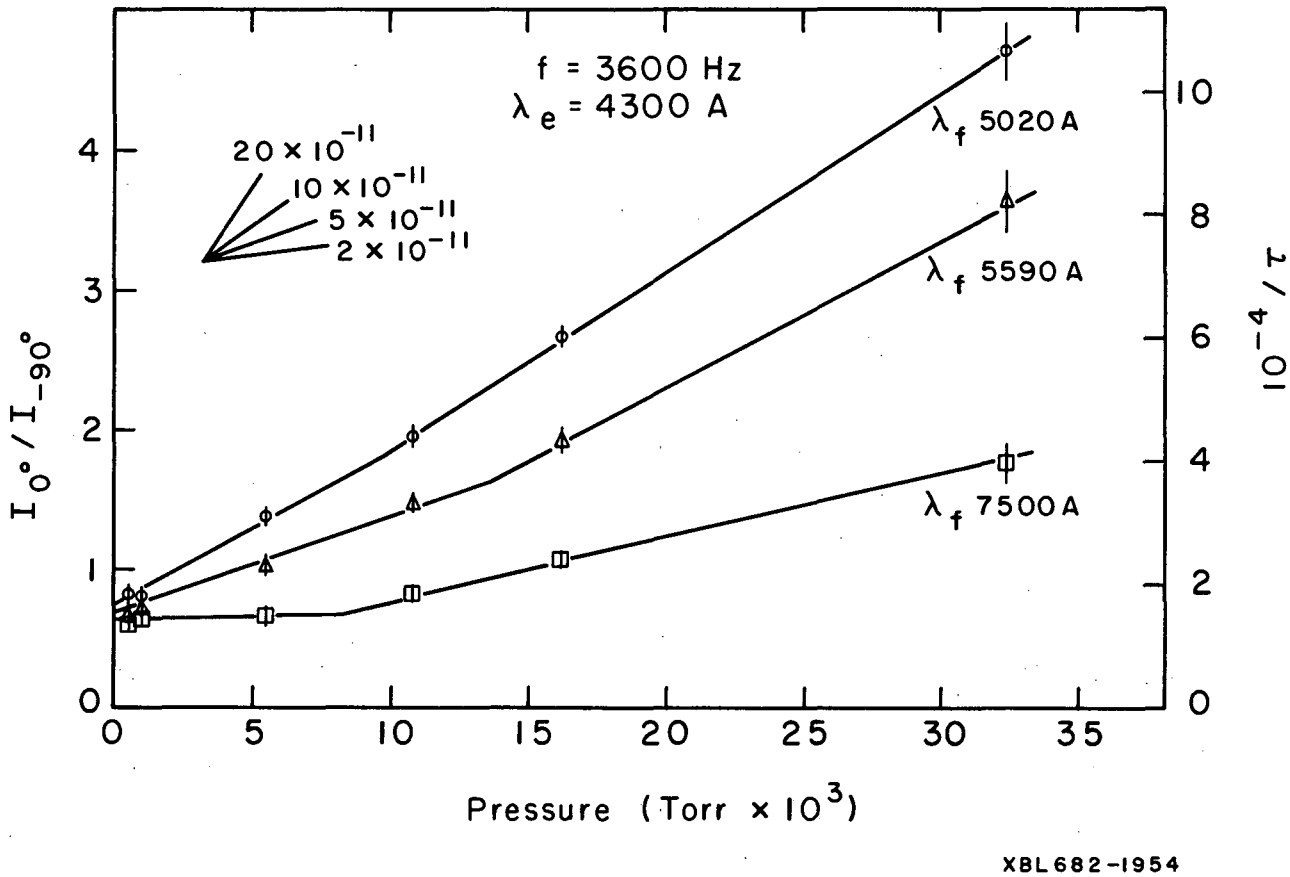

Fig. IE.21-3 Inverse lifetime plot of NO_2 fluorescense excited at 4300A.

electronic states of IF. These require a knowledge of only the vibrational and rotational spectroscopic constants of the molecules; their disadvantage is that they do not yield analytic expressions for the vibrational wave functions. Zare has developed computer programs which give numerical solutions to the Schrodinger equation using these potentials,[6] and hence the Franck-Condon factors may be computed numerically.

Our primary concern is to follow the populations of the various vibrational levels of the $^3\Pi_{0^+}$ state as a function of total pressure, M gas diluent, and flow rates of the reactant gases. The actual vibrational-translational energy-transfer cross sections can be obtained from these data once the radiative lifetime has been experimentally determined.

1. R. A. Durie, Proc. Roy. Soc. (London) A207, 388 (1951).
2. R. A. Durie, Can. J. Phys. 44, 337 (1966).
3. R. Rydberg, Z. Physik 73, 376 (1931).
4. O. Klein, Z. Physik 76, 226 (1932).
5. A. L. G. Rees, Proc. Phys. Soc. (London) A59, 998 (1947).
6. R. N. Zare, J. Chem. Phys. 40, 1934 (1964).

23. HYDROGEN-ATOM SPECTROMETER

Philip Dow and Harold S. Johnston

We have been constructing a microwave Zeeman-modulated cavity resonance spectrometer to measure the H-atom concentration in the $H + D_2 \rightarrow HD + D$ reaction, by monitoring the hydrogen 21-cm, zero-field transition. This spectrometer resembles previous instruments built by Wittke[1] and the various hydrogen maser groups.[2] The requirements of high field and stringent homogeneity limit commercial ESR spectrometers to small sample volumes. By going to low fields (12 gauss max) we can increase the size of the sample volume to 1.6 liters. This suppresses surface reactions and increases the signal power and the Q of the cavity.

We have designed a novel magnet system, consisting of two pairs of Helmholtz coils oriented at right angles to each other. The current in one set is 90-deg out of phase with the other. Thus the quasi-static field is a rotating vector (280 Hz) of slowly varying amplitude. The signal power appears at the frequency of the first overtone (560 Hz). The advantages of the system are (1) modulation and signal frequencies are separated, (2) the coils are driven by ac rather than dc amplifiers, and (3) the signal is proportional to absorption, not its derivative.

The prototype cavity was made of silver-plated brass, wiped with a tarnish-preventive silicone. Although the wall thickness (3.6 mm) is small compared to the skin depth at 280 Hz (8 mm), powerful eddy currents are set up which shield the field inside the cavity by an order of magnitude. This severely restricts the dynamic range of the instrument. We are making a new cavity of silver-plated fiberglass-reinforced epoxy to solve this problem. Furthermore, the new cavity will have a small coefficient of thermal expansion, and will allow the present brass screw mechanism for adjusting the cavity length to function as a temperature-compensating post. The frequency sensitivity of the cavity will be reduced from 24 to 8 KHz/°C. Further reduction of the thermal instability can be accomplished by a small dielectric plunger driven by a thermocouple. The AFC, a frequency modulation system,[3] has been upgraded to increase the carrier power of the klystron and to improve the regulation to the extent that the frequency stability of the klystron is wholly determined by the environmental stability of the cavity.

The sample cell consists of two concentric cylinders of fused quartz to avoid undue dielectric losses. The outer cylinder serves as a thermostat. The end plates are of GE-150 quartz, so that the spectrometer can be used in conjunction with photochemical studies.

1. J. P. Wittke, A Redetermination of the Hyperfine Splitting in the Ground State of Atomic Hydrogen (Ph.D. Thesis), Princeton University, 1955 .
2. D. Kleppner, H. C. Berg, S. B. Crampton, N. F. Ramsey, R. F. C. Vessott, H. E. Peters, and J. Vanier, Phys. Rev. 138A, 972 (1965); D. Kleppner, H. M. Goldenberg, and N. F. Ramsey, Phys. Rev. 126, 603 (1962).
3. K. W. Lamers, ESR Spectrometer for Gaseous Media, UCRL-17306, October 1967.

24. RESEARCH PLANS FOR CALENDAR YEAR 1968

Harold S. Johnston

The molecular-modulation technique is now in operation with detection of ultraviolet and infrared spectra of intermediates. The method is being extended for use on a mass spectrometer. Kinetic and spectroscopic studies of the ClO and ClOO radicals will continue, including the reaction of ClOO with CO. The kinetics of the HOO radical will be studied by determinations of modulation amplitude and phase as a function of reactant concentrations (H_2O_2 and O_3) and ultraviolet flashing frequency, with observations at 1127 cm^{-1} in the infrared. In infrared, ultraviolet, and mass spectral systems, an attempt will be made to observe and characterize the CH_3OO free radical.

Studies in the molecular dynamics of excited molecules will continue. The chemiluminescence of IF as produced in the low-pressure $I_2 + F_2$ reaction will be analyzed in terms of population of IF-excited vibronic states and the change in this population as a function of collision rates. The fluorescence of NO_2 will be further studied as a function of pressure, input-radiation wave length, and fluorescence wave length.

The hydrogen-atom microwave spectrometer will be used to measure hydrogen atom concentrations in chemical and photochemical reactions.

Theoretical studies are under way to attempt to interpret experimental data we obtained two years ago on the thermal ionization of O_2 and N_2 and of Xe at high temperatures (5000 to 11,000°K).

25. 1967 PUBLICATIONS

Harold S. Johnston and Associates

Technical Journals

1. H. S. Johnston, G. E. McGraw, T. T. Paukert, L. W. Richards, and J. van den Bogaerde, Molecular Modulation Spectroscopy. I. New Method for Observing Infrared Spectra of Free Radicals, Proc. Nat. Acad. Sci. 57, 1146 (1967).
2. S. W. Mayer, L. Schieler, and H. S. Johnston, Computation of High-Temperature Rate Constants for Bimolecular Reactions of Combustion Products, presented at the Eleventh International Symposium on Combustion, The Combustion Institute, Pittsburg Pa., 1967.

26. SEMICLASSICAL PHASE SHIFTS FOR LOW-ENERGY "ORBITING" COLLISIONS*

Ronald R. Herm

In treating the elastic scattering of atoms or molecules subject to a spherically symmetric potential, a full partial wave quantum mechanical calculation can be prohibitively time consuming due to the large number of partial waves which contribute. On the other hand, the information concerning the intermolecular potential which is obtained from scattering experiments is often derived from the special quantal features which are observed. These observed quantal features have previously been incorporated into a modified classical scattering theory through the development of a semiclassical theory employing the "JWKB" expression for the phase shift. Previous numerical comparisons with exact quantal solutions have indicated that the JWKB is, in general, a very good approximation, although it is found to fail for low incident energies where classically the phenomena of orbiting collisions are expected.

In the work described here, a semiclassical expression for the phase shift valid for incident energies near a maximum in the effective potential, previously derived by Ford et al.,[1] was re-expressed in terms of the JWKB classical phase integrals with simple correction terms to incorporate the quantal features of tunnelling and the uncertainty principle. It was shown that semiclassical phase shifts in this low energy realm could easily be calculated for any collision partners, energy, and impact parameter from this expression and tables of reduced JWKB phase integrals. Tables of reduced phase integrals were prepared for a Lennard-Jones (12-6) potential; semiclassical phase shifts computed from these tables were found to be in good agreement with previously published values obtained by integrating Schrödinger's equation. Finally, the qualitative nature of the quantal corrections to the classical total and differential cross sections and collision lifetime in this low-energy realm was discussed.

* Work on this study is complete; it is described by R. R. Herm in J. Chem. Phys. 47, 4290 (1967); UCRL-17512, July 1967.

1. K. W. Ford, D. L. Hill, M. Wakano, and J. A. Wheeler, Ann. Phys. (N.Y.) 7, 239 (1959).

27. CROSSED-MOLECULAR-BEAM INVESTIGATIONS OF THERMAL Li ATOM REACTIONS

David D. Parrish and Ronald R. Herm

An apparatus has been constructed to investigate the reactive scattering from two crossed molecular beams with thermal energies and full Maxwellian velocity distributions. This equipment is to be used to measure product angular distributions, partitionings of reaction energy, and total reaction cross sections for the reactions of Li, Na, and Ba atoms with a variety of halogen-containing molecules.

The vacuum chamber was assembled in June of 1967. Since then, the component parts of the apparatus have been tested and, where necessary, modified so that they are now performing properly. Thus, the alkali species are detected by ionization on a hot tungsten surface followed by mass analysis in a 1 in. radius magnet and subsequent detection by electron-multiplier amplification. Detector noise levels at the Li peak have been reduced to less than 100 counts/sec under operating conditions. The inhomogeneous deflecting-magnet state selector (which distinguishes scattered reactants and products) has been calibrated; over 90% of a broad (0.030 in. FWHM) Li beam at 1100°K is easily deflected aside by this field. Scattered Li signals have been observed at wide laboratory angles which are considerably above the apparatus noise level.

Following a rather minor modification of the detector assembly to eliminate some "ghosts" (undesirable reflections of the main alkali beam onto the detector) which currently appear in the angular distribution, reactive scattering studies will be continued. Preliminary experiments, where the measured angular distributions have been somewhat distorted by the presence of these "ghosts", have indicated that the LiBr formed in the Li + Br_2 reaction may possess more kinetic recoil energy than do the alkali halide products of

the analogous K, Rb, and Cs + Br_2 reactions. In other respects, the Li atom reaction resembles the features previously reported for the K, Rb, and Cs + Br_2 reactions.

28. CROSSED-MOLECULAR-BEAM INVESTIGATION OF INELASTIC SCATTERING BY TIME-OF-FLIGHT ANALYSIS

David D. Parrish and Ronald R. Herm

An apparatus is being constructed to investigate the inelastic scattering of alkali atoms by a crossed beam of thermal-energy molecules. The differential cross section for inelastic scattering of alkali atoms will be determined as a function of the relative translational energy in the collision. Initial experiments will search for vibrational changes in molecular collision partners which will not react with the alkali metal and for which there is evidence that the features of the collision cannot be explained in terms of two-body forces; an obvious example is the K + SO_2 collision for which gas kinetic and molecular-beam data indicate the formation of a long-lived K-SO_2 complex.

The vacuum chamber built for the Li-atom reaction studies will be used to house the equipment for these experiments. A slotted-disk velocity selector has been constructed to provide a monoenergetic alkali beam (velocity resolution of ~5%) for a short time, ~8μsec, with a pulse repetition frequency on the order of 1 KHz. This selector has been successfully run under vacuum at speeds as high as 20,000 rpm for long periods without any detrimental effects; it is designed to rotate as fast as 40,000 rpm, where it will transmit atoms moving at 7×10^5 cm/sec.

The burst of monoenergetic atoms will be scattered by the crossed beam onto a surface-ionization detector and mass analyzer which is mounted a known distance from the scattering volume on a rotatable platform. Individual ions will be counted. Electronics have been built to open a counter at a certain time after the atoms have left the selector; the counter is then turned off after a chosen time has elapsed. Delay and channel times are continuously and independently variable from ~20 nsec to seconds. In this manner, the distribution in flight times will be directly measured; the distribution in the scattered atom's velocity, in turn, may be determined from these data.

Experimental pursuit of this problem has been delayed for a few months pending construction of a cryogenically pumped vacuum chamber to house the alkali atom source and slotted-disk velocity selector.

29. RESEARCH PLANS FOR CALENDAR YEAR 1968

Ronald R. Herm

Reactions of thermal energy Li, Na, and Ba atoms with a number of halogen-containing compounds will be studied in crossed molecular beams. The angular distributions of the alkali halide product, the reaction-energy partitionings, the total reaction cross sections, and other reaction features will be determined. The data collected will be compared with the predictions of the electron-transfer reaction model which has been proposed to account for the analogous K, Rb, and Cs reactions, and with the results of Monte Carlo calculations on assumed potential-energy surfaces.

Distribution in flight time of K and Na atoms scattered by nonreactive molecules will be measured. The differential cross section for inelastic scattering of K and Na from SO_2 and Na from CsCl, CsBr, and CsI will be determined as a function of initial translational energy. The probability of a "sticky" collision leading to a change in internal energy of a collision partner will thus have been evaluated.

A bakeable high vacuum chamber housing a quadrupole residual gas analyzer will be built to mount in the existing larger vacuum chamber on a rotating seal. A F atom source will be constructed and crossed-beam studies will determine detailed features of the transfer reactions

$$F + \text{hydrocarbon} \rightarrow HF + \text{radical}$$

An attempt will be made to measure the temperature dependence or noise level permitting, the velocity dependence of sensitized fluorescence, i.e. of collisions of the form

$$Hg^* + Tl \rightarrow Tl^* + Hg,$$

when the asterisk represents electronic excitation.

30. 1967 PUBLICATIONS

Ronald R. Herm and Associates

Technical Journals

1. J. H. Birely, R. R. Herm, K. R. Wilson, and D. R. Herschbach, Molecular-Beam Kinetics; Reactions of K, Rb, and Cs with Br_2 and I_2, J. Chem. Phys. 47, 993 (1967).
2. R. R. Herm, Semiclassical Phase Shifts for Low Energy "Orbiting" Collisions, J. Chem. Phys. 47, 4290 (1967).
3. D. Villarejo, R. R. Herm, and M. G. Inghram, Measurement of Threshold Electrons in Photoionization of Ar, Kr, and Xe, J. Chem. Phys. 46, 4995 (1967).

31. THE ELECTRON DISTRIBUTION IN TRANSITION METAL COMPLEXES

Charles B. Harris

The electron distributions in transition metal complexes have been studied by nuclear quadrupole resonance spectroscopy. In particular, the Co^{59} nuclear quadrupole resonances have been found in the orthocarborane complexes of Co[III]. A comparison of the quadrupole coupling constants in these compounds with those of cobalticinium perchlorate, ferrocene and ferrocinium have led to a unified picture of the electron distributions in a cyclopentadienyl transition metal bond or an orthocarborane transition metal bond. In particular, it can be shown that in Fe(II) and Co[III] sandwich compounds, roughly 0.5±0.1 electrons are back excepted into the Π^* orbitals of a cyclopentadienyl moiety. Also it can be shown that about 0.4±0.1 of an electron is donated by the cyclopentadienyl moiety into the $3d_{xz}$ and $3d_{yz}$ orbitals of the transition metal.

From an analysis of the uv and visible spectrum of cobalticinium perchlorate and ferrocene plus an analysis of the quadrupole coupling constants of Co^{59} and Fe^{57m}, obtained from Mossbauer results, we have calculated an effective Fe^{57m} nuclear electric quadrupole moment. A value of 0.175±0.02 barns has been determined. This value compares favorably with the best calculated value of 0.2 barns.

An analysis of the rhenium^{185} and rhenium^{187} nuclear quadrupole resonance in dirhenium decacarbonyl suggests that nuclear quadrupole resonance spectroscopy may be very powerful in analyzing the anisotropic thermovibrations of solids. In particular, the ideal point symmetry at the rhenium nucleus requires an asymmetry parameter of 0.0, however, the observed value is about 0.6. An explanation for the discrepancy has been put forth based on an analysis of the anisotropic temperature tensors obtained from the single crystal X-ray diffraction data in a variety of di-metal decacarbonyl isomorphs.

Because the interaction of electrons with nuclei are very sensitive to the molecular motions of a solid, it has been possible to study the dynamical behavior of a transition metal cyclopentadienyl bond in the solid state. Temperature dependent nuclear quadrupole resonance experiments have allowed us to determine the rotational or tortional barriers of the cyclopentadienyl and pyrolle in a few manganese tricarbonyl complexes.

32. RESEARCH PLANS FOR CALENDAR YEAR 1968

Charles B. Harris

The research to be carried out in the calendar year of 1968 will be basically an extension of the present work in progress. A spin-echo nuclear quadrupole resonance spectrometer is currently being developed in order to facilitate the discovery and elucidation of resonances having an inherent short spin-spin relaxation time. It is hoped that such a spectrometer will allow the discovery of many new resonances of compounds and nuclei heretofore undiscovered.

33. 1967 PUBLICATIONS

Charles B. Harris and Associates

Technical Journals

1. F. A. Cotton and C. B. Harris, Molecular Orbital Calculations for Complexes of Heavier Transition Elements. III. The Metal-Metal Bonding and Electronic Structure of $Re_2Cl_8^{2-}$, Inorg. Chem. 6, 924 (1967).
2. F. A. Cotton and C. B. Harris, Molecular Orbital Calculations for Complexes of Heavier Transition Elements. II. Hexachloro Complexes of Tetravalent Rhenium, Osmium, Iridium, and Platinum, Inorg. Chem. 6, 376 (1967).
3. F. A. Cotton and C. B. Harris, Molecular Orbital Calculations for Complexes of Heavier Transition Elements. I. Study of Parameter Variations in the Case of Tetrachloroplatinate(II), Inorg. Chem. 6, 369 (1967).
4. F. A. Cotton, C. B. Harris and J. J. Wise, Extended Hückel Calculations of the Molecular Orbitals in Bis(β-ketoenolate) Complexes of Copper(II) and Nickel(II), Inorg. Chem. 6, 909 (1967).

UCRL Reports

1. M. D. Fayer and C. B. Harris, A Fast Sweep Nuclear Quadrupole Resonance Spectrometer, UCRL-17860, October 1967.
2. C. B. Harris, The Rhenium Nuclear Quadrupole Resonance Spectra in Dirhenium Decacarbonyl, UCRL-17874, October 1967.

34. THERMODYNAMICS AND MOLECULAR STATE OF STRONG ACIDS

Richard W. Duerst, Wayne E. Gargrave, and Otto Redlich

The precise determination of nuclear

magnetic resonance (NMR) in the full range of the systems HNO_3-DNO_3-water and $HClO_4$-$DClO_4$-water has furnished information exceeding previous expectations. The complete interpretation of the data leads to the following results, some of which have been known for a long time:

(a) In the lower range (mole fraction $x < 0.5$) the NMR shifts depend on the degree of dissociation.

(b) The preference[1,2,3] of the hydrogen ion for H over D with a properly defined exchange equilibrium constant 1.5 is confirmed. The limiting slopes s_1 are related to the fraction

$$r = D/(H + D)$$

and the limiting slopes

$$s_{10} = s_1 \text{ for } r = 0, \quad s_{11} = s_1 \text{ for } r = 1$$

by the equation

$$1/s_1 = (1 - r)/s_{10} + r/s_{11}.$$

(c) Dissociation and H-preference of the hydrated hydrogen ion furnish a quantitative representation of the data for all isotopic mixtures in the lower range. Hydration numbers of 1.5 to 2 are obtained. The strengths of HNO_3 and DNO_3 are not appreciably different.

(d) The dimerization of HNO_3 in the upper range ($x > 0.5$) is corroborated.

(e) Degrees of dissociation of $HClO_4$ for concentrations near $x = 0.5$ and in the upper range have been obtained. The approach to complete dissociation of water dissolved in nearly anhydrous perchloric acid is safely confirmed.

(f) Deuterium substitution makes the decline of the shift with concentration in the upper range much steeper. This perplexing fact is explained by solvation of the hydrogen ion by $HClO_4$.

(g) The shift of the proton has the same value for $HClO_4$ and $DClO_4$ ($r = 0.998$). This shows that the acid is monomeric and that the influence of the environment of the molecule on the shift is small.

For the calculation of dissociation constants the activity coefficients of nitric acid have been revised on the basis of data of several authors. A new, very sensitive consistency test has been introduced. If the vapor is a perfect gas mixture, one defines by means of the partial pressures p_1 and p_2

$$Q = (1 - x) \log p_1 + x \log p_2$$

and plots Q, marking also the slopes

$$dQ/dx = \log(p_2/p_1).$$

Consistent data can be connected by a smooth curve satisfying the calculated slopes.

Activity coefficients of perchloric acid have been derived from Mascherpa's[4] measurements of the total pressure. The calculation, though conventional in principle, is difficult for a vapor-pressure curve with an extremely low azeotropic value.

A measure for the concentration of undissociated sulfuric acid in moderately concentrated solutions is given by the initial rate of the reaction

$$H_2O_2 + H_2SO_4 = H_2SO_5 + H_2O.$$

Older data[5] were confirmed. All results were compared with the activity and the acidity of sulfuric acid. Deuterium substitution ($r = 0.87$) has no influence on the rate. This is in accord with the assumption that the concentration of the undissociated molecule, not that of the ions, is rate-controlling.

1. A. J. Kresge and A. L. Allred, J. Am. Chem. Soc. 85, 1541 (1963).
2. V. Gold, Proc. Chem. Soc. 1963, 141.
3. K. Heinziger and R. E. Weston, J. Chem. Phys. 42, 272 (1965).
4. G. Mascherpa, Revue de Chimie Minérale 2, 379 (1965).
5. J. M. Monger and O. Redlich, J. Phys. Chem. 60, 797 (1956).

35. THERMODYNAMIC-CALCULATION METHODS

Victoria B. T. Ngo and Otto Redlich

Thermodynamic calculations, in principle established by the work of Gibbs and G. N. Lewis, can be carried out in a great variety of schemes and procedures. The choice between various correct methods is a matter of efficiency, important in technical applications.

As the result of practical experience, certain general guide lines and routines can be proposed. For routine computations it is usually advisable to derive first algebraically all relations between the data and the quantities finally desired. Then one critically surveys the available data. For the actual computation one uses a tabular arrangement. In the preparation of automatic computation similar steps must be followed.

The advantage of numerous rules is obvious as soon as they are formulated. A few examples: For a tabular computation one devises first a procedure which assigns one

line for each operation carried out directly (or by slide rule or desk calculator). No part of the computation is performed on separate sheets. The computation for each set of data is carried out in one column. The advantages of this procedure are speed of computation, easy detection of errors, and convenience in checking. Another rule refers to a graphical computation based on data to be exploited with full accuracy. The scale factors must be chosen so that the data points scatter. If this choice is not practically possible, a deviation function must be introduced.

An abstract discussion of such guide lines and numerous rules does not appear to be helpful. The best presentation will be a small collection of carefully discussed sample calculations. Two examples of this kind have been prepared. In the first, the combustion of sulfur or pyrite or zinc sulfide with various excess ratios of air is followed by the contact process. One of the objectives of this calculation is the determination of the concentration and amounts (per ton of sulfuric acid) of sulfur dioxide in the stack gas. In the second example, the limits of possible explosion of various mixtures of acetic acid, hydrogen peroxide, and water have been investigated. The assembly of the results in a ternary diagram illustrates the compact presentation of complicated data.

The preparation of more examples is planned.

36. FUNDAMENTAL THERMODYNAMICS

Otto Redlich

Sixty years have passed since G. N. Lewis[1] inaugurated the continual, healthy development of applied thermodynamics. This development has been of outstanding technical importance. At about the same time Carathéodory[2] proposed some ideas on the basis of thermodynamics that rightly are considered the starting point of modern fundamental theory. Why has the development in this field been so unsatisfactory that a concept as fundamental as work has never been defined or explained in any textbook?

The reason can be found to some extent in Carathéodory's paper. His objective was to develop thermodynamics up to the second law with the rigor of modern axiomatics. Unfortunately he restricted the discussion from the start to work done against external pressure, obviously implying that the generalization to other kinds of work is entirely unproblematical.

This shortcoming has been more than just a minor flaw in Carathéodory's brilliant achievements. His transformation of variables and his discussion of their meaning is neither cogent nor lucid, precisely because he started from a restricted set of variables (volumes and pressures), believed to be intuitively meaningful.

Carathéodory tries to justify the restriction of variables by quoting Gibbs.[3] But the first sentence of Gibbs' famous paper makes it clear that his objective is the application rather than the derivation of the principles of thermodynamics. Temporary restrictions are perfectly in order in his case, but not for Carathéodory's objective.

Several later authors refined the axiomatic derivations in extreme detail. None considered the meanings of the concepts and arbitrary assumptions from which their discussions started. Their efforts have been without results: They played a game with chips that were not interconvertible with the real money of physical concepts.

A first step towards a clarification of the basic concepts was made a few years ago.[4] Further work is in progress. Some historical facts explain misunderstandings in the literature.

1. G. N. Lewis, Proc. Amer. Acad. 43, 259 (1907); Z. Phys. Chem. 61, 129 (1907).
2. C. Carathéodory, Math. Ann. 67, 355 (1909).
3. J. W. Gibbs, Trans. Connecticut Acad. 2, 382 (1873).
4. O. Redlich, J. Phys. Chem. 66, 585 (1962).

37. LEACHING OF CLAY WITH ACIDS

Irundi Edelweiss and Otto Redlich

Bauxite, the traditional raw material for the production of aluminum, is available only in tropical and subtropical regions. A reasonably cheap process for the extraction of alumina from clay would offer very important economic advantages. Numerous methods have been developed. The most promising ones may be those based on the leaching of clay with sulfurous acid. In this group the leaching agent can be easily recovered and the separation of iron from aluminum can be achieved without difficulty by keeping iron in the ferrous state.

A process for leaching clay with sulfurous acid under elevated pressure has been developed in a series of patents by inventors of T. Goldschmidt A. G. in Germany. Elevated pressure is avoided in a combined process[1] in which about

two-thirds of the alumina is extracted by sulfurous acid, and the last third by sulfuric acid. Boiling of the leach liquor results in an easily filtrable precipitate of basic aluminum sulfate free of iron.

The serious obstacle for the practical realization of both processes is the silica content of the product. Conventionally the tolerance for SiO_2/Al_2O_3 is 0.02 wt.-%. Acid leaching results in a silica content of nearly 2%, intolerable in the electrolytic reduction. Recently the addition of an alkaline step (similar to Bayer's process) to the high-pressure leach has been proposed, but the cost of this double process is obviously excessive.

The combined sulfurous-sulfuric acid process would be highly promising if the silica content could be reduced to the usual specification value at a reasonable expense. The great economic importance of obtaining alumina close to the reduction plant, and especially close to water power, suggests that every lead to the removal of silica should be explored.

It is astonishing that leaching of various clays with sulfurous or sulfuric acid under usual conditions always results in approximately equal silica ratios. One may tentatively conclude that this amount of silica is bound in the clay in a special, soluble form. Consequently, one may try to find a special preleaching procedure that will remove the soluble silica without extracting an appreciable fraction of the alumina.

Experiments were started with sulfuric acid. In a large range of concentrations and leaching time, little change of the SiO_2/Al_2O_3 ratio was observed. Finally the removal of substantial amounts of silica was achieved by leaching with an acid containing about 0.01 moles H_2SO_4 per liter. A large amount of acid (750 ml for 5 g clay) and long leaching times (about 10 hours at boiling temperature) were required. By this method as much as 0.15 g SiO_2 were removed from 5 g clay. The residue, leached for 3 hours at 100°C with 100 ml 4 M sulfuric acid, furnished 1.4 g Al_2O_3 with a SiO_2/Al_2O_3 ratio of 0.29%. This and similar tests show that there is a sizable effect in the expected direction. The result, however, is still far from satisfactory, and considerable improvement would be required for a technically sound process.

At present, a combination of sulfurous acid leaching with a preleaching step to remove silica is being investigated.

1. O. Redlich, C. C. March, M. F. Adams, F. H. Sharp, E. K. Holt, and J. E. Taylor, Ind. Eng. Chem. 38, 1181 (1946).

38. RESEARCH PLANS FOR CALENDAR YEAR 1968

Otto Redlich

Thermodynamics and Molecular State of Solutions

Completion of computations and reports is planned.

Thermodynamic Calculation Methods

A number of other examples, covering a variety of computation methods and also the most important processes of the chemical industry will be prepared.

Fundamental Thermodynamics

The program of research in fundamental thermodynamics will be continued.

Leaching of Clay with Acids

The search for reduction of the silica content in extracted alumina will be pursued.

39. 1967 PUBLICATIONS

Otto Redlich and Associates

Technical Journals

1. A. Merbach, Ionization of Strong Electrolytes. IX. Proton Magnetic Resonance in the Ternary System HNO_3-DNO_3-H_2O-D_2O, J. Chem. Phys. 46, 3450 (1967).

UCRL Reports

1. Richard Duerst, Ionization of Strong Electrolytes. X. Proton Magnetic Resonance of the Ternary System $HClO_4$-$DClO_4$-H_2O-D_2O, UCRL-17532, June 1967.
2. W. E. Gargrave, On the Molecular Structure of Strong Acids (M.S. Thesis), UCRL-17915, December 1967.
3. O. Redlich, W. E. Gargrave, and W. D. Krostek, Thermodynamics of Solutions. XII. Consistency of Sparse Data. Activities of Nitric and Perchloric Acids, UCRL-17694, July 1967.

F. NUCLEAR SCIENCE

MOLECULAR-BEAM MASS SPECTROMETRY

1. GAS ANALYSIS BY MODULATED MOLECULAR-BEAM MASS SPECTROMETRY

Donald R. Olander and William Waddel*

A method of gas analysis utilizing modulated molecular-beam mass spectrometry has been developed and tested. A sketch of the system is shown in Fig. IF.1-1. The gas to be analyzed is contained at pressures up to 20 Torr in an inlet tube from which a molecular beam issues through a small orifice. The molecular beam is collimated and directed through the ionizer of the spectrometer. By employing differential pumping, a modulated molecular beam, and lock-in amplification, a partial pressure of 9×10^{-13} Torr was detected in a beam with an equivalent pressure of 6×10^{-7} Torr (1.5 ppm). Based on the observed signal-to-noise ratio, it is estimated that the minimum partial pressure that could be detected in this beam is about 6×10^{-14} Torr (0.1 ppm). Two different types of noise-averaging devices were employed, a narrow-band lock-in amplifier and an analog-to-digital computer. The molecular isotopes of oxygen were studied to determine the sensitivity of the system. The results are shown in Table IF.1-I. The precision and accuracy of the results are better than 5%, even in the ppm range. Two distinct advantages

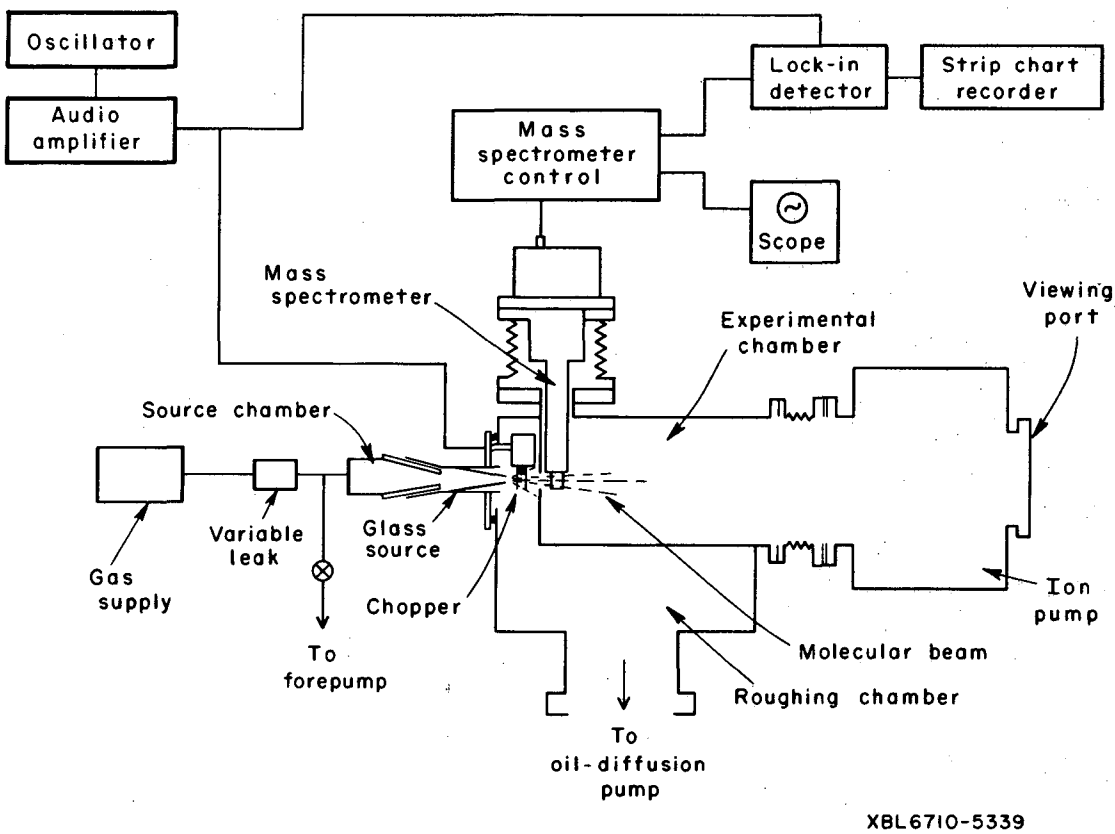

Fig. IF.1-1 Device to measure angular distribution from molecular-beam sources.

Table IF.1-I. Isotope ratios in molecular oxygen.

Isotope	m/e	Output signal relative to Mass 32	Predicted[a]	Accuracy
$O^{16}O^{16}$	32	1	1	--
$O^{16}O^{17}$	33	$(7.6\pm0.22)\times10^{-4}$	7.4×10^{-4}	+2.7
$O^{16}O^{18}$	34	$(3.9\pm0.10)\times10^{-3}$	4.0×10^{-3}	-2.5
$O^{17}O^{18}$	35	$(1.43\pm0.13)\times10^{-6}$	1.5×10^{-6}	-4.7
$O^{18}O^{18}$	36	$(3.8\pm0.0)\times10^{-6}$	4.0×10^{-6}	-5.0

a. The predicted molecular isotope abundances are calculated by assuming a statistical combination of the known atomic abundances of O^{16}, O^{17}, and O^{18}.

of this system are the ability to work at relatively high source pressures and the insensitivity of the method to background gases in the vacuum chamber, whose contribution to the mass spectrum is effectively suppressed by the phase-sensitive detection technique.

* Present address: Battelle Pacific Northwest Laboratory, Richland, Washington.

2. CHARACTERIZATION OF MOLECULAR-BEAM SOURCES

Richard Jones and Donald R. Olander

The performance of a molecular-beam source is an important factor in experiments involving scattering, reaction, or analysis of molecular beams. The most significant characteristic of the source is the ratio of the beam intensity along the center line to the total effusion rate. For a specified center line beam intensity, lower total effusion rates mean smaller pumping requirements and improved signal-to-background ratios.

The center line beam-to-total effusion flux ratio can be determined by measurement of the angular distribution pattern from the source. For an ideal thin-walled orifice source, this ratio is fixed by the fact that the angular-emission pattern follows the cosine law. There are a number of source configurations involving many long channels which can provide angular distributions which are much more peaked than that of an ideal orifice. Among these are the krinkly foil source developed by Zacharias,[1] the etched-wire-in-epoxy source developed by Hanes,[2] and multichannel sources constructed by microdrilling or electron-beam drilling.

The device that has been developed to measure the angular distribution pattern of a source before it is accepted for a molecular beam experiment is shown in Fig. IF.2-1. It consists of a vacuum chamber in which the source and a detecting probe or "sniffer" are mounted. The sniffer consists of a single capillary facing the source tip and connected to a standard helium-leak detector. The probe can be rotated ±45-deg about the source tip in order to trace out the angular distribution of the effusing flux. The source conductance is also measured by the pressure decay of a large ballast tank in the feed line. A beam flag to interrupt the direct-flight flux from the source to the detector is used to measure the helium background in the system.

The system has been tested on a single capillary source, and the leak rate and angular-emission pattern were in satisfactory agreement with theoretical predictions. The krinkly foil source used in the tantalum-hydrogen study reported in Sec. IF.3 was also tested. A sketch of the construction of this source is shown in Fig. IF.2-2. This source was found to suffer from excessive gas leakage around the bottom of the foil pack, and as a result, gave only a 30% improvement over an ideal thin-walled orifice source.

The beam source used in the gas-analysis apparatus described in Sec. IF.1 was a single capillary hand drawn from Pyrex tubing. The diameter at the source tip was 240μ. A typical angular distribution pattern from this source is shown in Fig. IF.2-3, along with the pattern of a cosine emitter of the same total flux. Although the drawn source does provide a more peaked angular distribution than the cosine source, the hand-drawn construction resulted in an off-axis intensity maximum. Since in a molecular beam experiment, the source is generally followed by a small collimating orifice along the axis of the source tube, the deviation of the beam maximum from the axis evident in Fig. IF.2-3 markedly decreases its efficiency.

Sources consisting of 100 very small holes drilled in a quartz plate by electron-beam drilling are currently being tested for eventual use in surface-reaction studies with molecular beams.

1. J. G. King and J. R. Zacharias, Advan. Electron. Electron Phys. 6, 1 (1956).
2. G. R. Hanes, J. Appl. Phys. 31, 2171 (1960).

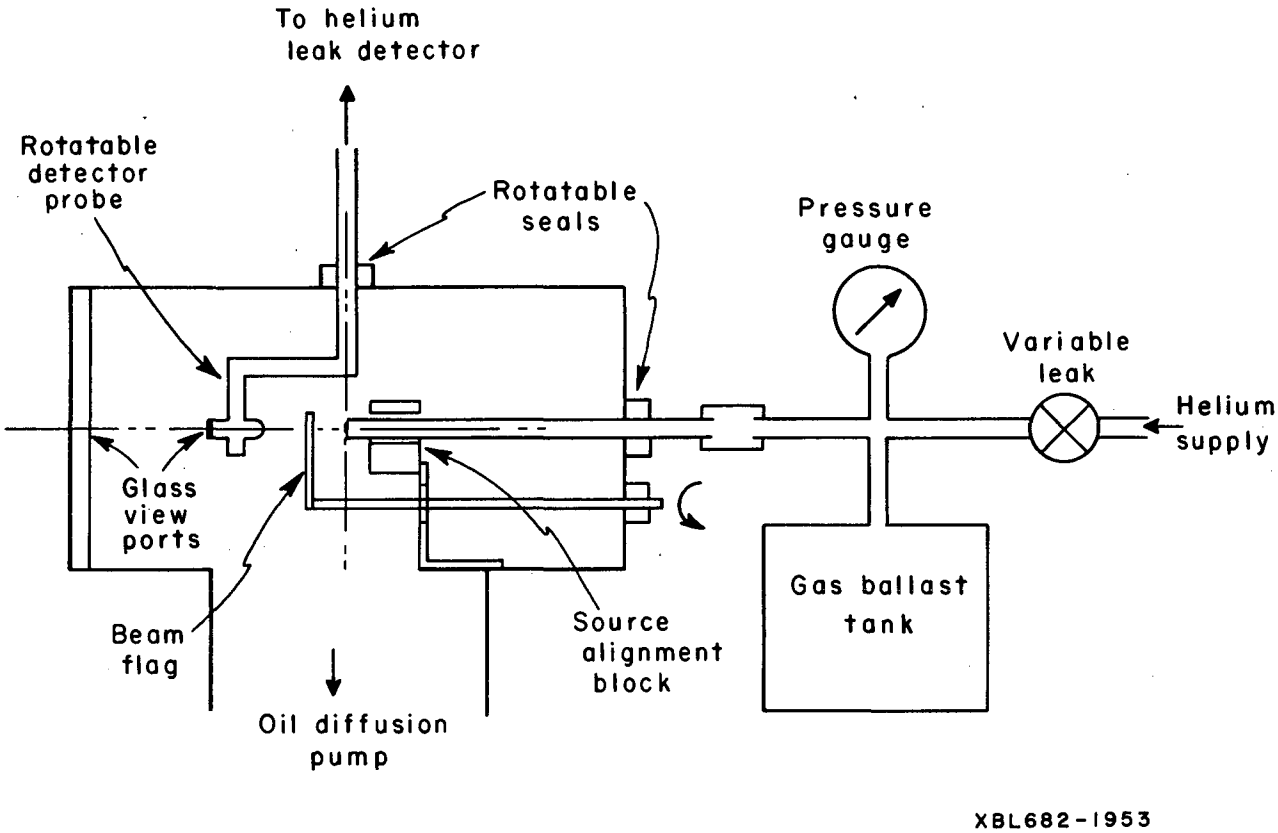

Fig. IF.2-1. Device to measure angular distribution from molecular-beam sources.

3. DISSOCIATION OF HYDROGEN ON TANTALUM USING A MODULATED MOLECULAR-BEAM TECHNIQUE*

Robert A. Krakowski† and Donald R. Olander

A molecular-beam mass-spectrometric apparatus has been developed to study the kinetics of gas-solid reactions at low pressures. The system has been used in an investigation of the dissociation of hydrogen on tantalum. A modulated beam of molecular hydrogen, formed by effusion from a source of Fig. IF2-2, impinged upon the tantalum target. The reflected H_2 and H atoms emitted after surface dissociation were monitored by a mass spectrometer in the vacuum system. The beams were modulated and the products measured by a phase-sensitive detector to improve the signal-to-noise characteristics of the detection system. The degree of dissociation was studied as a function of the surface temperature, beam temperature, and beam intensity. Experimental results have been analyzed in terms of phenomenological first- and second-order kinetic models. Within the pressure (3×10^{-8} to 3×10^{-7} Torr) and temperature (1000 to 2500°K) ranges studied, the data agreed best with the first-order mechanism, and yielded 65 kcal/mole for the hydrogen-metal bond energy. At a given temperature, dissociation increased with the beam temperature with an apparent activation energy of 1.4 kcal/mole, which was independent of the surface temperature. The rate of dissociation varied linearly with the beam intensity. Mixed hydrogen-deuterium beams were employed to investigate the isotope exchange reaction, and within the sensitivity of the detection system, exchange did not take place. Hydrogen solubility in the metal bulk and surface diffusion have been considered as possible sources for the observed nonequilibrium behavior.

* Abstract of a paper to be published in J. Chem. Phys.

† Present address: Chemistry Department, EURATOM, Ispra, Italy.

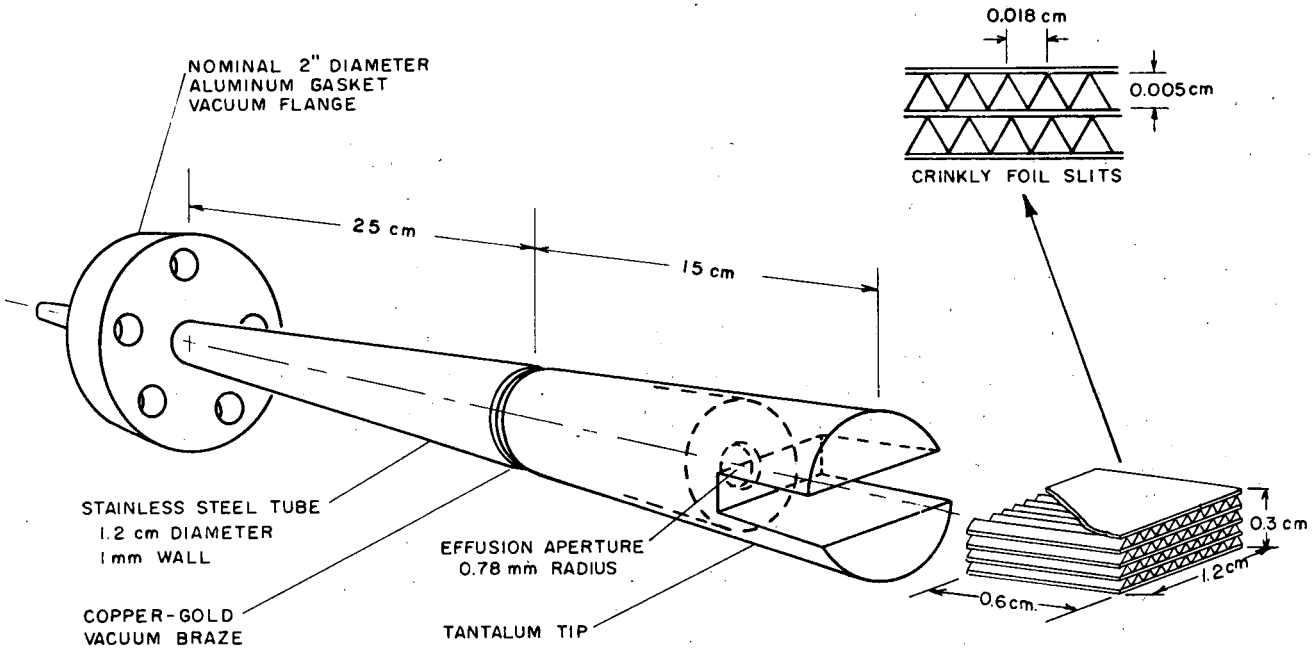

XBL 672-554

Fig. IF.2-2. Detail of Knudsen cell and multiple-channel array.

LIQUID-METAL RESEARCH

4. VISCOSITY DETERMINATIONS

James Finucane and Donald R. Olander

The purpose of this project is to develop an experimental system for the study of the properties of materials at high temperature. The goal is to develop an apparatus capable of determining the viscosity of materials, ultimately up to a temperature of 2500°C. The system is also designed to handle materials that react with atmospheric gases, such as oxygen, by providing a reduced pressure environment, a pressure usually less than 10^{-6} mm of Hg.

The viscosity is determined by the torsion-pendulum method. Design, construction, and initial testing of the vacuum system and the heater system have now been completed. Preparation and chemical analysis of the various compositions of uranium-chromium alloys is being finished. Work is now proceeding on the development of computer programs required for the data processing and on the calibration of the torsion-pendulum system prior to the final viscosity determinations.

5. TRANSIENT DIFFUSION IN A COMPOSITE SLAB*

Paul Concus† and Donald R. Olander

The transient response of two finite slabs initially containing nonequilibrium amounts of a transferable solute or at different temperatures is a problem of practical importance. Such a situation may occur in the thermal equilibrium of a solute distributing between two immiscible liquid layers contacted at their mutual interface. The latter application is of particular use in the distribution of solutes between two liquid metals where agitation to promote rapid attainment to equilibrium is not feasible.

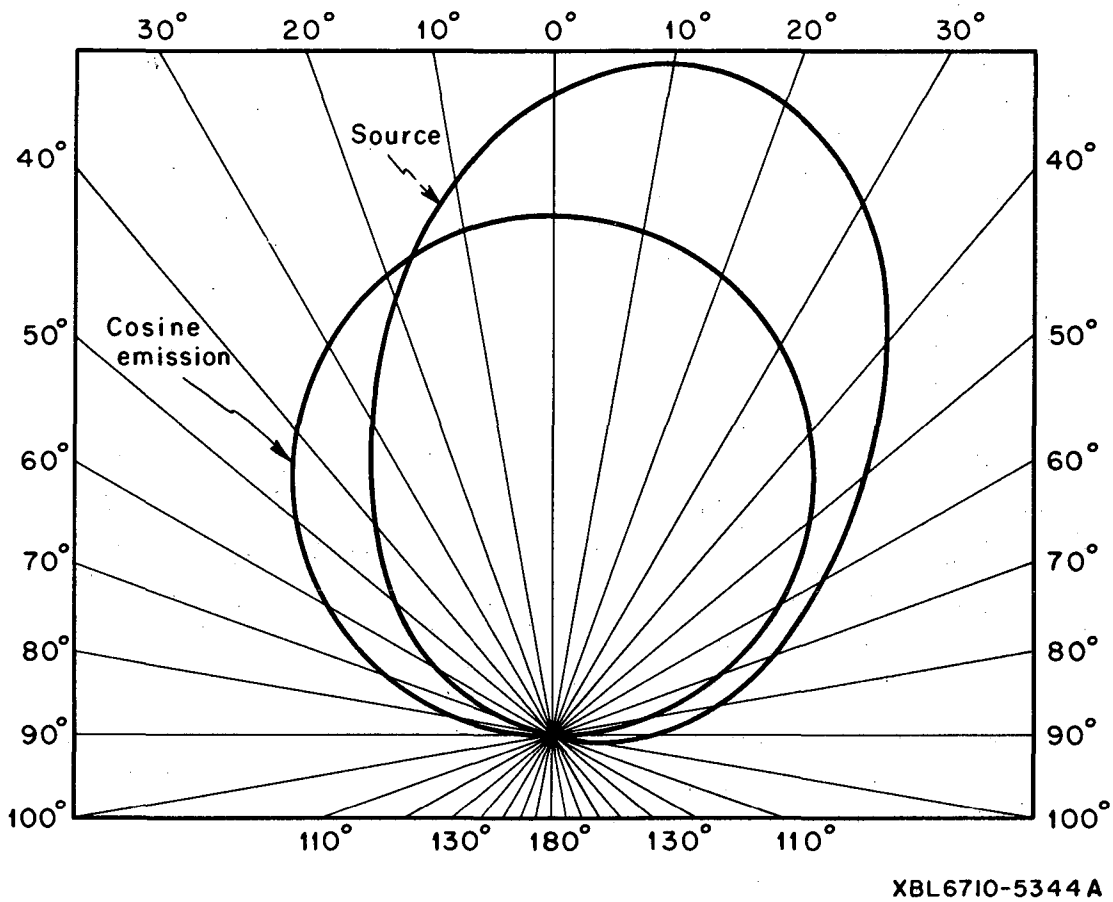

Fig. IF.2-3. Angular distribution of glass source.

Movement of the solute occurs by molecular diffusion in the two liquids which may have different diffusion coefficients. The layers are of finite thickness in the direction perpendicular to the interface but are assumed to be of infinite extent laterally. No transfer occurs across the outer boundaries of the two layers. The concentrations on the two sides of the interface are related by a distribution coefficient. The quantity of interest is the time variation of the ratio of the average concentrations in the two phases, which approaches the distribution coefficient at infinite time.

Fick's second law for the two phases subject to appropriate boundary conditions is solved in terms of an eigenfunction series. The approach to equilibrium is depicted graphically for a few values of the governing parameters which are the thickness ratio of the two layers, the diffusivity ratio of the two phases, and the distribution coefficient. With the aid of tables that have been prepared, the solution may be calculated for a larger range of values covering the region of practical interest.

* To be published in Int. J. Heat Mass Transfer.

† Mathematics and Computing Division, Lawrence Radiation Laboratory.

ROTATING-DISK STUDIES

6. CONDENSATION-ENHANCED VAPORIZATION OF HIGH-TEMPERATURE SOLIDS

Ronald Omberg and Donald R. Olander

The enhancement of diffusion-limited vaporization by condensation within the boundary layer is being investigated. Normally, diffusion-limited vaporization rates assume that condensation does not occur close enough to the surface to locally modify the vapor concentration profile. This assumption predicts a lower limit to the vaporization rate, since condensation near the surface provides a vapor

sink and hence increases the gradient at the vaporizing surface. The maximum vaporization rate occurs when the vapor concentration is equal to the equilibrium vapor pressure at the local temperature in the boundary layer. These two limits can differ by a factor of ten or more.

A model has been developed which incorporates the principles of homogeneous nucleation kinetics into the boundary-layer equations. The model has been put in the form of a coupled set of inhomogeneous partial differential equations with variable coefficients. The equations represent conservation of monomer (diffusing vapor) and condensed droplets, which are swept along with the flow during growth.

Enhancement of the vaporization rate predicted from the effect of boundary-layer nucleation is being measured experimentally using a rotating disk as the solid surface. High purity iron is evaporated into argon at atmospheric pressure and at temperatures just below the melting point. Effort this past year has been on accurate measurement of the rotating-surface temperature by optical pyrometry and on finding a disk holder material which does not react with or stick to iron at high temperatures. Graphite formed iron carbides and made rate measurements by weight loss impossible, but boron nitride appears suitable.

7. REFRACTORY METAL OXIDATION

John S. Schofill and Donald R. Olander

A high-temperature rotating-disk apparatus to study the reaction of molybdenum and oxygen to produce volatile molybdenum oxides has been completed and experimentation begun. The apparatus design is similar to that used for the metal-vaporization studies. However, in the present experiment, condensation of the reaction product in the boundary layer is avoided by preheating the reactant gas to the solid temperature before contacting. The precisely known flow patterns about a rotating disk permit accurate evaluation of diffusional limitations to the overall rate. Reproducible data in the temperature range 840 to 960°C and for an oxygen concentration of 2% in argon have been obtained. In this region, the overall rate is 90% controlled by the surface chemical reaction which shows an activation energy of 28 kcal/mole.

8. RESEARCH PLANS FOR CALENDAR YEAR 1968

Donald R. Olander

The gas-analysis molecular-beam apparatus will be utilized to follow the course of chemical reaction in a gas subjected to ionizing radiation. We will attempt to analyze the stable products and active intermediates of the reaction by modulated-molecular-beam mass spectrometry. The ionizing radiation will be the 1-MeV proton beam from a Van de Graaff accelerator, and the chemical reaction will be the conversion of oxygen to ozone, with oxygen atoms as the active intermediate.

The surface kinetic molecular-beam apparatus has been modified to increase its sensitivity and will be used in the investigation of the reactions of pyrolytic graphite and gases such as H_2, O_2, and CO_2. We also plan to investigate the germanium-iodine reaction with the germanium in both the liquid and solid states.

The liquid-metal viscometer will be used to measure the viscosity of liquid uranium and uranium-chromium alloys from 900 to 1400°C.

Numerical solution of the homogeneous nucleation-boundary layer transport equations will be sought. The experimental work in this area will consist of measurement of the vaporization rates of iron and chromium at temperatures from 1200 to 1600°C in argon and helium atmospheres.

The refractory-metal oxidation experiment will be conducted at higher temperatures (up to 1300°C) in order to determine the region in which diffusional limitations begin to affect the overall rate of oxidation. In the reaction-controlled region at low-temperatures, the oxygen partial pressure will be varied to permit determination of the order of the surface reaction.

Nonequilibrium vaporization produced by the rapid heatup of a solid surface by laser pulses will be studied mass-spectrometrically.

9. 1967 PUBLICATIONS

Donald R. Olander and Associates

Technical Journals

1. D. R. Olander, Uranium Chlorination in Fused Salts, A.I.Ch.E. J. 13, 191 (1967).
2. D. R. Olander, Surface Chemical Kinetics and Gas Phase Diffusion in the Germanium-Iodine Reaction, Ind. Eng. Chem. Fundamentals 6, 178 (1967).
3. D. R. Olander, Variable Property, Interfacial Velocity and Multicomponent Diffusion Effects in the Transport-Limited Reaction of Iodine and Germanium, Ind. Eng. Chem. Fundamentals Quart. 6, 188 (1967).
4. A. Pasternak and D. R. Olander, Diffusion in Liquid Metals, A.I.Ch.E. J. 13, 1052 (1967).
5. H. Shaked, D. R. Olander, and T. H. Pigford, Diffusion of Xenon in Uranium Monocarbide, Nucl. Sci. Eng. 29, 122 (1967).

UCRL Reports

1. P. Concus and D. R. Olander, Transient Diffusion in a Composite Slab, UCRL-17607, June 1967.
2. Daniel Koenig, Determination of Work-Function Distribution on Metal Surfaces from Surface Ionization, paper presented at Meeting on Physical Electronics, MIT; UCRL-17437, March 1967.
3. R. A. Krakowski, Dissociation of Hydrogen on Tantalum Using a Modulated Molecular Beam Technique (Ph.D. Thesis), UCRL-17336, March 1967.
4. R. Krakowski and D. Olander, Dissociation of Hydrogen on Tantalum Using a Modulated Molecular Beam Technique, UCRL-17336-Rev., June 1967.
5. A. D. Pasternak and D. R. Olander, Mass Transfer between Immiscible Liquid Metals, UCRL-17190-Rev., May 1967.
6. William Waddel, Development of a High-Pressure Mass Spectrometric Gas Analysis System (M.S. Thesis), UCRL-17866, December 1967.

Metallurgy

II. METALLURGY

A. CRYSTAL IMPERFECTIONS

1. STRESS-INDUCED MOVEMENT OF TWIN BOUNDARIES IN ZINC*

Roger E. Cooper† and Jack Washburn

Stress and temperature dependences of the rate of twin-boundary motion have been studied in zinc. Single-crystal tensile specimens with a ⟨1$\bar{1}$00⟩ axis and containing a single twin were used. Below about 176°K the stress required for widening of the twin exceeded that for nucleation of additional twins, and therefore no motion could be observed. Above this temperature, the resolved shear stress required for boundary motion increased with increasing boundary velocity. For the temperature range near room temperature, the apparent activation volume associated with the motion was $2.8(\pm1.8)\times10^4$ Å^3. The rate of boundary motion was also temperature-dependent; the apparent activation energy being 7100(±2500) cal/mole. The critical stress for motion was increased and the activation volume was decreased by prior twisting of the specimen, which caused basal slip and multiplication of 1/3 ⟨2$\bar{1}\bar{1}$0⟩ dislocations. Also consistent with the idea that dislocations in the crystal ahead of the advancing twin boundary may have constituted the primary barrier to its motion was the observation that some regions of crystal were by-passed by the growing twin, leaving lens-shaped islands of untwinned material within the twin.

* Abstract from Acta Met. 15, 639 (1967).
† Present address: AWRE, Aldermaston, Berks., England.

2. PLASTIC DEFORMATION OF CUPROUS OXIDE

Gerard Vagnard* and Jack Washburn

Slip-line and transmission-electron-microscopy observations on the plastic deformation of cuprous oxide were made on large-grained polycrystalline specimens. The specimens were prepared by the complete oxidation of OFHC copper strips in air followed by a high temperature anneal. Plastic deformation in this material was found to take place by motion of ⟨100⟩ dislocations on {100} glide planes. Some dislocation segments of ⟨110⟩ Burgers vector were present but were probably formed by recombination reactions between ⟨100⟩ dislocations (See Fig. IIA.2-1). The unusual structure of Cu_2O, which can be described as two interpenetrating and identical frameworks of copper and oxygen which are not cross-connected by any primary copper-oxygen bonds, did not result in any unusual behavior of dislocations. The effect of temperature on plasticity was explained in the same way as for other materials of less complex structure such as MgO.

* Present address: IRSID, Seine et Oise, France.

3. EFFECT OF INITIAL DISLOCATION DENSITY ON SINGLE-SLIP STRAIN HARDENING OF COPPER

Jack Washburn and Gollapudi Murty*

Copper crystals in which different dislocation densities were introduced by multiple slip were subsequently deformed in tension in single slip. In all cases three stages were found on the stress-strain curves. Detailed observations of surface slip markings were carried out on all specimens. It was shown that Stage I in prestrained specimens was due to progressive deformation starting at points of stress concentration and propagating through the gauge length. Stress-strain curves and shear-strain distribution were found to change in a regular way with initial dislocation density; the results from as-grown specimens are seen as part of a homologous series which includes all of the results from prestrained specimens. Therefore it is suggested that Stage I in pure copper is at least partly due to unavoidable prestrains during cooling, handling, and pre-yield loading.

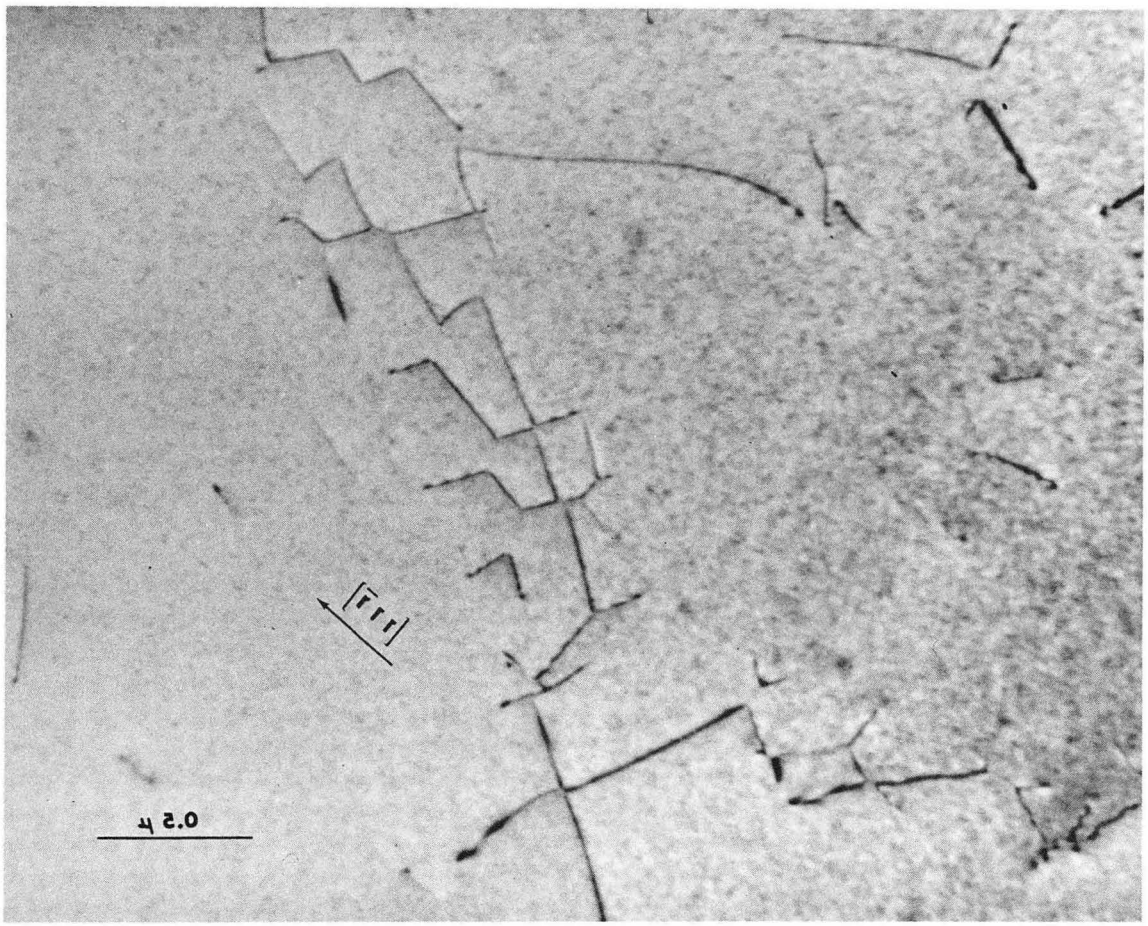

XBB 672-1154

Fig. IIA.2-1. Two-dimensional network of dislocations in cuprous oxide deformed 12% at 600°C. [011] dislocation segments in the network are out of contrast (the foil has an {112} orientation).

Linking of slip clusters to form groups that grow entirely across the specimen was found during all stages of deformation, even for as-grown crystals. Surface slip markings that were formed at a given stress level, whether in Stage I of a prestrained crystal or in Stages II or III of an as-grown crystal, were found to be similar. It was suggested that the type of instability of the dislocation substructure that is responsible for clustering of slip into definite bands and the existence of Stage I in prestrained specimens also develops gradually in a specimen deformed from the start in single slip. It was also suggested that the decrease in hardening rate in Stage III is associated with the instability of dense three-dimensional dislocation tangles within which the net Burgers vector is nearly zero.

---

* Present address: Department of Metallurgy, Kanpur, India.

4. ANNEALING OF STACKING-FAULT TETRAHEDRA IN GOLD

Michael Yokota and Jack Washburn

The annealing of stacking-fault tetrahedra in thin foils of gold was studied by transmission electron microscopy. Tetrahedra, in the size range 200 to 2000Å were observed to collapse to stacking-fault triangles during heating at 300°C. The frequency with which they collapsed increased with their increasing size. In the same temperature range stacking fault loops shrunk in size, while tetrahedra that had not collapsed did not. Figure IIA.4-1 shows these effects in an area containing tetrahedra of a wide size distribution. The complete sequence of annealing steps from collapse of the tetrahedra to shrinkage of the loops at 300°C is illustrated.

In Fig. IIA.4-1b the largest of the stacking-fault tetrahedra 1, 2, and 3 have collapsed to triangular stacking-fault loops. In Fig. IIA.4-1d smaller tetrahedra 4 and 5 have collapsed, and by Fig. IIA.4-1f the small tetrahedra 7, 8, 9, and 10 have finally collapsed. Tetrahedra, such as 11, did not change in size.

Sides of the stacking-fault loops always remained accurately parallel to ⟨110⟩ directions during shrinkage. This fact, together with the results of diffraction-contrast experiments on these loops was considered to be strong experimental evidence for dissociation of the 1/3⟨111⟩ Frank partials in gold into 1/6⟨110⟩ stair rod and 1/6⟨112⟩ Shockley partial dislocations.

5. CLIMB OF PERFECT AND IMPERFECT DISLOCATIONS IN ALUMINUM

Jean-Pierre Tartour and Jack Washburn

The kinetics of climb of dislocation loops obtained by quenching 99.999% pure aluminum single crystals has been studied. Annealings were carried out in a temperature-controlled oil bath, following electron-microscopy observations. A typical annealing sequence for Frank loops is shown in Fig. IIA.5-1. Annealing curves for loops 1 and 4 are shown in Fig. IIA.5-2. It can be seen that, after line-tension correction, the experimental points fit a straight line very closely. Systematically higher rates of shrinkage were observed for loops close to the surface, such as 1 in Fig. IIA.5-2, suggesting that even in thin foils diffusion may be rate-controlling. A comparative study of perfect prismatic-loop and Frank-loop annealing gave an estimated value of 110 ergs/cm^2 for the stacking-fault energy of aluminum and 1.23 eV for the activation energy of the climb process.

6. LIQUID-HELIUM FIELD-ION MICROSCOPE FOR RADIATION DAMAGE INVESTIGATIONS

Pierre Petroff* and Jack Washburn

A field-ion microscope has been constructed which allows in situ irradiation of a metal specimen at a temperature close to 5°K. It has been used with the 88-in. cyclotron at Berkeley which provides 10-MeV protons. The design permits "field off" irradiation of the specimen, as well as in situ temperature cycling. Figure IIA.6-1 illustrates the main features of the instrument.

* Present address: Faculte de Science, Orsay, France.

7. FIELD-ION MICROSCOPE INVESTIGATION OF RADIATION DAMAGE IN IRIDIUM BOMBARDED WITH 10-MeV PROTONS

Pierre Petroff* and Jack Washburn

Well-annealed iridium specimens were irradiated at 5°K with 10-MeV protons in situ in a field-ion microscope attached to the 88-in. cyclotron at Berkeley. Because of the atomic scale resolution of the field-ion microscope, point defects and their clusters could be directly observed at the surface and in the bulk of the irradiated specimens.

The low-temperature surface damage caused by bombardment with 10-MeV protons was mostly composed of ejected surface atoms. A larger surface damage was observed during irradiation with the imaging field applied to the specimen and has been related to the lowering in the binding energy of the surface atoms when the electrostatic field is applied to the specimen.

Interstitials were identified as extra-bright dots which popped up to the surface upon an increase of the field applied to the specimen. Pairs of extra-bright dots may sometimes be caused by a single interstitial rather than a diinterstitial. A typical field-evaporation sequence showing the arrival of an interstitial atom at the surface is shown in Fig. IIA.7-1.

The annealing behavior of the defects, as observed from the surface changes and the variations in the bulk interstitial

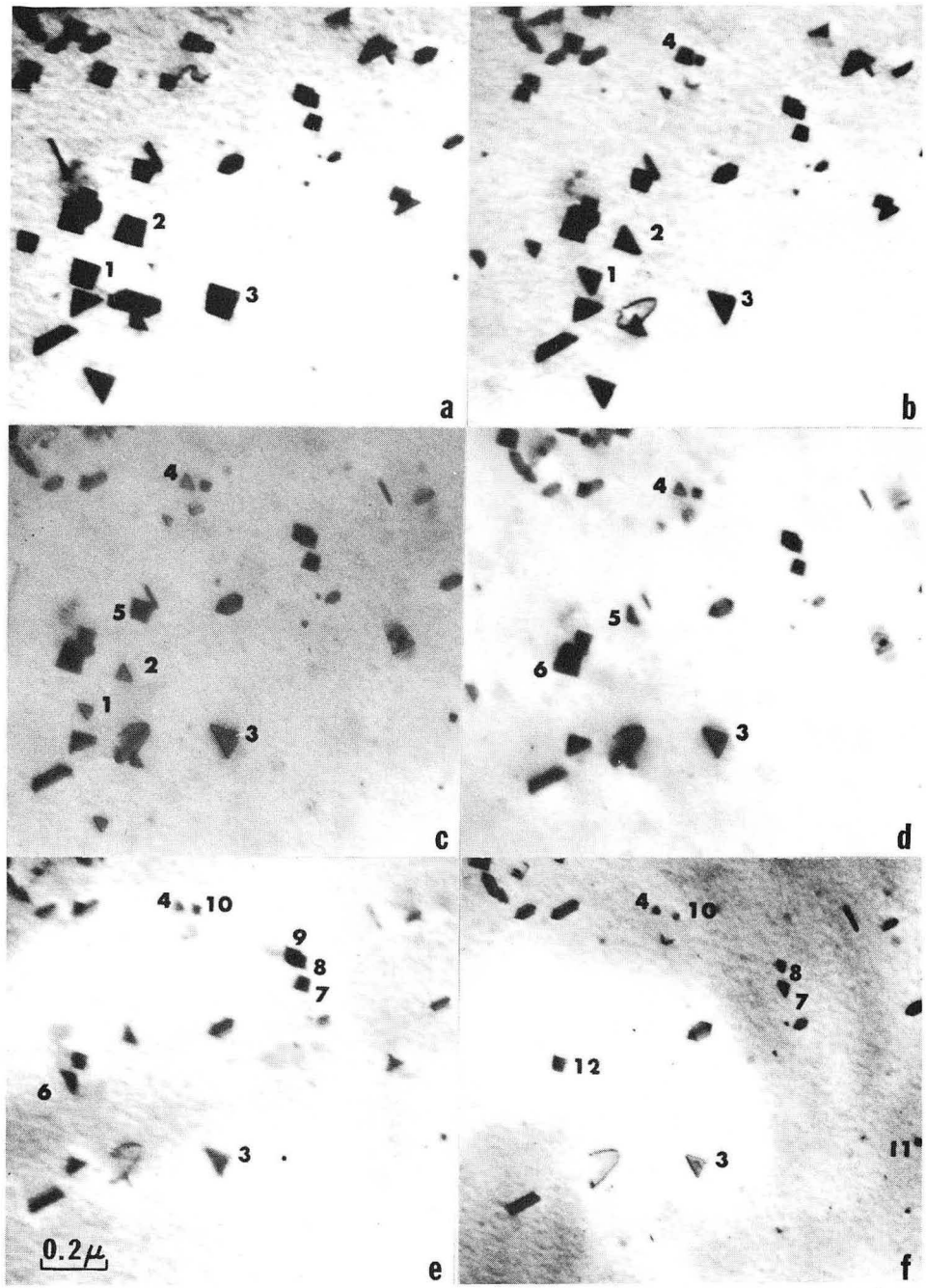

XBB 682-854

Fig. IIA.4-1 Collapse of stacking-fault tetrahedra to triangular Frank sessile loops. The same area is shown after annealing at 300°C for various total times up to 34 hours. (a) 15 min; (b) 2-1/4 hr; (c) 5-1/4 hr; (d) 9-1/4 hr; (e) 17-1/4 hr; (f) 34-1/4 hr.

concentration, showed that interstitials migrate to the surface in the temperature range 14 to 40°K.

The effects of the irradiation temperature were also investigated. Large voids and dislocation loops were observed in the specimens irradiated at room temperature.

* Present address: Faculte de Science, Orsay, France.

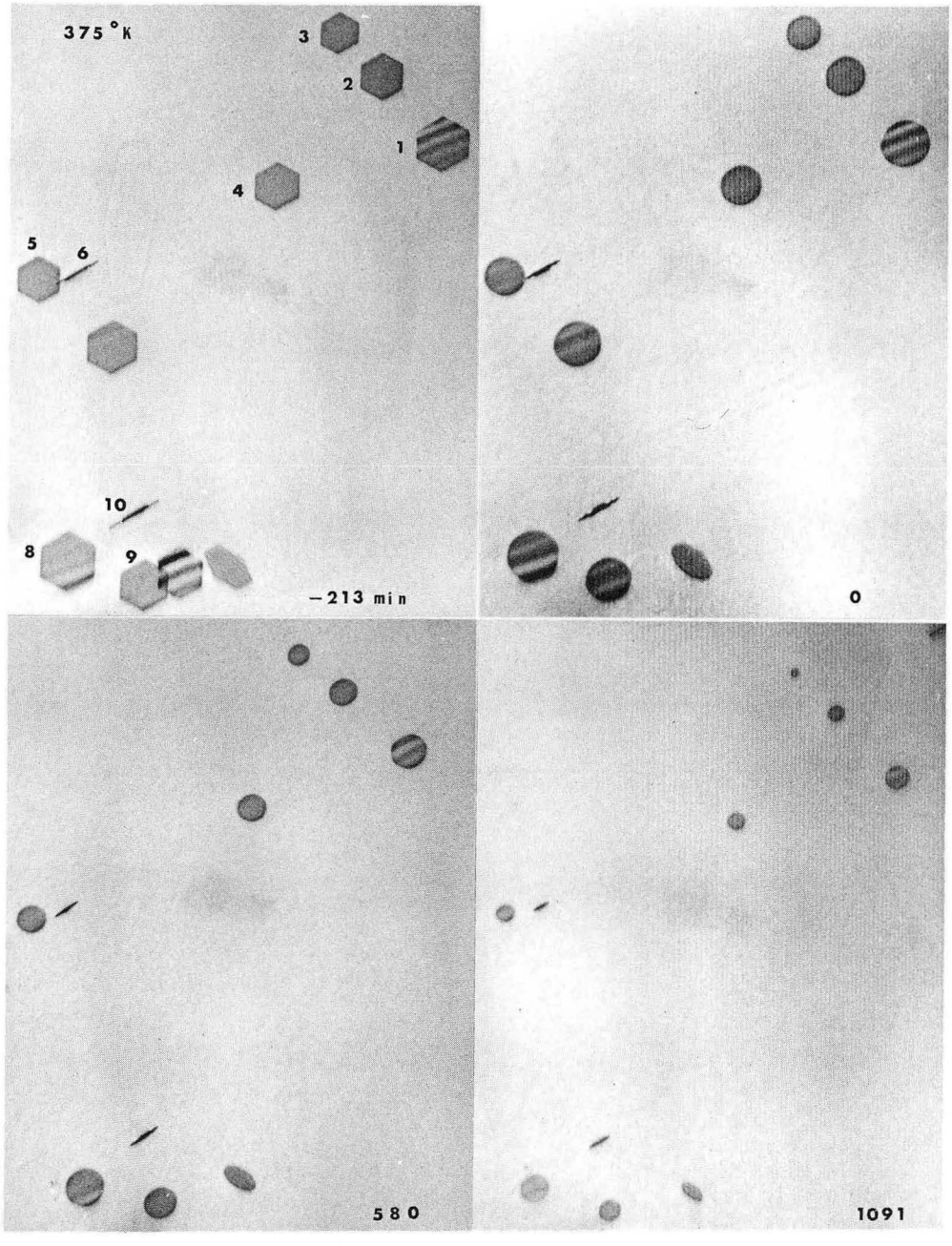

XBB 682-853

Fig. IIA.5-1 Climb of 1/3 ⟨111⟩ dislocations at 375°K in aluminum.

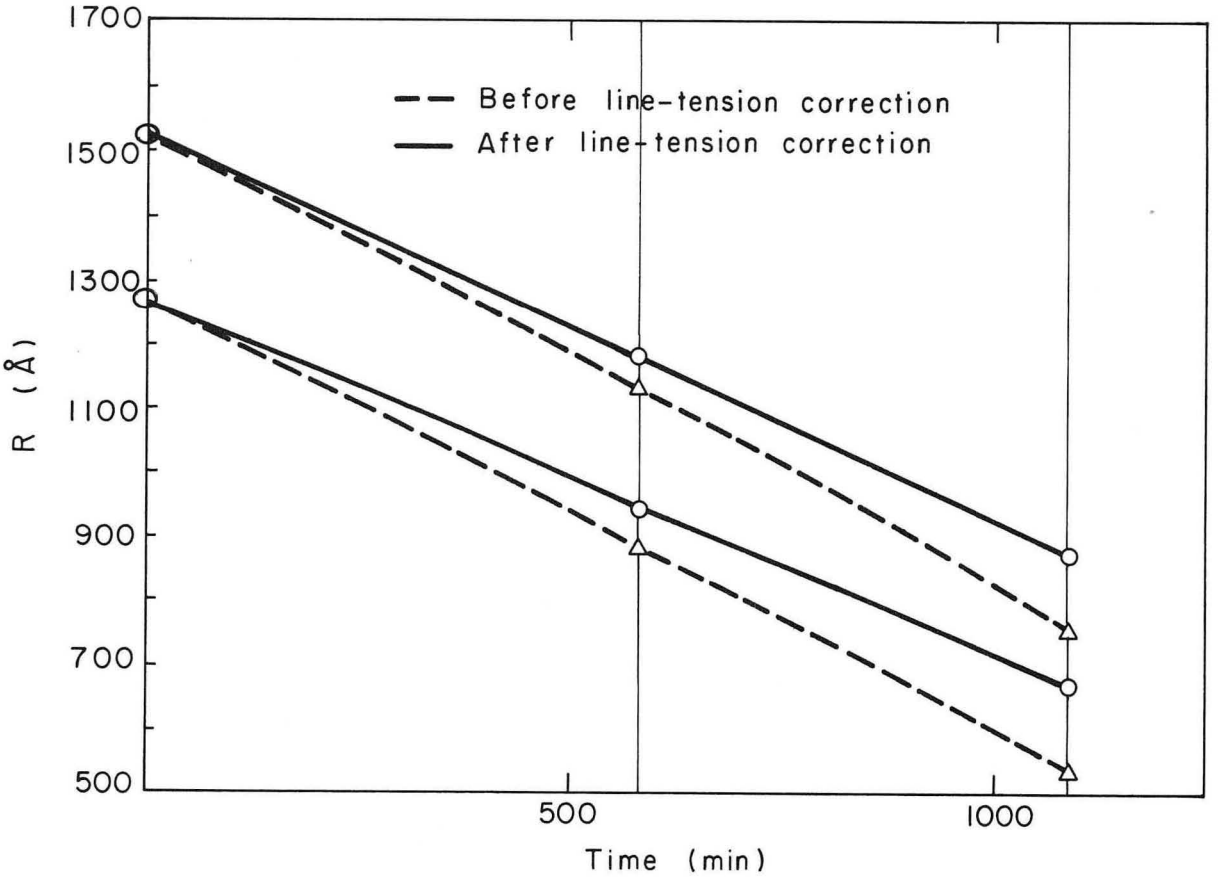

Fig. IIA.5-2 Corrected shrinkage rates for loops 1 and 4 in Fig. IIA.5-1.

8. RESEARCH PLANS FOR CALENDAR YEAR 1968

Jack Washburn

A field-ion microscope study of radiation damage in iridium is being continued. Specimens are being irradiated at 300°K in the Berkeley 88-in. cyclotron. Growth of defect clusters during annealing is being followed by resistivity and direct field-ion microscope observations.

X-ray topography techniques are being applied to the measurement of dislocation velocity in silicon. This work will be extended to study conservative and nonconservative motion of dislocations in magnesium. Eventually it should be possible to get reliable information concerning stress and temperature dependence of dislocation velocity for both climb and glide motions.

The mechanism of slip-band formation in a work-hardened metal is being studied by deforming copper crystals in multiple slip and then making transmission electron microscope observations after small amounts of additional deformation in single slip. This work is an extension of previous surface-replica observations of slip bands.

Dislocation etch-pit studies of the very early stages of plastic deformation of polycrystalline copper are in progress. It has been shown that at stresses far below the yield stress, dislocation multiplication begins at a few sources in the surface grains but not in interior grains.

The 650-kV electron microscope which will be put into operation during 1968 will permit observation of foils of aluminum and other light elements that are thick enough to avoid

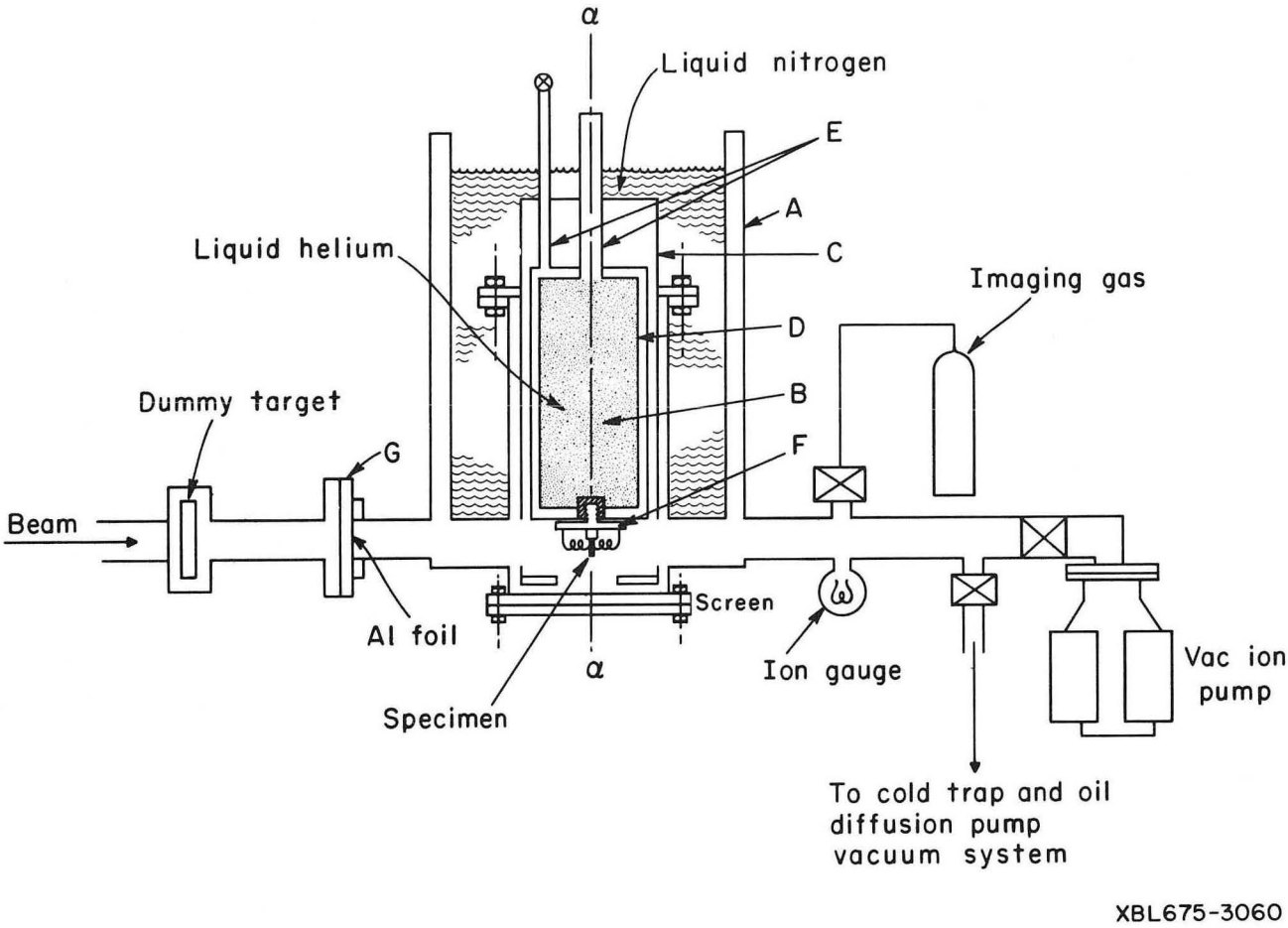

Fig. IIA.6-1. Liquid-helium field-ion microscope:
(A) stainless steel liquid-nitrogen dewar;
(B) liquid-helium cold finger;
(C) silver-plated copper heat shield;
(D) vacuum jacket;
(E) thin-walled stainless steel tubes;
(F) alumina specimen holder and copper clamping block.

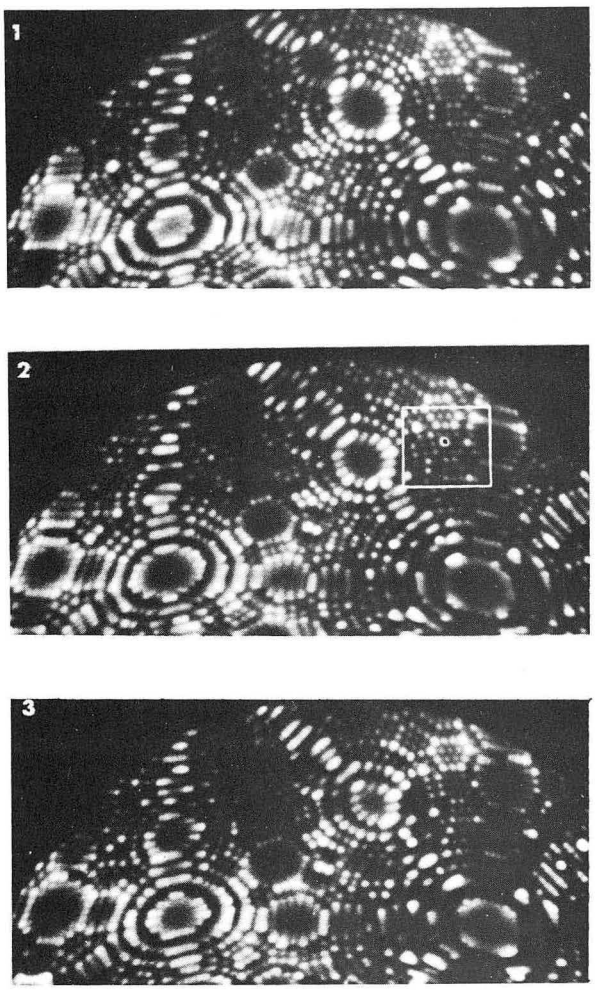

XBB 676-3525

Fig. IIA.7-1 Pictures 1 to 3 show a field-evaporation sequence of an irradiated specimen with an interstitial arriving at the surface on top of a plane which did not field-evaporate.

Research Plans (Continued)

many of the difficulties encountered with deformation-stage experiments on conventional foils. Systematic dynamic measurements of dislocation velocity under known applied stresses may become possible as an extension of the x-ray topographic studies.

9. 1967 PUBLICATIONS

Jack Washburn and Associates

Technical Journals

1. E. Levine, J. Washburn, and G. Thomas, Diffusion-Induced Defects in Silicon, I. J. Appl. Phys. 38, 81 (1967).
2. E. Levine, J. Washburn, and G. Thomas, Diffusion-Induced Defects in Silcon, II. J. Appl. Phys. 38, 87 (1967).
3. J. Washburn and R. E. Cooper, Stress-Induced Movement of Twin Boundaries in Zinc, Acta Met. 15, 639 (1967).
4. J. Washburn and G. Murty, Effect of Initial Dislocation Density on the Stress-Strain Curve and on Surface Indication of Slip in Copper, Can. J. Phys. 45, 523 (1967).
5. J. Washburn and P. C. J. Gallagher, The Formation of Extrinsic-Intrinsic Faulting, Phil. Mag. 15, 969 (1967).
6. J. Washburn, Crystal Imperfections in An Atomistic Approach to the Nature and Properties of Materials, Joseph A. Pask, ed. (John Wiley and Sons, Inc., New York, 1967), p. 103.
7. J. Washburn and T. Cass, Dislocation Dipoles in MgO, J. Physique 27, Supplement to Nos. 7-8, C3-168 (1966).
8. J. Washburn and G. Murty, Effect of Initial Dislocation Density on Single-Slip Strain Hardening of Copper, in Proceedings of the International Conference on the Strength of Metals and Alloys, Tokyo, Japan, September 4-8, 1967 (to be published); see also UCRL-17774, August 1967.
9. J. Washburn, A Survey of Techniques for the Direct Observation of Structure and Crystal Imperfections, in Techniques of Metal Research, Vol. 2, Part 1, R. Bunshah, ed. (John Wiley and Sons, Inc., New York, 1968), Chapter 1; see all UCRL-16948, February 1967.
10. M. J. Yokota and J. Washburn, Annealing of Stacking-Fault Tetrahedra in Gold, Phil. Mag. 16, 459 (1967).

UCRL Reports

1. P. Petroff and J. Washburn, A Liquid Helium Field-Ion Microscope for Radiation Damage Investigations, UCRL-17347-Rev., May 1967.
2. P. Petroff, A Field-Ion Microscope Investigation of Radiation Damage in Iridium Bombarded with 10-MeV Protons (Ph.D. Thesis), UCRL-17633, July 1967.
3. G. Vagnard and J. Washburn, Plastic Deformation of Cuprous Oxide, UCRL-17420, April 1967.

B. KINETICS OF DISLOCATION MECHANISMS

1. THEORETICAL STUDIES

John E. Dorn

The statistics of the cutting of randomly distributed point obstacles by a dislocation has been studied. The macroscopic flow stress at 0°K was deduced on the basis of nonuniformities in the motion of the dislocation. The results are in overall agreement with the computer experiments of Foreman and Makin.[1]

In an investigation of the interaction of dislocations with stationary Cottrell solute-atom atmospheres, it has been found that the force-distance diagram can be adequately represented by the equation

$$\frac{\tau_b}{\tau_{0b}} = \frac{X}{X_0}\left[\frac{2n}{\left(\frac{X}{X_0}\right)^2 + 2n-1}\right]^n ,$$

in which τ_{0b} is the maximum force per unit length of dislocation, X_0 is the distance that the dislocation has moved from the center of the equilibrium cloud, and n is determined from the equilibrium temperature. By using a method similar to that used by Dorn and Rajnak, the activation energy required to activate escape of the dislocation from the cloud can be calculated. The results of the theory will be tested experimentally by measurement of the stresses required to move low-angle tilt boundaries in pure and alloyed Zn crystals.

The Dorn-Rajnak approach to the Peierls process has been extended by taking into account the rearrangements of the core of screw dislocations in bcc structures. In this way the model is able to explain the observed asymmetries of yielding and slip in bcc metals.

1. A. J. E. Foreman and M. F. Makin, Phil. Mag. 14, 911 (1966).

2. EXPERIMENTAL INVESTIGATIONS

John E. Dorn

a. Deformation at Low Temperatures

The effect of interstitial C on the plastic behavior of Mo single crystals was studied. A ZrH_2 purification technique was used to lower the C content on previously zone-refined Mo. It was found that the athermal stress level is indeed lowered by purification, while the thermally activated components of the stress are not affected by it. The controlling mechanism is, seemingly, the Peierls process in agreement with the results on Fe-2% Mn of Wynblatt and Dorn.

A thermally activated mechanism was shown to be operative below 115°K in a study of the effect of temperature and strain rate on the flow stress of polycrystalline Mg-14 wt.% Li-1.5 wt.% Al. The process was satisfactorily interpreted in terms of the Dorn-Rajnak theory of the Peierls mechanism, the deformation being controlled by the rate of nucleation of pairs of kinks.

Two studies on the mechanical behavior of ordered alloys have been completed.

The flow stress of ordered and disordered fcc Cu_3Au has been investigated from 20 to 420°K. The thermally activated deformation mechanisms were shown to be operative below 100°K and 340°K for the ordered and disordered alloy, respectively. These results have been interpreted in terms of a pseudo-Peierls mechanism, due to the splitting of the cores of screw dislocations on several planes. Furthermore, it is suggested that, in the case of the disordered alloy, the intersection mechanism is operative in the range 225 to 340°K.

The effect of orientation on the rate of strain hardening of ordered β-phase AgMg (CsCl structure) was investigated. It was found that specimens oriented near the [001] direction exhibited a two stage stress-strain curve, with an easy-glide region followed by moderate strain hardening. On the other hand, specimens oriented near [011] and [111] directions presented parabolic stress-strain curves, with very high strain-hardening rates. The anisotropic strain hardening behavior is consistent with the athermal formation of barriers by the creation of antiphase boundary tubes. These are formed by the motion of nonaligned jogs on each of the dislocations of the glide superdislocation. The jogs result from intersection of mobile forest dislocations.

b. Investigation of Creep of Fe-4% Si

Strain rate $\dot{\gamma}$ was shown to obey (in the range 650 to 1100°K) the relationship

$$\dot{\gamma} = K \frac{\tau^{5.75}}{\tau G^{5.75}} \exp(-g/RT),$$

where K is a constant, τ the applied shear stress, G the shear modulus, g the free activation energy for creep, R the gas constant, and T the absolute temperature.

A steep increase of the apparent activation energy with increasing temperature takes place over the magnetic transformation range, 925 to 1035°K, reaching a maximum at the curve temperature. This increase is in good agreement with the known decrease in free energy of activation for diffusion.

The creep behavior over the entire range of temperatures was found to be in agreement with the dislocation climb mechanism.

c. Electrical Resistivity

The changes in electrical resistivity as a result of both the addition of 0.1% Al to Cu and of prestraining were studied.

The electrical resistivity was shown to be proportional to the square of the scattering charge of the alloying element. An increase of resistance was detected in specimens annealed at 90 and 113°K.

d. Dynamic Behavior

Experiments were carried out to study the effects of prestrain and the addition of 0.04 at.% and 2 at.% Cu + Al single crystals, on the damping of dislocations in accord with the previous results of Ferguson, Kumar, and Dorn. A linear dependence of the shear stress with shear strain rate was found. However, both the stress level and the slope of the linear relation were higher, particularly in the Al-2 at.% Cu alloy, which had been age-hardened to form Guinier-Preston zones.

3. RESEARCH PLANS FOR CALENDAR YEAR 1968

John E. Dorn

Recent theoretical developments have shown the necessity for further investigation of the asymmetric properties of both the flow stress and slip systems in bcc metals. A rationalization of these effects is intended by deforming high-purity Mo single crystals followed by slip-line trace analysis for each case.

The effects of temperature and strain rate on the CRSS of AgMg as a function of orientation will be investigated in order to ascertain whether the same mechanism is operative at both the [001] and rapid-hardening orientations.

Both tensile and creep testing will be used to investigate a steel containing 0.20% C and 4% Mo with the object of studying the effects of tempering, carbide formation, and strain aging.

In order to compare with previous measurements of the damping constant for pure Al, the temperature dependence of the shear stress will be studied for both the prestrained and alloyed Al single crystals.

The specimen chamber of a new high-velocity impact gun is in the final stages of construction. It will allow tests to be conducted at much higher stresses and strain rates (about 10^5 per sec) and hence provide data in the very high strain-rate region. Such data are necessary for explaining the mechanism of dislocation behavior in the near-relativistic velocity region:

$$\left(\frac{V_{dislocation}}{V_{sound}} \simeq 1 \right).$$

4. 1967 PUBLICATIONS

John E. Dorn and Associates

Technical Journals

1. Ching-Yao Cheng, P. Wynblatt, and J. E. Dorn, Vacancy Models for Concentrated Binary Alloys. Part I: Short-Range Ordered and Clustered Alloys, Acta Met. 15, 1035 (1967).
2. Ching-Yao Cheng, P. Wynblatt, and J. E. Dorn, Vacancy Models for Concentrated Binary Alloys. Part II: Long-Range Ordered Alloys, Acta Met. 15, 1045 (1967).
3. B. Y. Chirouze, D. M. Schwartz, and J. E. Dorn, The Mechanism of Basal Creep in Mg-12 At.% Li from 500 to 885°K, Trans. Quarterly 60, 51 (1967).
4. W. G. Ferguson, F. E. Hauser, and J. E. Dorn, Dislocation Damping in Zn Single Crystals, Brit. J. Appl. Phys. 18, 411 (1967).
5. W. G. Ferguson, A. Kumar, and J. E. Dorn, Dislocation Damping in Al at High Strain Rates, J. Appl. Phys. 38, 1863 (1967).
6. P. Guyot, Camel-Humps Peierls Hills in Iron, Phys. Stat. Sol. 19, [2] K95 (1967).
7. P. Guyot and J. E. Dorn, A Critical Review of the Peierls Mechanism, Can. J. Phys. 45, 983 (1967).
8. S. Lau, S. Ranji, A. H. Mukherjee, G. Thomas, and J. E. Dorn, Dislocation Mechanisms in Single Crystals of Tantalum and Molybdenum at Low Temperatures, Acta Met. 15, 237 (1967).
9. D. M. Schwartz, J. B. Mitchell, and J. E. Dorn, The Mechanism of Prismatic Creep in Mg-12 At -% Li, Acta Met. 15, 485 (1967).

UCRL Reports

1. O. Abo-el-Fotoh, J. B. Mitchell, and J. E. Dorn, The Low Temperature Thermally Activated Deformation Mechanisms for bcc Magnesium-Lithium-Aluminum Alloy, UCRL-17769, August 1967.
2. Ching-Yao Cheng, Vacancy Models for Concentrated Binary Alloys (Ph.D. Thesis), UCRL-17462, University of California, Berkeley, April 1967.
3. Ching-Yao Cheng, A. Karim, T. G. Langdon, and J. E. Dorn, Creep Mechanisms in Fe-4% Si Alloy, UCRL-17730, August 1967.
4. J. E. Dorn, Low Temperature Dislocation Mechanisms, presented at the Battelle Colloquium on Dislocation Dynamics, Seattle, May 1-5, 1967; UCRL-17521, April 1967.
5. P. Guyot, T. Stefansky, and J. E. Dorn, Nonuniformities in the Motion of a Dislocation through a Random Array of Point Obstacles, UCRL-17848, September 1967.
6. T. G. Langdon and J. E. Dorn, Low Temperature Dislocations Mechanisms in Ordered and Disordered Cu_3Au, UCRL-17863, October 1967.
7. R. P. Malatesta, Resistometric Observation of the Annealing Characteristics of a Tensile-Loaded Cu-Al Alloy (M.S. Thesis), UCRL-17799, University of California, Berkeley, September 1967.
8. J. B. Mitchell, Strain Hardening of Long-Range Ordered AgMg Single Crystals (Ph.D. Thesis), UCRL-17894, University of California, Berkeley, November 1967.

C. RELATION OF STRUCTURE TO PROPERTIES IN CRYSTALS

1. ON FATIGUE-INDUCED REVERSION AND OVERAGING IN DISPERSION-STRENGTHENED ALLOY SYSTEMS*

C. Laird† and Gareth Thomas

The low fatigue strength/U.T.S. ratios of dispersion-strengthened aluminum alloys may be explained by the presence of transgranular, precipitate-free bands in their microstructures. Since transgranular crack initiation and growth is frequently observed in such alloys, these bands appear to be as weak as the other type of precipitate-free band which is associated with grain boundaries. It has been suggested that the bands are formed by fatigue-induced reversion of the precipitates. An alternative suggestion for their formation, viz., that the bands develop naturally as part of the precipitate aging sequence, was proposed and tested by examination of the structures, using transmission electron microscopy, in Al-4% Cu and Al-5.57%Zn-2.50%Mg alloys both before and after cycling. Since bands with equal frequency of occurrence and similar structures have been observed in both situations, strong support for the aging inhomogeneity hypothesis has been obtained, i.e., fatigue cracks initiate in the soft, precipitate-free regions already existing in the alloys. Previous circumstantial evidence for the reversion viewpoint has been reconsidered and can be interpreted as also supporting the aging inhomogeneity hypothesis. While the latter is preferred on the basis of more direct evidence, the reversion mechanism may operate in a few isolated cases, such as in the fatigue of Fe-C alloys.

---

* J. Fracture Mechanics 3, 81 (1967).
† Scientific Laboratory, Ford Motor Company, Dearborn, Michigan.

2. COMMENTS ON SURFACE OXIDE FILMS AND THE LIFETIME OF VACANCIES IN THIN CRYSTALS*

Alf Eikum† and Gareth Thomas

During annealing experiments in the electron microscope, prismatic dislocation loops and helices have been observed to grow in thin foils prepared from quenched and aged samples

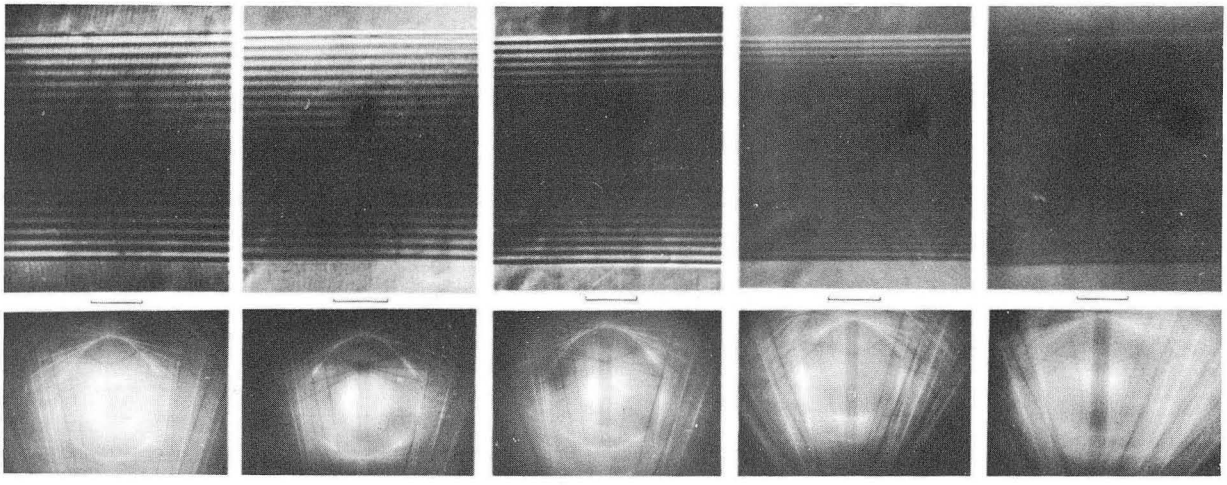

XBB 679-5634

Fig. IIC.3-1. The same area of a silicon foil showing the loss of fringe contrast due to absorption upon reduction of the voltage. (a) 1200 kV; (b) 1000 kV; (c) 750 kV; (d) 500 kV; (e) 300 kV. The corresponding diffraction patterns show that the orientation remains constant with systematic [111] reflections operating. Thickness ~3μ.

of supersaturated aluminum-magnesium alloys. Growth in pure aluminum or dilute aluminum-magnesium alloys has not been reported. It has been suggested recently that the excess vacancies required for growth are residual quenched-in vacancies that were not able to sink at external surfaces due to the presence of an impervious oxide film.

The oxide mechanism fails to account for the fact that growth has not been observed in pure aluminum and dilute aluminum alloys. This point and others concerning the lifetime of vacancies in thin crystals have been discussed.

* Phil. Mag. 15, 261 (1967).

† Present address: Boeing Scientific Research Laboratories, Seattle, Washington.

3. ELECTRON MICROSCOPY AT HIGH VOLTAGES*

Gareth Thomas

Experiments have been conducted to investigate the useful thickness limits as a function of voltage under routine operating conditions for silicon and stainless steel. The criterion adopted for this limit was that thickness at which fringe contrast at faults was destroyed by absorption. Figure IIC.3-1 shows an example for silicon, and Fig. IIC.3-2 summarizes the results obtained.

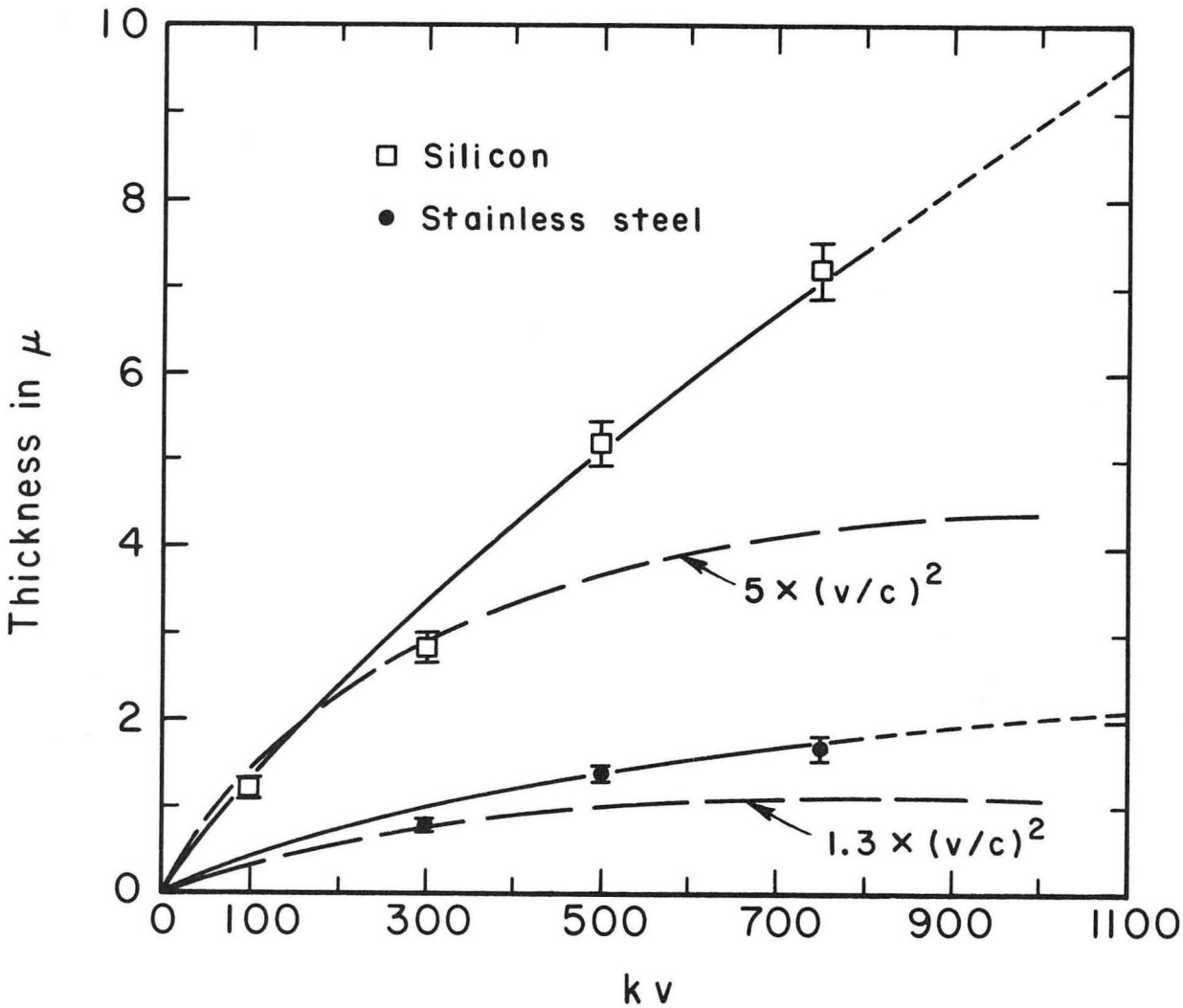

XBL679-5291

Fig. IIC.3-2. Plot of the thickness limit for silicon and stainless steel determined from experiments such as those shown in Figs. IIC.3-1, 3 (systematic ⟨111⟩ reflections). It can be seen that the limits are not proportional to $(v/c)^2$.

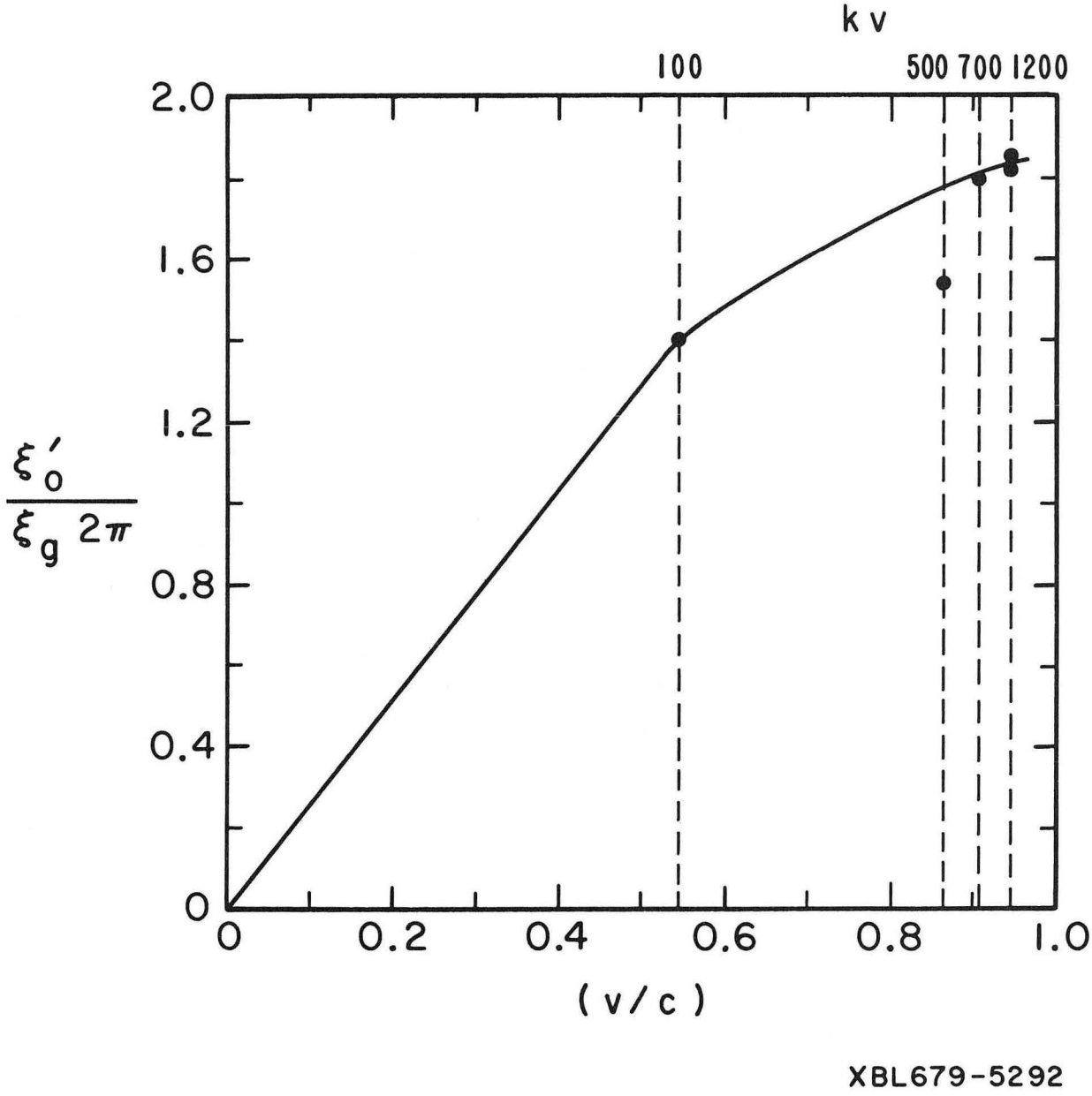

Fig. IIC.3-3. Plot of the dimensionless factor $[\xi_0'/2\pi\xi_g]$ against (v/c) for silicon; mainly systematic ⟨111⟩ conditions except at higher voltages.

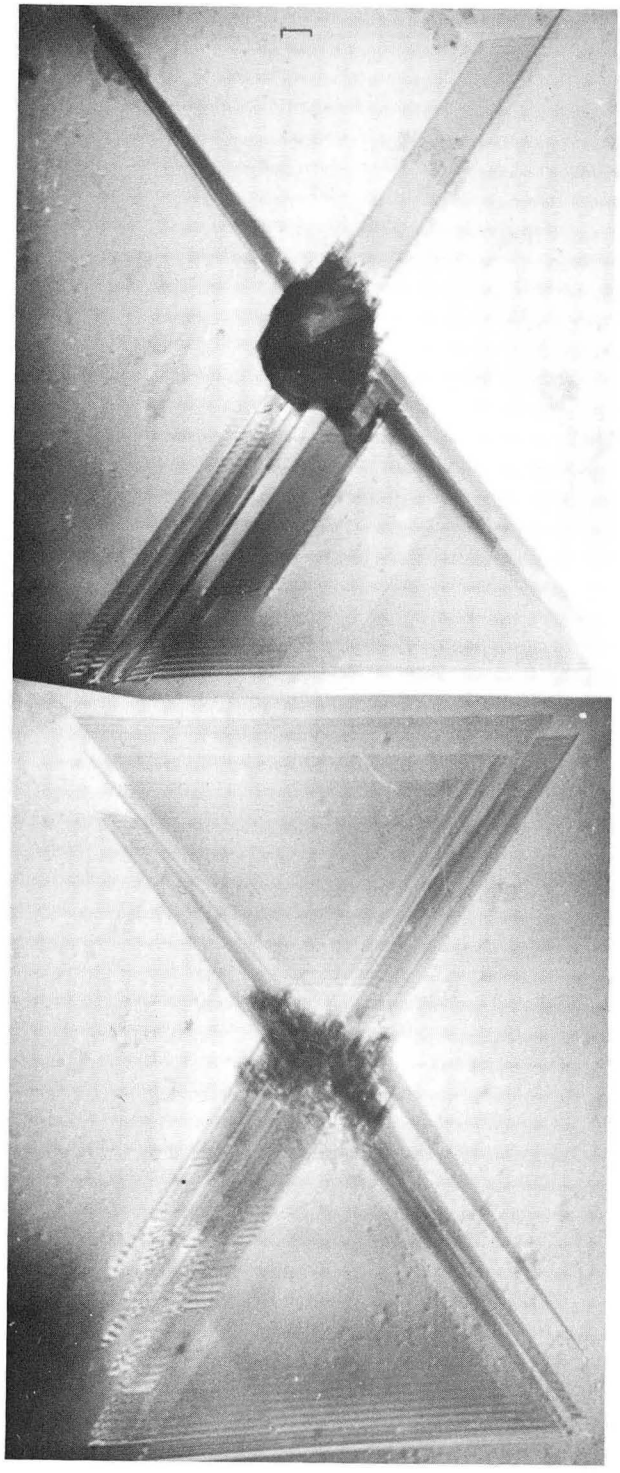

XBB 679-5633

It can be seen that penetration increases with voltage, but the rate of increase falls off with increasing atomic number, presumably because of greater absorption. Furthermore, it appears that there is not much benefit beyond 500 kV, except for the light elements.

The nonlinear behavior of the transmissive power (inverse of the mean absorption coefficient) with voltage observed by others for MgO was also found for silicon (Fig. IIC. 3-3). The anomaly is attributed to the operation of multiple beams at high voltage.

An application to the study of interfaces showed that the high penetration enables matrix-substrates to be much more easily studied than at 100 kV. Fig. IIC. 3-4 shows the generation of stacking faults from impurities at the substrate-epitaxial layer in silicon.

I wish to acknowledge the assistance of Prof. G. Dupuoy and the Electron Optics Laboratory, Toulouse, France, and Dr. V. E. Cosslett of the Cavendish Laboratory, Cambridge, England which enabled me to carry out these experiments.

---

* Abstract from UCRL-17842, September 1967; Phil. Mag. (in press).

Fig. IIC.3-4. Origin of stacking faults from inclusions at the substrate-epitaxial layer interface in silicon. Thickness of the layer ~6.1/4μ; photographed at 1 MeV.

4. STRUCTURE AND PROPERTIES OF Fe/Ni/Co/Ti MARAGING STEEL*

I-Lin Cheng and Gareth Thomas

The structure and properties of an alloy of Fe-20Ni-24Co-0.07Al-0.2Ti were investigated. Figure IIC.4-1 shows the stress-strain curves of the alloy following heat treatment. Although good strength is obtained by aging the martensite, there is a serious loss in ductility. This is attributed to lath and grain boundary precipitation (Fig. IIC.4-2).

The dark-field technique was used to investigate the onset of precipitation. The precipitates form uniformly in the highly dislocated martensite laths and were identified as Ni_3Ti using electron diffraction from foils and extraction replicas, x-ray analysis using the XMA probe attachment to the Siemens microscope, and normal microprobe techniques (Fig. IIC.4-3). The overaging was shown to correspond to reversion to austenite, and not to growth of the Ni_3Ti phase. The η Ni_3Ti phase forms as plates with the relation $(0001)_\eta // (110)_\alpha$; $[2\bar{1}\bar{1}0]_\eta // [1\bar{1}1]_\alpha$.

We conclude that cobalt has little benefit in strengthening, and no evidence was obtained for ordering of the matrix.

After plastic deformation the precipitates were observed to deform with the matrix (Fig. IIC.4-4). The strength of the alloy is due primarily to dispersion strengthening.

---

* Abstract from UCRL-17803, September 1967; Trans. ASM (in press, 1968).

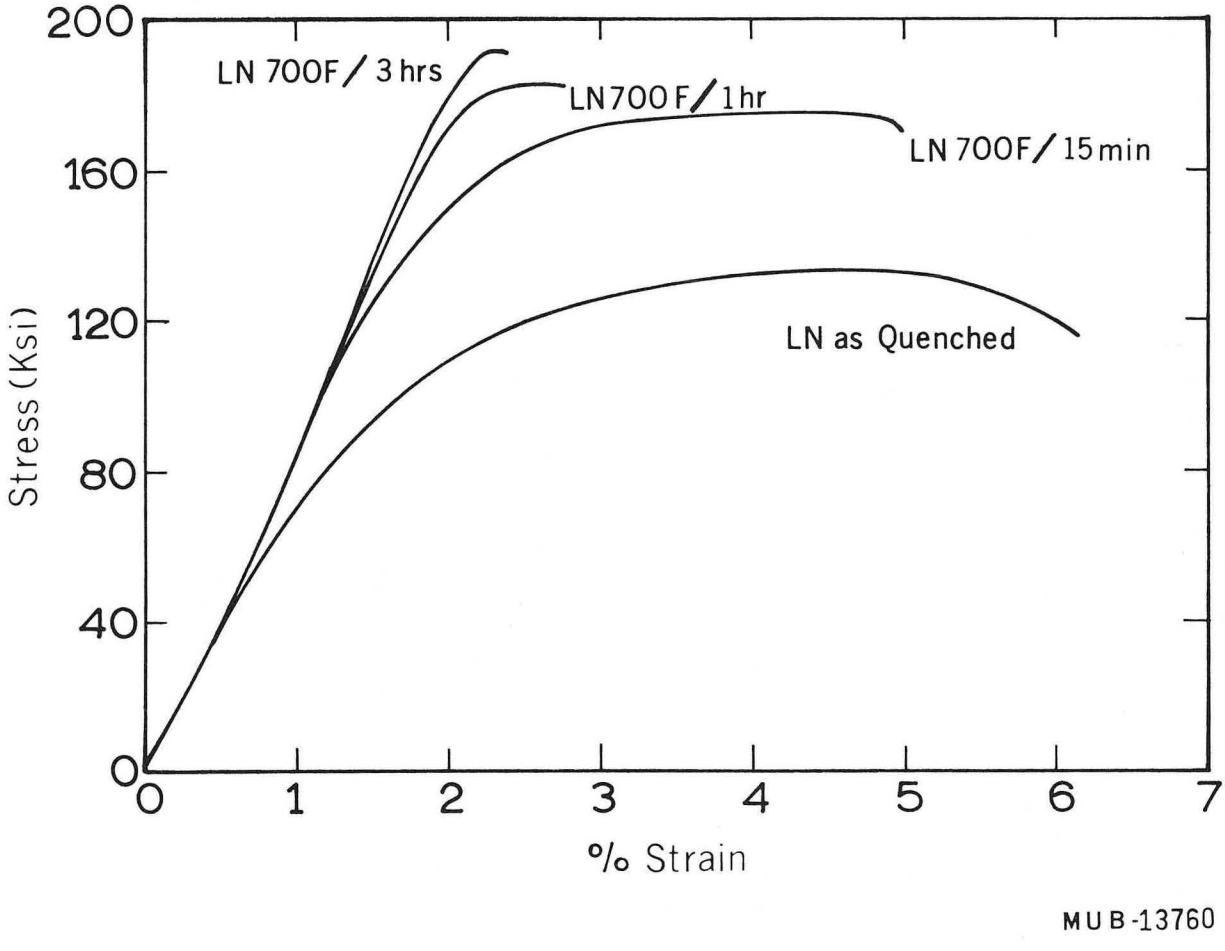

Fig. IIC.4-1. Stress-strain curves of aged alloys after quenching in liquid nitrogen.

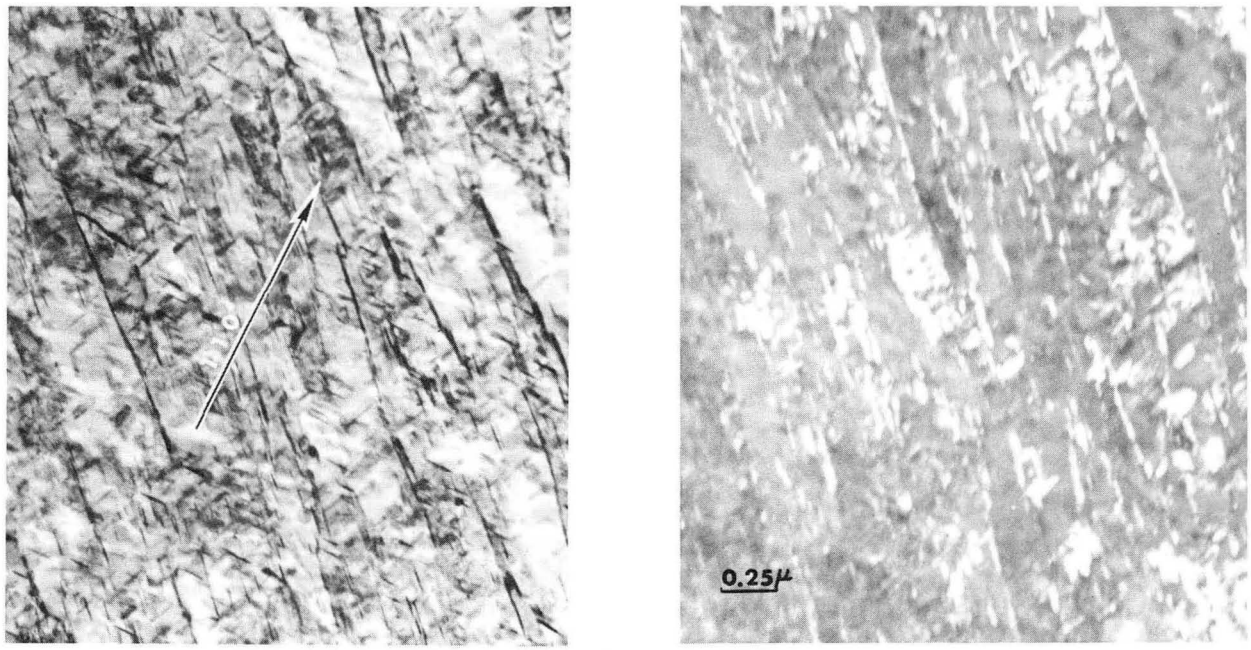

(a) (b) XBB 679-5310

Fig. IIC.4-2. Alloy aged for 3 hr at 900°F after LN quench. (a) Bright field, (b) gun-tilt dark field (using Ni_3Ti reflections) showing both matrix and boundary precipitates of Ni_3Ti.

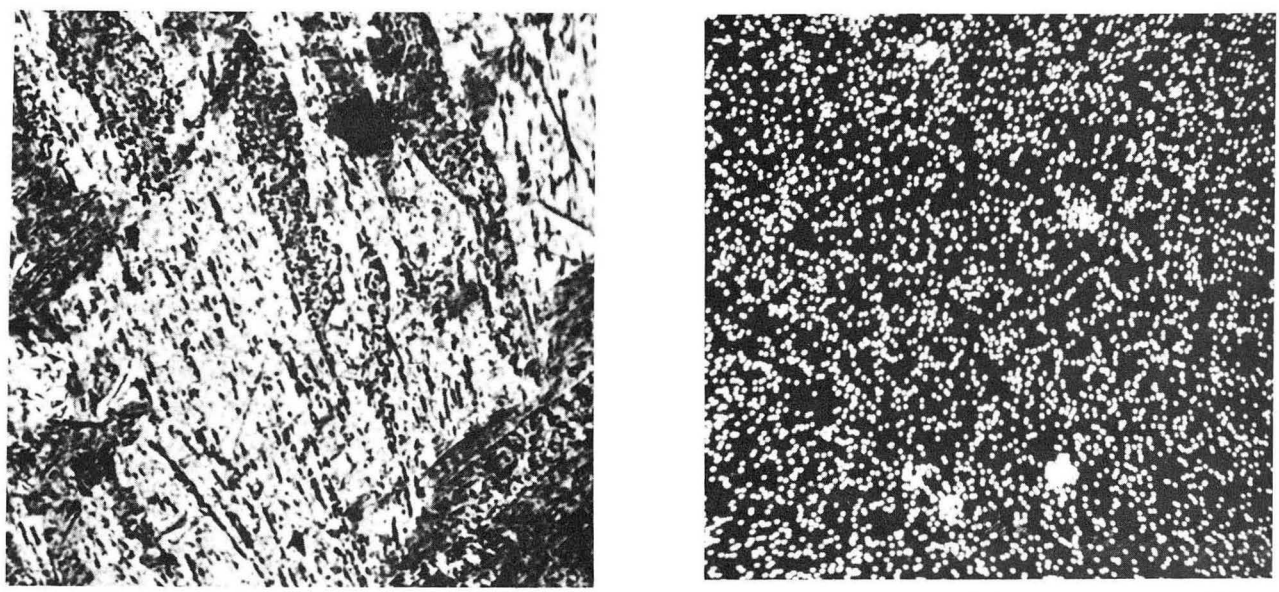

(a) (b) IM 2483

Fig. IIC.4-3. Electron-beam probe analysis. (a) optical photograph (×550), (b) x-ray image area using TiK_α.

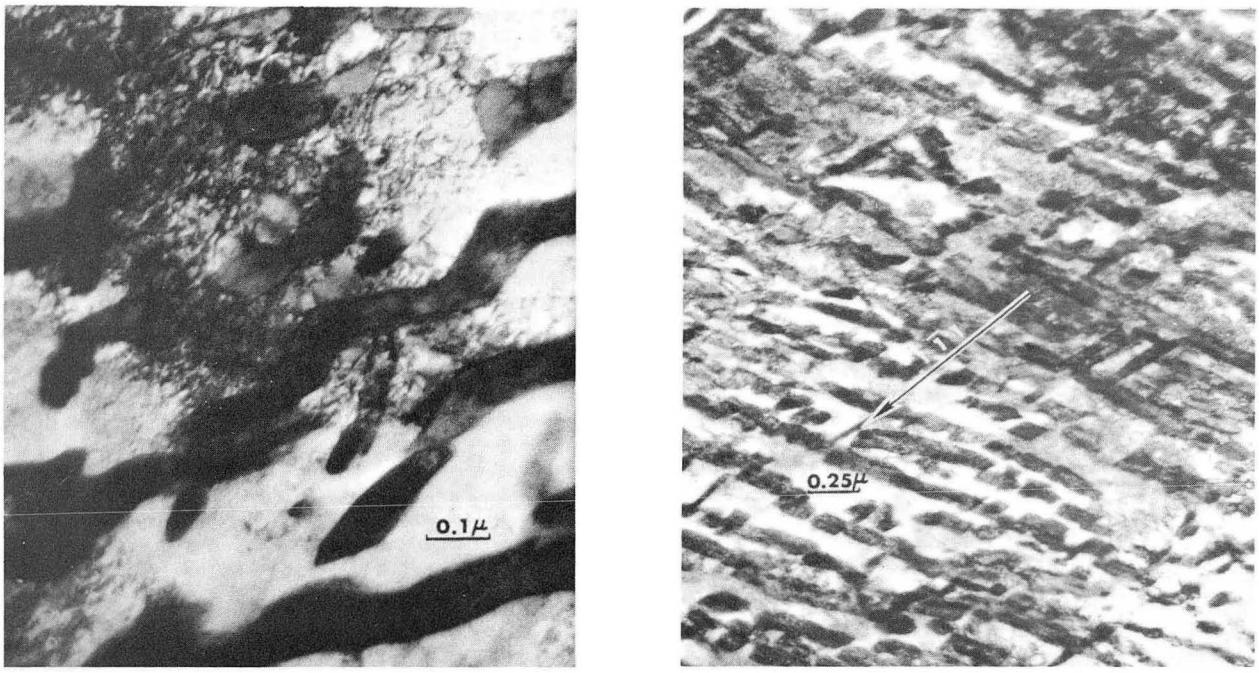

(a) (b) XBB 679-5306

Fig. IIC.4-4. Thin foil of alloy aged 12 hr at 900°F after 30% cold rolling. (a) shows shearing of particles in the matrix in ⟨111⟩; (b) shows shearing and fracture of boundary particles.

5. ELECTRON MICROSCOPE OBSERVATIONS OF TWINNING AND PHASE TRANSFORMATIONS IN InS CRYSTALS*

Alexander G. Fitzgerald† and Gareth Thomas

Thin crystals of indium sulfide with the crystal structures corresponding to the compositions InS and In_6S_7 have been grown by means of a chemical transport reaction. Phase transitions have been induced by beam heating in the electron microscope and have been identified by electron diffraction.

Crystals of InS occasionally contain twins when examined in the electron microscope. The twins presumably originate during the growth process. When these crystals are subjected to high-intensity electron irradiation in the electron microscope, large numbers of twins are nucleated. On continued electron irradiation, structural transformations occur in these crystals. Crystals with the orthorhombic InS structure transform to the monoclinic In_6S_7 structure (Fig. IIC.5-1) and, on further electron irradiation, an additional transformation to the tetragonal In_2S_3 structure occurs.

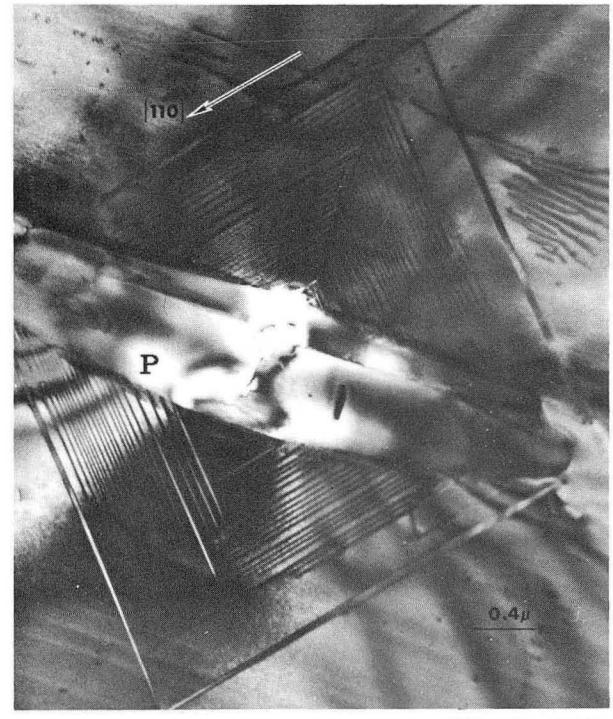

XBB 679-5113

Fig. IIC.5-1. Area of an InS crystal showing twins and the new phase P, which has the monoclinic In_6S_7 crystal structure.

When crystals with the monoclinic In_6S_7 structure are subjected to high electron-beam intensities in the electron microscope, a structural transformation also occurs, and the crystals transform to the tetragonal In_2S_3 structure (Figs. IIC.5-2 and 5-3).

We conclude that crystals of InS grown by chemical transport reactions are non-stoichiometric and are probably sulfur-rich.

* Abstract from UCRL-17764, August 1967; Phys. Stat. Solidi 25, 263 (1968).
† Present address: Department of Physics, University of St. Andrews, Dundee, Scotland.

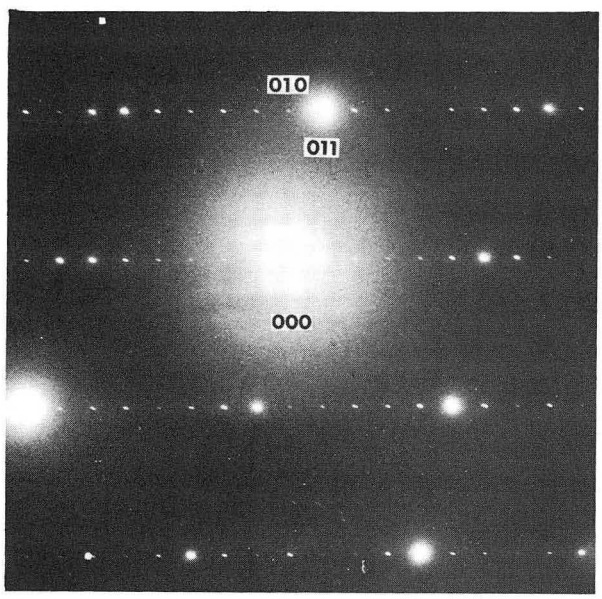

XBB 679-5125

Fig. IIC.5-2. Electron-diffraction pattern from In_6S_7 crystal with [100] zone axis in this monoclinic structure.

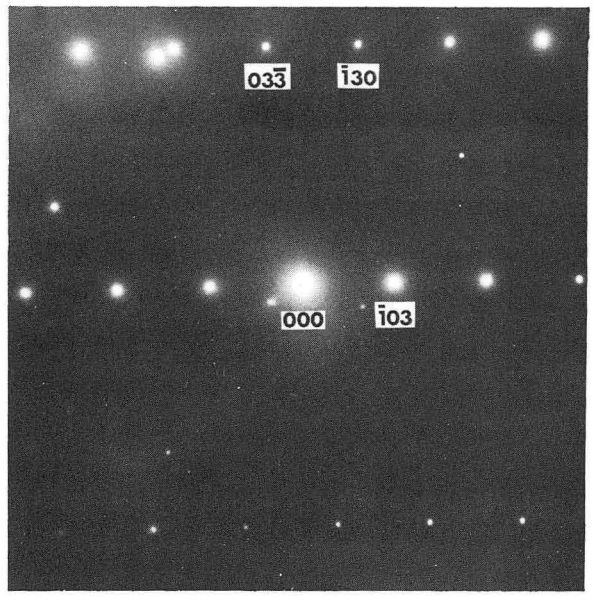

XBB 679-5126

Fig. IIC.5-3. Electron-diffraction pattern from transformed region of the crystal produced by heating this In_6S_7 crystal in the electron beam. This is $(31\bar{1})$ the reciprocal lattice section in the tetragonal In_2S_3 structure.

6. INDICES OF PLANES AND DIRECTIONS IN HCP CRYSTALS*

Paul Okamoto and Gareth Thomas

In a recent paper, Partridge and Gardiner[1] pointed out that errors may arise in the indexing of diffraction patterns from hcp crystals unless care is taken to distinguish between formulae based on the three- and four-axis hexagonal systems. It was also stated that because it is impossible to construct a reciprocal lattice based on the four-axis reference basis, indexing of reciprocal lattice planes in terms of the Miller-Bravais notation is meaningless.

However, we wish to point out that it is possible to construct a four-axis hexagonal lattice in reciprocal space having all the characteristics of the conventional reciprocal lattice.[2] The four-axis "reciprocal" lattice follows directly from the conventional Miller-to-Miller-Bravais transformation for planar indices, i.e., $(hk\ell) \rightarrow (hki\ell)$, where $h+k+i = 0$ as usual. In this case, the basis vectors along the three close-packed directions in the reciprocal space have fractional indices of the form $1/3\ \langle 2\bar{1}\bar{1}0\rangle$. Thus not all reciprocal lattice points have rational indices, but those that do coincide with conventional reciprocal-lattice points. Those that do not cannot represent real crystal planes and, therefore, will not register as reflections in an actual diffraction pattern. From this point of view, the four-axis and the conventional reciprocal lattices are physically indistinguishable (Fig. IIC.6-1).

The four-axis "reciprocal" lattice not only has all of the characteristics of the conventional one, but also has several additional properties which makes it, as far as the interpretation of electron-diffraction patterns and images are concerned, the most convenient one to use.

First of all, the basis vectors of the four-axis reciprocal lattice define the hexagonal prism forming the first Brillouin zone, and since the orientation of the latter is identical to the hexagons of the direct lattice, the close-packed directions in both coincide and have the same indicial form, viz., $\langle 2\bar{1}\bar{1}0\rangle$. Consequently, the crystallographic relationships between a diffraction pattern and its image can be related more easily.

Secondly, since both the direct and "reciprocal" lattices are described in terms of four-axis hexagonal systems, crystallographic relationships such as those relating the indices of a plane and its normal; the magnitude of vectors and interplanar spacings and angles can be obtained through elementary vector algebra using the four-index Miller-Bravais notation throughout. Moreover, in addition to their relative simplicity, the formulae possess symmetry properties unique to this system. Therefore, by using the Miller-Bravais notation throughout the indexing procedures,

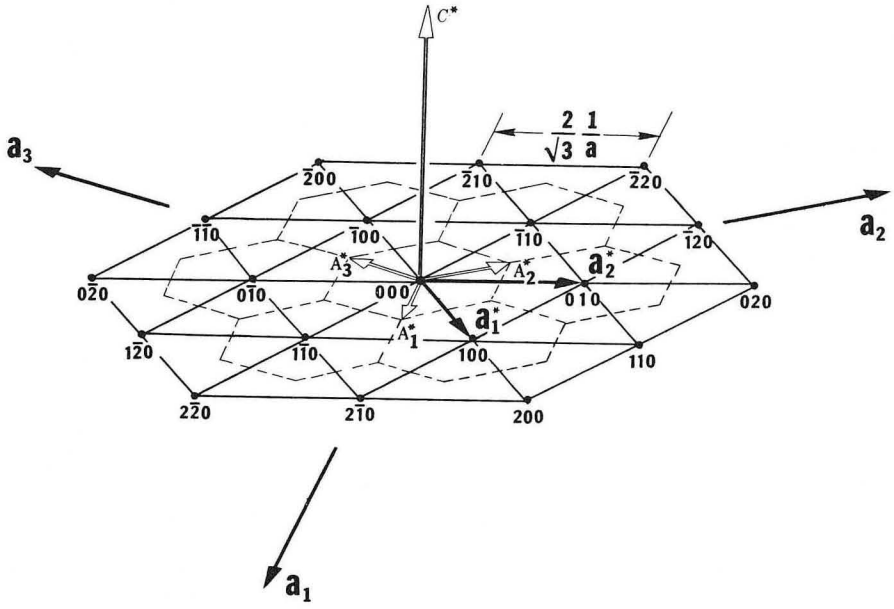

XBL 674-1429

Fig. IIC.6-1. The [0001] reciprocal-lattice plane showing the relationship between the four-axis and the conventional reciprocal-lattice basis vectors. (See text for further explanation.)

most of the sources of error pointed out by Partridge and Gardiner[1] can be avoided.

Finally, it can be shown from simple geometrical arguments that, contrary to the statement of Partridge and Gardiner,[1] the indexing of reciprocal lattice planes in terms of Miller-Bravais indices can be quite meaningful. In fact the Miller-Bravais indices (uvtw)* of a reciprocal lattice plane are also the components of its normal [uvtw] in direct space, and furthermore, its magnitude is inversely proportional to the interplanar spacing d* of the (uvtw)* reciprocal lattice planes.

---

* Abstracted from Scripta Met. 1, 25 (1967).

1. P. G. Partridge and R. W. Gardiner, Acta Met. 15, 387 (1967).
2. P. R. Okamoto and G. Thomas, UCRL-17413, April 1967; Phys. Stat. Solidi (in press).

7. RESEARCH PLANS FOR CALENDAR YEAR 1968

Gareth Thomas

a. New Programs

High-Voltage Microscopy

A Hitachi 650-kV microscope will be installed in July 1968. Advantage will be taken of the increased penetration that is possible with increasing voltage. Topics to be investigated include (a) electron-diffraction contrast and absorption phenomena, (b) determination of transparency limits, (c) applications to thick foils, and (d) applications to nonmetals, particularly ceramic systems.

Joint projects with Professor Washburn's group will include studies of dislocation behavior in thick foils.

Velocity Analysis

A velocity-analyzing lens is being built for incorporation into one of our Siemens microscopes. This lens will enable us to select the energy spectrum and to measure the characteristic plasmon losses. In this way we will be able to carry out qualitative chemical analysis to about 50Å resolution in addition to obtaining the normal images and diffraction patterns. Applications include studies of spinodal decomposition, grain boundaries, and solute segregation, e.g. temper embrittlement, etc., in addition to applications to the study of absorption (inelastic scattering) and contrast.

b. Cooperative Program on Biological Materials

Gareth Thomas, IMRD, and R. M. Glaeser, Donner Laboratories

The electron microscope is being used for electron-diffraction studies with biological specimens that are not more than 1000 to 2000Å thick and not more than a few microns on edge. The usual selected-area technique has been used to obtain wide-angle diffraction patterns (repeat distances on the order of 1 to 10Å) from a variety of crystalline amino acids. Low-angle diffraction experiments were used for low-angle studies with (1) 880Å polystyrene spheres in hexagonal close-packed array, (2) longitudinal thin sections of striated muscle, and (3) crystalline ℓ-valine. A 15-μ-diam condenser-aperture limits the field examined in diffraction to approximately 10μ, and improves the clarity of the diffraction patterns. Electron diffraction thus enjoys the advantages that (a) single crystals of very small dimensions and/or microscopic domains of large specimens can be examined, (b) photographic recording of data is very rapid (on the order of 10 sec), and (c) direct high-resolution images of the same (microscopic) sample can be recorded. One of the most important results of this study has been to prove that the Fourier contrast (interference contrast) mechanism must necessarily be considered in the interpretation of ordered biological structures with repeat distances of 10Å or more. This approach will be continued.

c. Continuing Projects

i. Comparison of the structure and properties of bainitic and martensitic alloys based on Fe/Ni/Co/C in the strength range 150,000 to 250,000 psi (yield).

ii. The role of dislocations and precipitates on the strength of steels after various thermal-mechanical treatments.

iii. Investigation of the role of interstitial order and/or precipitation on the ductile-brittle transition phenomenon in Group V metals. Ta-C is the system under investigation; work includes field-ion microscopy.

iv. Inelastic scattering and absorption of electrons in crystals. Measurement of absorption parameters and effects on image contrast, particularly for small defects. Kikuchi diffraction and effects on contrast.

v. Spinodal decomposition; direct observations by hot-stage microscopy. Investigations of the spinodal in Fe/Ni/Al. Use of Lorentz microscopy in quantitative microscopy of spinodal systems.

vi. Structural characteristics of A15 compounds and their relation to superconductivity. The work will include field-ion microscopy. (Joint project with Professor E. R. Parker's group.)

vii. Structural modifications in ultrahigh-strength steels and relation to properties. (Joint project with Professors E. R. Parker and V. F. Zackay's groups.)

8. 1967 PUBLICATIONS

Gareth Thomas and Associates

Technical Journals

1. A. Eikum and G. Thomas, Surface Oxide Films and the Lifetime of Vacancies in Thin Crystals, Phil. Mag. 15, 261 (1967).
2. S. S. Lau, S. Ranji, A. K. Mukherjee, G. Thomas, and J. E. Dorn, Dislocation Mechanisms in Single Crystals of Tantalum and Molybdenum at Low Temperatures, Acta Met. 15, 237 (1967).
3. E. Levine, J. Washburn, and G. Thomas, Diffusion-Induced Defects in Silicon. Part I, J. Appl. Phys. 38, 81 (1967).
4. E. Levine, J. Washburn, and G. Thomas, Diffusion-Induced Defects in Silicon. Part II, J. Appl. Phys. 38, 87 (1967).
5. P. R. Okamoto, E. Levine, and G. Thomas, Kikuchi Maps for hcp and bcc Crystals, J. Appl. Phys. 38, 289 (1967).
6. P. R. Okamoto and G. Thomas, Comments on "Indices of Planes and Directions in hcp Crystals," Scripta Met. 1, 25 (1967).
7. P. R. Okamoto and G. Thomas, Dislocation Substructure in Single Crystals of Hexagonal Ag-Al Oriented for Prismatic Slip, Acta Met. 15, 1325 (1967).
8. S. Ranganathan, H. B. Lyon, and G. Thomas, Computer Simulation of Field Ion Images of Hexagonal Structures and Superlattices, J. Appl. Phys. 38, 4957 (1967).
9. P. Rao and G. Thomas, Defects in Neutron-Irradiated Molybdenum, Acta Met. 15, 1153 (1967).
10. G. Thomas, High Temperature Electron Microscopy, in High-Temperature, High-Resolution Metallography, Proceedings of a Symposium sponsored by the Ferrous Metallurgy Committee, Institute of Metals Division, The Metallurgical Society, AIME, Chicago, Illinois, Feb. 15, 1965, (Gordon and Breach Science Publishers, New York, 1967) p. 217.
11. G. Thomas and C. Laird, On Fatigue-Induced Reversion and Overaging in Dispersion Strengthened Alloy Systems, Fracture Mechanics 3, 81 (1967).
12. G. Thomas and V. C. Kannan, Reply to "Comment on Dislocation Climb and Determination of Stacking-Fault Energies in Al and Al-1% Mg," J. Appl. Phys. 38, 4076 (1967).

UCRL Reports

1. K. H. G. Ashbee and J. W. Heavens, Brillouin Zone Boundary Construction for Indexing Bragg Contours and Kikuchi Lines, UCRL-17614, June 1967.
2. I-Lin Cheng, An Electron Microscopic Study of Maraging Steel (M.S. Thesis), UCRL-17334, January 1967.
3. I-Lin Cheng and G. Thomas, Structure and Properties of Fe-Ni-Co-Ti Maraging Steel, UCRL-17803, September 1967.
4. A. G. Fitzgerald and G. Thomas, Electron Microscope Observations of Twinning and Phase Transformations in Indium Sulfide Crystals, UCRL-17764, August 1967.
5. P. R. Okamoto and G. Thomas, On the Four-axis Hexagonal Reciprocal Lattice and Its Use in the Indexing of Transmission Electron Diffraction Patterns, UCRL-17413, April 1967.
6. N. V. Durai Raghavan and S. Ranganathan, Field Ion Microscopy, UCRL-17447, March 1967.
7. N. V. Durai Raghavan, A Field Ion Microscope Study of the Ta-Mo System, (Ph.D. Thesis), UCRL-17711, August 1967.
8. S. Ranganathan, Field Ion Microscopic Observations of Dislocation Structures at Grain Boundaries, UCRL-17331, May 1967.
9. G. Thomas, Experiments at High-Voltage Electron Microscopy, UCRL-17842, September 1967.
10. R. E. Villagrana, The Detection and Analysis of Modulated Ferromagnetic Structures by Transmission Electron Microscopy and Diffraction (Ph.D. Thesis), UCRL-17345, August 1967.

D. HIGH-STRENGTH MATERIALS

Earl R. Parker and Victor F. Zackay

The useful strength of alloys is essentially established by the degree of ductility present. For example, the use of iron-base alloys is restricted above 200,000 psi and virtually prohibited above 300,000 psi because of the lack of ductility. Because of this ductility restriction, metals are used at a fraction of their theoretical strength, i.e., 10 to 15 percent for the common structural metals. Thus, 85 to 90 percent of the potential strength of iron remains unexplored and unexploited due to lack of ductility. These upper regions of the strength of iron are the object of a current study.

By considerations of continuum mechanics and dislocation and alloy theory it has been possible to design and produce alloys with three to five times the ductility of conventional alloys at the same strength level. The essential analytical feature of this research has been to show that failure of high strength alloys is caused by lack of uniform ductility and that premature failure by necking (high local ductility) can be prevented by substantially increasing the rate of strain hardening. The increased rate of strain hardening is produced by causing a strain-induced transformation to occur in a precipitation-hardened austenitic steel. These studies suggest that steels can be made having a strength of 750,000 psi and an elongation of 30 percent. These principles that govern the behavior of iron-base alloys are of course applicable to any metal or alloy exhibiting a strain-induced transformation. Several metals showing this type of transformation are titanium and zirconium.

Another topic of study is the fundamental nature of fracture at high strength levels. Plastics are used as model systems exhibiting all the detailed features associated with the fracture of metals. The added feature of transparency greatly aids in developing quantitative theories of fracture toughness.

1. QUANTITATIVE INVESTIGATION OF THE STRAIN-INDUCED MARTENSITIC TRANSFORMATION IN HIGH STRENGTH STEELS*

Bertrand de Miramon† and Martin D. Merz

Three nitrogen containing TRIP steels which exhibit high strength and good ductility

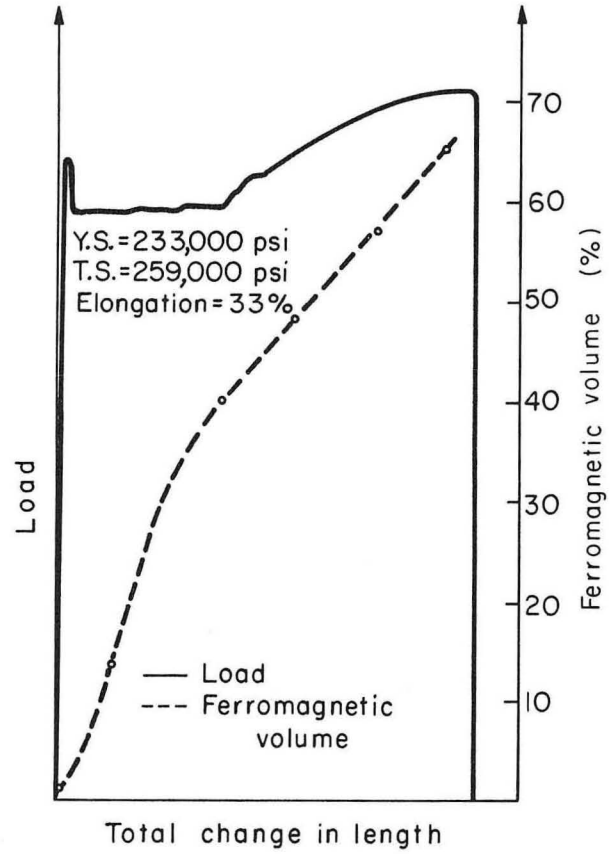

Fig. IID.1-1. Alloy II - Load displacement curve and corresponding ferromagnetic volume. Prior treatment 450°C - 80%. Short gage specimen.

Alloy	Fe	Cr	V	Mn	Ni	Si	Mo	N	C
I	bal	8	-	13	-	-	-	0.21	-
II	bal	9	-	2.5	7.5	1.8	3	0.09	0.25
III	bal	9.6	1.0	2.4	7.4	1.8	1.1	0.07	0.27

were investigated. An apparatus was constructed to measure the production of ferromagnetic phase (martensite) during a tensile test.

The alloy compositions studied are given above.

Figure IID.1-1 shows a load elongation curve for alloy II which had been austenitized and then deformed 80% at 450°C. As can be seen the amount of ferromagnetic phase increases with straining until at fracture approximately 65% of the austenite has been converted to martensite. This particular processing treatment results in an excellent combination of strength (yield strength = 233,000 psi) and elongation (33%).

There appears to be no relationship between the amount of martensite transformed at a given strain in a specimen and the total elongation of that specimen. Figure IID.1-2 shows the relationship between elongation and percent of martensite prior to testing. It appears that an amount of martensite between 4 and 7% is detrimental to elongation, whereas an amount between 10 and 15% enhances elongation.

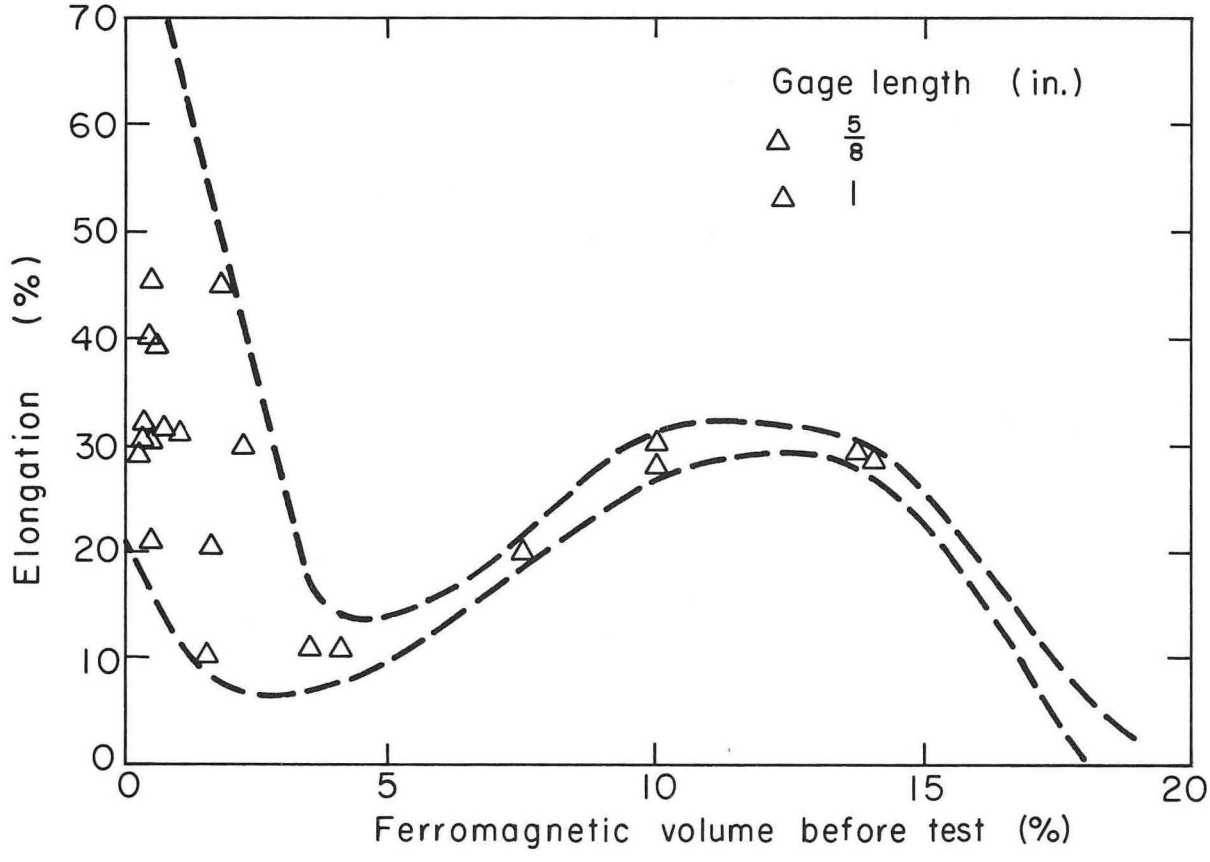

XBL682-1958

Fig. IID.1-2. Alloy II - Elongation of various TRIP steels as a function of amount of martensite present prior to testing.

Many of the TRIP steel specimens deform by the passage of a strain load down the length of the specimen. In the present work it was verified that the martensitic transformation occurs in this region as it progresses along the specimen and that very little transformation occurs outside this region.

* Abstract from UCRL-17849, September 1967.
† Now serving with the Armed French Forces.

2. EFFECT OF TEST TEMPERATURE ON THE MECHANICAL PROPERTIES OF METASTABLE AUSTENITIC STEELS*

Govind R. Chanani and Martin D. Merz

A series of TRIP steels of varying carbon content were tested at temperatures between -196 and 200°C. The compositions of the steels investigated are given in Table IID.2-I.

Table IID.2-I. Composition of investigated steels.

Alloy	Fe	Ni	Cr	Mn	Si	Mo	C
j	bal	7.7	12.2	0.68	1.6	4.1	0.05
k	bal	7.7	11.6	8.60	1.3	2.5	0.07
l	bal	7.7	11.8	0.61	1.5	3.0	0.16
m	bal	7.7	12.0	0.52	0.7	3.2	0.20

These steels were austenitized at 1100°C, cooled to room temperature, and subsequently deformed 80% at various temperatures between 250 and 550°C. These treatments give room-temperature properties as shown in Fig. IID.2-1. For maximum elongation there appears to be an optimum deformation temperature at 450°C for the three steels of highest carbon content. The lowest carbon steel was strongly magnetic prior to testing.

The variation in tensile properties with test temperature is shown in Fig. IID.2-2.

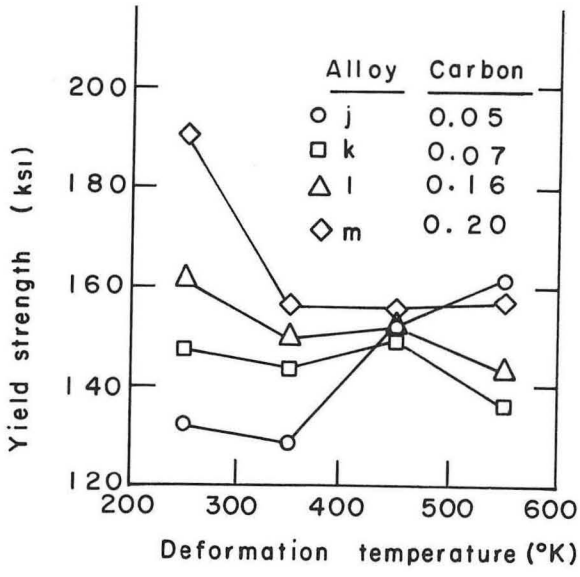

Fig. IID.2-1. Yield strength and elongation at -196°C vs deformation temperature for different alloys as indicated after 80% deformation.

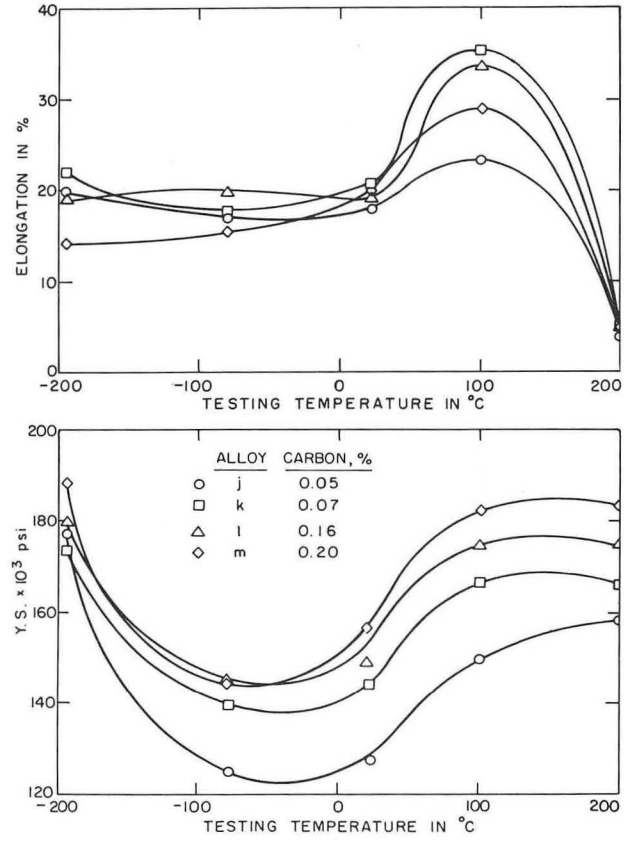

Fig. IID.2-2. Yield strength and elongation vs testing temperature in °C for different alloys as indicated after 80% deformation at 350°C.

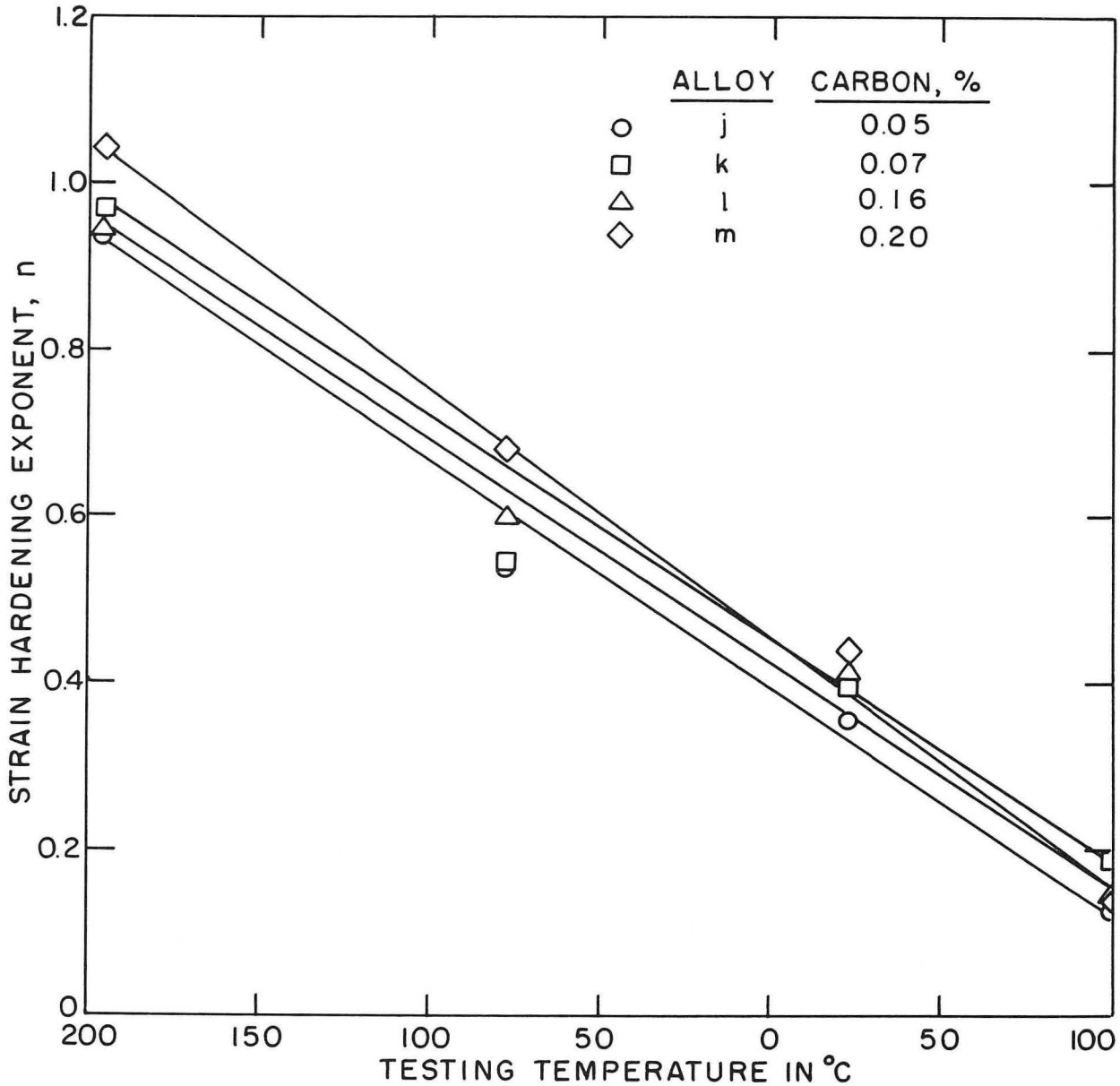

XBL 678-4844

Fig. IID.2-3. Strain-hardening exponent, n, vs testing temperature in °C for different alloys as indicated after 80% deformation at 350°C.

It should be noted that the yield and ultimate strengths are the highest at a carbon level of about 0.20%. Other data on higher carbon TRIP steels show a peak in elongation at about 0.29% carbon and also that the strength increases with increasing carbon level. Raising the carbon level above about 0.30% for this series of steels is not beneficial, probably because of undissolved carbides at the higher carbon level which embrittle the material.

The strain-hardening characteristics of these steels were evaluated and the value of n (in the equation $\sigma = K \epsilon^n$) is shown versus test temperatures in Fig. IID.2-3. It can be seen that n is very large at low temperatures

(approaching unity as compared to about 0.4 for a conventional stainless steel). There seems to be no correlation between n and total elongation. TRIP steels fracture before general necking occurs and therefore an elongation criterion based on strain to necking should have no application in these materials. It is therefore not surprising to find no connection between n (which is equal to the strain at necking) and elongation. TRIP steels are however able to resist necking at low strains due to their high work-hardening rate.

* Abstract of UCRL-17805, September 1967.

3. MICROSTRUCTURE AND PLANE-STRAIN FRACTURE TOUGHNESS OF HIGH-STRENGTH ALUMINUM ALLOYS*

Peter J. Guest and Martin D. Merz

The plane-strain fracture toughness of precipitation hardening high-strength 7075-aluminum alloy has been determined in the fully precipitation hardened condition and compared with the overaged and underaged conditions at predetermined stress levels less than the yield strength. Plane-strain fracture toughness values were determined using the "pop-in" technique employing single-edge-notched large and small type specimens. The results show that the plane-strain fracture toughness was markedly improved for both underaged and overaged conditions accompanied by a corresponding minimal loss in yield strength, as shown in Fig. IID.3-1. The underaged condition exhibited higher toughness than the overaged condition at equivalent yield-strength levels. It can be seen that a K_{Ic} value of 61 ksi-in$^{1/2}$ at a yield strength of 66 ksi was obtained by a suitable underaging treatment, compared to 38 ksi-in$^{1/2}$ at 77 ksi yield strength in the commercially available T6 condition. This is a substantial increase in fracture toughness with little sacrifice in strength. It was also found that the work required to cause crack propagation increases considerably for underaging and overaging, with a larger increase for the underaged condition, over the fully precipitation-hardened condition. The plane-strain fracture toughness was found to increase with increasing strain hardening exponent.

* Abstract from UCRL-17872, October 1967.

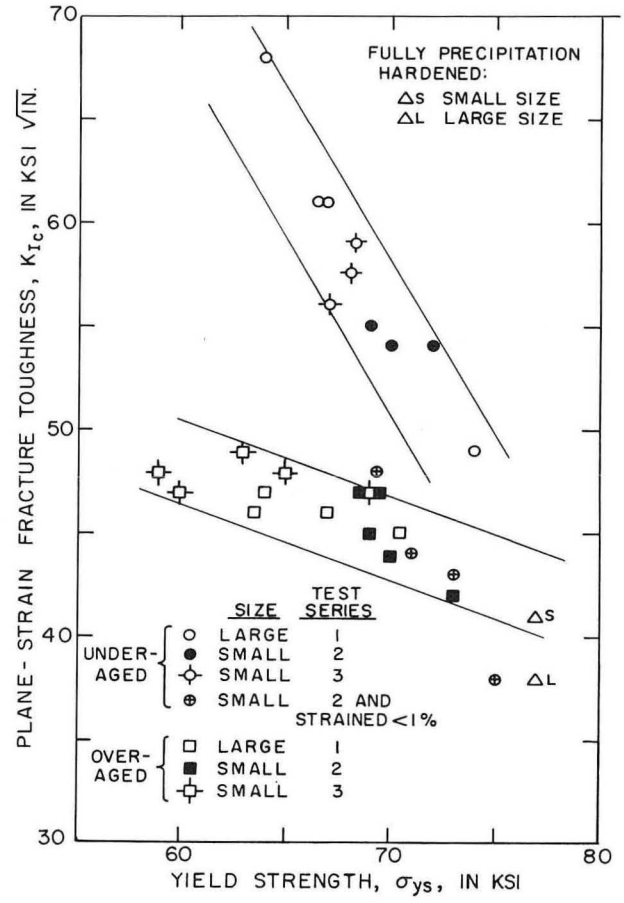

Fig. IID.3-1. The plane-strain fracture toughness values determined by "pop-in" method for high-strength 7075-T6 for all specimens versus yield strength.

4. NOTCH TOUGHNESS VARIATIONS IN STEELS WITH THE SAME TENSILE PROPERTIES

Yosef Katz and Martin D. Merz

Variation of fracture toughness in a low-carbon H-11 steel has been investigated. Specimens were deformed at three temperatures above the M_s prior to transformation. In addition a second series of specimens was isothermally transformed at temperatures the same as the deformation temperatures. Little variation in tensile properties was found within each

series. The fracture toughness, as measured with a single-edge-notched specimen is shown for the two series in Fig. IID.4-1. It can be seen that the peak toughness for the ausformed material (deformed 50% above M_s) occurs at 410°C, whereas the peak toughness of the isothermally transformed specimens occurs at 375°C.

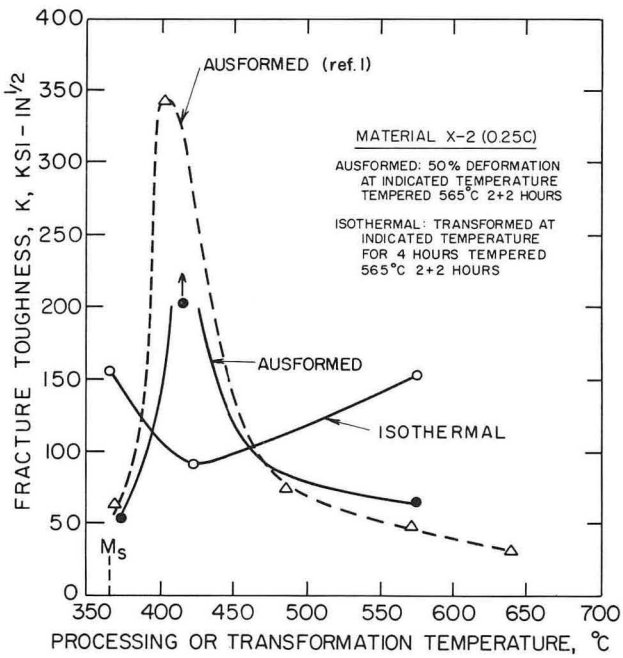

XBL 679-4984

Fig. IID.4-1. Variation in fracture toughness with processing temperature.

The peak toughness in the steel has been associated with the appearance of a tough second phase, namely lower bainite. Deformation causes this phase to appear at a higher temperature than when the specimens are isothermally transformed. Figure IID.4-2 shows the fracture specimens for the two series. Large amounts of plastic deformation occur around the crack for the tough material (ausformed 410°C, and isothermal 375 and 575°C). The other specimens failed in a brittle catastrophic manner. Examination of the advancing crack tip at high magnification revealed that the crack moved along carbide-matrix interfaces for these low toughness specimens. This study has stressed the importance of local variations in structure which may drastically affect toughness with little effect on tensile properties. The presence of a tough second phase such as lower bainite has been shown to improve toughness markedly in this steel.

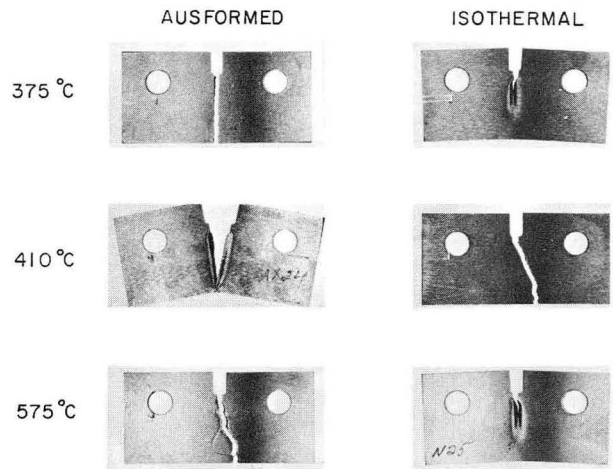

XBB 670-5722

Fig. IID.4-2. Fracture toughness specimens showing fracture appearance for ausformed and isothermally transformed material.

5. EFFECT OF A STRAIN-INDUCED TRANSFORMATION ON THE TOUGHNESS OF HIGH-STRENGTH STEELS

Christian P. Laporte,† Peter Hemmings, William Gerberich, and Martin D. Merz

An effort has been made to evaluate the fracture toughness of certain high-strength TRIP alloys. A preliminary invesitgation revealed the importance of using wide specimens (width > 3 in.) in order to contain the large plastic transformation zone in elastic surroundings. Preliminary results on smaller specimens do indicate however that TRIP steels are not as sensitive to changes in test temperature as conventional steels. Most conventional high-strength steels (i.e., maraging and quenched and tempered martensitic steels) have relatively poor toughness at cryogenic temperatures, even though their room-temperature toughnesses are adequate. It would be of great advantage to find a high-strength material which retains toughness to low temperatures.

Several room-temperature tests have been made on notched TRIP specimens of adequate width to give a value of plane-stress fracture toughness, K_C. A value of 250 ksi-in$^{1/2}$ at a yield strength of 225 ksi has been measured. This particular steel has an elongation of 30% and ultimate strength of 245 ksi in uniaxial tension. The alloy composition is given below.

Fe	Cr	Ni	Mo	Mn	Si	C
bal	9.0	9.0	4.9	2.5	2.0	0.26

The alloy was austenitized 3/4 hr. at 1050°C

and reduced 80% at 450°C. Work is also in progress to evaluate the fatigue properties of this material.

† Now serving with French Armed Forces.

6. FRACTURE TOUGHNESS OF PLASTICS

Leland Key and Yosef Katz

A program to investigate the use of fracture mechanics for quantitative evaluation of the resistance to fracture of plastics has been completed during this year. Single-edge-notch fracture specimens were prepared from polystyrene, polycarbonate, acrylic, and a vinyl chloride-vinyl acetate copolymer; the plane strain-fracture toughness values obtained for these commercially important plastics are shown in Table IID.6-I. The effects of temperature and loading rate on the fracture toughness of polycarbonate and acrylic were evaluated by testing single-edge-notch specimens in the range -150 to +75°C and at 10^{-3} to 5 cm/min. Figure IID.6-1 shows the observed temperature dependence of fracture toughness. Figure IID.6-2 shows the transition from a flat fracture to a fracture with shear lips observed with polycarbonate in the range -50°C to room temperature.

Table IID.6-I. Fracture toughness of plastics.

Material	K_{Ic} ksi(in.)$^{1/2}$
Polystyrene	1.64
Polycarbonate	3.29
Acrylic	0.99
Vinyl Chloride-vinyl acetate	3.71

Extensive but reproducible variations in

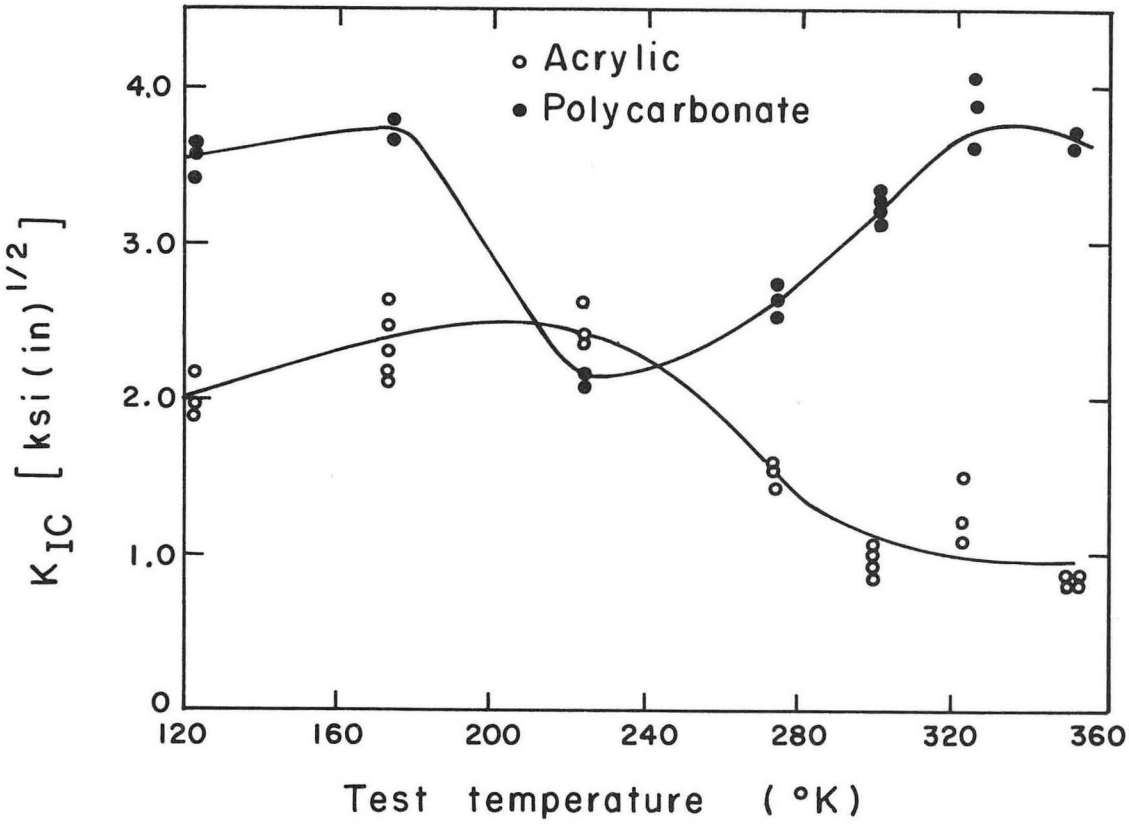

XBL682-1959

Fig. IID.6-1. Effect of temperature on fracture toughness.

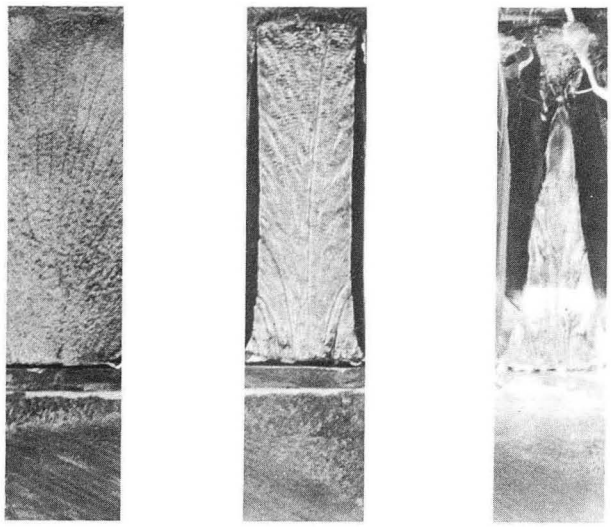

a b c

XBB 6711-6659

Fig. IID.6-2. Macrographs of polycarbonate single-edge-notch fracture specimens, tested at (a) -50°C, (b) 0°C, (c) room temperature. Specimens are 0.250×1 in.

fracture surface morphology were observed by optical fractography. These differences in topography corresponded closely to variations in fracture toughness, increased toughness being associated with a higher density of surface markings. Figure IID.6-3 shows the

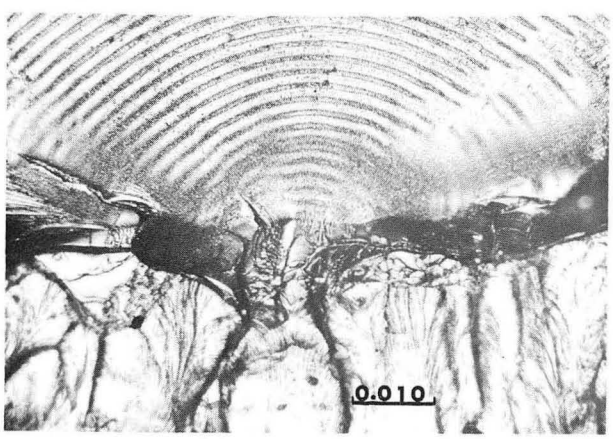

XBB 682-852

Fig. IID.6-3. Fracture initiation site in a polycarbonate single-edge-notch specimen tested at 5 cm/min and room temperature. Fracture propagated upward from razor-cut notch.

region of fracture initiation in a polycarbonate specimen tested at 5 cm/min.

An additional objective of this work was to evaluate the variability of fracture toughness as measured with several types of specimens.

7. FRACTURE TOUGHNESS OF PRECIPITATION-HARDENING ALUMINUM ALLOYS

David Porter

A knowledge of the effect of volume-fraction size and distribution of precipitates on the fracture toughness of precipitation-hardening alloys is important in alloy design. This information is necessary for the selection of the correct composition and heat treatment of precipitation alloys. However, the literature is lacking in this information. Six alloys in the Al-Cu system were solution-treated, quenched, and aged at various temperatures to give a variety of volume fractions, sizes, and distributions of precipitates. After heat treatment the fracture toughness and other mechanical properties were measured. Similar studies were carried out in the Al-Ag and Al-Zn systems.

8. RESEARCH PLANS FOR CALENDAR YEAR 1968

Victor F. Zackay and Earl R. Parker

Plane-Strain Fracture Toughness of TRIP Steels

The determination of the important engineering parameter K_{Ic} (plane-strain fracture toughness) in TRIP steels is in progress and will be completed during the coming year. Thick sections (thickness > 1/2 in.) are being fabricated in these steels in order to achieve the plane strain condition in notched specimens. Attempts will be made to optimize alloy composition and processing treatment with respect to this parameter.

Cyclic Straining of TRIP Steels

An MTS 150-ton-capacity testing machine capable of tension-compression cycling up to 20 Hz will be used to explore the cyclic-ductility characteristics of TRIP steels. These steels show extraordinary elongation in tensile tests, and it is of fundamental importance to see if such elongation can be utilized under conditions of cyclic plastic deformation. Such tests will give the low cycle fatigue properties of these alloys.

Corrosion and Stress-Corrosion Characteristics of Materials

A program is being initiated to evaluate the corrosion and stress-corrosion resistance of high-strength steels. The initial stage of this program will be to compare the corrosion behavior of TRIP steels to conventional stainless steels, using anodic dissolution in oxalic acid, nitric-hydrofluoric acid, and ferric sulfate-sulfuric acid solutions.

A single-edge-notched specimen of suitable geometry to give a constant stress-intensity factor over a range of crack lengths is being considered for use in stress-corrosion studies. Such a specimen would allow a more fundamental evaluation of crack growth rate without the added complication of changing stress intensity as the crack grows, as is the case in most studies.

Stress Wave Emission

Elastic waves emitted from growing cracks will be studied in both polymeric and metallic materials. One purpose of these studies will be to establish the relationship between available elastic energy and emitted stress-wave energy so that microflow growth may be evaluated quantitatively. Other studies will consider the slow crack-growth processes in two-phase composites and alloys undergoing stress-corrosion cracking (SCC). The objective is to formulate a critical stress, strain, or displacement criterion for the step-wise growth process in the two-phase materials; and to measure the kinetics of the SCC process such that an activation energy may be unambiguously determined.

An attempt will also be made to evaluate other sources of stress-wave emission such as the martensitic transformation and mechanical twinning. If successful, this would be utilized to monitor strain-induced transformations and, perhaps, isothermal martensitic transformations.

Fracture of Cracked Tungsten Single Crystals

A program to investigate the tensile fracture behavior of tungsten single crystals containing crack-like flaws of a specified size has been started. Cleavage cracks are introduced into the crystals by a spark-discharge technique which allows the size and location of the crack to be controlled. The tensile behavior of these crystals will be studied as a function of test temperature and the relative orientation of the crack plane and tensile axis. Cracks will be introduced in some specimens prior to loading to evaluate the initiation of fracture from an existing crack. In other specimens, the crack will be introduced after loading the specimen to produce a running crack and thus allow evaluation of crack propagation separately from initiation.

The macroscopic behavior will be analyzed using the methods of fracture mechanics. The microscopic behavior and particularly the significance of slip behavior in the neighborhood of the crack will be evaluated by dislocation etch-pit techniques.

9. 1967 PUBLICATIONS

Earl R. Parker, Victor F. Zackay, and Associates

Technical Journals

1. R. W. Carpenter, Growth of Modulated Structure in Gold-Platinum Alloys, Acta Met. 15, 1567 (1967).
2. R. W. Carpenter, Deformation and Fracture of Au-Pt Polycrystals Strengthened by Spinodal Decomposition, Acta Met. 15, 1297 (1967).
3. E. R. Parker and V. F. Zackay, Origin and Nature of Microstructure, in An Atomistic Approach to the Nature and Properties of Materials, J. A. Pask, ed., (John Wiley and Sons, New York, 1967). p. 205.
4. E. R. Parker, ed., Materials Data Book for Engineers and Scientists, (McGraw-Hill Book Co., New York, 1967).
5. D. Porter, The Decomposition of Tungsten-Chromium Solid Solution, Acta Met. 15, 721 (1967).
6. V. F. Zackay, W. W. Gerberich, R. Busch, and E. R. Parker, Strength of Dynamically Strain Aged Alloy Steels, Int. J. Frac. Mech. 2, 638 (1966).
7. V. F. Zackay, E. Parker, D. Fahr, and R. Busch, The Enhancement of Ductility in High-Strength Steels, Trans. ASM Quart. 60, 2 (1967).

UCRL Reports

1. G. Chanani, The Strength and Ductility of Metastable Austenitic Steels as a Function of Composition and Test Temperatures (M.S. Thesis), UCRL-17805, September 1967.
2. P. J. Guest, The Microstructure and Plane Strain Fracture Toughness of High-Strength Aluminum Alloys (M.S. Thesis), UCRL-17872, October 1967.
3. L. Hartsough, V. F. Zackay, and E. R. Parker, High-Field Characteristics of $Nb_3(Al,Ge)$, UCRL-17761, August 1961.

4. C. P. Laporte, Effect of a Strain-Induced Transformation on the Toughness of High-Strength Materials (M.S. Thesis), UCRL-17812, September 1967.
5. B. de Miramon, Quantitative Investigation of Strain-Induced Strengthening in Steel (M.S. Thesis), UCRL-17849, September 1967.
6. G. Walter, Investigation of the Application of Spinodal Theory to the Palladium-Iridium System (M.S. Thesis), UCRL-17470, May 1967.

E. HIGH-FIELD SUPERCONDUCTIVITY

Leo Brewer, Earl R. Parker, and Victor F. Zackay

This research is directed toward increasing our understanding of the structural factors that influence the properties of high-field superconductors. The critical current density is the property of greatest interest and its dependence on the defect structure and microstructure is being given the greatest research emphasis.

1. SINGLE-PHASE AND POLYPHASE ALLOY SYSTEMS

Masaki Suenaga, Jean Olson, and Kenneth Ralls*

Although the critical magnetic fields of solid-solution alloys of transition metals are not as high as those of intermetallic compounds such as Nb_3Sn, the alloys are still attractive for medium magnetic field-strength applications because of their ease of fabrication to useful shapes. At the present time the highest critical field in binary alloys is found in the Nb-Ti system. The major factor in limiting upper critical fields of these alloys is thought to be preferential Pauli-paramagnetic lowering of normal-state free energy. However, it is possible to increase this superconducting-state paramagnetism which is responsible for lowering the superconducting-state free energy. The increase of superconducting-state paramagnetism of an alloy can be accomplished by addition of large-atomic-number elements to the alloy. Hence, it is likely that higher critical-field alloys can be made, for example, by the addition of Ta to the Nb-Ti binary system.

Our investigation which was completed this year shows that slightly higher critical fields can be obtained with ternary alloys, i.e., Nb-Ti-Ta, compared to fields obtained with the binary alloy Nb-Ti, although the critical temperatures of the alloys decrease. Critical temperatures and fields are shown in Figs. IIE.1-1 and IIE.1-2, respectively. In Fig. IIE.1-3 critical temperatures, T_c, normal resistivity, ρ_N, the Pauli-paramagnetic limit critical field, Hp, and the measured critical field, H_{c2}, are plotted for 64 at.% Ti alloys with varying Nb and Ta. All parameters with the exception of the measured critical fields decrease with increased replacement of Ta. The decrease of T_c and ρ_N tends to decrease critical fields. However, the fact that very sharp increases in H_{c2} are observed with addition of Ta clearly indicates that the spin-orbit-scattering effect is playing the dominant role in the observed variation of critical fields in Fig. IIE.1-3. This behavior suggests that the presence of a peak in the critical-field plot (Fig. IIE.1-2) of the ternary alloy system is possible.

Critical currents of some of the ternary alloys were investigated, and it was found that they were slightly lower than those of a Westinghouse Nb-Ti wire. However, it is highly likely that higher critical currents will be attained with appropriate processing of the alloys.

Effects of fine precipitates on critical currents of a type-II superconductor were considered in a 30Nb-70Zr alloy. It was previously found that the type, distribution, and sizes of the precipitates are very critical in establishing the critical current densities of a superconductor. Results from a simple calculation on the flux pinning by the nonsuperconducting precipitates indicate that the Lorentz parameter, $\alpha_c \cong (J \times B)/c$, is inversely proportional to $d^{1/2}$ for $R > d$ and to d for $R < d$, where d is half of the interparticle spacing, and R is the radius of curvature of a pinned flux line. Current research is in process for obtaining further experimental confirmation of this dependence with the use of a Nb-1% Zr-O alloy.

Superconducting critical temperatures, T_c, and the effect of metallurgical treatments on the critical temperatures of Ta-Zr alloys were investigated. It was found that the superconducting transition temperature for alloys quenched from a one-phase (bcc) region exhibits a maximum of 7.5°K near 15 at.% Zr. The maximum T_c at 4.85 valence electrons per atom is in accord with De Sorbo's correlation which

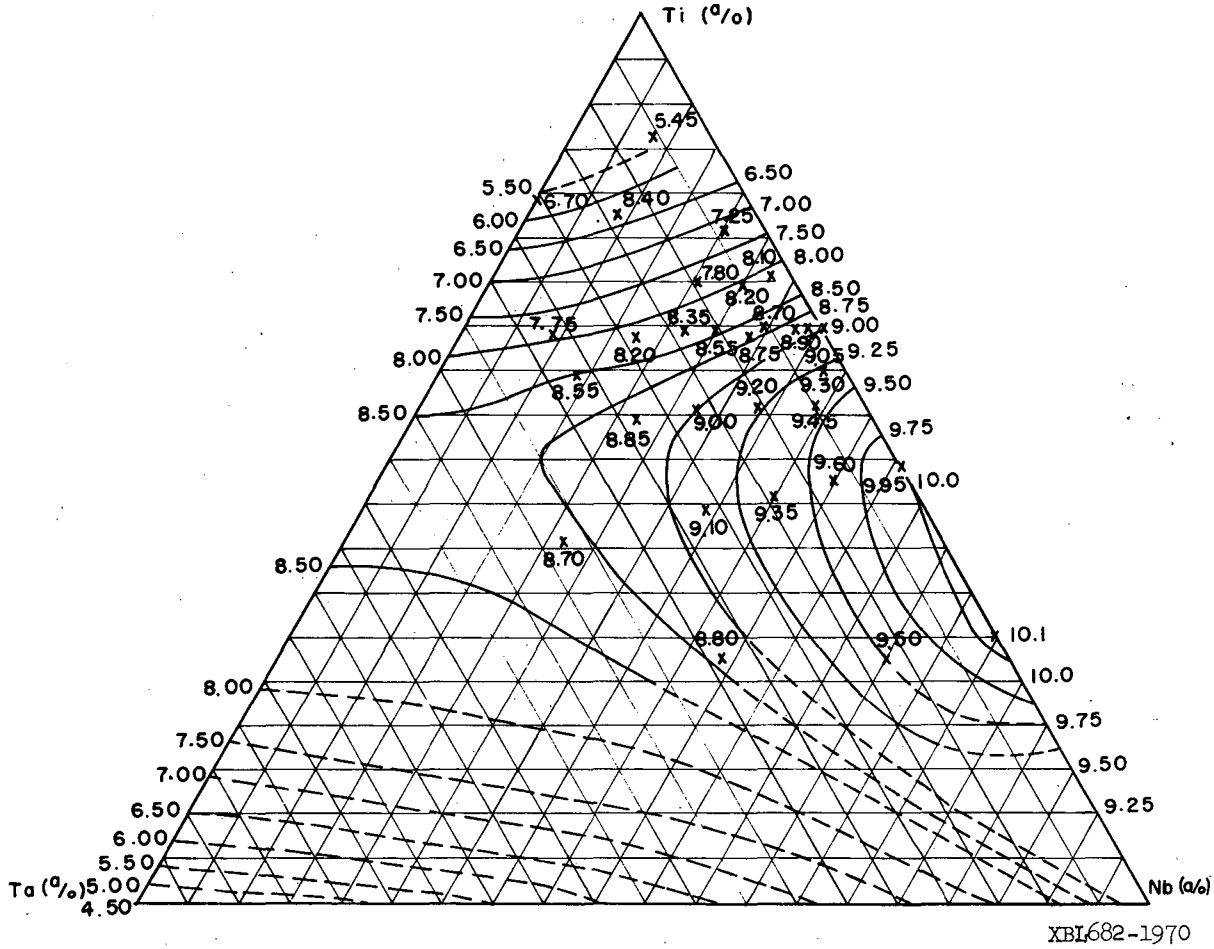

Fig. IIE.1-1 The variation of T_c with composition in the ternary system Ti-Nb-Ta.

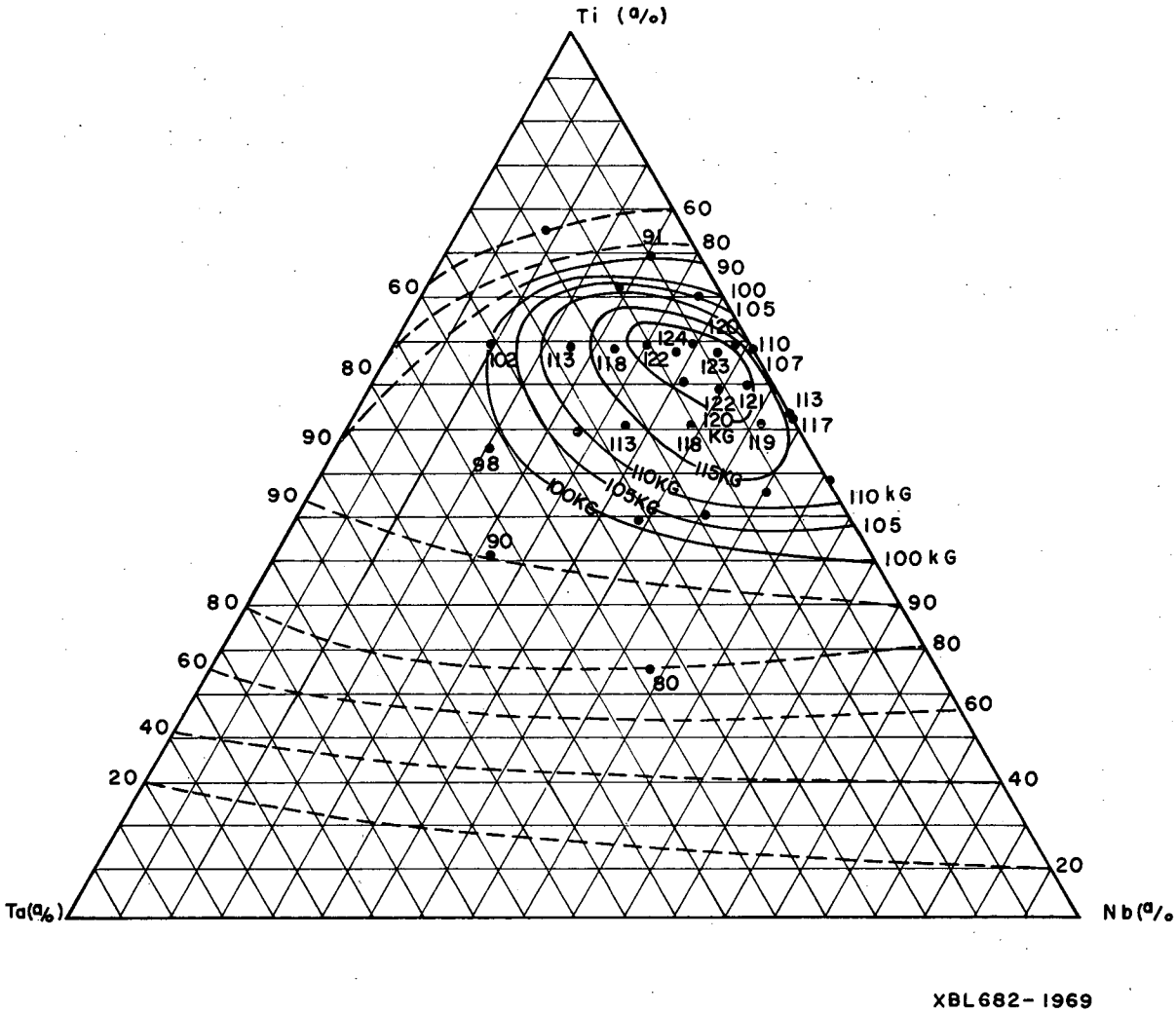

Fig. IIE.1-2 The variation of H_{c2} with composition in the ternary system Ti-Nb-Ta

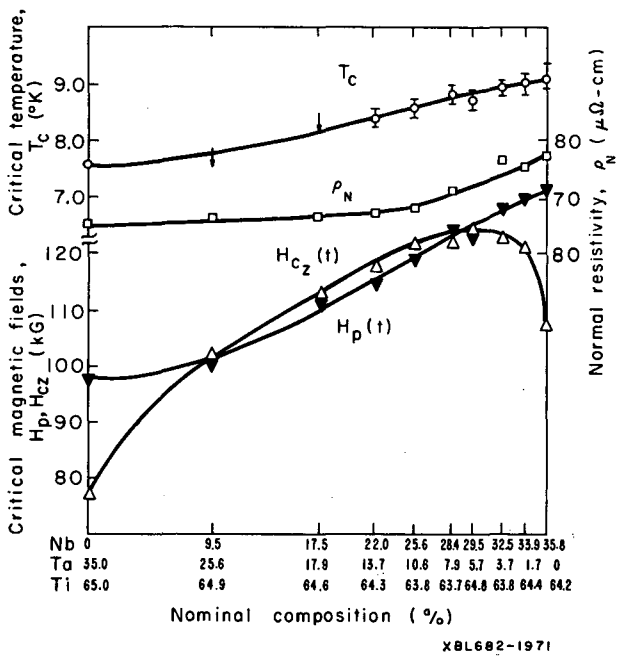

Fig. IIE.1-3. Variations of critical temperature, T_c, normal-state resistivity, ρ_N, the paramagnetic-limit critical fields, H_p, and measured critical fields, H_{c2} along constant 64 at.% Ti line on the ternary diagram.

utilizes an effective electron-to-atom ratio. Annealing of the alloys within the miscibility gap tends to form two bcc phases which differ in composition. The critical temperatures of annealed alloys are determined by the compositions of resultant phases, and it was observed that observed critical temperatures of annealed polyphase alloys were well in accord with the critical temperatures of the single-phase alloys of the same composition.

† Present address: Department of Physics, University of Austin, Texas.

2. INTERMETALLIC AND CERAMIC COMPOUNDS

The superconducting properties of two intermetallic compounds, $Nb_3(Al_xGe_{1-x})_1$ and Nb-Sn-C, have been investigated.

a. $Nb_3(Al_xGe_{1-x})$

Larry D. Hartsough

The discovery by Matthias et al. earlier this year of a T_c of 20.05°K for a well-ordered alloy of nominal composition $Nb_3(Al_{0.8}Ge_{0.2})$, prompted our investigation into the effect of alloy additions to Nb_3Al. The superconducting properties T_c, J_c, and H were compared for single-phase Nb_3Al and for an alloy of nominal composition $[Nb_3(Al_{0.8}Ge_{0.2})]$. After an anneal for three days at 950°C, the Nb_3Al had a broad T_c centered at 16.8°K, while the T_c for the $Nb_3(Al_{0.8}Ge_{0.2})$ was sharp at 18.7°K. Although the increase in T_c was not as high as previously observed, the J_c vs H curves for the two samples differed significantly. Figures IIE.2-1 and IIE.2-2 show the results obtained

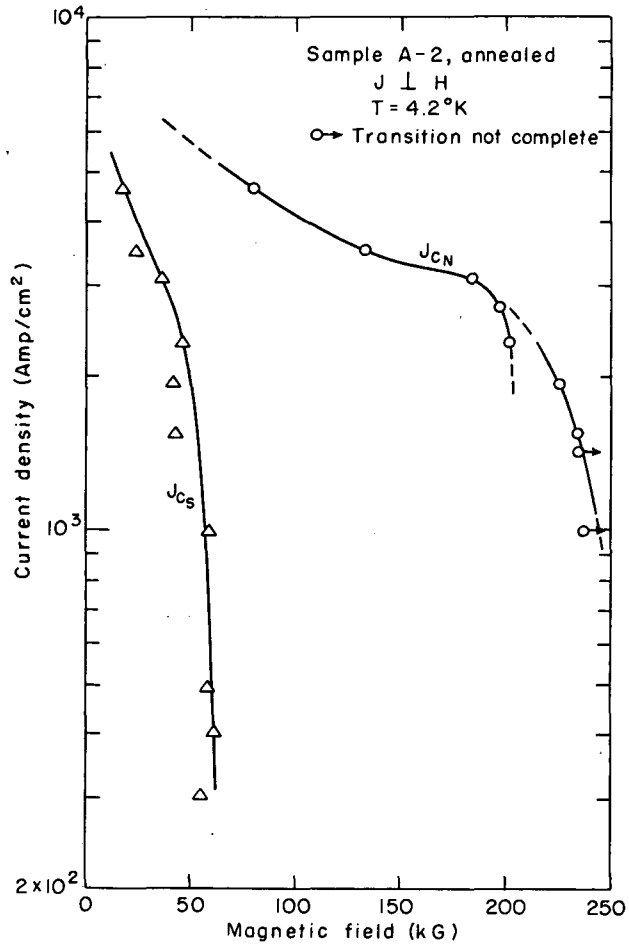

Fig. IIE.2-1. J_c vs H for single-phase Nb_3Al containing 22% Al; T_c = 16.8°K.

by a pulsed-field technique, for which the pulse rise time was 9 to 11 msec. Figure IIE.2-1 shows data for the Nb_3Al, while Fig. IIE.2-2 represents the J_c vs H curve for the $Nb_3(Al_{0.8}Ge_{0.2})$ alloy, corrected for sample

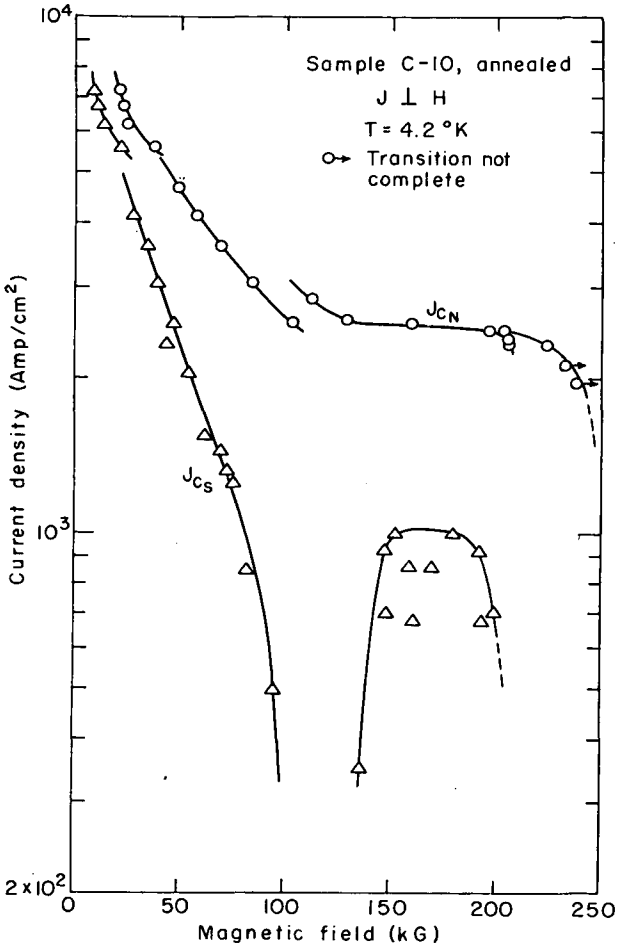

ABL 6712-1965

Fig. IIE.2-2. J_c vs H for Nb alloy of nominal composition 75Nb-20Al-5Ge; T_c = 18.7°K.

heating at high current densities. The onset of resistance, J_{cs}, is significantly higher for the germanium-bearing alloy. Moreover, the peak effect and the fact that the resistance in the "valley" was less than 10% of full normal indicate that the steady-field characteristics of the $Nb_3(Al_{0.8}Ge_{0.2})$ alloy may be even better than shown here.

Because of the limitation in the pulsed-magnetic field equipment, it was not possible to determine the upper critical field, H_{c2} (4.2°K) of the alloys. However, as indicated in Fig. IIE.2-2, H_{c2} (4.2°K) is well above 220 kG, which is probably higher than that of Nb_3Sn.

The microstructures of the Nb-Al-Ge alloys exhibited a marked degree of coring with respect to Ge content. The last liquid to solidify is relatively rich in Ge, while the primary phase is transformed to Nb solid solution. The secondary or continuous phase which determines the measured T_c, was analyzed with a microprobe. Microprobe analysis on a system such as Nb-Al-Ge does not give completely accurate results, because the correction for atomic-number effect, which can be quite large, is not precisely known. However, an approximate correction for this effect was used for the required analyses. The Nb-Al-Ge alloy with highest onset T_c (19.0°K) has a composition near $Nb_3(Al_{0.75}Ge_{0.25})$ for the "secondary" phase, with the total minor elements (Al + Ge) equal to about 24.2 at.%.

In an effort to determine the effect of stoichiometry on the T_c of Nb_3Al, small amounts of As were added. Since As has an e/a of 5 (according to Matthias' rule) and is nearly the same size as Al, its substitutional for Nb on Al-type sites in Nb_3Al would affect neither e/a nor the lattice constant appreciably. The only intermediate phases which have been reported for the Nb-As system are $NbAs_2$, NbAs, and Nb_3As (Ti_3P-type structure). Thus, it is not likely that much As is soluble in Nb_3Al. It was observed that almost 1.4 at.% As dissolves in Nb_3Al under normal conditions of solidification and that this amount has no appreciable effect on T_c.

b. Nb-Sn-C SYSTEM

Jean Chabanne,† Roger Goolsby, and Russell Jones

The superconducting properties of a sintered Nb-Sn-C body have been established. The sintered product consists of grains of NbC surrounded by a thin film of Nb_3Sn. The thickness of the grain boundary Nb_3Sn can be controlled to some extent by varying the heat treatment and composition of the product. The effect of the thickness variation on superconducting properties was investigated. We have found in one case an upper critical field (the magnetic field where the resistive transition was completed) of 240 kG at 4.2°K. Because of the limitation in the pulsed magnet apparatus, the measured critical magnetic field corresponding to the critical field, H_{c2} (4.2°K), is still uncertain. The critical current densities of the compound seem to be lower than that of Nb_3Sn processed in other ways. However, it is not clear at this moment whether the lower current capability is due to

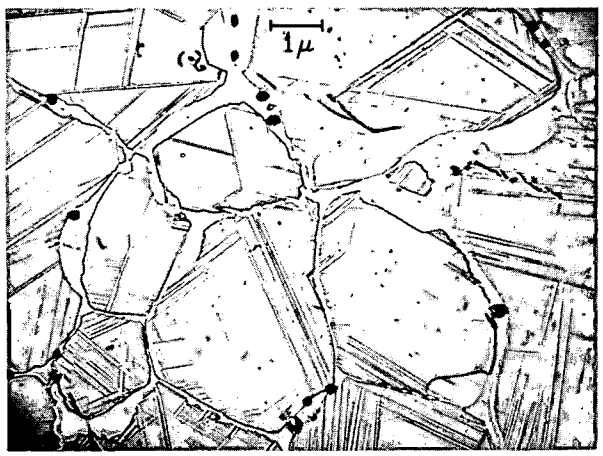

XBB6710-6117

Fig. IIE.3-1. Micrograph showing the grain boundary Nb_3Sn.

weak flux pinning in the sintered product, or to effects resulting from the discontinuity of the boundary Nb_3Sn. By appropriate processing of the sintered product, the established critical temperature of 18.2°K was attained. The photomicrograph, Fig. IIE.3-1, of the sintered product shows the grain-boundary film of Nb_3Sn around the matrix NbC grains.

† Now serving with the French Armed Forces, France.

3. RESEARCH PLANS FOR CALENDAR YEAR 1968

Leo Brewer, Earl R. Parker, and Victor F. Zackay

Projects currently in progress will be continued. Experimental studies of the flux-pinning mechanism in Nb-1% Zr-O alloy in steady magnetic fields will be made to prove the theoretical prediction previously mentioned. Investigation of compounds will continue, with emphasis on the study or properties, especially that of high critical magnetic field. Systems similar to Nb-Sn-C will be investigated. Progress has been made in building a new pulsed magnet which is capable of producing magnetic fields well above 250 kG.

Also under consideration are ac properties of type-II superconductors. An intensive review on ac loss in superconductors has been made. Although it seems that losses in superconductors under ac applications are inescapable, it appears that there are some means of reducing these losses. An object of the research in 1968 is to characterize the structural and compositional factors influencing these losses.

4. 1967 PUBLICATIONS

Leo Brewer, Earl R. Parker, Victor F. Zackay, and Associates

Technical Journals

1. R. G. Boyd, Nucleation of Superconductivity at a Tunneling Barrier of High Transmissivity, Phys. Rev. 153, 444 (1967).
2. M. W. Williams, K. M. Ralls, and M. R. Pickus, Superconductivity of Cubic Niobium Carbonitrides, J. Phys. Chem. Solids 28, 333 (1967).
3. M. Suenaga, J. O'Brien, V. Zackay, and K. M. Ralls, Effects of Low-Temperature Aging on the Resistive Transition of Superconducting 70Zr-30Nb in Pulsed Magnetic Fields, Trans. AIME 239, 992 (1967).

UCRL Reports

1. Z. J. Olson, Investigation of High Field Superconducting Compounds (Ph.D. Thesis), UCRL-17550, May 1967.
2. L. Hartsough, V. Zackay, and E. R. Parker, High Field Characteristics of Nb_3 (Al, Ge), UCRL-17761, August 1967.
3. J. Chabanne, Effect of the Microstructure on the Superconductive Properties of Nb_3Sn in a NbC matrix (M.S. Thesis), UCRL-17826, September 1967.
4. L. Hartsough, The Effect of Ternary Additions on the Superconducting Properties of Nb_3Al (M.S. Thesis), UCRL-17982, December 1967.

5. SUPERCONDUCTIVITY IN ALLOY SYSTEMS

Marshal F. Merriam†

This research is directed toward applying superconducting transition-temperature measurements to the study of electronic structure effects in alloys. Studies of T_c vs alloy composition have proved to be a very sensitive way to detect small shifts in normal-state free energy, such as arise from Fermi surface - Brillouin zone interactions.

During the early part of 1967 the equipment necessary for the preparation of alloys was completed and put into use. Also the necessary low-temperature facility was finished and put into operation during 1967.

† Currently on sabbatical leave, Indian Institute of Technology, Kanpur, India.

6. THE LOW-TEMPERATURE FACILITY

Eckhard Nembach

The equipment for measuring the transition temperatures T_c of superconductors has been finished. The transition is detected by the change of the mutual inductance of two coaxial coils. To speed up measurements six such coil pairs, each for one specimen, are enclosed in a heavy copper block, which also contains the germanium resistors used as thermometers. Each coil-pair consists of a primary and a secondary; the output of the latter is amplified, and together with the resistance of the thermometers is recorded on a multichannel recorder. Attached to the copper block is a heater. The whole assembly is enclosed in a copper box, which is filled at room temperature with 760-Torr helium gas. At the beginning of a run, this box is immersed into liquid helium to cool the specimens well below T_c, then the box is raised above the level of the liquid helium. A temperature-sweep-rate of about 0.003°K/min is established by heating the copper block constantly, but varying the evaporation rate of the helium by changing the power input in a resistor placed in the liquid helium. For T_c between 3 and 4°K one pumps on the helium. For lower values of T_c a sweep-rate can be established by placing the box in the helium and either sweeping the pumping speed or the power input into the heater wound on the copper block. The achieved accuracy of T_c depends on the quality of the sample as well as on the temperature range. At about 7°K the relative limits of error of T_c are less than 0.0005°K.

7. SUPERCONDUCTING TRANSITION TEMPERATURES OF Pb-In ALLOYS*

Eckhard Nembach

About 50 lead-indium alloy samples, covering the whole solubility range from 0-65 at.% In, have been measured. The results are shown in Fig. IIE.7-1, together with three points measured by W. Meissner et al.[1] T. Claeson's data on Pb-Tl are also given.[2] The two differences between the indium and thallium alloys are:

1. Indium affects T_c much less than thallium does.
2. Though 20 specimens with compositions between 46 and 54 at.% In have been tested, no deviations from a continuous decrease of T_c with increasing In content have been detected. This is in contrast to T. Claeson's results for Pb-Tl alloys.

* Abstracted from UCRL-17905, November 1967.

1. W. Meissner, H. Franz, and H. Westerhoff, Ann. Physik 13, 505 (1962).
2. T. Claeson, Phys. Rev. 147, 340 (1966).

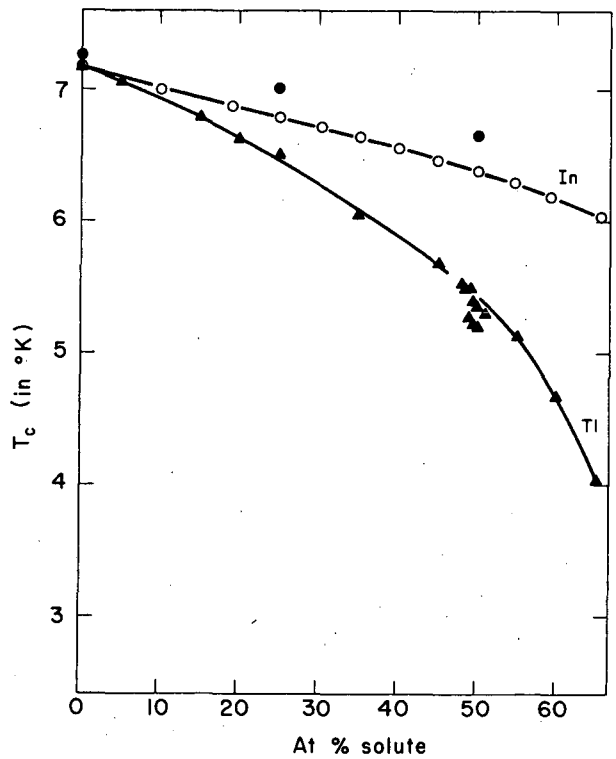

XBL670-5320

Fig. IIE.7-1. Critical temperature versus composition.

○ In, this investigation
● In, W. Meissner et al.
▲ Tl, T. Claeson

8. SUPERCONDUCTING TRANSITION TEMPERATURES OF VARIOUS LEAD-BASE ALLOYS*

Eckhard Nembach

Values of T_c for lead-base alloys with up to 7 at.% Cd, Hg, In, Tl, Sb, Bi, and Sn have been measured. The results are shown in Fig. IIE.8-1 and Fig. IIE.8-2. With the exception of Cd, dT_c/dx (x is the solute concentration) is always larger for the lighter solute than for the heavier one of the same group of the periodic table. Tin alloys have to be compared with pure lead. This increase in T_c is, according to J. Appel,[1] due to a change in the phonon spectrum caused by the light solute.

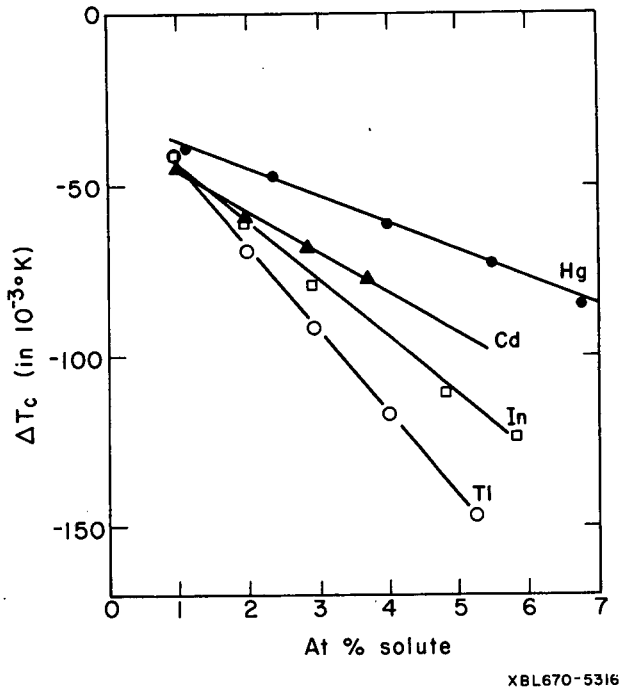

Fig. IIE.8-1. T_c for various dilute Pb-base alloys minus T_c for pure Pb.

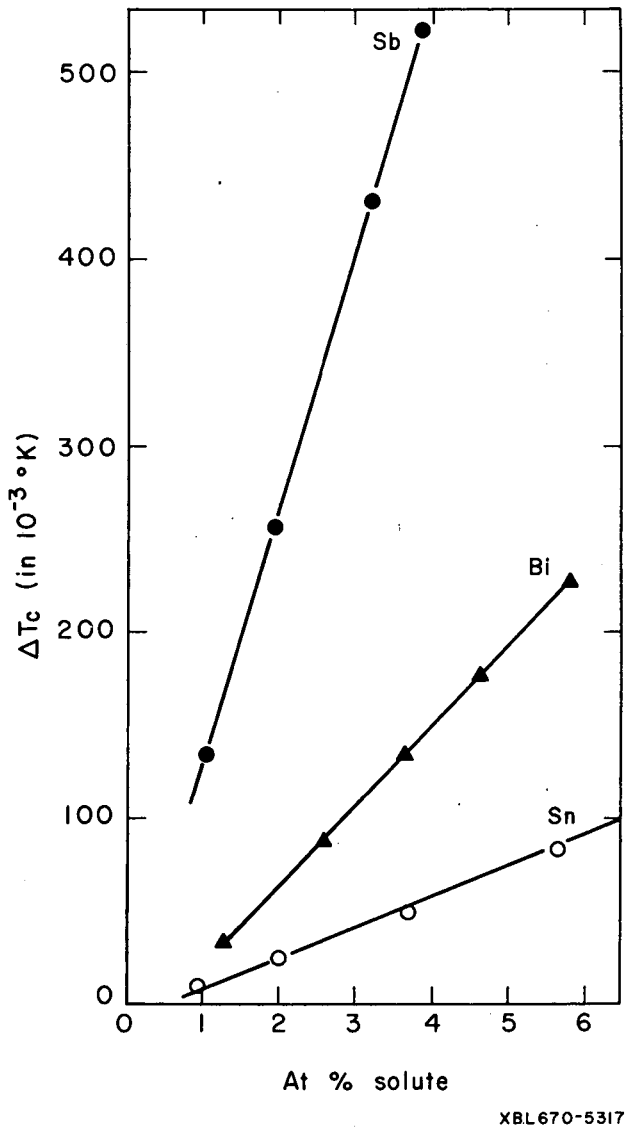

Fig. IIE.8-2. T_c for various dilute Pb-base alloys minus T_c for pure Pb.

* Abstracted from UCRL-17905, November 1967.
1. J. Appel, Phys. Rev. 156, 421 (1967).

9. RESEARCH PLANS FOR CALENDAR YEAR 1968

Marshal F. Merriam and Robert Hammond

In investigating the superconducting temperatures T_c of Pb-In alloys, it has been found that in the composition range between 40 and 60 at.% some phase changes occur below room temperature. These will be investigated by measuring T_c and by low-temperature X-ray work.

The experiments of T. Claeson on Pb-Tl alloys are going to be checked to find out what really caused the special behavior of the 50% Tl samples.

A study has been started of the In-Mg solid-solution alloy system in order to see if anomalies appear at the solute concentrations corresponding to the critical electron/atom values, according to the Fermi surface-Brillouin zone interaction. Later the In-Li system will be investigated, as will the In-Bi system.

10. 1967 PUBLICATIONS

Marshal Merriam and Associates

Technical Journals

1. M. F. Merriam, J. Hagen, and H. L. Luo, Superconductivity in the Alloy System Indium-Thallium, Phys. Rev. 154, 424 (1967).

UCRL Reports

1. E. Nembach, Superconducting Transition Temperatures of Various Lead-Base Alloys, UCRL-17905, November 1967.

F. THERMODYNAMICS OF METAL SYSTEMS

1. A THERMODYNAMIC STUDY OF THE HEAT OF ORDERING IN CuPt*

Gerald W. Geiken, Raymond L. Orr, and Ralph Hultgren

The heat of formation of the equiatomic copper-platinum alloy, CuPt, has been measured as a function of temperature over the range 360 to 1155°K by means of liquid-tin solution calorimetry. Above a critical temperature, T_c, of about 1100°K, CuPt has a disordered fcc structure. Below T_c the alloy forms an ordered superlattice with Cu and Pt atoms occupying sites on alternate (111) planes, with an accompanying slight rhombohedral distortion. From measurements of the rhombohedral angle as a function of temperature, Walker[1] deduced that the degree of long-range order, S, is virtually constant and equal to 1.0 up to a temperature of about 773°K, after which disordering sets in, until at 1073°K, S has decreased to about 0.8. The degree of long-range order then drops discontinuously to 0 at about 1100°K.

The results of the calorimetric measurements show that the heat of formation decreases from -4010 cal/g-atom at 360°K to -4140 cal/g-atom at 900°K. It then increases to a value of -3070 cal/g-atom at 1100°K, at which there appears to be a discontinuous change to the disordered alloy having a heat of formation of -2630 cal/g-atom. The total disordering energy of the alloy, as calculated from the difference between the heats of formation at 900 and 1100°K, is 1510±100 cal/g-atom. Of this total amount, 440 cal/g-atom is absorbed in a first-order transition at 1100°K, and the remainder in a second-order process over a temperature range of about 200°K. This behavior is similar to that observed in AuCu.[2]

The total entropy change for the disordering process is obtained as 1.44 cal/deg g-atom, which is only slightly greater than the calculated configurational entropy change, 1.38 cal/deg g-atom. The good agreement between these values suggests that any contribution to the total entropy change arising from thermal entropy differences between the ordered and disordered states must be small.

* Abstracted from UCRL-17615, June 1967.

1. C. B. Walker, J. Appl. Phys. 23, 118 (1952).
2. R. L. Orr, J. Luciat-Labry, and R. Hultgren, Acta Met. 8, 431 (1960).

2. THERMODYNAMICS OF THE SILVER-SILICON SYSTEM BY DROP CALORIMETRY*

Thomas A. Corn and Ralph Hultgren

The thermodynamic properties of liquid Ag-Si alloys from X_{Si} = 0.00 to 0.32 at 1500°K have been determined by a variation of the Oelsen technique, i.e., from heat-content measurements alone, using the diphenyl-ether Bunsen-type drop calorimeter. Heat contents with respect to 300°K were measured as a function of temperature between 1000 and 1520°K, both within single- and two-phase regions. On cooling to 300°K in the calorimeter, the alloys decomposed into pure $Ag_{(s)}$ + $Si_{(s)}$. Heats of formation of the alloys were obtained from the differences between their heat contents and those of the pure elements. Gibbs energies and entropies of formation of the alloys at 1500°K were then obtained through integration of the Gibbs-Helmholtz equation.

The heats of formation of the liquid alloys at 1500°K are negative from X_{Si} = 0 to ~0.2, beyond which they become increasingly more positive to X_{Si} = 0.32. The Gibbs energies of formation, however, show positive deviations from ideality over the entire range of composition studied. Limiting values at X_{Si} = 0 and 1500°K are found to be $\Delta\bar{H}_{Si}$ = -3810±500 cal/g-atom and γ°_{Si} = 2.80(+0.38, -0.16), both with respect to supercooled $Si_{(\ell)}$.

From the heat-content measurements on pure silver, its heat of fusion was determined to be 2607 cal/g-atom, which agrees well with previous direct measurements.

* Abstracted from UCRL-17946, December 1967.

3. VAPOR PRESSURE OF THALLIUM AND ACTIVITY MEASUREMENTS ON LIQUID SILVER-THALLIUM ALLOYS BY THE TORSION EFFUSION METHOD*

Pierre J. Desré,† Donald T. Hawkins, and Ralph Hultgren

The vapor pressure of pure thallium was measured in the temperature range 931-996°K using the torsion effusion method. The resulting $\Delta H_{v,298}$ = 43520(±100) cal per g-atom is in excellent agreement with previously determined values.

Vapor pressures of thallium above seven silver-thallium alloys ranging from 33 to 90 at.% thallium were measured at 975°K. The calculated activities of thallium show a positive deviation from Raoult's Law and scatter less than previous data obtained using the emf technique.[1] Activities of silver and integral Gibbs energies of formation were calculated through integration of the Gibbs-Duhem relationship.

* Abstracted from UCRL-17828, December 1967.
† Present address: Faculté des Sciences, Metallurgie et Electrometallurgie, Université de Grenoble, Grenoble, France.
1. J. Terpilowski, E. Kundys, and H. H. Slaby, Arch. Hutnictwa 6, 137 (1961).

4. LOW-TEMPERATURE HEAT CAPACITY OF AuCu

Donald T. Hawkins and Ralph Hultgren

A study has been initiated concerning the effects of ordering on the low-temperature thermal properties of the equiatomic gold-copper alloy, AuCu. Low-temperature heat capacities of a highly ordered and a quenched disordered alloy will be measured from 15 to 298°K. From these and other data, the zero-point entropies of the alloys will be obtained.

The experimental apparatus, an isothermal heat-capacity calorimeter designed to operate from liquid-hydrogen temperatures to room temperature[1] has been improved and put in good operating condition. Performance of the apparatus is now being checked by means of measurements of the heat capacity of pure copper. Upon completion of these runs, measurements will be made on pure gold and the alloys.

1. M. C. Huffstutler, Jr. (Ph.D. Thesis), University of California, Berkeley, October 1961.

5. HEAT CAPACITY AND HEAT OF DECOMPOSITION OF AUSTENITE

Hong-il Yoon and Ralph Hultgren

The liquid-metal solution calorimeter is being adapted for use in measurements of some thermodynamic properties of austenite, which will be studied by high-temperature drop calorimetry. Samples of austenite which have been held and equilibrated at various temperatures within its stable range will be dropped into a newly designed calorimeter receptacle held at some temperature below the eutectoid decomposition temperature. The heat capacity of austenite and the heat effect accompanying its decomposition into ferrite and cementite will be measured.

The calorimeter receptacle has been constructed, and several calibration and check runs using samples of pure platinum and iron have been made. The results have revealed the existence of some experimental difficulties which need to be analyzed and resolved before measurements on the alloys are initiated.

6. EVALUATION OF THERMODYNAMIC DATA

Ralph Hultgren, Molly Gleiser, Kenneth K. Kelley, Raymond L. Orr, Elias Plaza* and Gollakota Somayajulu

The project for the evaluation of thermodynamic data of metallic systems, the first phase of which was published in book form,[1] is being continued and extended to include some semimetallic elements and compounds. Current evaluations as they are completed are being distributed in loose-leaf form to all those requesting them. During 1967, evaluations of data and tables of selected values were distributed for the systems, Ac, Cd, Co, Cr, Dy, Er, Eu, Fe, Gd, Ho, Lu, Mg, Mn, Nd, Ni, Pr, Sc, Sm, Tb, Th, Ti, Tm, U, Y, Yb, Zr, Ag-Zr, Al-Th, Al-Zr, B-Zr, Be-Zr, Bi-Th, C-Cr, C-Mn, C-Mo, C-Th, C-Zr, Cd-Pb, Cd-Zr, Co-Nb, Co-Ti, Cr-Ni, Cr-V, Fe-Ti, Fe-V, Fe-Zr, Hg-Th, In-Sb, In-Zr, Mg-Th, Mn-Ti, Mo-Ti, Mo-U, Nb-Zr, Pb-Sn, Pb-Th, Sb-Zr, Si-Th, Si-Ti, Si-Zr, Sn-Zr, Th-Zn, Ti-V, Ti-Zr, U-Zr, and Zn-Zr.

Evaluations have been completed and are being readied for distribution for the systems La, C-U, Cd-Mg, Cr-Mo, Cr-Ti, Mo-Ir, Mo-Nb, Mo-Re, Mo-Ru, Mo-Tc, and Ni-Ti.

The reference file and associated Termatrex searching system now contain 12,500 references, primarily to thermodynamic and phase-equilibrium data. New references are being

incorporated at a rate of approximately 80 per month.

* Present address: Department of Metallurgy, Universidad Nacional de Ingenieria, Lima, Peru.

1. R. Hultgren, R. L. Orr, P. D. Anderson, and K. K. Kelley, Selected Values of Thermodynamic Properties of Metals and Alloys (John Wiley and Sons, Inc., New York, 1963).

7. RESEARCH PLANS FOR CALENDAR YEAR 1968

Ralph Hultgren

Measurements of the low-temperature heat capacities of copper, gold, and the equiatomic gold-copper alloy, AuCu, in both the fully ordered and quenched disordered states, will be continued. From these and other data, the zero-point entropies of the alloys will be obtained. Differences in properties of the ordered and disordered states will be interpreted in terms of atomic bonding and configurations in the two states.

The study of the thermodynamics of the decomposition of austenite by means of high-temperature drop calorimetry will be continued. Attempts will be made to resolve existing experimental difficulties which have been encountered in adapting the liquid-metal solution calorimeter for these measurements. The heat capacity of austenite and the heat effect accompanying its decomposition into ferrite and cementite will be measured.

Heats of formation of the three solid phases in the indium-lead system will be determined by means of liquid-tin solution calorimetry.

Evaluation of published thermodynamic data for additional metallic and semimetallic systems as well as revisions of previous evaluations will be continued. Evaluations are now in progress for Be, Ca, Ce, Sb, Al-Ti, B-Mo, B-Ti, Co-Mo, Fe-Mo, Fe-Si, H-Ti, H-Zr, Mo-N, Mo-Ni, Mo-Os, Mo-Pd, Mo-Pu, Mo-Si, Mo-V, N-Ti, N-Zr, Nb-In, Nb-Os, Nb-Pd, Nb-Pt, Nb-Rh, Nb-Sn, Sn-Ti, and Ta-Si.

8. 1967 PUBLICATIONS

Ralph Hultgren and Associates

Technical Journals

1. R. W. Carpenter, R. L. Orr, and R. Hultgren, Heats of Formation of Au_3Zn and AuZn, Trans. Met. Soc. AIME 239, 107 (1967).
2. Y. A. Chang and R. Hultgren, High-Temperature Heat Contents of Three Alpha Brass Alloys, J. Chem. Eng. Data 12, 98 (1967).
3. Y. A. Chang, L. Himmel, and J. P. Neumann, Thermal Expansion and Elastic Constants of β'-AgMg. II. Single-Crystal Elastic Constants from 77 to 750°K, J. Appl. Phys. 38 649 (1967).
4. D. T. Hawkins and R. Hultgren, Vapor Pressure of Lead and Activity Measurements on Liquid Lead-Tin Alloys by the Torsion Effusion Method, Trans. Met. Soc. AIME 239, 1046 (1967).
5. R. Hultgren, Interatomic Forces and Chemical Bonding Energies, in An Atomistic Approach to the Nature and Properties of Materials, Joseph A. Pask, Ed. (John Wiley and Sons, Inc., New York, 1967), pp. 52-73.
6. R. Hultgren, Additional Data Needed to Establish the Thermodynamic Properties of Alloying Systems, in Applications of Fundamental Thermodynamics to Metallurgical Processes, G. R. Fitterer, Ed. (Gordon and Breach, New York, 1967), pp. 5-10.
7. R. Hultgren, Problems and Progress in the Thermodynamics of Metals and Alloys, J. Metals 19, 1 (1967).
8. R. Hultgren and Raymond L. Orr, Some Energy Measurements Related to Structure of Metallic Liquids, Rev. Int. Hautes Temper. et Refract. 4, 123 (1967).
9. R. L. Orr and J. Chipman, Thermodynamic Functions of Iron, Trans. Met. Soc. AIME 239, 630 (1967).

UCRL Reports

1. T. A. Corn, The Thermodynamics of the Silver-Silicon System by Drop Calorimetry (M.S. Thesis), UCRL-17946, December 1967.
2. P. J. Desré, D. T. Hawkins, and R. Hultgren, Vapor Pressure of Thallium and Activity Measurements on Liquid Silver-Thallium Alloys by the Torsion Effusion Method, UCRL-17828, December 1967.
3. G. W. Geiken, A. Thermodynamic Study of the Heat of Ordering in CuPt (M.S. Thesis), UCRL-17615, June 1967.
4. E. M. Plaza, Thermodynamics of Solid and Liquid AuSn and Heat Contents of Gold and Tin (M.S. Thesis), UCRL-17401, Feb. 1967.

Ceramic Science

III. CERAMIC SCIENCE

A. HIGH TEMPERATURE REACTIONS

1. SUBLIMATION OF PRASEODYMIUM FLUORIDE*

Harry B. Skinner and Alan W. Searcy

The equilibrium and Langmuir sublimation pressures of praseodymium fluoride were measured by the torsion technique from 1424 to 1586°K. Graphite torsion cells containing the praseodymium fluoride powder were suspended in a tungsten hairpin furnace. Torsion deflection measurements were taken to the nearest 0.005-deg with a modified goniometer. Temperatures were measured by means of a dummy graphite cell located directly below the effusion cell which had previously been calibrated by measuring temperatures in both cells at a series of power settings.

The equilibrium pressure is given in the experimental range by the expression

$$\log P_{atm} = -(2.109\pm0.012)\ \frac{10^4}{T} + 9.371\pm0.082,$$

where the quoted errors are the standard deviations from the least-squares fit of 77 data points. To insure that molecular flow conditions prevailed, measurements were made only under conditions for which λ/d, the calculated ratio of mean free path to orifice diameter, exceeded 0.80 although no failure of molecular flow was found with λ/d ratios as low as 0.40 by Mar and Searcy.

The heat of sublimation at 298.15°K was calculated by the second-law and third-law methods. It was necessary to estimate the heat capacities and free-energy functions for both the solid and the gas.

The heat of sublimation at 298.15°K was calculated to be 106.6 kcal/mole by the second-law method and 103.3 kcal/mole by the third-law method. Estimated probable error in the experimental technique and approximated thermochemical data cause a ±5 kcal/mole uncertainty in second- and third-law values. However, because no measured data for closely related materials are available to compare with the estimates, the uncertainties in third-law calculations may have been seriously underestimated. Since second-law calculations are relatively insensitive to errors in the estimates of these data, the second-law analysis was given principal weight in fixing $\Delta H^\circ_{298.15}$ as 106.5±5 kcal/mole.

Comparison of equilibrium sublimation pressures with Langmuir sublimation pressures from the (0001) crystal face yielded an apparent evaporation coefficient of 1.00±0.04 in the experimental range.

However microscopic examination of the evaporated Langmuir surfaces revealed surface features similar but more pronounced than those observed by Mar and Searcy in the evaporation of lanthanum fluoride. In consideration of the pitting and fissuring observed for the Langmuir surfaces, the true evaporation coefficient is fixed as 0.9±0.1 for the (0001) face.

* Abstract from UCRL-17804, September 1967.

2. EXCHANGE OF ENERGY BETWEEN TUNGSTEN AT HIGH TEMPERATURES AND GASES AT ROOM TEMPERATURE*

Mahn Jick Lim† and Alan W. Searcy

The exchange of energy between a tungsten filament and room-temperature neon, nitrogen, argon, krypton, and mixtures of argon with oxygen were determined over a wide range of filament temperatures and gas pressures. For the study, the apparatus of DePoorter and Searcy[1] was modified to operate at improved vacuum and improved sensitivity to the energy exchange.

For nonreactive gases, the thermal-accomodation coefficient was found to be independent of gas pressures between 10^{-7} and 5×10^{-5} atm. Figure IIIA.2-1 shows data for argon as an example.

The dependence of thermal accommodation coefficients for the noble gases and for nitrogen on temperature are all of similar complex forms (Fig. IIIA.2-2). The variations for these gases are believed to reflect primarily

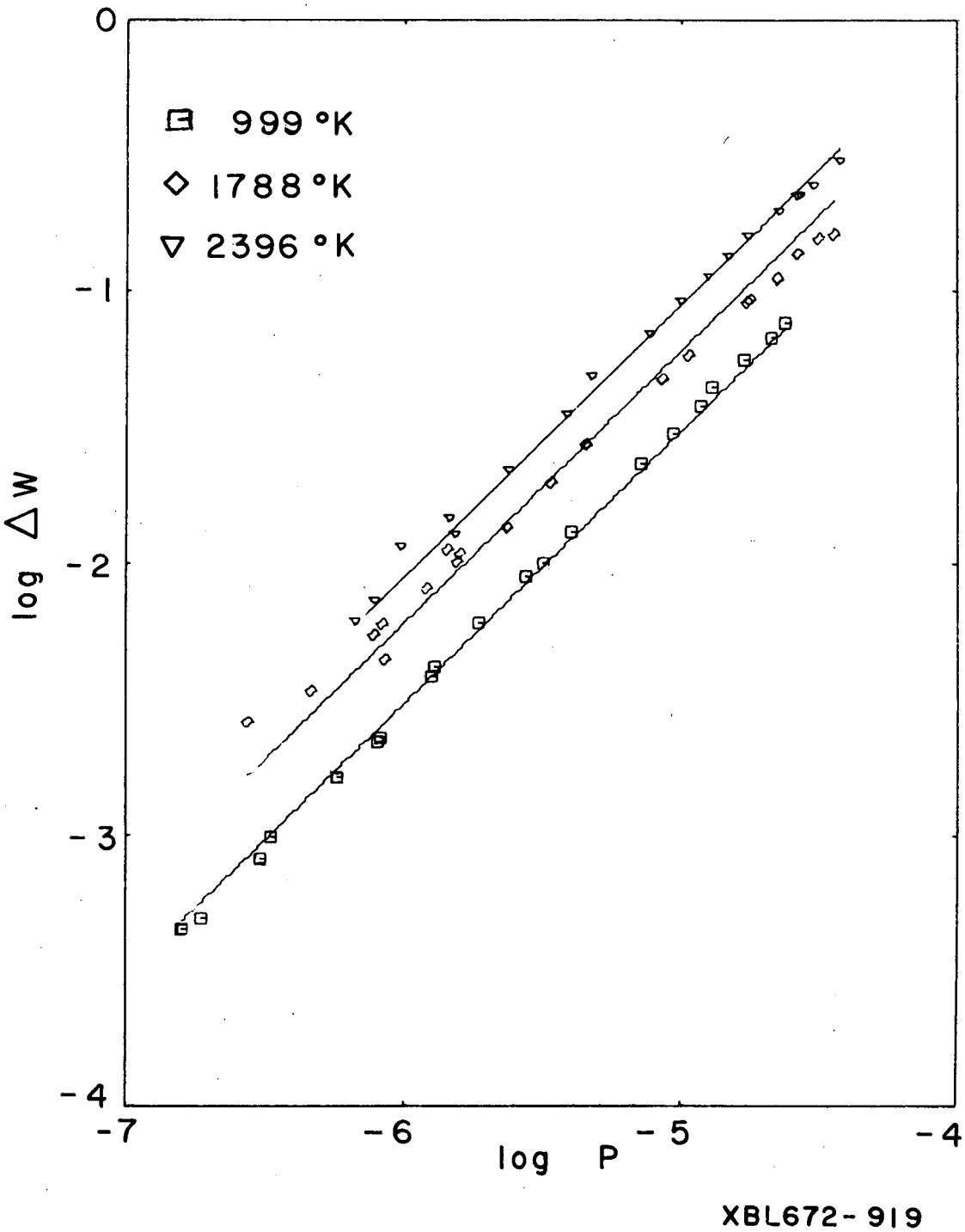

Fig. IIIA.2-1. Power loss vs argon pressure. ΔW is in watts/cm^2; P in atm.

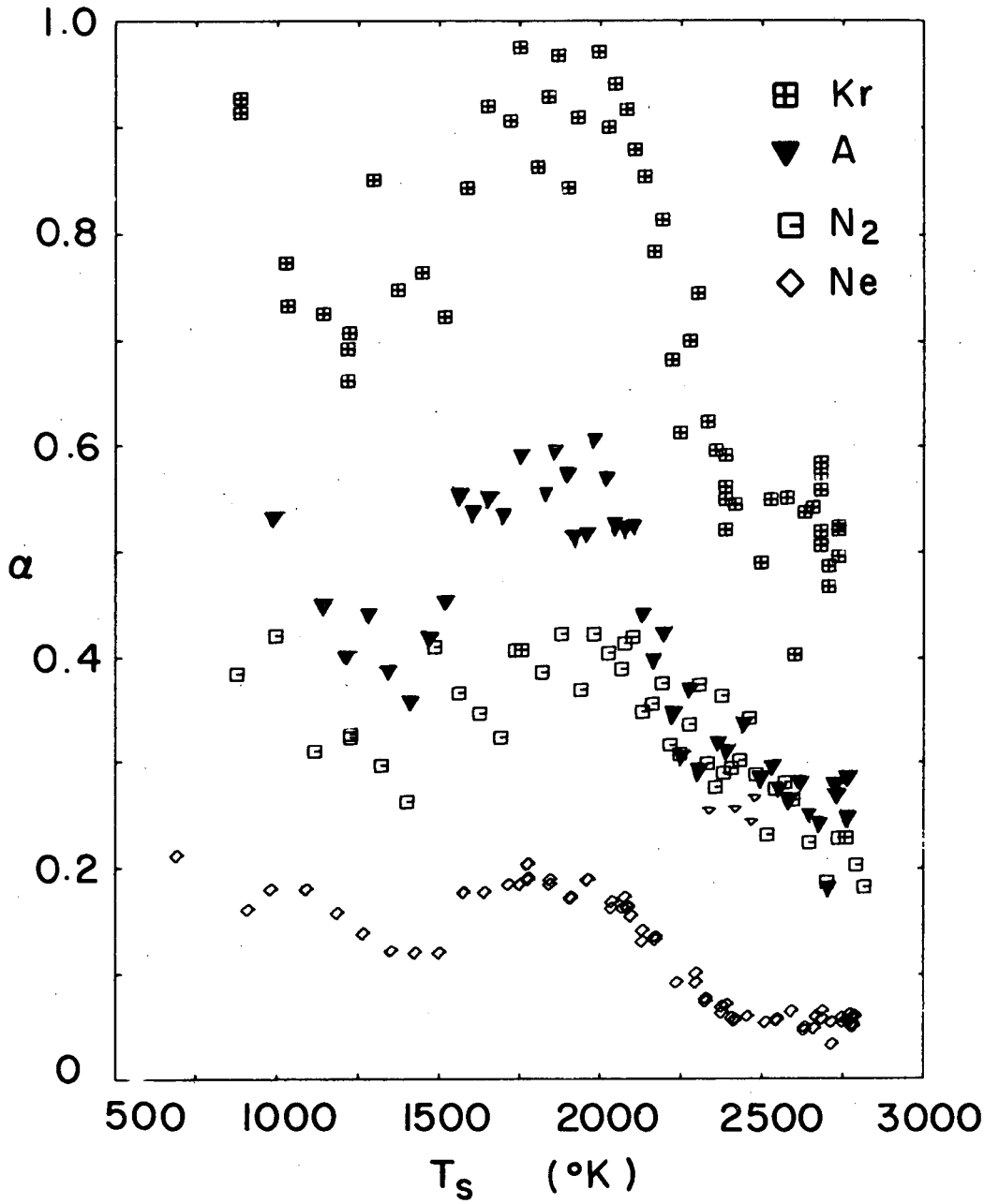

Fig. IIIA. 2-2. Thermal accommodation coefficient (α_1) vs tungsten temperature.

changes in the fraction of coverage of adsorbed surface impurities and in surface structures. All show maximum thermal accommodation coefficients near 2000°K.

For oxygen, below 1500°K, the energy exchange phenomenon is very similar to those for various nonreactive gases (Fig. IIIA.2-3). In the temperature range from 1500 to 1800°K an

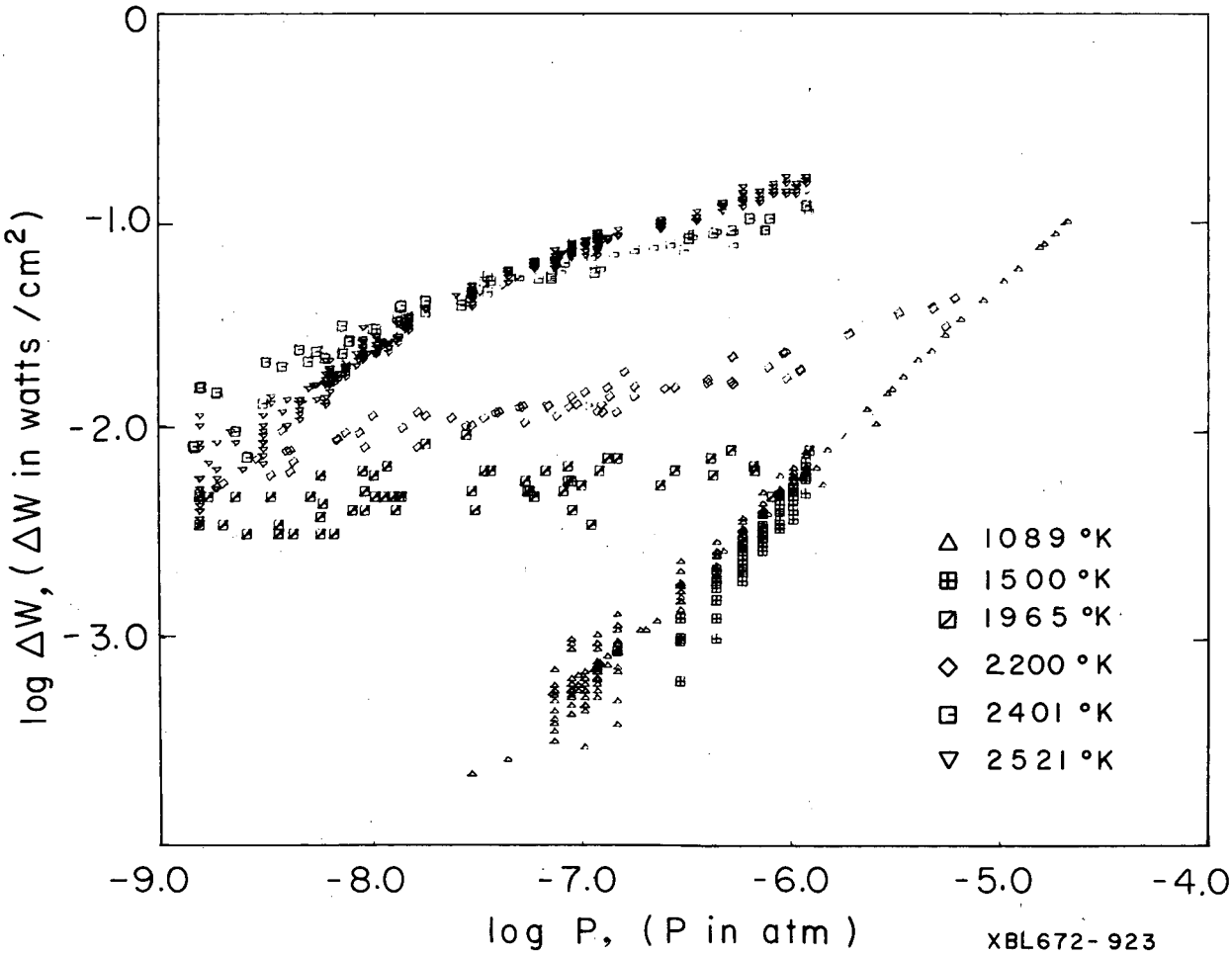

Fig. IIIA.2-3. Endothermic energy exchange rate vs oxygen pressures at different tungsten temperatures.

exothermic energy exchange occurs that is nearly independent of gas pressure. Above 1900°K, where the exchange is again endothermic, the pressure dependence of the energy exchange becomes more pronounced as the solid temperature is further raised (Fig. IIIA.2-3). At very low oxygen pressures, an abnormally high apparent energy exchange was observed. This was presumably due to an instantaneous change in carbon content which caused a change in the electrical resistance, and due to large errors in the measurement of energy exchange at low pressures. For oxygen, nitric oxide, and nitrous oxide, the energy exchange at about 2600°K is high enough to support the conclusion that essentially all incident molecules react.

The energy exchanges of mixtures of neon with krypton are essentially the arithmetic sums of the energy exchanges of the individual species at 2142°K. The same was found for argon-oxygen mixtures at 2528°K, but at 1740 and 2200°K departure from this simple addition rule was found, especially for higher oxygen mole fractions.

* Abstract from UCRL-17395, April 1967.

† Present address: Western Electric Co., Engineering Research Center, P. O. Box 900, Princeton, New Jersey.

1. G. L. DePoorter and A. W. Searcy, J. Chem. Phys. 39, 925 (1963).

3. VAPOR SPECIES OF THE BARIUM-OXYGEN SYSTEM*

Ray S. Newbury,† George W. Barton, Jr.,† and Alan W. Searcy

Mass spectrometric and vacuum thermobalance studies of barium oxide between 1365 and 1917°K yield for the equilibrium pressure of BaO gas

$$\log P_{atm} = -22{,}610/T + 7.90.$$

The enthalpy for the reaction BaO(g) = BaO(g) was calculated to be $\Delta H^{\circ}_{298} = 110.9 \pm 2.8$ kcal/mole by the second-law method. The third-law data are consistent with this value if a $^3\Pi$ state is assumed to be at or near (within a few hundred cm^{-1}) the ground state of BaO(g)

The heat of sublimation of the dimer $Ba_2O_2(g)$ was found from the mass spectrometer study to be about 142 kcal/mole, and the heat of the reaction BaO(g) + Ba(g) = $Ba_2O(g)$ was found to be -73±15 kcal/mole at 1800°K. No reaction of barium oxide at 1800°K with $O_2(g)$ at pressures up to 10^{-3} atm was detected.

* From the Ph.D. Thesis of R.S.N. Experimental work performed at Livermore LRL. J. Chem. Phys. (in press).
† Affiliated with Chemistry Division, Lawrence Radiation Laboratory, Livermore, California.

4. A STUDY OF THE FREE ENERGY AND ENTHALPY OF FORMATION OF $Al_2S_3(s)$

Oddvin Herstad and Alan W. Searcy

The equilibrium between $Al_2S_3(s)$ and HCl(g) has been measured in the temperature range 575 to 829°K by the transpiration method. Argon and HCl(g) were brought together through separate gas flowmeters and led into the reaction chamber. The composition of the ingoing mixture of gas could be determined roughly from the readings of the meters, and could be changed by changing the flow rate either of HCl or argon. After equilibration with Al_2S_3 the gas mixture, then consisting of Ar, HCl(g), $H_2S(g)$, $AlCl_3(g)$, and $Al_2Cl(g)$, was led through an ice-water-cooled condenser where the aluminum chloride was condensed. The residual gas was successively bubbled through distilled water and N/10 NaOH to absorb HCl and H_2S, respectively. The total amount of argon was measured at the outlet of the apparatus by a gas volume meter.

From analysis of the concentrations of aluminum chloride, hydrogen sulfide, and hydrogen chloride in the transport gas and known data for the dimer-monomer equilibrium for aluminum trichloride, the free energy of the reaction $Al_2S_3(s) + 6HCl(g) = 2AlCl_3(g) + 3H_2S(g)$ was found to be -5300-5.0T cal. A third-law calculation of the enthalpy of formation of Al_2S_3 at 298°K yielded -156±4.5 kcal/mole. This value is to be compared with the previous discordant value of -147 from heat-of-solution measurements and -121.6 + -172.9 obtained by direct combustion.

5. EQUILIBRIUM AND NONEQUILIBRIUM SUBLIMATION OF ZINC SULFIDE AND OF CADMIUM TELLURIDE

Bette A. H. Blank and Alan W. Searcy

The torsion-effusion method was used to measure equilibrium vapor pressures of zinc sulfide and of cadmium telluride. The torsion-Langmuir method was used to measure free surface sublimation from the basal (001) planes of hexagonal single crystals of each substance.

The equilibrium constant for the dissociation sublimation reaction ZnS(s) = Zn(g) + 1/2 $S_2(g)$ is

$$\log K = 3/2 \log P_T - 0.4147$$

$$= -\left(\frac{88.438\ 2.609}{4.576}\right) \cdot 10^3/T + 9.671 \pm 0.509.$$

From a second-law treatment of the data, the heat of the reaction at 298°K is calculated to be 88.4 kcal/mole of ZnS, and from comparison of the torsion-effusion and torsion-Langmuir data, the evaporation coefficient is found to be 0.3±0.1 in the experimental range.

For the reaction CdTe(s) = Cd(g)+;/2Te(g), log K is [(66.37±4.57)/4.576] + 8.75±1.09, the heat of the reaction at 298°K is 65.37 kcal/mole of CdTe, and the evaporation coefficient is 0.8±0.2.

6. RESEARCH PLANS FOR CALENDAR YEAR 1968

Alan W. Searcy

The apparatus, which employs a quadrupole mass spectrometer as a detector of species deflected in the field of our inhomogeneous field magnet, will be applied during the coming year to identification of the low-lying electronic states of high temperature vapor species.

A mass spectrometer study of the polymeric

vapor species of chromium (VI) oxide was completed during 1967. Double-oven experiments designed to establish the stabilities of vapor species of oxidation state between V and VI will be carried out in 1968.

The vapor pressure of stannous fluoride is under investigation by the torsion-effusion method. The study should be completed during 1968.

Studies of the kinetics of free surface sublimation of single crystals of zinc will continue. Particular emphasis is being placed on correlation of the surface structure and orientation with the rate of sublimation as measured by the torsion-Langmuir method.

Studies of the effect of atmospheres of various gases on the kinetics of effusion and free surface sublimation of magnesium nitride will continue by the torsion-effusion and torsion-Langmuir techniques. The apparatus is being fitted with a quadrupole mass spectrometer, which will facilitate characterization of the vapor and gaseous species present under various reaction conditions.

A mass spectrometer will be employed to study the kinetics of free surface sublimation of magnesium oxide single crystals. The surface structures that correspond to non-steady-state and steady-state sublimation in vacuum will be determined by microscopic examination.

A tube furnace and microbalance have been constructed for use in the coming year on a more detailed study of the effect of chemical composition and incident light on the kinetics of sublimation of single crystals of zinc oxide and possibly of chemically related solids.

A transpiration and mass spectrometer study will be made of the reaction of $Al_2O_3(s)$ and $Al(\ell)$ with hydrogen. We hope to prepare and study gaseous AlOH.

7. 1967 PUBLICATIONS

Alan W. Searcy and Associates

Technical Journals

1. C. L. Hoenig and A. W. Searcy, Vapor Pressure, Enthalpy, Evaporation Coefficient, and Enthalpy of Activation of the Beryllium Nitride (Be_3N_2) Decomposition Reaction, J. Am. Ceram. Soc. 50, 460 (1967).
2. R. W. Mar and A. W. Searcy, The Vapor Pressure, Heat of Sublimation, and Evaporation Coefficient of Lanthanum Fluoride, J. Phys. Chem. 71, 888 (1967).

UCRL Reports

1. M. J. Lim, The Exchange of Energy Between Tungsten at High Temperatures and Gases at Room Temperature (Ph.D. Thesis), UCRL-17395, April 1967.
2. H. B. Skinner, The Heat of Sublimation and the Evaporation Coefficient of Praseodymium Trifluoride (M.S. Thesis), UCRL-17804, September 1967.

B. MICROSTRUCTURE AND BEHAVIOR OF CERAMIC MATERIALS: GLASS AND CERAMIC-METAL SYSTEMS

Joseph A. Pask

An objective of this program is to contribute to the development of a fundamental understanding of the factors involved in obtaining ceramic materials with controlled character, which includes microstructure, and of the relationship of character to mechanical behavior at room and high temperatures. This objective involves studies on the kinetics and mechanisms of solid-state reactions, which in general play a part in the development of microstructure. It also involves studies on the mechanisms responsible for the mechanical behavior of single crystals, and on the application of such knowledge to the understanding of the behavior of polycrystalline ceramic materials.

A second objective of this program is concerned with structural, thermodynamic and electrochemical studies of glass, glass-metal, and ceramic-metal systems. It deals with studies related to wetting, bonding, and the nature of the interfaces between such phases, to the thermodynamics and kinetics of chemical reactions at such interfaces, and to the kinetics and mechanisms of dissolution and diffusion in glasses.

1. DIFFUSION OF IRON AND NICKEL INTO SINGLE-CRYSTAL MgO*

Stuart L. Blank† and Joseph A. Pask

The diffusion kinetics in the Fe-MgO, NiO-MgO, and Fe_2O_3-MgO systems were investigated, with particular emphasis placed on the relationship between atomistic mechamisms and structural changes. The existence of Fe^{+3} ions and their location in the lattice in the Fe-MgO (vacuum) and Fe_2O_3-MgO (air) systems were determined by the use of electron paramagnetic resonance, and optical spectroscopy. The location of Fe^{+2} was investigated using optical spectroscopy. The occurrence of Fe^{+3} ions in tetrahedral symmetry in MgO was associated with structural changes that were responsible for variations in the activation energy for diffusion in the Fe-MgO and Fe_2O_3-MgO systems. The presence of chemically created vacancies in all of the systems increased the diffusivities and placed them in the extrinsic range. The concentration vs penetration curves were obtained using the electron microprobe analyzer. The diffusion studies showed that in vacuum iron reacts with MgO in the temperature range 1100 to 1350°C according to the reaction

$$xFe + MgO = Fe_xO + Mg.$$

The subsequent diffusion of iron into MgO was found to follow the relations:

at 1150°C $D = 8.1\times10^{-12}\ e^{0.346\,[Fe]}$

at 1250°C $D = 1.6\times10^{-11}\ e^{0.398\,[Fe]}$

at 1350°C $D = 2.4\times10^{-11}\ e^{0.438\,[Fe]}$

The temperature dependence was found to be:

at 5 a/o Fe $D = 6.34\times10^{-7}\ e^{-29.6\ kcal/RT}$

at 10 a/o Fe $D = 4.49\times10^{-6}\ e^{-32.9\ kcal/RT}$

at 15 a/o Fe $D = 5.04\times10^{-5}\ e^{-37.7\ kcal/RT}$

at 20 a/o Fe $D = 8.40\times10^{-4}\ e^{-43.5\ kcal/RT}$

The diffusion results in the NiO-MgO system in vacuum show no concentration dependence of either the D_o term or the activation energy and are represented by $D = 9.82\times10^{-6}\ \exp(-45.5\ kcal/RT)$. However, in air the diffusivity was concentration-dependent, but the activation energy was found to be constant. The air results are:

at 1200°C $D = 1.75\times10^{-12}\ e^{0.0537\,[Ni]}$

at 1300°C $D = 4.1\times10^{-12}\ e^{0.0537\,[Ni]}$

at 1370°C $D = 7.6\times10^{-12}\ e^{0.0537\,[Ni]}$

at 1400°C $D = 1.05\times10^{-11}\ e^{0.0537\,[Ni]}$

The temperature dependence was found to follow the relationships:

at 10 a/o $D = 6.31\times10^{-6} \exp(-42.8 \text{ kcal/RT})$

at 20 a/o $D = 1.05\times10^{-5} \exp(-42.8 \text{ kcal/RT})$

at 30 a/o $D = 1.96\times10^{-5} \exp(-42.8 \text{ kcal/RT})$

at 40 a/o $D = 3.16\times10^{-5} \exp(-42.8 \text{ kcal/RT})$.

The diffusion kinetics in the Fe_2O_3-MgO system were found to obey the relation: $D = 8.83 \exp(-74.6 \text{ kcal/RT})$ in the temperature range 1200 to 1400°C. This relation is for an average composition in the diffusion zone resulting from the approximation used to solve the 3-phase 2-moving-boundary diffusion problem.

* Abstract from S. L. Blank, UCRL-17411, March 1967.
† Present address: U.S. Army Materials Research Laboratory, Watertown, Massachusetts 02172.

2. DIFFUSION IN THE CaO-NiO SYSTEM

Marvin Appel and Joseph A. Pask

The objectives of this study program are to investigate solid-state diffusion in a binary oxide system in which there is limited solid solubility and no compound formation. A CaO-NiO diffusion couple satisfies this criterion with the additional advantages: (a) The eutectic is at 1720°C so that considerable diffusion will occur in times of the order of one week over a temperature range of 1300 to 1600°C, and (b) single crystals of these oxides are readily available.

A complete series of single-crystal vs single-crystal-diffusion anneals has been made in air at various times and temperatures. The diffusion couples were sectioned, and concentration vs distance profiles were determined with an electron microprobe. Computer programs were developed in Fortran, and extensive use was made of a CDC 6600 computer to correct the raw microprobe data for background, drift, dead time, absorption, and fluorescence. A Cal-Comp plotter was used to plot the data automatically as concentration vs distance profiles.

A Kirkendall or moving-boundary effect has been observed in this system with the NiO-rich phase growing at the expense of the CaO-rich phase. The Ca^{+2} diffuses much more quickly in the NiO-rich phase than the Ni^{+2} in the CaO-rich phase. Electroneutrality relative to the moving boundary is maintained by a net O^{-2} flow in the direction of Ca^{+2} diffusion.

As a consequence of this two-phase diffusion study, portions of the NiO-CaO phase diagram have been redetermined. There was no correlation between maximum solubility and annealing time for the various runs, and so it may be assumed that an equilibrium concentration was always maintained at the phase boundary. The maximum solubilities in mole-% of CaO in NiO and NiO in CaO, respectively, are shown in Table IIIB.2-I.

Table IIIB.2-I. Maximum solubilities.

Temp. (°C)	CaO in NiO (mole-%)	NiO in CaO (mole-%)
1352	8.25	4.25
1420	11.0	6.0
1525	12.5	7.0

NiO and MgO are of nearly the same lattice spacing (4.172 and 4.203Å, respectively) and form a complete series of solid solutions at all temperatures below the melting point. A single-crystal vs single-crystal-diffusion anneal was made at 1346°C for 173:26 hr. A previously reported Kirkendall effect and concentration-dependent diffusivity were verified. The Mg^{+2} diffusion exceeds that of the Ni^{+2}. A Boltzmann-Matano analysis of the two respective, continuous concentration profiles showed the following concentration dependences for the respective diffusivities, with Ni concentration expressed in atomic percent:

$$D_{Ni} = 7.50\times10^{-12} \exp[(0.0594\pm0.0064)\ Ni]$$

$$D_{Mg} = 1.13\times10^{-12} \exp[(0.1778\pm0.0268)\ Mg].$$

The Ni diffusivity compares very well with the value $D_{Ni} = 7.6\times10^{-12} \exp[0.0537\ Ni]$ determined by Blank* for a couple at 1372°C.

To determine the diffusivities and activation energies in the two-phase system, the equation for Fick's second law in one dimension, $dc/dt = d/dx(D\ dc/dx)$, must be solved with $D = D(c)$. No solution presently exists for this equation which satisfies the conditions of our problem. Attempts are being made to modify the Boltzmann-Matano solution so that it may be applied to a concentration profile that is discontinuous across the phase boundary.

CaO is stoichiometric in air, but NiO is not. There is a Ni vacancy concentration proportional to

$$P_{O_2}^{1/6}.$$

The characteristics of diffusion in this system may therefore be different <u>in vacuo</u> than in air.

Consequently, a series of CaO-NiO diffusion anneals are currently being made in vacuo to determine what effect, if any, NiO stoichiometry will have on the diffusion characteristics.

* See Section IIIB.1.

3. EFFECT OF LITHIUM FLUORIDE ON THE DENSIFICATION OF MAGNESIUM OXIDE*

Patrick E. Hart† and Joseph A. Pask

Studies on the densification by pressure sintering of magnesium oxide compacts containing an additive of 1/2 to 10% lithium fluoride have been continued.[1] Identification and analysis of the mechanisms involved in this fabrication process was a primary objective.

Densification may be considered to be a three-step process with the first two steps occurring in the fabrication die, and the last step, annealing, after pressing. The first stage in the die is a rapid process and is believed to be similar to the rearrangement stage that has been observed by several authors. Depending on fabrication parameters, i.e., temperature, pressure, and initial lithium fluoride content, this initial stage may take place up to densities as high as 90% of theoretical, relative to pure magnesium oxide. Experimental evidence indicates that the second stage of densification in the die is controlled by flow of a lithium fluoride-rich phase along magnesia grain boundaries and its expulsion from the compact. Transport of magnesium oxide is also achieved through this phase by means of a solution-precipitation process. This analysis in this stage is valid for samples with densities ranging from 91 to 99.5%. These two stages are not distinct but are separated by a transition range. The annealing stage is controlled by the evaporation of lithium fluoride from the sample surface. Samples having densities of 99.1% or more, after hot pressing, become transparent during the last annealing stage and reach essentially the theoretical density of MgO.

* Abstracted in part from UCRL-17978, December 1967.

† Present address: Battelle Northwest, Richland, Washington.

1. M. W. Benecke, N. E. Olson, and J. A. Pask, Effect of LiF on Hot-Pressing of MgO, J. Am. Ceram. Soc. 50, 365 (1967).

4. PHASE DISTRIBUTION IN MULTIPHASE MAGNESIA AND FORSTERITE BODIES

Abbaraju P. Raju,† Ilhan A. Aksay, and Joseph A. Pask

The geometrical distribution of phases (microstructure) is critical in the performance of refractory materials at high temperatures. An understanding of the various factors affecting the distribution of a liquid phase (at the firing temperatures) in the presence of one or two solid phases is helpful in the production of controlled microstructure, and in turn, a ceramic body with controlled properties. Wetting experiments in the systems MgO-liquid and forsterite (Mg_2SiO_4)-liquid were performed with this objective in mind.

Contact angles of liquids of monticellite ($CaO \cdot MgO \cdot SiO_2$) composition, containing Cr_2O_3 and Fe_2O_3, on single crystals of MgO were measured at 1550°C in air. The contact angle of monticellite liquid on MgO was 45-deg. The angle decreased when either Fe_2O_3 or Cr_2O_3 was added to the monticellite. Fe_2O_3-containing liquids reached a constant value of 15 to 16° above about 3% Fe_2O_3 in the liquid, and the Cr_2O_3-containing liquids reached a value of about 0° above about 3% Cr_2O_3. The possible operative mechanisms are under investigation. Efforts to measure contact angles of liquids containing CaO, MgO, and SiO_2 on sintered polycrystalline forsterite specimens met with difficulties because of a reaction at the interface.

Studies are continuing to determine the factors that play a role in the microstructure development of a system containing a liquid phase.

† Present address: Ceramics Group, Research Department, National Lead Company, Niagara Falls, New York.

5. INVESTIGATION OF THE REACTIONS BETWEEN Al_2O_3 AND SiO_2

Robert F. Davis* and Joseph A. Pask

A comprehensive review[1] of the literature concerning mullite ($3Al_2O_3 \cdot SiO_2$) has revealed not only wide disagreement in the much-researched phase relations in the Al_2O_3-SiO_2 system, but also confusing and often conflicting reports of the mechanisms, reaction kinetics, and results in the formation of this material. Studies have been undertaken to

resolve some of the discrepancies with an objective of developing a highly dense, non-vitreous mullite body.

An investigation of the diffusion between single-crystal Al_2O_3 and fused silica has been started, together with the derivation or modification of the mathematical, microprobe, and computer methods of analysis necessary for a system of this type. Mathematical equations have been derived to describe the reaction for a doubly moving boundary in a three-phase system. Through the development of a three-phase polishing technique, microprobe analysis of the couple can now be carried out and these data corrected for background, drift, dead time, absorption, and fluorescence by a computer program developed for the CDC 6600. A program has been written that will plot these results with the aid of the Cal-Comp plotter.

* Edward Orton, Jr., Ceramic Foundation Fellow.

1. Prepared as a chapter for a book entitled, Oxide Refractories, edited by A. M. Alper (to be published by Academic Press).

6. EFFECT OF MICROSTRUCTURE ON THE DEFORMATION OF POLYCRYSTALLINE MgO*

Terence G. Langdon† and Joseph A. Pask

The effect of varying porosity on the deformation of polycrystalline MgO was investigated using specimens of varying density and with pores located primarily either along the grain boundaries or within the grains. Specimens were deformed in compression in the temperature range from room temperature to 1400°C, under conditions of constant force rate with an initial rate of 20 psi/sec. The results showed that for specimens of a similar density (~98% theoretical density) the stress-strain behavior was critically dependent both on the location of the pores and on the average size of the pores with respect to the grain size. With relatively large pores located intergranually or for specimens of theoretical density, substantial ductility occurred only at temperatures of 1200°C and greater. For specimens containing pores of small number and size along grain boundaries or small transgranular pores in clusters, ductility was apparent at temperatures as low as ~800°C.

* Based on a paper presented at the Twentieth Annual Pacific Coast Regional Meeting of the American Ceramic Society, San Francisco, California, November 1967.

† Present address: Department of Surface Physics, Cavendish Laboratory, University of Cambridge, Cambridge, England.

7. CREEP OF POLYCRYSTALLINE MAGNESIUM OXIDE

Terence G. Langdon,† John Sherohman, and Joseph A. Pask

Although a number of papers have been published on the creep of polycrystalline MgO, many of these early results are difficult to analyze due to the use of material of varying porosity. To overcome this problem, creep tests were carried out on fully dense MgO produced by hot-pressing high-purity powder with LiF as an additive.* Tests were conducted in compression at 1200°C for a wide range of stresses and for three different grain sizes. The results show that, for all of these grain sizes, the creep rate is related to the stress through an exponent of $n \sim 3$ to 4, thereby excluding Herring-Nabarro diffusional creep as the rate-controlling mechanism.

These creep specimens will be used to measure the contribution of grain-boundary sliding to the total strain.

† Present address: Department of Surface Physics, Cavendish Laboratory, University of Cambridge, Cambridge, England.

* See Section IIIB.3.

8. GRAIN-BOUNDARY SLIDING AT HIGH TEMPERATURES*

Terence G. Langdon†

Grain-boundary sliding is an extremely important process in the deformation of materials at high temperatures, particularly since a high incidence of sliding may lead to the formation of small voids or cavities in the boundaries, and the linking of these will ultimately give rise to intergranular failure. In this paper, the various methods available for measuring grain-boundary sliding are reviewed and emphasis placed on the analysis of such measurements to give meaningful results.

Two methods of measuring grain-boundary sliding are depicted in Figs. IIIB.8-1 and 8-2, both obtained on a magnesium alloy creep-tested at 200°C. In Fig. IIIB.8-1, the boundary offsets are revealed by interference fringes; in Fig. IIIB.8-2, by a transverse marker line scribed prior to testing.

The methods described are applicable to both ceramic and metallic materials.

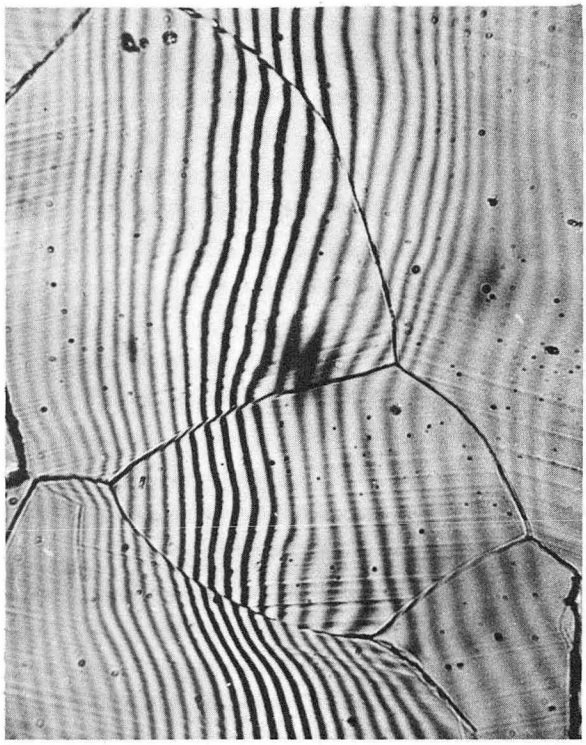

XBB 673-1378

Fig. IIIB.8-1. Grain-boundary offsets revealed by interference fringes. Magnesium alloy strained 1.5% at 200°C (x386).

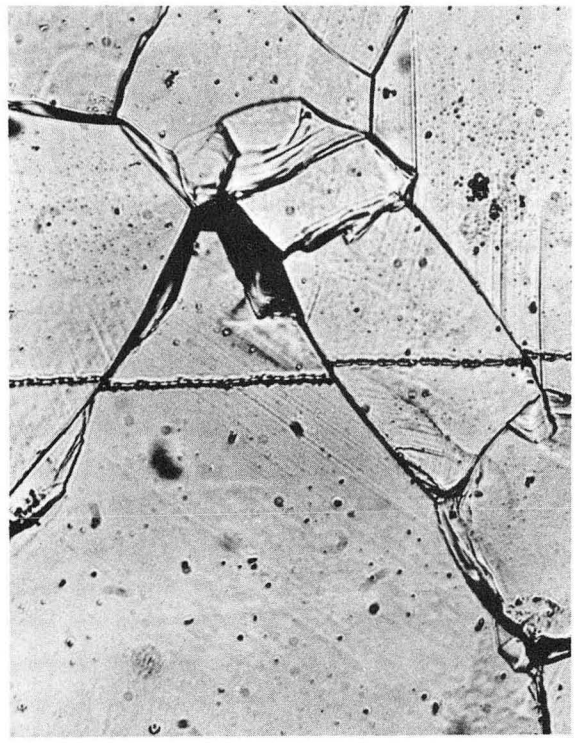

XBB 673-1377

Fig. IIIB.8-2. Offsets revealed by a transverse marker line on a magnesium alloy strained 2.5% at 200°C. Stress axis horizontal (x382).

* Abstracted from UCRL-17442, August 1967, part of which was expanded into a paper presented at the annual meeting of AIME in Cleveland, Ohio, October 1967, UCRL-17832.
† Present address: Department of Surface Physics, Cavendish Laboratory, University of Cambridge, Cambridge, England.

9. VOID FORMATION IN NICKEL AND SILVER DURING CREEP*

Terence G. Langdon†

In a recent study of void formation in nickel and silver, Price[1,2] concluded that primary creep was due to deformation within the grains, and that the transition to secondary creep marked the onset of general grain-boundary sliding. However, this view is contrary to the extensive evidence now available in the literature, where sliding is generally found to decrease, or remain constant, with increasing strain throughout the primary and secondary regions.

* Abstracted from UCRL-17821, September 1967.
† Present address: Department of Surface Physics, Cavendish Laboratory, University of Cambridge, Cambridge, England.

1. C. E. Price, Acta Met. 15, 1249 (1967).
2. C. E. Price, Acta Met. 14, 1781 (1966).

10. CREEP OF POLYCRYSTALLINE LiF

Terence G. Langdon† and Donald R. Cropper

While the creep of pure polycrystalline metals is fairly well documented for temperatures greater than ~0.5 T_m, where T_m is the melting point in degrees Kelvin, there is at present only limited information on the creep behavior in polystalline ceramics. Creep tests were carried out on theoretically dense polycrystalline LiF at temperatures from 300 to 550°C.

Polycrystalline rods which were prepared by extrusion and recrystallization of single crystals were cut into cylindrical specimens

with length:diameter ratios of about 1.5 and loaded in compression. Stress dependence was determined at a constant temperature by applying a stress, waiting until steady-state creep was established, changing the stress level instantaneously, and observing the new steady-state creep rate. As many as five or six stress changes were made on a single specimen. The data were plotted as ratios of strain rate after a change to strain rate before a change ($\dot{\epsilon}_2/\dot{\epsilon}_1$) versus the corresponding ratios of stresses (σ_2/σ_1). A logarithmic plot of these data for five temperatures and two grain sizes (~160 and ~3000μ) is shown in Fig. IIIB.10-1.

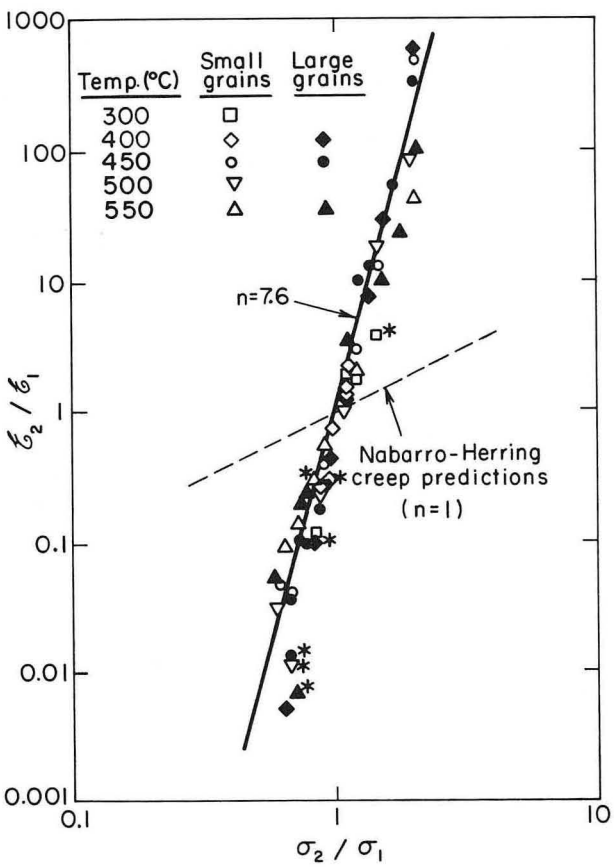

XBL682-1965

Fig. IIIB.10-1. Steady-state strain-rate ratios vs applied-stress ratios for creep of polycrystalline LiF in compression.

The data points indicated by an asterisk (from the first change in stress) fall off the line because steady-state creep probably had not been established prior to the stress change. The slope of the line indicates that the steady-state creep rate is proportional to the 7.6 power of the applied stress.

The temperature dependence was evaluated between 400 and 550°C by observing the effect of a rapid temperature change of about 25°C on the strain rate at constant applied stress. The average of 13 values for the activation energy for creep obtained in this manner gave the result $\Delta H_c = 50.1 \pm 9.8$ kcal/mole. This value agrees with that reported for diffusion of fluorine ion in LiF, $\Delta H_d = 50$ kcal/mole.

Thus it may be concluded that steady-state creep in polycrystalline LiF between 0.5 and 0.75 T_m can be described by the equation

$$\dot{\epsilon} = A^{\sim 7.6} \exp\left(-\frac{50.1 \pm 9.8 \text{kcal/mole}}{RT}\right).$$

Although the stress dependence is somewhat higher than that predicted by present dislocation theories of high-temperature creep, it is felt that a dislocation mechanism, possibly climb of edge dislocations or motion of jogged-screw dislocations, is rate controlling. The agreement between the activation energy for creep and that for fluorine-ion diffusion in LiF suggests that the motion of F^- ions is the limiting step in the process.

† Present address: Department of Surface Physics, Cavendish Laboratory, University of Cambridge, Cambridge, England.

11. CREEP OF LiF SINGLE CRYSTALS

Donald R. Cropper and Joseph A. Pask

One creep machine has been modified and a duplicate apparatus has been constructed in preparation for creep studies on single-crystal LiF in compression and in double shear. The principal modification was conversion from intermittent dial-gage monitoring of deformation to continuous electronic recording of deformation vs time. A technique has been developed for preparing "dumbbell" shaped double-shear specimens from single crystal blanks by cutting with a diamond-impregnated resin wheel.

Results from MgO studies have suggested that resistance to intersections by dislocations on orthogonal {110} slip planes below about 1250°C (~0.5 T_m) control the mode of deformation. Thus using direct shear on a single {110} slip plane below 0.5 T_m for LiF (~300°C) should isolate the deformation contribution of dislocation motion alone rather than the motion-plus-intersection mode observed for the ⟨001⟩-oriented compression specimens over the same temperature range.

It is felt that understanding creep in a

model material such as LiF will contribute greatly to the development of the more refractory members of the NaCl structure family, i.e., MgO. A direct verification of this principle may result from comparison of LiF creep results with those obtained on MgO single crystals.

12. PLASTIC BUCKLING AND CREEP OF MgO SINGLE CRYSTALS

Donald R. Cropper and Joseph A. Pask

Studies on conditions likely to result in plastic buckling during compression tests have been continued. Calculations have shown that formulae obtained from continuum mechanics may be used to accurately predict the compressive load at which a single-crystal column becomes unstable. Supplemental experimental work has shown that buckling can be eliminated by proper choice of specimen geometry and/or end constraints. The large degree of scatter previously observed in compression creep tests is substantially reduced when plastic buckling is eliminated.

Creep testing will be performed on a number of MgO single crystals with dimensions chosen to eliminate buckling. These crystals will be deformed in compression at temperatures between 1300°C (slightly above 0.5 T_m) and the maximum temperature of the furnace available, about 1600°C. In this temperature range the resistance to intersection of dislocations moving on orthogonal {110} slip planes should be minimized and diffusion-controlled dislocation climb mechanisms should be controlling.

13. KINETICS OF INTERFACIAL REACTION AND DIFFUSION IN THE SYSTEM IRON-SODIUM DISILICATE GLASS*

Marcus P. Borom† and Joseph A. Pask

The kinetics of the surface-reaction and diffusion processes occurring in the system iron-molten sodium disilicate glass were studied in a neutral atmosphere in the temperature range 900 to 1100°C. A method was established for treatment of the solution of the diffusion equation for the case of surface-reaction-controlled diffusion when there is no prior knowledge of the equilibrium relationships for the system. The temperature dependences of the diffusion and exchange coefficients, together with the temperature dependence of the equilibrium concentration of iron are given.

The diffusion in the glass was found to occur through the interdiffusion of iron and sodium ions in a constant silica matrix. The rate-controlling step in the reaction was determined in terms of the structural changes occurring at the glass/iron interface and arising from the poor wetting nature of the system.

---

* Abstracted from M. P. Borom and J. A. Pask, Phys. Chem. Glasses 8, 5 (1967).
† Present address: Research and Development Center, General Electric Co., Schenectady, New York.

14. ELECTROCHEMICAL AND CONDUCTIVITY STUDIES IN GLASS

Richard N. Schweinberg and Joseph A. Pask

Studies on electrical properties of the system $FeO-Na_2O \cdot 2SiO_2$ in the molten state have been initiated with the original scope including conductivity, polarization, and current-efficiency measurements. The current-efficiency measurements, whereby the electronic and ionic conductivity contributions could be separated using Faraday's law and observed weight changes of the electrodes, have been suspended. It was found that the weight changes produced from the application of a constant dc potential (0.1 to 0.4 V) could not be reliably reproduced using the present experimental setup.

Difficulties were encountered in making stable homogeneous glasses with FeO content from 20% to approximately 42%, the saturation limit. Studies were thus concerned with compositions having less than 20% FeO. An atmosphere of 10/1 CO to CO_2 is used to control the oxidation states of iron in the temperature range 1000 to 1100°C. Conductivity and polarization measurements were performed using parallel-plate electrodes of iron and/or platinum.

15. DISSOLUTION AND DIFFUSION STUDIES IN GLASS

Alton M. Lacy and Joseph A. Pask

Comparative studies of the diffusion rates of iron, cobalt, and nickel ions, dissolving from solid oxides into sodium disilicate glass have been undertaken in order to lay a groundwork for understanding those factors that govern the motion of the ions in glassy silicate solution. Interest is focused both on the properties of the ions themselves, such as charge, size, and ionic polarizability; and on

the variation in the hypothetical glass structure as the oxygen/silicon ratio is altered in the diffusion process. The latter results from dissolution of a network-modifying oxide and the associated diffusion of the component ions to eliminate chemical potential gradients and, at the same time, to maintain electrical neutrality.

Concurrently with the specific work of sample preparation and analysis, a study of the ternary nature of silicate systems has been initiated. Specifically, the work is oriented toward an in-depth understanding of the applicability of binary mathematics to systems that are, in reality, ternary in nature (i.e., two cations and one anion). The applicability of "metallic" diffusion mathematics to ionic solutions is also being studied. The ability to correctly interpret mathematical output in terms of atomistic processes rests squarely on a proper fundamental understanding of the analysis appropriate to the situation at hand.

16. CERAMIC-METAL INTERFACES

John J. Brennan and Joseph A. Pask

Studies on wetting and adherence in the Al-Al_2O_3 system have been continued. Specifically, research was conducted on the effect of the nature of the alumina surface on its wetting by molten aluminum. The pretreatment of the alumina surface affected the wetting characteristics as shown in Fig. IIIB.16-1. If alumina is heated in vacuum to above 1000°C, a complex surface structure is formed.[1] The LEED pattern for this high-temperature surface is retained on lowering the temperature below 1000°C, but some loss of intensity and resolution results on exposure of the alumina surface to the atmosphere. This surface at temperatures above about 1000°C has a higher surface energy and is reactive with aluminum; as a result contact angles decrease below 90-deg in sessile-drop experiments. Hydroxylated alumina surfaces also affect the sessile-drop experiments.

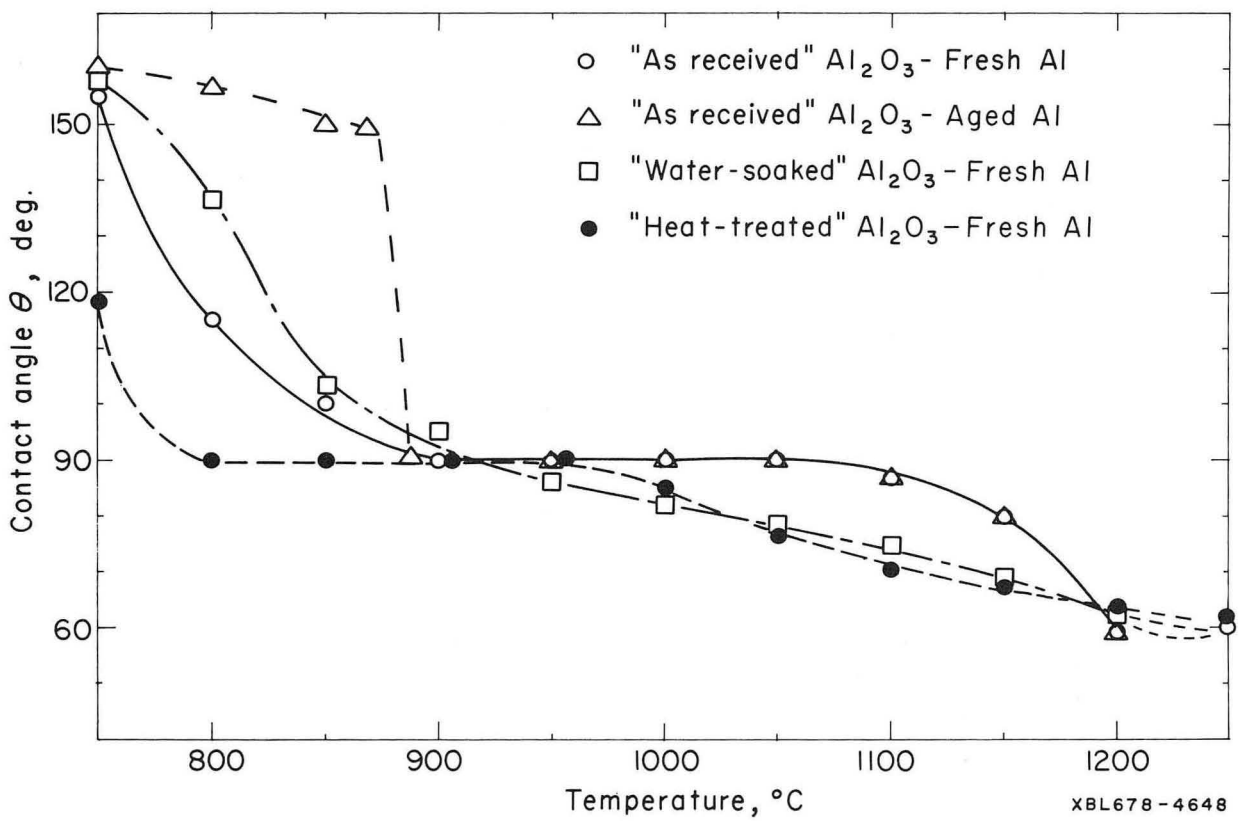

Fig. IIIB.16-1. Change in contact angle with temperature for the system Al-Al_2O_3 with different surface treatments.

Further studies will be made of alumina surfaces and their modification in order to realize wetting of alumina by aluminum at temperatures slightly above the melting point of aluminum.

1. J. M. Charig, Low-Energy Electron Diffraction Observations of α-Alumina, Appl. Phys. Letters 10, 139 (1967); and private communication.

17. RESEARCH PLANS FOR CALENDAR YEAR 1968

Joseph A. Pask

Solid-State Reactions

Studies on the mechanisms and kinetics of diffusion in NiO-MgO and NiO-CaO couples, using single crystals in all cases, are continuing. These couples allow development of interrelationships, since the former system shows complete solid solution and the latter, limited solid solution. The effect of NiO stoichiometry on diffusion characteristics will be determined by an additional series of diffusion anneals in vacuum. Attempts will be made to modify the Boltzmann-Matano solution of the equation for Fick's second law in one dimension to apply to a concentration profile with a discontinuity across the phase boundary.

Studies of the reactions between fused silica and alumina to form mullite ($3Al_2O_3 \cdot 2SiO_2$) are continuing. Diffusion couples of fused silica-Al_2O_3, fused silica-mullite, and fused aluminum silicate-Al_2O_3 are being used to provide kinetic data and information on the steps of the mechanisms in the formation of mullite. This information will then be utilized in an effort to develop a fully dense polycrystalline mullite body.

Development of Microstructures

Studies of the factors that play a role in the development of microstructure, or the distribution of phases, in two-phase systems are continuing. The systems being used are MgO-glass and Mg_2SiO_4-glass. The glasses in both cases are of varying composition in order to achieve a variation in interfacial energies and a variation in reactivity at the interfaces. Relationships between these variations and the nature of the microstructure will be determined.

Mechanical Behavior

Constant-stress-rate (stress-strain) and constant-load (creep) tests will be made on single-crystal specimens of LiF properly shaped for loading in double compressive shear and oriented so that flow is realized only on a single-slip system, thus avoiding complications brought about by intersections with other slip systems. The nature of these complications will be indicated by comparing these results with those obtained by compressive loading of specimens oriented for flow on a conjugate pair of slip systems.

Constant-load tests in compression will also be made on single-crystal specimens of MgO oriented for flow on a conjugate pair of slip systems. The thickness-to-length ratio will be controlled to avoid the occurrence of buckling during creep.

Glass Studies

Studies on the dissolution of network-modifying oxides in a binary oxide glass and the associated diffusion of the component ions to eliminate chemical potential gradients and, at the same time, to maintain electrical neutrality are continuing. Studies of ternary diffusion in a binary oxide silicate system (i.e., two cations and an anion) will also be undertaken to (a) correlate self-diffusion coefficients with the chemical diffusivities observed at elevated temperatures and (b) study the role of oxygen in modifying both the diffusion of cations and the structure of the glass.

Electrical conductivity studies on sodium disilicate glasses containing up to 20 wt.% of FeO in the temperature range of 1000 to 1100°C are continuing. Conductivity and polarization measurements are being performed using parallel-electrodes of iron and/or platinum.

Ceramic-Metal Interfaces

Studies are continuing on the wettability of sapphire by molten aluminum. Relationships will be determined between modifications of alumina surfaces and their wettability by molten aluminum at temperatures slightly above the melting point of aluminum.

18. 1967 PUBLICATIONS

Joseph A. Pask and Associates

Technical Journals

1. R. L. Bell, C. Graeme-Barber, and T. G. Langdon, The Contribution of Grain Boundary Sliding to the Overall Strain of a Polycrystal, Trans. AIME 239, 1821 (1967).
2. R. L. Bell and T. G. Langdon, An Investigation of Grain-Boundary Sliding During Creep, J. Mat. Sci. 2, 313 (1967).
3. M. W. Benecke, N. E. Olson, and J. A. Pask, Effect of LiF on Hot Pressing of MgO, J. Am. Ceram. Soc. 50, 365 (1967).
4. M. P. Borom, J. A. Longwell, and J. A. Pask, Reactions between Metallic Iron and Cobalt Oxide-Bearing Sodium Disilicate Glass, J. Am. Ceram. Soc. 50 (2), 61 (1967).
5. M. P. Borom and J. A. Pask, Kinetics of the Interfacial Reaction and Diffusion Processes in the System Iron-Sodium Disilicate Glass, Phys. Chem. Glasses 8, 194 (1967).
6. T. G. Langdon, Thinning of Polycrystalline MgO for Transmission Electron Microscopy, Rev. Sci. Instr. 38, 125 (1967).
7. J. A. Pask, Editor, An Atomistic Approach to the Nature and Properties of Materials (John Wiley and Sons, Inc., New York, 1967), p. 477.

UCRL Reports

1. S. L. Blank, The Kinetics and Mechanisms of the Diffusion of Iron and Nickel in Single Crystals of Magnesium Oxide (Ph.D. Thesis), UCRL-17411, May 1967.
2. P. E. Hart, The Activated Hot Pressing of Magnesium Oxide, (Ph.D. Thesis), UCRL-17978, December 1967.
3. T. G. Langdon, Grain Boundary Sliding at High Temperatures, UCRL-17442, August 1967.
4. T. G. Langdon, Comment on Void Formation in Nickel and Silver During Creep, UCRL-17821, September 1967.
5. T. G. Langdon, An Assessment of the Use of Dimensional Changes to Determine Grain Strain During Creep, presented at AIME Fall Meeting, Cleveland, Ohio, October 1967, UCRL-17832.

C. DEVELOPMENT AND BEHAVIOR OF MICROSTRUCTURES IN CERAMIC SYSTEMS

Richard M. Fulrath

The principal objective of this research is to understand the relationship between the microstructure of ceramic materials and the physical and mechanical properties. To produce required microstructures, conventional processing of ceramics and unique fabrication techniques are employed.

1. HIGH-TEMPERATURE PHASE EQUILIBRIA IN THE LEAD TITANATE-LEAD ZIRCONATE SYSTEM*

Ronald L. Moon† and Richard M. Fulrath

Lead zirconate titanate is currently the primary crystalline solid used for ceramic piezoelectric transducers. Even though it is so widely used, little is known about the phase relationships existing at high temperatures. Since the solids are formed at temperatures between 1100 to 1300°C by sintering or hot-pressing methods, information of this nature is necessary for understanding the mechanisms involved in forming dense polycrystalline bodies.

The purpose of this study was (1) to investigate whether any high-temperature phases exist in this system and (2) to determine the solidus and liquidus temperatures of the proposed binary system.

Lead zirconate titanate compositions are prepared by calcining a mixture of reagent grade PbO, ZrO_2, and TiO_2. Lead zirconate titanate (PZT) powders which were formed by calcining at 800°C for 200 hr were demonstrated to be inhomogeneous (Fig. IIIC.1-1). The calcined powders showed broad ill-defined X-ray diffractometer peaks in the back-reflection region. Treating the powders at 1200°C for 1-1/2 hr produced well-defined peaks which were the resolved $K\alpha_1$-$K\alpha_2$ doublet.

The region between the Curie and liquidus temperatures was determined to be a solid solution for all compositions. X-ray, differential thermal, and thermal analysis failed to detect any phase transitions.

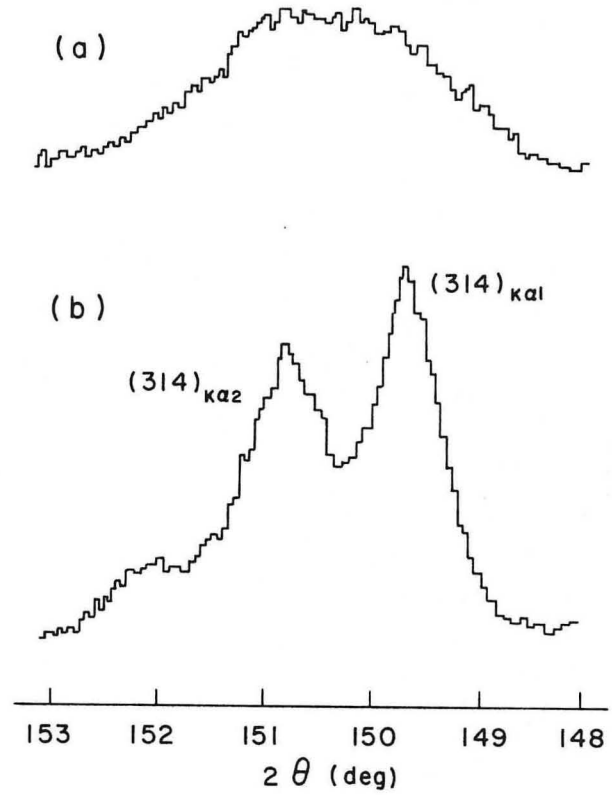

XBL682-1966

Fig. IIIC.1-1. Diffractometer pattern of the (314) peak of $Pb(Zr_{0.20},Ti_{0.80})O_3$ illustrating the inhomogeneity of calcined powders under CuKα radiation. (a) Calcined powder; (b) after the calcined powder has been heated at 1200°C for 1.5 hr.

Additional experiments in the solid-solution region which were conducted in vacuum at 1050 and 1100°C showed the loss of PbO from the surface of a lead zirconate titanate sample to be by incongruent sublimation. The sample's surface was examined by X-ray diffractometry which detected the presence of new phases following a loss of weight in vacuum. The phases that appeared for a given composition

of lead titanate-lead zirconate were compatible with the reaction diagram at 1100°C for the $PbO-TiO_2-ZrO_2$ system.[1,2] In the reaction diagram the line at 50 mole-% PbO represents the $PbTiO_3-PbZrO_3$ binary. If a sample of a given lead zirconate titanate composition becomes deficient in PbO the stable phases which can exist below 50 mole-% PbO are ZrO_2, TiO_2, $ZrTiO_4$, and PZT of a different $PbZrO_3/PbTiO_3$ ratio. The exact phases that appear depend on the $ZrO_2 \cdot TiO_2$ ratio and are in agreement with those predicted by the reaction diagram.

Lead titanate was determined by thermal analysis to melt congruently at 1286±3°C. Similar experiments with $PbZrO_3$ were unsuccessful due to rapid crucible attacks above 1500°C.

The phases present at high temperatures have been determined recently by quenching methods.[3] The quenching method is subject to error and cannot be exclusively used to determine phase diagrams. In a complex oxide system the possibility of nucleating a nonequilibrium phase from the melt on cooling because of lower surface-energy considerations is always present. If nonequilibrium phases preferentially nucleate, the phases detected at room temperature will have little relationship to those at high temperature. The results of quenching analysis then must be substantiated by an independent method such as thermal analysis. Heating-curve analysis can verify whether the phase relationships obtained by quenching methods are indicative of the high-temperature situation since nucleation and growth considerations will not affect the observed phase transitions. Cooling curve analysis can show the general trend of the phase transitions, providing nonequilibrium phases do not nucleate, but will indicate lower transition temperatures because of super-cooling and segregation in the solid; this type of behavior was observed for this system.

The results of the heating analysis showed a peritectic reaction occurring above 1360°C which previous quenching studies identified as solid-solution lead zirconium titanate decomposing to liquid, ZrO_2, and PZT which is rich in $PbZrO_3$ (Fig. IIIC.1-2). The peritectic horizontal extended from 15 mole-% $PbZrO_3$ to 45 mole-% $PbZrO_3$, and showed a simple melting behavior characteristic of a solid solution. The comparison between the phase diagram determined by thermal and quenching analysis is shown in Fig. IIIC.1-3. The lower temperatures obtained by heating analysis, particularly the solidus temperature, are probably due to the greater sensitivity of thermal analysis.

As a result of the decomposition reaction, the $PbZrO_3-PbTiO_3$ phase diagram cannot be considered a pseudobinary, but merely a vertical section in the $PbO-TiO_2-ZrO_2$ ternary system.

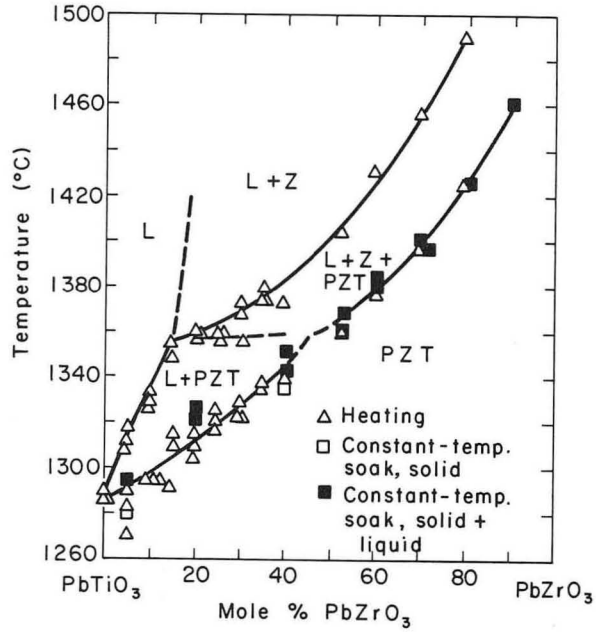

Fig. IIIC.1-2. Phase diagram determined by heating-curve analysis. L = liquid; Z = ZrO_2-rich solid; PZT = lead zirconate titanate.

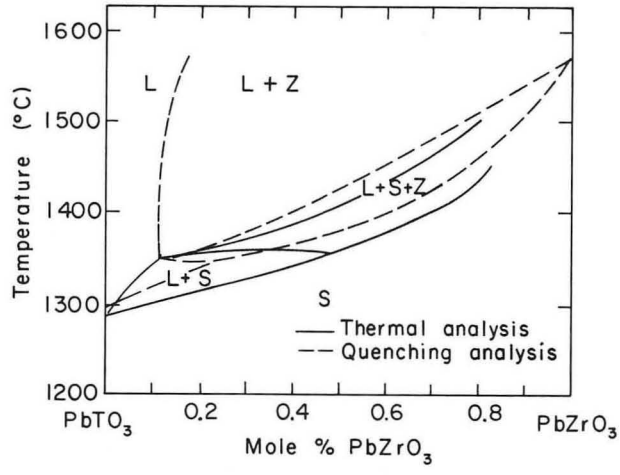

Fig. IIIC.1-3. Comparative phase diagrams based on thermal analysis and quenching. L = liquid, Z = ZrO_2-rich solid; S = lead zirconate titanate.

* Abstracted from R. L. Moon, High Temperature Phase Equilibria in the Lead Titanate - Lead Zirconate System (Ph.D. Thesis), UCRL-17545, May, 1967.

† Present address: Imperial College, London, England.

1. T. Ikeda, T. Okano, and M. Watanabe, A Ternary System $PbO-TiO_2$, Japan J. Appl. Phys. 1, 218 (1962).
2. A. H. Webster, R. C. MacDonald, and W. S. Boroman, The System $PbO-ZrO_2-TiO_2$ at 1100°C, J. Can. Ceram. Soc. 34, 97 (1965).
3. S. Fushimi and T. Ikeda, Phase Equilibrium in the System $PbO-TiO_2-ZrO_2$, J. Am. Ceram. Soc. 50, 129 (1967).

2. DIFFERENTIAL THERMAL CALORIMETRY*

Patrick S. Nicholson† and Richard M. Fulrath

Following a heat-transfer investigation, the differential thermal calorimeter, designed by Barner[1] was modified. The new design facilitated the accurate control of temperature gradients within the system. This control, it was postulated, would greatly improve the accuracy of the instrument. The design of the

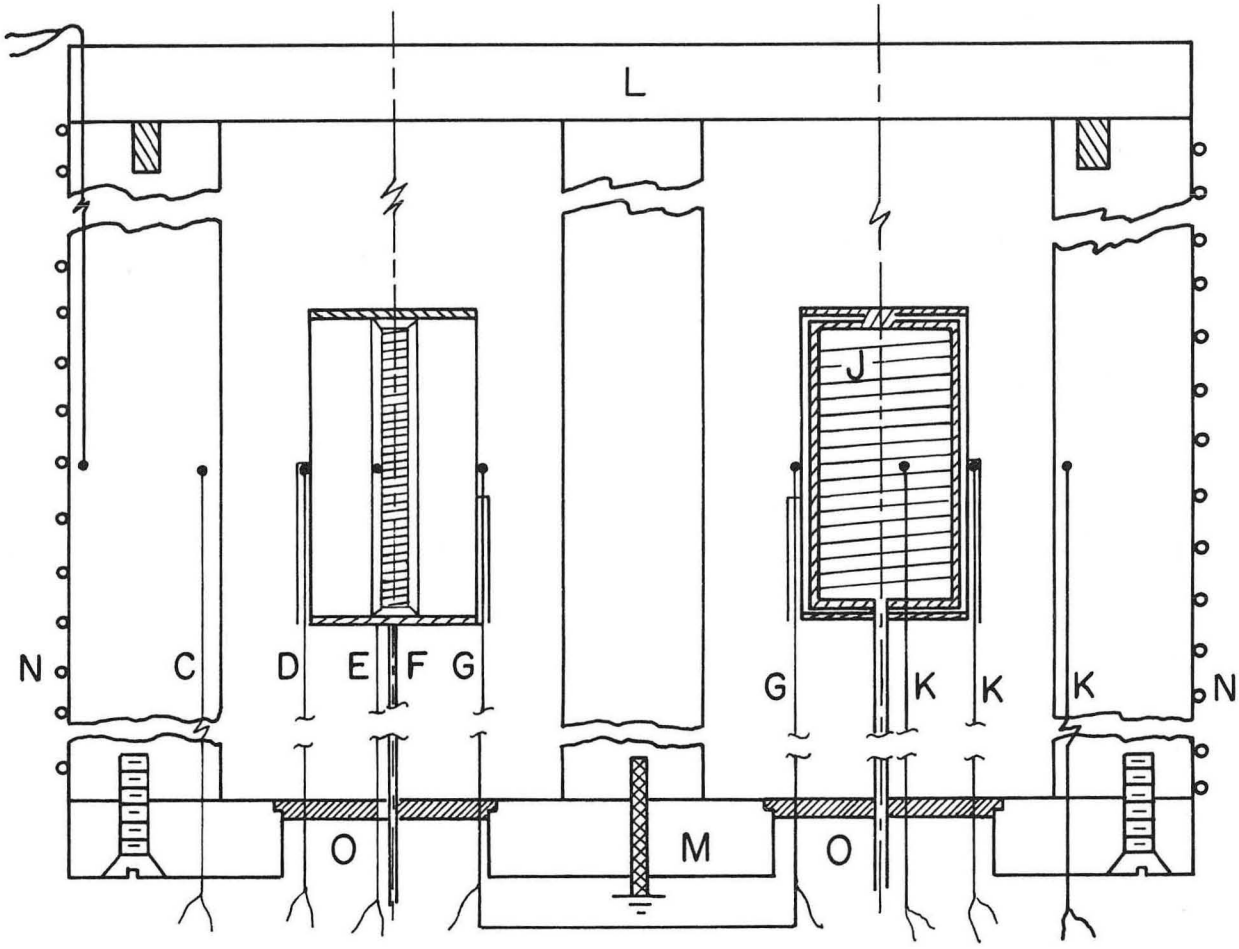

XBL682-1964

Fig. IIIC.2-1. Differential calorimeter design. A. Sample in sample cell; B. zirconia powder around each cell; C. chromel-alumel (C-A) thermocouple for measuring the nickel block temperature; D. C-A thermocouple differentially linked with C for comparing the temperature of the outer wall of the sample cell with that of the nickel block; E. C-A thermocouple linked differentially with C for comparing the temperatures of the sample-cell heater wall and that of the nickel block; F. sample cell heater leads; G. platinum-platinum/10% rhodium differential thermocouple used to control the power input to the control cell J; H. C-A thermocouple controlling the main furnace N; J. boron nitride control-cell heater; K. temperature-gradient thermocouples for the control cell; L. nickel top; M. nickel bottom; N. main-furnace winding; and O. boron nitride inserts.

modified differential thermal calorimeter shown in Fig. IIIC.2-1.

A large block of nickel has two parallel holes drilled through it. In the center of each hole is placed one of the calorimeter cells. The intervening space between the cell and the periphery of the cavity in which it sits is filled with zirconia powder. Utilization of a large nickel block guarantees that each cell is in an identical isothermal environment. A small Kanthal heater is located in the center of each cell. These heaters are wound on boron nitride formers and the cell end-caps are also boron nitride. The design of the two-cell heaters is not the same; however they both have the same electrical resistance. The cells were also designed to have identical heat capacities. Cell A contains the sample, and the other cell is left empty. The power to the sample cell is maintained constant at all times. The control of empty-cell power is variable. The temperatures of the outer walls of the two cells are maintained equal by varying the power input to the control cell. The input power to both cells is measured by wattmeters, and their output recorded on a two-pen recorder. Hence any reaction taking place in the sample is directly measured, and a power/time trace obtained. The area of the resulting peak gives a measure of the heat of the reaction taking place in the sample. By leaving the control cell empty, the change in the heat content of the sample can also be estimated. Thermocouples C, D, E, and G enter through the base of the nickel block via boron nitride inserts. C, D, and E are linked differentially in such a way that E records the

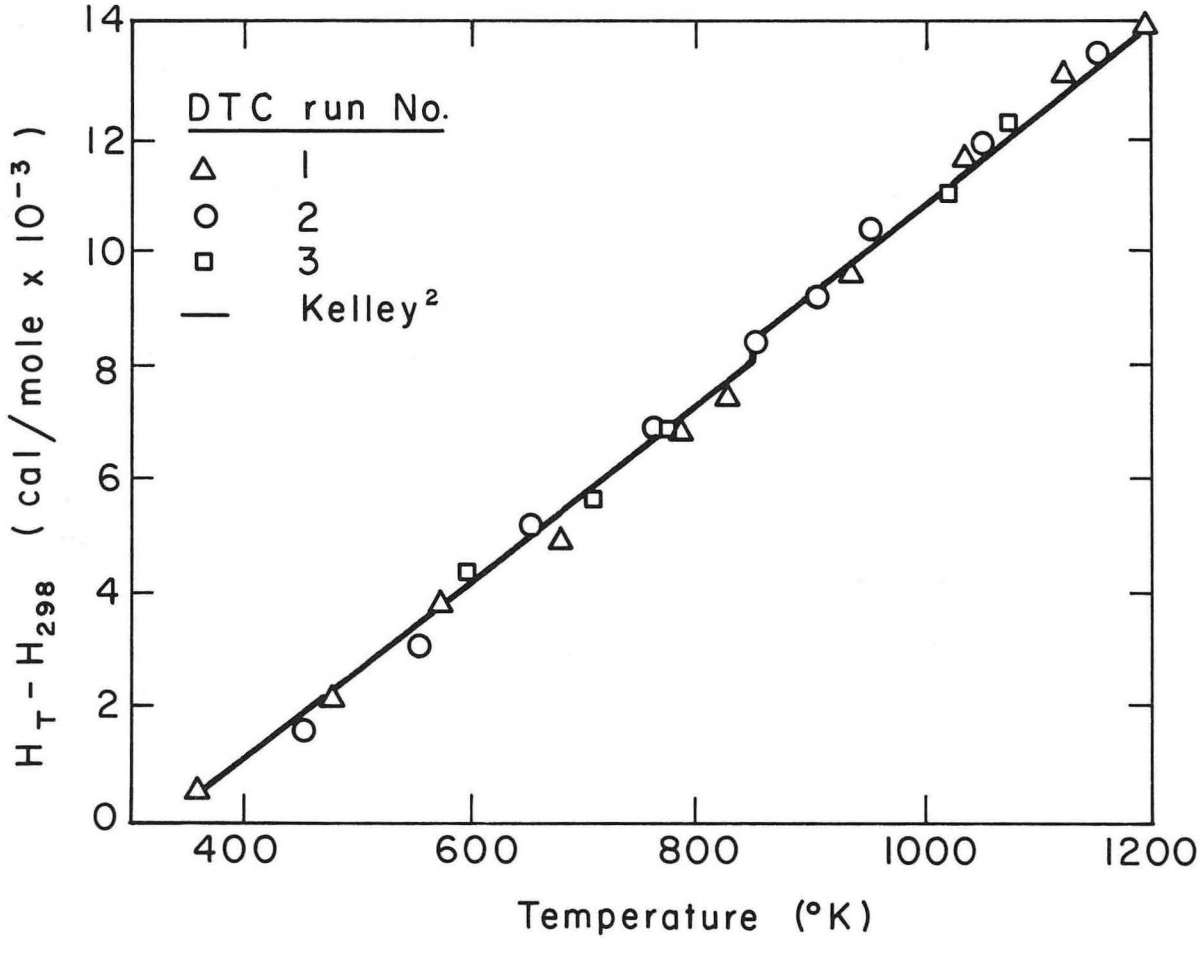

XBL682-1963

Fig. IIIC.2-2. Total heat content of SiO_2 vs temperature.

actual temperature and C and D the differential gradients from this temperature. G is the differential couple whose signal controls the power input to the control cell. This differential signal is maintained at zero at all times. Thermocouple H monitors the block temperature and controls the power input to the furnace winding. This winding is located on the outer circumference of the nickel block. Boron nitride is used at various points in the DTC complex to ensure low electrical leakage and low thermal conductivity at high temperatures. The intervening ZrO_2 powder acts as both a heat sink and a heat insulator. It is this powder that facilitates the control of the heat flow in the system. Heat must flow out of the cells at all times, and a powder insulation ensures that this condition can be met by decreasing convection and radiative heat transfer. Thermocouples C, D, and E monitor this condition continuously. The useful range of the instrument is from room temperature to 1100°C.

The differential thermal calorimeter just described was calibrated by measuring the heat content of SiO_2 (quartz) and α-alumina up to 1100°C. The SiO_2 results were compared with those of Kelley[2] and the α-Al_2O_3 results with those of Furukawa et al.[3] The comparisons are shown in Figs. IIIC.2-2 and IIIC.2-3. In these figures the solid line represents the accepted literature values[2,3] and the points the DTC data. An accuracy of ±2% was observed. The accuracy of Barner's design was ±25%.

After the accuracy of the modified design was demonstrated, the thermodynamic properties of kaolinite were measured. The 550°C endothermic enthalpy was measured as 40 kcal/mole, and this figure agrees well with accepted literature values. The 980°C exothermic enthalpy was found to be 9 kcal/mole. This figure throws new light on the mechanism of this reaction. It is postulated that most of the heat release observed at this temperature accompanies the crystallization,

$$SiO_2(\text{amorphous}) \rightarrow SiO_2(\beta\text{-quartz}).$$

This explanation correlates many previously unexplained observations reported in the literature.

* Abstracted from P. S. Nicholson, Differential Thermal Calorimetric Determination of the Thermodynamic Properties of Kaolinite (Ph.D. Thesis) UCRL-17820, September 1967.

† Present address: Department of Ceramics, University of Utah, Salt Lake City, Utah.

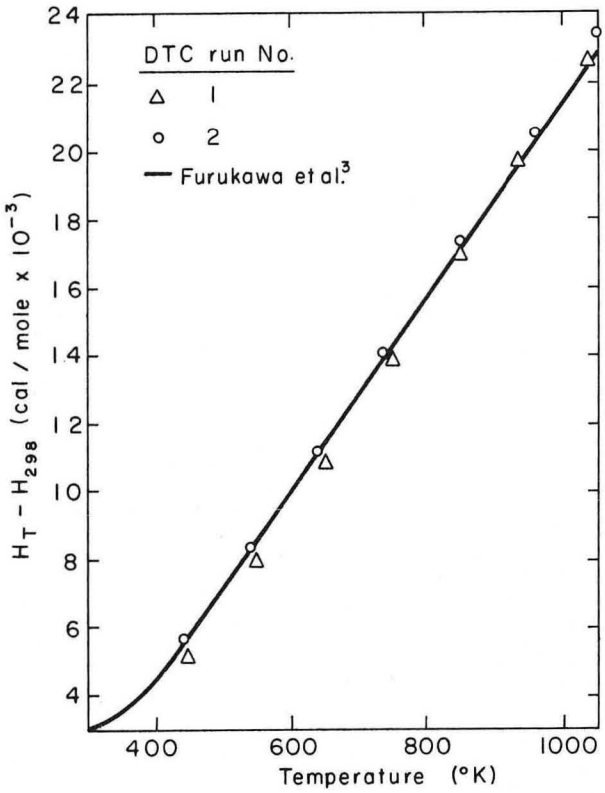

XBL682-1961

Fig. IIIC.2-3. Total heat content of Al_2O_3 vs temperature.

1. J. O. Barner, Design of a Differential Calorimeter Suitable for Measurement at High Temperature Heats of Solid-State Reactions, UCRL-10631, January 1963.
2. K. K. Kelley, Contribution to the Data on Theoretical Metallurgy, U. S. Bureau of Mines Bulletin 601, U. S. Government Printing Office, Washington, D.C., 1962.
3. G. T. Furukawa, T. B. Douglas, R. E. McCoskey, and D. C. Ginnings, Thermal Properties of Aluminum Oxide from 0° to 1200°K, Nat. Bur. Std. Res. Paper 2694, 57, 67 (1956).

3. RADIOFREQUENCY PLASMA MICROSPHEROIDIZATION OF CERAMICS*

Randolph T. Tremper† and Richard M. Fulrath

Several studies have been made on the use of the rf induction-coupled plasma jet for the spheroidization of ceramic particles in the 30-150 micron range. The most notable of these

works is that by Hedger and Hall.[1] The most significant problem associated with rf plasma spheroidization has been found to be the injection of the particles into the plasma flame. A thorough literature search has shown that little or no work has been done in this area.

It was desirable to be able to force the powder through the high-temperature center of the plasma. Therefore, it was necessary to be able to produce a highly directed flow of particles with a high enough velocity to drive them through the center of the turbulent plasma. Thus, an injection nozzle had to be designed which would give laminar flow of the particles over a wide range of velocities. The laminar flow requirement is necessary to assure that no spraying of particles occurs at the orifice.

The injection nozzle supplied with the plasma generator contained both of the two major factors which can produce turbulence in a flowstream; abrupt cross-sectional area changes and a very small orifice. The flow patterns produced at two velocities are shown in Fig. IIIC.3-1, which demonstrates the spraying effect caused by turbulent flow.

After several intermediate nozzles had been designed, built, and tested, a final design was decided upon; this is shown in Fig. IIIC.3-2. Here, all abrupt cross-sectional area changes have been eliminated, and an intermediate inside diameter has been chosen to be a compromise between excessive friction and excessive gas flow. The resulting flow patterns are shown in Fig. IIIC.3-3, where it can be seen that a highly directed laminar flow is produced with no spraying effect at the orifice.

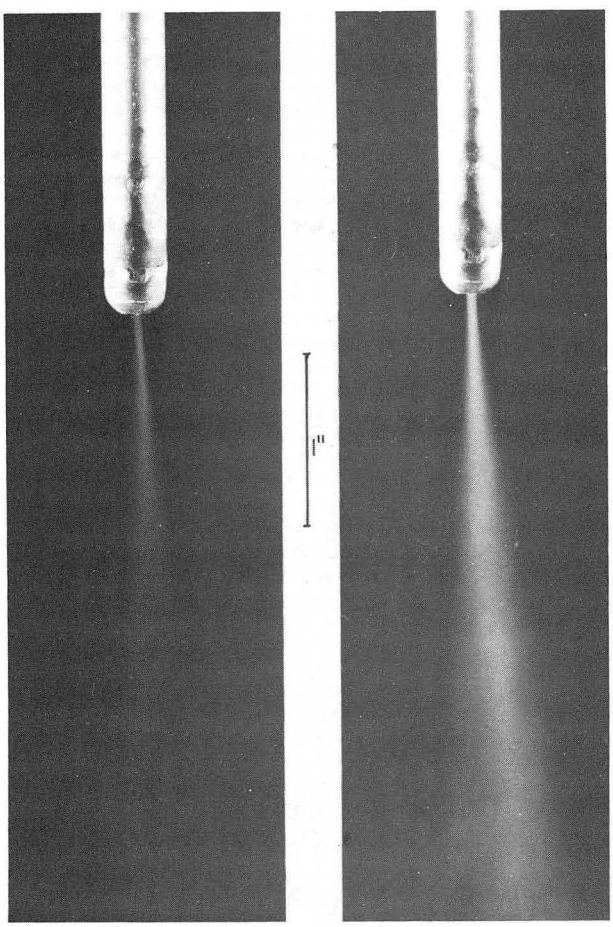

XBB 6712-6671-A

Fig. IIIC.3-1. Flow patterns of factory supplied nozzles: (a) 30 ft/sec, (b) 70 ft/sec. Patterns made with CO_2-water vapor mixture.

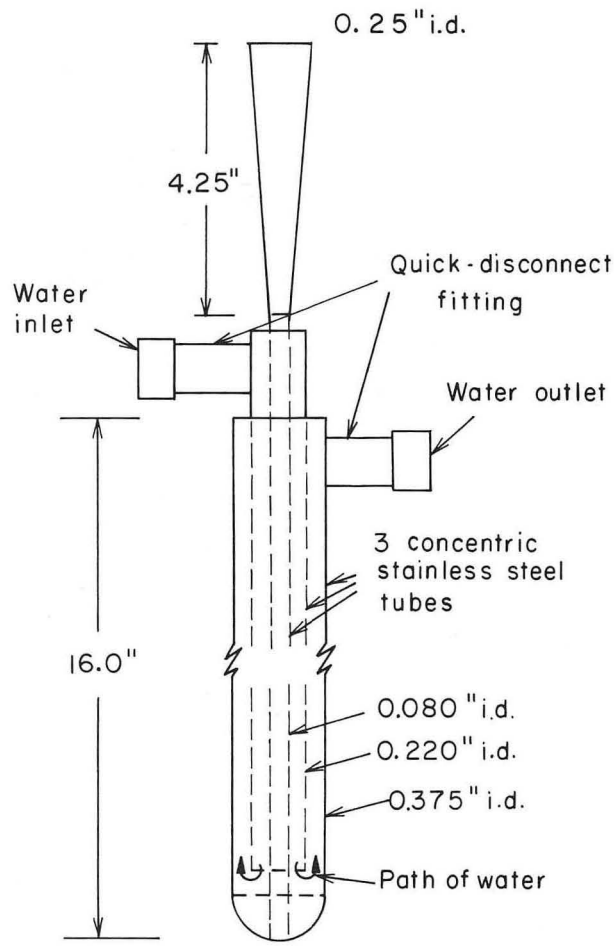

XBL682-1962

Fig. IIIC.3-2. Fourth and final nozzle design.

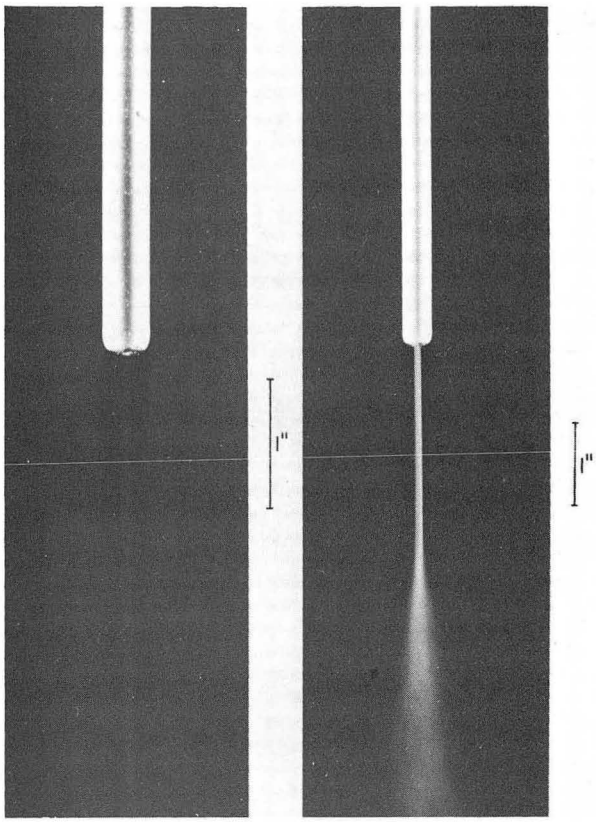

XBB 6712-6672-A

Fig. IIIC.3-3. Flow patterns of final nozzle: (a) 30 ft/sec, (b) 80 ft/sec.

By means of this nozzle, SiO_2, NiO, and Al_2O_3 in the 30 to 70-μ range were spheroidized successfully. The Al_2O_3 spheres, which were produced from powders of the alpha phase had been converted largely to the metastable gamma and delta phases, as also reported by Das[2] in work with a dc plasma jet.

---

* Abstracted from R. T. Tremper, R-F Plasma Microspheroidization of Ceramics, UCRL-17896, December 1967.

† Present address: University of Utah, Salt Lake City, Utah.

1. H. J. Hedger and A. R. Hall, Preliminary Observations on the Use of the Induction-Coupled Plasma Torch for the Preparation of Spherical Powder, Powder Met. 8, 65 (1961).
2. A. S. Das and R. M. Fulrath, Liquid Solid Transformation Kinetics in Al_2O_3, in Reactivity of Solids (Elsevier, Amsterdam, 1965), pp. 31-44.

4. EFFECT OF PRESSURE ON HIGH-TEMPERATURE DISSOLUTION*

Mark A. Stett and Richard Fulrath

Physical properties such as compressive strength of ceramic shapes of clay and zirconia have been enhanced by the application of pressure during a chemical reaction leading to high-density bodies. Chemical reactions can occur at lower temperatures under an applied pressure. The process of dissolution can also be affected by an applied pressure. The dissolution process consists of two steps, the entry of atoms of solute into the solvent and a subsequent diffusion of these atoms through the solvent. Either of these steps can be rate-controlling. The self-diffusion coefficient of lead has been shown to decrease with increased pressure. The other step, the entry, is shown to be inhibited by an applied hydrostatic pressure in a specific model system.

Composites of sodium disilicate glass and oxidized nickel microspheres were hot-pressed at zero, 250, and 1000 psi and examined in an electron-beam microprobe. Photographs were taken of the oscilloscope image of nickel around a sphere in each case. The background concentration of nickel can be seen around an untreated oxidized sphere in Fig. IIIC.4-1. This concentration was measured with a counter and found to be 0.2 wt.%, and a correction was made for this in each of the following values. Figure IIIC.4-2 shows the nickel concentration around an oxidized nickel sphere in a composite that was treated at 900°C and zero pressure. Measured concentrations were 5.1, 4.7, 5.0, and 4.7 wt.%. The nickel concentrations around spheres in composites formed at 900°C for 2 hr in vacuum and at 250 and 1000 psi can be seen in Fig. IIIC.4-3 and IIIC.4-4 respectively. Measured concentrations were 2.6 wt.% for the 250-psi sample and 0.4 wt.% for the 1000-psi sample.

The saturation concentration of a solute in a solvent is an accurate measure of the concentration of the liquidus in a binary system at a given temperature. With a relatively long length of time at temperature, the saturation concentration will be reached and will be, in effect, the measured concentration in the solvent. A plot of these compositions as a function of pressure would therefore yield the liquidus as a function of pressure at a given temperature. This function is shown in the plot of the nonequilibrium liquidus in Fig. IIIC.4-5. One can see that it is the correct shape as would be predicted from free-energy concentrations.

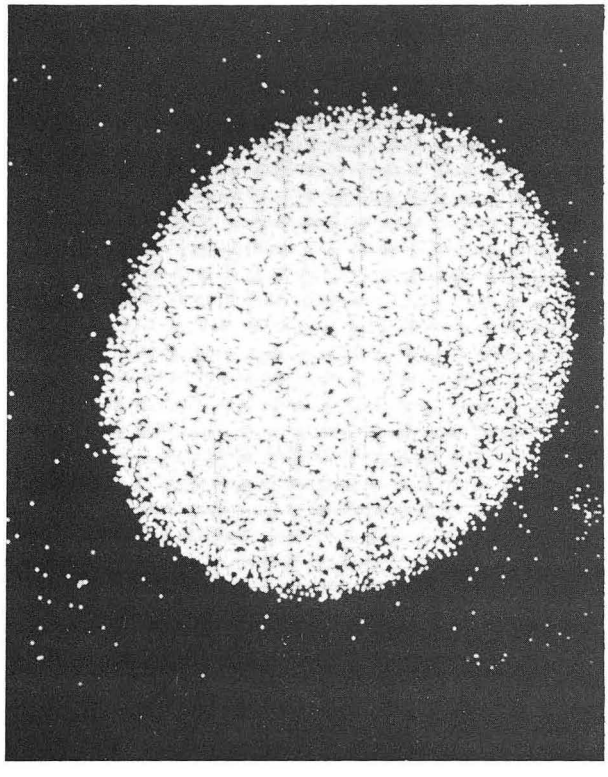

XBB 672-712

Fig. IIIC.4-1. Oscilloscope photograph showing background Ni concentration about an untreated sphere.

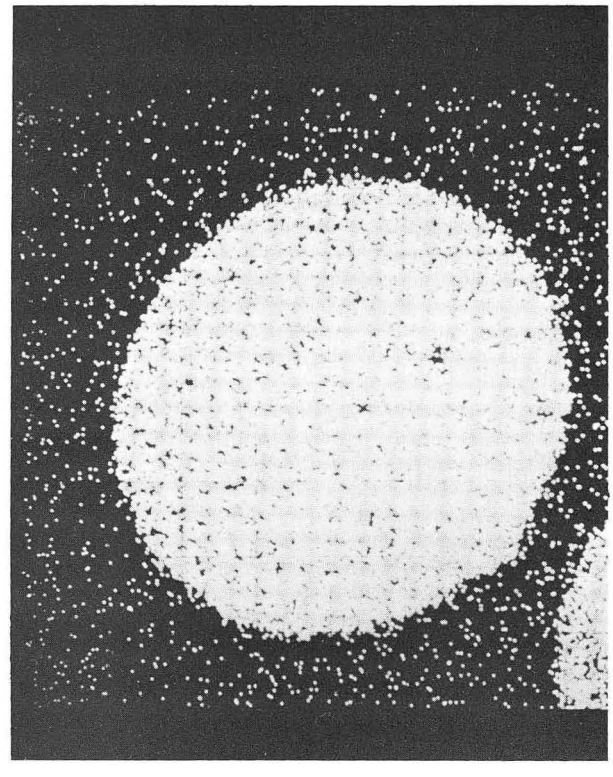

XBB 672-711

Fig. IIIC.4-2. Oscilloscope photograph showing Ni concentration about a sphere in a composite formed at 900°C and zero psi for 2 hr.

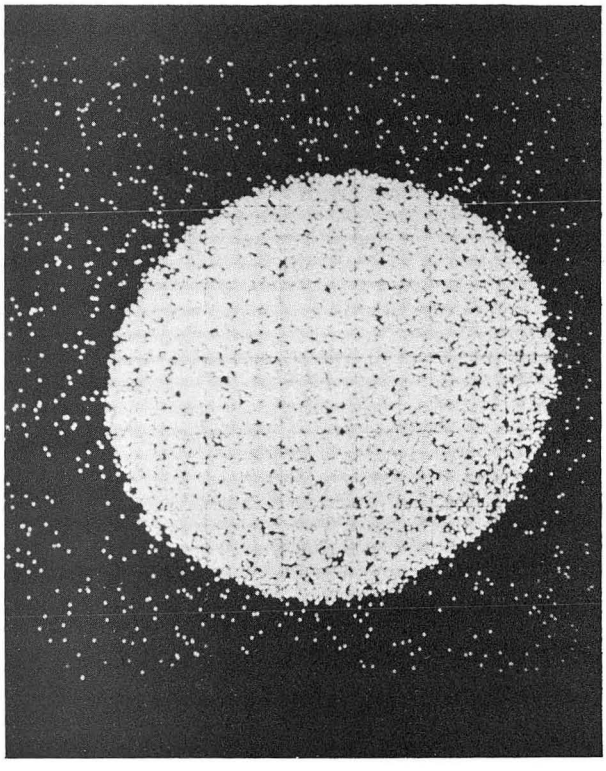

XBB 672-709

Fig. IIIC.4-3. Oscilloscope photograph showing Ni concentration about a sphere in a composite formed at 900°C and 250 psi for 2 hr.

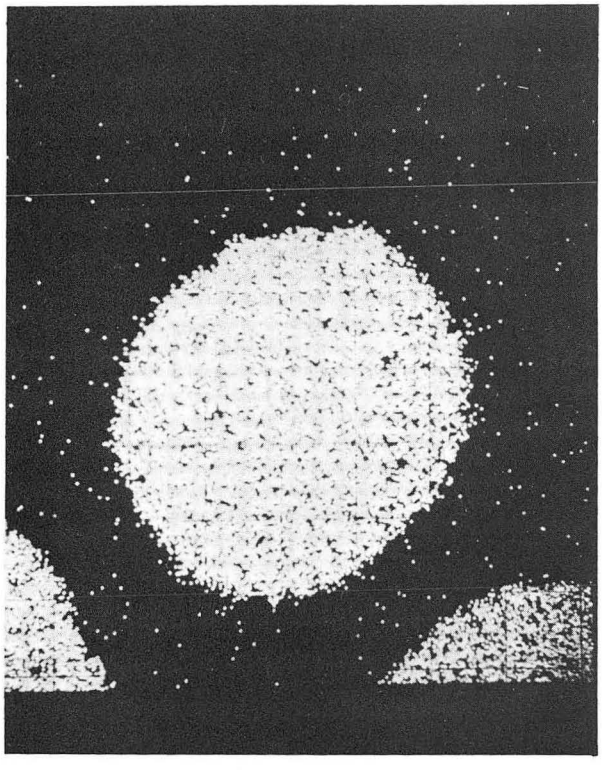

XBB 672-710

Fig. IIIC.4-4. Oscilloscope photograph showing Ni concentration about a sphere in a composite formed at 900°C and 1000 psi for 2 hr.

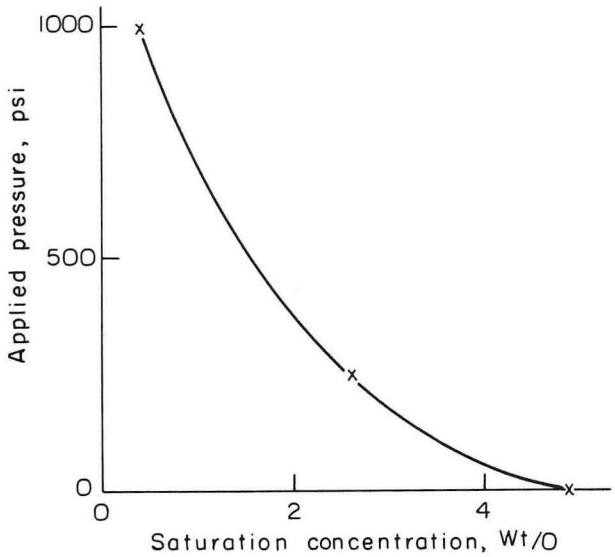

XBL676-4090

Fig. IIIC.4-5. Effect of pressure on saturation concentration.

In all cases the concentration was constant deep in the matrix, indicating that the entry step was affected by the pressure. Had the diffusion step only been affected by the pressure, there would have been a concentration gradient in the matrix.

* Abstracted from M. A. Stett and R. M. Fulrath, Effect of Pressure on High-Temperature Dissolution, UCRL-17410, February 1967.

5. RESEARCH PLANS FOR CALENDAR YEAR 1968

Richard M. Fulrath

Composite Materials with Ceramic Matrices

Fracture in dispersion-strengthened glass has been shown to be related to the mean free path in the glass matrix. When nondeformable crystalline particles of a single particle size are used for the dispersed phase, fabrication limitations are encountered as to the maximum volume fraction of dispersed phase obtainable. Therefore, testing of the fracture theory is limited. With two sizes of microspheres of a nondeformable crystalline material, improved packing characteristics allow increased volume fractions of a dispersed phase to be incorporated into a glass matrix by vacuum hot-pressing. The subsequent reduction of the mean free path should provide a suitable model for extending the experimental conformation of the proposed fracture theory. Work has been initiated in this area and will continue during the coming year.

Previous studies have indicated that interfacial relations between the dispersed phase and the matrix have a marked affect on the fracture propagation path. Work on developing this relationship further has been initiated and will be pursued.

Ferroelectric Ceramics

The lead zirconate titanate system, one of major polycrystalline piezoelectric transducer materials, is still under study. During 1967 it was established that no secondary phases or minimum melting occurred in the high-temperature phase-equilibrium diagram which could aid sintering.

The first area of PZT research seeks to correlate the final microstructure of a sintered sample with the processing variables involved. Small changes in the presintering treatment of the material have been shown to cause a substantial variation in the final density as a function of increased impurity content and decreased particle size from ball milling has been studied. Separating these two variables will be the primary area of study. A smaller increase in density was noted with change in firing atmosphere with higher densities resulting from a greater percent of oxygen in the atmosphere. Further work is planned in establishing the sintering mechanism of PZT so that sintering may be optimized with respect to all the variables concerned.

The second area of investigation has been in the utilization of hot-pressing techniques in the fabrication of 99+% theoretically dense PZT samples. Experimentation into the optimal temperature, pressure, atmosphere, and die material has been undertaken. Initial investigation shows that PZT is very reactive with many, normally used die materials. This has led to the adoption of platinum as a container material during the pressing operation. Lead zirconium titanate also appears to be very sensitive to the ambient atmosphere. Experimentation into the effect of an atmosphere of argon, and of oxygen, as well as vacuum has been studied. Reduction of lead is of prime importance and as such has eliminated the use

of graphite as a die material. Work thus far shows that a high-density undoped sample of PZT can be obtained. These samples should show varied electrical properties as compared with previously reported data because the effect of porosity has been reduced to a minimum.

Subsequent investigation will be carried out as to the effect of known additives on the sintering characteristics and electrical properties of PZT as compared with the now producable high-density undoped material. Recent published reports have indicated that additives of bismuth aid densification through the addition of vacancies to the lattice. The effects of Bi and Al as well as their combined effects on both densification mechanisms and electrical properties are presently being investigated. The role these two ions play should prove an aid in the production of commercially usable lead zirconium titanate products.

The increasing interest in devitrified glass ferroelectric materials has prompted questions about the relation of microstructure to macroscopic properties. In order to evaluate the relative importance of the many variables, e.g. the dielectric and mechanical properties of the matrix and the dispersed crystalline phase, model systems will be constructed that allow independent variation of each parameter. The derived relations should aid in optimizing the nature of interactions in two phase systems.

Gas Permeation through Ceramics

Previous work on helium permeation in polycrystalline ceramic bodies has indicated that helium diffuses through the grain boundaires. This observation led to initiation of studies on helium permeation in simple glasses to determine permeation mechanisms. Fused quartz was chosen because it is the most elementary inorganic glass system. Although considerable work has been done on helium permeation in fused quartz, very little account has been taken of the effect of the presence of "water" as OH in the SiO_2 structure. The water which is introduced in the fabrication process of fused quartz may be present up to 6000 ppm.

Data have been obtained for the permeation of helium in fused quartz on samples directly from fabrication. These data compare fairly well with the literature except for small deviations at low temperatures. The explanation of these deviations is currently under investigation.

Plans for the current year include building a suitable system for saturating the glass samples with water vapor. After this is completed specimens will be tested as received, desaturated, and saturated. The data received from these tests should indicate the effect of OH on the permeation of helium in the SiO_2 network. The same experimental procedure will be repeated using diatomic molecules such as hydrogen. The data generated in this part of the program will be used in the second or theoretical phase.

The theoretical phase of this work will involve the extension of Studt's theoretical prediction of solubility-coefficient temperature dependence[1] (derived using statistical thermodynamics). Two approaches are contemplated:

(a) Apply current equations for helium solution to different solubility-site geometries expected for various "water" contents.

(b) Derive equations for H_2 solution (considering both "water" and network-modifier content) for both physical and chemical solubility.

In addition, a comprehensive review of the literature in the field will allow a summary of the current model of gas-permeation mechanisms in glass. This information may suggest additional experimental work, e.g., the use of Sieverts' method[2] to obtain more accurate solubility data than obtainable from dynamic permeation experiments.

Differential Thermal Calorimetry

The differential calorimeter can be used to give thermodynamic data obtainable only with much more effort by other means. It involves measuring the amount of power needed to heat a weighed sample over that needed to heat an empty sample holder in the same environment. Although some good results have been achieved with present equipment, there are some problems that have placed limitations on its use. Further work is planned to overcome some of the problems in heat flow in the system. The major work for the next year then is the redesign of the equipment to remove some of the limitations and facilitate its use.

1. P. L. Studt, Mechanism of Gaseous Permeation through Glass, Single-Crystal Silicon, and Germanium; and Stress-Enhanced Gaseous Permeation through Alumina Bodies, (Ph.D. Thesis), UCRL-10466, September 1962.
2. A. Sieverts and G. Zapf, Iron and Nitrogen, Z. Physik. Chem. (Leipzig) A172, 314 (1935).

6. 1967 PUBLICATIONS

Richard M. Fulrath and Associates

Technical Journals

1. R. L. Bertolotti and R. M. Fulrath, Effect of Micromechanical Stress Concentrations on Strength of Porous Glass, J. Am. Ceram. Soc. 50, 11 (1967).
2. D.P.H. Hasselman and R.M. Fulrath, Micromechanical Stress Concentrations in Two-Phase Brittle-Matrix Ceramic Composites, J. Am. Ceram. Soc. 50, 8 (1967).
3. M. A. Stett and R. M. Fulrath, Chemical Reactions in a Hot-Pressed Al_2O_3 Glass Composite, J. Am. Ceram. Soc. 50, 12 (1967).

UCRL Reports

1. R. L. Bertolotti and R. M. Fulrath, Micromechanical Stress Concentration Effects on Strength of Porous Brittle Ceramics, UCRL-17082-Rev., April 1967.
2. D. P. H. Hasselman and R. M. Fulrath, Mechanical Properties of Continuous-Matrix, Dispersed-Phase Ceramic Systems, chapter in book "Ceramic Microstructures," (J. Wiley and Sons, New York, in press).
3. R. L. Moon, High-Temperature Phase Equilibria in the Lead Titanate - Lead Zirconate System (Ph.D. Thesis), UCRL-17545, May 1967.
4. P. S. Nicholson, Differential Thermal Calorimetric Determination of the Thermodynamic Properties of Kaolinite (Ph.D. Thesis), UCRL-17820, September 1967.
5. M. A. Stett and R. M. Fulrath, Effect of Pressure on High-Temperature Dissolution, UCRL-17410, February 1967.
6. M. A. Stett and R. M. Fulrath, Chemical Reaction in a Hot-Pressed Al_2O_3 Glass Composite, UCRL-16892-Rev. II, April 1967.
7. M. A. Stett and R. M. Fulrath, Dissolution of Al_2O_3 in $Na_2O \cdot 2SiO_2$ Glass, UCRL-17516, April 1967.
8. R. T. Tremper, R-F Plasma Microspheroidization of Ceramics (M.S. Thesis), UCRL-17896, December 1967.

Solid-State Physics

IV. SOLID-STATE PHYSICS

A. THEORETICAL SOLID-STATE PHYSICS

1. ELECTRONIC STRUCTURE OF SOLIDS

Marvin L. Cohen

We have analyzed the optical structure of semiconductors and insulators using the Empirical Pseudopotential Method[1] (EPM). This method yields accurate electronic band structures and also allows calculation of various optical constants such as the frequency-dependent dielectric constant.

The EPM is very flexible. It can be applied to many different types of materials. For example, the method has been used successfully for narrow-gap semiconductors such as SnTe and for wide-gap insulators like MgO. In both of the above examples, the optical constants were computed; for example, for MgO the energy range considered was 7 to 28 eV. We have recently completed similar calculations for NaCl.

This work will be continued and extended to include analysis of other crystals.

1. M. L. Cohen and T. K. Bergstresser, Phys. Rev. 141, 789 (1966).

2. SUPERCONDUCTIVITY IN DEGENERATE SEMICONDUCTORS

Marvin L. Cohen

A low-temperature refrigerator is being built by Dr. T. Thorp, who is a postdoctoral research associate with our group. This refrigerator will be capable of achieving very low temperatures so that studies can be made of the superconducting properties of degenerate semiconductors and semimetals.[1]

1. M. L. Cohen, Phys. Rev. 134, A511 (1964).

3. RESEARCH PLANS FOR CALENDAR YEAR 1968

Marvin L. Cohen

We plan to extend our work using the Empirical Pseudopotential Method to other crystals. Also some properties of superconducting semiconductors will be examined at low temperatures.

4. 1967 PUBLICATIONS

Marvin L. Cohen and Associates

1. M. L. Cohen and P. J. Lin, Ultraviolet Optical Properties and Electronic Band Structure of Magnesium Oxide, Phys. Rev. 155, 992-996 (1967).
2. M. L. Cohen, P. J. Lin, and W. Saslow, Analysis of the Optical Properties and Electronic Structure of SnTe Using the Empirical Pseudopotential Method, Solid State Commun. 5, 893 (1967).
3. M. L. Cohen, C. Y. Fong, and W. Saslow, Pseudopotential Calculation of the Optical Constants of MgO from 7-28 eV, Phys. Rev. to be published.
4. Y. R. Shen, M. Y. Au Yang, and M. Cohen, Theory of Self-Trapped Filaments of Light, Phys. Rev. Letters 19, 1171 (1967).

B. MAGNETIC PROPERTIES OF SOLIDS

Alan M. Portis

1. ANTIFERROMAGNETIC RELAXATION

A very careful study of magnetic resonance in $CsMnF_3$ in the vicinity of its ordering temperature has been completed. In contrast to antiferromagnets like $KMnF_3$, which are cubic and show little line broadening, $CsMnF_3$, which is hexagonal, shows a sharp increase in linewidth near the transition. The theoretical situation is complex and possibly contradictory, but it is hoped that the experimental results will serve as a guide to which kinds of approximations are reasonable.

2. MAGNETIC AND ELECTRICAL PROPERTIES OF MnAu

The temperature dependence of the electrical resistivity of single-crystal MnAu has been successfully interpreted as originating from spin disorder scattering. A one-band model appears to be adequate for the conduction electrons. The d electrons are treated as localized with an assumed correlation.

3. SPIN WAVE PROPAGATION

A great deal of effort has been expended to obtain high-quality nickel films which could then be used in a study of the temperature dependence of the spin wave spectrum over a large temperature range. We have succeeded in preparing better films than have been obtained elsewhere and temperature studies are now in progress.

4. NUCLEAR RESONANCE IN FERROMAGNETIC ALLOYS

Dilute alloys of copper in nickel have been prepared and studies have been made of nuclear relaxation. It is found that the copper nuclear relaxation is unusually slow, in support of models which assume little or no magnetic moment at the copper site.

5. NUCLEAR DOUBLE RESONANCE IN FERROMAGNETIC ALLOYS

Attempts to observe nuclear double resonance have been impeded by an unexpected but interesting effect. High-amplitude radio-frequency fields are evidently capable of producing discontinuous but coherent wall displacements. We have observed nuclear absorption at 200 MHz derived by a 1-MHz applied field. Thus, we are observing the 200'th harmonic in nuclear resonance. Now that this effect is fully understood, we expect that we can control it in such a way that it does not interfere with our double-resonance studies.

6. RESEARCH PLANS FOR CALENDAR YEAR 1968

Alan M. Portis

Spin Wave Propagation

With the availability of high-quality nickel films, we plan to do a careful study of the temperature dependence of the spin wave spectrum. We hope that our results can be correlated with neutron-diffraction studies which are being planned at Brookhaven. In addition we hope to be able to prepare and study alloy films such as Ni:Cu and Ni:Rh.

Nuclear Resonance in Ferromagnetic Alloys

We hope to study other nickel-base alloys and possibly extend the work to cobalt- and iron-base alloys. We believe that the relaxation studies are a more sensitive indication of the local hole density in the d band than is either the magnetization or the observed hyperfine field. We expect that with further studies the systematics of the local magnetization will become apparent.

Nuclear Double Resonance in Ferromagnetic Alloys

We are optimistic that the double-resonance

technique will make possible very high resolution spectra, permitting a much more exact test of theory than has been possible up to now.

Nearly Ferromagnetic Metals

We hope to investigate electron resonance in intermetallic systems that are nearly ferromagnetic. This area is of considerable theoretical interest as it is felt that the origin of ferromagnetic ordering in metals may be best understood from this point of view. As yet there have been few microscopic studies of such systems. Electron resonance would be an extremely useful addition.

7. 1967 PUBLICATIONS

Alan M. Portis and Associates

Technical Journals

1. A. M. Portis, Physics of Metals, in VIIIth Latin American School of Physics, Caracas, Venezuela, July 1966, M. Bemporad, editor, (Gordon and Breach, Inc., New York, in press).
2. M. B. Salamon, Magnetic Relaxation in Nickel Above the Curie Temperature, Phys. Rev. 155, 224 (1967).
3. L. B. Welsh, Properties of the Mn^{55} Nuclear Magnetic Resonance Modes in $CsMnF_3$, Phys. Rev. 156, 370 (1967).

C. FAR-INFRARED PROPERTIES OF SOLIDS

1. CONSTRUCTION OF FAR-INFRARED APPARATUS

George C. Brackett, Richard R. Joyce, and Paul L. Richards

A pulsed gas laser yielding fixed frequencies in the far-infrared has been constructed for use as a light source in the spectroscopy of systems where parameters such as an applied magnetic field may be used to vary absorption frequencies. Repetitively pulsed output stable enough for lock-in detection has been achieved with two gases, water and isopropylamine vapors, at the frequencies listed in Table IVC.1-I.

Table IVC.1-I. Laser frequencies.

Vapor	Frequencies (cm^{-1})
Isopropylamine	32.2
	29.7
Water	126.4
	127.5
	136.2
	209.7
	211.6

Further development is expected to produce numerous other frequencies from water vapor and emission from iodine cyanide vapor at frequencies as low as 13 cm^{-1}. The higher output powers (relative to other standard sources) made available by stimulated emission promise to be useful in many applications.

Construction of a superconducting magnet system was completed which permits infrared transmission measurements of solid samples at any temperature between 1.5 and 300°K and in magnetic fields up to 55 kOe. A number of Ga-doped Ge, far-infrared, bolometer detectors for operation at liquid-helium temperatures were constructed for use with the magnet system and other cryogenic sample holders.

A tunable far-infrared Fabry-Pérot interferometer has been constructed for use as a variable frequency monochromator and filter. It is expected that this interferometer will be of special use in selecting modes of the water-vapor laser.

Two far-infrared interferometers were completed for use as Fourier-transform spectrometers. One, a 6-in. Michelson interferometer was begun last year and is currently used in crystalline field studies. The other, a 12-in. lamellar grating interferometer, was constructed in the Physics Department several years ago as a rapid-scan interferometer. It has been converted for use with digital Fourier transformation and is being used in the study of the Josephson effect.

2. LOW-LYING ENERGY LEVELS OF A SINGLE d-ELECTRON

Richard R. Joyce and Paul L. Richards

When Ti^{3+} or V^{4+} ions are substituted for Al^{3+} in Al_2O_3, the tenfold-degenerate free-ion ground level is split into five Kramers doublets. The combined effect of the trigonal crystalline field and spin-orbit coupling leaves the $E_{3/2}$ doublet lying lowest. The next higher levels are a ${}_1E_{1/2}$ doublet at energy δ_1 and a ${}_2D_{1/2}$ doublet at energy δ_2. The values of δ_1 and δ_2 were measured for $Al_2O_3:Ti^{3+}$ and for $Al_2O_3:V^{4+}$ by observing the frequencies of far-infrared absorption lines at 4.2°K. The g values for the splittings of the $E_{3/2}$ and ${}_1E_{1/2}$ levels were obtained for the same samples by transmission measurements in magnetic fields up to 50 kOe. Figure IVC.2-1 shows the splittings of the line at energy δ_1 as a function of H parallel to the optic axis. The effective g values for this line are $1/2(g_0 \pm g_1)$ where g_0 and g_1 give the splittings of the $E_{3/2}$ and ${}_1E_{1/2}$ levels. For H perpendicular to the optic axis no broadening or splitting was seen. The line at energy δ_2 was too broad to observe splittings in either sample. The results in Table IC.2-I are in good agreement with microwave measurements of g_0, but comparison of our values of g_1 with a recent theoretical prediction that includes the effect of dynamic Jahn-Teller distortions shows that single d-electron systems are still imperfectly

Table IVC.2-I. Theoretical predictions and experimental results for $Al_2O:Ti^{3+}$ and $Al_2O_3:V^{4+}$

Sample	Theoretical predictions[1]		Experimental Results	
$Al_2O_3:Ti^{3+}$	$\delta_1 = 43\ cm^{-1}$	$g_{0\parallel} = 1.18$	$\delta_1 = 37.8\ cm^{-1}$	$g_{0\parallel} = 1.06$
		$g_0 = 0$		$g_{0\perp} < 0.2$
	$\delta_2 = 107\ cm^{-1}$	$g_{1\parallel} = -2.5$	$\delta_2 = 107\ cm^{-1}$	$g_{1\parallel} = 2.0$
		$g_{1\perp} < -0.2$		$g_{1\perp} < 0.2$
$Al_2O_3:V^{4+}$	$\delta_1 = 21.4\ cm^{-1}$	$g_{0\parallel} = 1.7$	$\delta_1 = 28.1\ cm^{-1}$	$g_{0\parallel} = 1.5$
		$g_{0\perp} = 0$		$g_{0\perp} = 0.2$
	$\delta_2 = 63.4\ cm^{-1}$	$g_{1\parallel} = -1.9$	$\delta_2 = 53\ cm^{-1}$	$g_{1\parallel} = 1.5$
		$g_{1\perp} < 0.5$		$g_{1\perp} = 0.2$

1. R. M. Macfarlane, J. Y. Wong, and M. D. Sturge, Dynamic Jahn-Teller Effect in Octahedrally Coordinated d^1 Impurity Systems, Phys. Rev. 166, 250 (1968).

understood. The agreement is good enough, however, to confirm the assignment of the 37.8 cm^{-1} line to Ti^{3+} ions. Recent publications have attributed it to impurity-induced lattice modes and to a Cr^{3+} pair line.

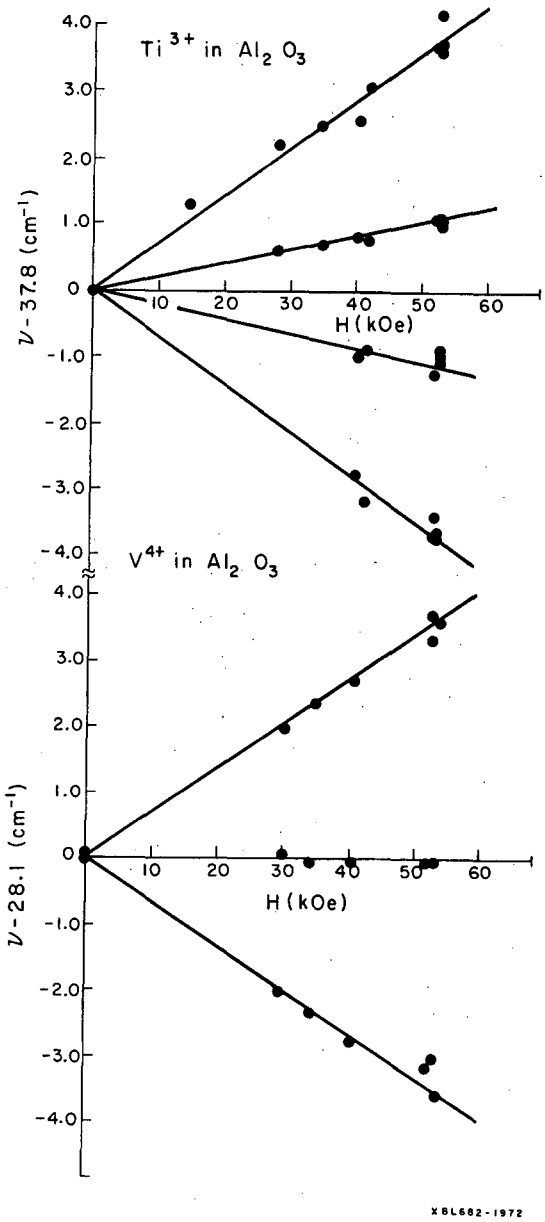

Fig. IVC.2-1. Line splittings at energy δ_1 as a function of the field parallel to the optic axis for Ti^{3+} and V^{4+} in Al_2O_3.

3. LOW-LYING ENERGY LEVELS OF INTERMEDIATE- AND HIGH-SPIN Fe^{3+}

George C. Brackett and Paul L. Richards

The low-lying energy levels of the ferric (Fe^{3+}) ion in several compounds with a large axial crystalline field have been studied by the methods of far-infrared Fourier transform spectroscopy. Among the samples under study are several hemin compounds. The magnetic properties of these compounds may be described by the approximate spin Hamiltonian $\mathcal{H} = \beta \underline{H} \cdot \underline{g} \cdot \underline{S} + D[S_z^2 - 1/3\, S(S+1)]$. Since, in general $g_\perp \gg g_\parallel$, sharp absorption lines corresponding to $g_\perp$ can be observed in randomly oriented powder specimens even at large fields. A typical plot of absorption frequency versus field is shown in Fig. IVC.3-1. Thus, far these measurements have yielded values for the axial crystalline field parameter D listed in Table IVC.3-I.

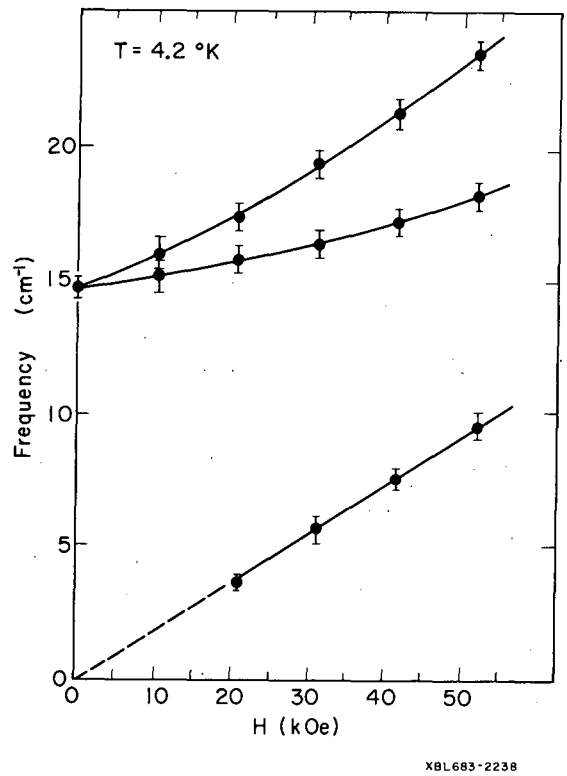

Fig. IVC.3-1. Bis (N N diethyl dithiocarbamato) ferric bromide.

4. JOSEPHSON JUNCTION AS A FAR-INFRARED DETECTOR

Paul L. Richards and Stewart A. Sterling

Point-contact Josephson tunnel junctions between two superconductors couple strongly to high-frequency radiation and potentially make fast sensitive detectors and mixers of far-infrared radiation. The detection mechanism involves beating between the ac Josephson currents, whose frequency $\omega = 2eV/\hbar$ is fixed by the bias voltage V, and currents induced by incident infrared. An attempt was made to verify the theoretically predicted frequency dependence of the ac Josephson current amplitude

Table IVC.3-I. Experimental values of the crystalline field parameter D for various compounds.

Compound	S	D(cm^{-1})
Deuteroporphyrin IX dimethyl ester Fe^{3+} azide	5/2	7.3
Bis (N, N dimethyl dithiocarbamato) Fe^{3+} chloride	3/2	-2.1
Bis (N, N diisopropyl dithiocarbamato) Fe^{3+} chloride	3/2	-2.3
Bis (N, N diethyl dithiocarbamato) Fe^{3+} bromide	3/2	7.4
Bis (N, N diethyl dithiocarbamato) Fe^{3+} chloride	3/2	-2.0

by measuring the spectral response of a Nb point-contact detector in the 2 to 30-cm^{-1} frequency region. It was found however that the detector sensitivity peaks strongly at frequencies governed primarily by unavoidable resonances in the detector surroundings. A stable means of mounting and adjusting point contacts has been devised and the resonant modes of one conical and two cylindrical cavities studies in the submillimeter wave region in an attempt to identify the observed peaks and to construct a useful detector geometry.

Two types of response peaks are identified in cavities with low $Q \approx 10$. Usually, peaks in detector sensitivity are comparable in sharpness to the cavity Q. This seems to represent a linear response to the radiation incident on the junction. Occasionally very much sharper peaks of opposite sign are seen, which seem to be due to nonlinear coupling of the Josephson currents to specific cavity modes. In higher-Q cavities, the dc I-V characteristic shows current steps analogous to those arising from resonant modes in evaporated-film Josephson junctions. This phenomenon can be viewed as a strong coupling between the ac Josephson current and the resonant-cavity modes and mixing of the infrared radiation with this ac current.

In connection with this project, a student laboratory demonstration experiment on the Josephson effect has been developed. Point-contact Josephson junctions mounted to a probe inserted into a storage vessel of liquid helium are now being used in the Berkeley Advanced Undergraduate Physics Laboratory to study the ac Josephson effect and flux quantization in superconductors.

5. RESEARCH PLANS FOR CALENDAR YEAR 1968

Paul L. Richards

Study of the interaction of far-infrared radiation with point-contact Josephson junctions will be continued. Attempts will be made to observe mixing between two far-infrared frequencies using the laser.

Studies of the low-lying energy levels of transition-metal ions by far-infrared spectroscopy will be continued with special attention to materials which are of biological interest, such as hemoglobin and myoglobin.

Two experiments have been started which have not yet yielded any results: A search is being made for a far-infrared absorption in the 3 to 20-cm^{-1} region due to a zero-wave vector libron mode in the ordered state of solid hydrogen with ortho concentrations greater than 70%. A mode has been predicted which is in many ways analogous to antiferromagnetic resonance. Rather than magnons, the fundamental excitations of this system are quantized hindered rotations of molecular quadrupole moments or librons.

A search is being made in collaboration with Prof. Y. R. Shen for far-infrared radiation produced by beating between two Q-switched ruby lasers focused into a quartz mixing crystal. One of the lasers is cooled sufficiently to obtain a difference frequency of $\approx 10\ cm^{-1}$. A high-speed InSb electronic bolometer (Putley detector) and appropriate filters are being used in the search for emitted far-infrared radiation.

In addition to these projects it is anticipated that a study of cyclotron resonance in metals will be started during 1968. The measurements will be made with the laser and

the superconducting magnet system. The primary goals will be, (i) to see far-infrared cyclotron resonance in metals, and (ii) to search for effects of phonon interactions on the resonances.

6. 1967 PUBLICATIONS

Paul L. Richards and Associates

Technical Journals

1. G. Feher and P. L. Richards, Determination of the Zero Field Splitting D in Heme Chloride, in Proceedings of the International Conference on Magnetic Resonance in Biological Systems, Stockholm, 1966.
2. P. L. Richards, Far Infrared Absorption by Two-Magnon Excitations in Antiferromagnets, J. Appl. Phys. 38, 1500 (1967).
3. P. L. Richards, Fourier Transform Spectroscopy, in Millimeter and Submillimeter Waves, D. Martin, Editor (North Holland, Amsterdam, 1967).
4. P. L. Richards, W. S. Caughey, H. Eberspaecher, G. Feher, and M. Malley, Determination of the Zero Field Splitting of Fe^{+++} in Several Hemin Compounds, J. Chem. Phys. Commun. 47, 1187 (1967).

D. SUPERCONDUCTIVITY

Gene Rochlin

Some initial results on flux jumping have been obtained which demonstrate that flux bundles entering a type-II superconductor follow a Poisson distribution, with remarkably high probabilities for large ($\sim 10^3$ fluxoid) bundles at certain values of applied magnetic field.

The ordinary tunneling work has just gotten underway, and the equipment is now operational. We anticipate results on several problems shortly. Both Josephson experiments have been partially set up. On one, a He^3 refrigerator-quenched vacuum evaporator device has been renovated and will be operational in the near future. On the other, the microwave assembly and cavity have been assembled and tested at room temperature, and we are awaiting the completion of our cryogenic equipment.

We have also done some preliminary investigation on the effect of organometallic cyclopentadiene compounds on the transition temperature of superconductors, although thus far we have obtained only null results.

1. RESEARCH PLANS FOR CALENDAR YEAR 1968

Gene Rochlin

Our investigation of flux-jumping statistics in a variety of materials and situations will be continued during 1968. We will attempt to get both Josephson-effect experiments operational. The effects of the cyclopentadiene compounds on superconductors will be studied further. The "ordinary" tunneling research will be continued in order to investigate "zero-bias" anomalies, energy-gap anisotropies, etc., and to examine the usefulness of superconducting tunnel junctions as Raman spectrometers.

2. 1967 PUBLICATIONS

Gene Rochlin and Associates

Technical Journals

1. G. I. Rochlin, Determination of the Anisotropy of the Energy Gap in Superconducting Pb by Superconductive Tunneling, Phys. Rev. 153, 513 (1967).

E. EXPERIMENTAL SOLID-STATE PHYSICS AND QUANTUM ELECTRONICS

1. OPTICAL PROPERTIES OF SOLIDS

Ricardo Zucca and Yuen Ron Shen

This project was actually started in the summer of 1967 when Mr. R. Zucca joined our group. A provisional setup was constructed to test the basic principle of a frequency-modulated differential reflectometer. Several difficulties have been encountered and solved. The electronic part of the system was designed and is being constructed.

2. SPONTANEOUS SCATTERING OF LIGHT

Harold Rosen, F. Stenman, and Yuen Ron Shen

A Raman spectrometer consisting of a Spex double monochromator, a Spectra Physics He-Ne laser, and a photon-counting detecting system has been set up for performing high-sensitivity and high-resolution Raman spectroscopy. It is now being used to study the molecular interaction between I_2 and various solvents. Results of the experiments yield information about the possible existence of I_2-complex.

3. ULTRASHORT LIGHT PULSES

John Shelton and Yuen Ron Shen

This project was started in late September of 1967. The laser system was designed and constructed in the Physics Department shops and is now being tested.

4. NONLINEAR OPTICS

Theory

Yuen Ron Shen

Nonlinear interaction of light with matter was described from the quantum-statistical point of view. It was shown that the nonlinear optical effects depend strongly on the statistical properties of the light fields. Measurements of the statistics of the output fields may yield information about the statistics of the input fields and the properties of the medium.

As to the problem of self-trapped filaments of laser light observed in liquids, we have presented a calculation modeled after the theory of phase transitions. The resulting state was shown to be similar to the Abrokosov vortex state in superconductors.

Experiments

Michael Loy, D. Faries, J. Shaham, and R. Ribotta

The self-focusing of a laser beam in many liquids has been studied. It was shown that the optical Kerr effect and electrostriction cannot explain the temperature variation of self-focusing in some liquid. Forward-stimulated Brillouin scattering seems important in such cases. The generation of stimulated Raman and Brillouin radiation in liquids has been measured. The effect of self-focusing and self-trapping on the forward-backward asymmetry in the Stokes generation was studied. Other qualitative features in the stimulated Raman and Brillouin scattering have been explained.

5. RESEARCH PLANS FOR CALENDAR YEAR 1968

Yuen Ron Shen

A low-temperature optical dewar will be constructed for experiments using the differential reflectometer. After the entire system is in shape, experiments on the Frank-Keldysh effect and on ferromagnetic semiconductors (if crystals are available) will be conducted. The dewar system will also be used in light-scattering experiments to probe the infrared properties of magnetic crystals. Molecular interaction will be investigated using Raman spectroscopy. The data could be helpful to the understanding of possible field-induced phase transformation in liquids. Experiments will be done on self-focusing and self-trapping of ruby laser beams. They would yield more information about the formation and the characteristics of the self-trapped filaments. Other

nonlinear optical experiments will be performed using a setup of two independent but simultaneously Q-switched lasers. Measurements of Optical phonon lifetimes will be measured using ultra-short pulses.

6. 1967 PUBLICATIONS

Yuen Ron Shen and Associates

Technical Journals

1. Y. R. Shen, Scattering of Light by Magnons, J. Appl. Phys. 38, 1490 (1967).
2. Y. R. Shen, Quantum Statistics of Nonlinear Optics, Phys. Rev. 155, 921 (1967).
3. Y. R. Shen and Y. J. Shaham, Self-Focusing and Stimulated Raman and Brillouin Effects in Liquids, Phys. Rev. 163, 224 (1967).
4. Y. R. Shen, Quantum Theory of Nonlinear Optics, International School of Physics "Enrico Fermi". XLII Course-Quantum Optics, July 31 to August 19, 1967, Varenna, Italy.
5. Y. R. Shen, M. Y. Au Yang, and M. Cohen, Theory of Self-Trapped Filaments of Light, Phys. Rev. Letters 19, 1171 (1967).

F. NUCLEAR-SPIN INTERACTIONS

1. A SCHEME FOR NMR-NQR DETECTION IN SOLIDS: C^{13} AND DEUTERIUM IN PARADICHLOROBENZENE*

Michael Schwab and Erwin L. Hahn

In a deuterium-enriched sample of solid paradichlorobenzene, the deuterium NQR and NMR of naturally abundant C^{13} have been observed. An ordered Cl^{35} quadrupole system cools the proton magnetic-spin reservoir in zero field, which in turn is coupled either to the deuterium system in zero field or to the C^{13} system in a low magnetic field (~150 gauss). Onset of double resonance is measured by the reduction of the Cl^{35} magnetization signal following recoupling of the Cl^{35} to the proton spin reservoir. The long proton T_1 (~45 sec in zero field, 50 min in 150 gauss) provides a metastable proton-spin-ordered state that can be coupled to unknown spin interactions. In a 12% deuterated sample a deuterium NQR doublet was measured at 138 kHz with ~5 kHz splitting. The naturally abundant (1.1%) C^{13} NMR was measured at a number of different field values with both audio and phase-shift saturation. Its linewidth was measured to be ~7 kHz, and the optimum double resonance rate was ~100 ms^{-1}. All measurements were made at 77°K.

* Supported in part by the National Science Foundation and the Office of Naval Research.

2. LEVEL-CROSSING DETECTION OF NQR TRANSITIONS*

Jackson C. Koo and Erwin L. Hahn

The nuclear electric-quadrupole interaction of N^{14} in phenothiazine at zero magnetic field has been observed by means of a level crossing method. Values of $e^2qQ/\hbar=4$, 240±10 kHz, asymmetry parameter η = 0.226±0.005, and spin-lattice relaxation time T_1 = 63±1 sec were deduced from the experiment at 77°K. Protons, initially polarized in a high dc magnetic field, are adiabatically demagnetized into zero field. In the demagnetized state the NQR of a N^{14} transition is saturated, and following proton remagnetization the change in proton signal reflects N^{14} saturation via level crossing which permits spin population exchange. For a long NQR relaxation time, this method can be two to three orders of magnitude more sensitive than direct resonance methods. Proton saturation in zero field can be induced by forbidden transitions involving the N^{14} NQR spectrum. For large η and integer spin I, properties associated with spin quenching[1] prevent observation of double-resonance coupling between N^{14} and the proton system.

* Supported in part by the National Science Foundation and the Office of Naval Research.

1. G. W. Leppelmeier and E. L. Hahn, Phys. Rev. 141, 724 (1966).

3. ZERO-FIELD, FREE-PRECESSION MEASUREMENTS OF THE HYPERFINE INTERACTION IN CESIUM^{133} VAPOR*

J. W. Shaner, S.A. Miller,† and Erwin L. Hahn

Free-induction decay in zero magnetic field of coherent microwave emission from the hyperfine levels of Cs vapor, excited from thermal equilibrium, has been measured to determine T_2 due to spin-exchange collisions. Measurements have been carried out from 120 to 240 °C corresponding to Cs densities from 4.5×10^{13} to 6×10^{15} cm^{-3}. If we assume that spin exchange completely dephases the radiating atom, our results for T_2 and the exchange cross section are in fair agreement with those of Moos[1] for higher temperature and intermediate magnetic field. We have also observed spin echoes for the Cs hyperfine system. T_1 measurements by a 90° - 90° pulse sequence have indicated no large difference between T_1 and T_2 for Cs densities below 3×10^{14} cm^{-3}.

* Supported in part by the National Science Foundation and the Office of Naval Research.
† Now at Naval Weapons Center, Corona, Calif.

1. H. W. Moos and R. H. Sands, Phys. Rev. 135, A591 (1964).

4. NUCLEAR SPIN DOUBLE RESONANCE IN KH_2PO_4

D. Stehlik

A nuclear double resonance apparatus used in previous work on other crystals was available for the above experiment. Improvement was necessary to detect the A-spin proton signal, indicating a receiver recovery of 15 - 20 μsec. Work is under way to construct a detection system with about 5 μsec recovery time. Furthermore a shorter 90°-pulse of 2 μsec is achieved using a one-coil arrangement.

The idea of the KH_2PO_4 experiment is to detect deuterium in its natural abundance by observing its coupling interaction with the proton system. Extensive studies of the deuterium resonance in completely deuterated crystals of ferroelectric KDP (KH_2PO_4) provide us with the following information.

1. The electric-field gradient tensor.
2. The spin- and domain-wall motions.

However, conclusions regarding the deuterium in KH_2PO_4 and also the behavior of the protons are limited. The double resonance method offers the direct observation of deuterium in KH_2PO_4.

Our earlier studies of the proton signal in KH_2PO_4 at the temperature of liquid N_2 indicated a very poor signal-to-noise ratio (especially during irradiation of an additional rf-field; this was attributed to the piezoelectric property of KH_2PO_4).

However, our first very recent measurements with a rather large crystal at room temperature indicated no strong piezoelectric effect on the signal by the additional irradiation, but an observable sensitivity to vibrational effects.

The proton signal gives the following information:

1. The free induction decay is time modulated depending upon the crystal orientation. This gives us properties of the proton-NMR-line shape and provides the possibility to determine the crystal orientation.
2. The study of the spin-lattice relaxation time T_1 gives the high field $T_1 = 35$ sec. However, the decay of the signal in the spin locked adiabatic demagnetized state exhibits two unexpected and interesting properties:
   a. The decay constant is much shorter, more than a factor of 10.
   b. The decay is a superposition of two exponentials decay curves with different time constants.

Next experimental steps are as follows:

1. Look for the naturally abundant deuterium resonance at room temperature.
2. Study the temperature dependence of the different relaxation times, and if possible, also of the deuterium resonance.
3. Apply the double resonance method to other solid state systems.

A successful study of naturally abundant deuterium, as it is coupled in the ferro-electric state in KH_2PO_4, will show directly its motional behavior in the environment of heavier, more abundant protons. Its tunneling properties will therefore not be altered by the usual procedure of enriching the sample with deuterium, an expedient necessary in order to see the NMR signal by standard techniques.

5. 1967 PUBLICATIONS

Erwin L. Hahn and Associates

Technical Journals

1. E. L. Hahn, Developments in Nuclear Double Resonance Spectroscopy, in Proceedings 14th Colloque Ampere, Ljubljana, Yugoslavia, (North Holland Publishing Co., 1967).
2. D. E. MacLoughlin and E. L. Hahn, Zero Field Nuclear Spin Relaxation and Resonance Absorption in Superconducting Aluminum, Phys. Rev. 159, 359 (1967).
3. S. L. McCall and E. L. Hahn, Self-Induced Transparency by Pulsed Coherent Light, Phys. Rev. Letters 18, 901 (1967).

Appendices

APPENDICES

IMRD STAFF FOR 1967

CHEMISTRY

Principal Investigator	Postdoctoral Fellows and Other Scientists	Graduate Students
Leo Brewer	J. Link B. Meyer G. Moore *L. Phillips J. Smith	*L. Bajema P. Cunningham *S. Currie D. Green H. Johansen B. King *R. Kortzeborn *A. Morello *D. Solan J. Tellinghuisen J. Wang P. Wengert
George Jura	J. Burton *R. Holmes	J. Pryzbylinski L. Rose W. Stark *C. Wu
Ronald Herm		D. Parrish S. Lin *L. Loh
William Jolly	P. Kuznesof K. Wynne	*R. Dreyfuss *P. Finn D. Hendrickson S. Lipp R. Patton *L. Prizant D. Rustad *K. Strom F. Wang J. Webster
Charles Harris		*M. Buckley R. Millikan *M. Silverman
Robert Connick	*K. Kustin *A. Von Zelewsky J. Vriesenga K. Wuthrich	H. Charles M. Judkins R. Lee *M. Silverman

* Participant Status

Principal Investigator	Postdoctoral Fellows and Other Scientists	Graduate Students
Rollie J. Myers	C. Arrington A. Bauder	W. Batchelder J. Chang J. Feiffer A. Jindo P. McKinney C. Pao D. Pratt *J. Smith C. Talcott *J. Tevebaugh *A. Wilkerson
Norman Phillips	J. Brock J. Ho C. Waterfield	M. Conway J. Hoffer G. Schwartz B. Triplett S. Wang
Charles W. Tobias	F. Baucke D. Landolt	R. Acosta R. Alkire K. Beach *C. Bon H. Cheh J. Earhart J. Jorne K. Kinoshita K. Kojima J. Selman
Bruce Mahan	E. Gislason R. Lambert Y. Lee I. Walker	M. Cheng A. Falick W. Gentry R. Horton M. Mosesman C. Tsao A. Werner
Rolf Muller	H. Gerischer R. Steiger	C. Churchman R. Gupta
Edward Grens III		J. Bert R. Levy *G. Long J. Roussillon
Otto Redlich	R. Duerst	*I. Edelweiss W. Gargrave V. Ngo

* Participant Status

Principal Investigator	Postdoctoral Fellows and Other Scientists	Graduate Students
Harold Johnston	*E. Marti	*P. Dow S. Gabelnick T. Paukert S. Schwartz J. Van den Bogaerde
John Newman		T. Chapman L. Hseuh V. Mirathe P. Milios P. Sih K. Tan
Gabor Somorjai	*A. Mattera A. Morgan J. Morabito	J. Davy H. Farrell T. French R. Goodman J. Lester C. Lou H. Lyon W. Szeto L. West
	NUCLEAR SCIENCE	
Donald Olander		J. Finucane *R. Jones R. Krakowski *V. Kruger R. Omberg C. Portwood J. Schofill W. Waddell
	METALLURGY	
John Dorn	C. Cheng P. Guyot M. Victoria	M. Abo-El-Fotoh K. Amin J. Bird C. Dharan *L. Jacobson *A. Karim S. Lau C. Liu R. Malatesta *R. Niccolls T. Stefansky

* Participant Status

Principal Investigator	Postdoctoral Fellows and Other Scientists	Graduate Students
Earl Parker	S. Antolovich K. Ralls	S. Ambekker C. Bruggeman J. Chabanne P. Guest R. Goolsby L. Hartsough R. Jones P. Key *W. Ludemann Z. Olson D. Porter M. Suenaga G. Walter
Gareth Thomas	K. Ashbee E. Butler A. Fitzgerald P. Petroff S. Ranganathan *E. Sturcken R. Villagrana	W. Bell I. Cheng S. Das N. Durai Raghavan J. Hall *D. Huang P. Manganon P. Okamoto P. Rao E. Rozovsky
Jack Washburn	G. Vagnard	V. Kannan T. Kosel Y. Miura A. Nes J. Tartour T. Trebert G. Vellaikal M. Yokota
Ralph Hultgren	P. Desai M. Gleiser K. Kelly R. Orr G. Somayajulu	T. Corn D. Hawkins E. Plaza H. Yoon
Victor Zackay	W. Gerberich M. Merz	J. Challande G. Chanani Y. Chung B. de Miramon J. Dunning D. Fahr Y. Katz J. Hall P. Hemmings C. La Porte E. Page

* Participant Status

Principal Investigator	Postdoctoral Fellows and Other Scientists	Graduate Students
Marshal Merriam Robert Hammond	* M. Heller H. King E. Nembach	G. Geiken
	CERAMICS	
Joseph Pask	J. Guiot *M. Koltermann T. Langdon	I. Aksay M. Appel S. Blank J. Brennan D. Cropper R. Davis P. Hart A. Lacy A. Raju R. Schweinberg
Alan Searcy	O. Herstad D. Meschi	J. Austin R. Coyle J. Dudash R. Leonard M. Lim R. Mar H. Skinner C. Washburn
Richard Fulrath		R. Atkin J. Masaryk R. Moon P. Nicholson Y. Nivas J. Playter G. Pryor B. Semans J. Shackleford M. Stett R. Tremper
	PHYSICS	
Erwin Hahn	D. Stehlik	*J. Koo R. Macklin *D. McArthur *S. McCall *L. Riley M. Schwab *J. Shaner
Marvin Cohen	T. Thorp	*C. Fong *J. Walter
Gene Rochlin		M. Jack J. Sweet

* Participant Status

Principal Investigator	Postdoctoral Fellows and Other Scientists	Graduate Students
Alan Portis		M. Bancroft E. Katz W. Holzer J. Siebert E. Shaw
Paul Richards	K. Gehring	G. Brackett *B. Enders R. Joyce S. Sterling
Y. Ron Shen	*R. Ribotta R. Roland	*M. Loy H. Rosen J. Shelton R. Zucca

* Participant Status

DEGREES AWARDED

Ph.D. Degrees

1. Stuart L. Blank, The Kinetics and Mechanisms of the Diffusion of Iron and Nickel in Single Crystals of Magnesium Oxide (UCRL-17411, May 1967).
2. James J. Burton, I. Relaxations in a Molecular Crystal; II. The Fermi Momentum of Aluminum from 0 to 100 Kilobars (UCRL-17479, May 1967).
3. Thomas W. Chapman, The Transport Properties of Concentrated Electrolytic Solutions (UCRL-17768, November 1967).
4. Huk Yuk Cheh, On the Mechanisms of Electrolytic Gas Evolution (UCRL-17324, February 1967).
5. Ching-Yao Cheng, Vacancy Models for Concentrated Binary Alloys (UCRL-17462, April 1967).
6. Nathapet Varadachari Durai-Raghavan, A Field Ion Microscope Study of the Ta-Mo System (UCRL-17711, August 1967).
7. Arnold M. Falick, An EPR Study of the O_2 ($^1\Delta_g$) Molecule (UCRL-17453, June 1967).
8. William R. Gentry, A Beam Study of $N_2^+ + H_2$ HD, D_2 Reaction Dynamics (UCRL-17813, September 1967).
9. Patrick E. Hart, The Activated Hot Pressing of Magnesium Oxide (UCRL-17978, December 1967).
10. Malcolm R. Judkins, Nuclear Magnetic Resonance Relaxation of Oxygen-17 in Aqueous Solutions of Ferric Ion (UCRL-17561, May 1967).
11. Robert A. Krakowski, Dissociation of Hydrogen on Tantalum Using a Modulated Molecular Beam Technique (UCRL-17336, March 1967).
12. Joseph E. Lester, Kinetics of Vaporization of Sodium Chloride (UCRL-17794, November 1967).
13. Robert E. Levy, Response Mode Analysis and Control of Multivariable Chemical Processes: Application to Distillation (UCRL-17480, June 1967).
14. Mahn Jick Lim, The Exchange of Energy Between Tungsten at High Temperatures and Gases at Room Temperature (UCRL-17395, May 1967).
15. Hylan B. Lyon, Jr., Low Energy Electron Diffraction Study of Low Index Platinum Single Crystal Surfaces (UCRL-17549, June 1967).
16. David McArthur, Nuclear Double Resonance Dynamics (UCRL-17468, July 1967).
17. Jack B. Mitchell, Strain Hardening of Long Range Ordered AgMg Single Crystals (UCRL-17894, November 1967).
18. Ronald L. Moon, High Temperature Phase Equilibria in the Lead Titanate - Lead Zirconate System (UCRL-17545, May 1967).
19. Patrick S. Nicholson, Differential Thermal Calorimetric Determination of the Thermodynamic Properties of Kaolinite (UCRL-17820, September 1967).
20. Zelma J. Olson, Investigation of High Field Superconducting Compounds (UCRL-17550, May 1967).
21. Pierre Petroff, A Field Ion Microscope Investigation of Radiation Damage in Iridium Bombarded with 10-MeV Protons (UCRL-17633, July 1967).
22. David W. Pratt, Magnetic Resonance Spectra of VCl_4 and Other Paramagnetic Species (UCRL-17406, May 1967).
23. Douglas S. Rustad, I. Reactions of Silane, Germane and Stannane with Metal- and Amide-Ammonia Solutions; II. Preparation and Reactions of Potassium Germyltrihydroborate, $KGeH_3BH_3$ (UCRL-17602, June 1967).
24. Walter Stark, Jr., Thermal Pulsing of Metals Under High Pressure (UCRL-17454, April 1967).
25. Carolyn Talcott, Electron Spin Resonance Studies of Radicals Produced by Electrolysis (UCRL-17743, September 1967).
26. Robert E. Villagrana, The Detection and Analysis of Modulated Ferromagnetic Structures by Transmission Electron Microscopy and Diffraction, (UCRL-17345, August 1967).

M. S. Degrees

1. Mohamed Osama Abo-el-Fotoh, The Low Temperature Thermally Activated Deformation Mechanisms for bcc Mg-Li-Al Alloy (UCRL-17449, April 1967).
2. Joel Lawrence Bert, Combustion of Heptane Droplets in a Hot Gas Flow (UCRL-17438, September 1967).
3. Jean Chabanne, Effect of the Microstructure on the Superconductive Properties of Nb_3Sn in a NbC Matrix (UCRL-17826, September 1967).
4. Govind R. Chanani, The Strength and Ductility of Metastable Austenitic Steels as a Function of Composition and Test Temperatures (UCRL-17805, September 1967).
5. I-Lin Cheng, An Electron Microscopic Study of Maraging Steel (UCRL-17334, March 1967).
6. Thomas A. Corn, The Thermodynamics of the Silver-Silicon System by Drop Calorimetry (UCRL-17946, December 1967).
7. Jonathan P. Earhart, The Viscosity of Concentrated Solutions of Calcium in Liquid Ammonia in the Temperature Interval of -40°C to -70°C (UCRL-17858, October 1967).
8. Wayne E. Gargrave, On the Molecular Structure of Strong Acids (UCRL-17915, December 1967).
9. Gerald Wayne Geiken, A Thermodynamic Study of the Heat of Ordering in CuPt (UCRL-17615, June 1967).
10. Peter J. Guest, The Microstructure and Plane Strain Fracture Toughness of High Strength Aluminum Alloys (UCRL-17872, October 1967).
11. Larry Hartsough, The Effect of Ternary Additions on the Superconducting Properties of Nb_3Al (UCRL-17982, December 1967).
12. Christian P. LaPorte, Effect of a Strain Induced Transformation on the Toughness of High Strength Materials (UCRL-17810, September 1967).
13. Gordon A. Long, Ignition of Fuel Droplets in Hot Stagnant Gases (UCRL-17811, September 1967).
14. Ronald P. Malatesta, Resistometric Observation of the Annealing Characteristics of a Tensile-Loaded Cu-Al Alloy (UCRL-17799, September 1967).
15. Paul Milios, A Theoretical Analysis of the Moving Boundary Measurement of Transference Numbers (UCRL-17807, September 1967).
16. Bertrand de Miramon, Quantitative Investigation of Strain Induced Strengthening in Steel (UCRL-17849, September 1967).
17. Elias M. Plaza, Thermodynamics of Solid and Liquid AuSn and Heat Contents of Gold and Tin (UCRL-17401, February 1967).
18. Jean Pierre Roussillon, The Effect of Periodic Meniscus Displacements on the Performance of Porous Gas Electrodes (UCRL-17594, August 1967).
19. Harry B. Skinner, Jr., The Heat of Sublimation and the Evaporation Coefficient of Praseodymium Trifluoride (UCRL-17804, September 1967).
20. Randolph T. Tremper, R-F Plasma Microspheroidization of Ceramics (UCRL-17896, December 1967).
21. William Waddel, Development of a High Pressure Mass Spectrometric Gas Analysis System (UCRL-17866, December 1967).
22. Gordon A. Walter, Investigation of the Application of Spinodal Theory to the Palladium-Iridium System (UCRL-17470, May 1967).

1967 RESEARCH SEMINARS

Application of Spinodal Theory to the Palladium-Iridium System

Electron Spin Resonance of Transition-Metal Compounds at Liquid-Helium Temperatures

Magnetic and Temperature Effects on the Zero-Bias-Tunnelling Anomaly

The Wetting of Aluminum Oxide by Liquid Aluminum

Towards Better Understanding of Solute-Solute Interactions in Liquid Metals

On the Mechanism of Electrolytic Gas Evolution

Dissociation of Hydrogen on Tantalum Using Modulated Molecular-Beam Technique

Application of X-Ray Techniques to Materials Problems in the Atomic Energy Field

Some Studies of the Coordination of Vanadyl Complexes in Aqueous Solutions

Heat-Capacity Measurements at Static High Pressure

An Electron Microscopic Study of Maraging Steel

Determination of Transference Numbers by the Moving-Boundary Method

Surface-Structure Analysis with Slow Electrons

Electrodeposition as a Chemical Process

Chemisorbed Gas Structures on Metals

Batteries for Vehicle Propulsion

The Effect of Periodic Meniscus Displacements on the Performance of Porous Gas Electrodes

Ionization of Strong Electrolytes. Temperature Coefficient of Dissociation of the $DClO_4$-$HClO_4$-D_2O-H_2O System by Proton Magnetic Resonance

The Structure of the Electrode Double Layer

Vacancy Concentrations in Concentrated Binary Alloys

Application of the Electron Microprobe to Metallurgical Problems in the U.S.S.R.

Reactive Fabrication Studies in Oxide and Metal Systems

Computer Simulation of Field-Ion Microscope Images

The Effect of Plastic Instability on Mechanical Property Measurements of MgO Loaded in Compression

The Superconducting Transition Temperature of Ultrathin Films

Velocity Analysis in Electron Microscopy

A Field-Ion Microscope Investigation of Radiation Damage in Iridium Bombarded with 10-Mev Protons

The Fermi Momentum of Aluminum from 0 to 100 Kilobars

The Transport Properties of Concentrated Electrolytic Solutions

Nuclear Spin Relaxation in Ferromagnetic Alloys

High Temperature Thermal Properties of AuSn

A Nitrogen-14 Nuclear Magnetic Resonance Study of Sulfur Nitride (S_4N_4) - Ammonia Solutions and Other Reactions of Sulfur Nitride

Effects of Surface Roughness and Turbulence on the Mass-Transfer Properties of Spherical Particles

Ab Initio Calculations on the High-Temperature Properties of BeO, MgO, and C_2

Infrared Spectra of Group V, VI, and VII Gaseous Oxides and Oxohalides

The Viscosity of Concentrated Solutions of Metallic Calcium in Liquid Ammonia

On the Relationship between Fracture Toughness and Tensile Behavior
Impurity Effects in Sintering Lead Zirconate Titanate
Surface Physics Investigated by Particle Bombardment
Calculation of the Diffusion-Layer Thickness on Membranes in an Electrodyalitic Apparatus
Propylene Carbonate as Nonaqueous Solvent for Electrochemical Measurements
The Microstructure and Plane-Strain Fracture Toughness of High-Strength Aluminum Alloys
ESR Hyperfine Coupling Parameter for PI Conjugated Radicals Containing N-14
The Strength of Nickel-Base Super Alloys
Molecular-Beam Studies of Scandium Monofluoride
Kinetics of NO_2 Electronic Fluorescence
The Heat of Sublimation and the Evaporation Coefficient of Praseodymium Fluoride
Fracture Mechanisms in Filled Polymers
Crystal-Growth Morphology as a Function of Entropy Change During Freezing

Key-Word-Plus-Title Subject and Author Index

KEY-WORD-PLUS-TITLE SUBJECT AND AUTHOR INDEX

The following pages are an alphabetical permuted index of the material in this report. Author's names are included. The index was prepared by the IBM-1401 computer using the key-word-plus-title program KWPT. All significant words are indexed; insignificant words have been automatically rejected by the computer. In some cases, the titles have been edited slightly to ensure proper word combination during automatic indexing and to provide maximum meaningful information.

Indexed terms are alphabetized and displayed in the left column of the index. The middle column shows the complete title and authors. The page number is given in the right column. Following the word index is the number index, which treats numbers as key words.

Your comments about the usefulness of this index and possible improvements are invited. Address such comments to Miss Gloria Smith, who is responsible for the automated indexing, or to the editor, Mr. Gerald Behman.

ACID	THE AQUATION OF THE NITRO PENTAAMMINE COBALT(III) ION IN SULFURIC ACID SOLUTIONS. A. D. HARRIS, R. STEWART, D. HENDRICKSON, AND W. L. JOLLY.	16
ACID	PROTON MAGNETIC-RESONANCE SPECTRA OF RHODIUM AND IRIDIUM COMPLEXES IN SULFURIC ACID. D. N. HENDRICKSON AND W. L. JOLLY.	16
ACIDS	STUDIES OF WEAK ACIDS. W. L. JOLLY.	10
ACIDS	DEPROTONATION OF WEAK ACIDS. W. L. JOLLY.	11
ACIDS	REACTION OF POTASSIUM GERMYL WITH LEWIS ACIDS. D. S. RUSTAD, P. M. KUZNESOF, AND W. L. JOLLY.	12
ACIDS	THERMODYNAMICS AND MOLECULAR STATE OF STRONG ACIDS. R. W. DUERST, W. E. GARGRAVE, AND O. REDLICH.	94
ACIDS	LEACHING OF CLAY WITH ACIDS. I. EDELWEISS AND O. REDLICH.	96
ADDUCTS	ADDUCTS OF SULFUR NITRIDE WITH BORON TRIHALIDES AND ANTIMONY PENTACHLORIDE. K. J. WYNNE AND W. L. JOLLY.	14
AKSAY	PHASE DISTRIBUTION IN MULTIPHASE MAGNESIA AND FORSTERITE BODIES. A. P. RAJU, I. A. AKSAY, AND J. A. PASK.	163
ALKALI	REVERSIBILITY OF THE REACTION OF ALKALI METALS WITH LIQUID AMMONIA. E. J. KIRSCHKE AND W. L. JOLLY.	17
ALKIRE	REACTION DISTRIBUTION IN FLOODED POROUS ELECTRODES. R. ALKIRE, E. A. GRENS II, AND C. W. TOBIAS.	51
ALLOY	TRANSITION-METAL ALLOY SYSTEMS. P. WENGERT.	24
ALLOY	HEAT CAPACITY OF A NI-RH ALLOY. N. E. PHILLIPS, B. B. TRIPLETT, AND D. W. WOODY.	28
ALLOY	ON FATIGUE-INDUCED REVERSION AND OVERAGING IN DISPERSION-STRENGTHENED ALLOY SYSTEMS. C. LAIRD AND G. THOMAS.	119
ALLOY	SINGLE-PHASE AND POLYPHASE ALLOY SYSTEMS. M. SUENAGA, J. OLSON, AND K. RALLS.	141
ALLOY	SUPERCONDUCTIVITY IN ALLOY SYSTEMS. M. F. MERRIAM.	146
ALLOYS	HEAT CAPACITY OF DILUTE FE IN CU ALLOYS. J. C. F. BROCK AND N. E. PHILLIPS.	27
ALLOYS	FRACTURE TOUGHNESS OF PRECIPITATION-HARDENING ALUMINUM ALLOYS. D. PORTER.	138
ALLOYS	VAPOR PRESSURE OF THALLIUM AND ACTIVITY MEASUREMENTS ON LIQUID SILVER-THALLIUM ALLOYS BY THE TORSION-EFFUSION METHOD. P. J. DESRE, D. T. HAWKINS, AND R. HULTGREN.	152
ALLOYS	MICROSTRUCTURE AND PLANE-STRAIN FRACTURE TOUGHNESS OF HIGH-STRENGTH ALUMINUM ALLOYS. P. J. GUEST AND M. D. MERZ.	135
ALLOYS	SUPERCONDUCTING TRANSITION TEMPERATURES OF VARIOUS LEAD-BASE ALLOYS. E. NEMBACH.	147
ALLOYS	SUPERCONDUCTING TRANSITION TEMPERATURES OF LEAD-INDIUM ALLOYS. E. NEMBACH.	147
ALLOYS	NUCLEAR RESONANCE IN FERROMAGNETIC ALLOYS. A. M. PORTIS.	185
ALLOYS	NUCLEAR DOUBLE RESONANCE IN FERROMAGNETIC ALLOYS. A. M. PORTIS.	185
ALPHA-ALUMINA	LOW-ENERGY ELECTRON-DIFFRACTION STUDY OF ALPHA-ALUMINA (AL2O3) AND QUARTZ (SIO2) SURFACES. T. M. FRENCH, J. MORABITO, AND G. A. SOMORJAI.	44
ALUMINUM	THE FERMI MOMENTUM OF ALUMINUM FROM 0 TO 100 KBARS. J. J. BURTON AND G. JURA.	34
ALUMINUM	FRACTURE TOUGHNESS OF PRECIPITATION-HARDENING ALUMINUM ALLOYS. D. PORTER.	138
ALUMINUM	LOW-ENERGY ELECTRON-DIFFRACTION STUDY OF ALUMINUM. H. H. FARRELL AND G. A. SOMORJAI.	44
ALUMINUM	CLIMB OF PERFECT AND IMPERFECT DISLOCATIONS IN ALUMINUM. J. TARTOUR AND J. WASHBURN.	109
ALUMINUM	MICROSTRUCTURE AND PLANE-STRAIN FRACTURE TOUGHNESS OF HIGH-STRENGTH ALUMINUM ALLOYS. P. J. GUEST AND M. D. MERZ.	135
AL2O3	INVESTIGATION OF THE REACTIONS BETWEEN AL2O3 AND SIO2. R. F. DAVIS AND J. A. PASK.	163
AMIDE	REACTIONS OF SILANE, GERMANE, AND STANNANE WITH METAL-AMMONIA AND AMIDE-AMMONIA SOLUTIONS. D. S. RUSTAD AND W. L. JOLLY.	11
AMMONIA	S4N4 AMMONIA SOLUTIONS. K. J. WYNNE AND W. L. JOLLY.	15
AMMONIA	STUDIES IN LIQUID AMMONIA. W. L. JOLLY.	17
AMMONIA	KINETICS OF METAL-ACID REACTIONS IN LIQUID AMMONIA. L. PRIZANT AND W. L. JOLLY.	17
AMMONIA	REACTIONS OF SILANE, GERMANE, AND STANNANE WITH METAL-AMMONIA AND AMIDE-AMMONIA SOLUTIONS. D. S. RUSTAD AND W. L. JOLLY.	11
AMMONIA	A GLASS PH ELECTRODE IN LIQUID AMMONIA. R. SHIURBA AND W. L. JOLLY.	17

AMMONIA	VISCOSITY OF CONCENTRATED SOLUTIONS OF CALCIUM IN LIQUID AMMONIA FROM -40 TO -70 DEGREES C. J. P. EARHART AND C. W. TOBIAS.	53
AMMONIA	REVERSIBILITY OF THE REACTION OF ALKALI METALS WITH LIQUID AMMONIA. E. J. KIRSCHKE AND W. L. JOLLY.	17
ANIONS	ESR SPECTRA OF THE RADICAL ANIONS OF METHYL-SUBSTITUTED NITROSOBENZENES. C. L. TALCOTT AND R. J. MYERS.	84
ANNEALING	ANNEALING OF STACKING-FAULT TETRAHEDRA IN GOLD. M. YOKOTA AND J. WASHBURN.	109
ANTIFERROMAGNETIC	ANTIFERROMAGNETIC RELAXATION. A. M. PORTIS.	185
ANTIMONY	ADDUCTS OF SULFUR NITRIDE WITH BORON TRIHALIDES AND ANTIMONY PENTACHLORIDE. K. J. WYNNE AND W. L. JOLLY.	14
ANTIMONY	REACTIONS OF DISULFUR DINITRIDE WITH ANTIMONY PENTACHLORIDE AND BORON TRIHALIDES. R. L. PATTON AND W. L. JOLLY.	14
APPEL	DIFFUSION IN THE CAO-NIO SYSTEM. M. APPEL AND J. A. PASK.	162
AQUATION	THE AQUATION OF THE NITRO PENTAAMMINE COBALT(III) ION IN SULFURIC ACID SOLUTIONS. A. D. HARRIS, R. STEWART, D. HENDRICKSON, AND W. L. JOLLY.	16
AQUEOUS	NMR RELAXATION OF OXYGEN-17 BY FERRIC ION IN AQUEOUS SOLUTION. M. R. JUDKINS.	7
ARSENIDE	EVAPORATION MECHANISM OF GALLIUM ARSENIDE SINGLE CRYSTALS. C. LOU AND G. A. SOMORJAI.	39
ASSIGNMENTS	LEAST-SQUARES-ADJUSTED ASSIGNMENTS FOR THE ESR SPECTRA OF FREE RADICALS IN SOLUTION. A. BAUDER, R. PAO, AND R. J. MEYERS.	80
ATOMS	RADIATIVE LIFETIMES OF EXCITED ELECTRONIC STATES OF ATOMS AND MOLECULES. P. T. CUNNINGHAM.	21
ATOMS	PSEUDOPOTENTIAL CALCULATIONS ON ATOMS AND DIATOMIC MOLECULES. J. TELLINGHUISEN.	22
ATOMS	THE MEAN DISPLACEMENT OF SURFACE ATOMS IN PALLADIUM AND LEAD SINGLE CRYSTALS. R. M. GOODMAN, H. H. FARRELL, AND G. A. SOMORJAI.	43
AUCU	LOW-TEMPERATURE HEAT CAPACITY OF AUCU. D. T. HAWKINS AND R. HULTGREN.	152
AUSTENITE	HEAT CAPACITY AND HEAT OF DECOMPOSITION OF AUSTENITE. H. I. YOON AND R. HULTGREN.	152
AUSTENITIC	EFFECT OF TEST TEMPERATURE ON THE MECHANICAL PROPERTIES OF METASTABLE AUSTENITIC STEELS. G. R. CHANANI AND M. D. MERZ.	133
AWARDED	DEGREES AWARDED.	205
BARIUM-OXYGEN	VAPOR SPECIES OF THE BARIUM-OXYGEN SYSTEM. R. S. NEWBURY, G. W. BARTON, JR., AND A. W. SEARCY.	159
BARTON	VAPOR SPECIES OF THE BARIUM-OXYGEN SYSTEM. R. S. NEWBURY, G. W. BARTON, JR., AND A. W. SEARCY.	159
BASICITY	INTRINSIC BASICITY OF THE HYDROXIDE ION. W. L. JOLLY.	10
BATCHELDER	ESR SPECTRA NEAR 1 DEGREE KELVIN. D. W. PRATT, A. JINDO, W. T. BATCHELDER, AND R. J. MYERS.	83
BAUCKE	THALLIUM - THALLOUS HALIDE REFERENCE ELECTRODES IN PROPYLENE CARBONATE. F. G. K. BAUCKE AND C. W. TOBIAS.	54
BAUCKE	ROTATING-DISK SYSTEM FOR METAL DEPOSITION FROM NONAQUEOUS SOLVENTS. F. G. K. BAUCKE, D. LANDOLT, AND C. W. TOBIAS.	55
BAUDER	LEAST-SQUARES-ADJUSTED ASSIGNMENTS FOR THE ESR SPECTRA OF FREE RADICALS IN SOLUTION. A. BAUDER, R. PAO, AND R. J. MEYERS.	80
BCC	HEAT CAPACITY OF SOLID BCC AND HCP HELIUM-4. J. K. HOFFER AND N. E. PHILLIPS.	28
BEACH	TRAVELLING-LASER INTERFEROMETER FOR MASS-TRANSFER STUDIES. K. W. BEACH, R. H. MULLER, AND C. W. TOBIAS.	50
BLANK	DIFFUSION OF IRON AND NICKEL INTO SINGLE-CRYSTAL MGO. S. L. BLANK AND J. A. PASK.	161
BLANK	EQUILIBRIUM AND NONEQUILIBRIUM SUBLIMATION OF ZINC SULFIDE AND OF CADMIUM TELLURIDE. B. A. H. BLANK AND A. W. SEARCY.	159
BOMBARDED	FIELD-ION MICROSCOPE INVESTIGATION OF RADIATION DAMAGE IN IRIDIUM BOMBARDED WITH 10-MEV PROTONS. P. PETROFF AND J. WASHBURN.	109
BON	SUPERSATURATION DURING ELECTROLYTIC GAS EVOLUTION. C. BON AND C. W. TOBIAS.	51
BOROM	KINETICS OF INTERFACIAL REACTION AND DIFFUSION IN THE SYSTEM IRON-SODIUM DISILICATE GLASS. M. P. BOROM AND J. A. PASK.	167
BORON	ADDUCTS OF SULFUR NITRIDE WITH BORON TRIHALIDES AND ANTIMONY PENTACHLORIDE. K. J. WYNNE AND W. L. JOLLY.	14
BORON	BORON HYDRIDE CHEMISTRY. W. L. JOLLY, T. SCHMITT, AND F. WANG.	13
BORON	REACTIONS OF DISULFUR DINITRIDE WITH ANTIMONY PENTACHLORIDE AND BORON TRIHALIDES. R. L. PATTON AND W. L. JOLLY.	14

BOUNDARIES	STRESS-INDUCED MOVEMENT OF TWIN BOUNDARIES IN ZINC. R. E. COOPER AND J. WASHBURN.	107
BRACKETT	CONSTRUCTION OF FAR-INFRARED APPARATUS. G. C. BRACKETT, R. R. JOYCE, AND P. L. RICHARDS.	187
BRACKETT	LOW-LYING ENERGY LEVELS OF INTERMEDIATE-SPIN AND HIGH-SPIN FE3+. G. C. BRACKETT AND P. L. RICHARDS.	189
BRENNAN	CERAMIC-METAL INTERFACES. J. J. BRENNAN AND J. A. PASK.	168
BREWER	GENERAL INTRODUCTION. L. BREWER AND V. ZACKAY.	1
BREWER	RESEARCH PLANS FOR 1968. L. BREWER.	24
BREWER	HIGH-FIELD SUPERCONDUCTIVITY. L. BREWER, E. R. PARKER, AND V. F. ZACKAY.	141
BREWER	RESEARCH PLANS FOR 1968. L. BREWER, E. R. PARKER, AND V. F. ZACKAY.	146
BREWER	1967 PUBLICATIONS. L. BREWER, E. R. PARKER, V. F. ZACKAY AND ASSOCIATES.	146
BREWER	1967 PUBLICATIONS. L. BREWER AND ASSOCIATES.	25
BROCK	HEAT CAPACITY OF DILUTE FE IN CU ALLOYS. J. C. F. BROCK AND N. E. PHILLIPS.	27
BROCK	HEAT CAPACITY OF MOLYBDENUM. J. C. F. BROCK AND N. E. PHILLIPS.	32
BUCKLING	PLASTIC BUCKLING AND CREEP OF MGO SINGLE CRYSTALS. D. R. CROPPER AND J. A. PASK.	167
BURTON	THE FERMI MOMENTUM OF ALUMINUM FROM 0 TO 100 KBARS. J. J. BURTON AND G. JURA.	34
BURTON	SURFACE-PHASE TRANSFORMATIONS ON A MOLECULAR SURFACE. J. J. BURTON AND G. JURA.	35
CADMIUM	EQUILIBRIUM AND NONEQUILIBRIUM SUBLIMATION OF ZINC SULFIDE AND OF CADMIUM TELLURIDE. B. A. H. BLANK AND A. W. SEARCY.	159
CALCIUM	VISCOSITY OF CONCENTRATED SOLUTIONS OF CALCIUM IN LIQUID AMMONIA FROM -40 TO -70 DEGREES C. J. P. EARHART AND C. W. TOBIAS.	53
CALCULATION	THERMODYNAMIC CALCULATION METHODS. V. B. T. NGO AND O. REDLICH.	95
CALCULATIONS	MAGNESIUM OXIDE SPECTRUM AND CALCULATIONS. D. GREEN.	23
CALCULATIONS	PSEUDOPOTENTIAL CALCULATIONS ON ATOMS AND DIATOMIC MOLECULES. J. TELLINGHUISEN.	22
CALORIMETRY	SURFACE CALORIMETRY. R. H. MULLER AND R. C. GUPTA.	49
CALORIMETRY	DIFFERENTIAL THERMAL CALORIMETRY. P. S. NICHOLSON AND R. M. FULRATH.	173
CALORIMETRY	THERMODYNAMICS OF THE SILVER-SILICON SYSTEM BY DROP CALORIMETRY. T. A. CORN AND R. HULTGREN.	151
CAO-NIO	DIFFUSION IN THE CAO-NIO SYSTEM. M. APPEL AND J. A. PASK.	162
CAPACITIES	HEAT CAPACITIES OF METALS UNDER PRESSURE. W. STARK AND G. JURA.	37
CAPTURE	CAPTURE RADIUS FOR ION RECOMBINATION. E. K. PARKS.	73
CARBONATE	THALLIUM - THALLOUS HALIDE REFERENCE ELECTRODES IN PROPYLENE CARBONATE. F. G. K. BAUCKE AND C. W. TOBIAS.	54
CATHODIC	OPTICAL STUDY OF CATHODIC GAS EVOLUTION DURING HIGH-CURRENT-DENSITY ELECTROLYSIS. D. LANDOLT, K. KINOSHITA, R. H. MULLER, AND C. W. TOBIAS.	59
CELL	CONCENTRATION PROFILE AND DIFFUSION COEFFICIENT IN A STAGNANT DIFFUSION CELL. L. HSUEH AND J. NEWMAN.	63
CELLS	POTENTIALS OF CELLS WITH LIQUID JUNCTIONS. W. H. SMYRL AND J. NEWMAN.	69
CERAMIC	INTERMETALLIC AND CERAMIC COMPOUNDS -- NB3(AL(X)GE(1-X)). L. D. HARTSOUGH.	144
CERAMIC	INTERMETALLIC AND CERAMIC COMPOUNDS -- NB-SN-C SYSTEM. J. CHABANNE, R. GOOLSBY, AND R. JONES.	145
CERAMIC	MICROSTRUCTURE AND BEHAVIOR OF CERAMIC MATERIALS -- GLASS AND CERAMIC-METAL SYSTEMS. J. A. PASK.	161
CERAMIC	DEVELOPMENT AND BEHAVIOR OF MICROSTRUCTURES IN CERAMIC SYSTEMS. R. M. FULRATH.	171
CERAMIC-METAL	MICROSTRUCTURE AND BEHAVIOR OF CERAMIC MATERIALS -- GLASS AND CERAMIC-METAL SYSTEMS. J. A. PASK.	161
CERAMIC-METAL	CERAMIC-METAL INTERFACES. J. J. BRENNAN AND J. A. PASK.	168
CERAMICS	RADIOFREQUENCY PLASMA MICROSPHEROIDIZATION OF CERAMICS. R. T. TREMPER AND R. M. FULRATH.	175
CESIUM-33	ZERO-FIELD, FREE-PRECESSION MEASUREMENTS OF THE HYPERFINE INTERACTION IN CESIUM-33 VAPOR. J. W. SHANER, S. A. MILLER, AND E. L. HAHN.	197
CHABANNE	INTERMETALLIC AND CERAMIC COMPOUNDS -- NB-SN-C SYSTEM. J. CHABANNE, R. GOOLSBY, AND R. JONES.	145
CHANANI	EFFECT OF TEST TEMPERATURE ON THE MECHANICAL PROPERTIES OF METASTABLE AUSTENITIC STEELS. G. R. CHANANI AND M. D. MERZ.	133
CHANG	TEMPERATURE DEPENDENCE OF THE EPR SPECTRUM OF HEXAQUACOPPER-II IN WATER. J. J. CHANG AND R. J. MYERS.	82

CHAPMAN	TRANSPORT PROPERTIES OF CONCENTRATED ELECTROLYTIC SOLUTIONS. T. W. CHAPMAN AND J. NEWMAN.	61
CHARLES	WATER EXCHANGE ON TI(III). H. CHARLES.	9
CHEMICAL	NITROGEN NMR CHEMICAL SHIFTS. D. N. HENDRICKSON AND P. M. KUZNESOF.	18
CHEMILUMINESCENCE	CHEMILUMINESCENCE FROM IF. S. D. GABELNICK AND H. S. JOHNSTON.	88
CHEMISTRY	THE CHEMISTRY OF STANNANE. J. R. WEBSTER AND W. L. JOLLY.	13
CHEMISTRY	SULFUR-NITROGEN CHEMISTRY. W. L. JOLLY.	14
CHEMISTRY	BORON HYDRIDE CHEMISTRY. W. L. JOLLY, T. SCHMITT, AND F. WANG.	13
CHENG	STRUCTURE AND PROPERTIES OF FE/NI/CO/TI MARAGING STEEL. I. L. CHENG AND G. THOMAS.	123
CHENG	MOLECULAR FRAGMENTATION BY ELECTRON IMPACT. M. H. CHENG AND B. H. MAHAN.	77
CHLORIDE	EVAPORATION MECHANISM OF SODIUM CHLORIDE. J. E. LESTER AND G. A. SOMORJAI.	39
CHLORIDES	SULFUR-NITROGEN CHLORIDES. W. L. JOLLY AND K. D. MAGUIRE.	15
CHLORINE-35	NMR SPECTRA OF CHLORINE-35 IN LIQUID VCL4 AND TICL4. D. W. PRATT AND R. J. MEYERS.	84
CLATHRATE	HEAT CAPACITY OF SOME SILVER CLATHRATE SALTS. M. M. CONWAY AND N. E. PHILLIPS.	31
CLAY	LEACHING OF CLAY WITH ACIDS. I. EDELWEISS AND O. REDLICH.	96
CLEAN	STUDIES OF THE CLEAN (100), (111), AND (110) CRYSTAL FACES OF PLATINUM. H. B. LYON AND G. A. SOMORJAI.	43
CLIMB	CLIMB OF PERFECT AND IMPERFECT DISLOCATIONS IN ALUMINUM. J. TARTOUR AND J. WASHBURN.	109
COBALT	STUDIES OF PENTAAMMINE COMPLEXES OF COBALT, RHODIUM, AND IRIDIUM. W. L. JOLLY.	16
COCONDENSATION	INORGANIC SYNTHESES IN LOW-TEMPERATURE MATRICES, NONAQUEOUS SOLVENTS, AND COCONDENSATION SYSTEMS. D. SOLAN, J. L. F. WANG, AND B. A. KING.	21
COHEN	THEORETICAL SOLID-STATE PHYSICS. M. L. COHEN.	183
COHEN	ELECTRONIC STRUCTURE OF SOLIDS. M. L. COHEN.	183
COHEN	SUPERCONDUCTIVITY IN DEGENERATE SEMICONDUCTORS. M. L. COHEN.	183
COHEN	RESEARCH PLANS FOR 1968. M. L. COHEN.	183
COHEN	1967 PUBLICATIONS. M. L. COHEN AND ASSOCIATES.	183
COLLISIONAL	THE COLLISIONAL-RADIATIVE REACTION OF SINGLET-DELTA OXYGEN. A. M. FALICK AND B. H. MAHAN.	74
COLLISIONS	SEMICLASSICAL PHASE SHIFTS FOR LOW-ENERGY ORBITING COLLISIONS. R. R. HERM.	92
COMPILATIONS	COMPILATIONS. N. LOFGREN.	24
COMPLEXED	OXYGEN-17 NMR STUDIES OF WATER EXCHANGE OF PARTIALLY COMPLEXED VANADYL ION. K. WUTHRICH.	7
COMPLEXES	STUDIES OF PENTAAMMINE COMPLEXES OF COBALT, RHODIUM, AND IRIDIUM. W. L. JOLLY.	16
COMPLEXES	ELECTRON DISTRIBUTION IN TRANSITION-METAL COMPLEXES. C. B. HARRIS.	94
COMPLEXES	PROTON MAGNETIC-RESONANCE SPECTRA OF RHODIUM AND IRIDIUM COMPLEXES IN SULFURIC ACID. D. N. HENDRICKSON AND W. L. JOLLY.	16
COMPLEXING	EFFECT OF COMPLEXING ON LIFETIMES OF WATER MOLECULES IN THE FIRST COORDINATION SPHERE OF NICKEL ION. K. KUSTIN.	8
COMPOSITE	TRANSIENT DIFFUSION IN A COMPOSITE SLAB. P. CONCUS AND D. R. OLANDER.	102
COMPOUNDS	STUDIES OF MISCELLANEOUS NITROGEN COMPOUNDS.	17
COMPOUNDS	INTERMETALLIC AND CERAMIC COMPOUNDS -- NB3(AL(X)GE(1-X)). L. D. HARTSOUGH.	144
COMPOUNDS	INTERMETALLIC AND CERAMIC COMPOUNDS -- NB-SN-C SYSTEM. J. CHABANNE, R. GOOLSBY, AND R. JONES.	145
COMPRESSED	CONSTANT-VOLUME HEAT CAPACITY OF COMPRESSED HELIUM-II. C. G. WATERFIELD, J. K. HOFFER, AND N. E. PHILLIPS.	29
CONCENTRATION	CONCENTRATION PROFILE AND DIFFUSION COEFFICIENT IN A STAGNANT DIFFUSION CELL. L. HSUEH AND J. NEWMAN.	63
CONCUS	TRANSIENT DIFFUSION IN A COMPOSITE SLAB. P. CONCUS AND D. R. OLANDER.	102
CONDENSATION	CONDENSATION-ENHANCED VAPORIZATION OF HIGH-TEMPERATURE SOLIDS. R. OMBERG AND D. R. OLANDER.	103
CONDUCTIVITY	ELECTROCHEMICAL AND CONDUCTIVITY STUDIES IN GLASS. R. N. SCHWEINBERG AND J. A. PASK.	167
CONNICK	RESEARCH PLANS FOR 1968. R. E. CONNICK.	9
CONNICK	1967 PUBLICATIONS. R. E. CONNICK AND ASSOCIATES.	10
CONSTANT-VOLUME	CONSTANT-VOLUME HEAT CAPACITY OF COMPRESSED HELIUM-II. C. G. WATERFIELD, J. K. HOFFER, AND N. E. PHILLIPS.	29
CONSTRUCTION	CONSTRUCTION OF FAR-INFRARED APPARATUS. G. C. BRACKETT, R. R. JOYCE, AND P. L. RICHARDS.	187

CONVECTION	LAMINAR FREE CONVECTION AT A VERTICAL PLATE IN THE PRESENCE OF SUPPORTING ELECTROLYTE. J. R. SELMAN AND J. NEWMAN.	66
CONVECTIVE	CURRENT AND POTENTIAL DISTRIBUTION IN CONVECTIVE MASS TRANSFER AT PLANE-PLATE ELECTRODES. J. R. SELMAN AND C. W. TOBIAS.	50
CONWAY	HEAT CAPACITY OF SOME SILVER CLATHRATE SALTS. M. M. CONWAY AND N. E. PHILLIPS.	31
CONWAY	HEAT CAPACITY OF METALS UNDER PRESSURE. S. S. B. WANG, M. M. CONWAY, AND N. E. PHILLIPS.	33
COOPER	STRESS-INDUCED MOVEMENT OF TWIN BOUNDARIES IN ZINC. R. E. COOPER AND J. WASHBURN.	107
COORDINATION	EFFECT OF COMPLEXING ON LIFETIMES OF WATER MOLECULES IN THE FIRST COORDINATION SPHERE OF NICKEL ION. K. KUSTIN.	8
COORDINATION	PROTON EXCHANGE FROM THE FIRST COORDINATION SPHERE OF HYDROLYTIC POLYMERS OF CHROMIUM(III). R. LEE.	8
COPPER	ELECTRODE POTENTIALS AND SURFACE CHARACTERISTICS IN HIGH-CURRENT-DENSITY COPPER DISSOLUTION. D. LANDOLT, K. KINOSHITA, R. MULLER, AND C. W. TOBIAS.	56
COPPER	STOICHIOMETRY OF COPPER DISSOLUTION AT HIGH CURRENT DENSITIES. K. KINOSHITA, D. LANDOLT, R. H. MULLER, AND C. W. TOBIAS.	55
COPPER	EFFECT OF INITIAL DISLOCATION DENSITY ON SINGLE-SLIP STRAIN HARDENING OF COPPER. J. WASHBURN AND G. MURTY.	107
CORN	THERMODYNAMICS OF THE SILVER-SILICON SYSTEM BY DROP CALORIMETRY. T. A. CORN AND R. HULTGREN.	151
COUPLED	NUMERICAL SOLUTION OF COUPLED ORDINARY DIFFERENTIAL EQUATIONS. J. NEWMAN.	70
CREEP	VOID FORMATION IN NICKEL AND SILVER DURING CREEP. T. G. LANGDON.	165
CREEP	CREEP OF LIF SINGLE CRYSTALS. D. R. CROPPER AND J. A. PASK.	166
CREEP	PLASTIC BUCKLING AND CREEP OF MGO SINGLE CRYSTALS. D. R. CROPPER AND J. A. PASK.	167
CREEP	CREEP OF POLYCRYSTALLINE MAGNESIUM OXIDE. T. G. LANGDON, J. SHEROHMAN, AND J. A. PASK.	164
CREEP	CREEP OF POLYCRYSTALLINE LIF. T. G. LANGDON AND D. R. CROPPER.	165
CROPPER	CREEP OF LIF SINGLE CRYSTALS. D. R. CROPPER AND J. A. PASK.	166
CROPPER	PLASTIC BUCKLING AND CREEP OF MGO SINGLE CRYSTALS. D. R. CROPPER AND J. A. PASK.	167
CROPPER	CREEP OF POLYCRYSTALLINE LIF. T. G. LANGDON AND D. R. CROPPER.	165
CROSSED-MOLECULAR	CROSSED-MOLECULAR-BEAM INVESTIGATION OF INELASTIC SCATTERING BY TIME-OF-FLIGHT ANALYSIS. D. D. PARRISH AND R. R. HERM.	93
CROSSED-MOLECULAR	CROSSED-MOLECULAR-BEAM INVESTIGATIONS OF THERMAL LI-ATOM REACTIONS. D. D. PARRISH AND R. R. HERM.	92
CRYSTAL	CRYSTAL IMPERFECTIONS. J. WASHBURN.	107
CRYSTAL	STUDIES OF THE CLEAN (100), (111), AND (110) CRYSTAL FACES OF PLATINUM. H. B. LYON AND G. A. SOMORJAI.	43
CRYSTALS	EVAPORATION RATE OF ICE SINGLE CRYSTALS. J. G. DAVY AND G. A. SOMORJAI.	43
CRYSTALS	SODIUM IN SILICON SINGLE CRYSTALS. W. SZETO AND G. A. SOMORJAI.	45
CRYSTALS	RELATION OF STRUCTURE TO PROPERTIES IN CRYSTALS. G. THOMAS.	119
CRYSTALS	ELECTRON-MICROSCOPE OBSERVATIONS OF TWINNING AND PHASE TRANSFORMATIONS IN INS CRYSTALS. A. G. FITZGERALD AND G. THOMAS.	125
CRYSTALS	INDICES OF PLANES AND DIRECTIONS IN HCP CRYSTALS. P. R. OKAMOTO AND G. THOMAS.	126
CRYSTALS	CREEP OF LIF SINGLE CRYSTALS. D. R. CROPPER AND J. A. PASK.	166
CRYSTALS	PLASTIC BUCKLING AND CREEP OF MGO SINGLE CRYSTALS. D. R. CROPPER AND J. A. PASK.	167
CRYSTALS	EVAPORATION MECHANISM OF GALLIUM ARSENIDE SINGLE CRYSTALS. C. LOU AND G. A. SOMORJAI.	39
CRYSTALS	COMMENTS ON SURFACE OXIDE FILMS AND THE LIFETIME OF VACANCIES IN THIN CRYSTALS. A. EIKUM AND G. THOMAS.	119
CRYSTALS	THE MEAN DISPLACEMENT OF SURFACE ATOMS IN PALLADIUM AND LEAD SINGLE CRYSTALS. R. M. GOODMAN, H. H. FARRELL, AND G. A. SOMORJAI.	43
CU	HEAT CAPACITY OF DILUTE FE IN CU ALLOYS. J. C. F. BROCK AND N. E. PHILLIPS.	27
CUNNINGHAM	RADIATIVE LIFETIMES OF EXCITED ELECTRONIC STATES OF ATOMS AND MOLECULES. P. T. CUNNINGHAM.	21

CUPROUS	PLASTIC DEFORMATION OF CUPROUS OXIDE. G. VAGNARD AND J. WASHBURN.	107
CUPT	THERMODYNAMIC STUDY OF THE HEAT OF ORDERING IN CUPT. G. W. GEIKEN, R. L. ORR, AND R. HULTGREN.	151
CURRENT	OPTICAL STUDY OF CATHODIC GAS EVOLUTION DURING HIGH CURRENT-DENSITY ELECTROLYSIS. D. LANDOLT, K. KINOSHITA, R. H. MULLER, AND C. W. TOBIAS.	59
CURRENT	CURRENT DISTRIBUTION ON A ROTATING-DISK ELECTRODE. V. MARATHE AND J. NEWMAN.	63
CURRENT	ELECTROLYSIS AT EXTREMELY HIGH CURRENT DENSITIES. C. W. TOBIAS.	55
CURRENT	CURRENT AND POTENTIAL DISTRIBUTION IN CONVECTIVE MASS-TRANSFER AT PLANE-PLATE ELECTRODES. J. R. SELMAN AND C. W. TOBIAS.	50
CURRENT-DENSITIES	STOICHIOMETRY OF COPPER DISSOLUTION AT HIGH CURRENT-DENSITIES. K. KINOSHITA, D. LANDOLT, R. H. MULLER, AND C. W. TOBIAS.	55
CURRENT-DENSITY	ELECTRODE POTENTIALS AND SURFACE CHARACTERISTICS IN HIGH CURRENT-DENSITY COPPER DISSOLUTION. D. LANDOLT, K. KINOSHITA, R. MULLER, AND C. W. TOBIAS.	56
CYLINDER	MASS TRANSFER TO THE REAR OF A CYLINDER AT HIGH SCHMITT NUMBERS. J. NEWMAN.	70
C13	A SCHEME FOR NMR-NQR DETECTION IN SOLIDS -- C13 AND DEUTERIUM IN PARADICHLOROBENZENE. M. SCHWAB AND E. L. HAHN.	197
D-ELECTRON	LOW-LYING ENERGY LEVELS OF A SINGLE D-ELECTRON. R. R. JOYCE AND P. L. RICHARDS.	187
DAVIS	INVESTIGATION OF THE REACTIONS BETWEEN AL203 AND SIO2. R. F. DAVIS AND J. A. PASK.	163
DAVY	EVAPORATION RATE OF ICE SINGLE CRYSTALS. J. G. DAVY AND G. A. SOMORJAI.	43
DE MIRAMON	QUANTITATIVE INVESTIGATION OF THE STRAIN-INDUCED MARTENSITIC TRANSFORMATION IN HIGH-STRENGTH STEELS. B. DE MIRAMON AND M. D. MERZ.	131
DECOMPOSITION	HEAT CAPACITY AND HEAT OF DECOMPOSITION OF AUSTENITE. H. I. YOON AND R. HULTGREN.	152
DEFORMATION	EFFECT OF MICROSTRUCTURE ON THE DEFORMATION OF POLYCRYSTALLINE MGO. T. G. LANGDON AND J. A. PASK.	164
DEFORMATION	PLASTIC DEFORMATION OF CUPROUS OXIDE. G. VAGNARD AND J. WASHBURN.	107
DEGENERATE	SUPERCONDUCTIVITY IN DEGENERATE SEMICONDUCTORS. M. L. COHEN.	183
DENSIFICATION	EFFECT OF LITHIUM FLUORIDE ON THE DENSIFICATION OF MAGNESIUM OXIDE. P. E. HART AND J. A. PASK.	163
DENSITIES	ELECTROLYSIS AT EXTREMELY HIGH CURRENT DENSITIES. C. W. TOBIAS.	55
DENSITY	OPTICAL STUDY OF CATHODIC GAS EVOLUTION DURING HIGH CURRENT-DENSITY ELECTROLYSIS. D. LANDOLT, K. KINOSHITA, R. H. MULLER, AND C. W. TOBIAS.	59
DENSITY	EFFECT OF INITIAL DISLOCATION DENSITY ON SINGLE-SLIP STRAIN HARDENING OF COPPER. J. WASHBURN AND G. MURTY.	107
DEPOSITION	ROTATING-DISK SYSTEM FOR METAL DEPOSITION FROM NONAQUEOUS SOLVENTS. F. G. K. BAUCKE, D. LANDOLT, AND C. W. TOBIAS.	55
DEPROTONATION	DEPROTONATION OF WEAK ACIDS. W. L. JOLLY.	11
DESRE	VAPOR PRESSURE OF THALLIUM AND ACTIVITY MEASUREMENTS ON LIQUID SILVER-THALLIUM ALLOYS BY THE TORSION-EFFUSION METHOD. P. J. DESRE, D. T. HAWKINS, AND R. HULTGREN.	152
DETECTION	A SCHEME FOR NMR-NQR DETECTION IN SOLIDS -- C13 AND DEUTERIUM IN PARADICHLOROBENZENE. M. SCHWAB AND E. L. HAHN.	197
DETECTION	LEVEL-CROSSING DETECTION OF NQR TRANSITIONS. J. C. KOO AND E. L. HAHN.	197
DETECTOR	JOSEPHSON JUNCTION AS A FAR-INFRARED DETECTOR. P. L. RICHARDS AND S. A. STERLING.	189
DEUTERIUM	A SCHEME FOR NMR-NQR DETECTION IN SOLIDS -- C13 AND DEUTERIUM IN PARADICHLOROBENZENE. M. SCHWAB AND E. L. HAHN.	197
DIATOMIC	PSEUDOPOTENTIAL CALCULATIONS ON ATOMS AND DIATOMIC MOLECULES. J. TELLINGHUISEN.	22
DIFFERENTIAL	NUMERICAL SOLUTION OF COUPLED ORDINARY DIFFERENTIAL EQUATIONS. J. NEWMAN.	70
DIFFERENTIAL	DIFFERENTIAL THERMAL CALORIMETRY. P. S. NICHOLSON AND R. M. FULRATH.	173
DIFFRACTION	SURFACE STUDIES BY LOW-ENERGY ELECTRON DIFFRACTION. G. A. SOMORJAI.	43

DIFFUSION	CONCENTRATION-PROFILE AND DIFFUSION COEFFICIENT IN A STAGNANT DIFFUSION CELL. L. HSUEH AND J. NEWMAN.	63
DIFFUSION	DIFFUSION OF IRON AND NICKEL INTO SINGLE-CRYSTAL MGO. S. L. BLANK AND J. A. PASK.	161
DIFFUSION	DIFFUSION IN THE CAO-NIO SYSTEM. M. APPEL AND J. A. PASK.	162
DIFFUSION	TRANSIENT DIFFUSION IN A COMPOSITE SLAB. P. CONCUS AND D. R. OLANDER.	102
DIFFUSION	KINETICS OF INTERFACIAL REACTION AND DIFFUSION IN THE SYSTEM IRON-SODIUM-DISILICATE GLASS. M. P. BOROM AND J. A. PASK.	167
DIFFUSION	DISSOLUTION AND DIFFUSION STUDIES IN GLASS. A. M. LACY AND J. A. PASK.	167
DIGERMANE	INVESTIGATION OF THE DISPROPORTIONATION OF DIGERMANE. R. DREYFUSS AND W. L. JOLLY.	12
DILUTION	HELIUM-3 - HELIUM-4 DILUTION REFRIGERATOR. B. B. TRIPLETT AND N. E. PHILLIPS.	33
DINITRIDE	REACTIONS OF DISULFUR DINITRIDE WITH ANTIMONY PENTACHLORIDE AND BORON TRIHALIDES. R. L. PATTON AND W. L. JOLLY.	14
DIOXIDE	RATE OF ATTACHMENT OF GASEOUS ELECTRONS TO NITROGEN DIOXIDE. B. H. MAHAN AND I. C. WALKER.	74
DIRECTIONS	INDICES OF PLANES AND DIRECTIONS IN HCP CRYSTALS. P. R. OKAMOTO AND G. THOMAS.	126
DISLOCATION	KINETICS OF DISLOCATION MECHANISMS. J. E. DORN.	115
DISLOCATION	EFFECT OF INITIAL DISLOCATION DENSITY ON SINGLE-SLIP STRAIN HARDENING OF COPPER. J. WASHBURN AND G. MURTY.	107
DISLOCATIONS	CLIMB OF PERFECT AND IMPERFECT DISLOCATIONS IN ALUMINUM. J. TARTOUR AND J. WASHBURN.	109
DISPERSION	ON FATIGUE-INDUCED REVERSION AND OVERAGING IN DISPERSION-STRENGTHENED ALLOY SYSTEMS. C. LAIRD AND G. THOMAS.	119
DISPLACEMENT	THE MEAN DISPLACEMENT OF SURFACE ATOMS IN PALLADIUM AND LEAD SINGLE CRYSTALS. R. M. GOODMAN, H. H. FARRELL, AND G. A. SOMORJAI.	43
DISPLACEMENTS	EFFECT OF PERIODIC MENISCUS DISPLACEMENTS ON THE PERFORMANCE OF POROUS GAS ELECTRODES. J. P. ROUSSILLON AND E. A. GRENS II.	53
DISPROPORTIONATION	INVESTIGATION OF THE DISPROPORTIONATION OF DIGERMANE. R. DREYFUSS AND W. L. JOLLY.	12
DISSOLUTION	ELECTRODE POTENTIALS AND SURFACE CHARACTERISTICS IN HIGH CURRENT-DENSITY COPPER DISSOLUTION. D. LANDOLT, K. KINOSHITA, R. MULLER, AND C. W. TOBIAS.	56
DISSOLUTION	EFFECT OF PRESSURE ON HIGH-TEMPERATURE DISSOLUTION. M. A. STETT AND R. M. FULRATH.	177
DISSOLUTION	STOICHIOMETRY OF COPPER DISSOLUTION AT HIGH CURRENT-DENSITIES. K. KINOSHITA, D. LANDOLT, R. H. MULLER, AND C. W. TOBIAS.	55
DISSOLUTION	DISSOLUTION AND DIFFUSION STUDIES IN GLASS. A. M. LACY AND J. A. PASK.	167
DISULFUR	REACTIONS OF DISULFUR DINITRIDE WITH ANTIMONY PENTACHLORIDE AND BORON TRIHALIDES. R. L. PATTON AND W. L. JOLLY.	14
DORN	KINETICS OF DISLOCATION MECHANISMS. J. E. DORN.	115
DORN	RESEARCH PLANS FOR 1968. J. E. DORN.	116
DORN	1967 PUBLICATIONS. J. E. DORN AND ASSOCIATES.	117
DOW	HYDROGEN-ATOM SPECTROMETER. P. DOW AND H. S. JOHNSTON.	91
DREYFUSS	INVESTIGATION OF THE DISPROPORTIONATION OF DIGERMANE. R. DREYFUSS AND W. L. JOLLY.	12
DROP	THERMODYNAMICS OF THE SILVER-SILICON SYSTEM BY DROP CALORIMETRY. T. A. CORN AND R. HULTGREN.	151
DUERST	THERMODYNAMICS AND MOLECULAR STATE OF STRONG ACIDS. R. W. DUERST, W. E. GARGRAVE, AND O. REDLICH.	94
DYNAMICS	DYNAMICS OF THE REACTION OF METHANE WITH NITROGEN-MOLECULE ION. E. A. GISLASON, C. W. TSAO, B. H. MAHAN, AND A. WERNER.	77
DYNAMICS	DYNAMICS OF POROUS ELECTRODES. C. W. TOBIAS.	51
EARHART	VISCOSITY OF CONCENTRATED SOLUTIONS OF CALCIUM IN LIQUID AMMONIA FROM -40 TO -70 DEGREES C. J. P. EARHART AND C. W. TOBIAS.	53
EDELWEISS	LEACHING OF CLAY WITH ACIDS. I. EDELWEISS AND O. REDLICH.	96
EIKUM	COMMENTS ON SURFACE OXIDE FILMS AND THE LIFETIME OF VACANCIES IN THIN CRYSTALS. A. EIKUM AND G. THOMAS.	119
ELECTRIC	MAGNETICAL AND ELECTRIC PROPERTIES OF MNAU. A. M. PORTIS.	185
ELECTROCHEMICAL	MASS TRANSFER AND ELECTROCHEMICAL SYSTEMS. J. NEWMAN.	69
ELECTROCHEMICAL	ELECTROCHEMICAL AND CONDUCTIVITY STUDIES IN GLASS. R. N. SCHWEINBERG AND J. A. PASK.	167
ELECTROCHEMISTRY	ELECTROCHEMISTRY IN NONAQUEOUS SOLVENTS. C. W. TOBIAS.	53
ELECTRODE	ELECTRODE POTENTIALS AND SURFACE CHARACTERISTICS IN HIGH-CURRENT-DENSITY COPPER DISSOLUTION. D. LANDOLT, K. KINOSHITA, R. MULLER, AND C. W. TOBIAS.	56

ELECTRODE	CURRENT DISTRIBUTION ON A ROTATING-DISK ELECTRODE. V. MARATHE AND J. NEWMAN.	63
ELECTRODE	A GLASS PH ELECTRODE IN LIQUID AMMONIA. R. SHIURBA AND W. L. JOLLY.	17
ELECTRODES	EFFECT OF PERIODIC MENISCUS DISPLACEMENTS ON THE PERFORMANCE OF POROUS GAS ELECTRODES. J. P. ROUSSILLON AND E. A. GRENS II.	53
ELECTRODES	THALLIUM - THALLOUS HALIDE REFERENCE ELECTRODES IN PROPYLENE CARBONATE. F. G. K. BAUCKE AND C. W. TOBIAS.	54
ELECTRODES	DYNAMICS OF POROUS ELECTRODES. C. W. TOBIAS.	51
ELECTRODES	CURRENT AND POTENTIAL DISTRIBUTION IN CONVECTIVE MASS TRANSFER AT PLANE-PLATE ELECTRODES. J. R. SELMAN AND C. W. TOBIAS.	50
ELECTRODES	REACTION DISTRIBUTION IN FLOODED POROUS ELECTRODES. R. ALKIRE, E. A. GRENS II, AND C. W. TOBIAS.	51
ELECTROLYSIS	OPTICAL STUDY OF CATHODIC GAS EVOLUTION DURING HIGH CURRENT-DENSITY ELECTROLYSIS. D. LANDOLT, K. KINOSHITA, R. H. MULLER, AND C. W. TOBIAS.	59
ELECTROLYSIS	ELECTROLYSIS AT EXTREMELY HIGH CURRENT DENSITIES. C. W. TOBIAS.	55
ELECTROLYTE	LAMINAR FREE CONVECTION AT A VERTICAL PLATE IN THE PRESENCE OF SUPPORTING ELECTROLYTE. J. R. SELMAN AND J. NEWMAN.	66
ELECTROLYTIC	SUPERSATURATION DURING ELECTROLYTIC GAS EVOLUTION. C. BON AND C. W. TOBIAS.	51
ELECTROLYTIC	TRANSPORT PROPERTIES OF CONCENTRATED ELECTROLYTIC SOLUTIONS. T. W. CHAPMAN AND J. NEWMAN.	61
ELECTRON	ELECTRON DISTRIBUTION IN TRANSITION-METAL COMPLEXES. C. B. HARRIS.	94
ELECTRON	ELECTRON MICROSCOPY AT HIGH VOLTAGES. G. THOMAS.	120
ELECTRON	ELECTRON-MICROSCOPE OBSERVATIONS OF TWINNING AND PHASE TRANSFORMATIONS IN INS CRYSTALS. A. G. FITZGERALD AND G. THOMAS.	125
ELECTRON	SURFACE STUDIES BY LOW-ENERGY ELECTRON DIFFRACTION. G. A. SOMORJAI.	43
ELECTRON	MOLECULAR FRAGMENTATION BY ELECTRON IMPACT. M. H. CHENG AND B. H. MAHAN.	77
ELECTRON	LOW-ENERGY ELECTRON-DIFFRACTION STUDY OF SOLID AND LIQUID LEAD. R. M. GOODMAN AND G. A. SOMORJAI.	44
ELECTRON	LOW-ENERGY ELECTRON-DIFFRACTION STUDY OF ALPHA-ALUMINA (AL2O3) AND QUARTZ (SIO2) SURFACES. T. M. FRENCH, J. MORABITO, AND G. A. SOMORJAI.	44
ELECTRON	LOW-ENERGY ELECTRON-DIFFRACTION STUDY OF ALUMINUM. H. H. FARRELL AND G. A. SOMORJAI.	44
ELECTRON	LOW-ENERGY ELECTRON-DIFFRACTION STUDIES AT LOW TEMPERATURES. J. MORABITO AND G. A. SOMORJAI.	44
ELECTRON	LOW-ENERGY ELECTRON-DIFFRACTION STUDY OF SURFACE REACTIONS ON (100) PLATINUM. A. E. MORGAN AND G. A. SOMORJAI.	44
ELECTRONIC	RADIATIVE LIFETIMES OF EXCITED ELECTRONIC STATES OF ATOMS AND MOLECULES. P. T. CUNNINGHAM.	21
ELECTRONIC	DETERMINATION OF THE ELECTRONIC PARTITION FUNCTION OF SCANDIUM MONOFLUORIDE BY MOLECULAR-BEAM FLUORESCENCE. D. GREEN.	23
ELECTRONIC	KINETICS OF NO2 ELECTRONIC FLUORESCENCE. S. E. SCHWARTZ AND H. S. JOHNSTON.	87
ELECTRONIC	ELECTRONIC STRUCTURE OF SOLIDS. M. L. COHEN.	183
ELECTRONICS	EXPERIMENTAL SOLID-STATE PHYSICS AND QUANTUM ELECTRONICS. Y. R. SHEN.	195
ELECTRONS	RATE OF ATTACHMENT OF GASEOUS ELECTRONS TO NITROGEN DIOXIDE. B. H. MAHAN AND I. C. WALKER.	74
ELECTROPOLISHING	MECHANISM OF ELECTROPOLISHING. K. KOJIMA AND C. W. TOBIAS.	59
ENERGY	PRODUCT ENERGY AND ANGULAR DISTRIBUTIONS FROM THE REACTION OF NITROGEN-MOLECULE ION WITH ISOTOPIC HYDROGEN MOLECULES. W. R. GENTRY, E. A. GISLASON, Y. T. LEE, B. H. MAHAN, AND C. W. TSAO.	75
ENERGY	EXCHANGE OF ENERGY BETWEEN TUNGSTEN AT HIGH TEMPERATURES AND GASES AT ROOM TEMPERATURE. M. J. LIM AND A. W. SEARCY.	155
ENERGY	LOW-LYING ENERGY LEVELS OF INTERMEDIATE-SPIN AND HIGH-SPIN FE3+. G. C. BRACKETT AND P. L. RICHARDS.	189
ENERGY	LOW-LYING ENERGY LEVELS OF A SINGLE D-ELECTRON. R. R. JOYCE AND P. L. RICHARDS.	187
ENTHALPY	A STUDY OF THE FREE-ENERGY AND ENTHALPY OF FORMATION OF AL2S3(S). O. HERSTAD AND A. W. SEARCY.	159
EPR	TEMPERATURE DEPENDENCE OF THE EPR SPECTRUM OF HEXAQUACOPPER-II IN WATER. J. J. CHANG AND R. J. MYERS.	82

EQUATIONS	NUMERICAL SOLUTION OF COUPLED ORDINARY DIFFERENTIAL EQUATIONS. J. NEWMAN.	70
EQUILIBRIA	HIGH-TEMPERATURE PHASE EQUILIBRIA IN THE LEAD-TITANATE - LEAD-ZIRCONATE SYSTEM. R. L. MOON AND R. M. FULRATH.	171
EQUILIBRIUM	EQUILIBRIUM AND NONEQUILIBRIUM SUBLIMATION OF ZINC SULFIDE AND OF CADMIUM TELLURIDE. B. A. H. BLANK AND A. W. SEARCY.	159
ESR	LEAST-SQUARES-ADJUSTED ASSIGNMENTS FOR THE ESR SPECTRA OF FREE RADICALS IN SOLUTION. A. BAUDER, R. PAO, AND R. J. MEYERS.	80
ESR	ESR SPECTRA NEAR 1 DEGREE KELVIN. D. W. PRATT, A. JINDO, W. T. BATCHELDER, AND R. J. MYERS.	83
ESR	ESR SPECTRA OF THE RADICAL ANIONS OF METHYL-SUBSTITUTED NITROSOBENZENES. C. L. TALCOTT AND R. J. MYERS.	84
EVAPORATION	EVAPORATION RATE OF ICE SINGLE CRYSTALS. J. G. DAVY AND G. A. SOMORJAI.	43
EVAPORATION	EVAPORATION MECHANISM OF SODIUM CHLORIDE. J. E. LESTER AND G. A. SOMORJAI.	39
EVAPORATION	EVAPORATION MECHANISM OF GALLIUM ARSENIDE SINGLE CRYSTALS. C. LOU AND G. A. SOMORJAI.	39
EVOLUTION	SUPERSATURATION DURING ELECTROLYTIC GAS EVOLUTION. C. BON AND C. W. TOBIAS.	51
EVOLUTION	OPTICAL STUDY OF CATHODIC GAS EVOLUTION DURING HIGH-CURRENT-DENSITY ELECTROLYSIS. D. LANDOLT, K. KINOSHITA, R. H. MULLER, AND C. W. TOBIAS.	59
EXCHANGE	OXYGEN-17 NMR STUDIES OF WATER EXCHANGE OF PARTIALLY COMPLEXED VANADYL ION. K. WUTHRICH.	7
EXCHANGE	WATER EXCHANGE ON TI(III). H. CHARLES.	9
EXCHANGE	PROTON EXCHANGE FROM THE FIRST COORDINATION SPHERE OF HYDROLYTIC POLYMERS OF CHROMIUM(III). R. LEE.	8
EXCHANGE	EXCHANGE OF ENERGY BETWEEN TUNGSTEN AT HIGH TEMPERATURES AND GASES AT ROOM TEMPERATURE. M. J. LIM AND A. W. SEARCY.	155
EXTREMELY	ELECTROLYSIS AT EXTREMELY HIGH CURRENT DENSITIES. C. W. TOBIAS.	55
FACES	STUDIES OF THE CLEAN (100), (111), AND (110) CRYSTAL FACES OF PLATINUM. H. B. LYON AND G. A. SOMORJAI.	43
FACILITY	THE LOW-TEMPERATURE FACILITY. E. NEMBACH.	147
FALICK	THE COLLISIONAL-RADIATIVE REACTION OF SINGLET-DELTA OXYGEN. A. M. FALICK AND B. H. MAHAN.	74
FAR-INFRARED	FAR-INFRARED PROPERTIES OF SOLIDS. P. L. RICHARDS.	187
FAR-INFRARED	CONSTRUCTION OF FAR-INFRARED APPARATUS. G. C. BRACKETT, R. R. JOYCE, AND P. L. RICHARDS.	187
FAR-INFRARED	JOSEPHSON JUNCTION AS A FAR-INFRARED DETECTOR. P. L. RICHARDS AND S. A. STERLING.	189
FARIES	NONLINEAR-OPTICS EXPERIMENTS. M. LOY, D. FARIES, J. SHAHAM, AND R. RIBOTTA.	195
FARRELL	LOW-ENERGY ELECTRON-DIFFRACTION STUDY OF ALUMINUM. H. H. FARRELL AND G. A. SOMORJAI.	44
FARRELL	THE MEAN DISPLACEMENT OF SURFACE ATOMS IN PALLADIUM AND LEAD SINGLE CRYSTALS. R. M. GOODMAN, H. H. FARRELL, AND G. A. SOMORJAI.	43
FATIGUE INDUCED	ON FATIGUE-INDUCED REVERSION AND OVERAGING IN DISPERSION-STRENGTHENED ALLOY SYSTEMS. C. LAIRD AND G. THOMAS.	119
FE	HEAT CAPACITY OF DILUTE FE IN CU ALLOYS. J. C. F. BROCK AND N. E. PHILLIPS.	27
FE/NI/CO/TI	STRUCTURE AND PROPERTIES OF FE/NI/CO/TI MARAGING STEEL. I. L. CHENG AND G. THOMAS.	123
FERMI	THE FERMI MOMENTUM OF ALUMINUM FROM 0 TO 100 KBARS. J. J. BURTON AND G. JURA.	34
FERRIC	NMR RELAXATION OF OXYGEN-17 BY FERRIC ION IN AQUEOUS SOLUTION. M. R. JUDKINS.	7
FERROMAGNETIC	NUCLEAR RESONANCE IN FERROMAGNETIC ALLOYS. A. M. PORTIS.	185
FERROMAGNETIC	NUCLEAR DOUBLE RESONANCE IN FERROMAGNETIC ALLOYS. A. M. PORTIS.	185
FE3	LOW-LYING ENERGY LEVELS OF INTERMEDIATE-SPIN AND HIGH-SPIN FE3+. G. C. BRACKETT AND P. L. RICHARDS.	189
FIELD ION	LIQUID-HELIUM FIELD-ION MICROSCOPE FOR RADIATION-DAMAGE INVESTIGATIONS. P. PETROFF AND J. WASHBURN.	109
FIELD ION	FIELD-ION MICROSCOPE INVESTIGATION OF RADIATION DAMAGE IN IRIDIUM BOMBARDED WITH 10-MEV PROTONS. P. PETROFF AND J. WASHBURN.	109
FILMS	COMMENTS ON SURFACE OXIDE FILMS AND THE LIFETIME OF VACANCIES IN THIN CRYSTALS. A. EIKUM AND G. THOMAS.	119
FINUCANE	VISCOSITY DETERMINATIONS. J. FINUCANE AND D. R. OLANDER.	102

FITZGERALD	ELECTRON-MICROSCOPE OBSERVATIONS OF TWINNING AND PHASE TRANSFORMATIONS IN INS CRYSTALS. A. G. FITZGERALD AND G. THOMAS.	125
FLOODED	REACTION DISTRIBUTION IN FLOODED POROUS ELECTRODES. R. ALKIRE, E. A. GRENS II, AND C. W. TOBIAS.	51
FLOW	FLOW TUNNEL WITH MOVING WALLS. P. H. SIH AND J. NEWMAN.	65
FLUORESCENCE	DETERMINATION OF THE ELECTRONIC PARTITION FUNCTION OF SCANDIUM MONOFLUORIDE BY MOLECULAR-BEAM FLUORESCENCE. D. GREEN.	23
FLUORESCENCE	KINETICS OF NO2 ELECTRONIC FLUORESCENCE. S. E. SCHWARTZ AND H. S. JOHNSTON.	87
FLUORIDE	SUBLIMATION OF PRASEODYMIUM FLUORIDE. H. B. SKINNER AND A. W. SEARCY.	155
FLUORIDE	EFFECT OF LITHIUM FLUORIDE ON THE DENSIFICATION OF MAGNESIUM OXIDE. P. E. HART AND J. A. PASK.	163
FORSTERITE	PHASE DISTRIBUTION IN MULTIPHASE MAGNESIA AND FORSTERITE BODIES. A. P. RAJU, I. A. AKSAY, AND J. A. PASK.	163
FRACTURE	FRACTURE TOUGHNESS OF PLASTICS. L. KEY AND Y. KATZ.	137
FRACTURE	FRACTURE TOUGHNESS OF PRECIPITATION-HARDENING ALUMINUM ALLOYS. D. PORTER.	138
FRACTURE	MICROSTRUCTURE AND PLANE-STRAIN FRACTURE TOUGHNESS OF HIGH-STRENGTH ALUMINUM ALLOYS. P. J. GUEST AND M. D. MERZ.	135
FRAGMENTATION	MOLECULAR FRAGMENTATION BY ELECTRON IMPACT. M. H. CHENG AND B. H. MAHAN.	77
FREE ENERGY	A STUDY OF THE FREE ENERGY AND ENTHALPY OF FORMATION OF AL2S3(S). O. HERSTAD AND A. W. SEARCY.	159
FREE PRECESSION	ZERO-FIELD, FREE-PRECESSION MEASUREMENTS OF THE HYPERFINE INTERACTION IN CESIUM-33 VAPOR. J. W. SHANER, S. A. MILLER, AND E. L. HAHN.	197
FREE RADICALS	SPECTRA AND LIFETIMES OF GAS-PHASE FREE RADICALS AT VERY LOW CONCENTRATIONS. H. S. JOHNSTON, E. D. MORRIS, JR., T. T. PAUKERT, AND J. VAN-DEN-BOGAERDE.	87
FRENCH	LOW-ENERGY ELECTRON-DIFFRACTION STUDY OF ALPHA-ALUMINA (AL2O3) AND QUARTZ (SIO2) SURFACES. T. M. FRENCH, J. MORABITO, AND G. A. SOMORJAI.	44
FULRATH	DEVELOPMENT AND BEHAVIOR OF MICROSTRUCTURES IN CERAMIC SYSTEMS. R. M. FULRATH.	171
FULRATH	DIFFERENTIAL THERMAL CALORIMETRY. P. S. NICHOLSON AND R. M. FULRATH.	173
FULRATH	RADIOFREQUENCY PLASMA MICROSPHEROIDIZATION OF CERAMICS. R. T. TREMPER AND R. M. FULRATH.	175
FULRATH	EFFECT OF PRESSURE ON HIGH-TEMPERATURE DISSOLUTION. M. A. STETT AND R. M. FULRATH.	177
FULRATH	RESEARCH PLANS FOR 1968. R. M. FULRATH.	180
FULRATH	HIGH-TEMPERATURE PHASE EQUILIBRIA IN THE LEAD-TITANATE - LEAD-ZIRCONATE SYSTEM. R. L. MOON AND R. M. FULRATH.	171
FULRATH	1967 PUBLICATIONS. R. M. FULRATH AND ASSOCIATES.	182
GABELNICK	CHEMILUMINESCENCE FROM IF. S. D. GABELNICK AND H. S. JOHNSTON.	88
GALLIUM	EVAPORATION MECHANISM OF GALLIUM ARSENIDE SINGLE CRYSTALS. C. LOU AND G. A. SOMORJAI.	39
GARGRAVE	THERMODYNAMICS AND MOLECULAR STATE OF STRONG ACIDS. R. W. DUERST, W. E. GARGRAVE, AND O. REDLICH.	94
GAS	SUPERSATURATION DURING ELECTROLYTIC GAS EVOLUTION. C. BON AND C. W. TOBIAS.	51
GAS	EFFECT OF PERIODIC MENISCUS DISPLACEMENTS ON THE PERFORMANCE OF POROUS GAS ELECTRODES. J. P. ROUSSILLON AND E. A. GRENS II.	53
GAS	OPTICAL STUDY OF CATHODIC GAS EVOLUTION DURING HIGH-CURRENT-DENSITY ELECTROLYSIS. D. LANDOLT, K. KINOSHITA, R. H. MULLER, AND C. W. TOBIAS.	59
GAS	GAS ANALYSIS BY MODULATED MOLECULAR-BEAM MASS SPECTROMETRY. D. R. OLANDER AND W. WADDEL.	99
GAS PHASE	SPECTRA AND LIFETIMES OF GAS-PHASE FREE RADICALS AT VERY LOW CONCENTRATIONS. H. S. JOHNSTON, E. D. MORRIS, JR., T. T. PAUKERT, AND J. VAN DEN BOGAERDE.	87
GASEOUS	RATE OF ATTACHMENT OF GASEOUS ELECTRONS TO NITROGEN DIOXIDE. B. H. MAHAN AND I. C. WALKER.	74
GASEOUS ION	GASEOUS-ION RECOMBINATION. V. B. H. MAHAN.	73
GASES	MASS SPECTROMETRY OF HIGH-PRESSURE IONIZED GASES. M. MOSESMAN AND B. H. MAHAN.	78
GASES	EXCHANGE OF ENERGY BETWEEN TUNGSTEN AT HIGH TEMPERATURES AND GASES AT ROOM TEMPERATURE. M. J. LIM AND A. W. SEARCY.	155
GEIKEN	THERMODYNAMIC STUDY OF THE HEAT OF ORDERING IN CUPT. G. W. GEIKEN, R. L. ORR, AND R. HULTGREN.	151

GENTRY	PRODUCT ENERGY AND ANGULAR DISTRIBUTIONS FROM THE REACTION OF NITROGEN-MOLECULE ION WITH ISOTOPIC HYDROGEN MOLECULES. W. R. GENTRY, E. A. GISLASON, Y. T. LEE, B. H. MAHAN, AND C. W. TSAO.	75
GENTRY	INELASTIC SCATTERING OF NITROGEN-MOLECULE ION BY HELIUM. W. R. GENTRY, E. A. GISLASON, B. H. MAHAN, AND C. W. TSAO.	74
GERBERICH	EFFECT OF A STRAIN-INDUCED TRANSFORMATION ON THE TOUGHNESS OF HIGH-STRENGTH STEELS. C. P. LAPORTE, P. HEMMINGS, W. GERBERICH, AND M. D. MERZ.	136
GERMANE	REACTIONS OF SILANE, GERMANE, AND STANNANE WITH METAL-AMMONIA AND AMIDE-AMMONIA SOLUTIONS. D. S. RUSTAD AND W. L. JOLLY.	11
GERMANIUM	STUDIES OF THE HYDRIDES OF SILICON, GERMANIUM, TIN, AND PHOSPHORUS.	11
GERMYL	REACTION OF POTASSIUM GERMYL WITH LEWIS ACIDS. D. S. RUSTAD, P. M. KUZNESOF, AND W. L. JOLLY.	12
GISLASON	PRODUCT ENERGY AND ANGULAR DISTRIBUTIONS FROM THE REACTION OF NITROGEN-MOLECULE ION WITH ISOTOPIC HYDROGEN MOLECULES. W. R. GENTRY, E. A. GISLASON, Y. T. LEE, B. H. MAHAN, AND C. W. TSAO.	75
GISLASON	DYNAMICS OF THE REACTION OF METHANE WITH NITROGEN-MOLECULE ION. E. A. GISLASON, C. W. TSAO, B. H. MAHAN, AND A. WERNER.	77
GISLASON	INELASTIC SCATTERING OF NITROGEN-MOLECULE ION BY HELIUM. W. R. GENTRY, E. A. GISLASON, B. H. MAHAN, AND C. W. TSAO.	74
GLASS	A GLASS PH ELECTRODE IN LIQUID AMMONIA. R. SHIURBA AND W. L. JOLLY.	17
GLASS	MICROSTRUCTURE AND BEHAVIOR OF CERAMIC MATERIALS -- GLASS AND CERAMIC-METAL SYSTEMS. J. A. PASK.	161
GLASS	KINETICS OF INTERFACIAL REACTION AND DIFFUSION IN THE SYSTEM IRON-SODIUM DISILICATE GLASS. M. P. BOROM AND J. A. PASK.	167
GLASS	ELECTROCHEMICAL AND CONDUCTIVITY STUDIES IN GLASS. R. N. SCHWEINBERG AND J. A. PASK.	167
GLASS	DISSOLUTION AND DIFFUSION STUDIES IN GLASS. A. M. LACY AND J. A. PASK.	167
GLEISER	EVALUATION OF THERMODYNAMIC DATA. R. HULTGREN, M. GLEISER, K. K. KELLEY, R. L. ORR, E. PLAZA, AND G. SOMAYAJULU.	152
GOKHALE	PHOSPHINE. S. D. GOKHALE AND W. L. JOLLY.	13
GOLD	ANNEALING OF STACKING-FAULT TETRAHEDRA IN GOLD. M. YOKOTA AND J. WASHBURN.	109
GOODMAN	LOW-ENERGY ELECTRON-DIFFRACTION STUDY OF SOLID AND LIQUID LEAD. R. M. GOODMAN AND G. A. SOMORJAI.	44
GOODMAN	THE MEAN DISPLACEMENT OF SURFACE ATOMS IN PALLADIUM AND LEAD SINGLE CRYSTALS. R. M. GOODMAN, H. H. FARRELL, AND G. A. SOMORJAI.	43
GOOLSBY	INTERMETALLIC AND CERAMIC COMPOUNDS -- NB-SN-C SYSTEM. J. CHABANNE, R. GOOLSBY, AND R. JONES.	145
GRAIN-BOUNDARY	GRAIN-BOUNDARY SLIDING AT HIGH TEMPERATURES. T. G. LANGDON.	164
GREEN	DETERMINATION OF THE ELECTRONIC PARTITION FUNCTION OF SCANDIUM MONOFLUORIDE BY MOLECULAR-BEAM FLUORESCENCE. D. GREEN.	23
GREEN	MAGNESIUM OXIDE SPECTRUM AND CALCULATIONS. D. GREEN.	23
GREEN	ANALYSIS OF ROTATIONAL PERTURBATIONS USING ISOTOPIC SHIFTS. D. GREEN AND H. JOHANSEN.	24
GRENS	EFFECT OF PERIODIC MENISCUS DISPLACEMENTS ON THE PERFORMANCE OF POROUS GAS ELECTRODES. J. P. ROUSSILLON AND E. A. GRENS II.	53
GRENS	REACTION DISTRIBUTION IN FLOODED POROUS ELECTRODES. R. ALKIRE, E. A. GRENS II, AND C. W. TOBIAS.	51
GUEST	MICROSTRUCTURE AND PLANE-STRAIN FRACTURE TOUGHNESS OF HIGH-STRENGTH ALUMINUM ALLOYS. P. J. GUEST AND M. D. MERZ.	135
GUPTA	SURFACE CALORIMETRY. R. H. MULLER AND R. C. GUPTA.	49
HAHN	NUCLEAR-SPIN INTERACTIONS. E. L. HAHN.	197
HAHN	A SCHEME FOR NMR-NQR DETECTION IN SOLIDS -- C13 AND DEUTERIUM IN PARADICHLOROBENZENE. M. SCHWAB AND E. L. HAHN.	197
HAHN	LEVEL-CROSSING DETECTION OF NQR TRANSITIONS. J. C. KOO AND E. L. HAHN.	197
HAHN	ZERO-FIELD, FREE-PRECESSION MEASUREMENTS OF THE HYPERFINE INTERACTION IN CESIUM-33 VAPOR. J. W. SHANER, S. A. MILLER, AND E. L. HAHN.	197
HAHN	1967 PUBLICATIONS. E. L. HAHN AND ASSOCIATES.	198

HALIDE	THALLIUM - THALLOUS HALIDE REFERENCE ELECTRODES IN PROPYLENE CARBONATE. F. G. K. BAUCKE, AND C. W. TOBIAS.	54
HAMMOND	RESEARCH PLANS FOR 1968. M. F. MERRIAM AND R. HAMMOND.	148
HARDENING	EFFECT OF INITIAL DISLOCATION DENSITY ON SINGLE-SLIP STRAIN HARDENING OF COPPER. J. WASHBURN AND G. MURTY.	107
HARRIS	ELECTRON DISTRIBUTION IN TRANSITION-METAL COMPLEXES. C. B. HARRIS.	94
HARRIS	THE AQUATION OF THE NITRO PENTAAMMINE COBALT(III) ION IN SULFURIC ACID SOLUTIONS. A. D. HARRIS, R. STEWART, D. HENDRICKSON, AND W. L. JOLLY.	16
HARRIS	RESEARCH PLANS FOR 1968. C. B. HARRIS.	94
HARRIS	1967 PUBLICATIONS. C. B. HARRIS.	94
HART	EFFECT OF LITHIUM FLUORIDE ON THE DENSIFICATION OF MAGNESIUM OXIDE. P. E. HART AND J. A. PASK.	163
HARTSOUGH	INTERMETALLIC AND CERAMIC COMPOUNDS -- NB3(AL(X)GE(1-X)). L. D. HARTSOUGH.	144
HAWKINS	VAPOR PRESSURE OF THALLIUM AND ACTIVITY MEASUREMENTS ON LIQUID SILVER-THALLIUM ALLOYS BY THE TORSION-EFFUSION METHOD. P. J. DESRE, D. T. HAWKINS, AND R. HULTGREN.	152
HAWKINS	LOW-TEMPERATURE HEAT CAPACITY OF AUCU. D. T. HAWKINS AND R. HULTGREN.	152
HCP	HEAT CAPACITY OF SOLID BCC AND HCP HELIUM-4. J. K. HOFFER AND N. E. PHILLIPS.	28
HCP	INDICES OF PLANES AND DIRECTIONS IN HCP CRYSTALS. P. R. OKAMOTO AND G. THOMAS.	126
HEAT	HEAT CAPACITY OF DILUTE FE IN CU ALLOYS. J. C. F. BROCK AND N. E. PHILLIPS.	27
HEAT	HEAT CAPACITY OF A NI-RH ALLOY. N. E. PHILLIPS, B. B. TRIPLETT, AND D. W. WOODY.	28
HEAT	CONSTANT-VOLUME HEAT CAPACITY OF COMPRESSED HELIUM-II. C. G. WATERFIELD, J. K. HOFFER, AND N. E. PHILLIPS.	29
HEAT	HEAT CAPACITY OF SOME SILVER CLATHRATE SALTS. M. M. CONWAY AND N. E. PHILLIPS.	31
HEAT	HEAT CAPACITY OF MOLYBDENUM. J. C. F. BROCK AND N. E. PHILLIPS.	32
HEAT	HEAT CAPACITY OF METALS UNDER PRESSURE. S. S. B. WANG, M. M. CONWAY, AND N. E. PHILLIPS.	33
HEAT	HEAT CAPACITIES OF METALS UNDER PRESSURE. W. STARK AND G. JURA.	37
HEAT	HEAT CAPACITY OF SOLID BCC AND HCP HELIUM-4. J. K. HOFFER AND N. E. PHILLIPS.	28
HEAT	THERMODYNAMIC STUDY OF THE HEAT OF ORDERING IN CUPT. G. W. GEIKEN, R. L. ORR, AND R. HULTGREN.	151
HEAT	HEAT CAPACITY AND HEAT OF DECOMPOSITION OF AUSTENITE. H. I. YOON AND R. HULTGREN.	152
HEAT CAPACITY	LOW-TEMPERATURE HEAT CAPACITY OF AUCU. D. T. HAWKINS AND R. HULTGREN.	152
HEAT CAPACITY	HEAT CAPACITY AND HEAT OF DECOMPOSITION OF AUSTENITE. H. I. YOON AND R. HULTGREN.	152
HELIUM	INELASTIC SCATTERING OF NITROGEN-MOLECULE ION BY HELIUM. W. R. GENTRY, E. A. GISLASON, B. H. MAHAN, AND C. W. TSAO.	74
HELIUM-II	CONSTANT-VOLUME HEAT CAPACITY OF COMPRESSED HELIUM-II. C. G. WATERFIELD, J. K. HOFFER, AND N. E. PHILLIPS.	29
HELIUM-3	HELIUM-3 - HELIUM-4 DILUTION REFRIGERATOR. B. B. TRIPLETT AND N. E. PHILLIPS.	33
HELIUM-4	HEAT CAPACITY OF SOLID BCC AND HCP HELIUM-4. J. K. HOFFER AND N. E. PHILLIPS.	28
HELIUM-4	MELTING CURVE OF HELIUM-4. N. E. PHILLIPS, J. K. HOFFER, AND C. G. WATERFIELD.	29
HELIUM-4	HELIUM-3 - HELIUM-4 DILUTION REFRIGERATOR. B. B. TRIPLETT AND N. E. PHILLIPS.	33
HEMMINGS	EFFECT OF A STRAIN-INDUCED TRANSFORMATION ON THE TOUGHNESS OF HIGH-STRENGTH STEELS. C. P. LAPORTE, P. HEMMINGS, W. GERBERICH, AND M. D. MERZ.	136
HENDRICKSON	MOLECULAR STRUCTURE OF SODIUM α-OXYHYPONITRITE. D. N. HENDRICKSON.	17
HENDRICKSON	NITROGEN NMR CHEMICAL SHIFTS. D. N. HENDRICKSON AND P. M. KUZNESOF.	18
HENDRICKSON	THE AQUATION OF THE NITRO PENTAAMMINE COBALT(III) ION IN SULFURIC ACID SOLUTIONS. A. D. HARRIS, R. STEWART, D. HENDRICKSON, AND W. L. JOLLY.	16
HENDRICKSON	PROTON MAGNETIC-RESONANCE SPECTRA OF RHODIUM AND IRIDIUM COMPLEXES IN SULFURIC ACID. D. N. HENDRICKSON AND W. L. JOLLY.	16
HERM	SEMICLASSICAL PHASE SHIFTS FOR LOW-ENERGY ORBITING COLLISIONS. R. R. HERM.	92

HERM CROSSED-MOLECULAR-BEAM INVESTIGATION OF INELASTIC SCATTERING BY TIME-OF-FLIGHT ANALYSIS. D. D. PARRISH AND R. R. HERM. 93
HERM CROSSED-MOLECULAR-BEAM INVESTIGATIONS OF THERMAL LI-ATOM REACTIONS. D. D. PARRISH AND R. R. HERM. 92
HERM RESEARCH PLANS FOR 1968. R. R. HERM. 93
HERM 1967 PUBLICATIONS. R. R. HERM AND ASSOCIATES. 93
HERSTAD A STUDY OF THE FREE-ENERGY AND ENTHALPY OF FORMATION OF AL2S3(S). O. HERSTAD AND A. W. SEARCY. 159
HEXAQUACOPPER-II TEMPERATURE DEPENDENCE OF THE EPR SPECTRUM OF HEXAQUACOPPER-II IN WATER. J. J. CHANG AND R. J. MYERS. 82
HIGH-FIELD HIGH-FIELD SUPERCONDUCTIVITY. L. BREWER, E. R. PARKER, AND V. F. ZACKAY. 141
HIGH-PRESSURE MASS SPECTROMETRY OF HIGH-PRESSURE IONIZED GASES. M. MOSESMAN AND B. H. MAHAN. 78
HIGH-SPIN LOW-LYING ENERGY LEVELS OF INTERMEDIATE-SPIN AND HIGH-SPIN FE3+. G. C. BRACKETT AND P. L. RICHARDS. 189
HIGH-STRENGTH HIGH-STRENGTH MATERIALS. E. R. PARKER AND V. F. ZACKAY. 131
HIGH-STRENGTH EFFECT OF A STRAIN-INDUCED TRANSFORMATION ON THE TOUGHNESS OF HIGH-STRENGTH STEELS. C. P. LAPORTE, P. HEMMINGS, W. GERBERICH, AND M. D. MERZ. 136
HIGH-STRENGTH QUANTITATIVE INVESTIGATION OF THE STRAIN-INDUCED MARTENSITIC TRANSFORMATION IN HIGH-STRENGTH STEELS. B. DE MIRAMON AND M. D. MERZ. 131
HIGH-STRENGTH MICROSTRUCTURE AND PLANE-STRAIN FRACTURE TOUGHNESS OF HIGH-STRENGTH ALUMINUM ALLOYS. P. J. GUEST AND M. D. MERZ. 135
HIGH-TEMPERATURE SPECTROSCOPIC INVESTIGATIONS OF HIGH-TEMPERATURE SPECIES TRAPPED AT LOW TEMPERATURES IN INERT MATRICES. J. L.-F. WANG, B. A. KING, AND C. B. MEYER. 21
HIGH-TEMPERATURE HIGH-TEMPERATURE VAPORIZATION MECHANISMS. G. A. SOMORJAI. 43
HIGH-TEMPERATURE CONDENSATION-ENHANCED VAPORIZATION OF HIGH-TEMPERATURE SOLIDS. R. OMBERG AND D. R. OLANDER. 103
HIGH-TEMPERATURE HIGH-TEMPERATURE REACTIONS. A. W. SEARCY. 155
HIGH-TEMPERATURE EFFECT OF PRESSURE ON HIGH-TEMPERATURE DISSOLUTION. M. A. STETT AND R. M. FULRATH. 177
HIGH-TEMPERATURE HIGH-TEMPERATURE PHASE EQUILIBRIA IN THE LEAD-TITANATE - LEAD-ZIRCONATE SYSTEM. R. L. MOON AND R. M. FULRATH. 171
HOFFER CONSTANT-VOLUME HEAT CAPACITY OF COMPRESSED HELIUM-II. C. G. WATERFIELD, J. K. HOFFER, AND N. E. PHILLIPS. 29
HOFFER HEAT CAPACITY OF SOLID BCC AND HCP HELIUM-4. J. K. HOFFER AND N. E. PHILLIPS. 28
HOFFER MELTING CURVE OF HELIUM-4. N. E. PHILLIPS, J. K. HOFFER, AND C. G. WATERFIELD. 29
HORTON ION-CYCLOTRON RESONANCE MASS SPECTROMETRY. R. HORTON, R. M. LAMBERT, AND B. H. MAHAN. 77
HSUEH CONCENTRATION PROFILE AND DIFFUSION COEFFICIENT IN A STAGNANT DIFFUSION CELL. L. HSUEH AND J. NEWMAN. 63
HULTGREN THERMODYNAMICS OF METAL SYSTEMS. R. HULTGREN. 151
HULTGREN VAPOR PRESSURE OF THALLIUM AND ACTIVITY MEASUREMENTS ON LIQUID SILVER-THALLIUM ALLOYS BY THE TORSION-EFFUSION METHOD. P. J. DESRE, D. T. HAWKINS, AND R. HULTGREN. 152
HULTGREN RESEARCH PLANS FOR 1968. R. HULTGREN. 153
HULTGREN THERMODYNAMIC STUDY OF THE HEAT OF ORDERING IN CUPT. G. W. GEIKEN, R. L. ORR, AND R. HULTGREN. 151
HULTGREN EVALUATION OF THERMODYNAMIC DATA. R. HULTGREN, M. GLEISER, K. K. KELLEY, R. L. ORR, E. PLAZA, AND G. SOMAYAJULU. 152
HULTGREN THERMODYNAMICS OF THE SILVER-SILICON SYSTEM BY DROP CALORIMETRY. T. A. CORN AND R. HULTGREN. 151
HULTGREN LOW-TEMPERATURE HEAT CAPACITY OF AUCU. D. T. HAWKINS AND R. HULTGREN. 152
HULTGREN HEAT CAPACITY AND HEAT OF DECOMPOSITION OF AUSTENITE. H. I. YOON AND R. HULTGREN. 152
HULTGREN 1967 PUBLICATIONS. R. HULTGREN AND ASSOCIATES. 153
HYDRIDE BORON HYDRIDE CHEMISTRY. W. L. JOLLY, T. SCHMITT, AND F. WANG. 13
HYDRIDES STUDIES OF THE HYDRIDES OF SILICON, GERMANIUM, TIN, AND PHOSPHORUS. 11
HYDROGEN PRODUCT ENERGY AND ANGULAR DISTRIBUTIONS FROM THE REACTION OF NITROGEN-MOLECULE ION WITH ISOTOPIC HYDROGEN MOLECULES. W. R. GENTRY, E. A. GISLASON, Y. T. LEE, B. H. MAHAN, AND C. W. TSAO. 75
HYDROGEN DISSOCIATION OF HYDROGEN ON TANTALUM USING A MODULATED MOLECULAR-BEAM TECHNIQUE. R. A. KRAKOWSKI AND D. R. OLANDER. 101

HYDROGEN ATOM	HYDROGEN-ATOM SPECTROMETER. P. DOW AND H. S. JOHNSTON.	91
HYDROLYTIC	PROTON EXCHANGE FROM THE FIRST COORDINATION SPHERE OF HYDROLYTIC POLYMERS OF CHROMIUM(III). R. LEE.	8
HYDROXIDE	INTRINSIC BASICITY OF THE HYDROXIDE ION. W. L. JOLLY.	10
HYPERFINE	ZERO-FIELD, FREE-PRECESSION MEASUREMENTS OF THE HYPERFINE INTERACTION IN CESIUM-33 VAPOR. J. W. SHANER, S. A. MILLER, AND E. L. HAHN.	197
H2SO4	S4N4-H2SO4 SOLUTIONS. S. LIPP AND W. L. JOLLY.	14
ICE	EVAPORATION RATE OF ICE SINGLE CRYSTALS. J. G. DAVY AND G. A. SOMORJAI.	43
IMPERFECT	CLIMB OF PERFECT AND IMPERFECT DISLOCATIONS IN ALUMINUM. J. TARTOUR AND J. WASHBURN.	109
IMPERFECTIONS	CRYSTAL IMPERFECTIONS. J. WASHBURN.	107
IMRD	IMRD STAFF FOR 1967.	199
INDICES	INDICES OF PLANES AND DIRECTIONS IN HCP CRYSTALS. P. R. OKAMOTO AND G. THOMAS.	126
INELASTIC	CROSSED-MOLECULAR-BEAM INVESTIGATION OF INELASTIC SCATTERING BY TIME-OF-FLIGHT ANALYSIS. D. D. PARRISH AND R. R. HERM.	93
INELASTIC	INELASTIC SCATTERING OF NITROGEN-MOLECULE ION BY HELIUM. W. R. GENTRY, E. A. GISLASON, B. H. MAHAN, AND C. W. TSAO.	74
INERT	SPECTROSCOPIC INVESTIGATIONS OF HIGH-TEMPERATURE SPECIES TRAPPED AT LOW TEMPERATURES IN INERT MATRICES. J. L.-F. WANG, B. A. KING, AND C. B. MEYER.	21
INORGANIC	INORGANIC SYNTHESES IN LOW-TEMPERATURE MATRICES, NONAQUEOUS SOLVENTS, AND COCONDENSATION SYSTEMS. D. SOLAN, J. L.-F. WANG, AND B. A. KING.	21
INS	ELECTRON MICROSCOPE OBSERVATIONS OF TWINNING AND PHASE TRANSFORMATIONS IN INS CRYSTALS. A. G. FITZGERALD AND G. THOMAS.	125
INTERFACES	CERAMIC-METAL INTERFACES. J. J. BRENNAN AND J. A. PASK.	168
INTERFACIAL	OPTICAL STUDIES OF INTERFACIAL PHENOMENA. R. H. MULLER AND R. F. STEIGER.	47
INTERFACIAL	KINETICS OF INTERFACIAL REACTION AND DIFFUSION IN THE SYSTEM IRON-SODIUM DISILICATE GLASS. M. P. BOROM AND J. A. PASK.	167
INTERFEROMETER	TRAVELLING-LASER INTERFEROMETER FOR MASS-TRANSFER STUDIES. K. W. BEACH, R. H. MULLER, AND C. W. TOBIAS.	50
INTERMEDIATE SPIN	LOW-LYING ENERGY LEVELS OF INTERMEDIATE-SPIN AND HIGH-SPIN FE3+. G. C. BRACKETT AND P. L. RICHARDS.	189
INTERMETALLIC	INTERMETALLIC AND CERAMIC COMPOUNDS -- NB3(AL(X)GE(1-X)). L. D. HARTSOUGH.	144
INTERMETALLIC	INTERMETALLIC AND CERAMIC COMPOUNDS -- NB-SN-C SYSTEM. J. CHABANNE, R. GOOLSBY, AND R. JONES.	145
INTRINSIC	INTRINSIC BASICITY OF THE HYDROXIDE ION. W. L. JOLLY.	10
IODINE	IODINE PREDISSOCIATION AND RECOMBINATION STUDIES. J. TELLINGHUISEN.	22
ION	OXYGEN-17 NMR STUDIES OF WATER EXCHANGE OF PARTIALLY COMPLEXED VANADYL ION. K. WUTHRICH.	7
ION	EFFECT OF COMPLEXING ON LIFETIMES OF WATER MOLECULES IN THE FIRST COORDINATION SPHERE OF NICKEL ION. K. KUSTIN.	8
ION	NMR RELAXATION OF OXYGEN-17 BY FERRIC ION IN AQUEOUS SOLUTION. M. R. JUDKINS.	7
ION	CAPTURE RADIUS FOR ION RECOMBINATION. E. K. PARKS.	73
ION	PRODUCT ENERGY AND ANGULAR DISTRIBUTIONS FROM THE REACTION OF NITROGEN-MOLECULE ION WITH ISOTOPIC HYDROGEN MOLECULES. W. R. GENTRY, E. A. GISLASON, Y. T. LEE, B. H. MAHAN, AND C. W. TSAO.	75
ION	DYNAMICS OF THE REACTION OF METHANE WITH NITROGEN-MOLECULE ION. E. A. GISLASON, C. W. TSAO, B. H. MAHAN, AND A. WERNER.	77
ION	INTRINSIC BASICITY OF THE HYDROXIDE ION. W. L. JOLLY.	10
ION	THE AQUATION OF THE NITRO PENTAAMMINE COBALT(III) ION IN SULFURIC ACID SOLUTIONS. A. D. HARRIS, R. STEWART, D. HENDRICKSON, AND W. L. JOLLY.	16
ION	INELASTIC SCATTERING OF NITROGEN-MOLECULE ION BY HELIUM. W. R. GENTRY, E. A. GISLASON, B. H. MAHAN, AND C. W. TSAO.	74
ION CYCLOTRON	ION-CYCLOTRON RESONANCE MASS SPECTROMETRY. R. HORTON, R. M. LAMBERT, AND B. H. MAHAN.	77
IONIC	FUNDAMENTAL STUDIES OF IONIC MASS TRANSFER. C. W. TOBIAS.	50
IONIZED	MASS SPECTROMETRY OF HIGH-PRESSURE IONIZED GASES. M. MOSESMAN AND B. H. MAHAN.	78
IRIDIUM	STUDIES OF PENTAAMMINE COMPLEXES OF COBALT, RHODIUM, AND IRIDIUM. W. L. JOLLY.	16
IRIDIUM	PROTON MAGNETIC RESONANCE SPECTRA OF RHODIUM AND IRIDIUM COMPLEXES IN SULFURIC ACID. D. N. HENDRICKSON AND W. L. JOLLY.	16

IRIDIUM	FIELD-ION MICROSCOPE INVESTIGATION OF RADIATION-DAMAGE IN IRIDIUM BOMBARDED WITH 10-MEV PROTONS. P. PETROFF AND J. WASHBURN.	109
IRON	DIFFUSION OF IRON AND NICKEL INTO SINGLE-CRYSTAL MGO. S. L. BLANK AND J. A. PASK.	161
IRON	KINETICS OF INTERFACIAL REACTION AND DIFFUSION IN THE SYSTEM IRON-SODIUM DISILICATE GLASS. M. P. BOROM AND J. A. PASK.	167
ISOTOPIC	ANALYSIS OF ROTATIONAL PERTURBATIONS USING ISOTOPIC SHIFTS. D. GREEN AND H. JOHANSEN.	24
ISOTOPIC	PRODUCT ENERGY AND ANGULAR DISTRIBUTIONS FROM THE REACTION OF NITROGEN-MOLECULE ION WITH ISOTOPIC HYDROGEN MOLECULES. W. R. GENTRY, E. A. GISLASON, Y. T. LEE, B. H. MAHAN, AND C. W. TSAO.	75
JINDO	ESR SPECTRA NEAR 1 DEGREE KELVIN. D. W. PRATT, A. JINDO, W. T. BATCHELDER, AND R. J. MYERS.	83
JOHANSEN	ANALYSIS OF ROTATIONAL PERTURBATIONS USING ISOTOPIC SHIFTS. D. GREEN AND H. JOHANSEN.	24
JOHNSTON	SPECTRA AND LIFETIMES OF GAS-PHASE FREE RADICALS AT VERY LOW CONCENTRATIONS. H. S. JOHNSTON, E. D. MORRIS, JR., T. T. PAUKERT, AND J. VAN DEN BOGAERDE.	87
JOHNSTON	CHEMILUMINESCENCE FROM IF. S. D. GABELNICK AND H. S. JOHNSTON.	88
JOHNSTON	HYDROGEN-ATOM SPECTROMETER. P. DOW AND H. S. JOHNSTON.	91
JOHNSTON	KINETICS OF NO2 ELECTRONIC FLUORESCENCE. S. E. SCHWARTZ AND H. S. JOHNSTON.	87
JOHNSTON	RESEARCH PLANS FOR 1968. H. S. JOHNSTON.	91
JOHNSTON	1967 PUBLICATIONS. H. S. JOHNSTON AND ASSOCIATES.	92
JOLLY	STUDIES OF WEAK ACIDS. W. L. JOLLY.	10
JOLLY	DEPROTONATION OF WEAK ACIDS. W. L. JOLLY.	11
JOLLY	REACTION OF POTASSIUM GERMYL WITH LEWIS ACIDS. D. S. RUSTAD, P. M. KUZNESOF, AND W. L. JOLLY.	12
JOLLY	THE CHEMISTRY OF STANNANE. J. R. WEBSTER AND W. L. JOLLY.	13
JOLLY	SULFUR NITROGEN CHEMISTRY. W. L. JOLLY.	14
JOLLY	S4N4 AMMONIA SOLUTIONS. K. J. WYNNE AND W. L. JOLLY.	15
JOLLY	STUDIES OF PENTAAMMINE COMPLEXES OF COBALT, RHODIUM, AND IRIDIUM. W. L. JOLLY.	16
JOLLY	STUDIES IN LIQUID AMMONIA. W. L. JOLLY.	17
JOLLY	KINETICS OF METAL-ACID REACTIONS IN LIQUID AMMONIA. L. PRIZANT AND W. L. JOLLY.	17
JOLLY	RESEARCH PLANS FOR 1968. W. L. JOLLY.	18
JOLLY	INTRINSIC BASICITY OF THE HYDROXIDE ION. W. L. JOLLY.	10
JOLLY	REACTIONS OF SILANE, GERMANE, AND STANNANE WITH METAL-AMMONIA AND AMIDE-AMMONIA SOLUTIONS. D. S. RUSTAD AND W. L. JOLLY.	11
JOLLY	INVESTIGATION OF THE DISPROPORTIONATION OF DIGERMANE. R. DREYFUSS AND W. L. JOLLY.	12
JOLLY	PHOSPHINE. S. D. GOKHALE AND W. L. JOLLY.	13
JOLLY	ADDUCTS OF SULFUR NITRIDE WITH BORON TRIHALIDES AND ANTIMONY PENTACHLORIDE. K. J. WYNNE AND W. L. JOLLY.	14
JOLLY	S4N4. M. VILLENA-BLANCO AND W. L. JOLLY.	15
JOLLY	THE AQUATION OF THE NITRO PENTAAMMINE COBALT(III) ION IN SULFURIC ACID SOLUTIONS. A. D. HARRIS, R. STEWART, D. HENDRICKSON, AND W. L. JOLLY.	16
JOLLY	A GLASS PH ELECTRODE IN LIQUID AMMONIA. R. SHIURBA AND W. L. JOLLY.	17
JOLLY	BORON HYDRIDE CHEMISTRY. W. L. JOLLY, T. SCHMITT, AND F. WANG.	13
JOLLY	STUDIES OF THE THERMAL SPLITTING OF S4N4. R. L. PATTON AND W. L. JOLLY.	14
JOLLY	SULFUR NITROGEN CHLORIDES. W. L. JOLLY AND K. D. MAGUIRE.	15
JOLLY	PROTON MAGNETIC-RESONANCE SPECTRA OF RHODIUM AND IRIDIUM COMPLEXES IN SULFURIC ACID. D. N. HENDRICKSON AND W. L. JOLLY.	16
JOLLY	REVERSIBILITY OF THE REACTION OF ALKALI METALS WITH LIQUID AMMONIA. E. J. KIRSCHKE AND W. L. JOLLY.	17
JOLLY	REACTIONS OF DISULFUR DINITRIDE WITH ANTIMONY PENTACHLORIDE AND BORON TRIHALIDES. R. L. PATTON AND W. L. JOLLY.	14
JOLLY	S4N4 H2SO4 SOLUTIONS. S. LIPP AND W. L. JOLLY.	14
JOLLY	1967 PUBLICATIONS. W. L. JOLLY AND ASSOCIATES.	19
JONES	CHARACTERIZATION OF MOLECULAR-BEAM SOURCES. R. JONES AND D. R. OLANDER.	100
JONES	INTERMETALLIC AND CERAMIC COMPOUNDS -- NB-SN-C SYSTEM. J. CHABANNE, R. GOOLSBY, AND R. JONES.	145
JOSEPHSON	JOSEPHSON JUNCTION AS A FAR-INFRARED DETECTOR. P. L. RICHARDS AND S. A. STERLING.	189

JOYCE CONSTRUCTION OF FAR-INFRARED APPARATUS. G. C. BRACKETT, R. R. JOYCE, AND P. L. RICHARDS. 187
JOYCE LOW-LYING ENERGY LEVELS OF A SINGLE D-ELECTRON. R. R. JOYCE AND P. L. RICHARDS. 187
JUDKINS NMR RELAXATION OF OXYGEN-17 BY FERRIC ION IN AQUEOUS SOLUTION. M. R. JUDKINS. 7
JUNCTION JOSEPHSON JUNCTION AS A FAR-INFRARED DETECTOR. P. L. RICHARDS AND S. A. STERLING. 189
JUNCTIONS POTENTIALS OF CELLS WITH LIQUID JUNCTIONS. W. H. SMYRL AND J. NEWMAN. 69
JURA THE FERMI MOMENTUM OF ALUMINUM FROM 0 TO 100 KBARS. J. J. BURTON AND G. JURA. 34
JURA SURFACE-PHASE TRANSFORMATIONS ON A MOLECULAR SURFACE. J. J. BURTON AND G. JURA. 35
JURA RESISTIVITY OF PHOSPHORUS. J. PRYZBYLINSKI AND G. JURA. 36
JURA HEAT CAPACITIES OF METALS UNDER PRESSURE. W. STARK AND G. JURA. 37
JURA RESEARCH PLANS FOR 1968. G. JURA. 38
JURA 1967 PUBLICATIONS. G. JURA AND ASSOCIATES. 39
KATZ NOTCH-TOUGHNESS VARIATIONS IN STEELS WITH THE SAME TENSILE PROPERTIES. Y. KATZ AND M. D. MERZ. 135
KATZ FRACTURE TOUGHNESS OF PLASTICS. L. KEY AND Y. KATZ. 137
KBARS THE FERMI MOMENTUM OF ALUMINUM FROM 0 TO 100 KBARS. J. J. BURTON AND G. JURA. 34
KELLEY EVALUATION OF THERMODYNAMIC DATA. R. HULTGREN, M. GLEISER, K. K. KELLEY, R. L. ORR, E. PLAZA, AND G. SOMAYAJULU. 152
KEY FRACTURE TOUGHNESS OF PLASTICS. L. KEY AND Y. KATZ. 137
KH2PO4 NUCLEAR SPIN DOUBLE RESONANCE IN KH2PO4. D. STEHLIK. 198
KINETICS KINETICS OF METAL-ACID REACTIONS IN LIQUID AMMONIA. L. PRIZANT AND W. L. JOLLY. 17
KINETICS VAPORIZATION KINETICS OF SOLIDS. G. A. SOMORJAI. 39
KINETICS KINETICS OF NO2 ELECTRONIC FLUORESCENCE. S. E. SCHWARTZ AND H. S. JOHNSTON. 87
KINETICS KINETICS OF DISLOCATION MECHANISMS. J. E. DORN. 115
KINETICS KINETICS OF INTERFACIAL REACTION AND DIFFUSION IN THE SYSTEM IRON-SODIUM DISILICATE GLASS. M. P. BOROM AND J. A. PASK. 167
KING SPECTROSCOPIC INVESTIGATIONS OF HIGH-TEMPERATURE SPECIES TRAPPED AT LOW TEMPERATURES IN INERT MATRICES. J. L.-F. WANG, B. A. KING, AND C. B. MEYER. 21
KING INORGANIC SYNTHESES IN LOW-TEMPERATURE MATRICES, NONAQUEOUS SOLVENTS, AND COCONDENSATION SYSTEMS. D. SOLAN, J. L.-F. WANG, AND B. A. KING. 21
KINOSHITA ELECTRODE POTENTIALS AND SURFACE CHARACTERISTICS IN HIGH-CURRENT-DENSITY COPPER DISSOLUTION. D. LANDOLT, K. KINOSHITA, R. MULLER, AND C. W. TOBIAS. 56
KINOSHITA OPTICAL STUDY OF CATHODIC GAS EVOLUTION DURING HIGH-CURRENT-DENSITY ELECTROLYSIS. D. LANDOLT, K. KINOSHITA, R. H. MULLER, AND C. W. TOBIAS. 59
KINOSHITA STOICHIOMETRY OF COPPER DISSOLUTION AT HIGH CURRENT DENSITIES. K. KINOSHITA, D. LANDOLT, R. H. MULLER, AND C. W. TOBIAS. 55
KIRSCHKE REVERSIBILITY OF THE REACTION OF ALKALI METALS WITH LIQUID AMMONIA. E. J. KIRSCHKE AND W. L. JOLLY. 17
KOJIMA MECHANISM OF ELECTROPOLISHING. K. KOJIMA AND C. W. TOBIAS. 59
KOO LEVEL-CROSSING DETECTION OF NQR TRANSITIONS. J. C. KOO AND E. L. HAHN. 197
KRAKOWSKI DISSOCIATION OF HYDROGEN ON TANTALUM USING A MODULATED MOLECULAR-BEAM TECHNIQUE. R. A. KRAKOWSKI AND D. R. OLANDER. 101
KUSTIN EFFECT OF COMPLEXING ON LIFETIMES OF WATER MOLECULES IN THE FIRST COORDINATION SPHERE OF NICKEL ION. K. KUSTIN. 8
KUZNESOF REACTION OF POTASSIUM GERMYL WITH LEWIS ACIDS. D. S. RUSTAD, P. M. KUZNESOF, AND W. L. JOLLY. 12
KUZNESOF NITROGEN NMR CHEMICAL SHIFTS. D. N. HENDRICKSON AND P. M. KUZNESOF. 18
LACY DISSOLUTION AND DIFFUSION STUDIES IN GLASS. A. M. LACY AND J. A. PASK. 167
LAIRD ON FATIGUE-INDUCED REVERSION AND OVERAGING IN DISPERSION-STRENGTHENED ALLOY SYSTEMS. C. LAIRD AND G. THOMAS. 119
LAMBERT ION-CYCLOTRON RESONANCE MASS SPECTROMETRY. R. HORTON, R. M. LAMBERT, AND B. H. MAHAN. 77
LAMINAR LAMINAR FREE CONVECTION AT A VERTICAL PLATE IN THE PRESENCE OF SUPPORTING ELECTROLYTE. J. R. SELMAN AND J. NEWMAN. 66
LANDOLT ROTATING-DISK SYSTEM FOR METAL DEPOSITION FROM NONAQUEOUS SOLVENTS. F. G. K. BAUCKE, D. LANDOLT, AND C. W. TOBIAS. 55

LANDOLT	ELECTRODE POTENTIALS AND SURFACE CHARACTERISTICS IN HIGH CURRENT-DENSITY COPPER DISSOLUTION. D. LANDOLT, K. KINOSHITA, R. MULLER, AND C. W. TOBIAS.	56
LANDOLT	OPTICAL STUDY OF CATHODIC GAS EVOLUTION DURING HIGH-CURRENT-DENSITY ELECTROLYSIS. D. LANDOLT, K. KINOSHITA, R. H. MULLER, AND C. W. TOBIAS.	59
LANDOLT	STOICHIOMETRY OF COPPER DISSOLUTION AT HIGH CURRENT-DENSITIES. K. KINOSHITA, D. LANDOLT, R. H. MULLER, AND C. W. TOBIAS.	55
LANGDON	EFFECT OF MICROSTRUCTURE ON THE DEFORMATION OF POLYCRYSTALLINE MGO. T. G. LANGDON AND J. A. PASK.	164
LANGDON	VOID FORMATION IN NICKEL AND SILVER DURING CREEP. T. G. LANGDON.	165
LANGDON	CREEP OF POLYCRYSTALLINE MAGNESIUM OXIDE. T. G. LANGDON, J. SHEROHMAN, AND J. A. PASK.	164
LANGDON	CREEP OF POLYCRYSTALLINE LIF. T. G. LANGDON AND D. R. CROPPER.	165
LANGDON	GRAIN-BOUNDARY SLIDING AT HIGH TEMPERATURES. T. G. LANGDON.	164
LAPORTE	EFFECT OF A STRAIN-INDUCED TRANSFORMATION ON THE TOUGHNESS OF HIGH-STRENGTH STEELS. C. P. LAPORTE, P. HEMMINGS, W. GERBERICH, AND M. D. MERZ.	136
LASER	TRAVELLING-LASER INTERFEROMETER FOR MASS-TRANSFER STUDIES. K. W. BEACH, R. H. MULLER, AND C. W. TOBIAS.	50
LEACHING	LEACHING OF CLAY WITH ACIDS. I. EDELWEISS AND O. REDLICH.	96
LEAD	LOW-ENERGY ELECTRON-DIFFRACTION STUDY OF SOLID AND LIQUID LEAD. R. M. GOODMAN AND G. A. SOMORJAI.	44
LEAD	HIGH-TEMPERATURE PHASE EQUILIBRIA IN THE LEAD-TITANATE - LEAD-ZIRCONATE SYSTEM. R. L. MOON AND R. M. FULRATH.	171
LEAD	THE MEAN DISPLACEMENT OF SURFACE ATOMS IN PALLADIUM AND LEAD SINGLE CRYSTALS. R. M. GOODMAN, H. H. FARRELL, AND G. A. SOMORJAI.	43
LEAD-BASE	SUPERCONDUCTING TRANSITION TEMPERATURES OF VARIOUS LEAD-BASE ALLOYS. E. NEMBACH.	147
LEAD-INDIUM	SUPERCONDUCTING TRANSITION TEMPERATURES OF LEAD-INDIUM ALLOYS. E. NEMBACH.	147
LEAD TITANATE	HIGH-TEMPERATURE PHASE EQUILIBRIA IN THE LEAD TITANATE - LEAD ZIRCONATE SYSTEM. R. L. MOON AND R. M. FULRATH.	171
LEAST-SQUARES	LEAST-SQUARES-ADJUSTED ASSIGNMENTS FOR THE ESR SPECTRA OF FREE RADICALS IN SOLUTION. A. BAUDER, R. PAO, AND R. J. MEYERS.	80
LEE	PROTON EXCHANGE FROM THE FIRST COORDINATION SPHERE OF HYDROLYTIC POLYMERS OF CHROMIUM(III). R. LEE.	8
LEE	PRODUCT ENERGY AND ANGULAR DISTRIBUTIONS FROM THE REACTION OF NITROGEN-MOLECULE ION WITH ISOTOPIC HYDROGEN MOLECULES. W. R. GENTRY, E. A. GISLASON, Y. T. LEE, B. H. MAHAN, AND C. W. TSAO.	75
LESTER	EVAPORATION MECHANISM OF SODIUM CHLORIDE. J. E. LESTER AND G. A. SOMORJAI.	39
LEVEL-CROSSING	LEVEL-CROSSING DETECTION OF NQR TRANSITIONS. J. C. KOO AND E. L. HAHN.	197
LEWIS	REACTION OF POTASSIUM GERMYL WITH LEWIS ACIDS. D. S. RUSTAD, P. M. KUZNESOF, AND W. L. JOLLY.	12
LI ATOM	CROSSED-MOLECULAR-BEAM INVESTIGATIONS OF THERMAL LI-ATOM REACTIONS. D. D. PARRISH AND R. R. HERM.	92
LIF	CREEP OF LIF SINGLE CRYSTALS. D. R. CROPPER AND J. A. PASK.	166
LIF	CREEP OF POLYCRYSTALLINE LIF. T. G. LANGDON AND D. R. CROPPER.	165
LIFETIME	COMMENTS ON SURFACE OXIDE FILMS AND THE LIFETIME OF VACANCIES IN THIN CRYSTALS. A. EIKUM AND G. THOMAS.	119
LIFETIMES	EFFECT OF COMPLEXING ON LIFETIMES OF WATER MOLECULES IN THE FIRST COORDINATION SPHERE OF NICKEL ION. K. KUSTIN.	8
LIFETIMES	RADIATIVE LIFETIMES OF EXCITED ELECTRONIC STATES OF ATOMS AND MOLECULES. P. T. CUNNINGHAM.	21
LIFETIMES	SPECTRA AND LIFETIMES OF GAS-PHASE FREE RADICALS AT VERY LOW CONCENTRATIONS. H. S. JOHNSTON, E. D. MORRIS, JR., T. T. PAUKERT, AND J. VAN DEN BOGAERDE.	87
LIM	EXCHANGE OF ENERGY BETWEEN TUNGSTEN AT HIGH TEMPERATURES AND GASES AT ROOM TEMPERATURE. M. J. LIM AND A. W. SEARCY.	155
LIPP	S4N4-H2SO4 SOLUTIONS. S. LIPP AND W. L. JOLLY.	14
LIQUID	STUDIES IN LIQUID AMMONIA. W. L. JOLLY.	17
LIQUID	KINETICS OF METAL-ACID REACTIONS IN LIQUID AMMONIA. L. PRIZANT AND W. L. JOLLY.	17

LIQUID LOW-ENERGY ELECTRON-DIFFRACTION STUDY OF SOLID AND LIQUID LEAD. R. M. GOODMAN AND G. A. SOMORJAI. 44
LIQUID POTENTIALS OF CELLS WITH LIQUID JUNCTIONS. W. H. SMYRL AND J. NEWMAN. 69
LIQUID A GLASS PH ELECTRODE IN LIQUID AMMONIA. R. SHIURBA AND W. L. JOLLY. 17
LIQUID VISCOSITY OF CONCENTRATED SOLUTIONS OF CALCIUM IN LIQUID AMMONIA FROM -40 TO -70 DEGREES C. J. P. EARHART AND C. W. TOBIAS. 53
LIQUID NMR SPECTRA OF CHLORINE-35 IN LIQUID VCL4 AND TICL4. D. W. PRATT AND R. J. MEYERS. 84
LIQUID VAPOR PRESSURE OF THALLIUM AND ACTIVITY MEASUREMENTS ON LIQUID SILVER-THALLIUM ALLOYS BY THE TORSION-EFFUSION METHOD. P. J. DESRE, D. T. HAWKINS, AND R. HULTGREN. 152
LIQUID REVERSIBILITY OF THE REACTION OF ALKALI METALS WITH LIQUID AMMONIA. E. J. KIRSCHKE AND W. L. JOLLY. 17
LIQUID HELIUM LIQUID-HELIUM FIELD-ION MICROSCOPE FOR RADIATION-DAMAGE INVESTIGATIONS. P. PETROFF AND J. WASHBURN. 109
LITHIUM EFFECT OF LITHIUM FLUORIDE ON THE DENSIFICATION OF MAGNESIUM OXIDE. P. E. HART AND J. A. PASK. 163
LOFGREN COMPILATIONS. N. LOFGREN. 24
LOU EVAPORATION MECHANISM OF GALLIUM ARSENIDE SINGLE CRYSTALS. C. LOU AND G. A. SOMORJAI. 39
LOW-ENERGY LOW-ENERGY ELECTRON-DIFFRACTION STUDY OF SOLID AND LIQUID LEAD. R. M. GOODMAN AND G. A. SOMORJAI. 44
LOW-ENERGY SEMICLASSICAL PHASE SHIFTS FOR LOW-ENERGY ORBITING COLLISIONS. R. R. HERM. 92
LOW-ENERGY LOW-ENERGY ELECTRON-DIFFRACTION STUDY OF ALPHA-ALUMINA (AL2O3) AND QUARTZ (SIO2) SURFACES. T. M. FRENCH, J. MORABITO, AND G. A. SOMORJAI. 44
LOW-ENERGY SURFACE STUDIES BY LOW-ENERGY ELECTRON DIFFRACTION. G. A. SOMORJAI. 43
LOW-ENERGY LOW-ENERGY ELECTRON-DIFFRACTION STUDY OF ALUMINUM. H. H. FARRELL AND G. A. SOMORJAI. 44
LOW-ENERGY LOW-ENERGY ELECTRON-DIFFRACTION STUDIES AT LOW TEMPERATURES. J. MORABITO AND G. A. SOMORJAI. 44
LOW-ENERGY LOW-ENERGY ELECTRON-DIFFRACTION STUDY OF SURFACE REACTIONS ON (100) PLATINUM. A. E. MORGAN AND G. A. SOMORJAI. 44
LOW-LYING LOW-LYING ENERGY LEVELS OF INTERMEDIATE-SPIN AND HIGH-SPIN FE3+. G. C. BRACKETT AND P. L. RICHARDS. 189
LOW-LYING LOW-LYING ENERGY LEVELS OF A SINGLE D-ELECTRON. R. R. JOYCE AND P. L. RICHARDS. 187
LOW-TEMPERATURE INORGANIC SYNTHESES IN LOW-TEMPERATURE MATRICES, NONAQUEOUS SOLVENTS, AND COCONDENSATION SYSTEMS. D. SOLAN, J. L.-F. WANG, AND B. A. KING. 21
LOW-TEMPERATURE THE LOW-TEMPERATURE FACILITY. E. NEMBACH. 147
LOW-TEMPERATURE LOW-TEMPERATURE HEAT-CAPACITY OF AUCU. D. T. HAWKINS AND R. HULTGREN. 152
LOY NONLINEAR-OPTICS EXPERIMENTS. M. LOY, D. FARIES, J. SHAHAM, AND R. RIBOTTA. 195
LYON STUDIES OF THE CLEAN (100), (111), AND (110) CRYSTAL FACES OF PLATINUM. H. B. LYON AND G. A. SOMORJAI. 43
MAGNESIA PHASE DISTRIBUTION IN MULTIPHASE MAGNESIA AND FORSTERITE BODIES. A. P. RAJU, I. A. AKSAY, AND J. A. PASK. 163
MAGNESIUM MAGNESIUM OXIDE SPECTRUM AND CALCULATIONS. D. GREEN. 23
MAGNESIUM EFFECT OF LITHIUM FLUORIDE ON THE DENSIFICATION OF MAGNESIUM OXIDE. P. E. HART AND J. A. PASK. 163
MAGNESIUM CREEP OF POLYCRYSTALLINE MAGNESIUM OXIDE. T. G. LANGDON, J. SHEROHMAN, AND J. A. PASK. 164
MAGNETIC MAGNETIC PROPERTIES OF SOLIDS. A. M. PORTIS. 185
MAGNETIC PROTON MAGNETIC RESONANCE SPECTRA OF RHODIUM AND IRIDIUM COMPLEXES IN SULFURIC ACID. D. N. HENDRICKSON AND W. L. JOLLY. 16
MAGNETICAL MAGNETICAL AND ELECTRIC PROPERTIES OF MNAU. A. M. PORTIS. 185
MAGUIRE SULFUR NITROGEN CHLORIDES. W. L. JOLLY AND K. D. MAGUIRE. 15
MAHAN RATE OF ATTACHMENT OF GASEOUS ELECTRONS TO NITROGEN DIOXIDE. B. H. MAHAN AND I. C. WALKER. 74
MAHAN PRODUCT ENERGY AND ANGULAR DISTRIBUTIONS FROM THE REACTION OF NITROGEN-MOLECULE ION WITH ISOTOPIC HYDROGEN MOLECULES. W. R. GENTRY, E. A. GISLASON, Y. T. LEE, B. H. MAHAN, AND C. W. TSAO. 75
MAHAN DYNAMICS OF THE REACTION OF METHANE WITH NITROGEN-MOLECULE ION. E. A. GISLASON, C. W. TSAO, B. H. MAHAN, AND A. WERNER. 77
MAHAN MASS SPECTROMETRY OF HIGH-PRESSURE IONIZED GASES. M. MOSESMAN AND B. H. MAHAN. 78

MAHAN	RESEARCH PLANS FOR 1968. B. H. MAHAN.	80
MAHAN	GASEOUS-ION RECOMBINATION. V. B. H. MAHAN.	73
MAHAN	THE COLLISIONAL-RADIATIVE REACTION OF SINGLET-DELTA OXYGEN. A. M. FALICK AND B. H. MAHAN.	74
MAHAN	ION-CYCLOTRON RESONANCE MASS SPECTROMETRY. R. HORTON, R. M. LAMBERT, AND B. H. MAHAN.	77
MAHAN	INELASTIC SCATTERING OF NITROGEN-MOLECULE ION BY HELIUM. W. R. GENTRY, E. A. GISLASON, B. H. MAHAN, AND C. W. TSAO.	74
MAHAN	MOLECULAR FRAGMENTATION BY ELECTRON IMPACT. M. H. CHENG AND B. H. MAHAN.	77
MAHAN	1967 PUBLICATIONS. B. H. MAHAN AND ASSOCIATES.	80
MARAGING	STRUCTURE AND PROPERTIES OF FE/NI/CO/TI MARAGING STEEL. I. L. CHENG AND G. THOMAS.	123
MARATHE	CURRENT DISTRIBUTION ON A ROTATING-DISK ELECTRODE. V. MARATHE AND J. NEWMAN.	63
MARTENSITIC	QUANTITATIVE INVESTIGATION OF THE STRAIN-INDUCED MARTENSITIC TRANSFORMATION IN HIGH-STRENGTH STEELS. B. DE MIRAMON AND M. D. MERZ.	131
MASS	FUNDAMENTAL STUDIES OF IONIC MASS TRANSFER. C. W. TOBIAS.	50
MASS	MASS TRANSFER TO THE REAR OF A CYLINDER AT HIGH SCHMITT NUMBERS. J. NEWMAN.	70
MASS	MASS TRANSFER AND ELECTROCHEMICAL SYSTEMS. J. NEWMAN.	69
MASS SPECTROMETRY	MASS SPECTROMETRY OF HIGH-PRESSURE IONIZED GASES. M. MOSESMAN AND B. H. MAHAN.	78
MASS SPECTROMETRY	GAS ANALYSIS BY MODULATED MOLECULAR-BEAM MASS SPECTROMETRY. D. R. OLANDER AND W. WADDEL.	99
MASS SPECTROMETRY	ION-CYCLOTRON RESONANCE MASS SPECTROMETRY. R. HORTON, R. M. LAMBERT, AND B. H. MAHAN.	77
MASS TRANSFER	TRAVELLING LASER INTERFEROMETER FOR MASS-TRANSFER STUDIES. K. W. BEACH, R. H. MULLER, AND C. W. TOBIAS.	50
MASS TRANSFER	CURRENT AND POTENTIAL DISTRIBUTION IN CONVECTIVE MASS TRANSFER AT PLANE-PLATE ELECTRODES. J. R. SELMAN AND C. W. TOBIAS.	50
MATERIALS	HIGH-STRENGTH MATERIALS. E. R. PARKER AND V. F. ZACKAY.	131
MATERIALS	MICROSTRUCTURE AND BEHAVIOR OF CERAMIC MATERIALS -- GLASS AND CERAMIC-METAL SYSTEMS. J. A. PASK.	161
MATRICES	SPECTROSCOPIC INVESTIGATIONS OF HIGH-TEMPERATURE SPECIES TRAPPED AT LOW TEMPERATURES IN INERT MATRICES. J. L.-F. WANG, B. A. KING, AND C. B. MEYER.	21
MATRICES	INORGANIC SYNTHESES IN LOW-TEMPERATURE MATRICES, NONAQUEOUS SOLVENTS, AND COCONDENSATION SYSTEMS. D. SOLAN, J. L.-F. WANG, AND B. A. KING.	21
MEASUREMENTS	VAPOR PRESSURE OF THALLIUM AND ACTIVITY MEASUREMENTS ON LIQUID SILVER-THALLIUM ALLOYS BY THE TORSION-EFFUSION METHOD. P. J. DESRE, D. T. HAWKINS, AND R. HULTGREN.	152
MEASUREMENTS	ZERO-FIELD, FREE-PRECESSION MEASUREMENTS OF THE HYPERFINE INTERACTION IN CESIUM-33 VAPOR. J. W. SHANER, S. A. MILLER, AND E. L. HAHN.	197
MECHANICAL	EFFECT OF TEST TEMPERATURE ON THE MECHANICAL PROPERTIES OF METASTABLE AUSTENITIC STEELS. G. R. CHANANI AND M. D. MERZ.	133
MELTING	MELTING CURVE OF HELIUM-4. N. E. PHILLIPS, J. K. HOFFER, AND C. G. WATERFIELD.	29
MENISCUS	EFFECT OF PERIODIC MENISCUS DISPLACEMENTS ON THE PERFORMANCE OF POROUS GAS ELECTRODES. J. P. ROUSSILLON AND E. A. GRENS II.	53
MERRIAM	SUPERCONDUCTIVITY IN ALLOY SYSTEMS. M. F. MERRIAM.	146
MERRIAM	RESEARCH PLANS FOR 1968. M. F. MERRIAM AND R. HAMMOND.	148
MERRIAM	1967 PUBLICATIONS. M. MERRIAM AND ASSOCIATES.	149
MERZ	EFFECT OF TEST TEMPERATURE ON THE MECHANICAL PROPERTIES OF METASTABLE AUSTENITIC STEELS. G. R. CHANANI AND M. D. MERZ.	133
MERZ	NOTCH-TOUGHNESS VARIATIONS IN STEELS WITH THE SAME TENSILE PROPERTIES. Y. KATZ AND M. D. MERZ.	135
MERZ	EFFECT OF A STRAIN-INDUCED TRANSFORMATION ON THE TOUGHNESS OF HIGH-STRENGTH STEELS. C. P. LAPORTE, P. HEMMINGS, W. GERBERICH, AND M. D. MERZ.	136
MERZ	QUANTITATIVE INVESTIGATION OF THE STRAIN-INDUCED MARTENSITIC TRANSFORMATION IN HIGH-STRENGTH STEELS. B. DE MIRAMON AND M. D. MERZ.	131
MERZ	MICROSTRUCTURE AND PLANE-STRAIN FRACTURE TOUGHNESS OF HIGH-STRENGTH ALUMINUM ALLOYS. P. J. GUEST AND M. D. MERZ.	135
METAL	ROTATING-DISK SYSTEM FOR METAL DEPOSITION FROM NONAQUEOUS SOLVENTS. F. G. K. BAUCKE, D. LANDOLT, AND C. W. TOBIAS.	55

METAL	REACTIONS OF SILANE, GERMANE, AND STANNANE WITH METAL-AMMONIA AND AMIDE-AMMONIA SOLUTIONS. D. S. RUSTAD AND W. L. JOLLY.	11
METAL	REFRACTORY METAL OXIDATION. J. S. SCHOFILL AND D. R. OLANDER.	104
METAL	THERMODYNAMICS OF METAL SYSTEMS. R. HULTGREN.	151
METAL-ACID	KINETICS OF METAL-ACID REACTIONS IN LIQUID AMMONIA. L. PRIZANT AND W. L. JOLLY.	17
METALS	HEAT CAPACITY OF METALS UNDER PRESSURE. S. S. B. WANG, M. M. CONWAY, AND N. E. PHILLIPS.	33
METALS	HEAT CAPACITIES OF METALS UNDER PRESSURE. W. STARK AND G. JURA.	37
METALS	REVERSIBILITY OF THE REACTION OF ALKALI METALS WITH LIQUID AMMONIA. E. J. KIRSCHKE AND W. L. JOLLY.	17
METASTABLE	EFFECT OF TEST TEMPERATURE ON THE MECHANICAL PROPERTIES OF METASTABLE AUSTENITIC STEELS. G. R. CHANANI AND M. D. MERZ.	133
METHANE	DYNAMICS OF THE REACTION OF METHANE WITH NITROGEN-MOLECULE ION. E. A. GISLASON, C. W. TSAO, B. H. MAHAN, AND A. WERNER.	77
METHYL-SUBSTITUTED	ESR SPECTRA OF THE RADICAL ANIONS OF METHYL-SUBSTITUTED NITROSOBENZENES. C. L. TALCOTT AND R. J. MYERS.	84
MEYER	SPECTROSCOPIC INVESTIGATIONS OF HIGH-TEMPERATURE SPECIES TRAPPED AT LOW TEMPERATURES IN INERT MATRICES. J. L.-F. WANG, B. A. KING, AND C. B. MEYER.	21
MEYERS	LEAST-SQUARES-ADJUSTED ASSIGNMENTS FOR THE ESR SPECTRA OF FREE RADICALS IN SOLUTION. A. BAUDER, R. PAO, AND R. J. MEYERS.	80
MEYERS	NMR SPECTRA OF CHLORINE-35 IN LIQUID VCL4 AND TICL4. D. W. PRATT AND R. J. MEYERS.	84
MGO	DIFFUSION OF IRON AND NICKEL INTO SINGLE-CRYSTAL MGO. S. L. BLANK AND J. A. PASK.	161
MGO	EFFECT OF MICROSTRUCTURE ON THE DEFORMATION OF POLYCRYSTALLINE MGO. T. G. LANGDON AND J. A. PASK.	164
MGO	PLASTIC BUCKLING AND CREEP OF MGO SINGLE CRYSTALS. D. R. CROPPER AND J. A. PASK.	167
MICROSCOPE	ELECTRON MICROSCOPE OBSERVATIONS OF TWINNING AND PHASE TRANSFORMATIONS IN INS CRYSTALS. A. G. FITZGERALD AND G. THOMAS.	125
MICROSCOPE	LIQUID-HELIUM FIELD-ION MICROSCOPE FOR RADIATION-DAMAGE INVESTIGATIONS. P. PETROFF AND J. WASHBURN.	109
MICROSCOPE	FIELD-ION MICROSCOPE INVESTIGATION OF RADIATION-DAMAGE IN IRIDIUM BOMBARDED WITH 10-MEV PROTONS. P. PETROFF AND J. WASHBURN.	109
MICROSCOPY	ELECTRON MICROSCOPY AT HIGH VOLTAGES. G. THOMAS.	120
MICROSPHEROID	RADIOFREQUENCY PLASMA MICROSPHEROIDIZATION OF CERAMICS. R. T. TREMPER AND R. M. FULRATH.	175
MICROSTRUCTURE	MICROSTRUCTURE AND BEHAVIOR OF CERAMIC MATERIALS -- GLASS AND CERAMIC-METAL SYSTEMS. J. A. PASK.	161
MICROSTRUCTURE	EFFECT OF MICROSTRUCTURE ON THE DEFORMATION OF POLYCRYSTALLINE MGO. T. G. LANGDON AND J. A. PASK.	164
MICROSTRUCTURE	MICROSTRUCTURE AND PLANE-STRAIN FRACTURE TOUGHNESS OF HIGH-STRENGTH ALUMINUM ALLOYS. P. J. GUEST AND M. D. MERZ.	135
MICROSTRUCTURES	DEVELOPMENT AND BEHAVIOR OF MICROSTRUCTURES IN CERAMIC SYSTEMS. R. M. FULRATH.	171
MILIOS	MOVING-BOUNDARY TRANSFERENCE NUMBERS. P. MILIOS AND J. NEWMAN.	62
MILLER	ZERO-FIELD, FREE-PRECESSION MEASUREMENTS OF THE HYPERFINE INTERACTION IN CESIUM-33 VAPOR. J. W. SHANER, S. A. MILLER, AND E. L. HAHN.	197
MNAU	MAGNETICAL AND ELECTRIC PROPERTIES OF MNAU. A. M. PORTIS.	185
MODULATED	GAS ANALYSIS BY MODULATED MOLECULAR-BEAM MASS SPECTROMETRY. D. R. OLANDER AND W. WADDEL.	99
MODULATED	DISSOCIATION OF HYDROGEN ON TANTALUM USING A MODULATED MOLECULAR-BEAM TECHNIQUE. R. A. KRAKOWSKI AND D. R. OLANDER.	101
MOLECULAR	MOLECULAR STRUCTURE OF SODIUM α-OXYHYPONITRITE. D. N. HENDRICKSON.	17
MOLECULAR	SURFACE-PHASE TRANSFORMATIONS ON A MOLECULAR SURFACE. J. J. BURTON AND G. JURA.	35
MOLECULAR	THERMODYNAMICS AND MOLECULAR STATE OF STRONG ACIDS. R. W. DUERST, W. E. GARGRAVE, AND O. REDLICH.	94
MOLECULAR	MOLECULAR FRAGMENTATION BY ELECTRON IMPACT. M. H. CHENG AND B. H. MAHAN.	77
MOLECULAR-BEAM	DETERMINATION OF THE ELECTRONIC PARTITION FUNCTION OF SCANDIUM MONOFLUORIDE BY MOLECULAR-BEAM FLUORESCENCE. D. GREEN.	23

MOLECULAR-BEAM GAS ANALYSIS BY MODULATED MOLECULAR-BEAM MASS SPECTROMETRY. D. R. OLANDER AND W. WADDEL. 99
MOLECULAR-BEAM CHARACTERIZATION OF MOLECULAR-BEAM SOURCES. R. JONES AND D. R. OLANDER. 100
MOLECULAR-BEAM DISSOCIATION OF HYDROGEN ON TANTALUM USING A MODULATED MOLECULAR-BEAM TECHNIQUE. R. A. KRAKOWSKI AND D. R. OLANDER. 101
MOLECULES EFFECT OF COMPLEXING ON LIFETIMES OF WATER MOLECULES IN THE FIRST COORDINATION SPHERE OF NICKEL ION. K. KUSTIN. 8
MOLECULES RADIATIVE LIFETIMES OF EXCITED ELECTRONIC STATES OF ATOMS AND MOLECULES. P. T. CUNNINGHAM. 21
MOLECULES PRODUCT ENERGY AND ANGULAR DISTRIBUTIONS FROM THE REACTION OF NITROGEN-MOLECULE ION WITH ISOTOPIC HYDROGEN MOLECULES. W. R. GENTRY, E. A. GISLASON, Y. T. LEE, B. H. MAHAN, AND C. W. TSAO. 75
MOLECULES PSEUDOPOTENTIAL CALCULATIONS ON ATOMS AND DIATOMIC MOLECULES. J. TELLINGHUISEN. 22
MOLYBDENUM HEAT CAPACITY OF MOLYBDENUM. J. C. F. BROCK AND N. E. PHILLIPS. 32
MOMENTUM THE FERMI MOMENTUM OF ALUMINUM FROM 0 TO 100 KBARS. J. J. BURTON AND G. JURA. 34
MONOFLUORIDE DETERMINATION OF THE ELECTRONIC PARTITION FUNCTION OF SCANDIUM MONOFLUORIDE BY MOLECULAR-BEAM FLUORESCENCE. D. GREEN. 23
MOON HIGH-TEMPERATURE PHASE EQUILIBRIA IN THE LEAD TITANATE - LEAD ZIRCONATE SYSTEM. R. L. MOON AND R. M. FULRATH. 171
MORABITO LOW-ENERGY ELECTRON-DIFFRACTION STUDY OF ALPHA-ALUMINA (AL2O3) AND QUARTZ (SIO2) SURFACES. T. M. FRENCH, J. MORABITO, AND G. A. SOMORJAI. 44
MORABITO LOW-ENERGY ELECTRON-DIFFRACTION STUDIES AT LOW TEMPERATURES. J. MORABITO AND G. A. SOMORJAI. 44
MORGAN LOW-ENERGY ELECTRON-DIFFRACTION STUDY OF SURFACE REACTIONS ON (100) PLATINUM. A. E. MORGAN AND G. A. SOMORJAI. 44
MORRIS SPECTRA AND LIFETIMES OF GAS-PHASE FREE RADICALS AT VERY LOW CONCENTRATIONS. H. S. JOHNSTON, E. D. MORRIS, JR., T. T. PAUKERT, AND J. VAN DEN BOGAERDE. 87
MOSESMAN MASS SPECTROMETRY OF HIGH-PRESSURE IONIZED GASES. M. MOSESMAN AND B. H. MAHAN. 78
MOVEMENT STRESS-INDUCED MOVEMENT OF TWIN BOUNDARIES IN ZINC. R. E. COOPER AND J. WASHBURN. 107
MOVING-BOUNDARY MOVING-BOUNDARY TRANSFERENCE NUMBERS. P. MILIOS AND J. NEWMAN. 62
MULLER OPTICAL STUDIES OF INTERFACIAL PHENOMENA. R. H. MULLER AND R. F. STEIGER. 47
MULLER SURFACE CALORIMETRY. R. H. MULLER AND R. C. GUPTA. 49
MULLER ELECTRODE POTENTIALS AND SURFACE CHARACTERISTICS IN HIGH-CURRENT-DENSITY COPPER DISSOLUTION. D. LANDOLT, K. KINOSHITA, R. MULLER, AND C. W. TOBIAS. 56
MULLER OPTICAL STUDY OF CATHODIC GAS EVOLUTION DURING HIGH-CURRENT-DENSITY ELECTROLYSIS. D. LANDOLT, K. KINOSHITA, R. H. MULLER, AND C. W. TOBIAS. 59
MULLER RESEARCH PLANS FOR 1968. R. H. MULLER. 49
MULLER TRAVELLING LASER INTERFEROMETER FOR MASS-TRANSFER STUDIES. K. W. BEACH, R. H. MULLER, AND C. W. TOBIAS. 50
MULLER STOICHIOMETRY OF COPPER DISSOLUTION AT HIGH CURRENT DENSITIES. K. KINOSHITA, D. LANDOLT, R. H. MULLER, AND C. W. TOBIAS. 55
MULLER 1967 PUBLICATIONS. R. H. MULLER AND ASSOCIATES. 50
MULTIPHASE PHASE DISTRIBUTION IN MULTIPHASE MAGNESIA AND FORSTERITE BODIES. A. P. RAJU, I. A. AKSAY, AND J. A. PASK. 163
MURTY EFFECT OF INITIAL DISLOCATION DENSITY ON SINGLE-SLIP STRAIN HARDENING OF COPPER. J. WASHBURN AND G. MURTY. 107
MYERS TEMPERATURE DEPENDENCE OF THE EPR SPECTRUM OF HEXAQUACOPPER-II IN WATER. J. J. CHANG AND R. J. MYERS. 82
MYERS ESR SPECTRA NEAR 1 DEGREE KELVIN. D. W. PRATT, A. JINDO, W. T. BATCHELDER, AND R. J. MYERS. 83
MYERS ESR SPECTRA OF THE RADICAL ANIONS OF METHYL-SUBSTITUTED NITROSOBENZENES. C. L. TALCOTT AND R. J. MYERS. 84
MYERS RESEARCH PLANS FOR 1968. R. J. MYERS. 86
MYERS 1967 PUBLICATIONS. R. J. MYERS. 86
NB-SN-C INTERMETALLIC AND CERAMIC COMPOUNDS -- NB-SN-C SYSTEM. J. CHABANNE, R. GOOLSBY, AND R. JONES. 145
NEMBACH THE LOW-TEMPERATURE FACILITY. E. NEMBACH. 147
NEMBACH SUPERCONDUCTING TRANSITION TEMPERATURES OF VARIOUS LEAD-BASE ALLOYS. E. NEMBACH. 147

NEMBACH	SUPERCONDUCTING TRANSITION TEMPERATURES OF LEAD-INDIUM ALLOYS. E. NEMBACH.	147
NEWBURY	VAPOR SPECIES OF THE BARIUM-OXYGEN SYSTEM. R. S. NEWBURY, G. W. BARTON, JR., AND A. W. SEARCY.	159
NEWMAN	TRANSPORT PROPERTIES OF CONCENTRATED ELECTROLYTIC SOLUTIONS. T. W. CHAPMAN AND J. NEWMAN.	61
NEWMAN	MOVING-BOUNDARY TRANSFERENCE NUMBERS. P. MILIOS AND J. NEWMAN.	62
NEWMAN	CURRENT DISTRIBUTION ON A ROTATING-DISK ELECTRODE. V. MARATHE AND J. NEWMAN.	63
NEWMAN	FLOW TUNNEL WITH MOVING WALLS. P. H. SIH AND J. NEWMAN.	65
NEWMAN	LAMINAR FREE CONVECTION AT A VERTICAL PLATE IN THE PRESENCE OF SUPPORTING ELECTROLYTE. J. R. SELMAN AND J. NEWMAN.	66
NEWMAN	POTENTIALS OF CELLS WITH LIQUID JUNCTIONS. W. H. SMYRL AND J. NEWMAN.	69
NEWMAN	MASS TRANSFER TO THE REAR OF A CYLINDER AT HIGH SCHMITT NUMBERS. J. NEWMAN.	70
NEWMAN	CONCENTRATION PROFILE AND DIFFUSION COEFFICIENT IN A STAGNANT DIFFUSION CELL. L. HSUEH AND J. NEWMAN.	63
NEWMAN	MASS TRANSFER AND ELECTROCHEMICAL SYSTEMS. J. NEWMAN.	69
NEWMAN	NUMERICAL SOLUTION OF COUPLED ORDINARY DIFFERENTIAL EQUATIONS. J. NEWMAN.	70
NEWMAN	RESEARCH PLANS FOR 1968. J. NEWMAN.	70
NEWMAN	1967 PUBLICATIONS. J. NEWMAN AND ASSOCIATES.	71
NGO	THERMODYNAMIC CALCULATION METHODS. V. B. T. NGO AND O. REDLICH.	95
NI-RH	HEAT CAPACITY OF A NI-RH ALLOY. N. E. PHILLIPS, B. B. TRIPLETT, AND D. W. WOODY.	28
NICHOLSON	DIFFERENTIAL THERMAL CALORIMETRY. P. S. NICHOLSON AND R. M. FULRATH.	173
NICKEL	EFFECT OF COMPLEXING ON LIFETIMES OF WATER MOLECULES IN THE FIRST COORDINATION SPHERE OF NICKEL ION. K. KUSTIN.	8
NICKEL	DIFFUSION OF IRON AND NICKEL INTO SINGLE-CRYSTAL MGO. S. L. BLANK AND J. A. PASK.	161
NICKEL	VOID FORMATION IN NICKEL AND SILVER DURING CREEP. T. G. LANGDON.	165
NITRIDE	ADDUCTS OF SULFUR NITRIDE WITH BORON TRIHALIDES AND ANTIMONY PENTACHLORIDE. K. J. WYNNE AND W. L. JOLLY.	14
NITRO	THE AQUATION OF THE NITRO PENTAAMMINE COBALT(III) ION IN SULFURIC ACID SOLUTIONS. A. D. HARRIS, R. STEWART, D. HENDRICKSON, AND W. L. JOLLY.	16
NITROGEN	SULFUR NITROGEN CHEMISTRY. W. L. JOLLY.	14
NITROGEN	STUDIES OF MISCELLANEOUS NITROGEN COMPOUNDS.	17
NITROGEN	NITROGEN NMR CHEMICAL SHIFTS. D. N. HENDRICKSON AND P. M. KUZNESOF.	18
NITROGEN	RATE OF ATTACHMENT OF GASEOUS ELECTRONS TO NITROGEN DIOXIDE. B. H. MAHAN AND I. C. WALKER.	74
NITROGEN	SULFUR NITROGEN CHLORIDES. W. L. JOLLY AND K. D. MAGUIRE.	15
NITROGEN MOLECULE	PRODUCT ENERGY AND ANGULAR DISTRIBUTIONS FROM THE REACTION OF NITROGEN-MOLECULE ION WITH ISOTOPIC HYDROGEN MOLECULES. W. R. GENTRY, E. A. GISLASON, Y. T. LEE, B. H. MAHAN, AND C. W. TSAO.	75
NITROGEN MOLECULE	DYNAMICS OF THE REACTION OF METHANE WITH NITROGEN-MOLECULE ION. E. A. GISLASON, C. W. TSAO, B. H. MAHAN, AND A. WERNER.	77
NITROGEN MOLECULE	INELASTIC SCATTERING OF NITROGEN-MOLECULE ION BY HELIUM. W. R. GENTRY, E. A. GISLASON, B. H. MAHAN, AND C. W. TSAO.	74
NITROSOBENZENES	ESR SPECTRA OF THE RADICAL ANIONS OF METHYL-SUBSTITUTED NITROSOBENZENES. C. L. TALCOTT AND R. J. MYERS.	84
NMR	OXYGEN-17 NMR STUDIES OF WATER EXCHANGE OF PARTIALLY COMPLEXED VANADYL ION. K. WUTHRICH.	7
NMR	NMR RELAXATION OF OXYGEN-17 BY FERRIC ION IN AQUEOUS SOLUTION. M. R. JUDKINS.	7
NMR	NITROGEN NMR CHEMICAL SHIFTS. D. N. HENDRICKSON AND P. M. KUZNESOF.	18
NMR	NMR SPECTRA OF CHLORINE-35 IN LIQUID VCL4 AND TICL4. D. W. PRATT AND R. J. MEYERS.	84
NMR-NQR	A SCHEME FOR NMR-NQR DETECTION IN SOLIDS -- C13 AND DEUTERIUM IN PARADICHLOROBENZENE. M. SCHWAB AND E. L. HAHN.	197
NONAQUEOUS	ELECTROCHEMISTRY IN NONAQUEOUS SOLVENTS. C. W. TOBIAS.	53
NONAQUEOUS	ROTATING-DISK SYSTEM FOR METAL DEPOSITION FROM NONAQUEOUS SOLVENTS. F. G. K. BAUCKE, D. LANDOLT, AND C. W. TOBIAS.	55
NONAQUEOUS	INORGANIC SYNTHESES IN LOW-TEMPERATURE MATRICES, NONAQUEOUS SOLVENTS, AND COCONDENSATION SYSTEMS. D. SOLAN, J. L.-F. WANG, AND B. A. KING.	21

NONEQUILIBRIUM EQUILIBRIUM AND NONEQUILIBRIUM SUBLIMATION OF ZINC SULFIDE AND OF CADMIUM TELLURIDE. B. A. H. BLANK AND A. W. SEARCY. 159
NONLINEAR OPTICS NONLINEAR-OPTICS THEORY. Y. R. SHEN. 195
NONLINEAR OPTICS NONLINEAR-OPTICS EXPERIMENTS. M. LOY, D. FARIES, J. SHAHAM, AND R. RIBOTTA. 195
NOTCH TOUGHNESS NOTCH-TOUGHNESS VARIATIONS IN STEELS WITH THE SAME TENSILE PROPERTIES. Y. KATZ AND M. D. MERZ. 135
NO2 KINETICS OF NO2 ELECTRONIC FLUORESCENCE. S. E. SCHWARTZ AND H. S. JOHNSTON. 87
NQR LEVEL-CROSSING DETECTION OF NQR TRANSITIONS. J. C. KOO AND E. L. HAHN. 197
NUCLEAR NUCLEAR-SPIN DOUBLE RESONANCE IN KH2PO4. D. STEHLIK. 198
NUCLEAR NUCLEAR RESONANCE IN FERROMAGNETIC ALLOYS. A. M. PORTIS. 185
NUCLEAR NUCLEAR DOUBLE RESONANCE IN FERROMAGNETIC ALLOYS. A. M. PORTIS. 185
NUCLEAR SPIN NUCLEAR-SPIN INTERACTIONS. E. L. HAHN. 197
NUMERICAL NUMERICAL SOLUTION OF COUPLED ORDINARY DIFFERENTIAL EQUATIONS. J. NEWMAN. 70
O-OXYHYPONITRITE MOLECULAR STRUCTURE OF SODIUM O-OXYHYPONITRITE. D. N. HENDRICKSON. 17
OKAMOTO INDICES OF PLANES AND DIRECTIONS IN HCP CRYSTALS. P. R. OKAMOTO AND G. THOMAS. 126
OLANDER GAS ANALYSIS BY MODULATED MOLECULAR-BEAM MASS SPECTROMETRY. D. R. OLANDER AND W. WADDEL. 99
OLANDER CHARACTERIZATION OF MOLECULAR-BEAM SOURCES. R. JONES AND D. R. OLANDER. 100
OLANDER DISSOCIATION OF HYDROGEN ON TANTALUM USING A MODULATED MOLECULAR-BEAM TECHNIQUE. R. A. KRAKOWSKI AND D. R. OLANDER. 101
OLANDER VISCOSITY DETERMINATIONS. J. FINUCANE AND D. R. OLANDER. 102
OLANDER CONDENSATION-ENHANCED VAPORIZATION OF HIGH-TEMPERATURE SOLIDS. R. OMBERG AND D. R. OLANDER. 103
OLANDER REFRACTORY-METAL OXIDATION. J. S. SCHOFILL AND D. R. OLANDER. 104
OLANDER TRANSIENT DIFFUSION IN A COMPOSITE SLAB. P. CONCUS AND D. R. OLANDER. 102
OLANDER RESEARCH PLANS FOR 1968. D. R. OLANDER. 104
OLANDER 1967 PUBLICATIONS. D. R. OLANDER AND ASSOCIATES. 105
OLSON SINGLE-PHASE AND POLYPHASE ALLOY SYSTEMS. M. SUENAGA, J. OLSON, AND K. RALLS. 141
OMBERG CONDENSATION-ENHANCED VAPORIZATION OF HIGH-TEMPERATURE SOLIDS. R. OMBERG AND D. R. OLANDER. 103
OPTICAL OPTICAL STUDIES OF INTERFACIAL PHENOMENA. R. H. MULLER AND R. F. STEIGER. 47
OPTICAL OPTICAL STUDY OF CATHODIC GAS EVOLUTION DURING HIGH-CURRENT-DENSITY ELECTROLYSIS. D. LANDOLT, K. KINOSHITA, R. H. MULLER, AND C. W. TOBIAS. 59
OPTICAL OPTICAL PROPERTIES OF SOLIDS. R. ZUCCA AND Y. R. SHEN. 195
ORBITING SEMICLASSICAL PHASE SHIFTS FOR LOW-ENERGY ORBITING COLLISIONS. R. R. HERM. 92
ORDINARY NUMERICAL SOLUTION OF COUPLED ORDINARY DIFFERENTIAL EQUATIONS. J. NEWMAN. 70
ORR THERMODYNAMIC STUDY OF THE HEAT OF ORDERING IN CUPT. G. W. GEIKEN, R. L. ORR, AND R. HULTGREN. 151
ORR EVALUATION OF THERMODYNAMIC DATA. R. HULTGREN, M. GLEISER, K. K. KELLEY, R. L. ORR, E. PLAZA, AND G. SOMAYAJULU. 152
OVERAGING ON FATIGUE-INDUCED REVERSION AND OVERAGING IN DISPERSION-STRENGTHENED ALLOY SYSTEMS. C. LAIRD AND G. THOMAS. 119
OXIDATION REFRACTORY-METAL OXIDATION. J. S. SCHOFILL AND D. R. OLANDER. 104
OXIDE MAGNESIUM OXIDE SPECTRUM AND CALCULATIONS. D. GREEN. 23
OXIDE EFFECT OF LITHIUM FLUORIDE ON THE DENSIFICATION OF MAGNESIUM OXIDE. P. E. HART AND J. A. PASK. 163
OXIDE PLASTIC DEFORMATION OF CUPROUS OXIDE. G. VAGNARD AND J. WASHBURN. 107
OXIDE COMMENTS ON SURFACE OXIDE FILMS AND THE LIFETIME OF VACANCIES IN THIN CRYSTALS. A. EIKUM AND G. THOMAS. 119
OXIDE CREEP OF POLYCRYSTALLINE MAGNESIUM OXIDE. T. G. LANGDON, J. SHEROHMAN, AND J. A. PASK. 164
OXYGEN THE COLLISIONAL-RADIATIVE REACTION OF SINGLET-DELTA OXYGEN. A. M. FALICK AND B. H. MAHAN. 74
OXYGEN-17 OXYGEN-17 NMR STUDIES OF WATER EXCHANGE OF PARTIALLY COMPLEXED VANADYL ION. K. WUTHRICH. 7
OXYGEN-17 NMR RELAXATION OF OXYGEN-17 BY FERRIC ION IN AQUEOUS SOLUTION. M. R. JUDKINS. 7

PALLADIUM	THE MEAN DISPLACEMENT OF SURFACE ATOMS IN PALLADIUM AND LEAD SINGLE CRYSTALS. R. M. GOODMAN, H. H. FARRELL, AND G. A. SOMORJAI.	43
PAO	LEAST-SQUARES-ADJUSTED ASSIGNMENTS FOR THE ESR SPECTRA OF FREE RADICALS IN SOLUTION. A. BAUDER, R. PAO, AND R. J. MEYERS.	80
PARADICHLOROBENZENE	A SCHEME FOR NMR-NQR DETECTION IN SOLIDS -- C13 AND DEUTERIUM IN PARADICHLOROBENZENE. M. SCHWAB AND E. L. HAHN.	197
PARKER	HIGH-STRENGTH MATERIALS. E. R. PARKER AND V. F. ZACKAY.	131
PARKER	RESEARCH PLANS FOR 1968. V. F. ZACKAY AND E. R. PARKER.	138
PARKER	1967 PUBLICATIONS. E. R. PARKER, V. F. ZACKAY AND ASSOCIATES.	139
PARKER	HIGH-FIELD SUPERCONDUCTIVITY. L. BREWER, E. R. PARKER, AND V. F. ZACKAY.	141
PARKER	RESEARCH PLANS FOR 1968. L. BREWER, E. R. PARKER, AND V. F. ZACKAY.	146
PARKER	1967 PUBLICATIONS. L. BREWER, E. R. PARKER, V. F. ZACKAY AND ASSOCIATES.	146
PARKS	CAPTURE RADIUS FOR ION RECOMBINATION. E. K. PARKS.	73
PARRISH	CROSSED-MOLECULAR-BEAM INVESTIGATION OF INELASTIC SCATTERING BY TIME-OF-FLIGHT ANALYSIS. D. D. PARRISH AND R. R. HERM.	93
PARRISH	CROSSED-MOLECULAR-BEAM INVESTIGATIONS OF THERMAL LI-ATOM REACTIONS. D. D. PARRISH AND R. R. HERM.	92
PARTITION	DETERMINATION OF THE ELECTRONIC PARTITION FUNCTION OF SCANDIUM MONOFLUORIDE BY MOLECULAR-BEAM FLUORESCENCE. D. GREEN.	23
PASK	DIFFUSION OF IRON AND NICKEL INTO SINGLE-CRYSTAL MGO. S. L. BLANK AND J. A. PASK.	161
PASK	MICROSTRUCTURE AND BEHAVIOR OF CERAMIC MATERIALS -- GLASS AND CERAMIC-METAL SYSTEMS. J. A. PASK.	161
PASK	DIFFUSION IN THE CAO-NIO SYSTEM. M. APPEL AND J. A. PASK.	162
PASK	EFFECT OF LITHIUM FLUORIDE ON THE DENSIFICATION OF MAGNESIUM OXIDE. P. E. HART AND J. A. PASK.	163
PASK	EFFECT OF MICROSTRUCTURE ON THE DEFORMATION OF POLYCRYSTALLINE MGO. T. G. LANGDON AND J. A. PASK.	164
PASK	CREEP OF LIF SINGLE CRYSTALS. D. R. CROPPER AND J. A. PASK.	166
PASK	PLASTIC BUCKLING AND CREEP OF MGO SINGLE CRYSTALS. D. R. CROPPER AND J. A. PASK.	167
PASK	CERAMIC-METAL INTERFACES. J. J. BRENNAN AND J. A. PASK.	168
PASK	RESEARCH PLANS FOR 1968. J. A. PASK.	169
PASK	PHASE DISTRIBUTION IN MULTIPHASE MAGNESIA AND FORSTERITE BODIES. A. P. RAJU, I. A. AKSAY, AND J. A. PASK.	163
PASK	CREEP OF POLYCRYSTALLINE MAGNESIUM OXIDE. T. G. LANGDON, J. SHEROHMAN, AND J. A. PASK.	164
PASK	KINETICS OF INTERFACIAL REACTION AND DIFFUSION IN THE SYSTEM IRON-SODIUM DISILICATE GLASS. M. P. BOROM AND J. A. PASK.	167
PASK	INVESTIGATION OF THE REACTIONS BETWEEN AL203 AND SIO2. R. F. DAVIS AND J. A. PASK.	163
PASK	ELECTROCHEMICAL AND CONDUCTIVITY STUDIES IN GLASS. R. N. SCHWEINBERG AND J. A. PASK.	167
PASK	DISSOLUTION AND DIFFUSION STUDIES IN GLASS. A. M. LACY AND J. A. PASK.	167
PASK	1967 PUBLICATIONS. J. A. PASK AND ASSOCIATES.	170
PATTON	STUDIES OF THE THERMAL SPLITTING OF S4N4. R. L. PATTON AND W. L. JOLLY.	14
PATTON	REACTIONS OF DISULFUR DINITRIDE WITH ANTIMONY PENTACHLORIDE AND BORON TRIHALIDES. R. L. PATTON AND W. L. JOLLY.	14
PAUKERT	SPECTRA AND LIFETIMES OF GAS-PHASE FREE RADICALS AT VERY LOW CONCENTRATIONS. H. S. JOHNSTON, E. D. MORRIS, JR., T. T. PAUKERT, AND J. VAN DEN BOGAERDE.	87
PENTAAMMINE	STUDIES OF PENTAAMMINE COMPLEXES OF COBALT, RHODIUM, AND IRIDIUM. W. L. JOLLY.	16
PENTAAMMINE	THE AQUATION OF THE NITRO PENTAAMMINE COBALT(III) ION IN SULFURIC ACID SOLUTIONS. A. D. HARRIS, R. STEWART, D. HENDRICKSON, AND W. L. JOLLY.	16
PENTACHLORIDE	ADDUCTS OF SULFUR NITRIDE WITH BORON TRIHALIDES AND ANTIMONY PENTACHLORIDE. K. J. WYNNE AND W. L. JOLLY.	14
PENTACHLORIDE	REACTIONS OF DISULFUR DINITRIDE WITH ANTIMONY PENTACHLORIDE AND BORON TRIHALIDES. R. L. PATTON AND W. L. JOLLY.	14
PERFECT	CLIMB OF PERFECT AND IMPERFECT DISLOCATIONS IN ALUMINUM. J. TARTOUR AND J. WASHBURN.	109
PERTURBATIONS	ANALYSIS OF ROTATIONAL PERTURBATIONS USING ISOTOPIC SHIFTS. D. GREEN AND H. JOHANSEN.	24

PETROFF	LIQUID-HELIUM FIELD-ION MICROSCOPE FOR RADIATION-DAMAGE INVESTIGATIONS. P. PETROFF AND J. WASHBURN.	--109
PETROFF	FIELD-ION MICROSCOPE INVESTIGATION OF RADIATION DAMAGE IN IRIDIUM BOMBARDED WITH 10-MEV PROTONS. P. PETROFF AND J. WASHBURN.	- --109
PH	A GLASS PH ELECTRODE IN LIQUID AMMONIA. R. SHIURBA AND W. L. JOLLY.	-17
PHASE SHIFTS	SEMICLASSICAL PHASE SHIFTS FOR LOW-ENERGY ORBITING COLLISIONS. R. R. HERM.	92
PHILLIPS	HEAT CAPACITY OF DILUTE FE IN CU ALLOYS. J. C. F. BROCK AND N. E. PHILLIPS.	27
PHILLIPS	HEAT CAPACITY OF A NI-RH ALLOY. N. E. PHILLIPS, B. B. TRIPLETT, AND D. W. WOODY.	28
PHILLIPS	CONSTANT-VOLUME HEAT CAPACITY OF COMPRESSED HELIUM-II. C. G. WATERFIELD, J. K. HOFFER, AND N. E. PHILLIPS.	29
PHILLIPS	HEAT CAPACITY OF SOME SILVER CLATHRATE SALTS. M. M. CONWAY AND N. E. PHILLIPS.	31
PHILLIPS	HEAT CAPACITY OF MOLYBDENUM. J. C. F. BROCK AND N. E. PHILLIPS.	32
PHILLIPS	HEAT CAPACITY OF METALS UNDER PRESSURE. S. S. B. WANG, M. M. CONWAY, AND N. E. PHILLIPS.	33
PHILLIPS	HEAT CAPACITY OF SOLID BCC AND HCP HELIUM-4. J. K. HOFFER AND N. E. PHILLIPS.	-28
PHILLIPS	MELTING CURVE OF HELIUM-4. N. E. PHILLIPS, J. K. HOFFER, AND C. G. WATERFIELD.	-29
PHILLIPS	HELIUM-3 HELIUM-4 DILUTION REFRIGERATOR. B. B. TRIPLETT AND N. E. PHILLIPS.	-33
PHILLIPS	RESEARCH PLANS FOR 1968. N. E. PHILLIPS.	--33
PHILLIPS	1967 PUBLICATIONS. N. E. PHILLIPS AND ASSOCIATES.	34
PHOSPHINE	PHOSPHINE. S. D. GOKHALE AND W. L. JOLLY.	-13
PHOSPHORUS	STUDIES OF THE HYDRIDES OF SILICON, GERMANIUM, TIN, AND PHOSPHORUS.	11
PHOSPHORUS	RESISTIVITY OF PHOSPHORUS. J. PRYZBYLINSKI AND G. JURA.	36
PHYSICS	THEORETICAL SOLID-STATE PHYSICS. M. L. COHEN.	183
PHYSICS	EXPERIMENTAL SOLID-STATE PHYSICS AND QUANTUM ELECTRONICS. Y. R. SHEN.	195
PLANE PLATE	CURRENT AND POTENTIAL DISTRIBUTION IN CONVECTIVE MASS-TRANSFER AT PLANE-PLATE ELECTRODES. J. R. SELMAN AND C. W. TOBIAS.	--50
PLANE STRAIN	MICROSTRUCTURE AND PLANE-STRAIN FRACTURE TOUGHNESS OF HIGH-STRENGTH ALUMINUM ALLOYS. P. J. GUEST AND M. D. MERZ.	-135
PLANES	INDICES OF PLANES AND DIRECTIONS IN HCP CRYSTALS. P. R. OKAMOTO AND G. THOMAS.	126
PLASMA	RADIOFREQUENCY PLASMA MICROSPHEROIDIZATION OF CERAMICS. R. T. TREMPER AND R. M. FULRATH.	175
PLASTIC	PLASTIC BUCKLING AND CREEP OF MGO SINGLE CRYSTALS. D. R. CROPPER AND J. A. PASK.	167
PLASTIC	PLASTIC DEFORMATION OF CUPROUS OXIDE. G. VAGNARD AND J. WASHBURN.	-107
PLASTICS	FRACTURE TOUGHNESS OF PLASTICS. L. KEY AND Y. KATZ.	137
PLATE	LAMINAR FREE CONVECTION AT A VERTICAL PLATE IN THE PRESENCE OF SUPPORTING ELECTROLYTE. J. R. SELMAN AND J. NEWMAN.	66
PLATINUM	STUDIES OF THE CLEAN (100), (111), AND (110) CRYSTAL FACES OF PLATINUM. H. B. LYON AND G. A. SOMORJAI.	---43
PLATINUM	LOW-ENERGY ELECTRON-DIFFRACTION STUDY OF SURFACE REACTIONS ON (100) PLATINUM. A. E. MORGAN AND G. A. SOMORJAI.	- ---44
PLAZA	EVALUATION OF THERMODYNAMIC DATA. R. HULTGREN, M. GLEISER, K. K. KELLEY, R. L. ORR, E. PLAZA, AND G. SOMAYAJULU.	-152
POLYCRYSTALLINE	EFFECT OF MICROSTRUCTURE ON THE DEFORMATION OF POLYCRYSTALLINE MGO. T. G. LANGDON AND J. A. PASK.	164
POLYCRYSTALLINE	CREEP OF POLYCRYSTALLINE MAGNESIUM OXIDE. T. G. LANGDON, J. SHEROHMAN, AND J. A. PASK.	-164
POLYCRYSTALLINE	CREEP OF POLYCRYSTALLINE LIF. T. G. LANGDON AND D. R. CROPPER.	-165
POLYMERS	PROTON EXCHANGE FROM THE FIRST COORDINATION SPHERE OF HYDROLYTIC POLYMERS OF CHROMIUM(III). R. LEE.	-8
POLYPHASE	SINGLE-PHASE AND POLYPHASE ALLOY SYSTEMS. M. SUENAGA, J. OLSON, AND K. RALLS.	141
POROUS	EFFECT OF PERIODIC MENISCUS DISPLACEMENTS ON THE PERFORMANCE OF POROUS GAS ELECTRODES. J. P. ROUSSILLON AND E. A. GRENS II.	53
POROUS	DYNAMICS OF POROUS ELECTRODES. C. W. TOBIAS.	-51
POROUS	REACTION DISTRIBUTION IN FLOODED POROUS ELECTRODES. R. ALKIRE, E. A. GRENS II, AND C. W. TOBIAS.	--51
PORTER	FRACTURE TOUGHNESS OF PRECIPITATION-HARDENING ALUMINUM ALLOYS. D. PORTER.	138

PORTIS	MAGNETIC PROPERTIES OF SOLIDS. A. M. PORTIS.	185
PORTIS	ANTIFERROMAGNETIC RELAXATION. A. M. PORTIS.	185
PORTIS	MAGNETICAL AND ELECTRIC PROPERTIES OF MNAU. A. M. PORTIS.	185
PORTIS	SPIN WAVE PROPAGATION. A. M. PORTIS.	185
PORTIS	NUCLEAR RESONANCE IN FERROMAGNETIC ALLOYS. A. M. PORTIS.	185
PORTIS	NUCLEAR DOUBLE RESONANCE IN FERROMAGNETIC ALLOYS. A. M. PORTIS.	185
PORTIS	RESEARCH PLANS FOR 1968. A. M. PORTIS.	185
PORTIS	1967 PUBLICATIONS. A. M. PORTIS AND ASSOCIATES.	186
POTASSIUM	REACTION OF POTASSIUM GERMYL WITH LEWIS ACIDS. D. S. RUSTAD, P. M. KUZNESOF, AND W. L. JOLLY.	12
PROPYLENE	THALLIUM - THALLOUS HALIDE REFERENCE ELECTRODES IN PROPYLENE CARBONATE. F. G. K. BAUCKE AND C. W. TOBIAS.	54
PRASEODYMIUM	SUBLIMATION OF PRASEODYMIUM FLUORIDE. H. B. SKINNER AND A. W. SEARCY.	155
PRATT	ESR SPECTRA NEAR 1 DEGREE KELVIN. D. W. PRATT, A. JINDO, W. T. BATCHELDER, AND R. J. MYERS.	83
PRATT	NMR SPECTRA OF CHLORINE-35 IN LIQUID VCL4 AND TICL4. D. W. PRATT AND R. J. MEYERS.	84
PRECIPITATION	FRACTURE TOUGHNESS OF PRECIPITATION-HARDENING ALUMINUM ALLOYS. D. PORTER.	138
PREDISSOCIATION	IODINE PREDISSOCIATION AND RECOMBINATION STUDIES. J. TELLINGHUISEN.	22
PRESSURE	HEAT CAPACITY OF METALS UNDER PRESSURE. S. S. B. WANG, M. M. CONWAY, AND N. E. PHILLIPS.	33
PRESSURE	HEAT CAPACITIES OF METALS UNDER PRESSURE. W. STARK AND G. JURA.	37
PRESSURE	EFFECT OF PRESSURE ON HIGH-TEMPERATURE DISSOLUTION. M. A. STETT AND R. M. FULRATH.	177
PRIZANT	KINETICS OF METAL-ACID REACTIONS IN LIQUID AMMONIA. L. PRIZANT AND W. L. JOLLY.	17
PRODUCT	PRODUCT ENERGY AND ANGULAR DISTRIBUTIONS FROM THE REACTION OF NITROGEN-MOLECULE ION WITH ISOTOPIC HYDROGEN MOLECULES. W. R. GENTRY, E. A. GISLASON, Y. T. LEE, B. H. MAHAN, AND C. W. TSAO.	75
PROPAGATION	SPIN WAVE PROPAGATION. A. M. PORTIS.	185
PROPERTIES	TRANSPORT PROPERTIES OF CONCENTRATED ELECTROLYTIC SOLUTIONS. T. W. CHAPMAN AND J. NEWMAN.	61
PROPERTIES	RELATION OF STRUCTURE TO PROPERTIES IN CRYSTALS. G. THOMAS.	119
PROPERTIES	STRUCTURE AND PROPERTIES OF FE/NI/CO/TI MARAGING STEEL. I. L. CHENG AND G. THOMAS.	123
PROPERTIES	EFFECT OF TEST TEMPERATURE ON THE MECHANICAL PROPERTIES OF METASTABLE AUSTENITIC STEELS. G. R. CHANANI AND M. D. MERZ.	133
PROPERTIES	NOTCH-TOUGHNESS VARIATIONS IN STEELS WITH THE SAME TENSILE PROPERTIES. Y. KATZ AND M. D. MERZ.	135
PROPERTIES	MAGNETIC PROPERTIES OF SOLIDS. A. M. PORTIS.	185
PROPERTIES	FAR-INFRARED PROPERTIES OF SOLIDS. P. L. RICHARDS.	187
PROPERTIES	OPTICAL PROPERTIES OF SOLIDS. R. ZUCCA AND Y. R. SHEN.	195
PROPERTIES	MAGNETICAL AND ELECTRIC PROPERTIES OF MNAU. A. M. PORTIS.	185
PROTON	PROTON EXCHANGE FROM THE FIRST COORDINATION SPHERE OF HYDROLYTIC POLYMERS OF CHROMIUM(III). R. LEE.	8
PROTON	PROTON MAGNETIC RESONANCE SPECTRA OF RHODIUM AND IRIDIUM COMPLEXES IN SULFURIC ACID. D. N. HENDRICKSON AND W. L. JOLLY.	16
PROTONS	FIELD-ION MICROSCOPE INVESTIGATION OF RADIATION DAMAGE IN IRIDIUM BOMBARDED WITH 10-MEV PROTONS. P. PETROFF AND J. WASHBURN.	109
PRYZBYLINSKI	RESISTIVITY OF PHOSPHORUS. J. PRYZBYLINSKI AND G. JURA.	36
PSEUDOPOTENTIAL	PSEUDOPOTENTIAL CALCULATIONS ON ATOMS AND DIATOMIC MOLECULES. J. TELLINGHUISEN.	22
PUBLICATIONS	1967 PUBLICATIONS. R. E. CONNICK AND ASSOCIATES.	10
PUBLICATIONS	1967 PUBLICATIONS. W. L. JOLLY AND ASSOCIATES.	19
PUBLICATIONS	1967 PUBLICATIONS. L. BREWER AND ASSOCIATES.	25
PUBLICATIONS	1967 PUBLICATIONS. N. E. PHILLIPS AND ASSOCIATES.	34
PUBLICATIONS	1967 PUBLICATIONS. G. JURA AND ASSOCIATES.	39
PUBLICATIONS	1967 PUBLICATIONS. R. H. MULLER AND ASSOCIATES.	50
PUBLICATIONS	1967 PUBLICATIONS. C. W. TOBIAS AND ASSOCIATES.	61
PUBLICATIONS	1967 PUBLICATIONS. J. NEWMAN AND ASSOCIATES.	71
PUBLICATIONS	1967 PUBLICATIONS. B. H. MAHAN AND ASSOCIATES.	80
PUBLICATIONS	1967 PUBLICATIONS. H. S. JOHNSTON AND ASSOCIATES.	92
PUBLICATIONS	1967 PUBLICATIONS. R. R. HERM AND ASSOCIATES.	93
PUBLICATIONS	1967 PUBLICATIONS. O. REDLICH AND ASSOCIATES.	97
PUBLICATIONS	1967 PUBLICATIONS. R. J. MYERS.	86
PUBLICATIONS	1967 PUBLICATIONS. D. R. OLANDER AND ASSOCIATES.	105
PUBLICATIONS	1967 PUBLICATIONS. J. WASHBURN AND ASSOCIATES.	114

PUBLICATIONS	1967 PUBLICATIONS. J. E. DORN AND ASSOCIATES.	117
PUBLICATIONS	1967 PUBLICATIONS. G. THOMAS AND ASSOCIATES.	129
PUBLICATIONS	1967 PUBLICATIONS. E. R. PARKER, V. F. ZACKAY AND ASSOCIATES.	139
PUBLICATIONS	1967 PUBLICATIONS. M. MERRIAM AND ASSOCIATES.	149
PUBLICATIONS	1967 PUBLICATIONS. A. W. SEARCY AND ASSOCIATES.	160
PUBLICATIONS	1967 PUBLICATIONS. J. A. PASK AND ASSOCIATES.	170
PUBLICATIONS	1967 PUBLICATIONS. R. M. FULRATH AND ASSOCIATES.	182
PUBLICATIONS	1967 PUBLICATIONS. A. M. PORTIS AND ASSOCIATES.	186
PUBLICATIONS	1967 PUBLICATIONS. P. L. RICHARDS AND ASSOCIATES.	191
PUBLICATIONS	1967 PUBLICATIONS. Y. R. SHEN AND ASSOCIATES.	196
PUBLICATIONS	1967 PUBLICATIONS. E. L. HAHN AND ASSOCIATES.	198
PUBLICATIONS	1967 PUBLICATIONS. C. B. HARRIS.	94
PUBLICATIONS	1967 PUBLICATIONS. L. BREWER, E. R. PARKER, V. F. ZACKAY AND ASSOCIATES.	146
PUBLICATIONS	1967 PUBLICATIONS. R. HULTGREN AND ASSOCIATES.	153
PUBLICATIONS	1967 PUBLICATIONS. G. A. SOMORJAI AND ASSOCIATES.	45
PUBLICATIONS	1967 PUBLICATIONS. G. ROCHLIN AND ASSOCIATES.	193
PUBLICATIONS	1967 PUBLICATIONS. M. L. COHEN AND ASSOCIATES.	183
PULSES	ULTRASHORT LIGHT PULSES. J. SHELTON AND Y. R. SHEN.	195
QUANTITATIVE	QUANTITATIVE INVESTIGATION OF THE STRAIN-INDUCED MARTENSITIC TRANSFORMATION IN HIGH-STRENGTH STEELS. B. DE MIRAMON AND M. D. MERZ.	131
QUANTUM	EXPERIMENTAL SOLID-STATE PHYSICS AND QUANTUM ELECTRONICS. Y. R. SHEN.	195
QUARTZ	LOW-ENERGY ELECTRON-DIFFRACTION STUDY OF ALPHA-ALUMINA (AL203) AND QUARTZ (SIO2) SURFACES. T. M. FRENCH, J. MORABITO, AND G. A. SOMORJAI.	44
RADIATION DAMAGE	LIQUID-HELIUM FIELD-ION MICROSCOPE FOR RADIATION-DAMAGE INVESTIGATIONS. P. PETROFF AND J. WASHBURN.	109
RADIATION DAMAGE	FIELD-ION MICROSCOPE INVESTIGATION OF RADIATION DAMAGE IN IRIDIUM BOMBARDED WITH 10-MEV PROTONS. P. PETROFF AND J. WASHBURN.	109
RADIATIVE	RADIATIVE LIFETIMES OF EXCITED ELECTRONIC STATES OF ATOMS AND MOLECULES. P. T. CUNNINGHAM.	21
RADICAL	ESR SPECTRA OF THE RADICAL ANIONS OF METHYL-SUBSTITUTED NITROSOBENZENES. C. L. TALCOTT AND R. J. MYERS.	84
RADICALS	LEAST-SQUARES-ADJUSTED ASSIGNMENTS FOR THE ESR SPECTRA OF FREE RADICALS IN SOLUTION. A. BAUDER, R. PAO, AND R. J. MEYERS.	80
RADIOFREQUENCY	RADIOFREQUENCY PLASMA MICROSPHEROIDIZATION OF CERAMICS. R. T. TREMPER AND R. M. FULRATH.	175
RADIUS	CAPTURE RADIUS FOR ION RECOMBINATION. E. K. PARKS.	73
RAJU	PHASE DISTRIBUTION IN MULTIPHASE MAGNESIA AND FORSTERITE BODIES. A. P. RAJU, I. A. AKSAY, AND J. A. PASK.	163
RALLS	SINGLE-PHASE AND POLYPHASE ALLOY SYSTEMS. M. SUENAGA, J. OLSON, AND K. RALLS.	141
REACTION	REACTION OF POTASSIUM GERMYL WITH LEWIS ACIDS. D. S. RUSTAD, P. M. KUZNESOF, AND W. L. JOLLY.	12
REACTION	PRODUCT ENERGY AND ANGULAR DISTRIBUTIONS FROM THE REACTION OF NITROGEN-MOLECULE ION WITH ISOTOPIC HYDROGEN MOLECULES. W. R. GENTRY, E. A. GISLASON, Y. T. LEE, B. H. MAHAN, AND C. W. TSAO.	75
REACTION	DYNAMICS OF THE REACTION OF METHANE WITH NITROGEN-MOLECULE ION. E. A. GISLASON, C. W. TSAO, B. H. MAHAN, AND A. WERNER.	77
REACTION	THE COLLISIONAL-RADIATIVE REACTION OF SINGLET-DELTA OXYGEN. A. M. FALICK AND B. H. MAHAN.	74
REACTION	REVERSIBILITY OF THE REACTION OF ALKALI METALS WITH LIQUID AMMONIA. E. J. KIRSCHKE AND W. L. JOLLY.	17
REACTION	REACTION DISTRIBUTION IN FLOODED POROUS ELECTRODES. R. ALKIRE, E. A. GRENS II, AND C. W. TOBIAS.	51
REACTION	KINETICS OF INTERFACIAL REACTION AND DIFFUSION IN THE SYSTEM IRON SODIUM DISILICATE GLASS. M. P. BOROM AND J. A. PASK.	167
REACTIONS	KINETICS OF METAL-ACID REACTIONS IN LIQUID AMMONIA. L. PRIZANT AND W. L. JOLLY.	17
REACTIONS	SOLID-STATE REACTIONS. G. A. SOMORJAI.	45
REACTIONS	REACTIONS OF SILANE, GERMANE, AND STANNANE WITH METAL-AMMONIA AND AMIDE-AMMONIA SOLUTIONS. D. S. RUSTAD AND W. L. JOLLY.	11
REACTIONS	CROSSED-MOLECULAR-BEAM INVESTIGATIONS OF THERMAL LI-ATOM REACTIONS. D. D. PARRISH AND R. R. HERM.	92
REACTIONS	HIGH-TEMPERATURE REACTIONS. A. W. SEARCY.	155
REACTIONS	REACTIONS OF DISULFUR DINITRIDE WITH ANTIMONY PENTACHLORIDE AND BORON TRIHALIDES. R. L. PATTON AND W. L. JOLLY.	14
REACTIONS	INVESTIGATION OF THE REACTIONS BETWEEN AL203 AND SIO2. R. F. DAVIS AND J. A. PASK.	163

RECOMBINATION	IODINE PREDISSOCIATION AND RECOMBINATION STUDIES. J. TELLINGHUISEN.	22
RECOMBINATION	CAPTURE RADIUS FOR ION RECOMBINATION. E. K. PARKS.	73
RECOMBINATION	GASEOUS-ION RECOMBINATION. V. B. H. MAHAN.	73
REDLICH	THERMODYNAMICS AND MOLECULAR STATE OF STRONG ACIDS. R. W. DUERST, W. E. GARGRAVE, AND O. REDLICH.	94
REDLICH	THERMODYNAMIC CALCULATION METHODS. V. B. T. NGO AND O. REDLICH.	95
REDLICH	FUNDAMENTAL THERMODYNAMICS. O. REDLICH.	96
REDLICH	RESEARCH PLANS FOR 1968. O. REDLICH.	97
REDLICH	LEACHING OF CLAY WITH ACIDS. I. EDELWEISS AND O. REDLICH.	96
REDLICH	1967 PUBLICATIONS. O. REDLICH AND ASSOCIATES.	97
REFRACTORY	REFRACTORY METAL OXIDATION. J. S. SCHOFILL AND D. R. OLANDER.	104
REFRIGERATOR	HELIUM-3 - HELIUM-4 DILUTION REFRIGERATOR. B. B. TRIPLETT AND N. E. PHILLIPS.	33
RELAXATION	NMR RELAXATION OF OXYGEN-17 BY FERRIC ION IN AQUEOUS SOLUTION. M. R. JUDKINS.	7
RELAXATION	ANTIFERROMAGNETIC RELAXATION. A. M. PORTIS.	185
RESEARCH PLANS	RESEARCH PLANS FOR 1968. R. E. CONNICK.	9
RESEARCH PLANS	RESEARCH PLANS FOR 1968. W. L. JOLLY.	18
RESEARCH PLANS	RESEARCH PLANS FOR 1968. L. BREWER.	24
RESEARCH PLANS	RESEARCH PLANS FOR 1968. C. W. TOBIAS.	60
RESEARCH PLANS	RESEARCH PLANS FOR 1968. B. H. MAHAN.	80
RESEARCH PLANS	RESEARCH PLANS FOR 1968. R. J. MYERS.	86
RESEARCH PLANS	RESEARCH PLANS FOR 1968. O. REDLICH.	97
RESEARCH PLANS	RESEARCH PLANS FOR 1968. R. H. MULLER.	49
RESEARCH PLANS	RESEARCH PLANS FOR 1968. H. S. JOHNSTON.	91
RESEARCH PLANS	RESEARCH PLANS FOR 1968. R. R. HERM.	93
RESEARCH PLANS	RESEARCH PLANS FOR 1968. C. B. HARRIS.	94
RESEARCH PLANS	RESEARCH PLANS FOR 1968. J. WASHBURN.	112
RESEARCH PLANS	RESEARCH PLANS FOR 1968. J. E. DORN.	116
RESEARCH PLANS	RESEARCH PLANS FOR 1968. G. THOMAS.	128
RESEARCH PLANS	RESEARCH PLANS FOR 1968. V. F. ZACKAY AND E. R. PARKER.	138
RESEARCH PLANS	RESEARCH PLANS FOR 1968. L. BREWER, E. R. PARKER, AND V. F. ZACKAY.	146
RESEARCH PLANS	RESEARCH PLANS FOR 1968. M. F. MERRIAM AND R. HAMMOND.	148
RESEARCH PLANS	RESEARCH PLANS FOR 1968. R. HULTGREN.	153
RESEARCH PLANS	RESEARCH PLANS FOR 1968. J. A. PASK.	169
RESEARCH PLANS	RESEARCH PLANS FOR 1968. R. M. FULRATH.	180
RESEARCH PLANS	RESEARCH PLANS FOR 1968. P. L. RICHARDS.	190
RESEARCH PLANS	RESEARCH PLANS FOR 1968. N. E. PHILLIPS.	33
RESEARCH PLANS	RESEARCH PLANS FOR 1968. G. A. SOMORJAI.	45
RESEARCH PLANS	RESEARCH PLANS FOR 1968. J. NEWMAN.	70
RESEARCH PLANS	RESEARCH PLANS FOR 1968. D. R. OLANDER.	104
RESEARCH PLANS	RESEARCH PLANS FOR 1968. G. ROCHLIN.	193
RESEARCH PLANS	RESEARCH PLANS FOR 1968. A. W. SEARCY.	159
RESEARCH PLANS	RESEARCH PLANS FOR 1968. M. L. COHEN.	183
RESEARCH PLANS	RESEARCH PLANS FOR 1968. A. M. PORTIS.	185
RESEARCH PLANS	RESEARCH PLANS FOR 1968. Y. R. SHEN.	195
RESISTIVITY	RESISTIVITY OF PHOSPHORUS. J. PRYZBYLINSKI AND G. JURA.	36
RESONANCE	ION-CYCLOTRON RESONANCE MASS SPECTROMETRY. R. HORTON, R. M. LAMBERT, AND B. H. MAHAN.	-77
RESONANCE	NUCLEAR-SPIN DOUBLE RESONANCE IN KH2PO4. D. STEHLIK.	198
RESONANCE	PROTON MAGNETIC-RESONANCE SPECTRA OF RHODIUM AND IRIDIUM COMPLEXES IN SULFURIC ACID. D. N. HENDRICKSON AND W. L. JOLLY.	16
RESONANCE	NUCLEAR RESONANCE IN FERROMAGNETIC ALLOYS. A. M. PORTIS.	185
RESONANCE	NUCLEAR DOUBLE RESONANCE IN FERROMAGNETIC ALLOYS. A. M. PORTIS.	185
REVERSIBILITY	REVERSIBILITY OF THE REACTION OF ALKALI METALS WITH LIQUID AMMONIA. E. J. KIRSCHKE AND W. L. JOLLY.	17
REVERSION	ON FATIGUE-INDUCED REVERSION AND OVERAGING IN DISPERSION-STRENGTHENED ALLOY SYSTEMS. C. LAIRD AND G. THOMAS.	119
RHODIUM	STUDIES OF PENTAAMMINE COMPLEXES OF COBALT, RHODIUM, AND IRIDIUM. W. L. JOLLY.	16
RHODIUM	PROTON MAGNETIC-RESONANCE SPECTRA OF RHODIUM AND IRIDIUM COMPLEXES IN SULFURIC ACID. D. N. HENDRICKSON AND W. L. JOLLY.	16
RIBOTTA	NONLINEAR-OPTICS EXPERIMENTS. M. LOY, D. FARIES, J. SHAHAM, AND R. RIBOTTA.	195
RICHARDS	FAR-INFRARED PROPERTIES OF SOLIDS. P. L. RICHARDS.	187
RICHARDS	RESEARCH PLANS FOR 1968. P. L. RICHARDS.	190
RICHARDS	CONSTRUCTION OF FAR-INFRARED APPARATUS. G. C. BRACKETT, R. R. JOYCE, AND P. L. RICHARDS.	187
RICHARDS	LOW-LYING ENERGY LEVELS OF INTERMEDIATE-SPIN AND HIGH-SPIN FE3+. G. C. BRACKETT AND P. L. RICHARDS.	189

RICHARDS	LOW-LYING ENERGY LEVELS OF A SINGLE D-ELECTRON. R. R. JOYCE AND P. L. RICHARDS.	187
RICHARDS	JOSEPHSON JUNCTION AS A FAR-INFRARED DETECTOR. P. L. RICHARDS AND S. A. STERLING.	189
RICHARDS	1967 PUBLICATIONS. P. L. RICHARDS AND ASSOCIATES.	191
ROCHLIN	SUPERCONDUCTIVITY. G. ROCHLIN.	193
ROCHLIN	RESEARCH PLANS FOR 1968. G. ROCHLIN.	193
ROCHLIN	1967 PUBLICATIONS. G. ROCHLIN AND ASSOCIATES.	193
ROSEN	SPONTANEOUS SCATTERING OF LIGHT. H. ROSEN, F. STENMAN, AND Y. R. SHEN.	195
ROTATING DISK	ROTATING-DISK SYSTEM FOR METAL DEPOSITION FROM NONAQUEOUS SOLVENTS. F. G. K. BAUCKE, D. LANDOLT, AND C. W. TOBIAS.	55
ROTATING DISK	CURRENT DISTRIBUTION ON A ROTATING-DISK ELECTRODE. V. MARATHE AND J. NEWMAN.	63
ROTATIONAL	ANALYSIS OF ROTATIONAL PERTURBATIONS USING ISOTOPIC SHIFTS. D. GREEN AND H. JOHANSEN.	24
ROUSSILLON	EFFECT OF PERIODIC MENISCUS DISPLACEMENTS ON THE PERFORMANCE OF POROUS GAS ELECTRODES. J. P. ROUSSILLON AND E. A. GRENS II.	53
RUSTAD	REACTION OF POTASSIUM GERMYL WITH LEWIS ACIDS. D. S. RUSTAD, P. M. KUZNESOF, AND W. L. JOLLY.	12
RUSTAD	REACTIONS OF SILANE, GERMANE, AND STANNANE WITH METAL-AMMONIA AND AMIDE-AMMONIA SOLUTIONS. D. S. RUSTAD AND W. L. JOLLY.	11
SALTS	HEAT CAPACITY OF SOME SILVER CLATHRATE SALTS. M. M. CONWAY AND N. E. PHILLIPS.	31
SCANDIUM	DETERMINATION OF THE ELECTRONIC PARTITION FUNCTION OF SCANDIUM MONOFLUORIDE BY MOLECULAR-BEAM FLUORESCENCE. D. GREEN.	23
SCATTERING	CROSSED-MOLECULAR-BEAM INVESTIGATION OF INELASTIC SCATTERING BY TIME-OF-FLIGHT ANALYSIS. D. D. PARRISH AND R. R. HERM.	93
SCATTERING	INELASTIC SCATTERING OF NITROGEN-MOLECULE ION BY HELIUM. W. R. GENTRY, E. A. GISLASON, B. H. MAHAN, AND C. W. TSAO.	74
SCATTERING	SPONTANEOUS SCATTERING OF LIGHT. H. ROSEN, F. STENMAN, AND Y. R. SHEN.	195
SCHMITT	MASS TRANSFER TO THE REAR OF A CYLINDER AT HIGH SCHMITT NUMBERS. J. NEWMAN.	70
SCHMITT	BORON HYDRIDE CHEMISTRY. W. L. JOLLY, T. SCHMITT, AND F. WANG.	13
SCHOFILL	REFRACTORY-METAL OXIDATION. J. S. SCHOFILL AND D. R. OLANDER.	104
SCHWAB	A SCHEME FOR NMR-NQR DETECTION IN SOLIDS -- C13 AND DEUTERIUM IN PARADICHLOROBENZENE. M. SCHWAB AND E. L. HAHN.	197
SCHWARTZ	KINETICS OF NO2 ELECTRONIC FLUORESCENCE. S. E. SCHWARTZ AND H. S. JOHNSTON.	87
SCHWEINBERG	ELECTROCHEMICAL AND CONDUCTIVITY STUDIES IN GLASS. R. N. SCHWEINBERG AND J. A. PASK.	167
SEARCY	HIGH-TEMPERATURE REACTIONS. A. W. SEARCY.	155
SEARCY	SUBLIMATION OF PRASEODYMIUM FLUORIDE. H. B. SKINNER AND A. W. SEARCY.	155
SEARCY	VAPOR SPECIES OF THE BARIUM-OXYGEN SYSTEM. R. S. NEWBURY, G. W. BARTON, JR., AND A. W. SEARCY.	159
SEARCY	EXCHANGE OF ENERGY BETWEEN TUNGSTEN AT HIGH TEMPERATURES AND GASES AT ROOM TEMPERATURE. M. J. LIM AND A. W. SEARCY.	155
SEARCY	A STUDY OF THE FREE ENERGY AND ENTHALPY OF FORMATION OF AL2S3(S). O. HERSTAD AND A. W. SEARCY.	159
SEARCY	EQUILIBRIUM AND NONEQUILIBRIUM SUBLIMATION OF ZINC SULFIDE AND OF CADMIUM TELLURIDE. B. A. H. BLANK AND A. W. SEARCY.	159
SEARCY	RESEARCH PLANS FOR 1968. A. W. SEARCY.	159
SEARCY AND ASSOCIAT	1967 PUBLICATIONS. A. W. SEARCY AND ASSOCIATES.	160
SELMAN	LAMINAR FREE CONVECTION AT A VERTICAL PLATE IN THE PRESENCE OF SUPPORTING ELECTROLYTE. J. R. SELMAN AND J. NEWMAN.	66
SELMAN	CURRENT AND POTENTIAL DISTRIBUTION IN CONVECTIVE MASS TRANSFER AT PLANE-PLATE ELECTRODES. J. R. SELMAN AND C. W. TOBIAS.	50
SEMICLASSICAL	SEMICLASSICAL PHASE SHIFTS FOR LOW-ENERGY ORBITING COLLISIONS. R. R. HERM.	92
SEMICONDUCTORS	SUPERCONDUCTIVITY IN DEGENERATE SEMICONDUCTORS. M. L. COHEN.	183
SEMINARS	1967 RESEARCH SEMINARS.	207

SHAHAM	NONLINEAR-OPTICS EXPERIMENTS. M. LOY, D. FARIES, J. SHAHAM, AND R. RIBOTTA.	195
SHANER	ZERO-FIELD, FREE-PRECESSION MEASUREMENTS OF THE HYPERFINE INTERACTION IN CESIUM-33 VAPOR. J. W. SHANER, S. A. MILLER, AND E. L. HAHN.	197
SHELTON	ULTRASHORT LIGHT PULSES. J. SHELTON AND Y. R. SHEN.	195
SHEN	EXPERIMENTAL SOLID-STATE PHYSICS AND QUANTUM ELECTRONICS. Y. R. SHEN.	195
SHEN	OPTICAL PROPERTIES OF SOLIDS. R. ZUCCA AND Y. R. SHEN.	195
SHEN	SPONTANEOUS SCATTERING OF LIGHT. H. ROSEN, F. STENMAN, AND Y. R. SHEN.	195
SHEN	ULTRASHORT LIGHT PULSES. J. SHELTON AND Y. R. SHEN.	195
SHEN	NONLINEAR-OPTICS THEORY. Y. R. SHEN.	195
SHEN	RESEARCH PLANS FOR 1968. Y. R. SHEN.	195
SHEN	1967 PUBLICATIONS. Y. R. SHEN AND ASSOCIATES.	196
SHEROHMAN	CREEP OF POLYCRYSTALLINE MAGNESIUM OXIDE. T. G. LANGDON, J. SHEROHMAN, AND J. A. PASK.	164
SHIFTS	NITROGEN NMR CHEMICAL SHIFTS. D. N. HENDRICKSON AND P. M. KUZNESOF.	18
SHIFTS	ANALYSIS OF ROTATIONAL PERTURBATIONS USING ISOTOPIC SHIFTS. D. GREEN AND H. JOHANSEN.	24
SHIURBA	A GLASS PH ELECTRODE IN LIQUID AMMONIA. R. SHIURBA AND W. L. JOLLY.	17
SIH	FLOW TUNNEL WITH MOVING WALLS. P. H. SIH AND J. NEWMAN.	65
SILANE	REACTIONS OF SILANE, GERMANE, AND STANNANE WITH METAL-AMMONIA AND AMIDE-AMMONIA SOLUTIONS. D. S. RUSTAD AND W. L. JOLLY.	11
SILICON	STUDIES OF THE HYDRIDES OF SILICON, GERMANIUM, TIN, AND PHOSPHORUS.	11
SILICON	SODIUM IN SILICON SINGLE CRYSTALS. W. SZETO AND G. A. SOMORJAI.	45
SILVER	HEAT CAPACITY OF SOME SILVER CLATHRATE SALTS. M. M. CONWAY AND N. E. PHILLIPS.	31
SILVER	VAPOR PRESSURE OF THALLIUM AND ACTIVITY MEASUREMENTS ON LIQUID SILVER-THALLIUM ALLOYS BY THE TORSION-EFFUSION METHOD. P. J. DESRE, D. T. HAWKINS, AND R. HULTGREN.	152
SILVER	VOID FORMATION IN NICKEL AND SILVER DURING CREEP. T. G. LANGDON.	165
SILVER-SILICON	THERMODYNAMICS OF THE SILVER-SILICON SYSTEM BY DROP CALORIMETRY. T. A. CORN AND R. HULTGREN.	151
SINGLE	EVAPORATION RATE OF ICE SINGLE CRYSTALS. J. G. DAVY AND G. A. SOMORJAI.	43
SINGLE	SODIUM IN SILICON SINGLE CRYSTALS. W. SZETO AND G. A. SOMORJAI.	45
SINGLE	CREEP OF LIF SINGLE CRYSTALS. D. R. CROPPER AND J. A. PASK.	166
SINGLE	PLASTIC BUCKLING AND CREEP OF MGO SINGLE CRYSTALS. D. R. CROPPER AND J. A. PASK.	167
SINGLE	EVAPORATION MECHANISM OF GALLIUM ARSENIDE SINGLE CRYSTALS. C. LOU AND G. A. SOMORJAI.	39
SINGLE	LOW-LYING ENERGY LEVELS OF A SINGLE D-ELECTRON. R. R. JOYCE AND P. L. RICHARDS.	187
SINGLE	THE MEAN DISPLACEMENT OF SURFACE ATOMS IN PALLADIUM AND LEAD SINGLE CRYSTALS. R. M. GOODMAN, H. H. FARRELL, AND G. A. SOMORJAI.	43
SINGLE CRYSTAL	DIFFUSION OF IRON AND NICKEL INTO SINGLE-CRYSTAL MGO. S. L. BLANK AND J. A. PASK.	161
SINGLE PHASE	SINGLE-PHASE AND POLYPHASE ALLOY SYSTEMS. M. SUENAGA, J. OLSON, AND K. RALLS.	141
SINGLE SLIP	EFFECT OF INITIAL DISLOCATION DENSITY ON SINGLE SLIP STRAIN HARDENING OF COPPER. J. WASHBURN AND G. MURTY.	107
SINGLET-DELTA	THE COLLISIONAL-RADIATIVE REACTION OF SINGLET-DELTA OXYGEN. A. M. FALICK AND B. H. MAHAN.	74
SIO2	INVESTIGATION OF THE REACTIONS BETWEEN AL2O3 AND SIO2. R. F. DAVIS AND J. A. PASK.	163
SKINNER	SUBLIMATION OF PRASEODYMIUM FLUORIDE. H. B. SKINNER AND A. W. SEARCY.	155
SLAB	TRANSIENT DIFFUSION IN A COMPOSITE SLAB. P. CONCUS AND D. R. OLANDER.	102
SLIDING	GRAIN-BOUNDARY SLIDING AT HIGH TEMPERATURES. T. G. LANGDON.	164
SMYRL	POTENTIALS OF CELLS WITH LIQUID JUNCTIONS. W. H. SMYRL AND J. NEWMAN.	69
SODIUM	MOLECULAR STRUCTURE OF SODIUM α-OXYHYPONITRITE. D. N. HENDRICKSON.	17
SODIUM	EVAPORATION MECHANISM OF SODIUM CHLORIDE. J. E. LESTER AND G. A. SOMORJAI.	39

SODIUM	SODIUM IN SILICON SINGLE CRYSTALS. W. SZETO AND G. A. SOMORJAI.	45
SODIUM DISILICATE	KINETICS OF INTERFACIAL REACTION AND DIFFUSION IN THE SYSTEM IRON-SODIUM DISILICATE GLASS. M. P. BOROM AND J. A. PASK.	167
SOLAN	INORGANIC SYNTHESES IN LOW-TEMPERATURE MATRICES, NONAQUEOUS SOLVENTS, AND COCONDENSATION SYSTEMS. D. SOLAN, J. L. F. WANG, AND B. A. KING.	21
SOLID	LOW-ENERGY ELECTRON-DIFFRACTION STUDY OF SOLID AND LIQUID LEAD. R. M. GOODMAN AND G. A. SOMORJAI.	44
SOLID	HEAT CAPACITY OF SOLID BCC AND HCP HELIUM-4. J. K. HOFFER AND N. E. PHILLIPS.	28
SOLID-STATE	SOLID-STATE REACTIONS. G. A. SOMORJAI.	45
SOLID-STATE	THEORETICAL SOLID-STATE PHYSICS. M. L. COHEN.	183
SOLID-STATE	EXPERIMENTAL SOLID-STATE PHYSICS AND QUANTUM ELECTRONICS. Y. R. SHEN.	195
SOLIDS	VAPORIZATION KINETICS OF SOLIDS. G. A. SOMORJAI.	39
SOLIDS	CONDENSATION-ENHANCED VAPORIZATION OF HIGH-TEMPERATURE SOLIDS. R. OMBERG AND D. R. OLANDER.	103
SOLIDS	MAGNETIC PROPERTIES OF SOLIDS. A. M. PORTIS.	185
SOLIDS	FAR-INFRARED PROPERTIES OF SOLIDS. P. L. RICHARDS.	187
SOLIDS	ELECTRONIC STRUCTURE OF SOLIDS. M. L. COHEN.	183
SOLIDS	OPTICAL PROPERTIES OF SOLIDS. R. ZUCCA AND Y. R. SHEN.	195
SOLIDS	A SCHEME FOR NMR-NQR DETECTION IN SOLIDS -- C13 AND DEUTERIUM IN PARADICHLOROBENZENE. M. SCHWAB AND E. L. HAHN.	197
SOLVENTS	ELECTROCHEMISTRY IN NONAQUEOUS SOLVENTS. C. W. TOBIAS.	53
SOLVENTS	ROTATING-DISK SYSTEM FOR METAL DEPOSITION FROM NONAQUEOUS SOLVENTS. F. G. K. BAUCKE, D. LANDOLT, AND C. W. TOBIAS.	55
SOLVENTS	INORGANIC SYNTHESES IN LOW-TEMPERATURE MATRICES, NONAQUEOUS SOLVENTS, AND COCONDENSATION SYSTEMS. D. SOLAN, J. L.-F. WANG, AND B. A. KING.	21
SOMAYAJULU	EVALUATION OF THERMODYNAMIC DATA. R. HULTGREN, M. GLEISER, K. K. KELLEY, R. L. ORR, E. PLAZA, AND G. SOMAYAJULU.	152
SOMORJAI	VAPORIZATION KINETICS OF SOLIDS. G. A. SOMORJAI.	39
SOMORJAI	EVAPORATION RATE OF ICE SINGLE CRYSTALS. J. G. DAVY AND G. A. SOMORJAI.	43
SOMORJAI	LOW-ENERGY ELECTRON-DIFFRACTION STUDY OF SOLID AND LIQUID LEAD. R. M. GOODMAN AND G. A. SOMORJAI.	44
SOMORJAI	SOLID-STATE REACTIONS. G. A. SOMORJAI.	45
SOMORJAI	EVAPORATION MECHANISM OF SODIUM CHLORIDE. J. E. LESTER AND G. A. SOMORJAI.	39
SOMORJAI	HIGH-TEMPERATURE VAPORIZATION MECHANISMS. G. A. SOMORJAI.	43
SOMORJAI	LOW-ENERGY ELECTRON-DIFFRACTION STUDY OF ALPHA-ALUMINA (AL2O3) AND QUARTZ (SIO2) SURFACES. T. M. FRENCH, J. MORABITO, AND G. A. SOMORJAI.	44
SOMORJAI	SODIUM IN SILICON SINGLE CRYSTALS. W. SZETO AND G. A. SOMORJAI.	45
SOMORJAI	EVAPORATION MECHANISM OF GALLIUM ARSENIDE SINGLE CRYSTALS. C. LOU AND G. A. SOMORJAI.	39
SOMORJAI	SURFACE STUDIES BY LOW-ENERGY ELECTRON DIFFRACTION. G. A. SOMORJAI.	43
SOMORJAI	LOW-ENERGY ELECTRON-DIFFRACTION STUDY OF ALUMINUM. H. H. FARRELL AND G. A. SOMORJAI.	44
SOMORJAI	RESEARCH PLANS FOR 1968. G. A. SOMORJAI.	45
SOMORJAI	STUDIES OF THE CLEAN (100), (111), AND (110) CRYSTAL FACES OF PLATINUM. H. B. LYON AND G. A. SOMORJAI.	43
SOMORJAI	LOW-ENERGY ELECTRON-DIFFRACTION STUDIES AT LOW TEMPERATURES. J. MORABITO AND G. A. SOMORJAI.	44
SOMORJAI	THE MEAN DISPLACEMENT OF SURFACE ATOMS IN PALLADIUM AND LEAD SINGLE CRYSTALS. R. M. GOODMAN, H. H. FARRELL, AND G. A. SOMORJAI.	43
SOMORJAI	LOW-ENERGY ELECTRON-DIFFRACTION STUDY OF SURFACE-REACTIONS ON (100) PLATINUM. A. E. MORGAN AND G. A. SOMORJAI.	44
SOMORJAI	1967 PUBLICATIONS. G. A. SOMORJAI	45
SPECIES	SPECTROSCOPIC INVESTIGATIONS OF HIGH-TEMPERATURE SPECIES TRAPPED AT LOW TEMPERATURES IN INERT MATRICES. J. L.-F. WANG, B. A. KING, AND C. B. MEYER.	21
SPECIES	VAPOR SPECIES OF THE BARIUM-OXYGEN SYSTEM. R. S. NEWBURY, G. W. BARTON, JR., AND A. W. SEARCY.	159
SPECTRA	LEAST-SQUARES-ADJUSTED ASSIGNMENTS FOR THE ESR SPECTRA OF FREE RADICALS IN SOLUTION. A. BAUDER, R. PAO, AND R. J. MEYERS.	80
SPECTRA	ESR SPECTRA NEAR 1 DEGREE KELVIN. D. W. PRATT, A. JINDO, W. T. BATCHELDER, AND R. J. MYERS.	83
SPECTRA	ESR SPECTRA OF THE RADICAL ANIONS OF METHYL-SUBSTITUTED NITROSOBENZENES. C. L. TALCOTT AND R. J. MYERS.	84

SPECTRA	SPECTRA AND LIFETIMES OF GAS-PHASE FREE RADICALS AT VERY LOW CONCENTRATIONS. H. S. JOHNSTON, E. D. MORRIS, JR., T. T. PAUKERT, AND J. VAN DEN BOGAERDE.	87
SPECTRA	NMR SPECTRA OF CHLORINE-35 IN LIQUID VCL4 AND TICL4. D. W. PRATT AND R. J. MEYERS.	84
SPECTRA	PROTON MAGNETIC-RESONANCE SPECTRA OF RHODIUM AND IRIDIUM COMPLEXES IN SULFURIC ACID. D. N. HENDRICKSON AND W. L. JOLLY.	16
SPECTROMETER	HYDROGEN-ATOM SPECTROMETER. P. DOW AND H. S. JOHNSTON.	91
SPECTROSCOPIC	SPECTROSCOPIC INVESTIGATIONS OF HIGH-TEMPERATURE SPECIES TRAPPED AT LOW TEMPERATURES IN INERT MATRICES. J. L.-F. WANG, B. A. KING, AND C. B. MEYER.	21
SPECTRUM	MAGNESIUM OXIDE SPECTRUM AND CALCULATIONS. D. GREEN.	23
SPECTRUM	TEMPERATURE DEPENDENCE OF THE EPR SPECTRUM OF HEXAQUACOPPER-II IN WATER. J. J. CHANG AND R. J. MYERS.	82
SPHERE	EFFECT OF COMPLEXING ON LIFETIMES OF WATER MOLECULES IN THE FIRST COORDINATION SPHERE OF NICKEL ION. K. KUSTIN.	8
SPHERE	PROTON EXCHANGE FROM THE FIRST COORDINATION SPHERE OF HYDROLYTIC POLYMERS OF CHROMIUM(III). R. LEE.	8
SPIN	NUCLEAR-SPIN DOUBLE RESONANCE IN KH2PO4. D. STEHLIK.	198
SPIN	SPIN WAVE PROPAGATION. A. M. PORTIS.	185
SPLITTING	STUDIES OF THE THERMAL SPLITTING OF S4N4. R. L. PATTON AND W. L. JOLLY.	14
STACKING FAULT	ANNEALING OF STACKING-FAULT TETRAHEDRA IN GOLD. M. YOKOTA AND J. WASHBURN.	109
STAFF	IMRD STAFF FOR 1967.	199
STAGNANT	CONCENTRATION PROFILE AND DIFFUSION COEFFICIENT IN A STAGNANT DIFFUSION CELL. L. HSUEH AND J. NEWMAN.	63
STANNANE	THE CHEMISTRY OF STANNANE. J. R. WEBSTER AND W. L. JOLLY.	13
STANNANE	REACTIONS OF SILANE, GERMANE, AND STANNANE WITH METAL-AMMONIA AND AMIDE-AMMONIA SOLUTIONS. D. S. RUSTAD AND W. L. JOLLY.	11
STARK	HEAT CAPACITIES OF METALS UNDER PRESSURE. W. STARK AND G. JURA.	37
STEEL	STRUCTURE AND PROPERTIES OF FE/NI/CO/TI MARAGING STEEL. I. L. CHENG AND G. THOMAS.	123
STEELS	EFFECT OF TEST TEMPERATURE ON THE MECHANICAL PROPERTIES OF METASTABLE AUSTENITIC STEELS. G. R. CHANANI AND M. D. MERZ.	133
STEELS	NOTCH-TOUGHNESS VARIATIONS IN STEELS WITH THE SAME TENSILE PROPERTIES. Y. KATZ AND M. D. MERZ.	135
STEELS	EFFECT OF A STRAIN-INDUCED TRANSFORMATION ON THE TOUGHNESS OF HIGH-STRENGTH STEELS. C. P. LAPORTE, P. HEMMINGS, W. GERBERICH, AND M. D. MERZ.	136
STEELS	QUANTITATIVE INVESTIGATION OF THE STRAIN-INDUCED MARTENSITIC TRANSFORMATION IN HIGH-STRENGTH STEELS. B. DE MIRAMON AND M. D. MERZ.	131
STEHLIK	NUCLEAR-SPIN DOUBLE RESONANCE IN KH2PO4. D. STEHLIK.	198
STEIGER	OPTICAL STUDIES OF INTERFACIAL PHENOMENA. R. H. MULLER AND R. F. STEIGER.	47
STENMAN	SPONTANEOUS SCATTERING OF LIGHT. H. ROSEN, F. STENMAN, AND Y. R. SHEN.	195
STERLING	JOSEPHSON JUNCTION AS A FAR-INFRARED DETECTOR. P. L. RICHARDS AND S. A. STERLING.	189
STETT	EFFECT OF PRESSURE ON HIGH-TEMPERATURE DISSOLUTION. M. A. STETT AND R. M. FULRATH.	177
STEWART	THE AQUATION OF THE NITRO PENTAAMMINE COBALT(III) ION IN SULFURIC ACID SOLUTIONS. A. D. HARRIS, R. STEWART, D. HENDRICKSON, AND W. L. JOLLY.	16
STOICHIOMETRY	STOICHIOMETRY OF COPPER DISSOLUTION AT HIGH CURRENT DENSITIES. K. KINOSHITA, D. LANDOLT, R. H. MULLER, AND C. W. TOBIAS.	55
STRAIN	EFFECT OF INITIAL DISLOCATION DENSITY ON SINGLE-SLIP STRAIN HARDENING OF COPPER. J. WASHBURN AND G. MURTY.	107
STRAIN-INDUCED	EFFECT OF A STRAIN-INDUCED TRANSFORMATION ON THE TOUGHNESS OF HIGH-STRENGTH STEELS. C. P. LAPORTE, P. HEMMINGS, W. GERBERICH, AND M. D. MERZ.	136
STRAIN-INDUCED	QUANTITATIVE INVESTIGATION OF THE STRAIN-INDUCED MARTENSITIC TRANSFORMATION IN HIGH-STRENGTH STEELS. B. DE MIRAMON AND M. D. MERZ.	131
STRESS-INDUCED	STRESS-INDUCED MOVEMENT OF TWIN BOUNDARIES IN ZINC. R. E. COOPER AND J. WASHBURN.	107
STRUCTURE	MOLECULAR STRUCTURE OF SODIUM α-OXYHYPONITRITE. D. N. HENDRICKSON.	17
STRUCTURE	RELATION OF STRUCTURE TO PROPERTIES IN CRYSTALS. G. THOMAS.	119

STRUCTURE	STRUCTURE AND PROPERTIES OF FE/NI/CO/TI MARAGING STEEL. I. L. CHENG AND G. THOMAS.	123
STRUCTURE	ELECTRONIC STRUCTURE OF SOLIDS. M. L. COHEN.	183
SUBLIMATION	SUBLIMATION OF PRASEODYMIUM FLUORIDE. H. B. SKINNER AND A. W. SEARCY.	155
SUBLIMATION	EQUILIBRIUM AND NONEQUILIBRIUM SUBLIMATION OF ZINC SULFIDE AND OF CADMIUM TELLURIDE. B. A. H. BLANK AND A. W. SEARCY.	159
SUENAGA	SINGLE-PHASE AND POLYPHASE ALLOY SYSTEMS. M. SUENAGA, J. OLSON, AND K. RALLS.	141
SULFIDE	EQUILIBRIUM AND NONEQUILIBRIUM SUBLIMATION OF ZINC SULFIDE AND OF CADMIUM TELLURIDE. B. A. H. BLANK AND A. W. SEARCY.	159
SULFUR	SULFUR NITROGEN CHEMISTRY. W. L. JOLLY.	14
SULFUR	ADDUCTS OF SULFUR NITRIDE WITH BORON TRIHALIDES AND ANTIMONY PENTACHLORIDE. K. J. WYNNE AND W. L. JOLLY.	14
SULFUR	SULFUR NITROGEN CHLORIDES. W. L. JOLLY AND K. D. MAGUIRE.	15
SULFURIC	THE AQUATION OF THE NITRO PENTAAMMINE COBALT(III) ION IN SULFURIC ACID SOLUTIONS. A. D. HARRIS, R. STEWART, D. HENDRICKSON, AND W. L. JOLLY.	16
SULFURIC	PROTON MAGNETIC-RESONANCE SPECTRA OF RHODIUM AND IRIDIUM COMPLEXES IN SULFURIC ACID. D. N. HENDRICKSON AND W. L. JOLLY.	16
SUPERCONDUCTING	SUPERCONDUCTING TRANSITION TEMPERATURES OF VARIOUS LEAD-BASE ALLOYS. E. NEMBACH.	147
SUPERCONDUCTING	SUPERCONDUCTING TRANSITION TEMPERATURES OF LEAD-INDIUM ALLOYS. E. NEMBACH.	147
SUPERCONDUCTIVITY	HIGH-FIELD SUPERCONDUCTIVITY. L. BREWER, E. R. PARKER, AND V. F. ZACKAY.	141
SUPERCONDUCTIVITY	SUPERCONDUCTIVITY IN ALLOY SYSTEMS. M. F. MERRIAM.	146
SUPERCONDUCTIVITY	SUPERCONDUCTIVITY. G. ROCHLIN.	193
SUPERCONDUCTIVITY	SUPERCONDUCTIVITY IN DEGENERATE SEMICONDUCTORS. M. L. COHEN.	183
SUPERSATURATION	SUPERSATURATION DURING ELECTROLYTIC GAS EVOLUTION. C. BON AND C. W. TOBIAS.	51
SURFACE	SURFACE-PHASE TRANSFORMATIONS ON A MOLECULAR SURFACE. J. J. BURTON AND G. JURA.	35
SURFACE	SURFACE CALORIMETRY. R. H. MULLER AND R. C. GUPTA.	49
SURFACE	ELECTRODE POTENTIALS AND SURFACE CHARACTERISTICS IN HIGH-CURRENT-DENSITY COPPER DISSOLUTION. D. LANDOLT, K. KINOSHITA, R. MULLER, AND C. W. TOBIAS.	56
SURFACE	SURFACE STUDIES BY LOW-ENERGY ELECTRON DIFFRACTION. G. A. SOMORJAI.	43
SURFACE	COMMENTS ON SURFACE OXIDE FILMS AND THE LIFETIME OF VACANCIES IN THIN CRYSTALS. A. EIKUM AND G. THOMAS.	119
SURFACE	THE MEAN DISPLACEMENT OF SURFACE ATOMS IN PALLADIUM AND LEAD SINGLE CRYSTALS. R. M. GOODMAN, H. H. FARRELL, AND G. A. SOMORJAI.	43
SURFACE-PHASE	SURFACE-PHASE TRANSFORMATIONS ON A MOLECULAR SURFACE. J. J. BURTON AND G. JURA.	35
SURFACE REACTIONS	LOW-ENERGY ELECTRON-DIFFRACTION STUDY OF SURFACE REACTIONS ON (100) PLATINUM. A. E. MORGAN AND G. A. SOMORJAI.	44
SURFACES	LOW-ENERGY ELECTRON-DIFFRACTION STUDY OF ALPHA-ALUMINA (AL2O3) AND QUARTZ (SIO2) SURFACES. T. M. FRENCH, J. MORABITO, AND G. A. SOMORJAI.	44
SYNTHESES	INORGANIC SYNTHESES IN LOW-TEMPERATURE MATRICES, NONAQUEOUS SOLVENTS, AND COCONDENSATION SYSTEMS. D. SOLAN, J. L.-F. WANG, AND B. A. KING.	21
SZETO	SODIUM IN SILICON SINGLE CRYSTALS. W. SZETO AND G. A. SOMORJAI.	45
S4N4	S4N4-AMMONIA SOLUTIONS. K. J. WYNNE AND W. L. JOLLY.	15
S4N4	S4N4. M. VILLENA-BLANCO AND W. L. JOLLY.	15
S4N4	STUDIES OF THE THERMAL SPLITTING OF S4N4. R. L. PATTON AND W. L. JOLLY.	14
S4N4	S4N4-H2SO4 SOLUTIONS. S. LIPP AND W. L. JOLLY.	14
TALCOTT	ESR SPECTRA OF THE RADICAL ANIONS OF METHYL-SUBSTITUTED NITROSOBENZENES. C. L. TALCOTT AND R. J. MYERS.	84
TANTALUM	DISSOCIATION OF HYDROGEN ON TANTALUM USING A MODULATED MOLECULAR-BEAM TECHNIQUE. R. A. KRAKOWSKI AND D. R. OLANDER.	101
TARTOUR	CLIMB OF PERFECT AND IMPERFECT DISLOCATIONS IN ALUMINUM. J. TARTOUR AND J. WASHBURN.	109

TELLINGHUISEN	IODINE PREDISSOCIATION AND RECOMBINATION STUDIES. J. TELLINGHUISEN.	22
TELLINGHUISEN	PSEUDOPOTENTIAL CALCULATIONS ON ATOMS AND DIATOMIC MOLECULES. J. TELLINGHUISEN.	22
TELLURIDE	EQUILIBRIUM AND NONEQUILIBRIUM SUBLIMATION OF ZINC SULFIDE AND OF CADMIUM TELLURIDE. B. A. H. BLANK AND A. W. SEARCY.	159
TEMPERATURE	TEMPERATURE DEPENDENCE OF THE EPR SPECTRUM OF HEXAQUACOPPER-II IN WATER. J. J. CHANG AND R. J. MYERS.	82
TEMPERATURE	EFFECT OF TEST TEMPERATURE ON THE MECHANICAL PROPERTIES OF METASTABLE AUSTENITIC STEELS. G. R. CHANANI AND M. D. MERZ.	133
TEMPERATURE	EXCHANGE OF ENERGY BETWEEN TUNGSTEN AT HIGH TEMPERATURES AND GASES AT ROOM TEMPERATURE. M. J. LIM AND A. W. SEARCY.	155
TEMPERATURES	SPECTROSCOPIC INVESTIGATIONS OF HIGH-TEMPERATURE SPECIES TRAPPED AT LOW TEMPERATURES IN INERT MATRICES. J. L.-F. WANG, B. A. KING, AND C. B. MEYER.	21
TEMPERATURES	SUPERCONDUCTING TRANSITION TEMPERATURES OF VARIOUS LEAD-BASE ALLOYS. E. NEMBACH.	147
TEMPERATURES	EXCHANGE OF ENERGY BETWEEN TUNGSTEN AT HIGH TEMPERATURES AND GASES AT ROOM TEMPERATURE. M. J. LIM AND A. W. SEARCY.	155
TEMPERATURES	LOW-ENERGY ELECTRON-DIFFRACTION STUDIES AT LOW TEMPERATURES. J. MORABITO AND G. A. SOMORJAI.	44
TEMPERATURES	SUPERCONDUCTING TRANSITION TEMPERATURES OF LEAD-INDIUM ALLOYS. E. NEMBACH.	147
TEMPERATURES	GRAIN-BOUNDARY SLIDING AT HIGH TEMPERATURES. T. G. LANGDON.	164
TENSILE	NOTCH-TOUGHNESS VARIATIONS IN STEELS WITH THE SAME TENSILE PROPERTIES. Y. KATZ AND M. D. MERZ.	135
TETRAHEDRA	ANNEALING OF STACKING-FAULT TETRAHEDRA IN GOLD. M. YOKOTA AND J. WASHBURN.	109
THALLIUM	THALLIUM - THALLOUS HALIDE REFERENCE ELECTRODES IN PROPYLENE CARBONATE. F. G. K. BAUCKE AND C. W. TOBIAS.	54
THALLIUM	VAPOR PRESSURE OF THALLIUM AND ACTIVITY MEASUREMENTS ON LIQUID SILVER-THALLIUM ALLOYS BY THE TORSION-EFFUSION METHOD. P. J. DESRE, D. T. HAWKINS, AND R. HULTGREN.	152
THALLOUS	THALLIUM - THALLOUS HALIDE REFERENCE ELECTRODES IN PROPYLENE CARBONATE. F. G. K. BAUCKE AND C. W. TOBIAS.	54
THERMAL	CROSSED-MOLECULAR-BEAM INVESTIGATIONS OF THERMAL LI-ATOM REACTIONS. D. D. PARRISH AND R. R. HERM.	92
THERMAL	DIFFERENTIAL THERMAL CALORIMETRY. P. S. NICHOLSON AND R. M. FULRATH.	173
THERMAL	STUDIES OF THE THERMAL SPLITTING OF S4N4. R. L. PATTON AND W. L. JOLLY.	14
THERMODYNAMIC	THERMODYNAMIC CALCULATION METHODS. V. B. T. NGO AND O. REDLICH.	95
THERMODYNAMIC	THERMODYNAMIC STUDY OF THE HEAT OF ORDERING IN CUPT. G. W. GEIKEN, R. L. ORR, AND R. HULTGREN.	151
THERMODYNAMIC	EVALUATION OF THERMODYNAMIC DATA. R. HULTGREN, M. GLEISER, K. K. KELLEY, R. L. ORR, E. PLAZA, AND G. SOMAYAJULU.	152
THERMODYNAMICS	THERMODYNAMICS AND MOLECULAR STATE OF STRONG ACIDS. R. W. DUERST, W. E. GARGRAVE, AND O. REDLICH.	94
THERMODYNAMICS	FUNDAMENTAL THERMODYNAMICS. O. REDLICH.	96
THERMODYNAMICS	THERMODYNAMICS OF METAL SYSTEMS. R. HULTGREN.	151
THERMODYNAMICS	THERMODYNAMICS OF THE SILVER-SILICON SYSTEM BY DROP CALORIMETRY. T. A. CORN AND R. HULTGREN.	151
THOMAS	RELATION OF STRUCTURE TO PROPERTIES IN CRYSTALS. G. THOMAS.	119
THOMAS	ON FATIGUE-INDUCED REVERSION AND OVERAGING IN DISPERSION-STRENGTHENED ALLOY SYSTEMS. C. LAIRD AND G. THOMAS.	119
THOMAS	ELECTRON MICROSCOPY AT HIGH VOLTAGES. G. THOMAS.	120
THOMAS	STRUCTURE AND PROPERTIES OF FE/NI/CO/TI MARAGING STEEL. I. L. CHENG AND G. THOMAS.	123
THOMAS	ELECTRON-MICROSCOPE OBSERVATIONS OF TWINNING AND PHASE TRANSFORMATIONS IN INS CRYSTALS. A. G. FITZGERALD AND G. THOMAS.	125
THOMAS	INDICES OF PLANES AND DIRECTIONS IN HCP CRYSTALS. P. R. OKAMOTO AND G. THOMAS.	126
THOMAS	RESEARCH PLANS FOR 1968. G. THOMAS.	128
THOMAS	COMMENTS ON SURFACE OXIDE FILMS AND THE LIFETIME OF VACANCIES IN THIN CRYSTALS. A. EIKUM AND G. THOMAS.	119
THOMAS	1967 PUBLICATIONS. G. THOMAS AND ASSOCIATES.	129

TICL4	NMR SPECTRA OF CHLORINE-35 IN LIQUID VCL4 AND TICL4. D. W. PRATT AND R. J. MEYERS.	84
TIME OF FLIGHT	CROSSED-MOLECULAR-BEAM INVESTIGATION OF INELASTIC SCATTERING BY TIME-OF-FLIGHT ANALYSIS. D. D. PARRISH AND R. R. HERM.	93
TIN	STUDIES OF THE HYDRIDES OF SILICON, GERMANIUM, TIN, AND PHOSPHORUS.	11
TOBIAS	FUNDAMENTAL STUDIES OF IONIC MASS TRANSFER. C. W. TOBIAS.	50
TOBIAS	SUPERSATURATION DURING ELECTROLYTIC GAS EVOLUTION. C. BON AND C. W. TOBIAS.	51
TOBIAS	ELECTROCHEMISTRY IN NONAQUEOUS SOLVENTS. C. W. TOBIAS.	53
TOBIAS	THALLIUM - THALLOUS HALIDE REFERENCE ELECTRODES IN PROPYLENE CARBONATE. F. G. K. BAUCKE AND C. W. TOBIAS.	54
TOBIAS	ROTATING-DISK SYSTEM FOR METAL DEPOSITION FROM NONAQUEOUS SOLVENTS. F. G. K. BAUCKE, D. LANDOLT, AND C. W. TOBIAS.	55
TOBIAS	ELECTRODE POTENTIALS AND SURFACE CHARACTERISTICS IN HIGH-CURRENT-DENSITY COPPER DISSOLUTION. D. LANDOLT, K. KINOSHITA, R. MULLER, AND C. W. TOBIAS.	56
TOBIAS	OPTICAL STUDY OF CATHODIC GAS EVOLUTION DURING HIGH-CURRENT-DENSITY ELECTROLYSIS. D. LANDOLT, K. KINOSHITA, R. H. MULLER, AND C. W. TOBIAS.	59
TOBIAS	RESEARCH PLANS FOR 1968. C. W. TOBIAS.	60
TOBIAS	TRAVELLING-LASER INTERFEROMETER FOR MASS-TRANSFER STUDIES. K. W. BEACH, R. H. MULLER, AND C. W. TOBIAS.	50
TOBIAS	DYNAMICS OF POROUS ELECTRODES. C. W. TOBIAS.	51
TOBIAS	VISCOSITY OF CONCENTRATED SOLUTIONS OF CALCIUM IN LIQUID AMMONIA FROM -40 TO -70 DEGREES C. J. P. EARHART AND C. W. TOBIAS.	53
TOBIAS	ELECTROLYSIS AT EXTREMELY HIGH CURRENT DENSITIES. C. W. TOBIAS.	55
TOBIAS	MECHANISM OF ELECTROPOLISHING. K. KOJIMA AND C. W. TOBIAS.	59
TOBIAS	CURRENT AND POTENTIAL DISTRIBUTION IN CONVECTIVE MASS TRANSFER AT PLANE-PLATE ELECTRODES. J. R. SELMAN AND C. W. TOBIAS.	50
TOBIAS	REACTION DISTRIBUTION IN FLOODED POROUS ELECTRODES. R. ALKIRE, E. A. GRENS II, AND C. W. TOBIAS.	51
TOBIAS	STOICHIOMETRY OF COPPER DISSOLUTION AT HIGH CURRENT-DENSITIES. K. KINOSHITA, D. LANDOLT, R. H. MULLER, AND C. W. TOBIAS.	55
TOBIAS	1967 PUBLICATIONS. C. W. TOBIAS AND ASSOCIATES.	61
TORSION EFFUSION	VAPOR PRESSURE OF THALLIUM AND ACTIVITY MEASUREMENTS ON LIQUID SILVER-THALLIUM ALLOYS BY THE TORSION-EFFUSION METHOD. P. J. DESRE, D. T. HAWKINS, AND R. HULTGREN.	152
TOUGHNESS	EFFECT OF A STRAIN-INDUCED TRANSFORMATION ON THE TOUGHNESS OF HIGH-STRENGTH STEELS. C. P. LAPORTE, P. HEMMINGS, W. GERBERICH, AND M. D. MERZ.	136
TOUGHNESS	FRACTURE TOUGHNESS OF PLASTICS. L. KEY AND Y. KATZ.	137
TOUGHNESS	FRACTURE TOUGHNESS OF PRECIPITATION-HARDENING ALUMINUM ALLOYS. D. PORTER.	138
TOUGHNESS	MICROSTRUCTURE AND PLANE-STRAIN FRACTURE TOUGHNESS OF HIGH-STRENGTH ALUMINUM ALLOYS. P. J. GUEST AND M. D. MERZ.	135
TRANSFER	FUNDAMENTAL STUDIES OF IONIC MASS TRANSFER. C. W. TOBIAS.	50
TRANSFER	MASS TRANSFER TO THE REAR OF A CYLINDER AT HIGH SCHMITT NUMBERS. J. NEWMAN.	70
TRANSFER	MASS TRANSFER AND ELECTROCHEMICAL SYSTEMS. J. NEWMAN.	69
TRANSFERENCE	MOVING-BOUNDARY TRANSFERENCE NUMBERS. P. MILIOS AND J. NEWMAN.	62
TRANSFORMATION	EFFECT OF A STRAIN-INDUCED TRANSFORMATION ON THE TOUGHNESS OF HIGH-STRENGTH STEELS. C. P. LAPORTE, P. HEMMINGS, W. GERBERICH, AND M. D. MERZ.	136
TRANSFORMATION	QUANTITATIVE INVESTIGATION OF THE STRAIN-INDUCED MARTENSITIC TRANSFORMATION IN HIGH-STRENGTH STEELS. B. DE MIRAMON AND M. D. MERZ.	131
TRANSFORMATIONS	SURFACE-PHASE TRANSFORMATIONS ON A MOLECULAR SURFACE. J. J. BURTON AND G. JURA.	35
TRANSFORMATIONS	ELECTRON-MICROSCOPE OBSERVATIONS OF TWINNING AND PHASE TRANSFORMATIONS IN INS CRYSTALS. A. G. FITZGERALD AND G. THOMAS.	125
TRANSITION	SUPERCONDUCTING TRANSITION TEMPERATURES OF VARIOUS LEAD-BASE ALLOYS. E. NEMBACH.	147
TRANSITION	SUPERCONDUCTING TRANSITION TEMPERATURES OF LEAD-INDIUM ALLOYS. E. NEMBACH.	147
TRANSITION METAL	TRANSITION-METAL ALLOY SYSTEMS. P. WENGERT.	24
TRANSITION METAL	ELECTRON DISTRIBUTION IN TRANSITION-METAL COMPLEXES. C. B. HARRIS.	94

TRANSITIONS LEVEL-CROSSING DETECTION OF NQR TRANSITIONS. J. C. KOO AND E. L. HAHN. 197
TRANSPORT TRANSPORT PROPERTIES OF CONCENTRATED ELECTROLYTIC SOLUTIONS. T. W. CHAPMAN AND J. NEWMAN. 61
TRAPPED SPECTROSCOPIC INVESTIGATIONS OF HIGH-TEMPERATURE SPECIES TRAPPED AT LOW TEMPERATURES IN INERT MATRICES. J. L.-F. WANG, B. A. KING, AND C. B. MEYER. 21
TRAVELLING TRAVELLING-LASER INTERFEROMETER FOR MASS-TRANSFER STUDIES. K. W. BEACH, R. H. MULLER, AND C. W. TOBIAS. 50
TREMPER RADIOFREQUENCY PLASMA MICROSPHEROIDIZATION OF CERAMICS. R. T. TREMPER AND R. M. FULRATH. 175
TRIHALIDES ADDUCTS OF SULFUR NITRIDE WITH BORON TRIHALIDES AND ANTIMONY PENTACHLORIDE. K. J. WYNNE AND W. L. JOLLY. 14
TRIHALIDES REACTIONS OF DISULFUR DINITRIDE WITH ANTIMONY PENTACHLORIDE AND BORON TRIHALIDES. R. L. PATTON AND W. L. JOLLY. 14
TRIPLETT HEAT CAPACITY OF A NI-RH ALLOY. N. E. PHILLIPS, B. B. TRIPLETT, AND D. W. WOODY. 28
TRIPLETT HELIUM-3 - HELIUM-4 DILUTION REFRIGERATOR. B. B. TRIPLETT AND N. E. PHILLIPS. 33
TSAO PRODUCT ENERGY AND ANGULAR DISTRIBUTIONS FROM THE REACTION OF NITROGEN-MOLECULE ION WITH ISOTOPIC HYDROGEN MOLECULES. W. R. GENTRY, E. A. GISLASON, Y. T. LEE, B. H. MAHAN, AND C. W. TSAO. 75
TSAO DYNAMICS OF THE REACTION OF METHANE WITH NITROGEN-MOLECULE ION. E. A. GISLASON, C. W. TSAO, B. H. MAHAN, AND A. WERNER. 77
TSAO INELASTIC SCATTERING OF NITROGEN-MOLECULE ION BY HELIUM. W. R. GENTRY, E. A. GISLASON, B. H. MAHAN, AND C. W. TSAO. 74
TUNGSTEN EXCHANGE OF ENERGY BETWEEN TUNGSTEN AT HIGH TEMPERATURES AND GASES AT ROOM TEMPERATURE. M. J. LIM AND A. W. SEARCY. 155
TUNNEL FLOW TUNNEL WITH MOVING WALLS. P. H. SIH AND J. NEWMAN. 65
TWIN STRESS-INDUCED MOVEMENT OF TWIN BOUNDARIES IN ZINC. R. E. COOPER AND J. WASHBURN. 107
TWINNING ELECTRON-MICROSCOPE OBSERVATIONS OF TWINNING AND PHASE TRANSFORMATIONS IN INS CRYSTALS. A. G. FITZGERALD AND G. THOMAS. 125
ULTRASHORT ULTRASHORT LIGHT PULSES. J. SHELTON AND Y. R. SHEN. 195
VACANCIES COMMENTS ON SURFACE OXIDE FILMS AND THE LIFETIME OF VACANCIES IN THIN CRYSTALS. A. EIKUM AND G. THOMAS. 119
VAGNARD PLASTIC DEFORMATION OF CUPROUS OXIDE. G. VAGNARD AND J. WASHBURN. 107
VAN DEN BOGAERDE SPECTRA AND LIFETIMES OF GAS-PHASE FREE RADICALS AT VERY LOW CONCENTRATIONS. H. S. JOHNSTON, E. D. MORRIS, JR., T. T. PAUKERT, AND J. VAN DEN BOGAERDE. 87
VANADYL OXYGEN-17 NMR STUDIES OF WATER EXCHANGE OF PARTIALLY COMPLEXED VANADYL ION. K. WUTHRICH. 7
VAPOR VAPOR SPECIES OF THE BARIUM-OXYGEN SYSTEM. R. S. NEWBURY, G. W. BARTON, JR., AND A. W. SEARCY. 159
VAPOR ZERO-FIELD, FREE-PRECESSION MEASUREMENTS OF THE HYPERFINE INTERACTION IN CESIUM-33 VAPOR. J. W. SHANER, S. A. MILLER, AND E. L. HAHN. 197
VAPOR PRESSURE VAPOR PRESSURE OF THALLIUM AND ACTIVITY MEASUREMENTS ON LIQUID SILVER-THALLIUM ALLOYS BY THE TORSION-EFFUSION METHOD. P. J. DESRE, D. T. HAWKINS, AND R. HULTGREN. 152
VAPORIZATION VAPORIZATION KINETICS OF SOLIDS. G. A. SOMORJAI. 39
VAPORIZATION HIGH-TEMPERATURE VAPORIZATION MECHANISMS. G. A. SOMORJAI. 43
VAPORIZATION CONDENSATION-ENHANCED VAPORIZATION OF HIGH-TEMPERATURE SOLIDS. R. OMBERG AND D. R. OLANDER. 103
VCL4 NMR SPECTRA OF CHLORINE-35 IN LIQUID VCL4 AND TICL4. D. W. PRATT AND R. J. MEYERS. 84
VERTICAL LAMINAR FREE CONVECTION AT A VERTICAL PLATE IN THE PRESENCE OF SUPPORTING ELECTROLYTE. J. R. SELMAN AND J. NEWMAN. 66
VILLENA-BLANCO S4N4. M. VILLENA-BLANCO AND W. L. JOLLY. 15
VISCOSITY VISCOSITY OF CONCENTRATED SOLUTIONS OF CALCIUM IN LIQUID AMMONIA FROM -40 TO -70 DEGREES C. J. P. EARHART AND C. W. TOBIAS. 53
VISCOSITY VISCOSITY DETERMINATIONS. J. FINUCANE AND D. R. OLANDER. 102
VOID VOID FORMATION IN NICKEL AND SILVER DURING CREEP. T. G. LANGDON. 165
VOLTAGES ELECTRON MICROSCOPY AT HIGH VOLTAGES. G. THOMAS. 120
WADDEL GAS ANALYSIS BY MODULATED MOLECULAR-BEAM MASS SPECTROMETRY. D. R. OLANDER AND W. WADDEL. 99
WALKER RATE OF ATTACHMENT OF GASEOUS ELECTRONS TO NITROGEN DIOXIDE. B. H. MAHAN AND I. C. WALKER. 74

WALLS	FLOW TUNNEL WITH MOVING WALLS. P. H. SIH AND J. NEWMAN.	65
WANG	SPECTROSCOPIC INVESTIGATIONS OF HIGH-TEMPERATURE SPECIES TRAPPED AT LOW TEMPERATURES IN INERT MATRICES. J. L.-F. WANG, B. A. KING, AND C. B. MEYER.	21
WANG	HEAT CAPACITY OF METALS UNDER PRESSURE. S. S. B. WANG, M. M. CONWAY, AND N. E. PHILLIPS.	33
WANG	INORGANIC SYNTHESES IN LOW-TEMPERATURE MATRICES, NONAQUEOUS SOLVENTS, AND COCONDENSATION SYSTEMS. D. SOLAN, J. L.-F. WANG, AND B. A. KING.	21
WANG	BORON HYDRIDE CHEMISTRY. W. L. JOLLY, T. SCHMITT, AND F. WANG.	13
WASHBURN	CRYSTAL IMPERFECTIONS. J. WASHBURN.	107
WASHBURN	STRESS-INDUCED MOVEMENT OF TWIN BOUNDARIES IN ZINC. R. E. COOPER AND J. WASHBURN.	107
WASHBURN	ANNEALING OF STACKING-FAULT TETRAHEDRA IN GOLD. M. YOKOTA AND J. WASHBURN.	109
WASHBURN	RESEARCH PLANS FOR 1968. J. WASHBURN.	112
WASHBURN	PLASTIC DEFORMATION OF CUPROUS OXIDE. G. VAGNARD AND J. WASHBURN.	107
WASHBURN	CLIMB OF PERFECT AND IMPERFECT DISLOCATIONS IN ALUMINUM. J. TARTOUR AND J. WASHBURN.	109
WASHBURN	EFFECT OF INITIAL DISLOCATION DENSITY ON SINGLE-SLIP STRAIN HARDENING OF COPPER. J. WASHBURN AND G. MURTY.	107
WASHBURN	LIQUID-HELIUM FIELD-ION MICROSCOPE FOR RADIATION DAMAGE INVESTIGATIONS. P. PETROFF AND J. WASHBURN.	109
WASHBURN	FIELD-ION MICROSCOPE INVESTIGATION OF RADIATION DAMAGE IN IRIDIUM BOMBARDED WITH 10-MEV PROTONS. P. PETROFF AND J. WASHBURN.	109
WASHBURN	1967 PUBLICATIONS. J. WASHBURN AND ASSOCIATES.	114
WATER	OXYGEN-17 NMR STUDIES OF WATER EXCHANGE OF PARTIALLY COMPLEXED VANADYL ION. K. WUTHRICH.	7
WATER	EFFECT OF COMPLEXING ON LIFETIMES OF WATER MOLECULES IN THE FIRST COORDINATION SPHERE OF NICKEL ION. K. KUSTIN.	8
WATER	WATER EXCHANGE ON TI(III). H. CHARLES.	9
WATER	TEMPERATURE DEPENDENCE OF THE EPR SPECTRUM OF HEXAQUACOPPER-II IN WATER. J. J. CHANG AND R. J. MYERS.	82
WATERFIELD	CONSTANT-VOLUME HEAT CAPACITY OF COMPRESSED HELIUM-II. C. G. WATERFIELD, J. K. HOFFER, AND N. E. PHILLIPS.	29
WATERFIELD	MELTING CURVE OF HELIUM-4. N. E. PHILLIPS, J. K. HOFFER, AND C. G. WATERFIELD.	29
WAVE	SPIN WAVE PROPAGATION. A. M. PORTIS.	185
WEBSTER	THE CHEMISTRY OF STANNANE. J. R. WEBSTER AND W. L. JOLLY.	13
WENGERT	TRANSITION-METAL ALLOY SYSTEMS. P. WENGERT.	24
WERNER	DYNAMICS OF THE REACTION OF METHANE WITH NITROGEN-MOLECULE ION. E. A. GISLASON, C. W. TSAO, B. H. MAHAN, AND A. WERNER.	77
WOODY	HEAT CAPACITY OF A NI-RH ALLOY. N. E. PHILLIPS, B. B. TRIPLETT, AND D. W. WOODY.	28
WUTHRICH	OXYGEN-17 NMR STUDIES OF WATER EXCHANGE OF PARTIALLY COMPLEXED VANADYL ION. K. WUTHRICH.	7
WYNNE	S4N4-AMMONIA SOLUTIONS. K. J. WYNNE AND W. L. JOLLY.	15
WYNNE	ADDUCTS OF SULFUR NITRIDE WITH BORON TRIHALIDES AND ANTIMONY PENTACHLORIDE. K. J. WYNNE AND W. L. JOLLY.	14
YOKOTA	ANNEALING OF STACKING-FAULT TETRAHEDRA IN GOLD. M. YOKOTA AND J. WASHBURN.	109
YOON	HEAT CAPACITY AND HEAT OF DECOMPOSITION OF AUSTENITE. H. I. YOON AND R. HULTGREN.	152
ZACKAY	GENERAL INTRODUCTION. L. BREWER AND V. ZACKAY.	1
ZACKAY	HIGH-STRENGTH MATERIALS. E. R. PARKER AND V. F. ZACKAY.	131
ZACKAY	RESEARCH PLANS FOR 1968. V. F. ZACKAY AND E. R. PARKER.	138
ZACKAY	HIGH-FIELD SUPERCONDUCTIVITY. L. BREWER, E. R. PARKER, AND V. F. ZACKAY.	141
ZACKAY	RESEARCH PLANS FOR 1968. L. BREWER, E. R. PARKER, AND V. F. ZACKAY.	146
ZACKAY	1967 PUBLICATIONS. E. R. PARKER, V. F. ZACKAY AND ASSOCIATES.	139
ZACKAY	1967 PUBLICATIONS. L. BREWER, E. R. PARKER, V. F. ZACKAY AND ASSOCIATES.	146
ZERO-FIELD	ZERO-FIELD, FREE-PRECESSION MEASUREMENTS OF THE HYPERFINE INTERACTION IN CESIUM-33 VAPOR. J. W. SHANER, S. A. MILLER, AND E. L. HAHN.	197
ZINC	STRESS-INDUCED MOVEMENT OF TWIN BOUNDARIES IN ZINC. R. E. COOPER AND J. WASHBURN.	107
ZINC	EQUILIBRIUM AND NONEQUILIBRIUM SUBLIMATION OF ZINC SULFIDE AND OF CADMIUM TELLURIDE. B. A. H. BLANK AND A. W. SEARCY.	159

ZIRCONATE	HIGH-TEMPERATURE PHASE EQUILIBRIA IN THE LEAD-TITANATE - LEAD-ZIRCONATE SYSTEM. R. L. MOON AND R. M. FULRATH.	-171
ZUCCA	OPTICAL PROPERTIES OF SOLIDS. R. ZUCCA AND Y. R. SHEN.	-195
1 DEGREE KELVIN	ESR SPECTRA NEAR 1 DEGREE KELVIN. D. W. PRATT, A. JINDO, W. T. BATCHELDER, AND R. J. MYERS.	83
10-MEV	FIELD-ION MICROSCOPE INVESTIGATION OF RADIATION DAMAGE IN IRIDIUM BOMBARDED WITH 10-MEV PROTONS. P. PETROFF AND J. WASHBURN.	- --109
100	THE FERMI MOMENTUM OF ALUMINUM FROM 0 TO 100 KBARS. J. J. BURTON AND G. JURA.	34
40	VISCOSITY OF CONCENTRATED SOLUTIONS OF CALCIUM IN LIQUID AMMONIA FROM -40 TO -70 DEGREES C. J. P. EARHART AND C. W. TOBIAS.	-53
70	VISCOSITY OF CONCENTRATED SOLUTIONS OF CALCIUM IN LIQUID AMMONIA FROM -40 TO -70 DEGREES C. J. P. EARHART AND C. W. TOBIAS.	-53

This report was prepared as an account of Government sponsored work. Neither the United States, nor the Commission, nor any person acting on behalf of the Commission:

A. Makes any warranty or representation, expressed or implied, with respect to the accuracy, completeness, or usefulness of the information contained in this report, or that the use of any information, apparatus, method, or process disclosed in this report may not infringe privately owned rights; or

B. Assumes any liabilities with respect to the use of, or for damages resulting from the use of any information, apparatus, method, or process disclosed in this report.

As used in the above, "person acting on behalf of the Commission" includes any employee or contractor of the Commission, or employee of such contractor, to the extent that such employee or contractor of the Commission, or employee of such contractor prepares, disseminates, or provides access to, any information pursuant to his employment or contract with the Commission, or his employment with such contractor.